frontiers | Research Topics

Acute-on-chronic liver failure: Systemic inflammation and immunosuppression, 2nd Edition

Edited by
Yu Shi, Yu-Chen Fan, Jonel Trebicka, Olaf Tyc and Xiaogang Xiang

Published in
Frontiers in Immunology

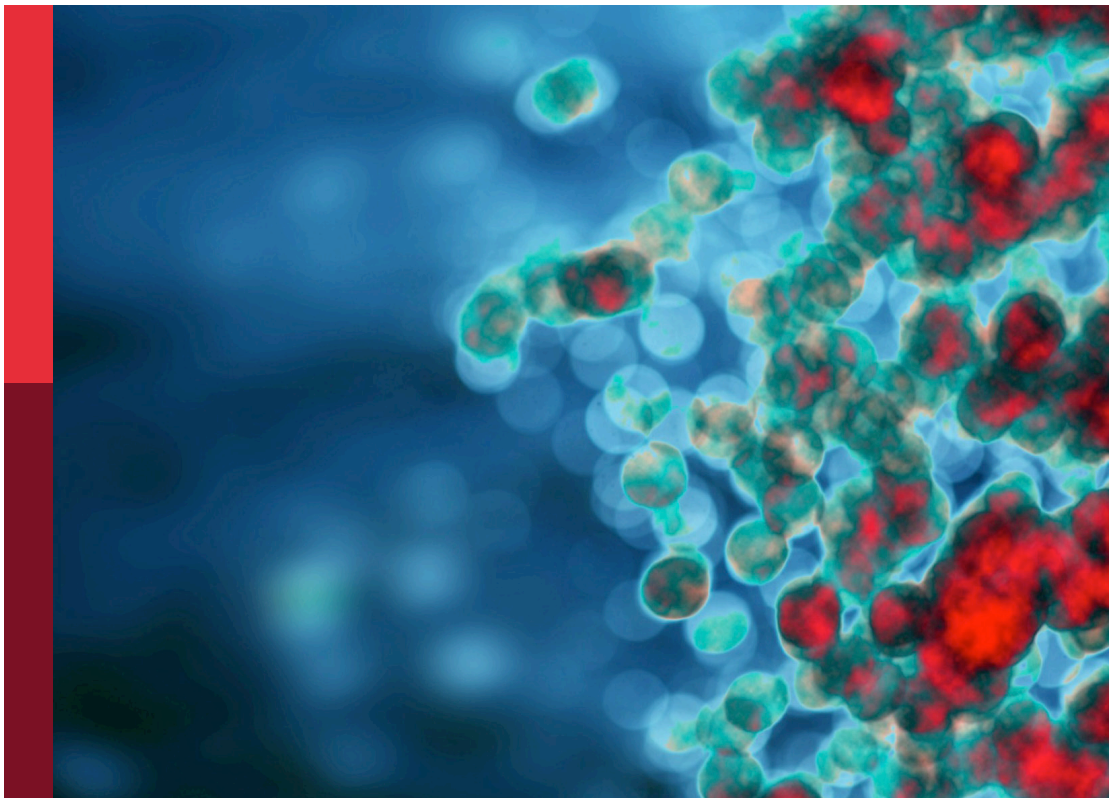

ISSN 1664-8714
ISBN 978-2-8325-3359-8
DOI 10.3389/978-2-8325-3359-8

About Frontiers

Frontiers is more than just an open access publisher of scholarly articles: it is a pioneering approach to the world of academia, radically improving the way scholarly research is managed. The grand vision of Frontiers is a world where all people have an equal opportunity to seek, share and generate knowledge. Frontiers provides immediate and permanent online open access to all its publications, but this alone is not enough to realize our grand goals.

Frontiers journal series

The Frontiers journal series is a multi-tier and interdisciplinary set of open-access, online journals, promising a paradigm shift from the current review, selection and dissemination processes in academic publishing. All Frontiers journals are driven by researchers for researchers; therefore, they constitute a service to the scholarly community. At the same time, the *Frontiers journal series* operates on a revolutionary invention, the tiered publishing system, initially addressing specific communities of scholars, and gradually climbing up to broader public understanding, thus serving the interests of the lay society, too.

Dedication to quality

Each Frontiers article is a landmark of the highest quality, thanks to genuinely collaborative interactions between authors and review editors, who include some of the world's best academicians. Research must be certified by peers before entering a stream of knowledge that may eventually reach the public - and shape society; therefore, Frontiers only applies the most rigorous and unbiased reviews. Frontiers revolutionizes research publishing by freely delivering the most outstanding research, evaluated with no bias from both the academic and social point of view. By applying the most advanced information technologies, Frontiers is catapulting scholarly publishing into a new generation.

What are Frontiers Research Topics?

Frontiers Research Topics are very popular trademarks of the *Frontiers journals series*: they are collections of at least ten articles, all centered on a particular subject. With their unique mix of varied contributions from Original Research to Review Articles, Frontiers Research Topics unify the most influential researchers, the latest key findings and historical advances in a hot research area.

Find out more on how to host your own Frontiers Research Topic or contribute to one as an author by contacting the Frontiers editorial office: frontiersin.org/about/contact

Acute-on-chronic liver failure: Systemic inflammation and immunosuppression, 2nd Edition

Topic editors

Yu Shi — Zhejiang University, China
Yu-Chen Fan — Shandong University, China
Jonel Trebicka — Goethe University Frankfurt, Germany
Olaf Tyc — University Hospital Frankfurt, Germany
Xiaogang Xiang — Shanghai Jiao Tong University, China

Citation

Shi, Y., Fan, Y.-C., Trebicka, J., Tyc, O., Xiang, X., eds. (2023). *Acute-on-chronic liver failure: Systemic inflammation and immunosuppression, 2nd Edition*. Lausanne: Frontiers Media SA. doi: 10.3389/978-2-8325-3359-8

Publisher's note: In this 2nd edition, the following article has been updated:

Tyc O, Shi Y, Fan Y-C, Trebicka J and Xiang X (2023) Editorial: Acute-on-chronic liver failure: systemic inflammation and immunosuppression. Front. Immunol. 14:1260749. doi: 10.3389/fimmu.2023.1260749

Table of contents

frontiers | Frontiers in Immunology

TYPE Editorial
PUBLISHED 15 August 2023
DOI 10.3389/fimmu.2023.1260749

OPEN ACCESS

EDITED AND REVIEWED BY
Pietro Ghezzi,
University of Urbino Carlo Bo, Italy

*CORRESPONDENCE
Yu Shi
zjushiyu@zju.edu.cn

RECEIVED 18 July 2023
ACCEPTED 02 August 2023
PUBLISHED 15 August 2023

CITATION
Tyc O, Shi Y, Fan Y-C, Trebicka J and Xiang X (2023) Editorial: Acute-on-chronic liver failure: systemic inflammation and immunosuppression. *Front. Immunol.* 14:1260749. doi: 10.3389/fimmu.2023.1260749

Editorial: Acute-on-chronic liver failure: systemic inflammation and immunosuppression

Olaf Tyc[1], Yu Shi[2]*, Yu-Chen Fan[3], Jonel Trebicka[4,5] and Xiaogang Xiang[6]

[1]Medical Clinic 1, University Hospital, Goethe University Frankfurt, Frankfurt, Germany, [2]State Key Laboratory for Diagnosis and Treatment of Infectious Diseases, Collaborative Innovation Center for Diagnosis and Treatment of Infectious Disease, National Clinical Research Center for Infectious Diseases, The First Affiliated Hospital, Zhejiang University School of Medicine, Hangzhou, China, [3]Department of Hepatology, Qilu Hospital, Shandong University, Jinan, China, [4]Department of Internal Medicine B, University Hospital of Münster, Münster, Germany, [5]European Foundation for the Study of Chronic Liver Failure (EF-CLIF), Barcelona, Spain, [6]Department of Infectious Diseases, Ruijin Hospital, School of Medicine, Shanghai Jiao Tong University, Shanghai, China

KEYWORDS

acute-on-chronic liver failure, systemic inflammation, immunosuppression, pathophysiological mechanisms, chronic liver disease

Editorial on the Research Topic
Acute-on-chronic liver failure: systemic inflammation and immunosuppression

Introduction

ACLF is a severe and often fatal condition that occurs in individuals with underlying chronic liver disease when acute events precipitate its development (1). Due to the lack of therapies for ACLF, except for liver transplantation, there is a critical need to investigate its pathophysiological mechanisms (2). It is well-established that systemic inflammation plays a significant role in driving ACLF (3). However, there is limited understanding of how systemic inflammation develops and how it affects organ functions. Additionally, immunosuppression, another immune dysfunction observed in ACLF, contributes to bacterial infections and worsens the overall condition (4). Unfortunately, little is known about the development of immunosuppression during ACLF and its underlying molecular mechanisms. Consequently, ACLF remains a major challenge for clinicians and researchers. The following articles present interesting findings in the field of Acute-on-chronic Liver Failure (ACLF).

Editorial on the Research Topic acute-on-chronic liver failure: systemic inflammation and immunosuppression

The first part of this Research Topic consists of investigations using biosamples from patients, which provide biomarkers and insights in potential immunological effects of specific drugs. The study of Sánchez-Rodríguez et al. investigates the role of CD5L (a macrophage anti-

inflammatory protein) and the specialized pro-resolving lipid mediators (SPMs) in the pathogenesis of acute-on-chronic liver failure (ACLF). The study revealed a progressive loss of circulating EVs as the disease progressed. Moreover, the content of CD5L in EVs exhibited differential changes during disease progression, with the highest levels observed in AD and a subsequent decrease in ACLF. This observation indicates a potential role of CD5L in regulating immune cell activation and the systemic inflammatory response. Hereby, monocytes are key cell type. Tong et al. reported about the effect of granulocyte colony stimulating factor (G-CSF) on switching the M1 pro-inflammatory state to M2 anti-inflammatory state of monocytes in ACLF patients from a randomized controlled trial. G-CSF therapy not only induces M1/M2 phenotype of monocyte but also attenuates pro-inflammatory cytokine secretion, but do not influence phagocytosis or oxidative burse capacity in patients with HBV-ACLF, which may lead to resolution of inflammation and ACLF recovery in selected patients. Maheshwari et al. analysed defects in phagocytic and oxidative burst capacity in ACLF monocytes in an animal model of ACLF. MSC therapy may correct the energy supply and eventually ameliorate hepatic injury and promote liver regeneration. Moreover, drug-induced liver injury (DILI) may also precipitate ACLF in few cases, which is shown in the prospective cohort study of Wang, M.-G. et al. The authors investigated the mechanisms underlying DILI due to anti- tuberculosis drugs (ATB) on diagnosed tuberculosis (TB) patients (Wang, M.-G. et al.). The authors analyzed urinary metabolic and microbial samples. The resulting data were submitted to machine learning techniques, which allowed the development of a prediction model for ATB-DILI based on the obtained metabolomics, microbiome, and clinical data.

The second topic was about to perform manipulations on disease model animals to provide insights into pathophysiological mechanisms of ACLF pathogenesis. MicroRNA (miRNA) is known to bind to specific sequences in target mRNAs and thereby silence gene translation. Tao et al. tested the therapeutic efficacy of miR-125b-5p supplement, which was depleted in the liver of HBV-ACLF patients in a model of liver failure induced by lipopolysaccharide (LPS) and D-galactosamine (D-GalN). The results showed that miR-125b-5p alleviated mouse ALF, most probably *via* Kelch-like ECH-associated protein 1 (Keap1) repression and up-regulation of the expression of nuclear factor (erythroid-derived 2)-like 2 (Nrf2) and Heme oxygenase-1 (HO-1).

By contrast, Qu et al. focused on the role of PEBP4 pathway, and using PDTC and TAK-242, that selectively inhibits the activity of NF-κB and TLR4, which can partially reverse the detrimental effect of PEBP4 depletion. The work of Qu et al. provides another candidate target for drugs that are partly in clinical testing as ACLF therapy. This part of the Research Topic is rounded-up by the work of Huang et al. investigating the role of mitophagy, in the pathogenesis of acute liver injury (ALI) caused by heat stroke (HS) which is a fatal form of heat injury. This study revealed a cytosolic p53-mediated impaired mitophagy in the pathogenesis of HS-ALI and highlights pharmacologic induction of mitophagy by inhibiting cytosolic p53 as a promising therapeutic approach for HS-ALI treatment. Also the work of Wang, J. et al. tested the therapeutic efficacy of phenethyl isothiocyanate (PEITC), a natural compound extracted from cruciferous vegetables, in an concanavalin A (ConA)-induced acute liver injury model and carbon tetrachloride (CCl4)-induced chronic liver injury model. Mechanically, PEITC inhibited hepatocyte pyroptosis by interacting with cysteine 191 of GSDMD with its specific structure –N=C=S, which may be a candidate drug for treating ALI.

The Research Topic also collected three up-to-dated literature reviews. The review of Qiang et al. incorporates the current research status related to ACLF and sheds light on the immune mechanisms underlying the development and progression of acute-on-chronic liver failure (ACLF). The authors discuss that the understanding of ACLF and its definition has been a subject of controversy discussion and definition differences among the liver-related research communities worldwide. In their review, the authors highlight the immune pathogenesis of ACLF and the importance of pathogen-associated molecular patterns (PAMPs) and damage-associated molecular patterns (DAMPs) in ACLF. Furthermore, the review of Hazrati et al. summarizes the mechanisms underlying the protective and therapeutic effects of MSCs and MCSs- derived extracellular vesicles (EVs) in liver diseases, involving differentiation into hepatocyte-like cells, inhibition of apoptosis and inflammation, promotion of growth factors production and hepatocyte proliferation, suppression of hepatic stellate cells (HSCs) and tissue-damaging immune cells.

Finally, the review of Ye et al. summarizes the evidences on the use of glucocorticoids in treating ACLF and ALF. The review article emphasizes the etiology of liver failure in evaluating glucocorticoid efficacy. The benefit of glucocorticoid therapy seems to be definite in AIH-induced liver failure, while controversial in HBV or drug-related ACLF or ALF. The authors highlighted the potential impact of dosing and timing of glucocorticoids use on the survival benefit and the lack of specific biomarkers to precisely guide the optimized use of glucocorticoids in these patients.

Author contributions

OT: Conceptualization, Writing – original draft. YS: Writing – original draft, Writing – review & editing. Y-CF: Investigation, Writing – original draft. JT: Data curation, Writing – original draft. XX: Formal Analysis, Writing – original draft.

Funding

OT was supported by the research funding program Landes-Offensive zur Entwicklung Wissenschaftlich-ökonomischer Exzellenz (LOEWE) of the State of Hesse (HMWK), Research Initiative ACLF-I. JT was supported by the German Research Foundation (DFG) project ID 403224013 – SFB 1382 (A09), by the German Federal Ministry of Education and Research (BMBF) for the DEEP-HCC project, and by the Hessian Ministry of Higher Education, Research and the Arts (HMWK) for the ENABLE and ACLF-I cluster projects. The MICROB-PREDICT (project ID 825694), DECISION (project ID 847949), GALAXY (project ID 668031), LIVERHOPE (project ID 731875), and IHMCSA (project ID 964590) projects have received funding from the European Union's Horizon 2020 research and innovation program. The manuscript reflects only the authors' views, and the European Commission is not responsible for any use that may

be made of the information it contains. The funders had no influence on the study design, data collection, and analysis, the decision to publish, or the preparation of the manuscript. This research received also funding from the Fundamental Research Funds for the Central Universities (2021FZZX001-41,226-2023-00127), Medical Health Science and Technology Project of Zhejiang Provincial Health Commission (No.2022490480), and Chinese National Natural Science Foundation (No.81870425).

Acknowledgments

We would like to thank all authors and reviewers who contributed to the Research Topic: "*Acute-on-chronic liver failure: systemic inflammation and immunosuppression*."

Conflict of interest

The authors declare that the research was conducted in the absence of any commercial or financial relationships that could be construed as a potential conflict of interest.

Publisher's note

References

1. Richard M, Marta T, Aleksander K, Paolo A, Marina B, Annalisa B, et al. EASL Clinical Practice Guidelines on acute-on-chronic liver failure. *J Hepatol* (2023) 79 (2):461–91. doi: 10.1016/j.jhep.2023.04.021

2. Luo J, Li J, Li P, Liang X, Hassan HM, Moreau R. Acute-on-chronic liver failure: far to go-a review. *Crit Care* (2023) 27:259. doi: 10.1186/s13054-023-04540-4

3. Arroyo V, Angeli P, Moreau R, Jalan R, Clària J, Trebicka J, et al. The systemic inflammation hypothesis: Towards a new paradigm of acute decompensation and multiorgan failure in cirrhosis. *J Hepatol* (2021) 74:670–85. doi: 10.1016/j.jhep.2020.11.048

4. Schierwagen R, Gu W, Brieger A, Brüne B, Ciesek S, Đikić I, et al. Pathogenetic mechanisms and therapeutic approaches of acute-to-chronic liver failure. *Am J Physiol Cell Physiol* (2023) 325:C129–40. doi: 10.1152/ajpcell.00101.2023

frontiers in Immunology

ORIGINAL RESEARCH
published: 31 January 2022
doi: 10.3389/fimmu.2022.825428

Direct Inhibition of GSDMD by PEITC Reduces Hepatocyte Pyroptosis and Alleviates Acute Liver Injury in Mice

Jie Wang[1†], Ke Shi[1†], Ning An[1], Shuaifei Li[1], Mei Bai[1], Xudong Wu[1], Yan Shen[1], Ronghui Du[1], Jingcai Cheng[2], Xuefeng Wu[1*] and Qiang Xu[1*]*

[1] State Key Laboratory of Pharmaceutical Biotechnology, Nanjing Drum Tower Hospital, School of Life Science, Nanjing University, Nanjing, China, [2] Drug R&D Institute, JC (Wuxi) Company, Inc., Wuxi, China

OPEN ACCESS

Edited by:
Haichao Wang,
Feinstein Institute for Medical Research, United States

Reviewed by:
Mohammad Asif Sherwani, University of Alabama at Birmingham, United States
Qinghua Hu, China Pharmaceutical University, China
Nattaya Konsue, Mae Fah Luang University, Thailand

***Correspondence:**
Jingcai Cheng
jcijcheng@163.com
Xuefeng Wu
wuxf@nju.edu.cn
Qiang Xu
molpharm@163.com

[†]These authors have contributed equally to this work

Specialty section:
This article was submitted to Inflammation, a section of the journal Frontiers in Immunology

Received: 30 November 2021
Accepted: 06 January 2022
Published: 31 January 2022

Citation:
Wang J, Shi K, An N, Li S, Bai M, Wu X, Shen Y, Du R, Cheng J, Wu X and Xu Q (2022) Direct Inhibition of GSDMD by PEITC Reduces Hepatocyte Pyroptosis and Alleviates Acute Liver Injury in Mice. Front. Immunol. 13:825428. doi: 10.3389/fimmu.2022.825428

Acute liver injury (ALI), often caused by viruses, alcohol, drugs, etc., is one of the most common clinical liver diseases. Although pyroptosis plays an important role in ALI, there is still a lack of effective clinical drugs related to this mechanism. Here, we show that phenethyl isothiocyanate (PEITC), a natural compound present in cruciferous vegetables, can significantly alleviate concanavalin A (ConA)-induced inflammatory liver damage and carbon tetrachloride (CCl_4)-induced chemical liver damage in a dose-dependent manner. PEITC dose-dependently reversed the ALI-induced increase in plasma levels of aspartate aminotransferase (AST), alanine aminotransferase (ALT), lactate dehydrogenase (LDH), tumor necrosis factor (TNF)-α, and interferon (IFN)-γ and reduced the protein levels of hepatocyte pyroptosis markers such as Nod-like receptor family pyrin domain containing 3 (NLRP3), cleaved caspase-1, and cleaved gasdermin D (GSDMD). *In vitro* experiments have also verified the inhibitory effect of PEITC on hepatocyte pyroptosis. Furthermore, PEITC inhibits pyroptosis by interacting with cysteine 191 of GSDMD. In summary, our findings establish a role for PEITC in rescuing hepatocyte pyroptosis *via* direct inhibition of GSDMD, which may provide a new potential therapeutic strategy for ALI.

Keywords: PEITC, pyroptosis, hepatocyte, gasdermin D, acute liver injury

INTRODUCTION

Acute liver injury (ALI) is one of the most common clinical liver diseases and is often caused by viruses, alcohol, drugs, etc. If it is not treated in time, it can easily develop into acute liver failure, chronic liver injury, or hepatocellular carcinoma, which seriously threatens human quality of life and health. The mechanisms and characteristics of ALI are very complex, including hepatocyte death, oxidative stress, inflammation, etc. Hepatocyte pyroptosis is particularly critical for liver damage in the development of liver inflammation into cirrhosis, liver fibrosis, and hepatocellular carcinoma (1–4). In mouse sepsis models induced by lipopolysaccharide (LPS), the level of pyroptosis is positively correlated with the severity of liver injury (5). Signaling pathways involved in pyroptosis in hepatocytes and nonparenchymal cells were significantly enhanced in concanavalin A (ConA)-induced mouse ALI models (6).

Pyroptosis is a programmed cell death mediated by gasdermin family proteins (7), and its activation mechanism is divided into classical pathways and nonclassical pathways according to whether it depends on caspase-1 (CASP1). In the classical pathway, CASP1 is recruited and activated by inflammasomes. Activated CASP1 cleaves gasdermin D (GSDMD) to produce an active GSDMD-N-terminal domain. The GSDMD-N-terminal domain translocates to the cell membrane to form membrane pores, resulting in pyroptosis. In the nonclassical pathway, human caspase-4, caspase-5, and mouse caspase-11 can be directly activated by LPS and then cleave GSDMD, causing pyroptosis (8–10). In addition, there is a pyroptosis pathway that depends on caspase-3, which is an executive protein of apoptosis. When apoptotic cells are not cleared in time, the expression levels of gasdermin E (GSDME) are upregulated by p53 and then specifically cleaved by caspase-3 to produce the GSDME N-terminal domain (11). Finally, the GSDME-N-terminal domain forms membrane pores to induce pyroptosis (11, 12).

Although the liver has a regenerative function, ALI may develop into acute liver failure with extremely high mortality if liver regeneration cannot offset a large number of hepatocyte deaths (13). When acute liver injury lasts for more than 1 month, it will develop into chronic liver injury and liver cancer. At present, there is still a lack of effective clinical drugs to prevent and treat ALI. Therefore, exploring the occurrence and development mechanisms of ALI and finding safe and effective hepatoprotective drugs are urgent problems for researchers to solve.

Phenethyl isothiocyanate (PEITC) is an isothiocyanate compound from the secondary metabolites of cruciferous plants hydrolyzed by myrosinase (14). Isothiocyanates are a class of compounds containing RN=C=S, in which R can be aliphatic or aromatic and the group =C=S has high reactive affinity with cysteine (15). PEITC has antibacterial, anti-inflammatory, antioxidant, and antitumor effects (16–19). This compound is reported as an effective inducer of nuclear factor erythroid 2-related factor 2 (NRF2) and can promote the expression of a variety of NRF2-driven antioxidant genes in different cell types (20, 21). It also suppresses translocation of nuclear factor kappa B (NF-κB) and phosphorylation of its upstream inhibitor IκBα, thereby inhibiting the production of inflammatory factors (22). In addition, many other studies show that PEITC at high doses also has the ability to reduce cancer cell invasion and migration, block the cell cycle, and induce apoptosis and autophagy in cancer cells with increased production of ROS (23–25). Moreover, as a widely distributed natural compound, PEITC actually has an excellent protective effect on vital organs in the human body, although it may have been ignored thus far.

In this study, we discovered that PEITC has a significant hepatoprotective effect, which reverses the increased levels of aspartate aminotransferase (AST), alanine aminotransferase (ALT), lactate dehydrogenase (LDH), tumor necrosis factor (TNF)-α, and interferon (IFN)-γ in mice with ALI. Furthermore, this effect of PEITC may be due to inhibition of hepatocyte pyroptosis *via* its unique structure of mercapten-targeting cysteine 191 of GSDMD.

MATERIALS AND METHODS

Chemicals and Reagents

PEITC was from JC (Wuxi) Company, Inc. (Wuxi, China). CCl_4 and olive oil were purchased from Nanjing Chemical Reagent Co., Ltd. (Nanjing, China). Lactate dehydrogenase (LDH) assay kit, alanine aminotransferase (ALT) assay kit, and aspartate aminotransferase (AST) assay kit were from Nanjing Jiancheng Bioengineering Institute (Nanjing, China). A mouse TNF-α ELISA kit and IFN-γ ELISA kit were purchased from Dakewe Biotech Co., Ltd. (Shenzhen, China). Dulbecco's modified Eagle's medium/nutrient mixture F-12 (DMEM/F12), Lipofectamine 3000, and Alexa Fluor 488-conjugated anti-rabbit IgG were purchased from Thermo Fisher Scientific (Waltham, MA, USA). ExFect Transfection Reagent was purchased from Vazyme (Nanjing, China). Dexamethasone, adenosine triphosphate (ATP), penicillin–streptomycin solution (100×), cell lysis buffer for Western blotting and immunoprecipitation, and RIPA lysis buffer were provided by Beyotime Biotechnology (Shanghai, China). Insulin-Transferrin-Selenium (ITS) Media Supplement (100×) was purchased from R&D Systems (Minneapolis, MN, USA). LPS and ConA were bought from Sigma-Aldrich (St. Louis, MO, USA). Necrosulfonamide (NSA) was purchased from MedChemExpress (Monmouth Junction, NJ, USA). Antibodies against β-tubulin, β-actin, and GAPDH were purchased from Abmart (Shanghai, China). Antibody against Nod-like receptor family pyrin domain containing 3 (NLRP3) was purchased from Cell Signaling Technology (Danvers, MA, USA). Anti-caspase-1 and anti-IL-1β antibodies were provided by Santa Cruz Biotechnology (Santa Cruz, CA, USA). Anti-GSDMD antibody was from Abcam (Cambridge, UK).

Animal Experiments

ICR male mice (6–8 weeks old) were purchased from the College of Veterinary Medicine Yangzhou University (Institute of Comparative Medicine, Yangzhou, China) and grown in an SPF-grade animal room at 21°C ± 2°C with a 12:12-h day-night cycle. PEITC (molecular mass: 163.24) is fat soluble, so it was dissolved in olive oil to the required concentrations.

ConA-Induced Acute Immune Liver Injury Model

Sixty ICR male mice were randomly divided into six groups: normal group, ConA-treated group, 7.5 mg/kg PEITC preadministered (pre) group, 15 mg/kg PEITC (pre) group, 30 mg/kg PEITC (pre) group, and 30 mg/kg PEITC postadministered (post) group. In the PEITC (pre) group, mice were given PEITC (7.5, 15, and 30 mg/kg, i.g.) for three consecutive days. After the last administration, the ConA-treated group, PEITC (pre) group, and PEITC (post) group were injected with 10 mg/kg ConA *via* the tail vein to induce an acute immune liver injury model. Half an hour after ConA

injection, the PEITC (post) group was given PEITC (30 mg/kg, i.g.). Eight hours after ConA injection, blood was collected, and serum was separated by centrifugation. The mice were then sacrificed and rapidly dissected, and the livers and spleens of the mice were removed and weighed. In addition, liver and spleen index were calculated. The lesions on the surface of liver and spleen tissues were photographed and recorded. At the same time, a piece of liver tissue was removed. One part was fixed with paraformaldehyde, embedded in paraffin and sectioned, and the other part was stored at −80°C.

CCl_4-Induced Acute Chemical Liver Injury Model

Male ICR mice were randomly divided into six groups: normal group, CCl_4 model group, 7.5 mg/kg PEITC (pre) group, 15 mg/kg PEITC (pre) group, 30 mg/kg PEITC (pre) group, and 30 mg/kg PEITC (post) group. In the PEITC (pre) group, mice were given PEITC (7.5, 15, and 30 mg/kg, i.g.) for three consecutive days. After the last administration, the CCl_4 model group, PEITC (pre) group and PEITC (post) group were injected with 0.2% (*v*/*v*) CCl_4 (10 ml/kg, i.p.) to induce acute chemical liver injury. Half an hour and 8 h after CCl_4 injection, the PEITC (post) group was given PEITC (30 mg/kg, i.g.). Sixteen hours after CCl_4 injection, blood was collected, mice were euthanized, and liver tissue samples were removed.

Analysis of Biochemical Indexes and Cytokine Levels

ALT, AST, and LDH activities were detected according to the instructions of the assay kits. The levels of serum TNF-α and IFN-γ were tested according to the instructions of ELISA kits.

Real-Time PCR

Total RNA of liver tissues was extracted with TRIzol and then reverse transcribed into cDNA (26). Real-time quantitative PCR was performed with a BioRad CFX96 Touch™ real-time PCR detection system (BioRad, Hercules, CA, USA). The amplification conditions were 95°C for 2 min, 1 cycle, denaturation at 95°C for 10 s, annealing at 60°C for 30 s, extension at 95°C for 10 s, and 45 cycles. The primer sequences used in our study were as follows: TNF-α forward, 5′-CCT GTA GCC CAC GTC GTA G-3′; TNF-α reverse, 5′-GGG AGT AGA CAA GGT ACA ACC C-3′; IFN-γ forward, 5′-ATG AAC GCT ACA CAC TGC ATC-3′; IFN-γ reverse, 5′-CCA TCC TTT TGC CAG TTC CTC-3′; CXCL-10 forward, 5′-CCA AGT GCT GCC GTC ATT TTC-3′; CXCL-10 reverse, 5′-GGC TCG CAG GGA TGA TTT CAA-3′; β-actin forward, 5′-GGC TGT ATT CCC CTC CAT CG-3′; and β-actin reverse, 5′-CCA GTT GGT AAC AAT GCC ATG T-3′.

Western Blot

Cells or liver tissues were lysed in lysis buffer with protease inhibitor cocktail for 30 min on ice, and the supernatants were collected after cell lysates were centrifuged at 12,000×*g* for 10 min. After the protein concentrations of each sample were measured, proteins were separated by sodium dodecyl sulfate–polyacrylamide gel electrophoresis (SDS-PAGE) and electrotransferred to polyvinylidene fluoride (PVDF) membranes (Millipore, Burlington, MA, USA). Different antibodies were incubated according to the molecular weight of target proteins for Western blotting.

Immunohistochemistry

Paraffin-embedded liver tissue sections were deparaffinized, rehydrated, subjected to antigen retrieval, blocked, and then incubated overnight at 4°C with antibodies against NLRP3, IL-1β, caspase-1, and GSDMD. After washing tissue sections with PBST, slides were stained according to the instructions of the anti-mouse/rabbit universal immunohistochemical detection kit (Proteintech, Wuhan, China) and finally counterstained with hematoxylin.

Cell Culture

The alpha mouse liver 12 (AML12) cell line and HEK293T cell line were obtained from the National Collection of Authenticated Cell Cultures (Shanghai, China). AML12 cells were cultured in DMEM/F12 medium supplemented with 10% fetal bovine serum (FBS), ITS media supplement (1×), 40 ng/ml dexamethasone, and penicillin–streptomycin solution (1×) under an atmosphere of 5% (*v*/*v*) CO_2 at 37°C. To induce the hepatocyte pyroptosis model, AML12 cells were treated with 100 ng/ml LPS for 3 h, then PEITC (0.3, 1, and 3 μM) for 1 h, and finally 5 mM ATP for 24 h. The cells were collected for subsequent experiments. HEK293T cells were cultured in DMEM supplemented with 10% FBS and penicillin–streptomycin solution (1×) under an atmosphere of 5% (*v*/*v*) CO_2 at 37°C.

Immunofluorescence Assay

AML12 cells were fixed, permeabilized, blocked, and then incubated overnight at 4°C with anti-GSDMD antibody. After washing with PBS, cells were exposed to Alexa Fluor 488-conjugated anti-rabbit IgG, and finally, cell nuclei were stained with DAPI.

Cell Transfection Assay

Mouse GSDMD WT-EGFP, human GSDMD WT-EGFP, and human GSDMD C191A-EGFP plasmids were purchased from General Biology (Anhui, China). The mouse GSDMD WT-EGFP plasmid was transfected into AML12 cells, and human GSDMD WT-EGFP or human GSDMD C191A-EGFP plasmid was transfected into HEK293T cells for subsequent experiments.

Cellular Thermal Shift Assay

After AML12 cells were incubated with DMSO or PEITC (3 μM) for 2 h, the cells were collected, washed, and resuspended in PBS. The cell suspension was divided into 10 aliquots and heated at the indicated temperatures. Finally, the cell supernatant at each temperature was analyzed by western blot. HEK293T cells transfected with human GSDMD WT-EGFP or human GSDMD C191A-EGFP plasmid were treated with DMSO, PEITC (3 μM) or NSA (3 μM) for 2 h, and the subsequent operations were basically the same as above.

Microscale Thermophoresis Assay

After the mouse GSDMD WT-EGFP plasmid was transiently transfected into AML12 cells for 24 h, the cells were lysed with

lysis buffer, and the supernatant was collected after centrifugation. PEITC was gradually diluted from 500 μM and added to an aliquot of cell lysis. They were mixed and sucked into Monolith NT.115 capillary tubes (Nanotemper Technologies, München, Germany). Finally, samples were detected by Monolith NT.115 (Nanotemper Technologies), and data were analyzed by MO.Affinity Analysis. HEK293T cells were transiently transfected with human GSDMD WT-EGFP or GSDMD C191A-EGFP plasmid for 24 h and then lysed with lysis buffer. The supernatant was collected after centrifugation. PEITC or NSA was gradually diluted from 500 μM and added to an aliquot of cell lysis. After samples were mixed, the subsequent operations were the same as above.

Electron Microscope

After the cell samples were fixed with prefixed electron microscopy fixative (Servicebio, Wuhan, China), they were sent to Wuhan Servicebio Co., Ltd. (Wuhan, China) to complete the electron microscope scan.

Statistical Analysis

The results are displayed as the mean ± SEM, and each experiment included triplicate sets. GraphPad Prism 8 Software (San Diego, CA, USA) was used to conduct all statistical analyses. Data were statistically evaluated by Student's *t*-test or one-way analysis of variance (ANOVA) followed by Bonferroni *post-hoc* test. $p < 0.05$ was considered significant.

RESULTS

PEITC Ameliorated ConA-Induced Acute Immune Liver Injury in Mice

The molecular structure of PEITC is presented in **Figure 1A**. PEITC had no significant effect on the body weight of mice in the ConA-induced acute immune liver injury model (data not shown), indicating the safety and low toxicity of PEITC. According to the schematic diagram of this experiment (**Figure 1B**), after the mice were euthanized, the livers of mice from each group were removed and photographed. Compared with the normal group, the liver from the ConA-treated group was obviously congested and enlarged, and the liver lesions of mice in the PEITC (preadministered) and PEITC (postadministered) groups improved (**Figure 1C**). The livers of mice from each group were weighed, and the ratio of weight to body weight was calculated. We found that the liver index of mice in the ConA-treated group was significantly higher than that in the normal group, while the liver index of mice treated with PEITC decreased in a dose-dependent manner (**Figure 1D**). At the same time, the spleens of mice in the ConA-treated group were congested and swollen, and the spleen lesions of mice treated with PEITC were inhibited (**Figure 1E**). The spleen index of mice in the ConA-treated group was significantly increased in comparison with that of the normal group, while the spleen index of mice from the PEITC (pre) and PEITC (post) groups decreased in a dose-dependent manner, indicating that PEITC has a protective effect on the liver and spleen of mice with ConA-induced acute immune liver injury (**Figure 1F**). Hematoxylin and eosin (H&E) staining of liver tissue sections of mice from each group showed that compared with the normal group, a large number of erythrocytes were deposited in the liver sinusoids, the liver cords were disorderly arranged and the necrotic foci were diffusely distributed in the ConA-treated group. In the PEITC (pre) and PEITC (post) groups, the liver structure recovered in a dose-dependent manner, and sinusoidal congestion and inflammatory cell infiltration were significantly reduced (**Figure 1G**). The above results indicated that PEITC can obviously improve the liver and spleen tissue pathology of mice with ConA-induced acute immune liver injury.

PEITC Reduced Hepatic Biochemical Indexes and Cytokine Levels

Next, we detected the levels of hepatic biochemical indexes ALT, AST, and LDH in the sera of mice from each group. The results showed that the levels of ALT, AST, and LDH in the ConA-treated group were significantly higher than those in the normal group, and PEITC inhibited the increase in ALT, AST, and LDH enzyme activities in the serum of ConA-treated mice in a dose-dependent manner (**Figure 2A**). ConA can activate macrophages, helper T cells, and natural killer T cells, which infiltrate the liver and produce a large number of proinflammatory cytokines, such as IFN-γ and TNF-α, as well as the chemokine CXCL-10. Here, we exploited ELISA to detect the effect of PEITC on the expression and secretion of inflammatory cytokines. PEITC significantly reversed the release of the inflammatory factors TNF-α and IFN-γ in the serum of ConA-treated mice (**Figure 2B**). In addition, PEITC also obviously downregulated the mRNA expression of TNF-α, IFN-γ, and CXCL-10 in the livers of mice with ALI (**Figure 2C**). These data indicated that PEITC can protect the liver and reduce cytokine levels in mice with ConA-induced acute immune liver injury.

PEITC Prevented Hepatocyte Pyroptosis Induced by ConA

Since hepatocyte death is one of the important mechanisms of ALI, we further explored whether PEITC can directly protect hepatocytes from cell death. PEITC has an excellent anti-inflammatory effect, and pyroptosis, which is highly related to inflammation, plays a critical role in the process of ALI; therefore, we will focus on the effect of PEITC on hepatocyte pyroptosis. First, we verified the existence of hepatocyte pyroptosis in the ConA-induced ALI model. Western blotting was used to detect the expression levels of the pyroptosis-related proteins NLRP3, pro-CASP1, cleaved CASP1, GSDMD, and GSDMD-N in the livers of mice treated with ConA. We found that the expression of NLRP3 was upregulated, and the key proteins CASP1 and GSDMD were activated and cleaved in mice with ConA-induced ALI (**Figures 3A, B**). ELISA results also showed that the activity of serum IL-1β in ConA-treated mice was increased (**Figure 3C**). At the same time, these data suggested that hepatocyte pyroptosis was the most significant

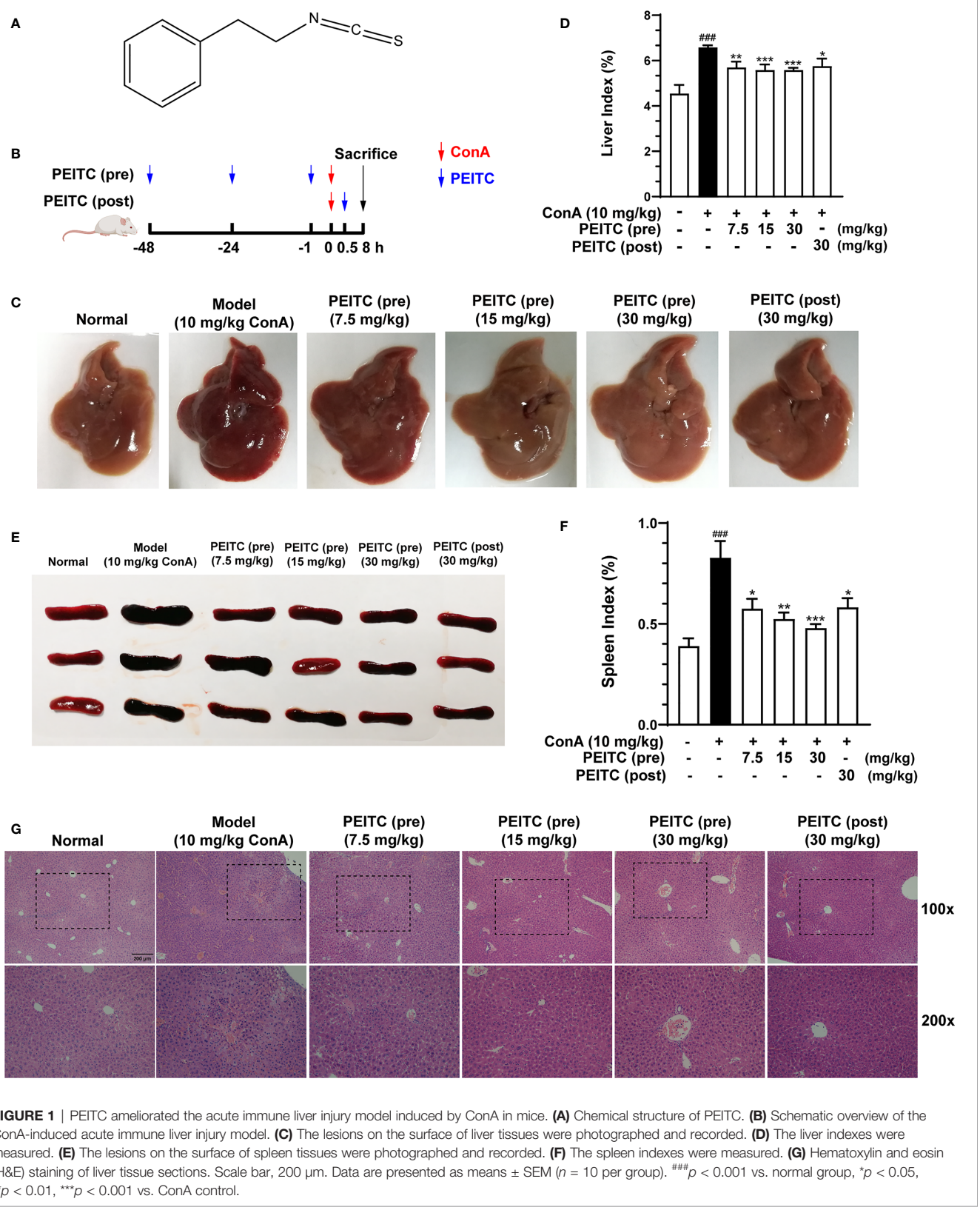

FIGURE 1 | PEITC ameliorated the acute immune liver injury model induced by ConA in mice. **(A)** Chemical structure of PEITC. **(B)** Schematic overview of the ConA-induced acute immune liver injury model. **(C)** The lesions on the surface of liver tissues were photographed and recorded. **(D)** The liver indexes were measured. **(E)** The lesions on the surface of spleen tissues were photographed and recorded. **(F)** The spleen indexes were measured. **(G)** Hematoxylin and eosin (H&E) staining of liver tissue sections. Scale bar, 200 μm. Data are presented as means ± SEM (n = 10 per group). $^{###}p < 0.001$ vs. normal group, $^{*}p < 0.05$, $^{**}p < 0.01$, $^{***}p < 0.001$ vs. ConA control.

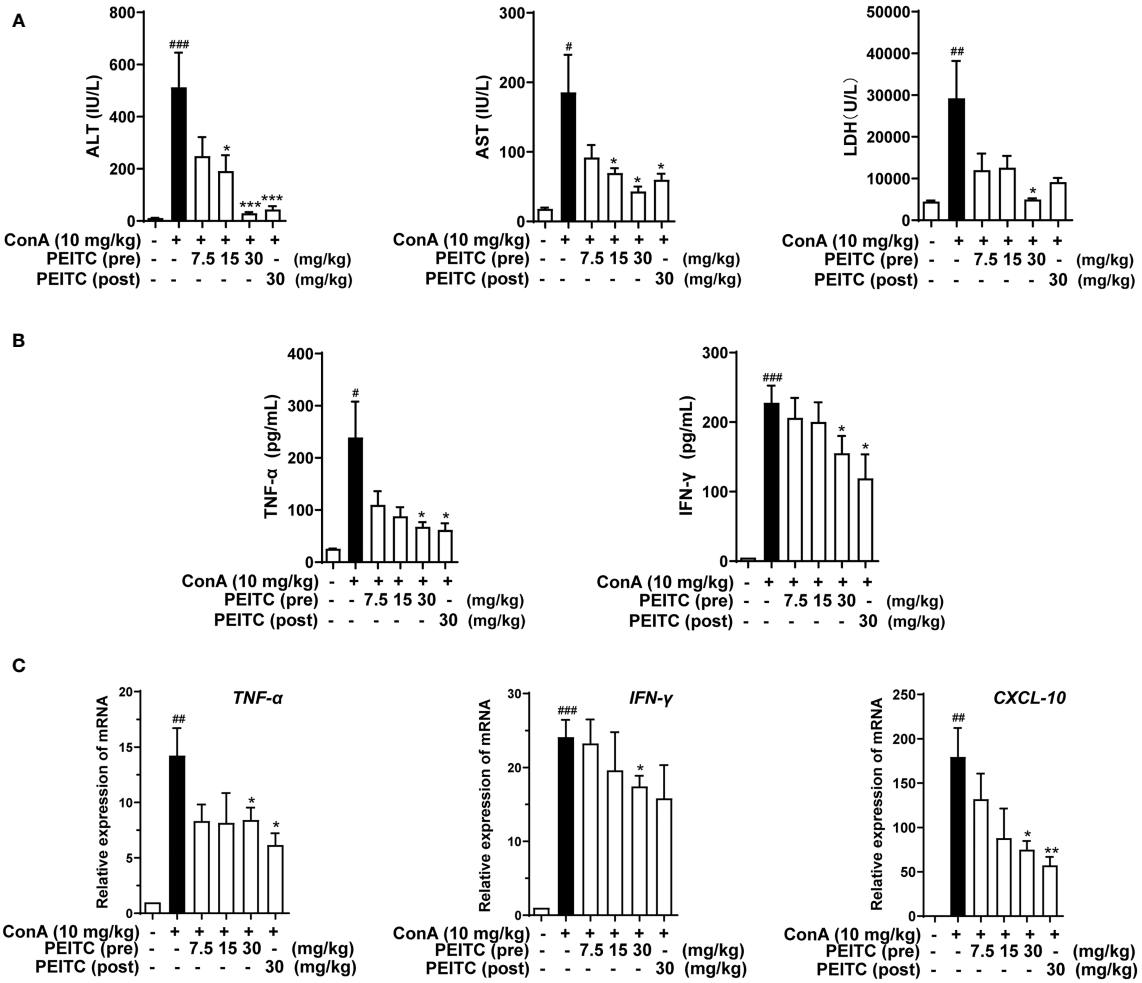

FIGURE 2 | PEITC reduced hepatic biochemical indexes and cytokine levels. **(A)** The levels of serum ALT, AST, and LDH. **(B)** Serum TNF-α and IFN-γ levels. **(C)** The mRNA expression levels of TNF-α, IFN-γ, and CXCL-10 in liver tissues. Data are presented as means ± SEM (n = 10 per group). $^{\#}p < 0.05$, $^{\#\#}p < 0.01$, $^{\#\#\#}p < 0.001$ vs. normal group, $^{*}p < 0.05$, $^{**}p < 0.01$, $^{***}p < 0.001$ vs. ConA control.

in mice when ConA was induced for 8 h. In the PEITC (pre) and PEITC (post) groups, the expression level of NLRP3 was downregulated, and the activation and cleavage of CASP1 and GSDMD were inhibited, indicating that PEITC can prevent ConA-induced ALI model mouse hepatocyte pyroptosis (**Figures 3D, E**).

PEITC Reduced the Expression Levels of Pyroptosis-Related Proteins

Next, we performed immunohistochemical analysis on liver sections of mice from each group. The results of immunohistochemistry showed that the expression levels of NLRP3, IL-1β, CASP1 (pro- and cleaved CASP1) and GSDMD (GSDMD and GSDMD-N) increased in the ConA-treated group compared with the normal group (**Figures 4A–E**). The PEITC (pre) and PEITC (post) groups inhibited the expression levels of NLRP3, IL-1β, CASP1 (pro- and cleaved CASP1), and GSDMD (GSDMD and GSDMD-N) in a dose-dependent manner. These results confirmed that PEITC can reduce the expression of pyroptosis-related proteins in ConA-treated mice.

PEITC Ameliorated Acute Chemical Liver Injury Model and Hepatocyte Pyroptosis Induced by CCl_4 in Mice

To verify the general inhibitory effect of PEITC on hepatocyte pyroptosis in different ALI models, we conducted experiments in CCl_4-induced acute chemical liver injury. The experimental process is shown in **Figure 5A**. We found that PEITC had no significant effect on the body weight of mice (data not shown). Compared with the normal group, the livers of mice in the CCl_4 model group were yellowish, with a large number of granular dots on the surface (**Figure 5B**). PEITC restored the normal color and texture of mouse liver to varying degrees in the PEITC (pre) and PEITC (post) groups. H&E staining also indicated that the livers of mice in the CCl_4 model group showed obvious damage, including hepatocyte necrosis, vacuolar degeneration,

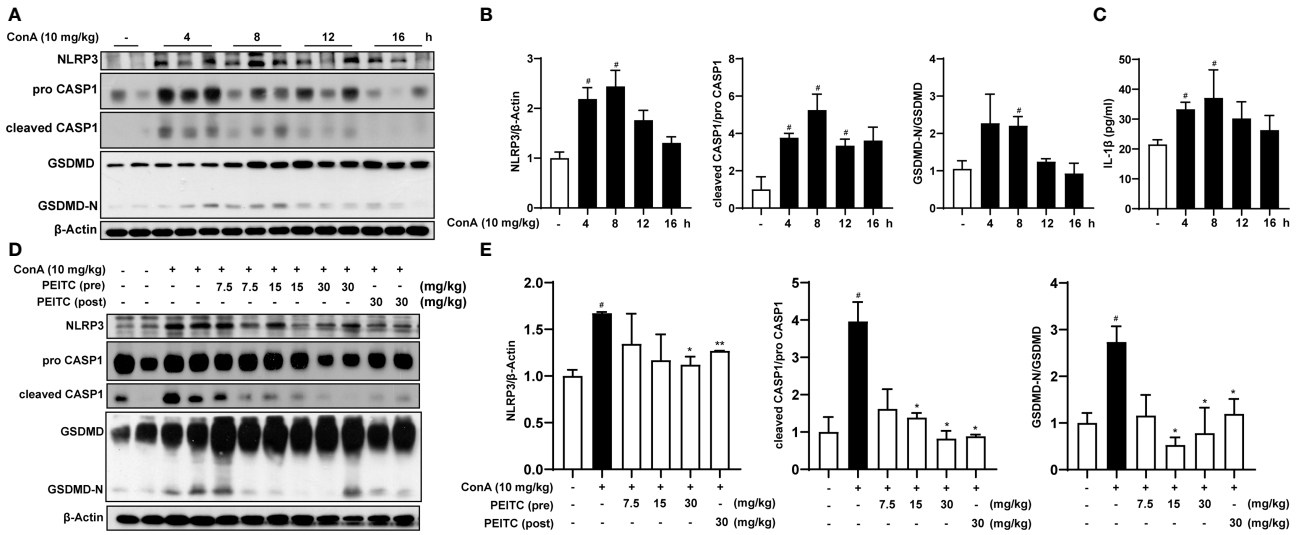

FIGURE 3 | PEITC prevented hepatocyte pyroptosis induced by ConA. **(A)** Immunoblot analysis of NLRP3, pro-CASP1, cleaved CASP1, GSDMD, GSDMD-N, and β-actin in liver tissues of mice induced by ConA (0, 4, 8, 12, and 16 h). **(B)** The relative protein levels of NLRP3/β-actin, cleaved CASP1/pro-CASP1, and GSDMD-N/GSDMD are displayed as histograms. **(C)** The expression levels of serum IL-1β. **(D, E)** Western blot and statistical analysis of NLRP3, pro-CASP1, cleaved CASP1, GSDMD, GSDMD-N, and β-actin. Data are presented as the means ± SEM (n = 6–10 per group). $^{\#}p < 0.05$ vs. normal group, $^{*}p < 0.05$, $^{**}p < 0.01$ vs. ConA control.

loss of hepatic cord structure, and a large amount of immune cell infiltration in the portal vein system (**Figure 5C**). Liver injury in mice from the PEITC (pre) and PEITC (post) groups showed a dose-dependent improvement. In addition, the levels of LDH, ALT and AST in the model group were also significantly higher than those in the normal group. The serum LDH, ALT and AST levels of mice in the PEITC (pre) and PEITC (post) groups were obviously reversed in a dose-dependent manner (**Figures 5D–F**). At the same time, we detected the expression levels of pyroptosis-related proteins in the liver of mice from each group and found that the liver of mice from the model group had significant hepatocyte pyroptosis, and the expression of pyroptosis-related proteins in the liver tissue of the PEITC (pre) and PEITC (post) groups was downregulated (**Figure 5G**). These data determined that PEITC can also improve CCl_4-induced acute chemical liver injury by inhibiting hepatocyte pyroptosis.

PEITC Inhibited AML12 Pyroptosis Induced by LPS and ATP *In Vitro*

We further verified the inhibitory role of PEITC on hepatocyte pyroptosis *in vitro*. Because pyroptosis has obvious morphological characteristics, we first observed the effect of PEITC on the morphology of pyroptotic cells through electron microscopy. The typical characteristics of pyroptosis in AML12 cells induced by LPS plus ATP include cell swelling, rupture of the cytoplasmic membrane, and intracellular vacuoles, while the morphology of AML12 cells treated with PEITC was restored, the plasma membrane was more complete, and intracellular vacuoles were reduced (**Figure 6A**). Immunoblot assays also showed that PEITC inhibited the increase in NLRP3 expression and the activation and cleavage of CASP1 and GSDMD in AML12 cells induced by LPS and ATP (**Figures 6B, C**). Furthermore, immunofluorescence results indicated that the expression level of GSDMD (GSDMD and GSDMD-N) increased and concentrated on the plasma membrane in AML12 cells induced by LPS plus ATP, while PEITC treatment reduced the GSDMD level in a dose-dependent manner (**Figure 6D**). These results verified the function of PEITC in inhibiting hepatocyte pyroptosis *in vitro*.

PEITC Directly Inhibited GSDMD by Interacting With Cysteine 191 of GSDMD

Since PEITC has a significant inhibitory effect on the cleavage of the pore-forming effector protein GSDMD during pyroptosis *in vivo* and *in vitro*, we tried to detect whether PEITC can directly interact with GSDMD. Molecular docking analysis predicted that PEITC binds to human GSDMD (PDB ID: 6N9O, -CDOCKER INTERACTION ENERGY = 28.859, data not shown). The cellular thermal shift assay (CETSA) showed that mouse GSDMD was completely degraded at 64°C in the DMSO group, while PEITC treatment accelerated the degradation of mouse GSDMD at 61°C and reduced the thermal stability of mouse GSDMD (**Figure 7A**). The MST results indicated that the Kd value between PEITC and mouse GSDMD was 308 nM (**Figure 7B**). PEITC has high reactive affinity for cysteine, and cysteine 191/192 of human/mouse GSDMD is essential to its membrane pore formation function. Therefore, we constructed a human GSDMD WT-EGFP plasmid and GSDMD C191A-EGFP plasmid for subsequent experiments and used NSA (inhibitor of GSDMD) as a positive control. By detecting the content of LDH in the medium supernatant, we found that the amount of LDH released from HEK293T cells transfected with C191A-GSDMD was less than that released from cells transfected with WT-GSDMD. PEITC and NSA inhibited the amount of LDH released

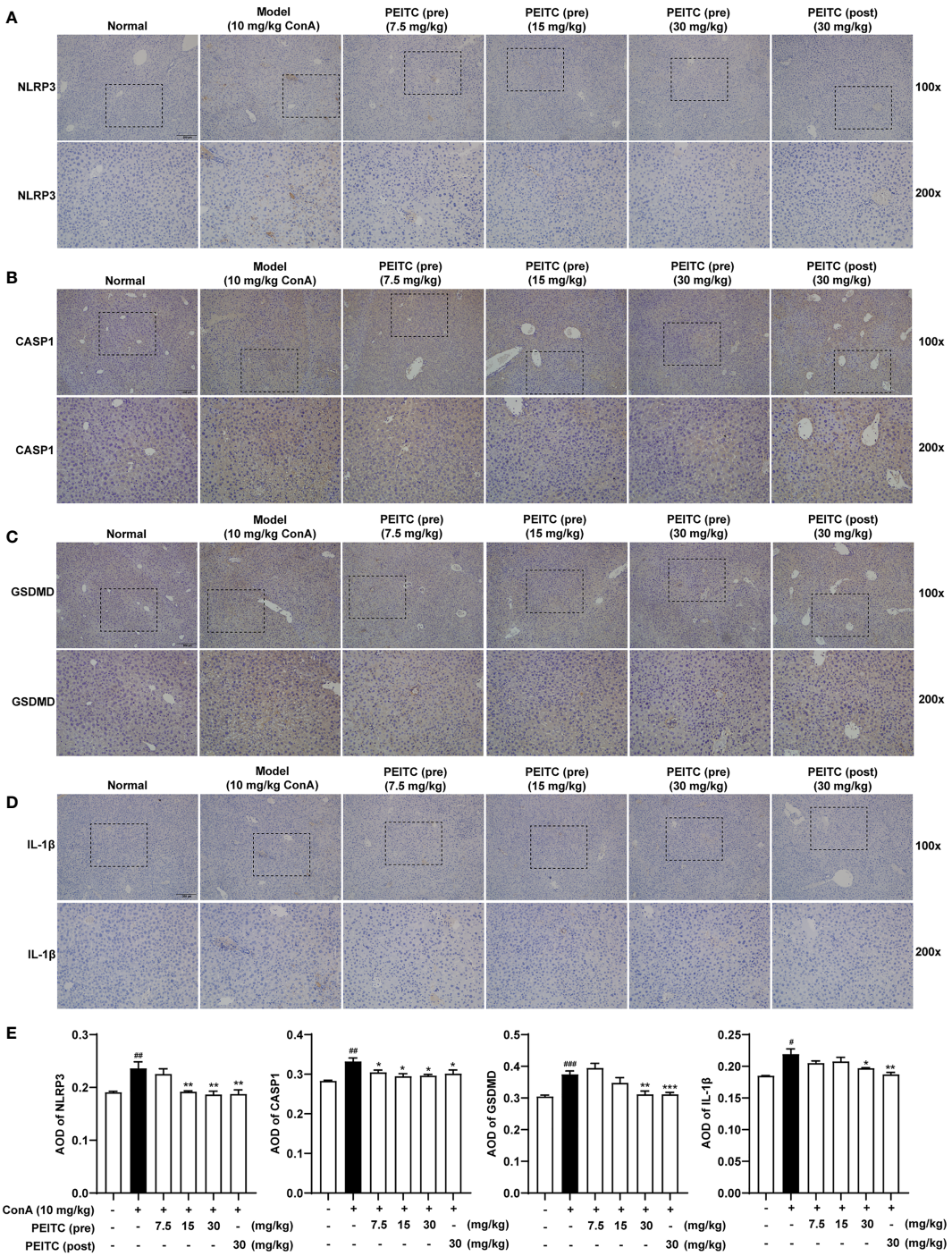

FIGURE 4 | PEITC reduced the expression levels of pyroptosis-related proteins. **(A–D)** Liver tissue sections from each group were stained for NLRP3, CASP1, GSDMD, and IL-1β. Scale bar, 200 μm. **(E)** The average optical densities (AOD) of NLRP3, CASP1, GSDMD, and IL-1β are displayed as histograms. Data are presented as means ± SEM (n = 10 per group). $^{\#}p < 0.05$, $^{\#\#}p < 0.01$, $^{\#\#\#}p < 0.001$ vs. normal group, $^{*}p < 0.05$, $^{**}p < 0.01$, $^{***}p < 0.001$ vs. ConA control.

from HEK293T cells transfected with WT-GSDMD (**Figure 7C**). The CETSA results showed that PEITC reduced the thermal stability of human WT-GSDMD, while NSA enhanced the thermal stability of human WT-GSDMD (**Figure 7D**). The MST results indicated that the Kd value between PEITC and human WT-GSDMD was 230 nM, and the Kd value between NSA and human WT-GSDMD was 11.2 μM (**Figure 7E**). However, PEITC and NSA had no significant effect on the

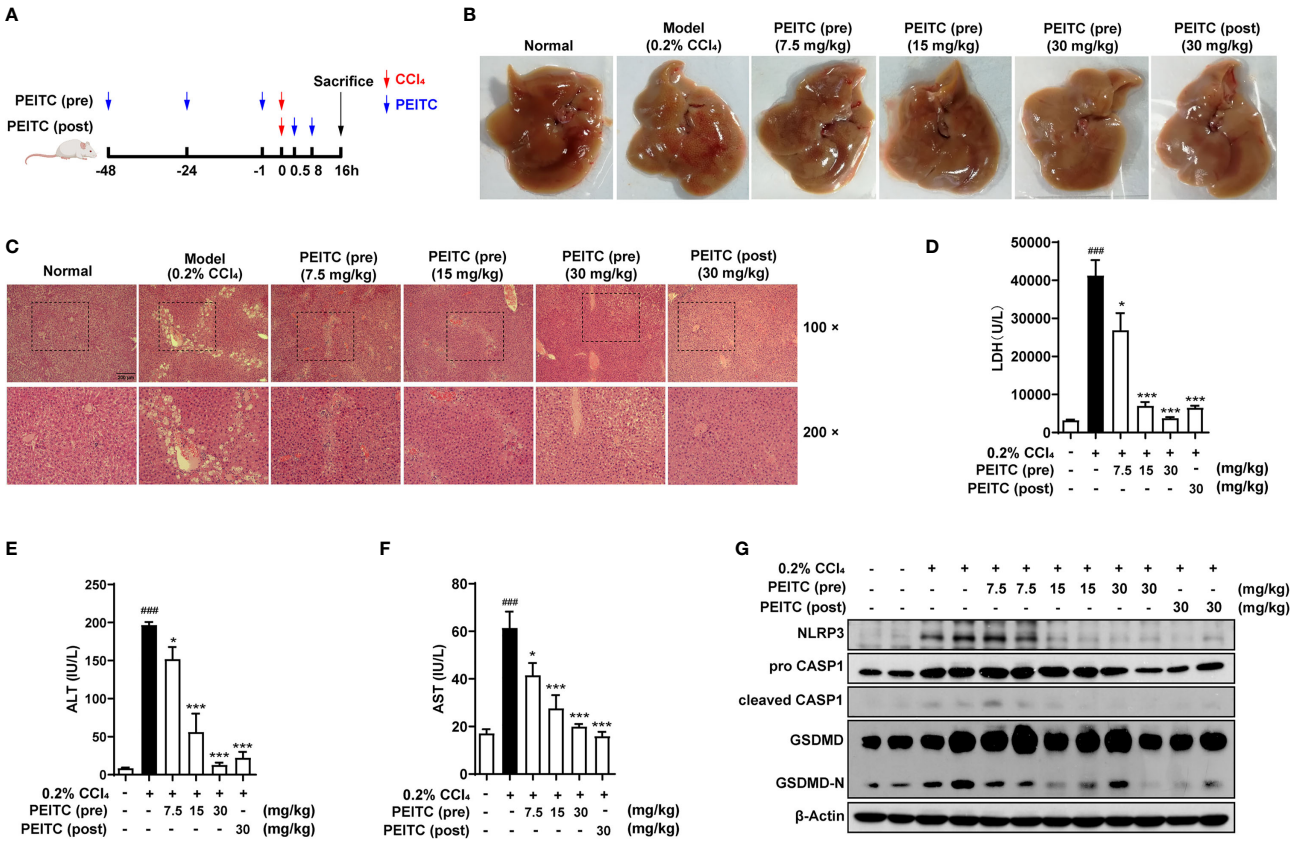

FIGURE 5 | PEITC ameliorated the acute chemical liver injury model and hepatocyte pyroptosis induced by CCl_4 in mice. **(A)** Schematic overview of the CCl_4-induced acute chemical liver injury model. **(B)** The lesions on the surface of liver tissues were photographed. **(C)** H&E staining of liver tissue sections. Scale bar, 200 μm. **(D–F)** The levels of serum LDH, ALT, and AST. **(G)** Western blot analysis of NLRP3, pro-CASP1, cleaved CASP1, GSDMD, GSDMD-N, and β-actin. Data are presented as the means ± SEM (n = 6–10 per group). $^{###}p < 0.001$ vs. normal group, $^{*}p < 0.05$, $^{***}p < 0.001$ vs. CCl_4 control.

thermal stability of human C191A-GSDMD, and PEITC and NSA did not bind to human C191A-GSDMD (**Figures 7F, G**). The above results confirmed that PEITC can directly bind to human GSDMD through cysteine 191 of GSDMD.

DISCUSSION

ALI is one of the most common clinical liver diseases with complicated pathogenesis. Since the liver is responsible for the material metabolism and detoxification of the body, it is very susceptible to damage (27). Parenchymal hepatocytes, Kupffer cells, lymphocytes, and hepatic stellate cells all play a role in the occurrence and development of ALI. The key features of ALI include cell death, inflammation, and oxidative stress (28, 29). Among them, hepatocyte pyroptosis may be particularly critical (6). However, there are very few drugs clinically used to protect the liver and to treat ALI. If ALI is not treated in time, it can easily develop into acute liver failure, chronic liver injury, or hepatocellular carcinoma, which seriously threatens human health and quality of life. Therefore, it is necessary to find clinical prevention and treatment drugs for ALI with fewer side effects and better curative effects.

PEITC has been reported to be used as an antibacterial, anti-inflammatory, antioxidant and anticancer agent (22, 30, 31). In a clinical trial about PEITC in the treatment of prostate hyperplasia, we found that many elderly patients had decreased liver function and increased serum transaminase levels, while the serum transaminase levels of elderly patients treated with PEITC significantly decreased. This suggests that PEITC may have a hepatoprotective function.

Here, we exploited a ConA-induced acute immune liver injury model and a CCl_4-induced acute chemical liver injury model to explore the hepatoprotective effect of PEITC (**Figures 1B**, **5A**). ConA, a kind of T-cell mitogen, can induce ALI in mice by activating T lymphocytes. ALI induced by CCl_4 can mimic the mechanism of ALI caused by chemical drugs. CCl_4 can cause the peroxidation of cell membrane lipids and proteins and destroy calcium ion channels to increase intracellular calcium ion concentrations, which will eventually lead to the death of liver cells and cause intracellular inflammation. PEITC significantly improved the ConA-

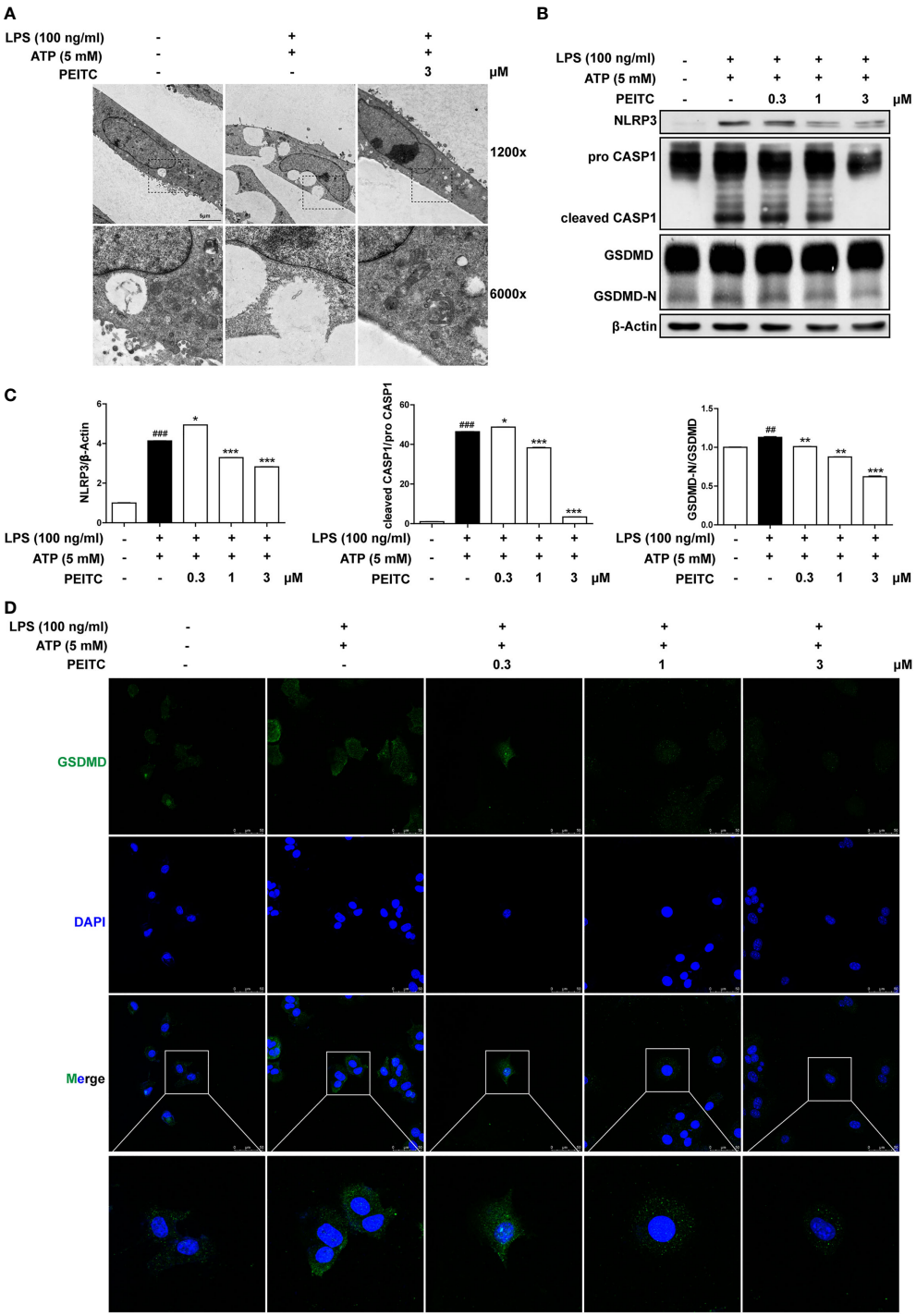

FIGURE 6 | PEITC inhibited pyroptosis in AML12 cells treated with LPS and ATP *in vitro*. **(A)** Representative electron micrographs of cell morphology from each group. Scale bar, 5 μm. **(B, C)** Immunoblot and statistical analysis of NLRP3, pro-CASP1, cleaved CASP1, GSDMD, GSDMD-N, and β-actin. **(D)** Immunofluorescence staining of GSDMD. Scale bar, 50 μm. Data are presented as means ± SEM. $^{\#\#}p < 0.01$, $^{\#\#\#}p < 0.001$ vs. blank, $^{*}p < 0.05$, $^{**}p < 0.01$ $^{***}p < 0.001$ vs. LPS+ATP control.

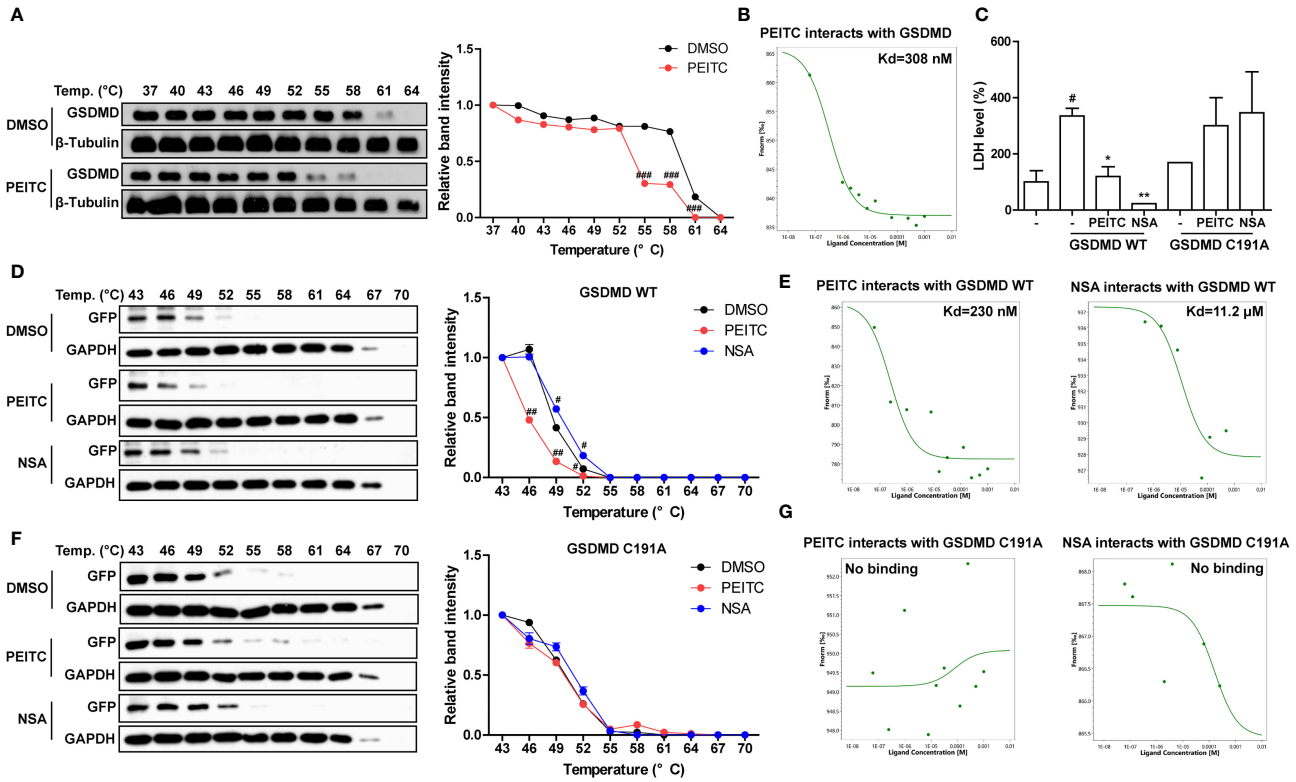

FIGURE 7 | PEITC directly inhibited GSDMD by interacting with cysteine 191 of GSDMD. **(A)** The effect of PEITC on the thermal stability of mouse GSDMD was detected by CETSA, and the line graph was used to show the remaining GSDMD amount at different temperatures. **(B)** The binding ability between PEITC and mouse GSDMD was detected by MST. **(C)** The secretion levels of LDH in cell culture supernatants. **(D)** The effect of PEITC and NSA on the thermal stability of human GSDMD WT. **(E)** The binding ability between human GSDMD WT and PEITC or NSA. **(F)** The effect of PEITC and NSA on the thermal stability of human GSDMD C191A. **(G)** The binding ability between human GSDMD C191A and PEITC or NSA. Data are presented as means ± SEM. $^{\#}p < 0.05$, $^{\#\#}p < 0.01$, $^{\#\#\#}p < 0.001$ vs. DMSO or blank, $^{*}p < 0.05$, $^{**}p < 0.01$ vs. GSDMD WT control.

induced acute immune liver injury model and CCl_4-induced acute chemical liver injury model. Compared with the model group, the normal structural units and material metabolism function of the liver in the PEITC (pre) group and PEITC (post) group were restored in a dose-dependent manner, and the activity of serum ALI-related biochemical indicators ALT, AST, and LDH was downregulated (**Figures 1**, **2A**, **5**). In addition, the expression and release of inflammatory factors were reduced in the livers of mice from the PEITC (pre) group and PEITC (post) group (**Figures 2B, C**, **4D**). It should be noted that pretreatment with PEITC (30 mg/kg) tended to have stronger effects on its inhibitory properties than posttreatment. PEITC is the most widely studied aromatic isothiocyanate with high bioavailability. This compound has rapid absorption, a low clearance rate and a high protein binding rate after oral administration, which may be due to its lipophilicity and low molecular weight (15). It has been reported that the peak time of plasma concentration is 2.6 ± 1.1 h and the half-life period is 4.9 ± 1.1 h after PEITC is orally taken (32). In our ALI experiment, PEITC was preadministered once a day for three consecutive days, while it was postadministered only once after ConA injection. Therefore, the blood drug concentrations in the PEITC (pre) group might be much higher than those in the PEITC (post) group when the livers were injured with ConA.

In a previous report, it was shown that in ConA-treated mice, pathogenic-elevated NLRP3, cleaved caspase-1 and IL-1β levels, as well as inflammatory cell death known as pyroptosis, occurred in the liver (6). Here, we verified for the first time that pyroptosis, with cleaved GSDMD and pore formation in the membrane as the gold standard, actually occurs during inflammatory ALI caused by ConA (**Figures 3**, **4C**, **6**). Moreover, in this study, we found that hepatocytes also experience notable pyroptosis in the process of CCl_4-induced chemical liver injury (**Figure 5**). Pyroptosis is a kind of programmed cell death that is characterized by the continuous expansion of cells until the rupture of the cell membrane. Under the electron microscope, it can be clearly seen that the cells underlying pyroptosis form a large number of vesicles. After that, pores will be formed on the cell membrane, the cell membrane will rupture, and the content will flow out, thus resulting in robust inflammation (33). These biochemical characteristics of pyroptosis are consistent with the phenomena revealed in this study. Furthermore, we found that PEITC reduced the production of NLRP3 and the cleavage of CASP1 and GSDMD in the livers of mice with ALI (**Figures 3D, E**, **4**, **5G**) and in

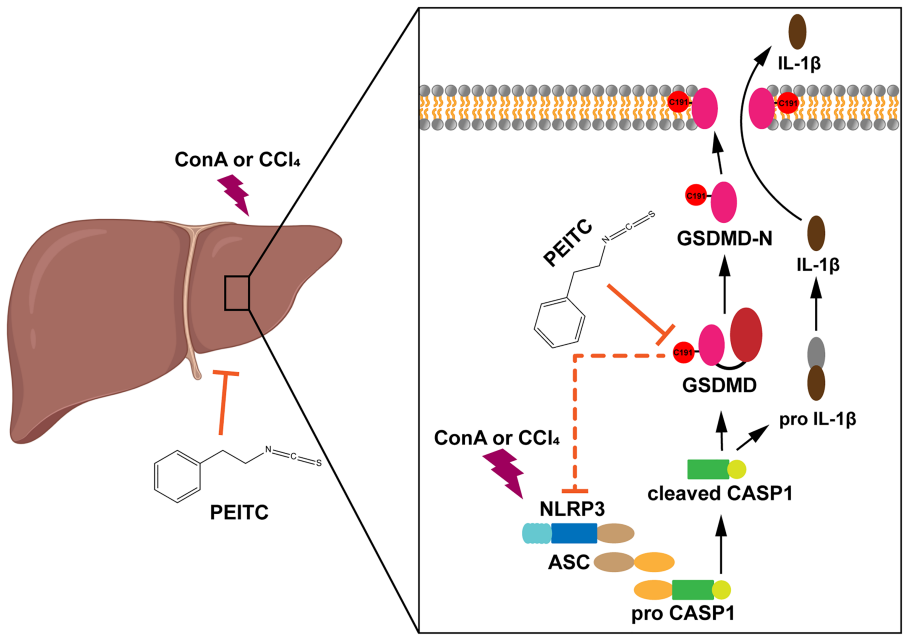

FIGURE 8 | Diagram of the effect of PEITC in inhibiting hepatocyte pyroptosis.

AML12 cells *in vitro* (**Figure 6**). These results indicate that PEITC can significantly inhibit pyroptosis in hepatocytes.

Previous research shows that scavenging ROS by *N*-acetyl-cysteine is an effective strategy to attenuate NLRP3 inflammasome activation and to suppress liver inflammation (6). PEITC has also been reported to significantly increase the activities of Nrf2 and a series of antioxidant enzymes in fibroblasts (21). Mechanistic studies showed that the anti-inflammatory effect of PEITC was driven, at least in part, by inhibiting the NLRP3 inflammasome pathway, as indicated by the downregulation of NLRP3, TXNIP, caspase-1, and IL-1β (34, 35). Our results also showed that PEITC can inhibit the expression of NLRP3 and the cleavage of CASP1 (upstream of GSDMD) both *in vivo* and *in vitro* (**Figures 3**, **4A, B**, **5G**, **6B, C**). We speculate that this may be partly due to its anti-inflammatory effects and partly resulted from feedback regulation in pyroptosis inhibition. Although we cannot rule out other sites of action and other mechanisms of PEITC that might indirectly lead to its suppressive effects on pyroptosis, the efficacy of PEITC may be mainly due to its direct inhibition of GSDMD in hepatocytes (**Figures 7A, B**). Cysteine 191/192 in human/mouse GSDMD is highly conserved and essential for the formation of its oligomerization and pyroptosis pores (36, 37). Since PEITC containing –N=C=S has high-reactive affinity with cysteine, we subsequently explored whether cysteine 191 of human GSDMD affects the function of PEITC and its binding to GSDMD. By detecting the content of LDH in the medium supernatant, we found that PEITC treatment reduced the release of LDH from HEK293T cells transfected with the GSDMD WT plasmid but had no significant effect on the release of LDH from cells transfected with GSDMD C191A (**Figure 7C**). In addition, compared with HEK293T cells with WT GSDMD, the release of LDH from cells with C191A GSDMD was reduced, which verified the critical role of cysteine 191 in GSDMD pyroptosis. The CETSA and MST assays showed that PEITC could bind to human WT-GSDMD but not C191A-GSDMD (**Figures 7D–G**). These results determined that PEITC can directly interact with cysteine 191 of GSDMD to inhibit hepatocyte pyroptosis.

In summary, our study reported for the first time the role of PEITC in inhibiting hepatocyte pyroptosis in ALI. We also found a new target of PEITC, GSDMD, and clarified the importance of cysteine 191 of GSDMD in the interaction between PEITC and GSDMD (**Figure 8**). These findings provide a new drug candidate for the clinical prevention and treatment of ALI.

DATA AVAILABILITY STATEMENT

The original contributions presented in the study are included in the article/**Supplementary Material**. Further inquiries can be directed to the corresponding authors.

ETHICS STATEMENT

The animal study was reviewed and approved by the Nanjing University Animal Care and Use Committee (NJU-ACUC).

AUTHOR CONTRIBUTIONS

JW, KS, NA, SL, and MB performed research and analyzed the data. JW, KS, and XFW designed the experiments and wrote the

paper. XDW, YS, and RD contributed experimental materials and gave suggestions in the formation. JC, XFW, and QX designed the research and obtained funding. All authors listed have made a substantial, direct, and intellectual contribution to the work and approved it for publication.

FUNDING

This work was supported by the National Key R&D Program of China (No. 2017YFA0506000), National Natural Science Foundation of China (Nos. 81773798, 82073910, 21937005), Natural Science Foundation of Jiangsu Province (BK20191253), and Wuxi Science and Technology Development Fund (CBE01G1650).

SUPPLEMENTARY MATERIAL

The Supplementary Material for this article can be found online at: https://www.frontiersin.org/articles/10.3389/fimmu.2022.825428/full#supplementary-material

REFERENCES

1. Heo MJ, Kim TH, You JS, Blaya D, Sancho-Bru P, Kim SG. Alcohol Dysregulates miR-148a in Hepatocytes Through FoxO1, Facilitating Pyroptosis. *via TXNIP overexpression Gut* (2019) 68(4):708–20. doi: 10.1136/gutjnl-2017-315123
2. Khanova E, Wu R, Wang W, Yan R, Chen Y, French SW, et al. Pyroptosis by Caspase11/4-Gasdermin-D Pathway in Alcoholic Hepatitis in Mice and Patients. *Hepatology* (2018) 67(5):1737–53. doi: 10.1002/hep.29645
3. Wei Q, Mu K, Li T, Zhang Y, Yang Z, Jia X, et al. Deregulation of the NLRP3 Inflammasome in Hepatic Parenchymal Cells During Liver Cancer Progression. *Lab Invest* (2014) 94(1):52–62. doi: 10.1038/labinvest.2013.126
4. Xu B, Jiang M, Chu Y, Wang W, Chen D, Li X, et al. Gasdermin D Plays a Key Role as a Pyroptosis Executor of Non-Alcoholic Steatohepatitis in Humans and Mice. *J Hepatol* (2018) 68(4):773–82. doi: 10.1016/j.jhep.2017.11.040
5. Chen YL, Xu G, Liang X, Wei J, Luo J, Chen GN, et al. Inhibition of Hepatic Cells Pyroptosis Attenuates CLP-Induced Acute Liver Injury. *Am J Transl Res* (2016) 8(12):5685–95.
6. Luan J, Zhang X, Wang S, Li Y, Fan J, Chen W, et al. NOD-Like Receptor Protein 3 Inflammasome-Dependent IL-1beta Accelerated ConA-Induced Hepatitis. *Front Immunol* (2018) 9:758. doi: 10.3389/fimmu.2018.00758
7. Broz P, Pelegrin P, Shao F. The Gasdermins, a Protein Family Executing Cell Death and Inflammation. *Nat Rev Immunol* (2020) 20(3):143–57. doi: 10.1038/s41577-019-0228-2
8. Wang K, Sun Q, Zhong X, Zeng M, Zeng H, Shi X, et al. Structural Mechanism for GSDMD Targeting by Autoprocessed Caspases in Pyroptosis. *Cell* (2020) 180(5):941–55.e20. doi: 10.1016/j.cell.2020.02.002
9. Shi J, Gao W, Shao F. Pyroptosis: Gasdermin-Mediated Programmed Necrotic Cell Death. *Trends Biochem Sci* (2017) 42(4):245–54. doi: 10.1016/j.tibs.2016.10.004
10. Guo H, Xie M, Zhou C, Zheng M. The Relevance of Pyroptosis in the Pathogenesis of Liver Diseases. *Life Sci* (2019) 223:69–73. doi: 10.1016/j.lfs.2019.02.060
11. Rogers C, Erkes DA, Nardone A, Aplin AE, Fernandes-Alnemri T, Alnemri ES. Gasdermin Pores Permeabilize Mitochondria to Augment Caspase-3 Activation During Apoptosis and Inflammasome Activation. *Nat Commun* (2019) 10(1):1689. doi: 10.1038/s41467-019-09397-2
12. Wang Y, Gao W, Shi X, Ding J, Liu W, He H, et al. Chemotherapy Drugs Induce Pyroptosis Through Caspase-3 Cleavage of a Gasdermin. *Nature* (2017) 547(7661):99–103. doi: 10.1038/nature22393
13. Riordan SM, Williams R. Mechanisms of Hepatocyte Injury, Multiorgan Failure, and Prognostic Criteria in Acute Liver Failure. *Semin Liver Dis* (2003) 23(3):203–15. doi: 10.1055/s-2003-42639
14. Powolny AA, Bommareddy A, Hahm ER, Normolle DP, Beumer JH, Nelson JB, et al. Chemopreventative Potential of the Cruciferous Vegetable Constituent Phenethyl Isothiocyanate in a Mouse Model of Prostate Cancer. *J Natl Cancer Inst* (2011) 103(7):571–84. doi: 10.1093/jnci/djr029
15. Brown KK, Hampton MB. Biological Targets of Isothiocyanates. *Biochim Biophys Acta* (2011) 1810(9):888–94. doi: 10.1016/j.bbagen.2011.06.004
16. Ioannides C, Konsue N. A Principal Mechanism for the Cancer Chemopreventive Activity of Phenethyl Isothiocyanate is Modulation of Carcinogen Metabolism. *Drug Metab Rev* (2015) 47(3):356–73. doi: 10.3109/03602532.2015.1058819
17. Yu R, Jiao JJ, Duh JL, Tan TH, Kong AN. Phenethyl Isothiocyanate, a Natural Chemopreventive Agent, Activates C-Jun N-Terminal Kinase 1. *Cancer Res* (1996) 56(13):2954–9.
18. Xiao D, Zeng Y, Choi S, Lew KL, Nelson JB, Singh SV. Caspase-Dependent Apoptosis Induction by Phenethyl Isothiocyanate, a Cruciferous Vegetable-Derived Cancer Chemopreventive Agent, is Mediated by Bak and Bax. *Clin Cancer Res* (2005) 11(7):2670–9. doi: 10.1158/1078-0432.CCR-04-1545
19. Aggarwal M, Saxena R, Sinclair E, Fu Y, Jacobs A, Dyba M, et al. Reactivation of Mutant P53 by a Dietary-Related Compound Phenethyl Isothiocyanate Inhibits Tumor Growth. *Cell Death Differ* (2016) 23(10):1615–27. doi: 10.1038/cdd.2016.48
20. Tan XL, Shi M, Tang H, Han W, Spivack SD. Candidate Dietary Phytochemicals Modulate Expression of Phase II Enzymes GSTP1 and NQO1 in Human Lung Cells. *J Nutr* (2010) 140(8):1404–10. doi: 10.3945/jn.110.121905
21. Ernst IM, Wagner AE, Schuemann C, Storm N, Hoppner W, Doring F, et al. Allyl-, Butyl- and Phenylethyl-Isothiocyanate Activate Nrf2 in Cultured Fibroblasts. *Pharmacol Res* (2011) 63(3):233–40. doi: 10.1016/j.phrs.2010.11.005
22. Sundaram MK, Preetha R, Haque S, Akhter N, Khan S, Ahmed S, et al. Dietary Isothiocyanates Inhibit Cancer Progression by Modulation of Epigenome. *Semin Cancer Biol* (2021) S1044-579X(20):30281–9. doi: 10.1016/j.semcancer.2020.12.021
23. Yu R, Mandlekar S, Harvey KJ, Ucker DS, Kong AN. Chemopreventive Isothiocyanates Induce Apoptosis and Caspase-3-Like Protease Activity. *Cancer Res* (1998) 58(3):402–8.
24. Huang C, Ma WY, Li J, Hecht SS, Dong Z. Essential Role of P53 in Phenethyl Isothiocyanate-Induced Apoptosis. *Cancer Res* (1998) 58(18):4102–6.
25. Gao N, Budhraja A, Cheng S, Liu EH, Chen J, Yang Z, et al. Phenethyl Isothiocyanate Exhibits Antileukemic Activity *In Vitro* and *In Vivo* by Inactivation of Akt and Activation of JNK Pathways. *Cell Death Dis* (2011) 2:e140. doi: 10.1038/cddis.2011.22
26. Wang J, Shi K, Li S, Chen L, Liu W, Wu X, et al. Meisoindigo Attenuates Dextran Sulfate Sodium-Induced Experimental Colitis via Its Inhibition of TAK1 in Macrophages. *Int Immunopharmacol* (2021) 101(Pt B):108239. doi: 10.1016/j.intimp.2021.108239
27. Davies SP, Terry LV, Wilkinson AL, Stamataki Z. Cell-In-Cell Structures in the Liver: A Tale of Four E's. *Front Immunol* (2020) 11:650. doi: 10.3389/fimmu.2020.00650
28. Hu C, Zhao L, Shen M, Wu Z, Li L. Autophagy Regulation is an Effective Strategy to Improve the Prognosis of Chemically Induced Acute Liver Injury Based on Experimental Studies. *J Cell Mol Med* (2020) 24(15):8315–25. doi: 10.1111/jcmm.15565
29. Bala S, Calenda CD, Catalano D, Babuta M, Kodys K, Nasser IA, et al. Deficiency of miR-208a Exacerbates CCl_4-Induced Acute Liver Injury in Mice by Activating Cell Death Pathways. *Hepatol Commun* (2020) 4(10):1487–501. doi: 10.1002/hep4.1540
30. Xiao D, Johnson CS, Trump DL, Singh SV. Proteasome-Mediated Degradation of Cell Division Cycle 25C and Cyclin-Dependent Kinase 1 in Phenethyl Isothiocyanate-Induced G2-M-Phase Cell Cycle Arrest in PC-3 Human Prostate Cancer Cells. *Mol Cancer Ther* (2004) 3(5):567–75.
31. Coscueta ER, Reis CA, Pintado M. Phenylethyl Isothiocyanate Extracted From Watercress By-Products With Aqueous Micellar Systems: Development and Optimisation. *Antioxidants (Basel)* (2020) 9(8):698. doi: 10.3390/antiox9080698
32. Ji Y, Morris ME. Determination of Phenethyl Isothiocyanate in Human Plasma and Urine by Ammonia Derivatization and Liquid Chromatography-Tandem Mass Spectrometry. *Anal Biochem* (2003) 323(1):39–47. doi: 10.1016/j.ab.2003.08.011

33. Yu J, Li S, Qi J, Chen Z, Wu Y, Guo J, et al. Cleavage of GSDME by Caspase-3 Determines Lobaplatin-Induced Pyroptosis in Colon Cancer Cells. *Cell Death Dis* (2019) 10(3):193. doi: 10.1038/s41419-019-1441-4
34. Jiang X, Li Y, Wang W, Han X, Han J, Chen M, et al. Nuclear Factor Erythroid 2 Related Factor 2 Activator JC-5411 Inhibits Atherosclerosis Through Suppression of Inflammation and Regulation of Lipid Metabolism. *Front Pharmacol* (2020) 11:532568. doi: 10.3389/fphar.2020.532568
35. Eisa NH, Khodir AE, El-Sherbiny M, Elsherbiny NM, Said E. Phenethyl Isothiocyanate Attenuates Diabetic Nephropathy *via* Modulation of Glycative/Oxidative/Inflammatory Signaling in Diabetic Rats. *BioMed Pharmacother* (2021) 142:111666. doi: 10.1016/j.biopha.2021.111666
36. Rathkey JK, Zhao J, Liu Z, Chen Y, Yang J, Kondolf HC, et al. Chemical Disruption of the Pyroptotic Pore-Forming Protein Gasdermin D Inhibits Inflammatory Cell Death and Sepsis. *Sci Immunol* (2018) 3(26):eaat2738. doi: 10.1126/sciimmunol.aat2738
37. Hu JJ, Liu X, Xia S, Zhang Z, Zhang Y, Zhao J, et al. FDA-Approved Disulfiram Inhibits Pyroptosis by Blocking Gasdermin D Pore Formation. *Nat Immunol* (2020) 21(7):736–45. doi: 10.1038/s41590-020-0669-6

Conflict of Interest: Author JC was employed by company JC (Wuxi) COMPANY, Inc.

The remaining authors declare that the research was conducted in the absence of any commercial or financial relationships that could be construed as a potential conflict of interest.

frontiers in Immunology

ORIGINAL RESEARCH
published: 07 March 2022
doi: 10.3389/fimmu.2022.842996

Reduced Plasma Extracellular Vesicle CD5L Content in Patients With Acute-On-Chronic Liver Failure: Interplay With Specialized Pro-Resolving Lipid Mediators

María Belen Sánchez-Rodríguez[1], Érica Téllez[2], Mireia Casulleras[1], Francesc E. Borràs[3], Vicente Arroyo[4], Joan Clària[1,4,5,6†] and Maria-Rosa Sarrias[2,6*†]*

[1] Biochemistry and Molecular Genetics Service, Hospital Clínic-Institut d'Investigacions Biomèdiques August Pi i Sunyer (IDIBAPS), Barcelona, Spain, [2] Innate Immunity Lab, Health Research Institute Germans Trias i Pujol (IGTP), Badalona, Spain, [3] Innovation in VEsicles and Cells for Application in Therapy (IVECAT), Health Research Institute Germans Trias i Pujol (IGTP), Badalona, Spain, [4] European Foundation for the Study of Chronic Liver Failure (EF Clif) and Grifols Chair, Barcelona, Spain, [5] Department of Biomedical Sciences, Universitat de Barcelona, Barcelona, Spain, [6] CIBER (Center of Biomedical Research in Network) of Hepatic and Digestive Diseases (CIBERehd), Barcelona, Spain

OPEN ACCESS

Edited by:
Jonel Trebicka,
Goethe University Frankfurt, Germany

Reviewed by:
Michael Praktiknjo,
University Hospital Bonn, Germany
Maximilian Joseph Brol,
University Hospital Frankfurt, Germany

***Correspondence:**
Joan Clària
jclaria@clinic.cat
Maria-Rosa Sarrias
mrsarrias@igtp.cat

†These authors have contributed equally to this work

Specialty section:
This article was submitted to Inflammation, a section of the journal Frontiers in Immunology

Received: 24 December 2021
Accepted: 11 February 2022
Published: 07 March 2022

Citation:
Sánchez-Rodríguez MB, Téllez É, Casulleras M, Borràs FE, Arroyo V, Clària J and Sarrias M-R (2022) Reduced Plasma Extracellular Vesicle CD5L Content in Patients With Acute-On-Chronic Liver Failure: Interplay With Specialized Pro-Resolving Lipid Mediators. Front. Immunol. 13:842996. doi: 10.3389/fimmu.2022.842996

Acute-on chronic liver failure (ACLF) is a syndrome that develops in patients with acutely decompensated cirrhosis (AD). It is characterized by a systemic hyperinflammatory state, leading to multiple organ failure. Our objective was to analyze macrophage anti-inflammatory protein CD5L in plasma extracellular vesicles (EVs) and assess its as yet unknown relationship with lipid mediators in ACLF. With this aim, EVs were purified by size exclusion chromatography from the plasma of healthy subjects (HS) (n=6) and patients with compensated cirrhosis (CC) (n=6), AD (n=11) and ACLF (n=11), which were defined as positive for CD9, CD5L and CD63 and their size, number, morphology and lipid mediator content were characterized by NTA, EM, and LC-MS/MS, respectively. Additionally, plasma CD5L was quantified by ELISA in 10 HS, 20 CC and 149 AD patients (69 ACLF). Moreover, macrophage CD5L expression and the biosynthesis of specialized lipid mediators (SPMs) were characterized *in vitro* in primary cells. Our results indicate that circulating EVs were significantly suppressed in cirrhosis, regardless of severity, and showed considerable alterations in CD5L and lipid mediator content as the disease progressed. In AD, levels of EV CD5L correlated best with those of the SPM RvE1. Analysis of total plasma supported these data and showed that, in ACLF, low CD5L levels were associated with circulatory ($p<0.001$), brain ($p<0.008$) and respiratory ($p<0.05$) failure (Mann-Whitney test). Functional studies in macrophages indicated a positive feedback loop between CD5L and RvE1 biosynthesis. In summary, we have determined a significant alteration of circulating EV contents in ACLF, with a loss of anti-inflammatory and pro-resolving molecules involved in the control of acute inflammation in this condition.

Keywords: macrophages, cirrhosis, resolution of inflammation, RvE1, lipid autacoids

INTRODUCTION

Cirrhosis is a progressive chronic liver disease characterized by extensive hepatic fibrosis, disruption of hepatic blood flow, portal hypertension and liver failure. During the evolution of the disease, compensated cirrhosis (CC) may lead to acutely decompensated cirrhosis (AD), involving the development of ascites, variceal hemorrhage and/or hepatic encephalopathy. AD is a risk factor for a fatal syndrome known as acute-on-chronic liver failure (ACLF) (1).

A hallmark of patients with cirrhosis and ACLF is systemic inflammation, which results in alterations of the number and function of circulating leukocyte components. In these patients, leukocytosis is a predictor of death and several features of unresolved inflammation and unremitting activation of immune cells (1, 2). Indeed, immune cells (i.e., polymorphonuclear leukocytes (PMNs), monocytes and T and B lymphocytes) are the main cellular players in systemic inflammation, and the activation of these cells is regulated by numerous factors, among them the protein CD5L (CD5-Like).

Produced mainly by macrophages, CD5L is a 40-kDa glycoprotein that plays diverse roles at the intersection between lipid homeostasis and the innate immune response and thus participates in many processes, including infection, atherosclerosis and cancer (3). In the context of inflammation, CD5L is emerging as a critical regulator of inflammation by inhibiting immune cell activation and preventing the secretion of pro-inflammatory cytokines by this cell population (3, 4).

Interestingly, this protein is enriched in extracellular vesicles (EVs) purified from plasma (5). The latter are cell-secreted nanovesicles present in human fluids, and their content provides a molecular fingerprint of the releasing cell and, importantly, its status. Given that EVs are enriched in highly selected biomolecules, which may comprise only a very small proportion of the total content of body fluids, they are a potential source of biomarkers in human disease. This feature can facilitate the discovery of biomarkers expressed at relatively low levels that would be difficult to determine in whole fluids (6). Importantly, CD5L modulates the processing of polyunsaturated fatty acids (PUFAs) and the formation of bioactive lipid mediators derived from these molecules (7). In fact, EVs released from immune cells, especially monocytes, macrophages and neutrophils, carry and deliver PUFA-derived bioactive lipids, protect bioactive lipid mediators from degradation, and are a nidus for the biosynthesis of specialized pro-resolving mediators (SPMs) (8, 9). The latter are endogenous lipids that orchestrate the resolution of inflammation, a tightly regulated process whose dysregulation is commonly associated with uncontrolled inflammation (10).

The term SPM embraces a family of chemically and functionally distinct lipid mediators derived from PUFAs and that have dual roles as stop-signals for inflammation and activators of its resolution (10, 11). For instance, SPMs pave the way for monocyte differentiation into phagocytic macrophages, facilitating the removal of dead or dying cells and bacterial clearance, as well as enhancing phagocyte efflux from inflamed tissues to draining lymph nodes to facilitate resolution (10, 11). In broad terms, the resolution of inflammation is an actively regulated process governed by an array of mediators (i.e., SPMs) as diverse as those that initiate inflammation.

In this study, we hypothesized that EVs circulating in plasma have key immunomodulatory potential in the context of chronic liver disease (12). Accordingly, the deregulation or loss of the immunomodulatory EV cargo in patients with advanced stages of liver disease, such as AD and ACLF, could contribute to the systemic hyperinflammatory status of these subjects. To explore this hypothesis, here we examined the plasma EV content of CD5L and bioactive lipid mediators during chronic liver disease progression and identified a novel functional link between CD5L and the SPM resolvin E1 (RvE1), two immunomodulatory signaling pathways that are impaired in ACLF.

MATERIALS AND METHODS

Patients and Biological Samples

The study used biobank plasma samples from 80 patients with AD cirrhosis without ACLF (a group hereafter called "AD") and 69 patients with AD cirrhosis with ACLF (a group hereafter called "ACLF") from the CANONIC study. The criteria for patient selection was based on availability of plasma samples at enrollment and intensive surveillance (clinical assessment) within the 28-day follow-up. The study also included 20 patients with compensated cirrhosis (a group hereafter called "CC"), who had clinically significant portal hypertension as indicated by presence of esophageal varices and/or high fibroscan liver stiffness, as well as 10 healthy subjects (HS) with matched sex and age. For the isolation of EVs, 6 plasma samples from HS, and pools of plasma samples (6 for CC, 11 for AD and 11 for ACLF) were analyzed. The pooling of plasma samples was needed to reach the volume required for EV extraction, and was performed at 4ºC to preserve the quality of the samples. All studies involving human samples were conducted following the Declaration of Helsinki principles and current legislation on the confidentiality of personal data and were approved by the Human Ethics Committee of the Hospital Clínic of Barcelona and Hospital Germans Trias i Pujol.

Human Monocyte-Derived Macrophage (HMDM) Cultures

PBMCs from 8 HS recruited at the Blood Bank of the Hospital Clínic of Barcelona were isolated from 20 mL of peripheral blood in EDTA tubes. Blood samples were centrifuged at 200 g for 10 min at room temperature (rt) to collect plasma, and sedimented cells were diluted with Dulbecco's Phosphate-Buffered Saline without calcium and magnesium ($DPBS^{-/-}$) up to a volume of 20 mL. Diluted blood was layered over 13.3 mL of Ficoll-Paque (GE Healthcare Life Sciences) and centrifuged at 500 g for 25 min. PBMCs were obtained from the mononuclear cell layer, incubated with pre-warmed ammonium-chloride-potassium lysis buffer for 10 min at rt to remove red blood cells, then centrifuged at 400 g for 5 min, and finally washed with $DPBS^{-/-}$. PBMCs were counted and resuspended in RPMI 1640 medium containing penicillin (100 U/mL), streptomycin (100 U/mL) and L-glutamine (4 mM). They were seeded at a density of $5x10^6$ cells/well with RPMI medium in 24-well plates. For peripheral blood monocyte differentiation into

macrophages, cells were allowed to attach at 37°C in a 5% CO_2 atmosphere for 2 h and non-adherent cells were discarded while adherent ones were incubated with fresh RPMI medium supplemented with 10% fetal bovine serum (FBS). The medium was replaced with fresh RPMI with 10% FBS after 2-3 days. After 5-6 days of culture in these conditions, HMDMs were grown for one day with FBS-free RPMI medium and were incubated for 6 h at 37°C in a 5% CO_2 atmosphere either with vehicle (0.007% ethanol) or 5S,12R,18R-trihydroxy-6Z,8E,10E,14Z,16E-eicosapentaenoic acid (RvE1) (10 nM) (Cayman Chemical, Ann Arbor, MI). After 2 h of incubation, lipopolysaccharide serotype O26:B6 (LPS) (Sigma-Aldrich, St Louis, MO) was added at 100 ng/mL together with fresh medium containing RvE1. After 6 h of incubation, the supernatants and cells were collected and stored at -80°C. In another set of experiments, HMDMs were incubated at 37°C in a 5% CO_2 atmosphere in the presence of either vehicle (1:10 $DPBS^{-/-}$ in RPMI) or recombinant human CD5L (catalog # 2797-CL-050, RD systems, Minneapolis, MN) (1 μg/mL) for 20 h and then exposed to LPS (100 ng/m) for 4 additional hours. At the end of the incubation period, the supernatants and cells were collected and stored at -80°C.

EV Purification

EVs were isolated from plasma by Size Exclusion Chromatography (SEC) as described before (13). Briefly, 1.5 mL of plasma was centrifuged at 2000 g for 1 min at 4°C and then loaded into 20 mL of Sepharose-CL2B (Sigma-Aldrich) previously packed into a Puriflash Dry Load Empty column (Interchim, France). Sample separation and elution were performed using filtered PBS. Thirty-five fractions of 0.5 mL were collected. Fractions 5 to 14 were analyzed for the expression of the tetraspanin-specific EV marker CD9 and CD5L by bead-based flow cytometry. Briefly, EVs were coupled to 4 μm aldehyde-sulphate latex beads (Invitrogen Ref A37304) for 15 min. Then, 1 mL of PBS containing 0.1% BSA and 0.01% Sodium Azide (coupling buffer) in PBS was added and EVs were incubated overnight at rt on rotation before incubation with anti-CD9 (RRID : AB_10627954) and anti CD5L (14) mAbs for 30 min at 4°C, followed by anti-mouse IgG-FITC antibody (BD Biosciences, San Jose, CA, ref. 555988, 1:100 dilution) for 30 min at 4°C. Unbound antibodies were washed off with coupling buffer by centrifugation at 2,000 *g* for 10 min between steps. Samples were analyzed using a FACSLyric flow cytometer (BD Biosciences). In this regard, 10,000 single beads per sample were examined, and mean fluorescence intensity (MFI, Flow Jo software, Tree Star, Ashland, OR) was used to compare different fractions. CD9-positive fractions were considered as EV-containing fractions. The 3 fractions containing the highest CD9 MFI were pooled for subsequent Nanoparticle Tracking Analysis (NTA) and cryo-electron microscopy studies. The protein concentration of each fraction was measured by bicinchoninic acid (BCA) assay, following the manufacturer´s instructions (Pierce, Thermo Fisher Scientific, Waltham, MA).

Western Blotting of EV

1.5 ml of eluted EVs were concentrated 8-fold by centrifugation at 2000 g for 20 min at 4°C, using a 100 kDa cutoff centricon (MerckMillipore, Darmstadt, Germany). THP1 cells, used as positive control, were grown in RPMI containing 10% FCS and P/S (14). Cell lysates were prepared in RIPA buffer (50 mmol/l Tris-HCl pH 8, 150 mmol/l NaCl, 1% Nonidet P-40, 0.1% SDS, 1% Triton X-100 plus proteinase inhibitors). Concentrated EVs or 30 μg of THP1 cell lysates were resolved in 10% SDS-polyacrylamide gels under non-reducing conditions and electrophoretically transferred to nitrocellulose membranes (Bio-Rad Laboratories). These were then blocked with Starting Block TBS buffer (Thermo Fisher) for 1 h at rt and incubated overnight at 4°C with anti-CD9 (Immunostep) or CD63 mAb (RRID : AB_396297) diluted in blocking buffer. The membranes were subsequently incubated for 60 min at rt with IRDye 800Cw-conjugated goat anti-mouse IgG (LI-COR Biosciences Lincoln, NE) (RRID : AB_621842) diluted in blocking buffer. Three 15-min washes between steps were performed with TBS-0.01% Tween 20 (Merck Millipore). Bound antibody was detected with an Odyssey Infrared Imager (LI-COR), and densitometric analysis was performed using the Odyssey V.3 software (LI-COR).

Nanoparticle Tracking Analysis

Size distribution and concentration of purified EVs (n=4/group) were determined in a NanoSight LM10 instrument (Malvern Instruments Ltd, Malvern, UK) equipped with a 638 nm laser and CCD camera (model F-033), and data were analyzed with the Nanoparticle Tracking Analysis (NTA) software version 3.2 (Build 3.1.46). The detection threshold was set to 5, and blur and Max Jump Distance were set to auto. Samples were diluted 10 or 20 times with PBS to reach the optimal concentration for instrument linearity: 20-120 particles/frame as advised by the manufacturer. Readings were taken on triplicates of 60 s at 30 frames per second (fps), at a camera level set to 16 and with manual monitoring of temperature.

Cryo-Electron Microscopy

Selected SEC fractions showing the highest MFI for CD9 marker were examined for EV size and morphology by cryo-electron microscopy (cryo-EM). A total of 3 preparations from each group were analyzed. Vitrified specimens were prepared by placing 3 μl of a sample on a Quantifoil® 1.2/1.3 TEM grid, which was blotted to a thin film and plunged into liquid ethane-N2(l) in the Leica EM CPC cryoworkstation (Leica, Wetzlar, Germany). The grids were transferred to a 626 Gatan cryoholder and kept at -179°C. Samples were analyzed with a Jeol JEM 2011 transmission electron microscope (Jeol, Tokyo, Japan) operating at 200 kV. Images were recorded on a Gatan Ultrascan 2000 cooled charge-coupled (CCD) camera with the Digital Micrograph software package (Gatan, Pleasanton, CA). Aliquots of 10 μL of samples were laid on formvar-Carbon EM grids, frozen, and immediately analyzed with a Jeol JEM 2011 transmission electron microscope operating at 200 kV. Samples were kept at -182°C during imaging (626 Gatan cryoholder). Images were recorded on a Gatan Ultrascan CCD camera under low electron dose conditions to minimize electron beam radiation.

mRNA Expression Analysis

Total RNA was isolated from cells using the TRIzol reagent and following the manufacturer's instructions. RNA concentrations

were assessed in a NanoDrop-1000 spectrophotometer (Thermo Fisher). cDNA synthesis from 200 to 1000 ng of total RNA was performed using the High-Capacity cDNA Archive Kit (Applied Biosystems, Foster City, CA). Real-time PCR analysis of human genes was performed in a 7900HT Fast System (Applied Biosystems) using commercial probes for arachidonate 5-lipoxygenase (5-LOX, Hs00167536_m1), arachidonate 15-lipoxygenases [15-LOX-1, Hs00993765_g1 and 15-LOX-2, type B Hs00153988_m1), arachidonate 12-lipoxygenase, 12S type (12-LOX, Hs00167524)], cytochrome P450 family 2 subfamily J member 2 (CYP2J2, Hs00356035_m1), prostaglandin-endoperoxide synthase 1 (COX-1, Hs00377726_m1), and 2 (COX-2, Hs00153133_m1), using β-actin (ACTB, Hs99999903_m1) as endogenous control. All probes were purchased from Thermo Fisher Scientific (Waltham, MA). Quantitative PCR results were analyzed with Sequence Detector 2.1 Software (Applied Biosystems). For CD5L expression probes (Hs.PT.56a.39293248) and glyceraldehyde 3-phosphate dehydrogenase (GAPDH, Hs.PT.39a.22214836) as endogenous control, were purchased from Integrated DNA Technologies (IDT, Iowa, United States). Relative quantification of gene expression was performed using the comparative CT method. The amount of target gene, normalized to ACTB and relative to a calibrator, was determined by the arithmetic equation 2-ΔΔCt, as described in the comparative CT method.

CD5L Expression Analyses

For analysis of CD5L expression, PBMCs were isolated from the buffy coats of healthy blood donors [provided by the Blood and Tissue Bank (Barcelona, Spain)] following the institutional standard operating procedures for blood donation and processing, including informed consent, as described previously (15). Briefly, PBMCs were purified by Ficoll-Paque (GE Healthcare) density gradient centrifugation and enriched in PB monocytes by adherence. Cells were allowed to differentiate to HMDMs for 10 days in RPMI-1640 2 mM glutamine (Lonza) supplemented with 10% heat-inactivated human AB serum (Sigma-Aldrich), 10% heat-inactivated fetal bovine serum (FBS, Lonza), 100 U/mL penicillin, and 100 μg/mL streptomycin (Sigma-Aldrich) in 6-well plates at a density of 10^6 cells/well. Twenty-four hours before the experiments, HMDMs were detached with accutase (Sigma-Aldrich) and placed on Millicell EZ slides (Merck Millipore) (10^5 cells/well). They were then stimulated for 72 h with RvE1 (10 nM) with or without 10 ng/ml LPS in Vehicle (Veh, 0.007% EtOH), or 40 ng/ml Dexamethasone (Kern pharma), used as positive control, as indicated. For mRNA expression analysis, cells were processed as detailed above. For immunofluorescence, cells were fixed with PBS containing 4% paraformaldehyde (Panreac) and incubated for 24 h at 4°C with mAb anti-CD5L in PBS containing 0.3% Triton X-100 and 10% human AB serum (Sigma-Aldrich). Cells were subsequently incubated for 1 h at rt with Alexa Fluor® 488 F(ab')2 fragment of goat anti-mouse IgG (Molecular Probes) in PBS containing 0.3% Triton X-100. Between steps, unbound antibodies were removed with three washes with PBS. Finally, nuclei were stained for 10 min at rt with PBS containing 800 nM Hoechst 33,258 solution (Sigma-Aldrich). They were then washed three times with PBS, and coverslips were mounted in Fluoromount media (Sigma-Aldrich) and left at 4°C overnight. The slides were examined under an Axio Observer Z1 DUO LSM 710 confocal system and analyzed with ZEN Black software (Carl Zeiss Microscopy GmbH) and ImageJ software, described previously (16).

Targeted Lipidomics

The extraction protocol and analysis of bioactive lipid mediators were performed as described by Le Faouder et al. (17), adapted by the Ambiotis SAS (Toulouse, France) standard operating procedure. Briefly, samples of plasma, cell supernatants and purified EVs were mixed with 0.4 mL of ice-cold methanol and held at -80°C for protein precipitation. Samples were then centrifuged and supernatants were collected. After removal of the organic solvent under a stream of nitrogen, samples were suspended in methanol and rapidly acidified to pH 3.5 with HCl. Acidified samples were then loaded into C-18 solid-phase extraction cartridges (Waters, Milford, MA), rapidly neutralized, and eluted with methyl formate. Eluate solvents were evaporated under a stream of nitrogen and residues were suspended in mobile phase for liquid chromatography analyses using an Exion LCAD U-HPLC system coupled to a Sciex QTRAP 6500+ MS-MS system (AB Sciex, Framingham, MA), equipped with an ESI source in negative ion mode.

Measurement of CD5L Levels by Enzyme-Linked Immunosorbent Assay (ELISA)

CD5L levels were assessed in plasma using an in-house developed sandwich ELISA assay, described in (14).

Measurement of Plasma Cytokines and Chemokines

Cytokine/chemokine levels were determined in 25 μl of plasma using a multiplexed bead-based immunoassay [Milliplex MAP Human Cytokine/Chemokine Magnetic Bead Panel (Merck Millipore, Darmstadt, Germany)] on a Luminex 100 Bioanalyzer (Luminex Corp., Austin, TX). The readouts were analyzed with the standard version of the Belysa software (Merck Millipore). A five-parameter logistic regression model was used to create standard curves (pg/mL) and to calculate the concentration of each sample.

Statistical Analysis

Results were expressed as mean ± SEM with the number of individual experiments detailed in the Figure Legends. Normal distribution was assessed by d'Agostino and Pearson normality test. Spearman's test was used for not normally distributed variables correlations. Correlations were calculated only between variables with more than 6 observations. Statistical evaluation of two groups was performed using Student's t test or the Mann-Whitney test. A p value of <0.05 was considered

statistically significant. All statistical analyses were performed using GraphPad Prism versions 5 and 8.

RESULTS

Progression of Chronic Liver Disease Alters the Amount of Plasma EVs and Their CD5L Content

To characterize the CD5L content of EVs, we purified EVs by SEC from total plasma from HS (n=6) and patients with liver cirrhosis at different stages of severity [CC (n=6), AD (n=11) and ACLF (n=11)]. The clinical and laboratory data for these patients are given in **Supplementary Table 1**. **Figure 1A** shows that the elution pattern was similar in all conditions and that EVs were successfully separated from the bulk of protein, as determined by the positivity for the EV-associated tetraspanin CD9 in bead-based flow cytometry and the BCA assay, respectively. These experiments showed that CD9 levels dropped dramatically at all stages of liver disease (CC, AD, ACLF) as compared to HS (**Figure 1B**). Western blotting confirmed reduced CD9 content in EVs from patients with cirrhosis (**Figure 1C**). Likewise, western blotting against the tetraspanin CD63, another constitutive marker of EV, further confirmed this suppression (**Figure 1D**). To further confirm the purification of EVs, a subset of SEC fractions was analyzed by NTA and processed for cryo-EM. NTA indicated the presence of particles with a similar mean size of 152 nm for all groups, and an average of 70 ± 36 particles/ml in HS and a much lower content, namely 20 ± 19, 41 ± 24 and 23 ± 15 particles/ml, in CC, AD and ACLF, respectively (**Figure 1E**). Cryo-EM confirmed that EV fractions contained round-shaped nanovesicles (**Figure 1F**). Of note, CD5L content was similar in EVs purified from HS and CC, while this parameter reached its highest value in AD and decreased in ACLF (**Figure 1G**). These observations can be better appreciated by plotting the MFI signal for CD5L against that for CD9 (CD5 vs. CD9 ratio), which showed a significant increase in CC vs. HS, a further increase in AD vs. CC and a significant reduction in ACLF as compared to AD (**Figure 1H**). Taken together, these results indicate a loss of circulating EVs at all stages of liver cirrhosis and a differential content in CD5L as the disease progressed.

Chronic Liver Disease Is Associated With Changes in the Profile of Bioactive Lipid Mediators in Plasma EVs

Since EVs are a nidus for the formation of bioactive lipid mediators, we next used LC-MS/MS to characterize the profile of lipid mediators in purified EVs. **Figure 2A** shows a schematic diagram of the lipid mediator biosynthesis from arachidonic acid (AA), eicosapentaenoic acid (EPA) and docosahexaenoic acid (DHA). The top five most abundant lipid mediators in EVs from HS were 12-hydroxyeicosatetraenoic acid (12-HETE) (produced by platelets), followed by 14-HDHA, TXB_2, 15-HETE and 17-HDHA (**Figure 2B**). The list of the top five abundant lipid mediators remained the same in EVs from patients with cirrhosis, except that TXB_2 was replaced by 5-HETE (**Figure 2B**). Other lipid mediators detected in EVs were LTB_4, PGE_2, 18-HEPE (the precursor of resolvins of the E-series), LXA_4 and LXB_4 (SPMs derived from 15-HETE), 14-HDHA-related SPMs (maresin [MaR] 1, MaR2 and 7(S)Mar1), resolvin (Rv) D5 (SPM derived from 17-HDHA), 6-keto-$PGF_{1\alpha}$ and a long list of other SPMs, including resolvins of the E- series (i.e. RvE2 and RvE1) and members of the D-series resolvins (RvD1, RvD2, RvD3 and RvD4) and protectins (PD1 and PDX) (**Figure 2B**). We next assigned each lipid mediator to its corresponding biosynthetic enzymatic pathway and identified that LOX-derived products were largely dominating the composition of EVs in patients with cirrhosis (**Figure 2C**). We also assigned each lipid mediator to the corresponding prostaglandin (PG), leukotriene (LT) or SPM family. The list of lipid mediators ascribed to each family is shown in **Supplementary Table 2**. In absolute values, EVs were predominantly enriched in SPMs and SPM intermediate precursors, followed by LTs and finally PGs (**Figure 2D**).

E-Series Resolvins Are Significantly Decreased in EVs From Patients With AD Cirrhosis That Develop ACLF

Since SPM were preponderant in the composition of lipid mediators in EVs, we then focused on the differences in SPM content in EVs between patients with AD cirrhosis that had developed ACLF and those patients with AD cirrhosis who hadn't. We categorized each SPM (including the SPM precursors) to the different SPM sub-families (see the list of SPMs ascribed to each sub-family in **Supplementary Table 3**). Interestingly, the EV content of the E-series precursor 18-HEPE was lower in AD patients with ACLF than in those without, and this was consistent with a significant loss of E-series resolvins in ACLF patients (**Figure 3**). This finding indicates that EVs from patients with AD cirrhosis lose their E-series SPM content during the development of ACLF. Furthermore, RvE1 showed the highest correlation with CD5L among the different lipid mediators (**Supplementary Figure 1**). Taken together, these findings suggest that at the most severe stages of liver disease (i.e., ACLF), there is a loss of pro-resolving pathways, which may favor the development of a systemic hyperinflammatory state, leading to organ dysfunction or failure.

Suppression of the Plasma Levels of CD5L in the Most Severe Stages of Advanced Liver Cirrhosis: Relationship With Extrahepatic Organ Failures

We next sought to compare the CD5L content in EVs to that in total plasma in a much larger cohort of patients by using ELISA. In these measurements, we included 10 HS, 20 CC, 80 AD without ACLF and 69 AD patients with ACLF. The baseline clinical and standard laboratory data of the patients included in

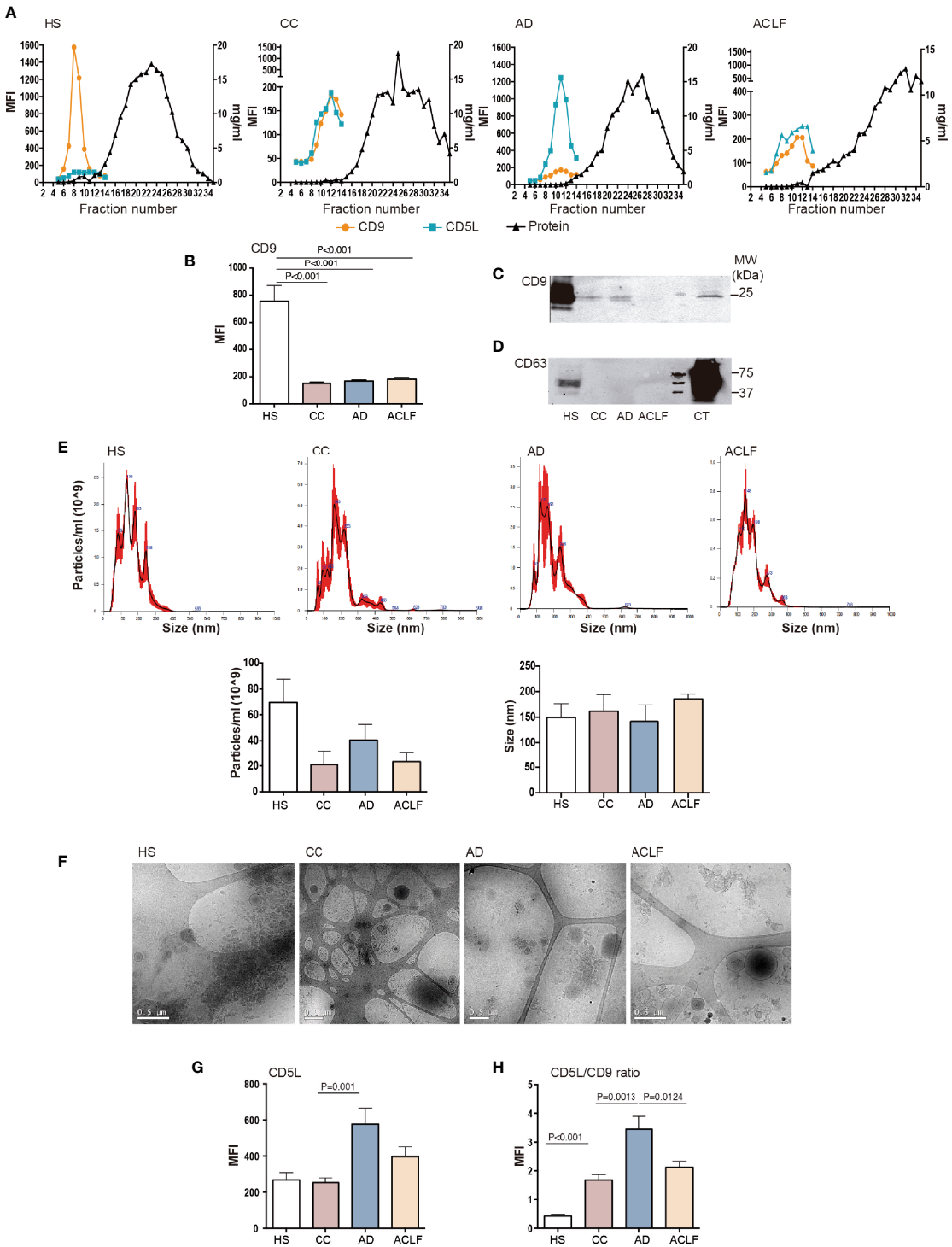

FIGURE 1 | EV characterization. Plasma fractions were pooled to generate n=6 HS, n=6 CC, n=11 AD and n=11 ACLF patient samples**. (A)** Upper panel: Representative graphs showing analysis of SEC eluted fractions. Left axis: Mean Fluorescence intensity (MFI) of EV markers CD9 and CD5L by bead-based flow cytometry. Right axis: protein elution was monitored by BCA. **(B)** CD9 MFI data of all samples analyzed. **(C)** Western blot of CD9 and **(D)** Western blot of CD63 in EVs and THP1 cell lysates, used as positive control (CT). **(E)** Upper panel: NTA of purified EVs from each group of patients. Lower panel: graph depicting particles/ml and size (nm) of the EV particles from 3 purifications. **(F)** Cryo-EM images confirmed EV presence in pooled fractions (F5-7) of SEC preparation from each group of patients. **(G)**. CD5L and **(H)** the ratio of CD5L vs. CD9 MFI data. Bars represent mean ± SEM. P values were calculated using the Mann-Whitney test. HS, healthy subject; CC, Compensated Cirrhotic; AD, Acute Decompensation without ACLF; ACLF, Acute-on-Chronic Liver Failure.

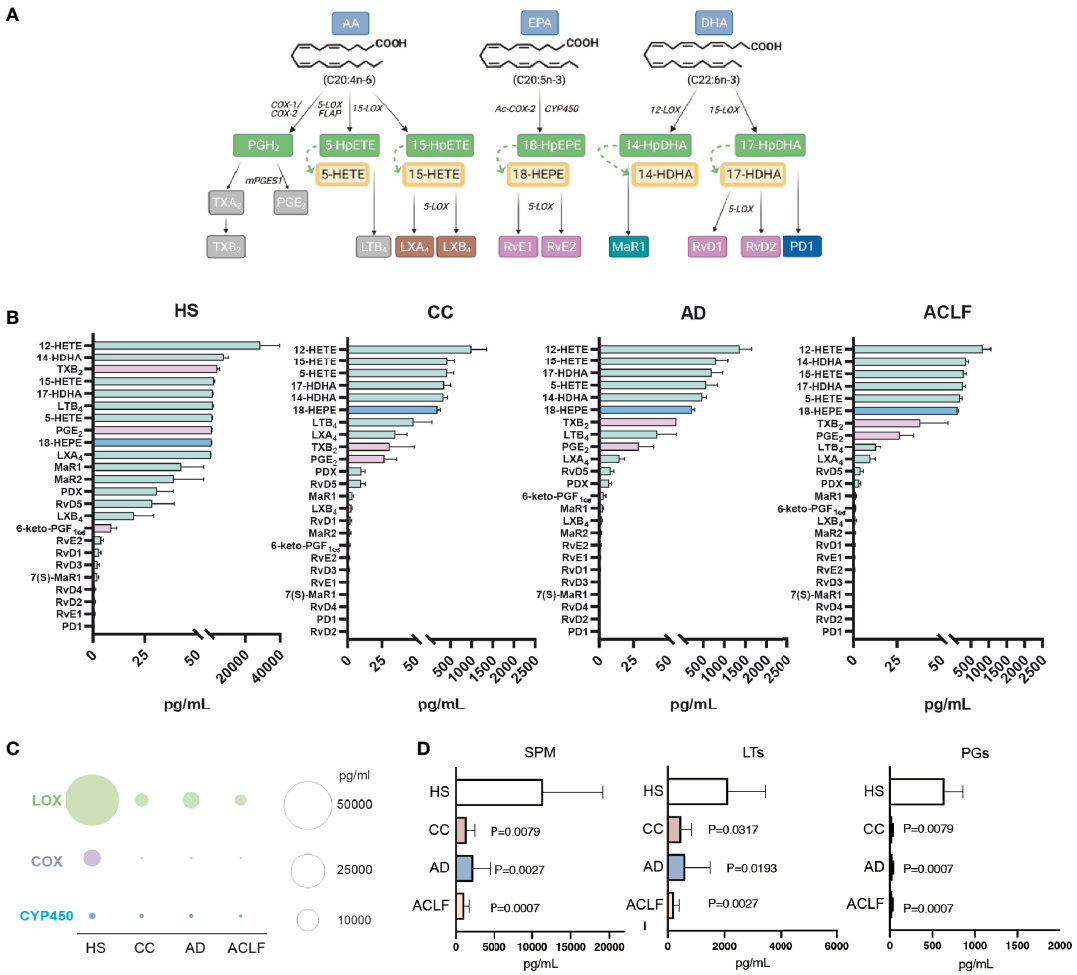

FIGURE 2 | Analysis of eicosanoid and SPM content by liquid chromatography-tandem mass spectrometry (LC-MS/MS)-based lipidomics in EV from HS (n= 5), CC (n=5), AD (n=10) and ACLF (n=10) patient samples. **(A)** Schematic diagram of SPM biosynthesis from arachidonic acid (AA), eicosapentaenoic acid (EPA) and docosahexaenoic acid (DHA). **(B)** Lipid mediators are ranked on the basis of their concentration (the highest on the top; the lowest on the bottom) in the four groups. Color of bars indicates the biosynthetic pathway of the lipid mediators: green-LOX, purple-COX, and blue-Cyp450. **(C, D)**. Total amount of lipid mediators calculated by the sum of the concentrations of each lipid mediator categorized according to the biosynthetic LOX, COX and CYP pathways **(C)**. or to the lipid mediator biochemical family **(D)**. Bars represent mean ± SEM. P values were calculated using the Mann-Whitney test. HS, healthy subject; CC, Compensated Cirrhotic; AD, Acute Decompensation without ACLF; ACLF, Acute-on-Chronic Liver Failure.

CD5L measurements are shown in **Supplementary Table 4**. The mean ± SEM plasma CD5L concentration as analyzed by ELISA in HS patients was 6.4 ± 0.6 μg/ml, while this parameter increased steadily in CC and AD patients, peaked in patients with ACLF (grade 1), and then dropped in those with the most severe forms of the disease (ACLF grades 2 and 3), reaching statistical significance in patients with ACLF grade 3 with respect to AD and ACLF grade 1 (**Figure 4A**). Remarkably, significantly lower levels of CD5L were observed in patients with either circulatory, brain or respiratory failure (**Figure 4B**), without apparent changes in their levels in patients with liver, coagulation or renal failure (**Supplementary Figure 2A**). No significant association was found between plasma levels of CD5L and bacterial infection, development of bacterial infection during hospitalization, or 28-day mortality (**Supplementary Figures 2B, C**). Levels of CD5L did not predict the clinical outcome of the patients but plasma levels were lower in those worsening than in those with improved or steady clinical course (mean ± SEM 14.07 ± 2.31 vs 16.08± 1.73 or 15,67 ± 0.96 μg/ml), although differences did not reach statistical significance (**Supplementary Figures 2D, E**). Of note, lower plasma levels of CD5L were present in patients with cirrhosis of alcohol etiology in comparison to those of hepatitis C virus origin, without reaching statistical significance (**Figure 4C**). Together, these findings suggest that development of extrahepatic organ failures (i.e. circulatory, brain or respiratory failures) in patients with well advanced and decompensated liver cirrhosis could be associated with defective circulating CD5L concentrations.

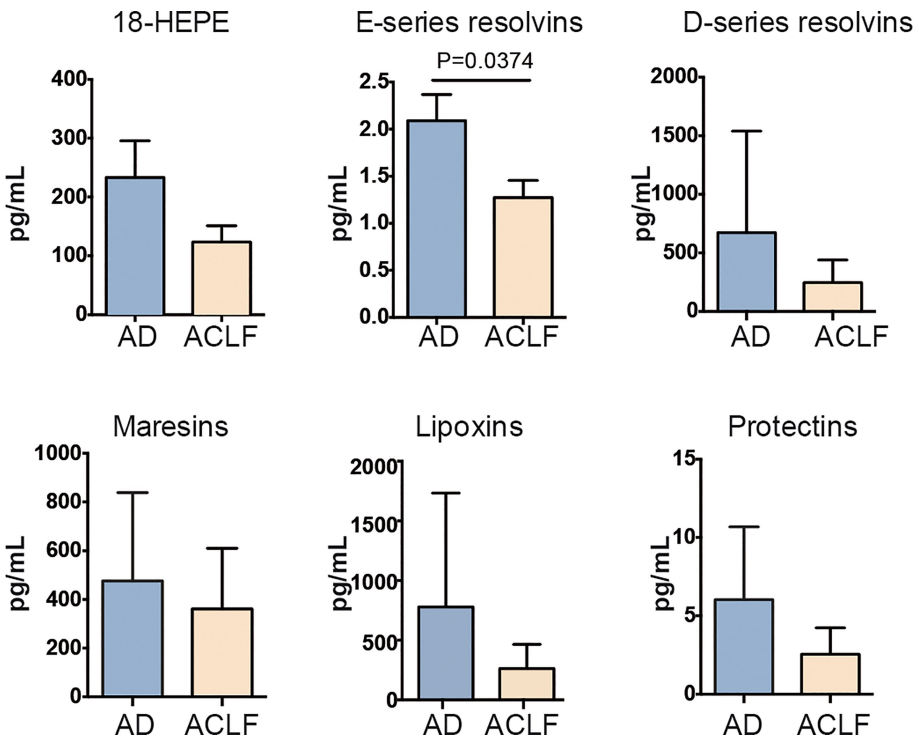

FIGURE 3 | Drop of E-series resolvins in EVs from ACLF patients. Individual SPM EV content in AD vs ACLF patients. Bars represent mean ± SEM. P values were calculated using the Mann-Whitney test. Data from AD (Acute Decompensation without ACLF) (n=10) and ACLF (Acute-on-Chronic Liver Failure) (n=10) patient samples.

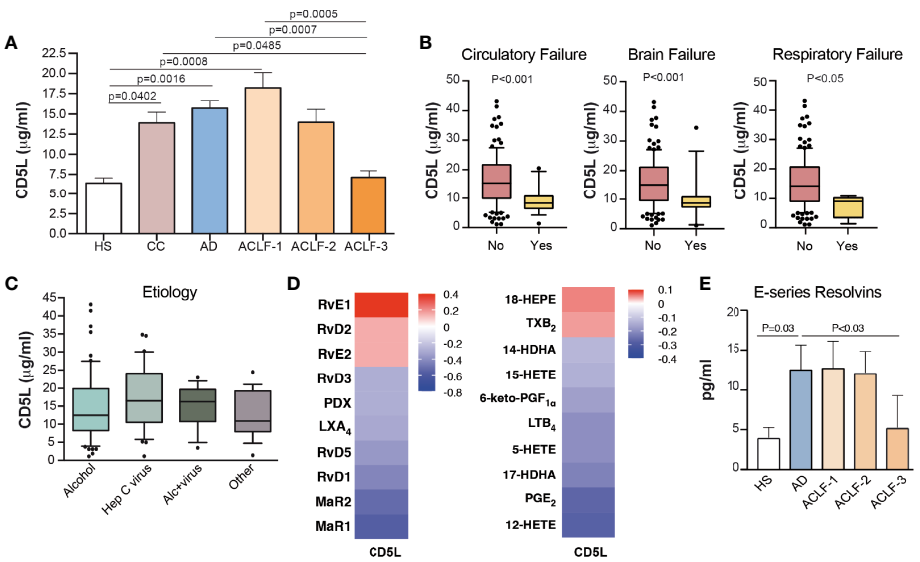

FIGURE 4 | Plasma CD5L levels and RvE1 decrease in ACLF. **(A)** Plasma levels of CD5L were measured by ELISA in HS (n=10), CC (n=20), AD (n=80) and ACLF (n=69) patient samples (ACLF-1 n=33, ACLF-2 n=21, ACLF-3 n=15). Bars indicate the mean values ± SEM for CD5L in each group. **(B)** Association of CD5L with circulatory (n=17), brain (n=17) and respiratory (n=4) failures. **(C)** Association of CD5L with alcohol (n=63), hepatitis C virus (Hep C virus, n=37), alcohol + hepatitis C virus (Alc+virus, n=17) and other (n=18) etiologies. Data represent median plus interquartile range. **(D)** Spearman´s correlation heat map with correlation coefficient between CD5L and lipid mediator concentration, determined by LC-MS/MS in the plasma of AD (n=10) and ACLF (n=15) patients. **(E)** E series Resolvins (RvE1 and RvE2) plasma concentration, determined as in D) and in additional n=5 HS. Bars represent mean ± SEM. D. P values were calculated using the Mann-Whitney test. HS: healthy subject; CC, Compensated Cirrhotic; AD, Acute Decompensation without ACLF; ACLF, Acute-on-Chronic Liver Failure.

Translation to the Systemic Circulation of the Defect in CD5L and RvE1 Levels

We next sought to investigate the impact of reduced plasma CD5L levels in the most severe forms of the disease with systemic inflammation. As shown in **Supplementary Figure 3A**, plasma CD5L levels showed a negative correlation with white blood cell (WBC) and platelet counts. In contrast, CD5L levels showed a highly significant positive correlation with IL-1α, IL-10, MCP-1 and IFNα2, and negative correlation with IL-17A (**Supplementary Figure 3B**). Of interest, CD5L significantly positively correlated with IgG concentration (**Supplementary Figure 3C**). We also correlated the CD5L content with the content of lipid mediators measured by LC-MS/MS in total plasma from 5 HS, 10 AD and 15 ACLF patients. This analysis revealed that CD5L strongly correlated with RvE1, as well as with its intermediate precursor 18-HEPE (**Figure 4D**). Additionally, plasma levels of E-series resolvins RvE1 and RvE2 were significantly suppressed in patients afflicted by grade 3 ACLF in comparison to patients with AD (**Figure 4E**). Overall, these data indicate that the pattern of suppression of anti-inflammatory and pro-resolving molecules (CD5L and RvE1) in the plasma of patients with cirrhosis parallels that seen in EVs, and that impairment of these endogenous braking signals is a hallmark in patients presenting the most severe forms of advanced liver cirrhosis.

Identification of a Positive Feedback Loop Between RvE1 and CD5L in Macrophages

To study whether there is a direct link and/or a causal relationship between CD5L and the biosynthesis of RvE1, we next carried out mechanistic studies in peripheral blood mononuclear cells (PBMCs) and macrophages derived from circulating peripheral blood monocytes from healthy donors (human monocyte-derived macrophages, HMDM). Given that HMDMs in culture express no detectable levels of CD5L protein (16, 18), we supplemented these cell cultures with recombinant human CD5L (rCD5L) and collected the supernatants to determine the levels of lipid mediators by LC-MS/MS. We also collected the cell extracts to assess the effects of rCD5L on the expression of genes involved in the SPM biosynthetic pathways in the presence of LPS (to mimic an inflammatory milieu). **Figure 5A** shows the effects of rCD5L on all the SPMs detected in the PBMCs supernatants. Unlike the AA-derived eicosanoids and the DHA-derived D-series resolvins, protectins and maresins, rCD5L induced a ~1.5-fold increase in the EPA-derived SPM RvE1. Consistent with enhanced RvE1 formation, in the presence of LPS, rCD5L upregulated the expression of COX-2 and CYP2J2 (**Figure 5B**), the two enzymes involved in the initial stages of RvE1 biosynthesis from EPA. rCD5L did not modify the LPS-induced downregulation of constitutive enzymes such as COX-1 and 5-LOX (**Figure 5C**) and did not affect the expression of 15-LOX-1 and -2 (**Figure 5D**). Conversely, when HMDMs were exposed to RvE1, the expression of CD5L mRNA and protein was increased, as observed by RT-qPCR (**Figure 5E**) and immunofluorescence microscopy using an anti-CD5L mAb (**Figure 5F**). Taken together, these data point to positive feedback between CD5L and the RvE1 axis in human macrophages.

DISCUSSION

Here we isolated and characterized EVs from the plasma of patients at different stages of liver disease, with a focus on ACLF. Given the alterations in EV composition in liver pathology, these structures have been proposed as a source of biomarkers, as well as potential tools for therapeutic intervention (12). Our results support this notion since we show that circulating CD5L and EV content of lipid mediators are not only altered in cirrhosis vs. healthy subjects but also differ between disease stages, namely compensated vs. decompensated with or without ACLF.

Previous findings suggest an increase in circulating liver-derived micro-vesicles (i.e., plasma cell-derived EVs) in cirrhosis (19–23). Additionally, it has been demonstrated that stressed hepatocytes in culture enhance the production of EVs (19), and a study showed that more EVs carrying ASPGRP hepatocyte marker are detected in SEC-purified serum of cirrhotic NASH patients than in healthy subjects (24). In contrast to these data, we observed a loss of circulating EVs in total plasma in compensated and also in decompensated cirrhosis. EV research is evolving rapidly, and various biomarkers and a range of purification methods may result in a different interpretation of the data. In this publication, it was agreed that SEC, the purification approach we used, is low recovery but specific method of purification, according to the Minimal information for studies of extracellular vesicles 2018 (25). More importantly, in our study, we did not aim to analyze hepatocyte-derived EVs but rather the global status of circulating EVs, since our focus was ACLF in decompensated cirrhosis and not liver centered. Although the central organ in these patients is the deteriorated liver, numerous organs or system dysfunctions are involved, such as renal, brain, circulatory, coagulation, respiratory and immune system, among others (26). Therefore, we analyzed circulating EVs regardless of their organ of origin and observed a significant loss of the number of plasma EVs in patients with cirrhosis and at advanced stages of the disease, as reflected by the lower levels of EV markers CD9 and CD63, and the number of particles indicated by NTA technology.

A limitation of our study is that we did not analyze markers of subcellular origin (e.g. phosphatidylserine as a marker for apoptotic bodies and Grp94 as ER marker) to understand the distribution and entity of purified EVs. Nevertheless, our main interest was the composition of isolated EVs and whether this parameter could provide insight into the possible physiological relationship between CD5L and lipid mediators. The results revealed that CD5L is present in EVs purified from plasma, in agreement with previous reports (5, 27). Interestingly, our data show that the EV cargo of CD5L undergoes significant changes during the course of liver pathology, thereby suggesting that CD5L is not a constitutive biomarker of circulating EVs. Of note, CD5L located in the EV fraction accounted for a very small portion of total plasma CD5L content (data not shown).

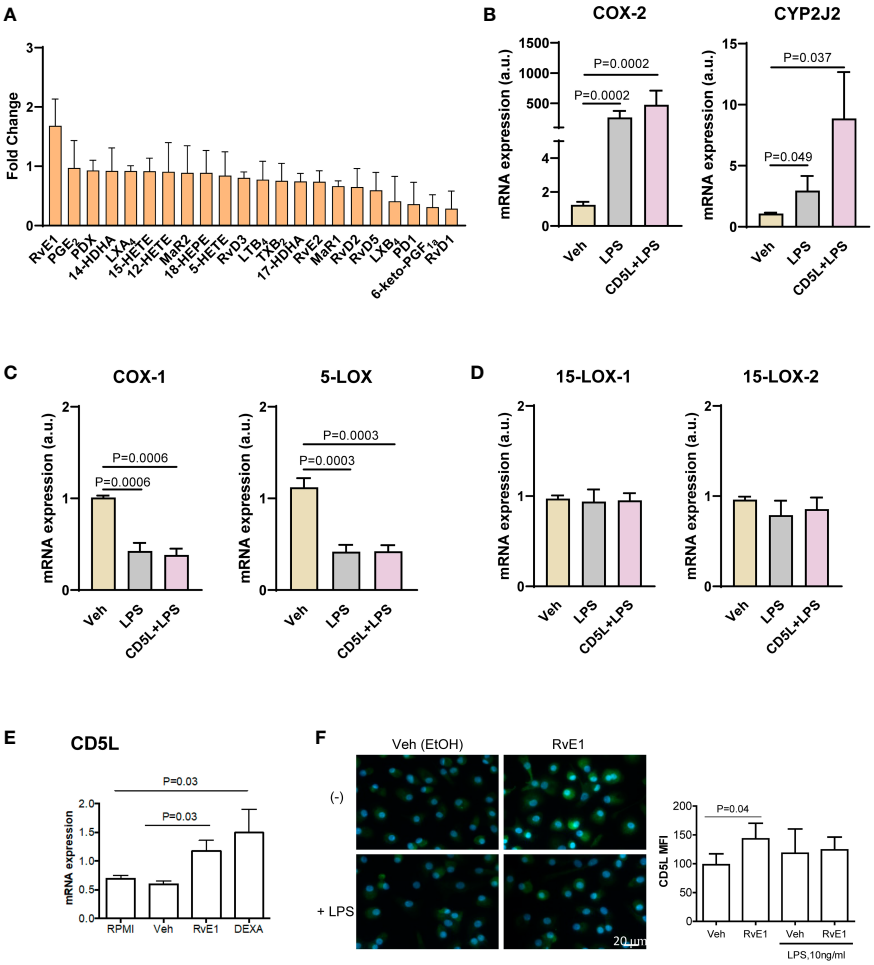

FIGURE 5 | Positive feed-back between CD5L and RvE1 synthesis in macrophages. Peripheral blood mononuclear cells (PBMCs) were isolated from the blood of healthy donors (n=8) by ficoll gradient centrifugation. **(A)** PBMCs were stimulated with 1 µg/ml CD5L or Vehicle (Veh, PBS) for 24 h, and SPMs in the supernatants were quantified by LC-MS/MS. **(B–D)** PBMCs were cultured for 7 days and differentiated into primary macrophages, which were stimulated with 1 µg/ml CD5L for 24 h with or without 100 ng/ml LPS during the last 4 h of culture, and the amount of mRNA encoding the indicated enzymes was quantified by RT-qPCR. **(E, F)** Human primary macrophages (n=5 donors) were treated for 72h with RvE1 (10 nM) with or without 10 ng/ml LPS in Vehicle (Veh, 0.007% EtOH), or 40 ng/ml Dexamethasone (DEXA), used as positive control. **(E)** The amount of mRNA encoding CD5L was measured by RT-qPCR. **(F)** Representative immunofluorescence images of CD5L (green) in primary treated Nuclei were stained with Hoechst (blue). Graphs show CD5L mean fluorescence intensity (MFI) ± SEM of 50 macrophages scored in random fields. Bars represent mean ± SEM. P values were calculated using the Mann-Whitney test.

Overall, our results reinforce the notion that circulating CD5L (in EVs and total plasma) is strongly associated with the severity of liver disease (14, 28–30). Regarding ACLF, we report for the first time a loss of circulating CD5L in this condition and a significant association with circulatory, brain and respiratory failure. The precise molecular events involved in this association are currently unknown. In contrast, CD5L systemic levels were not modified in bacterial infection, although the latter is associated with substantial morbidity and mortality in these patients. Previous studies have described that CD5L interacts with bacteria, thus pointing to a functional link with infection (31, 32). The heterogeneity of infectious agents in this cohort of patients may preclude the observation of systemic changes in CD5L related to infection. In blood, CD5L can circulate in its free form, in EVs, and in association with IgM but not IgG (33–35). In obesity, this IgM-CD5L association has a functional consequence, since it contributes to auto-antibody production (35). Little is known about its involvement in other contexts. However, in healthy individuals and in cirrhotic patients with liver cancer, IgM and CD5L levels are positively correlated (35, 36). In contrast, we found that CD5L was positively associated with IgG but not with IgM or IgA in AD cirrhosis and ACLF. Our results suggest that deregulation of immunoglobulin homeostasis in ACLF also affects the IgM-CD5L ratio. How CD5L distributes within the three compartments (i.e., free, EVs or IgM) in ACLF and the functional consequences of this distribution remains to be elucidated.

On the other hand, CD5L was found to be strongly positively correlated with IFNα2 and MCP1, two inflammatory mediators. In

this regard, patients presenting ACLF have been reported to show significantly higher levels of proinflammatory cytokines/chemokines, including TNF-α, MCP-1, IL-8, and IFN-γ, and also anti-inflammatory IL-10 than patients without ACLF (37). Further studies are needed to unravel the relationship between CD5L and these specific cytokines/chemokines in systemic inflammation. We previously hypothesized that the increase in CD5L during liver disease may be an adaptive response to liver damage and fibrosis that seeks to counteract inflammatory signaling (14). In ACLF, the loss of regulatory CD5L may contribute to failure to regulate inflammation. Additionally, a drop in SPMs would reduce the capacity to repair and regenerate damaged tissues.

Here we report that loss of SPMs and CD5L in EVs and total plasma may have a causal link, since CD5L and RvE1 are mutually upregulated in macrophages. The relationship between CD5L and lipid homeostasis is consistent with the findings of previous studies that showed that CD5L expression in macrophages is regulated by Liver X Receptor (LXR) (3, 38, 39), a transcription factor activated by oxysterols and specific intermediates in the cholesterol biosynthetic pathway that belongs to the nuclear receptor family (40). Moreover, in Th17 cells, CD5L modulates the processing of PUFAs and the formation of bioactive lipid mediators derived from these fatty acids, mainly evolutionarily conserved SPMs (7).

Liver macrophages are key players in most, if not all, inflammation-related liver disorders, including cirrhosis, because they respond to a wide array of activating signals. They are also capable of clearing apoptotic cells and debris, thus initiating the resolution of inflammation, tissue repair and regeneration. It is well known that SPMs play central roles in promoting these processes (41). Our results now suggest that mutual regulation of CD5L and RvE1 provides a novel link between innate immunity and lipid homeostasis. This finding may be highly relevant for understanding how macrophages regulate inflammation and its resolution.

DATA AVAILABILITY STATEMENT

The datasets presented in this article are not readily available because human sample clinical data will not be shared. Requests to access the datasets should be directed to M-R Sarrias, mrsarrias@igtp.cat; Joan Clària, jclaria@clinic.cat.

ETHICS STATEMENT

The studies involving human participants were reviewed and approved by Human Ethics Committee of the Hospital Clínic of Barcelona; Human Ethics Committee of the Hospital Germans Trias i Pujol. The patients/participants provided their written informed consent to participate in this study.

AUTHOR CONTRIBUTIONS

MBS-R, ET, and MC collected, analyzed and interpreted the data. FB and VA performed data analysis and interpretation. JC and M-RS contributed equally to literature search, study design, data analysis and interpretation, and writing. All authors contributed to the article and approved the submitted version.

FUNDING

This study was supported by the EF Clif, European Foundation for the study of chronic liver failure, a non-profit organization that receives unrestricted donations from the Cellex Foundation, Grifols and the European Union's Horizon 2020 research and innovation program (grant agreements 825694 and 847949). Additional funders were Instituto de Salud Carlos III (ISCIII), and ERDFs from the EU, 'Una manera de hacer Europa', PI19/00523 to M-RS and Ministerio de Ciencia e Innovacion (PID2019-105240RB-I00) to JC. The Innate Immunity lab is accredited as an Emergent Research group by the Catalan Agency for Management of University and Research Grants (2017-SGR-49). M-RS is a researcher from IGTP, a member of the CERCA network of institutes supported by the Health Department of the Government of Catalonia. JC laboratory at the Center Esther Koplowitz, IDIBAPS, is part of the CERCA Programme/Generalitat de Catalunya and is a Consolidated Research Group recognized by the Generalitat de Catalunya (2017SGR1449).

ACKNOWLEDGMENTS

We thank Marti de Cabo, Servei de Microscòpia, Facultat de Biociències, Universitat Autònoma de Barcelona, for his assistance with TEM. We thank Dr. Hernando A del Portillo (ICREA at ISGlobal/IGTP) for the use of the NTA apparatus and Ms. Paula Crego for technical assistance on its usage. We would also like to thank the technical assistance of Silvia Sanz.

SUPPLEMENTARY MATERIAL

The Supplementary Material for this article can be found online at: https://www.frontiersin.org/articles/10.3389/fimmu.2022.842996/full#supplementary-material

Supplementary Figure 1 | Spearman´s correlation heat map with correlation coefficient between CD5L and lipid mediator concentration in EVs, determined by LC-MS/MS in AD (n=10) and ACLF (n=15) patients pooled plasma.

Supplementary Figure 2 | (A). Association of CD5L plasma levels with clinical parameters: **(A)**. Organ failure: liver Yes n=34, No n=107, coagulation Yes n=20, No n=121, renal Yes n=37, No n=104. **(B)**. Bacterial infection: Yes n=15, No n=133, and development of bacterial infection during hospitalization: Yes n=44, No n=96. **(C)**. 28-day mortality: Yes n=31, No n=118. **(D)**. Disease course at 3-day follow-up: Steady n= 89, Improvement n=26, Worsening n=13. Data represent median plus interquartile range. AD steady course: no ACLF during follow-up. ACLF steady course: no change of ACLF grade. Improvement of ACLF: decrease of ACLF by at least one grade during follow-up. Worsening of AD or ACLF: development of ACLF or increase of ACLF by at least one grade during follow-up **(F)**. Table showing the distribution of patients analyzed for disease course according to ACLF grade at inclusion vs ACLF grade follow-up.

Supplementary Figure 3 | Correlation of plasma levels of CD5L in AD and ACLF with **(A)**. White blood cell (WBC), platelet counts and C-reactive protein. **(B)**. Circulating cytokines and chemokines. **(C)**. IgG concentration.

REFERENCES

1. Arroyo V, Moreau R, Jalan R. Acute-on-Chronic Liver Failure. *N Engl J Med* (2020) 382:2137–45. doi: 10.1056/NEJMra1914900
2. Moreau R, Jalan R, Gines P, Pavesi M, Angeli P, Cordoba J, et al. Acute-on-Chronic Liver Failure is a Distinct Syndrome That Develops in Patients With Acute Decompensation of Cirrhosis. *Gastroenterology* (2013) 144:1426–1437.e9. doi: 10.1053/j.gastro.2013.02.042
3. Sanchez-Moral L, Ràfols N, Martori C, Paul T, Téllez É, Sarrias MR. Multifaceted Roles of Cd5l in Infectious and Sterile Inflammation. *Int J Mol Sci* (2021) 22:1–14. doi: 10.3390/ijms22084076
4. Sanjurjo L, Aran G, Roher N, Valledor AF, Sarrias M-R. AIM/CD5L: A Key Protein in the Control of Immune Homeostasis and Inflammatory Disease. *J Leukoc Biol* (2015) 98:173–84. doi: 10.1189/jlb.3RU0215-074R
5. de Menezes-Neto A, Sáez MJF, Lozano-Ramos I, Segui-Barber J, Martin-Jaular L, Ullate JMEE, et al. Size-Exclusion Chromatography as a Stand-Alone Methodology Identifies Novel Markers in Mass Spectrometry Analyses of Plasma-Derived Vesicles From Healthy Individuals. *J Extracell Vesicles* (2015) 4:27378. doi: 10.1017/CBO9781107415324.004
6. Properzi F, Logozzi M, Fais S. Exosomes: The Future of Biomarkers in Medicine. *Biomark Med* (2013) 7:769–78. doi: 10.2217/bmm.13.63
7. Wang C, Yosef N, Gaublomme J, Wu C, Lee Y, Clish CB, et al. CD5L/AIM Regulates Lipid Biosynthesis and Restrains Th17 Cell Pathogenicity. *Cell* (2015) 163:1413–27. doi: 10.1016/j.cell.2015.10.068
8. Norling LV, Spite M, Yang R, Flower RJ, Perretti M, Serhan CN. Cutting Edge: Humanized Nano-Proresolving Medicines Mimic Inflammation-Resolution and Enhance Wound Healing. *J Immunol* (2011) 186:5543–7. doi: 10.4049/jimmunol.1003865
9. Dalli J, Serhan CN. Specific Lipid Mediator Signatures of Human Phagocytes: Microparticles Stimulate Macrophage Efferocytosis and Pro-Resolving Mediators. *Blood* (2012) 120:60–72. doi: 10.1182/blood-2012-04-423525
10. Serhan CN. Novel Pro-Resolving Lipid Mediators in Inflammation are Leads for Resolution Physiology. *Nature* (2014) 510:92–101. doi: 10.1038/nature13479.Novel
11. Clària J, Flores-Costa R, Duran-Güell M, López-Vicario C. Proresolving Lipid Mediators and Liver Disease. *Biochim Biophys Acta - Mol Cell Biol Lipids* (2021) 1866. doi: 10.1016/j.bbalip.2021.159023
12. Kostallari E, Valainathan S, Biquard L, Shah VH, Rautou PE. Role of Extracellular Vesicles in Liver Diseases and Their Therapeutic Potential. *Adv Drug Deliv Rev* (2021) 175:113816. doi: 10.1016/j.addr.2021.05.026
13. Monguió-Tortajada M, Morón-Font M, Gámez-Valero A, Carreras-Planella L, Borràs FE, Franquesa M. Extracellular-Vesicle Isolation From Different Biological Fluids by Size-Exclusion Chromatography. *Curr Protoc Stem Cell Biol* (2019) 49(1):e82. doi: 10.1002/cpsc.82
14. Bárcena C, Aran G, Perea L, Sanjurjo L, Téllez É, Oncins A, et al. CD5L is a Pleiotropic Player in Liver Fibrosis Controlling Damage, Fibrosis and Immune Cell Content. *EBioMedicine* (2019) 43:513–24. doi: 10.1016/j.ebiom.2019.04.052
15. Sanjurjo L, Amézaga N, Aran G, Naranjo-Gómez M, Arias L, Armengol C, et al. The Human CD5L/AIM-CD36 Axis: A Novel Autophagy Inducer in Macrophages That Modulates Inflammatory Responses. *Autophagy* (2015) 11:487–502. doi: 10.1080/15548627.2015.1017183
16. Sanjurjo L, Aran G, Téllez É, Amézaga N, Armengol C, López D, et al. CD5L Promotes M2 Macrophage Polarization Through Autophagy-Mediated Upregulation of ID3. *Front Immunol* (2018) 9:480. doi: 10.3389/fimmu.2018.00480
17. Le Faouder P, Baillif V, Spreadbury I, Motta JP, Rousset P, Chêne G, et al. LC-MS/MS Method for Rapid and Concomitant Quantification of Pro-Inflammatory and Pro-Resolving Polyunsaturated Fatty Acid Metabolites. *J Chromatogr B Anal Technol BioMed Life Sci* (2013) 932:123–33. doi: 10.1016/j.jchromb.2013.06.014
18. Amézaga N, Sanjurjo L, Julve J, Aran G, Pérez-Cabezas B, Bastos-Amador P, et al. Human Scavenger Protein AIM Increases Foam Cell Formation and CD36-Mediated Oxldl Uptake. *J Leukoc Biol* (2014) 95:509–20. doi: 10.1189/jlb.1212660
19. Verma VK, Li H, Wang R, Hirsova P, Mushref M, Liu Y, et al. Alcohol Stimulates Macrophage Activation Through Caspase-Dependent Hepatocyte Derived Release of CD40L Containing Extracellular Vesicles. *J Hepatol* (2016) 64:651–60. doi: 10.1016/j.jhep.2015.11.020
20. Sehrawat TS, Arab JP, Liu M, Amrollahi P, Wan M, Fan J, et al. Circulating Extracellular Vesicles Carrying Sphingolipid Cargo for the Diagnosis and Dynamic Risk Profiling of Alcoholic Hepatitis. *Hepatology* (2021) 73:571–85. doi: 10.1002/hep.31256
21. Julich-Haertel H, Urban SK, Krawczyk M, Willms A, Jankowski K, Patkowski W, et al. Cancer-Associated Circulating Large Extracellular Vesicles in Cholangiocarcinoma and Hepatocellular Carcinoma. *J Hepatol* (2017) 67:282–92. doi: 10.1016/j.jhep.2017.02.024
22. Payancé A, Silva-Junior G, Bissonnette J, Tanguy M, Pasquet B, Levi C, et al. Hepatocyte Microvesicle Levels Improve Prediction of Mortality in Patients With Cirrhosis. *Hepatology* (2018) 68:1508–18. doi: 10.1002/hep.29903
23. Kornek M, Lynch M, Mehta SH, Lai M, Exley M, Afdhal NH, et al. Circulating Microparticles as Disease-Specific Biomarkers of Severity of Inflammation in Patients With Hepatitis C or Nonalcoholic Steatohepatitis. *Gastroenterology* (2012) 143:448–58. doi: 10.1053/j.gastro.2012.04.031
24. Povero D, Yamashita H, Ren W, Subramanian MG, Myers RP, Eguchi A, et al. Characterization and Proteome of Circulating Extracellular Vesicles as Potential Biomarkers for NASH. *Hepatol Commun* (2020) 4:1263–78. doi: 10.1002/hep4.1556
25. Théry C, Witwer KW, Aikawa E, Alcaraz MJ, Anderson JD, Andriantsitohaina R, et al. Minimal Information for Studies of Extracellular Vesicles 2018 (MISEV2018): A Position Statement of the International Society for Extracellular Vesicles and Update of the MISEV2014 Guidelines. *J Extracell Vesicles* (2018) 7. doi: 10.1080/20013078.2018.1535750
26. Arroyo V, Moreau R, Kamath PS, Jalan R, Ginès P, Nevens F, et al. Acute-on-Chronic Liver Failure in Cirrhosis. *Nat Rev Dis Prim* (2016) 2:1–18. doi: 10.1038/nrdp.2016.41
27. Choi ES, Faruque H, Kim JH, Kim KJ, Choi JE, Kim BA, et al. CD5L as an Extracellular Vesicle-Derived Biomarker for Liquid Biopsy of Lung Cancer. *Diagnostics* (2021) 11:1–18. doi: 10.3390/diagnostics11040620
28. Gray J, Chattopadhyay D, Beale GS, Patman GL, Miele L, King BP, et al. A Proteomic Strategy to Identify Novel Serum Biomarkers for Liver Cirrhosis and Hepatocellular Cancer in Individuals With Fatty Liver Disease. *BMC Cancer* (2009) 9:271. doi: 10.1186/1471-2407-9-271
29. Gangadharan B, Antrobus R, Dwek RA, Zitzmann N. Novel Serum Biomarker Candidates for Liver Fibrosis in Hepatitis C Patients. *Clin Chem* (2007) 53:1792–9. doi: 10.1373/clinchem.2007.089144
30. Yamazaki T, Mori M, Arai S, Tateishi R, Abe M, Ban M, et al. Circulating AIM as an Indicator of Liver Damage and Hepatocellular Carcinoma in Humans. *PloS One* (2014) 9:e109123. doi: 10.1371/journal.pone.0109123
31. Sarrias M-R, Roselló S, Sánchez-Barbero F, Sierra JM, Vila J, Yélamos J, et al. A Role for Human Sp Alpha as a Pattern Recognition Receptor. *J Biol Chem* (2005) 280:35391–8. doi: 10.1074/jbc.M505042200
32. Gao X, Yan X, Zhang Q, Yin Y, Cao J. CD5L Contributes to the Pathogenesis of Methicillin-Resistant Staphylococcus Aureus-Induced Pneumonia. *Int Immunopharmacol* (2019) 72:40–7. doi: 10.1016/j.intimp.2019.03.057
33. Sarrias MRR, Padilla O, Monreal Y, Carrascal M, Abian J, Vives J, et al. Biochemical Characterization of Recombinant and Circulating Human Spalpha. *Tissue Antigens* (2004) 63:335–44. doi: 10.1111/j.0001-2815.2004.00193.x
34. Gebe JA, Llewellyn MBC, Hoggatt H, Aruffo A. Molecular Cloning, Genomic Organization and Cell-Binding Characteristics of Mouse Sp? *Immunology* (2000) 99:78–86. doi: 10.1046/j.1365-2567.2000.00903.x
35. Arai S, Maehara N, Iwamura Y, Honda Si, Nakashima K, Kai T, et al. Obesity-Associated Autoantibody Production Requires AIM to Retain the Immunoglobulin M Immune Complex on Follicular Dendritic Cells. *Cell Rep* (2013) 3:1187–98. doi: 10.1016/j.celrep.2013.03.006
36. Maehara N, Arai S, Mori M, Iwamura Y, Kurokawa J, Kai T, et al. Circulating AIM Prevents Hepatocellular Carcinoma Through Complement Activation. *Cell Rep* (2014) 9:61–74. doi: 10.1016/j.celrep.2014.08.058
37. Clària J, Stauber RE, Coenraad MJ, Moreau R, Jalan R, Pavesi M, et al. Systemic Inflammation in Decompensated Cirrhosis: Characterization and Role in Acute-on-Chronic Liver Failure. *Hepatology* (2016) 64:1249–64. doi: 10.1002/hep.28740
38. Joseph SB, Bradley MN, Castrillo A, Bruhn KW, Mak PA, Pei L, et al. LXR-Dependent Gene Expression is Important for Macrophage Survival and the Innate Immune Response. *Cell* (2004) 119:299–309. doi: 10.1016/j.cell.2004.09.032

39. Valledor AF, Hsu L, Ogawa S, Sawka-Verhelle D, Karin M, Glass CK. Activation of Liver X Receptors and Retinoid X Receptors Prevents Bacterial-Induced Macrophage Apoptosis. *Proc Natl Acad Sci USA* (2004) 101:17813–8. doi: 10.1073/pnas.0407749101
40. Glaría E, Letelier NA, Valledor AF. Integrating the Roles of Liver X Receptors in Inflammation and Infection: Mechanisms and Outcomes. *Curr Opin Pharmacol* (2020) 53:55–65. doi: 10.1016/j.coph.2020.05.001
41. Dalli J, Serhan CN. Pro-Resolving Mediators in Regulating and Conferring Macrophage Function. *Front Immunol* (2017) 8:1400. doi: 10.3389/fimmu.2017.01400

Conflict of Interest: A patent protecting monoclonal antibodies used herein for ELISA studies has been submitted to the European Patent Office.

Publisher's Note: All claims expressed in this article are solely those of the authors and do not necessarily represent those of their affiliated organizations, or those of the publisher, the editors and the reviewers. Any product that may be evaluated in this article, or claim that may be made by its manufacturer, is not guaranteed or endorsed by the publisher.

frontiers in Immunology

REVIEW
published: 16 March 2022
doi: 10.3389/fimmu.2022.846091

Glucocorticoid Treatment Strategies in Liver Failure

Chao Ye[1], *Wenyuan Li*[2]*, *Lei Li*[2] *and Kaiguang Zhang*[1]

[1] *Department of Gastroenterology, The First Affiliated Hospital of University of Science and Technology of China (USTC), Division of Life Sciences and Medicine, University of Science and Technology of China, Hefei, China,* [2] *Department of Infectious Diseases, The First Affiliated Hospital of University of Science and Technology of China (USTC), Division of Life Sciences and Medicine, University of Science and Technology of China, Hefei, China*

Liver failure is characterized by serious liver decompensation and high mortality. The activation of systemic immune responses and systemic inflammation are widely accepted as the core pathogenesis of liver failure. Glucocorticoids (GCs) are most regularly utilized to suppress excessive inflammatory reactions and immunological responses. GCs have been used in the clinical treatment of liver failure for nearly 60 years. While there has been no unanimity on the feasibility and application of GC treatment in liver failure until recently. The most recent trials have produced conflicting results when it comes to the dose and time for GC therapy of different etiology of liver failure. Our review outlines the issues and options in managing GC treatment in liver failure based on an investigation of the molecular mechanism that GC may give in the treatment.

Keywords: liver failure, glucocorticoids (GCs), inflammation suppression, immunosuppression, strategies

OPEN ACCESS

Edited by:
Yu Shi,
Zhejiang University, China

Reviewed by:
Su Lin,
First Affiliated Hospital of Fujian Medical University, China
Sukriti Baweja,
The Institution of Liver and Biliary Sciences (ILBS), India
Francesca M. Trovato,
King's College Hospital NHS Foundation Trust, United Kingdom

***Correspondence:**
Wenyuan Li
liwenyuan@ustc.edu.cn

Specialty section:
This article was submitted to Inflammation, a section of the journal Frontiers in Immunology

Received: *30 December 2021*
Accepted: *23 February 2022*
Published: *16 March 2022*

Citation:
Ye C, Li W, Li L and Zhang K (2022) Glucocorticoid Treatment Strategies in Liver Failure. Front. Immunol. 13:846091. doi: 10.3389/fimmu.2022.846091

1 INTRODUCTION

Liver failure (LF) is a life-threatening syndrome defined as the acute decompensation of liver function with varied etiology and multiple organ dysfunctions (1, 2). In China, viral hepatitis is the leading cause of liver failure, followed by alcohol and toxic drugs. Hepatitis B virus (HBV) related acute-on-chronic liver failure (ACLF) is the most common type of end-stage liver disease in chronic HBV infection patients, characterized by rapid deterioration, with muti-organ failure and high short-term mortality (3). At present, there is still no specific treatment of LF. Currently treatment is mostly based on comprehensive medical care, artificial liver support systems (ALSSs), and liver transplantation (LT). LT is an effective therapy even in patients at advanced stages, nevertheless, LT is limited by the availability of donor organs and the high medical cost, the mortality rate of LF remains high (4, 5).

Activation of immune response and systemic inflammation are considered as the key role of LF, glucocorticoids (GCs) have been used in the clinical treatment of LF for many years with the function that can rapidly suppress excessive inflammatory reactions and immune response. However, their usage has been contentious. For over half a century, there are numerous studies have been published (6–9). Although some clinical and experimental research are currently being conducted to determine the efficacy of GC treatment of LF, countries and organizations have yet to reach a consensus (10–15).

This study covers advances on the mechanism, value, existing difficulties, and application tactics of GC application in different etiology LF to identify ideas for further research in related domains and to provide assistance for the clinical management of LF.

2 THE MECHANISM OF GC TREATMENT IN LIVER FAILURE

2.1 The Core Pathogenesis of Liver Failure

Liver acts as an immune organ and plays a key role in innate immune defenses against pathogens (16–18). LF has the features of systemic inflammation, cellular immune depression, and progression to multiple organ dysfunction. Activation of systemic immune responses should be considered playing a significant role in the pathogenesis and prognosis of LF (19, 20). Cytokines also play a pivotal role in LF pathophysiology including hepatocellular death, extrahepatic complications, and hepatocyte regeneration. And cytokines mediated liver injuries are tightly associated with hepatocyte proliferation and regeneration (21, 22). Suppressor of cytokine signaling (SOCS) family, signal transducer and activator of transcription (STAT) and nuclear factor kB (NF-kB)-mediated pathways have been shown closely linked with liver injury (23, 24).

Patients with ALF and ACLF display evidence of a pro-inflammatory state with local liver inflammation, features of systemic inflammatory response syndrome (SIRS) and vascular endothelial dysfunction that drive progression to multi-organ failure (25). The sooner SIRS emerges, the worse the prognosis (26). "Endotoxin-macrophage-cytokine storm" is the core pathogenesis of liver failure (27). The immunological balance is disrupted in the latter stages of liver failure, resulting in "immune paralysis" and a reduction in the total number and activity of peripheral blood lymphocytes, both of which aided in the progression and exacerbation of LF (28–30).

The "first hit" in the "three hits hypothesis" is the initial immunological insult to the liver produced by viruses, medications, and other factors, which immediately leads to the degeneration and necrosis of hepatocytes. The loss of hepatic sinusoids, microvascular embolism, and microcirculation disturbances result in ischemia and hypoxia of liver tissue, as well as additional reperfusion damage, resulting in the "second hit". The liver's detoxifying and endotoxin-scavenging abilities were reduced by the first two strikes, resulting in intestinal endotoxin-induced endotoxemia, which released a significant number of inflammatory factors such as IL-6 and tumor necrosis factor α (TNF-α), culminating in the "third hit" (31–33). GCs can impede macrophage phagocytosis and antigen treatment, as well as reduce the generation of inflammatory cytokines, since they are the most often utilized anti-inflammatory and immunosuppressive medicines. As a result, there is a theoretical foundation for using GCs to treat liver failure.

2.2 Immune Response Inhibition and Anti-Inflammatory Mechanisms of GCs

GCs can swiftly suppress excessive immune response and inflammatory reaction. In addition to inhibiting cytotoxic liver damage, GC intervention in LF can also control humoral immunity. GCs can influence the fraction of CD4+ lymphocyte subsets that are distributed, raise the proportion of Treg cells, and boost the immunomodulatory activity of Treg cells, all of which contribute to increased negative inflammatory control (34). Furthermore, GCs can directly decrease CD8+ cell immunological activity and diminish cytotoxicity. ICAM-1 (intercellularcelladhesionmolecule-1, ICAM-1) is a part of the immunoglobulin superfamily which found on the cell membrane of hepatocytes and many other cells. ICAM-1-mediated cell adhesion is critical for cytotoxic T lymphocyte (CTL) attachment to hepatocytes and can improve CTL assault on target cells. At the receptor level, GCs can block the production of ICAM-1, effectively preventing CD8+ lymphocytes from attacking hepatocytes. Furthermore, GCs can minimize the liver tissue damage induced by T/NKT cell infiltration by inhibiting the killing impact of T/NKT cells (35, 36).

GCs can induce apoptosis of inflammatory cells and inhibit antigen presentation as well as the generation and release of proinflammatory cytokines including IL-1, IL-6, TNF-α, and IL-17 (37, 38). GCs can also boost the synthesis of the anti-inflammatory cytokine IL-10 and improve the negative control of inflammatory factor storms at the same time (37). Furthermore, through modulating the immunological signal transduction pathway, GCs can decrease the inflammatory response. Important negative cytokine regulatory factors include suppressor of cytokine signaling 1 (SOCS1), suppressor of cytokine signaling 2 (SOCS2), and interleukin-1 receptor-associated kinase M (IRAK-M) (39). GCs can improve the inhibitory impact of SOCS1 and SOCS2 on the JAK/STAT inflammatory signaling pathway, as well as the inhibitory effect of IRAK-M on the Toll-like receptor 4 (TLR4) inflammatory signaling pathway (40, 41). Nucleotide-binding oligomerisation domain-like receptors (NLRs) Family Pyrin Domain Containing 3 (NLRP3) is related to innate immunity and can produce proinflammatory cytokines *via* caspase-1 (42). NLRP3 has been found increased in HBV-related ACLF patients and downregulated by GCs in surviving patients (43). GCs can also cause lymphocytes to migrate out of blood vessels, reducing the number of lymphocytes in blood vessels. It may also enhance the local microcirculation of the liver, as well as lessen the disturbances of ischemia, hypoxia, and reperfusion of hepatocytes.

2.3 GCs Can Enhance the Protective Effect of Hepatocytes

By inhibiting caspase-8 activation and the mitochondria-dependent apoptosis pathway, dexamethasone (DEX) pretreatment protected hepatocytes from TNF-α, plus actinomycin D (ActD)-induced apoptosis (44). Considering that GCs are thought to have a significant stabilizing impact on cell membranes, they can prevent hepatocyte disintegration and necrosis, slowing the course of liver damage.

3 GC THERAPY IN DIFFERENT ETIOLOGY OF LIVER FAILURE

3.1 HBV Related ACLF

According to the evidence shows that HBV mainly causes liver damage through cytotoxic T-lymphocyte-mediated cytolytic

pathways in HBV-infected hepatocytes (45, 46), using GCs to treat severe hepatitis B infections is appropriate because of the particular effects of GCs to inhibit immune responses and prevent cytolysis in infecting hepatocytes (47). Multiple studies suggest that using GCs in the early period of severe hepatitis can help prevent liver cells necrosis and afford a possibility of liver regeneration (48–50) but might enhance HBV replication (51), and lead to LF (12, 52–54). Thus, GCs have not been widely used for the treatment of severe hepatitis B in clinic. However, in recent years, due to the new generation of nucleoside analogs (NA), using GCs to treat HBV related LF has become much safer (55–57).

Excessive systemic inflammation and susceptibility to infection are two pathophysiological characteristics of ACLF. Immunotherapies, such as glucocorticoids are effective on ACLF. Some studies have reported that GC treatment improve the survival rate of the patients with HBV-ACLF. A prospective multi-center clinical trial totally included 171 HBV-ACLF patients, 83 patients treated with methylprednisolone [1.5 mg/kg/day (day 1-3), 1 mg/kg/day (day 4-5), and 0.5 mg/kg/day (day 6-7)] for 7 days, the results showed methylprednisolone treatment can increase the 6-month survival rate of HBV-ACLF patients (27). And there is a retrospective study included 349 patients with HBV-ACLF in 2021. 155 patients used methylprednisolone or prednisone. The results showed that GC treatment could not improve the liver function of ACLF patients but might reduce their 28 days mortality rate (58). Similar results were also demonstrated by Zhao et al (59). No matter the patients used antivirus or not. The explanation for this might be that infectious complications are both the primary cause of ACLF and the leading cause of mortality from ACLF, these patients are susceptible immune paresis (60). Thus even though GC therapy did not improve liver function or short-term health, it may be required in critical patients. Nevertheless, this effect has not been validated by others. A retrospective, controlled trial with 31 HBV-related ACLF patients under dexamethasone injection for three times and followed up for 12 weeks, the results showed that dexamethasone cannot improve liver functions and 12-week survival rates of patients with HBV-related ACLF (61). A Ten-year cohort study in a University Hospital in East China also showed that steroid treatment did not improve transplant free survival in ACLF patients precipitated by hepatitis B (15).

The timing of GCs treatment in HBV-related ACLF is very important. Zhang et al. found that dexamethasone (10 mg/day, i.v.) for 5 days based on lamivudine (LMV) treatment is effective in improving the liver function and survival rate of patients with pre-ACLF (62). Another study included 87 patients with early-stage HBV-related subacute liver failure, 43 patients in the control group received LMV and routine integrated treatment, and those in the treatment group were given additional short-term low-dose glucocorticoid treatment. The results showed that GC treatment can improve survival rate and shorten the mean hospital stay of patients with HBV-related early-stage subacute liver failure patients (63). Thus, GCs should theoretically be able to control excessive systemic inflammation and hepatic inflammation in the early stages of ACLF, whereas they aggravate immune paralysis in the late stages. And another noteworthy issue is that nucleoside analog should be used as a basic treatment in HBV-ACLF patients. Overall, low dose, short term GC treatment combined with NA in the early stage of HBV-ACLF patients is safe and effective.

3.2 HBV Related ALF

Nearly half a century ago, researchers used double-blind, randomized trials of methylprednisolone(38-48mg/day) vs. placebo in severe viral hepatitis and showed the conclusion that methylprednisolone does not enhance survival in patients with severe viral hepatitis (6, 7). In 2006, Kotoh et al. used a high-dose methylprednisolone (1000 mg/day for 3 continuous days) to treat patients with severe acute hepatic failure and found methylprednisolone might effectively prevent the progression of severe acute hepatic failure (64). Fujiwara et al. used 1000 mg of methylprednisolone daily for 3 days followed by the reduced doses according to the treatment response in the early stage of viral acute liver failure, which indicated an effective suppressing of hepatocytes destruction and a slightly higher survival rate (65). And high dose of GCs treated in ALF did not significantly increase the incidence of infection (66). Then *Fujiwara* reported combination therapy with GCs and NA for HBV-ALF induces the rapid resolution of inflammation leading to a rapid recovery of the liver function. When it is administered at a sufficiently early stage, it would have a survival benefit and prevent persistent infection (67). In a whole, when treated in ALF, high dose GCs might be more effective, the early stage of the ascending period would be the best timing, and NA is also very important in HBV related ALF.

3.3 AIH Induced Liver Failure

Autoimmune hepatitis (AIH) is an immune-mediated necroinflammatory disease of the liver parenchyma. Although AIH is linked with minor symptoms in most patients, it can also be associated with severe symptoms and develop to ALF, or ACLF. Acute severe autoimmune hepatitis (AS-AIH) is a relatively rare cause of ALF, which is often neglected and delayed in treatment. The standard paradigm of management in acute AIH involved corticosteroid therapy. This can achieve a remission in more than 80% (68). However, GCs use in AIH-induced LF remains controversial. A single-center French study in 2007 looked at the role of GSs in patients with a severe presentation of AIH. They found that GC therapy is of little benefit in severe and fulminant forms of AIH; It may increase the risk of septic complications and should not delay liver transplantation (LT) (69). A retrospective analysis of patients with autoimmune, indeterminate, and drug-induced ALF included 66 patients with AIH. The study compared 25 patients who were given prednis(ol)one (median dosage 60 mg/day) with 41 patients who were not. GCs did not increase overall or spontaneous (without-LT) survival in autoimmune ALF. Furthermore, GCs use was linked to an increased mortality in the group of patients with the highest MELD scores (70). While there are also researchers suggested GCs should be considered as soon as possible in AS-AIH patients (71). Recently, a

retrospectively study enrolled 32 patients with AIH-induced ALF compared with 93 age- and sex-matched patients with chronic AIH (cAIH), the patients received prednis(ol)one with an average dose of 153.9 mg daily for the first group and from 61.8 mg daily for the second group. GCs therapy was not associated with high mortality or sepsis in AIH-induced ALF and suggested that GCs treatment of AIH-mediated ALF may improve the outcome (72). Another study included 128 AS-AIH patients, 115 (90%) were treated with GCs within a median of 6 (2–10) days of their admission to hospital. Seventy-eight patients (73%) received prednis(ol)one with a dosage of 1 mg/kg/d while 37 (27%) received 0.5 mg/kg/d. Thirteen patients (10%) did not receive GCs therapy, the results showed that non-treated patients were more seriously ill than treated patients (73). Zachou et al. present an open, real-world observational study included 34 AS-AIH patients were treated with either 1g methylprednisolone for 3 consecutive days followed by intravenous prednisolone (1mg/kg/day) or prednisolone (1.5mg/kg/day) from the beginning. And indicated that high-dose intravenous GCs in original AS-AIH seems safe and efficient as it prevents disease deterioration and the need of liver transplantation (74). A recent Asian-Pacific study included 82 patients with AIH induced ACLF. A survival benefit was demonstrated in those who received GCs. Moreover, patients with high MELD scores and encephalopathy had unfavorable responses to GCs (75). In general, GC treatment is effective in both ALF and ACLF induced by AIH. High doses are also relatively safe. GCs should be used as early as possible, with an increased risk if MELD score is very high or encephalopathy present.

3.4 Drug Induced Liver Failure

Drug-induced liver injury (DILI) is a liver toxicity induced by drugs or their metabolites. Patients with DILI may present with various clinical manifestations, ranging from abnormal liver function test results but without symptoms to ALF (76). For drug-induced ALF, there are two primary therapeutic options: a) fast depuration of the body from the toxic chemical to prevent additional aggressiveness before the agent reaches the liver; and b) administration of an antidote to prevent and/or stop the aggression once the toxin reaches the liver. The newest EASL clinical practice guidelines suggested that GCs are usually given when all else fails to produce results (77). In early trials, GC therapy for all kinds of ALF demonstrated limited benefits (70, 78). A single-centre retrospective study used two kinds of GCs administration methods (Methylprednisolone, range 60-120 mg/day or prednisone, range 40-60 mg/day for 3-5 days and then prednisone 20 mg/day and 5-10 mg weekly reduction) or (Methylprednisolone, range 60-120 mg/day for 3-5days) to treat severe drug-induced liver injury (DILI) patients. The results showed that short-term use of GCs can improve the liver injury and patient survival of severe DILI patients with hyperbilirubinemia (TBil >243 μmol/L) (79). GCs combined with ursodesoxycholic acid appears to be safe, and leads to a more rapid reduction in bilirubin and transaminases after severe DILI (80). However, opposite result was found by Wan et al. that prednisone was not beneficial for the treatment of severe DILI (81). Heretofore, among the several liver diseases, AIH is the most reliable clinical indication for GC treatment (82). In patients with suspected drug induced AIH who are receiving GCs therapy, withdrawal of treatment once the liver injury has resolved should be followed by careful monitoring (83). Antiepileptic drug-induced liver injury is commonly related with hypersensitivity symptoms and may respond to GCs treatment (84). GCs should be administered in patients with severe alcoholic hepatitis (AH) if there are no contraindications (85). Overall, drug-induced liver failure needs evidence of immunopathogenicity to restore the condition through GCs blocking immune responses.

4 THE APPLICATION STRATEGY OF GC TREATMENT IN LIVER FAILURE

4.1 The Dose and Timing of GC Treatment in Liver Failure

There is currently no consensus on the type and dosage of GCs used in LF. GC dose is generally controlled in methylprednisolone (1∼2mg/kg/d) according to current clinical studies. Kotoh et al. investigated the possibility of using high dose of GCs to treat LF. 17 ALF patients underwent three days treatment of 1000mg methylprednisolone daily, and 13 of them were cured without serious complications, two died, and two received LT (64). The relevance of high-dose GCs in the treatment of severe acute exacerbation of CHB and the early stage of ALF was explored by other researchers. They indicated a slim advantage in terms of survival and liver regeneration in the GC treated group, but there was no significant difference, whereas patients with a poor basic condition and advanced liver damage at the start of treatment had a poor prognosis (50, 65). It will not function if a high dose of GCs are given during LF due to a decrease in the number of GC receptors on the surface of cells in the liver tissue, and there may also be an increase in the likelihood of GC adverse effects because GCs have the potential to cause substantial liver damage (65, 86, 87). As a result, high-dose GCs are more usually used in ALF patients compared to ACLF patients. And not indicated for individuals particularly with poor basic condition. Low and medium doses are generally used. Currently, some researchers utilize 10 mg dexamethasone once a day for three days to treat patients with HBV-related ACLF. The results revealed that early in the course of a severe acute exacerbation of chronic hepatitis B, combined with standard treatment, low-dose, short-term glucocorticoid treatment dramatically decreased the probability of progression to liver failure and shortened hospitalization time, without raising the complication rate (88). Low doses of GCs primarily depress cellular immunity, but high doses of GCs lower humoral immunity by suppressing B cells and antibody generation (89). However, there are certain variances in the dosage of GC used for various reasons. Prednisone 40 mg/d, according to some research, can be taken early in alcohol induced LF (90). When AIH is induced to LF, an initial dose of 20-50 mg/d methylprednisolone is used to provide a stronger curative effect (91). Some studies employed 1.5 mg/kg/d as the beginning dose for CHB-related LF and eventually reached excellent outcomes after progressively lowering the dose according to the disease (92).

When the effectiveness of GC treatment cannot be established in a clinical setting, the concept of safety requires that any potential adverse effects of GCs be maintained within a manageable range. GCs can considerably lower the number of lymphocytes in circulation by inhibiting the presence of phagocytic cells to the antigen, promoting the destruction and disintegration of lymphocytes, and developing the removal of lymphocytes from blood vessels (93). Even though that GCs can raise the risk of infection and upper gastrointestinal bleeding, as well as other complications, their adverse effects are manageable. As a result, it is critical to screen for and monitor adverse effects in individuals with liver failure who are taking GCs.

GC intervention in the early stages of LF has been demonstrated in several studies to improve prognosis and minimize death (63). Zhao et al. believed that GCs should be utilized when the MELD score is less than 35, the HE score is less than 4, and the ALT level is ≥ 30 ULN (14). When the MELD score is less than 27 and hepatic encephalopathy is less than stage II in AIH-related LF, the benefit of GCs is greatest (94). However, until recently, there were no clear quantitative indicators for GC therapy in LF, we believe that the age, basic conditions, and complications of the patients should all be considered. As a result, more clinical experience should be very important for doctors.

4.2 Problems of GCs Application in Liver Failure

4.2.1 GC Resistance

Some ACLF patients have a low sensitivity to GCs treatment (95). GCs *via* binding to their intracellular receptor (GR) to have powerful anti-inflammatory activities. Decreased GR in many inflammatory diseases confers GC resistance (GCR) and undermines glucocorticoid therapy efficacy. GCR is clearly acquired through persistent inflammatory injury (96–98). Tjandra et al. reported a significant decrease in hepatic T lymphocyte GR mRNA and protein levels in experimental cholangitis rats, demonstrating that hepatic T cell resistance to increased cortisol levels is at least partially mediated by decreased GR expression (99). In AIH patients, GR expression in peripheral mononuclear cells was shown to be closely related with GCR and to impact the outcome of therapy and the degree of disease severity (100, 101). Moreover, there is a dynamic process in the immune state of LF. It is reported that inactivation of functional T cells is a key step in the progression of systemic immunological dysfunction in ALF (102). And proinflammatory cytokines are involved in the pathogenesis of ALF (103). Further studies reported that the serum cortisol level and the percentage of GR+T lymphocytes were significantly decreased in HBV-ACLF patients compared with CHB patients and healthy controls. The relative GR alpha mRNA expression was significant decreased in ACLF patients (95). Recently, Wang et al. noted that in ACLF patients, GR alpha expression was negatively regulated by miR-124a. MicroRNA-124a contributes to GCR in ACLF by negatively regulating GR alpha (104).

4.2.2 Side Effects of GC Therapy in Liver Failure

The immune system is depressed during GC therapy, which raises the risk of secondary infection and the spread and aggravation of the primary illness, as well as the chance of systemic infection and sepsis (14, 66, 105). According to the CANONIC research of the EASL chronic liver failure (EASL-CLIF) Alliance, almost a third of patients with ACLF will be complicated with bacterial infection. Similarly, the EASL-CLIF and the North American Federation of End-stage Liver Diseases (NACSELD) have discovered that some individuals with liver cirrhosis develop ACLF due to coinfection (106, 107). When LF strikes, the intestinal barrier weakens and microecological changes occur, allowing intestinal flora to migrate and endotoxin to enter the bloodstream, resulting in infection (108). At the same time, microorganisms increase the risk of infection after avoiding the immune system and entering the circulation owing to immune escape and immunological paralysis during LF (109). Furthermore, genetic variables have a role in raising the likelihood of coinfection in LF patients (110, 111).

Sepsis is a common complication of ACLF (112), GCs have been tested and widely used in sepsis patients (113). Although it is an acute systemic inflammatory disease, GCs are hardly useful in sepsis (114). One reason to explain the rather poor successes of GCs in sepsis is that a profound GCR has developed. GCR has already developed by the time sepsis are diagnosed and treated. Many researchers have described GCR in cohorts of sepsis patients. Levels of GR mRNA in peripheral mononuclear cells (PBMCs) were found reduced in sepsis children (115). And Dekelbab et al. reported reduced GR protein levels in some organs (such as liver, brain, muscle) during sepsis (116). An increased expression of miR124 was associated with reduced GR expression in T cells of sepsis patients was also reported (117). Furthermore, Guerrero et al. found a temporary increase of the dominant negative GR beta in PBMCs during sepsis (118). Sepsis is associated with GCR significantly, which might be due to a decrease in GR expression or response.

GCs can also suppress gastric mucus secretion while increasing stomach acid and pepsin secretion, resulting in ulcers, perforations, and gastrointestinal (GI) bleeding. As LF is associated with a high risk of severe GI bleeding, using GCs in LF will significantly increase the risk of causes. Although the specific mechanism by which GCs may cause GI bleeding is unknown, GCs may inhibit tissue repair, thus causing delayed wound healing (119). Furthermore, aberrant blood pressure may emerge because of the pharmacological properties of GCs, as well as electrolyte and blood glucose abnormalities, potentially increasing the risk of hepatic encephalopathy, hepatorenal syndrome, and other consequences in LF.

4.3 Strategies of GCs Application in Liver Failure

Secondary infection is one of the most serious concerns associated with the use of GCs in LF, posing a secondary threat to the prognosis. Antibiotic prophylaxis can avoid LF consequences including peritonitis and upper gastrointestinal bleeding (120). Currently, it is generally recommended to choose quinolones for prophylactic anti-infective treatment (121). Simultaneously, by increasing gut flora, stimulating

TABLE 1 | GC treatment in different etiology of liver failure.

Reference	Year	Nation	Etiology	Type/ Stage	Numbers of patients (total/GC treatment)	Intervention	Duration of therapy	Outcome
Gregory et al. (6)	1976	USA	HBV	ALF	29/14	Methylprednisolone (32–40 mg/day)	2 weeks	Do not improve prognosis
Greenber et al. (7)	1981	USA	HBV	ALF	16/8	Methylprednisolone (48 mg/day)	4 weeks	Do not improve prognosis
Ware et al. (8)	1981	USA	HBV	PLF	77/37	Prednisone (40 mg/day)	1 week	Do not improve prognosis and liver function
Rakela et al. (9)	1991	USA and Canada	Drug/hepatitis virus(A/B)	ALF	64/46	Hydrocortisone (400-800 mg/day)	Within 38 months	Do not improve prognosis
Kotoh et al. (64)	2006	Japan	HBV	ALF	34/17	Methylprednisolone (1000mg/day)	3 days	Prevent the ALF progression
Ichai et al. (69)	2007	France	AIH	ALF	16/8	Prednisone (1 mg/kg/d)	median of 2.5 days	Little benefit in severe and fulminant forms of AIH
Fujiwara et al. (50)	2010	Japan	HBV	ALF	10/10	Methylprednisolone (1000mg/day) or Prednisone (40-60 mg/day)	21-183 days	Required in the early stage
Zhang et al. (62)	2011	China	HBV	PLF	170/56	Dexamethasone (10 mg/day)	5 days	Improve prognosis and liver function
Wree et al. (80)	2011	UK	Drug	ALF	15/6	Prednisone (low dose)	3 days	Improve liver function (combined with ursodesoxycholic acid)
Zhao et al. (59)	2012	China	HBV	ACLF	56/30	Methylprednisolone (80 mg/day)	3 days	Improve prognosis
Karkhanis et al. (70)	2014	USA	HBV	ALF	361/62	Prednisone (40-60mg/d)	24-32.5 days	Do not improve prognosis
Zhu et al. (91)	2014	China	AIH	LF	22/7	Prednisolone (20-50 mg/d)	16-105 days	Improve prognosis
Fujiwara et al. (65)	2014	Japan	HBV	ALF	31/9	Methylprednisolone (1000mg/d)	3 days	Improved prognosis and liver regeneration
Chen et al. (61)	2014	China	HBV	ACLF	134/31	Dexamethasone (10 mg/d/person)	3 days	Do not improve prognosis and liver function
Zhao et al. (14)	2016	China	HBV	ALF SALF	73/34 165/21	Dexamethasone (5-30mg/d)	1-10 days	Improve prognosis
Yasui et al. (66)	2016	Japan	HBV	ALF	110/78	methylprednisolone (1,000 mg/d)	3 days	Do not increase the incidence of infection
Hu et al. (79)	2016	China	Drug	ALF	203/53	Methylprednisolone(60-120mg/d) or prednisolone (40-60mg/d)	3-5 days	Improve prognosis
Fujiwara et al. (67)	2018	Japan	HBV	ALF	19/14	Methylprednisolone (1,000 mg/d) or prednisolone (60 mg/d)	according to the response	Improve liver function (Combined with nucleoside analogs)
Anastasiou et al. (72)	2018	Germany	AIH	ALF	125/32	prednisone or prednisolone (60-500mg/d)	Not mention	Improve prognosis
Huang et al. (15)	2019	China	HBV	ACLF	293/162	Prednisone (1mg/kg) or methylprednisolone or dexamethasone	within 1 week	Do not improve prognosis (transplant free patients)
Zachou et al. (74)	2019	Greece	AIH	ALF	184/34	Prednisolone(1000mg/d)	3 days	Safe and efficient
Wan et al. (81)	2019	China	Drug	ALF	90/66	Prednisone (median 40mg/d)	7-86 days (median 21.5days)	Safe but not beneficial
Jia et al. (27)	2020	China	HBV	ACLF	171/83	methylprednisolone (1.5 mg/kg/day [day 1–3], 1 mg/kg/day [day 4–5], and 0.5 mg/kg/day [day 6–7])	7 days	Improve prognosis
Wu et al. (88)	2021	China	HBV	PLF	125/62	Dexamethasone (10mg/day)	3 days	Reduce the risk of progression
Xu et al. (58)	2021	China	HBV	ACLF	349/155	Methylprednisolone or Prednisone	28 days	Do not improve liver function, but improve prognosis

ALF, acute liver failure; PLF, preliver failure; ACLF, acute-on-chronic liver failure; LF, liver failure; SALF, sub-acute liver fail.

gastrointestinal peristalsis, managing autoimmunity, and strengthening nursing care, we can lower the chance of infection (122–124). Opportunistic fungal infections have emerged as a major cause of morbidity and mortality in immunocompromised patients including those who have received GC treatment (125). Although some studies have found that the prognosis of ACLF patients with fungal infection does not improve after active antifungal therapy, since all survivors have received antifungal therapy, it is still recommended to begin antifungal therapy as soon as possible in the early detection of fungal infection (126).

GI bleeding is common in LF patients, especially in ACLF patients with esophageal varices. The current GI bleeding in ALF patients is 1.5% (127). Patients who were taking high-dose glucocorticoids alone had a slight increased relative risk for developing GI bleeding (128). Pharmacologic suppression of stomach acid secretion has been proven to prevent GI bleeding (129, 130). Proton pump inhibitors (PPIs) are effective method to prevent peptic ulcer disease and GI bleeding in ALF (131). It is reported that in drug-induced liver injury, a PPI might be useful to prevent GI bleeding when GCs used (132). A study of HBV-related LF showed that GC therapy accompanied by prophylactic medication with PPI can prevent the severe side effects of GI bleeding of GC therapy (92). As a result, while using GCs in LF patients, more attention must be taken, and the stomach mucosa should be actively preserved to avoid GI bleeding.

Because of the immunosuppression caused by using GCs, LF patients with basic viral hepatitis may activate the virus. HBsAg positive LF patients should start antiviral therapy as soon as possible to inhibit virus replication. GCs can cause feelings of euphoria, excitation, sleeplessness, and even severe mental problems including hallucinations and insanity. It should be given special attention to patients' mental states. Medication should be discontinued as soon as significant mental problems are discovered. Patients taking GCs for a long time will develop osteoporosis, timely calcium supplement will be useful. Since the proposal of GCs in the treatment of LF has been controversial, its strong immunosuppressive effect and significant efficacy not only bring great temptation to us but also make us face the risk of serious adverse reactions.

5 CONCLUSIONS

Although the notion of administering GCs to treat LF has circulated for a long time, no conclusive evidence has been provided of its therapeutic efficacy. Some data was from non-randomized studies or carried out in small groups (62, 64, 67). Here, we summarized several published articles referred GC treatment in different status of LF in **Table 1**.

Given all of that, due to the intricate pathophysiology of LF, it is critical to investigate immunological manifestations with various etiologies. In the treatment of LF, we should personalize each patient's treatment plan, prioritize patient safety, monitor, and avoid any adverse responses to GCs in a timely manner, all of which will help patients obtain more benefit and improve their prognosis. To provide clinical professionals with a suitable treatment plan based on evidence-based medicine, further larger randomized clinical trials are required.

AUTHOR CONTRIBUTIONS

CY wrote this manuscript, WL designed this manuscript, LL and KZ provided literatures review. All authors contributed to the article and approved the submitted version.

FUNDING

Provincial natural science foundation of Anhui (1908085QH331).

REFERENCES

1. Xue R, Duan Z, Liu H, Chen L, Yu H, Ren M, et al. A Novel Dynamic Model for Predicting Outcome in Patients With Hepatitis B Virus Related Acute-on-Chronic Liver Failure. *Oncotarget* (2017) 8:108970–80. doi: 10.18632/oncotarget.22447
2. Singh T, Gupta N, Alkhouri N, Carey WD, Hanouneh IA. A Guide to Managing Acute Liver Failure. *Cleve Clin J Med* (2016) 83:453–62. doi: 10.3949/ccjm.83a.15101
3. Zhao RH, Shi Y, Zhao H, Wu W, Sheng JF. Acute-On-Chronic Liver Failure in Chronic Hepatitis B: An Update. *Expert Rev Gastroenterol Hepatol* (2018) 12:341–50. doi: 10.1080/17474124.2018.1426459
4. Asrani SK, Simonetto DA, Kamath PS. Acute-On-Chronic Liver Failure. *Clin Gastroenterol Hepatol* (2015) 13:2128–39. doi: 10.1016/j.cgh.2015.07.008
5. Singanayagam A, Bernal W. Update on Acute Liver Failure. *Curr Opin Crit Care* (2015) 21:134–41. doi: 10.1097/MCC.0000000000000187
6. Gregory PB, Knauer CM, Kempson RL, Miller R. Steroid Therapy in Severe Viral Hepatitis. A Double-Blind, Randomized Trial of Methyl-Prednisolone Versus Placebo. *New Engl J Med* (1976) 294:681–7. doi: 10.1056/NEJM197603252941301
7. Greenberg HB, Robinson WS, Knauer CM, Gregory PB. Hepatitis B Viral Markers in Severe Viral Hepatitis: Influence of Steroid Therapy. *Hepatol (Baltimore Md)* (1981) 1:54–7. doi: 10.1002/hep.1840010109
8. Ware AJ, Cuthbert JA, Shorey J, Gurian LE, Eigenbrodt EH, Combes B. A Prospective Trial of Steroid Therapy in Severe Viral Hepatitis. The Prognostic Significance of Bridging Necrosis. *Gastroenterology* (1981) 80:219–24. doi: 10.1016/0016-5085(81)90707-1
9. Rakela J, Mosley JW, Edwards VM, Govindarajan S, Alpert E. A Double-Blinded, Randomized Trial of Hydrocortisone in Acute Hepatic Failure. The Acute Hepatic Failure Study Group. *Digestive Dis Sci* (1991) 36:1223–8. doi: 10.1007/bf01307513
10. Wang F, Wang BY. Corticosteroids or non-Corticosteroids: A Fresh Perspective on Alcoholic Hepatitis Treatment. *Hepatobiliary Pancreat Dis Int* (2011) 10:458–64. doi: 10.1016/s1499-3872(11)60079-9
11. Yeoman AD, Westbrook RH, Zen Y, Bernal W, Al-Chalabi T, Wendon JA, et al. Prognosis of Acute Severe Autoimmune Hepatitis (AS-AIH): The Role of Corticosteroids in Modifying Outcome. *J Hepatol* (2014) 61:876–82. doi: 10.1016/j.jhep.2014.05.021
12. Yang CH, Wu TS, Chiu CT. Chronic Hepatitis B Reactivation: A Word of Caution Regarding the Use of Systemic Glucocorticosteroid Therapy. *Br J Dermatol* (2007) 157:587–90. doi: 10.1111/j.1365-2133.2007.08058.x
13. Ramachandran J, Sajith KG, Pal S, Rasak JV, Prakash JA, Ramakrishna B. Clinicopathological Profile and Management of Severe Autoimmune Hepatitis. *Trop Gastroenterol* (2014) 35:25–31. doi: 10.7869/tg.160

14. Zhao B, Zhang HY, Xie GJ, Liu HM, Chen Q, Li RF, et al. Evaluation of the Efficacy of Steroid Therapy on Acute Liver Failure. *Exp Ther Med* (2016) 12:3121–9. doi: 10.3892/etm.2016.3720
15. Huang C, Yu KK, Zheng JM, Li N. Steroid Treatment in Patients With Acute-on-Chronic Liver Failure Precipitated by Hepatitis B: A 10-Year Cohort Study in a University Hospital in East China. *J Dig Dis* (2019) 20:38–44. doi: 10.1111/1751-2980.12691
16. Gao B, Jeong WI, Tian Z. Liver: An Organ With Predominant Innate Immunity. *Hepatol (Baltimore Md)* (2008) 47:729–36. doi: 10.1002/hep.22034
17. Racanelli V, Rehermann B. The Liver as an Immunological Organ. *Hepatol (Baltimore Md)* (2006) 43:S54–62. doi: 10.1002/hep.21060
18. Crispe IN. The Liver as a Lymphoid Organ. *Annu Rev Immunol* (2009) 27:147–63. doi: 10.1146/annurev.immunol.021908.132629
19. Rolando N, Wade J, Davalos M, Wendon J, Philpott-Howard J, Williams R. The Systemic Inflammatory Response Syndrome in Acute Liver Failure. *Hepatol (Baltimore Md)* (2000) 32:734–9. doi: 10.1053/jhep.2000.17687
20. Wasmuth HE, Kunz D, Yagmur E, Timmer-Stranghoner A, Vidacek D, Siewert E, et al. Patients With Acute on Chronic Liver Failure Display "Sepsis-Like" Immune Paralysis. *J Hepatol* (2005) 42:195–201. doi: 10.1016/j.jhep.2004.10.019
21. Liu Q. Role of Cytokines in the Pathophysiology of Acute-on-Chronic Liver Failure. *Blood Purif* (2009) 28:331–41. doi: 10.1159/000232940
22. Li J, Zhu X, Liu F, Cai P, Sanders C, Lee WM, et al. Cytokine and Autoantibody Patterns in Acute Liver Failure. *J Immunotoxicol* (2010) 7:157–64. doi: 10.3109/15476910903501748
23. Yoshimura A, Naka T, Kubo M. SOCS Proteins, Cytokine Signalling and Immune Regulation. *Nat Rev Immunol* (2007) 7:454–65. doi: 10.1038/nri2093
24. Hong F, Jaruga B, Kim WH, Radaeva S, El-Assal ON, Tian Z, et al. Opposing Roles of STAT1 and STAT3 in T Cell-Mediated Hepatitis: Regulation by SOCS. *J Clin Invest* (2002) 110:1503–13. doi: 10.1172/JCI15841
25. Triantafyllou E, Woollard KJ, McPhail MJW, Antoniades CG, Possamai LA. The Role of Monocytes and Macrophages in Acute and Acute-On-Chronic Liver Failure. *Front Immunol* (2018) 9:2948. doi: 10.3389/fimmu.2018.02948
26. Jalan R, Gines P, Olson JC, Mookerjee RP, Moreau R, Garcia-Tsao G, et al. Acute-On Chronic Liver Failure. *J Hepatol* (2012) 57:1336–48. doi: 10.1016/j.jhep.2012.06.026
27. Jia L, Xue R, Zhu Y, Zhao J, Li J, He WP, et al. The Efficacy and Safety of Methylprednisolone in Hepatitis B Virus-Related Acute-on-Chronic Liver Failure: A Prospective Multi-Center Clinical Trial. *BMC Med* (2020) 18:383. doi: 10.1186/s12916-020-01814-4
28. Chen P, Wang YY, Chen C, Guan J, Zhu HH, Chen Z. The Immunological Roles in Acute-on-Chronic Liver Failure: An Update. *Hepatobiliary Pancreat Dis Int* (2019) 18:403–11. doi: 10.1016/j.hbpd.2019.07.003
29. Takeuchi O, Akira S. Pattern Recognition Receptors and Inflammation. *Cell* (2010) 140:805–20. doi: 10.1016/j.cell.2010.01.022
30. Dong X, Gong Y, Zeng H, Hao Y, Wang X, Hou J, et al. Imbalance Between Circulating CD4+ Regulatory T and Conventional T Lymphocytes in Patients With HBV-Related Acute-on-Chronic Liver Failure. *Liver International* (2013) 33:1517–26. doi: 10.1111/liv.12248
31. Ambrosino G, Naso A, Cillo U, Basso S, Feltracco P, Carraro P, et al. CYTOCHINES AND LIVER FAILURE: MODIFICATION OF TNF-A AND IL-6 IN PATIENTS WITH ACUTE ON CHRONIC LIVER DECOMPENSATION TRETED WITH MOLECULAR ADSORBENT RECYCLING SYSTEM (MARS). *Transplantation* (2004) 78:739. doi: 10.1097/00007890-200407271-02040
32. Malhi H, Gores GJ. Cellular and Molecular Mechanisms of Liver Injury. *Gastroenterology* (2008) 134:1641–54. doi: 10.1053/j.gastro.2008.03.002
33. Zhang Z, Zou ZS, Fu JL, Cai L, Jin L, Liu YJ, et al. Severe Dendritic Cell Perturbation Is Actively Involved in the Pathogenesis of Acute-on-Chronic Hepatitis B Liver Failure. *J Hepatol* (2008) 49:396–406. doi: 10.1016/j.jhep.2008.05.017
34. Kim EJ, Lee JG, Kim JY, Song SH, Joo DJ, Huh KH, et al. Enhanced Immune-Modulatory Effects of Thalidomide and Dexamethasone Co-Treatment on T Cell Subsets. *Immunology* (2017) 152:628–37. doi: 10.1111/imm.12804
35. Dejager L, Vandevyver S, Petta I, Libert C. Dominance of the Strongest: Inflammatory Cytokines Versus Glucocorticoids. *Cytokine Growth Factor Rev* (2014) 25:21–33. doi: 10.1016/j.cytogfr.2013.12.006
36. Kwon HJ, Won YS, Park O, Feng D, Gao B. Opposing Effects of Prednisolone Treatment on T/NKT Cell- and Hepatotoxin-Mediated Hepatitis in Mice. *Hepatol (Baltimore Md)* (2014) 59:1094–106. doi: 10.1002/hep.26748
37. Oakley RH, Cidlowski JA. The Biology of the Glucocorticoid Receptor: New Signaling Mechanisms in Health and Disease. *J Allergy Clin Immunol* (2013) 132:1033–44. doi: 10.1016/j.jaci.2013.09.007
38. Nagy P, Kiss A, Schnur J, Thorgeirsson SS. Dexamethasone Inhibits the Proliferation of Hepatocytes and Oval Cells But Not Bile Duct Cells in Rat Liver. *Hepatol (Baltimore Md)* (1998) 28:423–9. doi: 10.1002/hep.510280220
39. Linossi EM, Babon JJ, Hilton DJ, Nicholson SE. Suppression of Cytokine Signaling: The SOCS Perspective. *Cytokine Growth Factor Rev* (2013) 24:241–8. doi: 10.1016/j.cytogfr.2013.03.005
40. Philip AM, Vijayan MM. Stress-Immune-Growth Interactions: Cortisol Modulates Suppressors of Cytokine Signaling and JAK/STAT Pathway in Rainbow Trout Liver. *PLoS One* (2015) 10:e0129299. doi: 10.1371/journal.pone.0129299
41. Miyata M, Lee JY, Susuki-Miyata S, Wang WY, Xu H, Kai H, et al. Glucocorticoids Suppress Inflammation *via* the Upregulation of Negative Regulator IRAK-M. *Nat Commun* (2015) 6:6062. doi: 10.1038/ncomms7062
42. Wei Q, Mu K, Li T, Zhang Y, Yang Z, Jia X, et al. Deregulation of the NLRP3 Inflammasome in Hepatic Parenchymal Cells During Liver Cancer Progression. *Lab Invest* (2014) 94:52–62. doi: 10.1038/labinvest.2013.126
43. Zhao Q, Wu CS, Fang Y, Qian Y, Wang H, Fan YC, et al. Glucocorticoid Regulates NLRP3 in Acute-On-Chronic Hepatitis B Liver Failure. *Int J Med Sci* (2019) 16:461–9. doi: 10.7150/ijms.30424
44. Oh HY, Namkoong S, Lee SJ, Por E, Kim CK, Billiar TR, et al. Dexamethasone Protects Primary Cultured Hepatocytes From Death Receptor-Mediated Apoptosis by Upregulation of cFLIP. *Cell Death Diff* (2006) 13:512–23. doi: 10.1038/sj.cdd.4401771
45. Chisari FV, Ferrari C. Hepatitis B Virus Immunopathogenesis. *Annu Rev Immunol* (1995) 13:29–60. doi: 10.1146/annurev.iy.13.040195.000333
46. Kondo Y, Kobayashi K, Asabe S, Shiina M, Niitsuma H, Ueno Y, et al. Vigorous Response of Cytotoxic T Lymphocytes Associated With Systemic Activation of CD8 T Lymphocytes in Fulminant Hepatitis B. *Liver International* (2004) 24:561–7. doi: 10.1111/j.1478-3231.2004.0982.x
47. Higuchi N, Kato M, Kotoh K, Kohjima M, Aishima S, Nakamuta M, et al. Methylprednisolone Injection *via* the Portal Vein Suppresses Inflammation in Acute Liver Failure Induced in Rats by Lipopolysaccharide and D-Galactosamine. *Liver International* (2007) 27:1342–8. doi: 10.1111/j.1478-3231.2007.01590.x
48. Czaja AJ, Davis GL, Ludwig J, Taswell HF. Complete Resolution of Inflammatory Activity Following Corticosteroid Treatment of HBsAg-Negative Chronic Active Hepatitis. *Hepatol (Baltimore Md)* (1984) 4:622–7. doi: 10.1002/hep.1840040409
49. Dumortier J, Durupt S, Chevallier M, Trepo C, Zoulim F. Favorable Course of Hepatitis B Virus Reactivation With Hepatocellular Insufficiency by a Treatment Combining Corticoids, Foscarnet and Ganciclovir. *Gastroenterol Clin Biol* (1997) 21:982–6. doi: GCB-12-1997-21-12-0399-8320-101019-ART78
50. Fujiwara K, Yasui S, Okitsu K, Yonemitsu Y, Oda S, Yokosuka O. The Requirement for a Sufficient Period of Corticosteroid Treatment in Combination With Nucleoside Analogue for Severe Acute Exacerbation of Chronic Hepatitis B. *J Gastroenterol* (2010) 45:1255–62. doi: 10.1007/s00535-010-0280-y
51. Schalm SW, Summerskill WH, Gitnick GL, Elveback LR. Contrasting Features and Responses to Treatment of Severe Chronic Active Liver Disease With and Without Hepatitis BS Antigen. *Gut* (1976) 17:781–6. doi: 10.1136/gut.17.10.781
52. Tygstrup N AP, Juhl E. Steroids in Chronic B-Hepatitis. A Randomized, Double-Blind, Multinational Trial on the Effect of Low-Dose, Long-Term Treatment on Survival. A Trial Group of the European Association for the Study of the Liver. *Liver* (1986) 6:227–32. doi: 10.1111/j.1600-0676.1986.tb01070.x
53. Inadomi T, Saito T, Kaneko M, Hashimoto T, Suzuki H. Bullous Pemphigoid in an HB Virus Carrier: Interaction Between Corticosteroids and HB Virus. *J Dermatol* (1997) 24:179–83. doi: 10.1111/j.1346-8138.1997.tb02768.x
54. Zhang B, Wang J, Xu W, Wang L, Ni W. Fatal Reactivation of Occult Hepatitis B Virus Infection After Rituximab and Chemotherapy in

Lymphoma: Necessity of Antiviral Prophylaxis. *Onkologie* (2010) 33:537–9. doi: 10.1159/000319696
55. Shibolet O, Ilan Y, Gillis S, Hubert A, Shouval D, Safadi R. Lamivudine Therapy for Prevention of Immunosuppressive-Induced Hepatitis B Virus Reactivation in Hepatitis B Surface Antigen Carriers. *Blood* (2002) 100:391–6. doi: 10.1182/blood.v100.2.391
56. Lee WC, Wu MJ, Cheng CH, Chen CH, Shu KH, Lian JD. Lamivudine Is Effective for the Treatment of Reactivation of Hepatitis B Virus and Fulminant Hepatic Failure in Renal Transplant Recipients. *Am J Kidney Dis* (2001) 38:1074–81. doi: 10.1053/ajkd.2001.28607
57. Zhang XH, Feng R, Xu LP, Jiang Q, Jiang H, Fu HX, et al. Immunosuppressive Treatment Combined With Nucleoside Analog Is Superior to Nucleoside Analog Only in the Treatment of Severe Thrombocytopenia in Patients With Cirrhosis Associated With Hepatitis B in China: A Multicenter, Observational Study. *Platelets* (2015) 26:672–9. doi: 10.3109/09537104.2014.979339
58. Xu Y, Jiang Y, Li Y. Outcomes of Glucocorticoid Treatment in HBVAssociated Acute-On-Chronic Liver Failure Patients: A Retrospective Observational Study. *Turk J Gastroenterol* (2021) 32:473–80. doi: 10.5152/tjg.2021.20257
59. Zhao J, Zhang JY, Yu HW, He YL, Zhao JJ, Li J, et al. Improved Survival Ratios Correlate With Myeloid Dendritic Cell Restoration in Acute-on-Chronic Liver Failure Patients Receiving Methylprednisolone Therapy. *Cell Mol Immunol* (2012) 9:417–22. doi: 10.1038/cmi.2011.51
60. Bernsmeier C, Singanayagam A, Patel VC, Wendon J, Antoniades CG. Immunotherapy in the Treatment and Prevention of Infection in Acute-on-Chronic Liver Failure. *Immunotherapy* (2015) 7:641–54. doi: 10.2217/imt.15.27
61. Chen JF, Wang KW, Zhang SQ, Lei ZY, Xie JQ, Zhu JY, et al. Dexamethasone in Outcome of Patients With Hepatitis B Virus-Related Acute-on-Chronic Liver Failure. *J Gastroenterol Hepatol* (2014) 29:800–6. doi: 10.1111/jgh.12454
62. Zhang XQ, Jiang L, You JP, Liu YY, Peng J, Zhang HY, et al. Efficacy of Short-Term Dexamethasone Therapy in Acute-on-Chronic Pre-Liver Failure. *Hepatol Res* (2011) 41:46–53. doi: 10.1111/j.1872-034X.2010.00740.x
63. Wu JY, Li M, Zhang H. Effect of Glucocorticoid Treatment on the Clinical Outcome of Patients With Early-Stage Liver Failure. *Nan Fang Yi Ke Da Xue Xue Bao* (2011) 31:554–6.
64. Kotoh K, Enjoji M, Nakamuta M, Yoshimoto T, Kohjima M, Morizono S, et al. Arterial Steroid Injection Therapy Can Inhibit the Progression of Severe Acute Hepatic Failure Toward Fulminant Liver Failure. *World J Gastroenterol* (2006) 12:6678–82. doi: 10.3748/wjg.v12.i41.6678
65. Fujiwara K, Yasui S, Yonemitsu Y, Mikata R, Arai M, Kanda T, et al. Efficacy of High-Dose Corticosteroid in the Early Stage of Viral Acute Liver Failure. *Hepatol Res* (2014) 44:491–501. doi: 10.1111/hepr.12148
66. Yasui S, Fujiwara K, Haga Y, Nakamura M, Mikata R, Arai M, et al. Infectious Complications, Steroid Use and Timing for Emergency Liver Transplantation in Acute Liver Failure: Analysis in a Japanese Center. *J Hepato-Biliary-Pancreatic Sci* (2016) 23:756–62. doi: 10.1002/jhbp.399
67. Fujiwara K, Yasui S, Haga Y, Nakamura M, Yonemitsu Y, Arai M, et al. Early Combination Therapy With Corticosteroid and Nucleoside Analogue Induces Rapid Resolution of Inflammation in Acute Liver Failure Due to Transient Hepatitis B Virus Infection. *Intern Med* (2018) 57:1543–52. doi: 10.2169/internalmedicine.9670-17
68. Rahim MN, Liberal R, Miquel R, Heaton ND, Heneghan MA. Acute Severe Autoimmune Hepatitis: Corticosteroids or Liver Transplantation? *Liver Transpl* (2019) 25:946–59. doi: 10.1002/lt.25451
69. Ichai P, Duclos-Vallee JC, Guettier C, Hamida SB, Antonini T, Delvart V, et al. Usefulness of Corticosteroids for the Treatment of Severe and Fulminant Forms of Autoimmune Hepatitis. *Liver Transpl* (2007) 13:996–1003. doi: 10.1002/lt.21036
70. Karkhanis J, Verna EC, Chang MS, Stravitz RT, Schilsky M, Lee WM, et al. Steroid Use in Acute Liver Failure. *Hepatol (Baltimore Md)* (2014) 59:612–21. doi: 10.1002/hep.26678
71. Zheng L, Liu Y, Shang Y, Han Z, Han Y. Clinical Characteristics and Treatment Outcomes of Acute Severe Autoimmune Hepatitis. *BMC Gastroenterol* (2021) 21:93. doi: 10.1186/s12876-021-01653-4
72. Anastasiou OE, Dogan-Cavus B, Kucukoglu O, Baba H, Kahraman A, Gerken G, et al. Corticosteroid Therapy Improves the Outcome of Autoimmune Hepatitis-Induced Acute Liver Failure. *Digestion* (2018) 98:104–11. doi: 10.1159/000487940
73. De Martin E, Coilly A, Chazouilleres O, Roux O, Peron JM, Houssel-Debry P, et al. Early Liver Transplantation for Corticosteroid Non-Responders With Acute Severe Autoimmune Hepatitis: The SURFASA Score. *J Hepatol* (2021) 74:1325–34. doi: 10.1016/j.jhep.2020.12.033
74. Zachou K, Arvaniti P, Azariadis K, Lygoura V, Gatselis NK, Lyberopoulou A, et al. Prompt Initiation of High-Dose I.V. Corticosteroids Seems to Prevent Progression to Liver Failure in Patients With Original Acute Severe Autoimmune Hepatitis. *Hepatol Res* (2019) 49:96–104. doi: 10.1111/hepr.13252
75. Anand L, Choudhury A, Bihari C, Sharma BC, Kumar M, Maiwall R, et al. Flare of Autoimmune Hepatitis Causing Acute on Chronic Liver Failure: Diagnosis and Response to Corticosteroid Therapy. *Hepatol (Baltimore Md)* (2019) 70:587–96. doi: 10.1002/hep.30205
76. Chalasani NP, Maddur H, Russo MW, Wong RJ, Reddy KRPractice Parameters Committee of the American College of G. ACG Clinical Guideline: Diagnosis and Management of Idiosyncratic Drug-Induced Liver Injury. *Am J Gastroenterol* (2021) 116:878–98. doi: 10.14309/ajg.0000000000001259
77. European Association for the Study of the Liver, Electronic Address eee, Clinical Practice Guideline Panel C and Panel M, Representative EGB. EASL Clinical Practice Guidelines: Drug-Induced Liver Injury. *J Hepatol* (2019) 70:1222–61. doi: 10.1016/j.jhep.2019.02.014
78. Tujios SR, Lee WM. Acute Liver Failure Induced by Idiosyncratic Reaction to Drugs: Challenges in Diagnosis and Therapy. *Liver International* (2018) 38:6–14. doi: 10.1111/liv.13535
79. Hu PF, Wang PQ, Chen H, Hu XF, Xie QP, Shi J, et al. Beneficial Effect of Corticosteroids for Patients With Severe Drug-Induced Liver Injury. *J Dig Dis* (2016) 17:618–27. doi: 10.1111/1751-2980.12383
80. Wree A, Dechene A, Herzer K, Hilgard P, Syn WK, Gerken G, et al. Steroid and Ursodesoxycholic Acid Combination Therapy in Severe Drug-Induced Liver Injury. *Digestion* (2011) 84:54–9. doi: 10.1159/000322298
81. Wan YM, Wu JF, Li YH, Wu HM, Wu XN, Xu Y. Prednisone is Not Beneficial for the Treatment of Severe Drug-Induced Liver Injury: An Observational Study (STROBE Compliant). *Med (Baltimore)* (2019) 98:e15886. doi: 10.1097/MD.0000000000015886
82. European Association for the Study of the L. EASL Clinical Practice Guidelines: Autoimmune Hepatitis. *J Hepatol* (2015) 63:971–1004. doi: 10.1016/j.jhep.2015.06.030
83. Bjornsson ES, Bergmann O, Jonasson JG, Grondal G, Gudbjornsson B, Olafsson S. Drug-Induced Autoimmune Hepatitis: Response to Corticosteroids and Lack of Relapse After Cessation of Steroids. *Clin Gastroenterol Hepatol* (2017) 15:1635–6. doi: 10.1016/j.cgh.2017.05.027
84. Bjornsson E. Hepatotoxicity Associated With Antiepileptic Drugs. *Acta Neurol Scand* (2008) 118:281–90. doi: 10.1111/j.1600-0404.2008.01009.x
85. Singal AK, Bataller R, Ahn J, Kamath PS, Shah VH. ACG Clinical Guideline: Alcoholic Liver Disease. *Am J Gastroenterol* (2018) 113:175–94. doi: 10.1038/ajg.2017.469
86. D'Agnolo HM, Drenth JP. High-Dose Methylprednisolone-Induced Hepatitis in a Patient With Multiple Sclerosis: A Case Report and Brief Review of Literature. *Netherlands J Med* (2013) 71:199–202.
87. Oliveira AT, Lopes S, Cipriano MA, Sofia C. Induced Liver Injury After High-Dose Methylprednisolone in a Patient With Multiple Sclerosis. *BMJ Case Rep* (2015) 2015:bcr2015210722. doi: 10.1136/bcr-2015-210722
88. Zhe-Bin W, Ke W, Mo ZS, Zhen X, Yu-Bao Z, Ying Y, et al. Early, Short-Term, Low-Dose Glucocorticoid Therapy Effectively Blocks Progression of Severe Acute Exacerbation of Chronic Hepatitis B to Liver Failure. *Clin Res Hepatol Gastroenterol* (2021) 45:101505. doi: 10.1016/j.clinre.2020.07.010
89. Lim HY, Muller N, Herold MJ, van den Brandt J, Reichardt HM. Glucocorticoids Exert Opposing Effects on Macrophage Function Dependent on Their Concentration. *Immunology* (2007) 122:47–53. doi: 10.1111/j.1365-2567.2007.02611.x
90. Shasthry SM, Sarin SK. New Treatment Options for Alcoholic Hepatitis. *World J Gastroenterol* (2016) 22:3892–906. doi: 10.3748/wjg.v22.i15.3892
91. Zhu B, You SL, Wan ZH, Liu HL, Rong YH, Zang H, et al. Clinical Characteristics and Corticosteroid Therapy in Patients With

Autoimmune-Hepatitis-Induced Liver Failure. *World J Gastroenterol* (2014) 20:7473–9. doi: 10.3748/wjg.v20.i23.7473
92. Bockmann JH, Dandri M, Lüth S, Pannicke N, Lohse AW. Combined Glucocorticoid and Antiviral Therapy of Hepatitis B Virus-Related Liver Failure. *World J Gastroenterol* (2015) 21:2214–9. doi: 10.3748/wjg.v21.i7.2214
93. Hamalainen M, Lilja R, Kankaanranta H, Moilanen E. Inhibition of iNOS Expression and NO Production by Anti-Inflammatory Steroids. *Reversal Histone Deacetylase Inhibitors Pulm Pharmacol Ther* (2008) 21:331–9. doi: 10.1016/j.pupt.2007.08.003
94. Mendizabal M, Marciano S, Videla MG, Anders M, Zerega A, Balderramo DC, et al. Fulminant Presentation of Autoimmune Hepatitis: Clinical Features and Early Predictors of Corticosteroid Treatment Failure. *Eur J Gastroenterol Hepatol* (2015) 27:644–8. doi: 10.1097/meg.0000000000000353
95. Gao L, Wang JF, Xiang M, Fan YC, Zhang ZG, Wang K. Expression of Human Glucocorticoid Receptor in T Lymphocytes in Acute-on-Chronic Hepatitis B Liver Failure. *Digestive Dis Sci* (2011) 56:2605–12. doi: 10.1007/s10620-011-1656-4
96. Dendoncker K, Libert C. Glucocorticoid Resistance as a Major Drive in Sepsis Pathology. *Cytokine Growth Factor Rev* (2017) 35:85–96. doi: 10.1016/j.cytogfr.2017.04.002
97. Rodriguez JM, Monsalves-Alvarez M, Henriquez S, Llanos MN, Troncoso R. Glucocorticoid Resistance in Chronic Diseases. *Steroids* (2016) 115:182–92. doi: 10.1016/j.steroids.2016.09.010
98. Straub RH, Cutolo M. Glucocorticoids and Chronic Inflammation. *Rheumatol (Oxford)* (2016) 55:ii6–14. doi: 10.1093/rheumatology/kew348
99. Tjandra K, Le T, Swain MG. Glucocorticoid Receptors are Downregulated in Hepatic T Lymphocytes in Rats With Experimental Cholangitis. *Gut* (2003) 52:1363–70. doi: 10.1136/gut.52.9.1363
100. Rai T, Ohira H, Tojo J, Abe K, Yokokawa J, Takiguchi J, et al. Expression of Human Glucocorticoid Receptor in Lymphocytes of Patients With Autoimmune Hepatitis. *Hepatol Res* (2004) 29:148–52. doi: 10.1016/j.hepres.2004.03.004
101. Rai T, Monoe K, Kanno Y, Saito H, Takahashi A, Irisawa A, et al. Expression of Human Glucocorticoid Receptor Beta of Peripheral Blood Mononuclear Cells in Patients With Severe Autoimmune Hepatitis. *Fukushima J Med Sci* (2006) 52:65–70. doi: 10.5387/fms.52.65
102. Xing T, Li L, Cao H, Huang J. Altered Immune Function of Monocytes in Different Stages of Patients With Acute on Chronic Liver Failure. *Clin Exp Immunol* (2007) 147:184–8. doi: 10.1111/j.1365-2249.2006.03259.x
103. Bemeur C, Qu H, Desjardins P, Butterworth RF. IL-1 or TNF Receptor Gene Deletion Delays Onset of Encephalopathy and Attenuates Brain Edema in Experimental Acute Liver Failure. *Neurochem Int* (2010) 56:213–5. doi: 10.1016/j.neuint.2009.11.010
104. Wang X, Xu H, Wang Y, Shen C, Ma L, Zhao C. MicroRNA-124a Contributes to Glucocorticoid Resistance in Acute-on-Chronic Liver Failure by Negatively Regulating Glucocorticoid Receptor Alpha. *Ann Hepatol* (2020) 19:214–21. doi: 10.1016/j.aohep.2019.08.007
105. Thursz MR, Richardson P, Allison M, Austin A, Bowers M, Day CP, et al. Prednisolone or Pentoxifylline for Alcoholic Hepatitis. *N Engl J Med* (2015) 372:1619–28. doi: 10.1056/NEJMoa1412278
106. Moreau R, Jalan R, Gines P, Pavesi M, Angeli P, Cordoba J, et al. Acute-On-Chronic Liver Failure Is a Distinct Syndrome That Develops in Patients With Acute Decompensation of Cirrhosis. *Gastroenterology* (2013) 144:1426–37.e9. doi: 10.1053/j.gastro.2013.02.042
107. Bajaj JS, O'Leary JG, Reddy KR, Wong F, Olson JC, Subramanian RM, et al. Second Infections Independently Increase Mortality in Hospitalized Patients With Cirrhosis: The North American Consortium for the Study of End-Stage Liver Disease (NACSELD) Experience. *Hepatol (Baltimore Md)* (2012) 56:2328–35. doi: 10.1002/hep.25947
108. Bellot P, Francés R, Such J. Pathological Bacterial Translocation in Cirrhosis: Pathophysiology, Diagnosis and Clinical Implications. *Liver International* (2013) 33:31–9. doi: 10.1111/liv.12021
109. Wasmuth HE, Kunz D, Yagmur E, Timmer-Stranghöner A, Vidacek D, Siewert E, et al. Patients With Acute on Chronic Liver Failure Display "Sepsis-Like" Immune Paralysis. *J Hepatol* (2005) 42:195–201. doi: 10.1016/j.jhep.2004.10.019
110. Appenrodt B, Grünhage F, Gentemann MG, Thyssen L, Sauerbruch T, Lammert F. Nucleotide-Binding Oligomerization Domain Containing 2 (NOD2) Variants are Genetic Risk Factors for Death and Spontaneous Bacterial Peritonitis in Liver Cirrhosis. *Hepatol (Baltimore Md)* (2010) 51:1327–33. doi: 10.1002/hep.23440
111. Senkerikova R, de Mare-Bredemeijer E, Frankova S, Roelen D, Visseren T, Trunecka P, et al. Genetic Variation in TNFA Predicts Protection From Severe Bacterial Infections in Patients With End-Stage Liver Disease Awaiting Liver Transplantation. *J Hepatol* (2014) 60:773–81. doi: 10.1016/j.jhep.2013.12.011
112. Hernaez R, Sola E, Moreau R, Gines P. Acute-On-Chronic Liver Failure: An Update. *Gut* (2017) 66:541–53. doi: 10.1136/gutjnl-2016-312670
113. Prigent H, Maxime V, Annane D. Clinical Review: Corticotherapy in Sepsis. *Crit Care* (2004) 8:122–9. doi: 10.1186/cc2374
114. Salluh JI, Povoa P. Corticosteroids in Severe Sepsis and Septic Shock: A Concise Review. *Shock* (2017) 47:47–51. doi: 10.1097/SHK.0000000000000704
115. van den Akker EL, Koper JW, Joosten K, de Jong FH, Hazelzet JA, Lamberts SW, et al. Glucocorticoid Receptor mRNA Levels Are Selectively Decreased in Neutrophils of Children With Sepsis. *Intensive Care Med* (2009) 35:1247–54. doi: 10.1007/s00134-009-1468-6
116. Dekelbab BH, Witchel SF, DeFranco DB. TNF-Alpha and Glucocorticoid Receptor Interaction in L6 Muscle Cells: A Cooperative Downregulation of Myosin Heavy Chain. *Steroids* (2007) 72:705–12. doi: 10.1016/j.steroids.2007.05.007
117. Ledderose C, Mohnle P, Limbeck E, Schutz S, Weis F, Rink J, et al. Corticosteroid Resistance in Sepsis is Influenced by microRNA-124–Induced Downregulation of Glucocorticoid Receptor-Alpha. *Crit Care Med* (2012) 40:2745–53. doi: 10.1097/CCM.0b013e31825b8ebc
118. Guerrero J, Gatica HA, Rodriguez M, Estay R, Goecke IA. Septic Serum Induces Glucocorticoid Resistance and Modifies the Expression of Glucocorticoid Isoforms Receptors: A Prospective Cohort Study and *In Vitro* Experimental Assay. *Crit Care* (2013) 17:R107. doi: 10.1186/cc12774
119. Narum S, Westergren T, Klemp M. Corticosteroids and Risk of Gastrointestinal Bleeding: A Systematic Review and Meta-Analysis. *BMJ Open* (2014) 4:e004587. doi: 10.1136/bmjopen-2013-004587
120. Fernández J, Acevedo J, Wiest R, Gustot T, Amoros A, Deulofeu C, et al. Bacterial and Fungal Infections in Acute-on-Chronic Liver Failure: Prevalence, Characteristics and Impact on Prognosis. *Gut* (2018) 67:1870–80. doi: 10.1136/gutjnl-2017-314240
121. Strnad P, Tacke F, Koch A, Trautwein C. Liver - Guardian, Modifier and Target of Sepsis. *Nat Rev Gastroenterol Hepatol* (2017) 14:55–66. doi: 10.1038/nrgastro.2016.168
122. Victor DW3rd, Quigley EM. Microbial Therapy in Liver Disease: Probiotics Probe the Microbiome-Gut-Liver-Brain Axis. *Gastroenterology* (2014) 147:1216–8. doi: 10.1053/j.gastro.2014.10.023
123. Mookerjee RP, Pavesi M, Thomsen KL, Mehta G, Macnaughtan J, Bendtsen F, et al. Treatment With Non-Selective Beta Blockers Is Associated With Reduced Severity of Systemic Inflammation and Improved Survival of Patients With Acute-on-Chronic Liver Failure. *J Hepatol* (2016) 64:574–82. doi: 10.1016/j.jhep.2015.10.018
124. Madsen BS, Havelund T, Krag A. Targeting the Gut-Liver Axis in Cirrhosis: Antibiotics and non-Selective β-Blockers. *Adv Ther* (2013) 30:659–70. doi: 10.1007/s12325-013-0044-1
125. Lionakis MS, Kontoyiannis DP. Glucocorticoids and Invasive Fungal Infections. *Lancet* (2003) 362:1828–38. doi: 10.1016/S0140-6736(03)14904-5
126. Verma N, Singh S, Taneja S, Duseja A, Singh V, Dhiman RK, et al. Invasive Fungal Infections Amongst Patients With Acute-on-Chronic Liver Failure at High Risk for Fungal Infections. *Liver International* (2019) 39:503–13. doi: 10.1111/liv.13981
127. Acharya SK, Dasarathy S, Kumer TL, Sushma S, Prasanna KS, Tandon A, et al. Fulminant Hepatitis in a Tropical Population: Clinical Course, Cause, and Early Predictors of Outcome. *Hepatol (Baltimore Md)* (1996) 23:1448–55. doi: 10.1002/hep.510230622
128. Garcia Rodriguez LA, Lin KJ, Hernandez-Diaz S, Johansson S. Risk of Upper Gastrointestinal Bleeding With Low-Dose Acetylsalicylic Acid Alone and in Combination With Clopidogrel and Other Medications. *Circulation* (2011) 123:1108–15. doi: 10.1161/CIRCULATIONAHA.110.973008
129. Green FWJr., Kaplan MM, Curtis LE, Levine PH. Effect of Acid and Pepsin on Blood Coagulation and Platelet Aggregation. A Possible Contributor Prolonged Gastroduodenal Mucosal Hemorrhage. *Gastroenterology* (1978) 74:38–43. doi: 10.1016/0016-5085(78)90352-9

130. Yacyshyn BR, Thomson AB. Critical Review of Acid Suppression in Nonvariceal, Acute, Uppergastrointestinal Bleeding. *Dig Dis* (2000) 18:117–28. doi: 10.1159/000051385
131. Polson J, Lee WMAmerican Association for the Study of Liver D. AASLD Position Paper: The Management of Acute Liver Failure. *Hepatol (Baltimore Md)* (2005) 41:1179–97. doi: 10.1002/hep.20703
132. Hu PF, Xie WF. Corticosteroid Therapy in Drug-Induced Liver Injury: Pros and Cons. *J Dig Dis* (2019) 20:122–6. doi: 10.1111/1751-2980.12697

Conflict of Interest: The authors declare that the research was conducted in the absence of any commercial or financial relationships that could be construed as a potential conflict of interest.

Publisher's Note: All claims expressed in this article are solely those of the authors and do not necessarily represent those of their affiliated organizations, or those of the publisher, the editors and the reviewers. Any product that may be evaluated in this article, or claim that may be made by its manufacturer, is not guaranteed or endorsed by the publisher.

frontiers | Frontiers in Immunology

REVIEW
published: 07 April 2022
doi: 10.3389/fimmu.2022.865888

Mesenchymal Stromal/Stem Cells and Their Extracellular Vesicles Application in Acute and Chronic Inflammatory Liver Diseases: Emphasizing on the Anti-Fibrotic and Immunomodulatory Mechanisms

Ali Hazrati[1], *Kosar Malekpour*[2], *Sara Soudi*[1] *and Seyed Mahmoud Hashemi*[3]*

[1] Department of Immunology, Faculty of Medical Sciences, Tarbiat Modares University, Tehran, Iran, [2] Department of Immunology, School of Medicine, Iran University of Medical Sciences, Tehran, Iran, [3] Department of Immunology, School of Medicine, Shahid Beheshti University of Medical Sciences, Tehran, Iran

OPEN ACCESS

Edited by:
Yu-Chen Fan,
Shandong University, China

Reviewed by:
Ze-Hua Zhao,
Shandong University, China
Barbara Mara Klinkhammer,
University Hospital RWTH Aachen, Germany

***Correspondence:**
Seyed Mahmoud Hashemi
smmhashemi@sbmu.ac.ir

Specialty section:
This article was submitted to Inflammation, a section of the journal Frontiers in Immunology

Received: 30 January 2022
Accepted: 15 March 2022
Published: 07 April 2022

Citation:
Hazrati A, Malekpour K, Soudi S and Hashemi SM (2022) Mesenchymal Stromal/Stem Cells and Their Extracellular Vesicles Application in Acute and Chronic Inflammatory Liver Diseases: Emphasizing on the Anti-Fibrotic and Immunomodulatory Mechanisms. Front. Immunol. 13:865888. doi: 10.3389/fimmu.2022.865888

Various factors, including viral and bacterial infections, autoimmune responses, diabetes, drugs, alcohol abuse, and fat deposition, can damage liver tissue and impair its function. These factors affect the liver tissue and lead to acute and chronic liver damage, and if left untreated, can eventually lead to cirrhosis, fibrosis, and liver carcinoma. The main treatment for these disorders is liver transplantation. Still, given the few tissue donors, problems with tissue rejection, immunosuppression caused by medications taken while receiving tissue, and the high cost of transplantation, liver transplantation have been limited. Therefore, finding alternative treatments that do not have the mentioned problems is significant. Cell therapy is one of the treatments that has received a lot of attention today. Hepatocytes and mesenchymal stromal/stem cells (MSCs) are used in many patients to treat liver-related diseases. In the meantime, the use of mesenchymal stem cells has been studied more than other cells due to their favourable characteristics and has reduced the need for liver transplantation. These cells increase the regeneration and repair of liver tissue through various mechanisms, including migration to the site of liver injury, differentiation into liver cells, production of extracellular vesicles (EVs), secretion of various growth factors, and regulation of the immune system. Notably, cell therapy is not entirely excellent and has problems such as cell rejection, undesirable differentiation, accumulation in unwanted locations, and potential tumorigenesis. Therefore, the application of MSCs derived EVs, including exosomes, can help treat liver disease and prevent its progression. Exosomes can prevent apoptosis and induce proliferation by transferring different cargos to the target cell. In addition, these vesicles have been shown to transport hepatocyte growth factor (HGF) and can promote the hepatocytes'(one of the most important cells in the liver parenchyma) growths.

Keywords: MSCs, exosomes, liver disease, immunomodulation, inflammation, regeneration

1 INTRODUCTION

Inflammation is an immunological condition that has an important role in controlling microbial infections and is the basis of many natural physiological events of the body in healthy conditions (1). This physiological process plays a vital role in embryo implantation, tissue repair, fetal growth, etc. (2). These inflammations must be carefully regulated to maintain the homeostasis of various tissues and organs. Failure to control inflammation can lead to multiple injuries to the tissues involved and lead to the loss of part or all of that tissue (3). Hemostatic inflammation is an integral part of liver health, and treatment strategies should focus on reversing pathological inflammation to hemostatic inflammation (4).

The liver is one of the vital organs that has a great ability to regenerate itself due to liver cells' characteristics (5, 6). But when the amount of damage is so much and exceeds liver cells' ability to regenerate, the function of this tissue is impaired (7). Acute liver failure (ALF) is more common in adolescents and is associated with high mortality (8). In ALF, the metabolic and immunological function of the liver is impaired. It presents with manifestations such as blood coagulation defects, cardiovascular instability, liver encephalopathy, susceptibility to infection, and progressive multiple organ failure (9, 10). The interval between the onset of symptoms and the onset of hepatic encephalopathy distinguishes different forms of the disease (11). In this way, if the time between them is a few hours, it is called hyperacute liver failure (12), but if this interval occurs more slowly and lasts from a few days to a few weeks, it is called acute or sub-acute damage (13). Fibrosis is an intrinsic response to injury that maintains the integrity of the various organs involved in tissue damage due to extensive necrosis or apoptosis (14). Chronic liver disease occurs during persistent inflammation and is associated with the destruction and regeneration of the liver parenchyma, which eventually leads to fibrosis and cirrhosis. There are many different causes for chronic liver disease, autoimmune diseases, including long-term alcohol abuse, toxins, infections, genetic and metabolic disorders (15). For example, during myocardial infarction, fibrosis and collagen fibres become apparent by the end of the first week, preventing heart rupture by maintaining the heart's structure (16). Tissue fibrosis is also seen in the kidney after ischemia (17) and in the lung after H5N1 influenza and COVID-19 infection (18–20). **Figure 1** summarizes some acute and chronic liver diseases and the main mechanisms involved in these diseases development (**Figure 1**). It is worth noting that various treatments can prevent the progression of liver fibrosis (21) but do not lead to the reversion of fibrous tissue, and there is no definitive treatment for fibrosis.

There is currently no specific drug for treating liver disease, and many of the current treatments are used only in very acute cases due to their side effects (22). Therefore, there is an urgent need to find appropriate treatment methods to prevent liver disease progression and repair liver tissue. Today cell therapy is one of the fields that has raised many hopes and interests in the field of regenerative medicine. Cells such as mesenchymal stromal/stem cells, hepatocytes, hematopoietic cells, immune system cells and endothelial progenitor cells have been used in various studies to treat liver disease (23).

There are advantages and disadvantages to using each of these cells, which are summarized in **Table 1**. Among these cells, mesenchymal stem cells have been used extensively in studies due to their desirable properties and have shown promising results. The desirable characteristics of these cells are various isolation sources, easy isolation methods, easy culture methods, expansion and storage, low immunogenicity, self-renewal ability, ability to differentiate into different cell types, immunomodulatory properties, The ability to produce soluble factors such as exosomes and growth factors and the ability to migrate to the site of tissue damage were noted (39, 40). Due to the favourable properties of MSCs-derived extracellular vesicles (EVs), the therapeutic ability of these vesicles has been investigated. This review discusses the effect of inflammation on the progression of liver disease, the role of liver cells and immune cells in the pathogenesis of the liver disease, and studies of MSCs and their EVs (mechanisms).

2 INFLAMMATION ROLE IN LIVER DISEASES (LDS)

Under physiological conditions, the liver constantly contacts food-derived foreign proteins, drugs, chemicals, toxins, and intestinal microbiota (41). Kupffer cells (KCs) and dendritic cells (DCs), as well as circulating immune cells such as bone marrow-derived macrophages, natural killer (NK) cells, and neutrophils (42), play an important role in the formation of the liver immune microenvironment and hepatic immune responses (43).

Kupffer cells become highly active in the liver during this disease and produce inflammatory cytokines, including IL-1, IL-6, and TNF-α. In addition, due to the activation of other immune system cells that are recruited from the bloodstream to the liver tissue, systemic inflammation develops that can stimulate necrosis and apoptosis in hepatocytes (44, 45). Overall, inflammation, immune cells and liver cells inflammatory responses play an essential role in developing liver-related diseases (46).

Hepatic steatosis, or fatty liver disease (FLD), is the most common liver disease in the United States (47), occurs in response to alcohol, chemotherapy, toxins such as vanilla chloride, and insulin-related metabolic syndrome and can lead to liver tissue damage (48). This damage is associated with inflammation and fibrosis, alters hepatocyte gene expression, and leads to increased TLRs ligands, TGF-β, CXCL10, and IL-1A receptors (49). In hepatitis, activation of the NF-κB signaling pathway in activated hepatocytes has also been observed. In this pathway, the activated cells release several pro-inflammatory cytokines and chemokines such as TNF-α, IL-6, and CCL2, which mediate liver inflammation (50). Inflammation can lead to necrosis and necroptosis of liver cells (especially in hepatocytes) and result in releasing of a group of molecules called alarmin from them. Alarmins such as the high-mobility group B1 (HMGB1), IL-33, ATP, and formyl peptide is released from

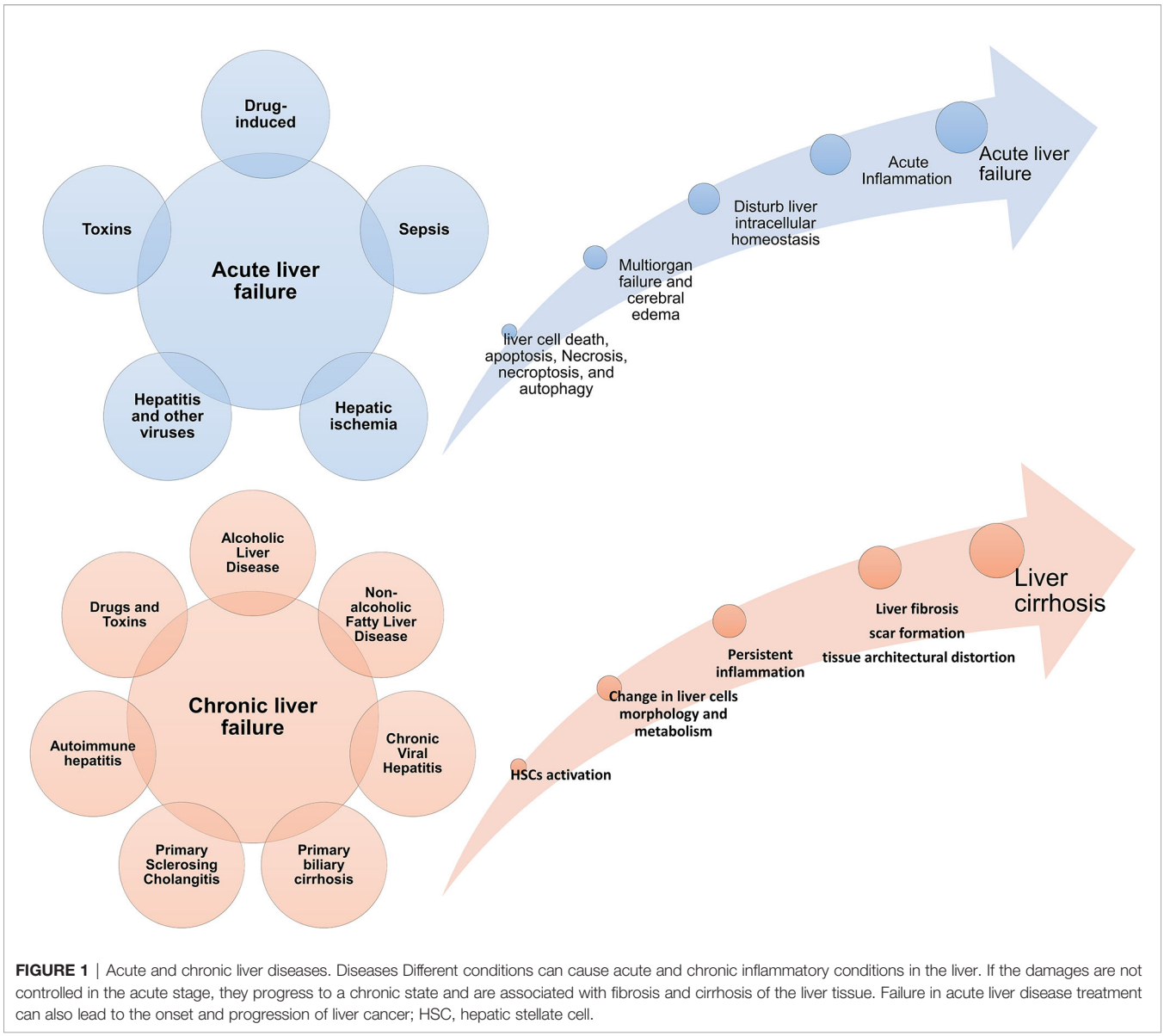

FIGURE 1 | Acute and chronic liver diseases. Diseases Different conditions can cause acute and chronic inflammatory conditions in the liver. If the damages are not controlled in the acute stage, they progress to a chronic state and are associated with fibrosis and cirrhosis of the liver tissue. Failure in acute liver disease treatment can also lead to the onset and progression of liver cancer; HSC, hepatic stellate cell.

necrotic cells (51). In fact, ATP and formyl peptide act as absorbers for neutrophils to the site of tissue damage in the liver. Activation of inflammasomes by reactive oxygen species (ROS) from damaged cells and other damage-associated molecular patterns (DAMPs) can also play a role in liver inflammation (52, 53). As a result of liver inflammation, extensive necrosis and apoptosis in hepatocytes eventually lead to loss of liver function (54). Therefore, controlling inflammatory responses is of particular importance and, if left untreated, can lead to fibrosis (55).

Fibrosis that has occurred in chronic liver disease and inflammation has been extensively studied, but its underlying mechanism in acute liver failure is still unclear (56). The progression of fibrosis leads to cirrhosis, hepatocellular carcinoma, liver failure, and portal hypertension (57). Liver fibrosis is caused by the activation of hepatic stellate cells (HSCs) and the extracellular matrix (ECM) deposition (58). When these cells are activated, the amount of vitamin A and adipogenic-related transcription factors decreases and leads to their differentiation into myofibroblasts, which are the main source of ECM production in liver fibrosis (59). In addition, HSCs contribute to the progression of liver fibrosis by producing inflammatory cytokines and chemokines (60). Immune system cells, especially KCs and circulating macrophages, play a significant role in the TGF-β1-mediated activation of the liver HSCs and increase their survival by the NF-κB-dependent manner (61). reactive oxygen species (ROS) production by KCs and macrophages is another fibrosis stimulant in hepatitis that stimulates the production of collagen 1 in HSCs/myofibroblasts (62).

In response to lipopolysaccharide (LPS), HSCs express chemokines such as IP-10, MCP-1, MIP-1α, MIP-1β, MIP-2,

TABLE 1 | Advantages and disadvantages of each cell in therapeutic applications.

Cell type	Advantage	Disadvantage	Ref.
Endothelial progenitor cells (EPCs)	Anti-fibrotic and pro-regenerative properties	Complicated isolation process, unclear clinical efficacy	(24, 25)
Hematopoietic stem cells	1. Pluripotency 2. Potential to self-renew	1. Requires bone marrow aspiration 2. Linage derivation (such as derivation to macrophages)	(26, 27)
Hepatoblasts (Fetal liver Stem Cells)	1. these cells are bipotent, being able to give rise to both hepatocytes and bile duct cells	1. Rarity of hepatoblasts 0.1% of fetal liver mass 2. Presence of oval cells in adult liver (make isolation an expansion difficult)	(28–30)
Hepatocytes	1. Key metabolic and synthetic cells of the liver 2. Suitable for replacing enzyme deficiency 3. Suitable for replacing metabolic disorders	1. Donor shortages 2. Limited engraftment and proliferation 3. Infection risk	(31, 32)
Immune cells	Relatively easy to isolate and culture	Potential ability to induce inflammatory storms	(33)
Induced pluripotent stem cells (iPS)	1. an unlimited source to produce hepatocytes-like cells *In vitro* 2. Lack of potential issues of allogenic rejection	1. Ethical concern 2. Malignancy potential 3. Low production efficiency	(34, 35)
MSCs	1. Relatively easy to isolate and culture 2. pluripotency 3. immunomodulatory and anti-inflammatory properties 4. Anti-fibrotic function 5. Extracellular signaling 6. Allograft potential 7. Diffreniatonal ability	1. Pro-tumor potential 2. Risks of isolation procedures 3. Malignancy potential 4. Risk of undesired migration to other organs such as lung and kidney	(36–38)

RANTES, and adhesive molecules E-selectin, ICAM-1, VCAM-1, and leading to migration of immune system cells into the liver (63). If liver fibrosis is left untreated, Cirrhosis develops. Cirrhosis is the end stage of progressive fibrosis that lacks effective and comprehensive medical treatment (64). Liver cancer is another consequence of fibrosis and liver inflammation.

Studies have identified the importance of inflammation-related signaling pathways and transcription factors, including STAT3 (55) and NF-κB (65), in liver cancer progression by four mechanisms. (1) Increases the expression of epithelial-to-mesenchymal transition (EMT) associated genes, including matrix metalloproteinases (MMPs) 2 and 9 (in breast cancer), E-cadherin, TWIST (in nasopharyngeal cancer), and cathepsins B. (2) Stimulates angiogenesis and increases tumor growth by regulating the expression of vascular endothelial growth factor (VEGF) (66). (3) Increases the expression of Bcl-2 members and cFLIP families and helps neoplastic cells proliferation and inhibit their apoptosis (67). (4) Increase production of inflammatory cytokines such as IL-1α, TNF-α, IL-1β, EGF-R, IL-6, and CCL2 (50, 68).

3 THE ROLE OF LIVER CELLS IN LIVER INFLAMMATION

There are some major types of cells in the liver that regulate liver different functions, including hepatocytes, hepatic sinusoidal endothelial cells (LSECs), bile epithelial cells (cholangiocytes), HSCs, and KCs (69). Each of these cells performs their specific function, and a defect in their function leads to a defect in the function of the liver (70). In addition, some of these cells play vital roles in regulating the liver microenvironment and participate in inflammation and immune responses (**Figure 2**).

3.1 Hepatocytes

Hepatocytes are the most abundant liver cells, which make up about 90% of its biomass, and are one of the main culprits in the liver's inflammatory response (71). In pathological conditions, hepatocytes produce different chemokines that trigger the immune system cells and create a complex local reaction at the site of infection (72). Hepatocytes express a large number and variety of pattern recognition receptors and identify different types of molecular patterns with pathogens and damage (PAMP, DAMP) (73). (1) Cell surface receptors such as quasi-tuft receptors such as TLR2,4; (2) Endosomal receptors such as TLR3 and (3) Cytoplasmic receptors, such as stimulators of IFN [STING] genes, members of the nucleotide-binding oligomerization domain (NOD) family, and retinoic acid 1 (RIG-1) induction gene (72). During the acute phase response, circulating levels of several proinflammatory cytokines, including IL-1a, TNF-a, and IL-6, increase (74). The most important cytokine affecting hepatocytes' function is IL-6 (75) and induces the expression of acute-phase proteins including serum amyloid A, reactive protein C, haptoglobin, α1-antichymotrypsin and fibrinogen (76).

Hepatocytes also interact with innate and acquired immune cells and activate or inhibit their responses by expressing different ligands. These cells express MIC-A, MIC-B, and CD1d (in mice, not humans) and thus interact with NK and NKT cells (76, 77). There is also evidence that these cells interact with T cells to alter their responses and regulate their function (78, 79).

3.2 Kpffer Cells (KCs)

Kupffer cells make up 20% of non-parenchymal cells in the liver and are located around the portal vein (80). Therefore, due to the potential and different functions of these cells, they play an important role in liver immunology, tissue homeostasis, as well as various liver diseases, including liver cancer, ischemia-

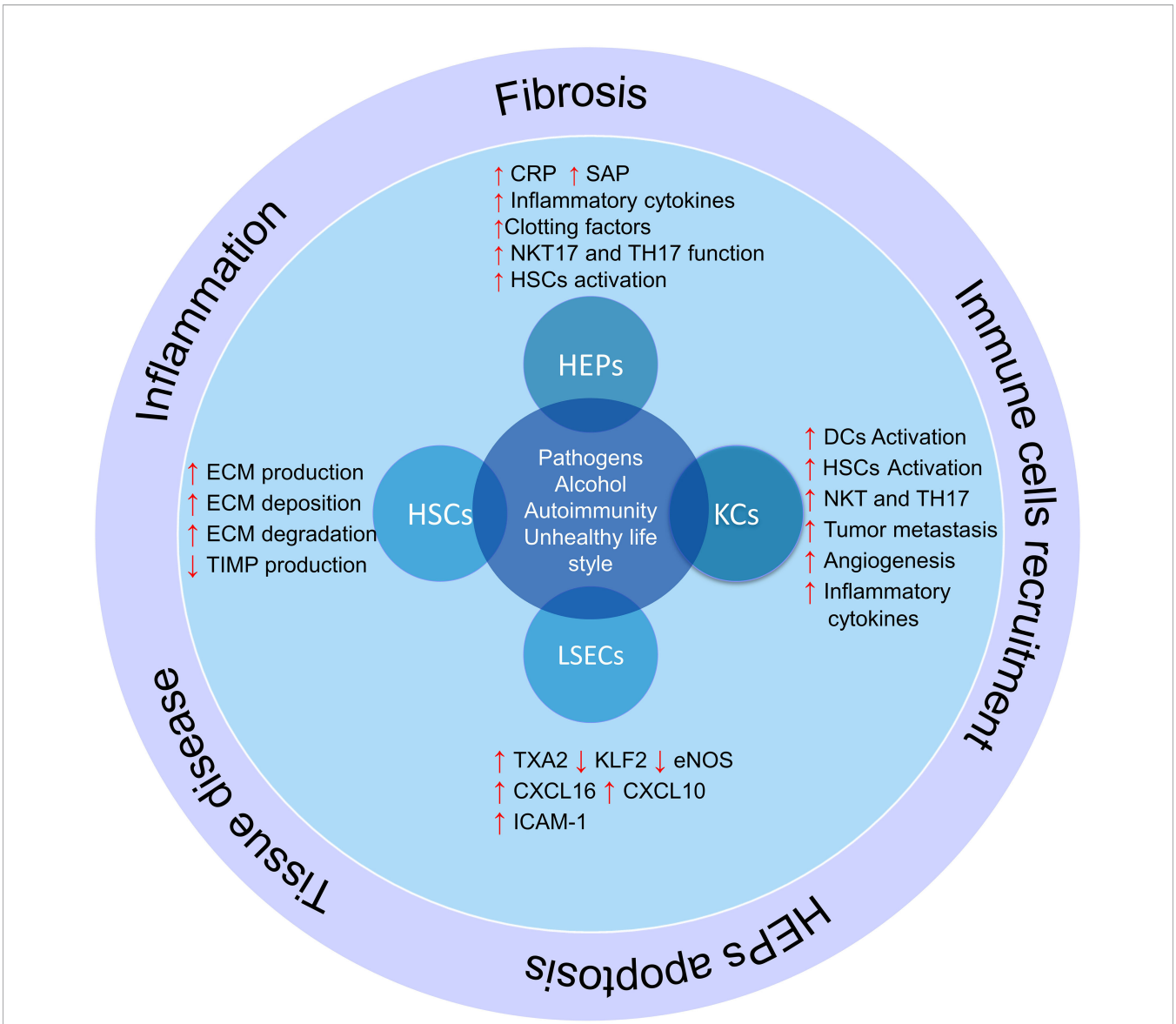

FIGURE 2 | The role of liver cells in inflammation and liver damage. Liver cells help produce and activate immune cells by producing cytokines and inflammatory chemokines. On the other hand, hepatic stellate cells produce fibrosis of the liver tissue and lose their function by producing different components of the extracellular matrix and differentiation into myofibroblasts in inflammatory conditions; HSCs, hepatic stellate cells; KCs, Kupffer cells; LSECs, hepatic sinusoidal endothelial cells; HEPs, Hepatocytes; DCs, Dendritic cells; ECM, extracellular matrix; TXA2, Thromboxane A2; KLF2, Krüppel factor 2 transcription factor; TIMP, Tissue inhibitors of matrix metalloproteinases.

reperfusion (I/R) injury, liver fibrosis and infectious diseases (81). Actually, different signals in the liver microenvironment, such as PAMPs and DAMPs, affect the function of Kupffer cells. For example, HMGB1 released by hepatocytes can activate KCs in Acetaminophen-induced liver injury (AILI), Non-alcoholic steatohepatitis (NASH), and I/R injury (82, 83).In liver diseases, KCs interact with other liver cells such as hepatocytes, cholangiocytes, LSECs, HSCs, and other immune cells. This interaction can exacerbate tissue damage or help to repair and regenerate the liver tissue depending on the type of cells and signalling pathways (81).

3.3 Hepatic Stellate Cells

HSCs, as another main cell of liver tissue, make up 13% of sinusoidal cells and 5 to 8% of all liver cells that perform various functions (84). Among the physiological roles of these cells is (1) synthesis of ECM, (2) regulation of sinusoidal blood flow, (3) storage of vitamin A and (4) synthesis of metalloproteinases (85). After various damage to liver tissue (cause inappropriate function) and apoptosis of its cells, HSCs loses their fat-rich granules and differentiate into trans-smooth muscle alpha-actin containing myofibroblasts, producing ECM and inflammatory cytokines (86). **Table 2** shows the different functions of these

TABLE 2 | Hepatic satellite cells role in different liver disease.

Type of disease	Inducing factors	Mechanism	Ref.
HCC	Hepatitis, Alcoholic liver diseases, and NASH	1. contribute to the formation of tumor microenvironment favorable for tumor growth 2. Activated HSCs in the tumor stroma continuously produce ECM 3. production of soluble factors favoring tumor growth, such as hepatocyte growth factor and TGF-β 4. production of proangiogenic factors such as vascular endothelial growth factor-A (VEGF-A) and MMP9	(87)
I/R liver injury	Ischemia and reperfusion in liver transplantation, imbalances in pH and electrolytes	1. interaction of $CD4^+$ T cells with HSCs before entering the hepatic parenchyma 2. induce the expansion of regulatory T cells (Protective)	(88–90)
Immune-induced hepatitis	Concanavalin A (ConA) and LPS	1. control $CD4^+$ T cell trafficking to liver parenchyma 2. contribution of HSCs to massive production of inflammatory cytokines and chemokines by intra- and extrahepatic immune cells in a paracrine manner	(91–93)
NASH	Increased intestinal permeability	1. The activation of HSCs by TLR4 (the production of chemokines and the expression of adhesion molecules ICAM-1 and VCAM-1 2. incensement in the interaction between HSCs and Kupffer cells	(94)
Viral hepatitis	Hepatitis B and C virus	1. inflammatory and fibrogenic responses by HSCs 2. cell proliferation and nonstructural proteins augment ICAM-1 expression and chemokine production through the NF-κB 3. induction cell migration and activation of several inflammatory pathways in response to CCL21 secreted by activated dendritic cells	(95)

HCC, Hepatocellular carcinoma; ECM, extracellular matrix; HSCs, hepatic stellate cells; MMPs, Matrix metalloproteinase; MSCs, Mesenchymal stromal/stem cells; I/R, Ischemia/reperfusion; NF-kB, Nuclear factor kappa-B; LPS, Lipopolysaccharide; TGF-β, Transforming growth factor-beta; NASH, Non-alcoholic steatohepatitis; TLR, Toll-like receptor.

cells and their role in liver inflammation in various diseases (**Table 2**).

3.4 Liver Sinusoidal Endothelial Cells

LSECs are one of the most specialized endothelial cells with high permeability and have the highest capacity for endocytosis that interface with blood cells on the one side and hepatocytes and HSCs on the other (96). Under pathological conditions, the function of LSECs is changed (97). Capillarization is a process that LSECs acquire vasoconstrictive, thrombotic, and proinflammatory properties (98). During I/R injury and hypoxia due to disruption of blood flow to the liver, LSECs become rounded cells due to vacuolation of the nuclei and reduced ATP supply. In addition, stress on blood flow to the liver leads to a decrease in the Krüppel factor 2 transcription factor (KLF2) in LSECs and its target genes, including the endothelial nitric oxide synthase (eNOS) (99). Since the expression of ICAM-1 and Stabilin-1 in LSECs increases during inflammation, the transmigration of immune cells increases to the liver tissue (100, 101). Expression of mentioned adhesion molecules by LSECs leads to platelet adhesion, vascular microthrombi formation, and platelet-activating factor (PAF) production by platelets, which activates neutrophils and increases ROS production and damages liver tissue (97).

In chronic inflammation, these cells lose their function and play a key role in the onset and progression of chronic liver disease through four processes: sinus capillary formation, angiogenesis, angiocrine signals, and vasoconstriction (102). Decreased NO produced by eNOS by decreased KLF2 activity and increased ROS leads to HSC activation, which is associated with the production and deposition of ECM, increased vasoconstrictors including TXA2 and endothelin-1, and the production of proinflammatory cytokines (103–105).

4 MESENCHYMAL STEM CELLS APPLICATION IN LDS

In vitro studies and co-culture of MSCs with liver tissue-derived cells can increase our understanding of their therapeutic properties and their effectiveness in the treatment of liver disease (106) (**Figure 3**). *In vivo* injections of MSCs into animals to treat various liver diseases have shown very promising results (107). These cells exert their therapeutic functions in laboratory models through various mechanisms (108), and in many studies, only some of the therapeutic aspects of these cells have been addressed. Overall these studies show that MSCs exert their therapeutic effect by modulating the immune environment and increasing the regeneration of liver tissue.

4.1 The Role of MSCs in Modulating Immune and Inflammatory Responses

Considering the significant role of immune cells in inflammation-induced liver damage, it is very important to evaluate the therapeutic effects of MSCs on localized hepatic inflammatory responses. MSCs perform their immunomodulatory functions by cell-cell interaction or by producing soluble factors such as cytokines and extracellular vesicles (**Figure 4**).

4.1.1 Impact on Differentiation and Function of DCs

A study by Yi Zhang et al. (109) Showed that injection of MSCs in the model of liver tissue damage induced by LPS and P. acnes (in mice) stimulates the differentiation of $CD11c^+$ $B220^-$ precursors to $CD11c^+$, $MHCII^{hi}$, $CD80^{low}$, $CD86^{low}$ tolerogenic dendritic cells. Further studies showed that MSC-derived prostaglandin E2 (PGE2) binds to the EP4 receptor on the surface of precursors of DCs and plays a key role in their differentiation into regulatory DCs in a phosphoinositide-3-kinase-dependent manner. These

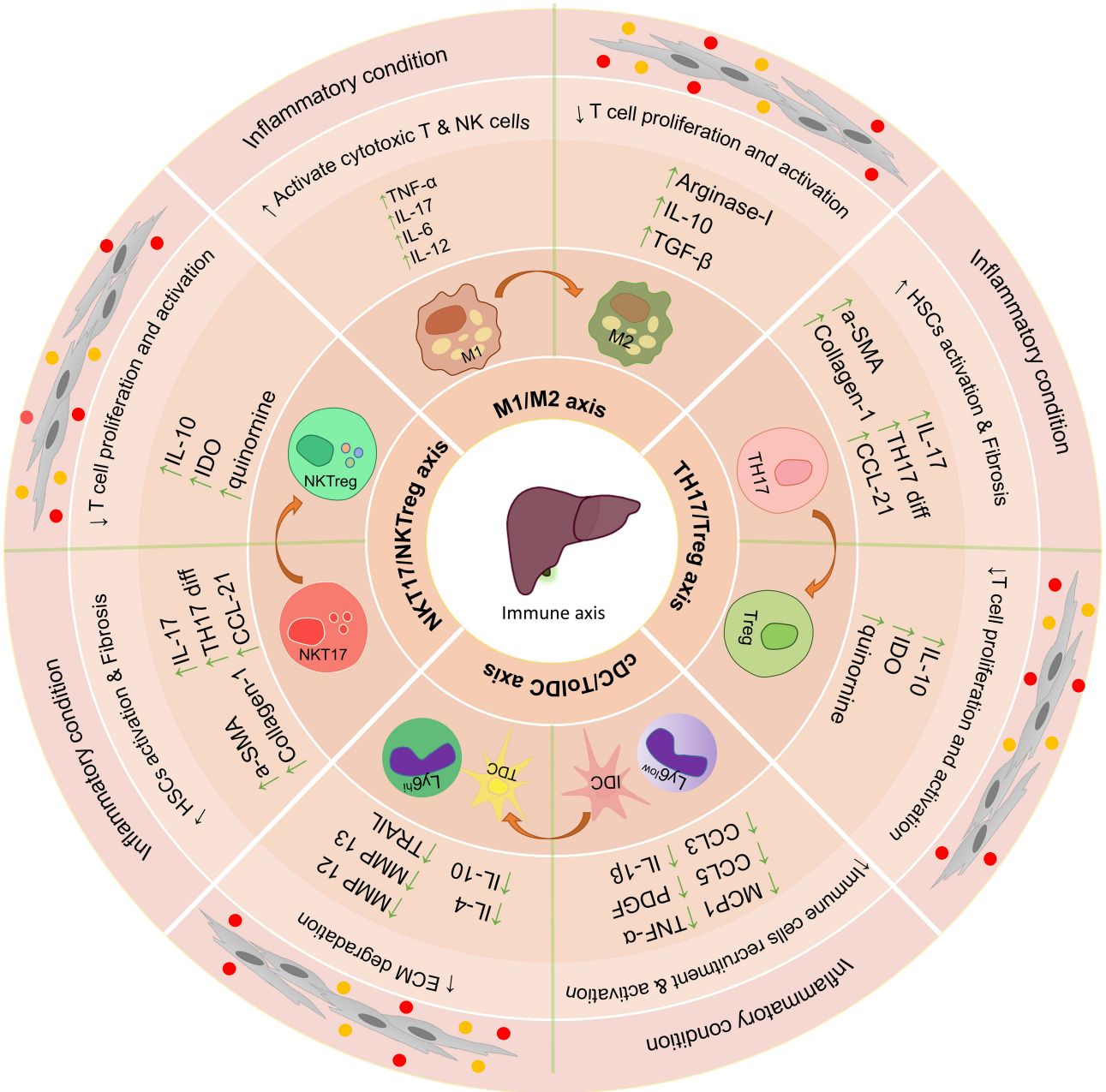

FIGURE 3 | The effect of using mesenchymal stem cells and extracellular vesicles on the important axis of the immune system in the liver. Immunomodulatory properties of mesenchymal stem cells and their extracellular vesicles lead to the suppression of inflammatory responses in the liver's microenvironment and increase anti-inflammatory responses. Some of the most important axis of the immune system involved in liver disease is TH17/Treg, NKT17/NKTreg, and M1/M2. The use of mesenchymal stem cells and extracellular vesicles leads to suppression of function Th17, NKT17, M1, and IDC and increase the differentiation and function of Treg, NKTreg, M2, and Tol DCs; HSCs, hepatic stellate cells; KCs, Kupffer cells; LSECs, hepatic sinusoidal endothelial cells; HEPs, Hepatocytes; Tol DCs, Tolerogenic dendritic cells; cDC, Classic dendritic cells; ECM, extracellular matrix; MSCs, Mesenchymal stromal/stem cells;, M1 Macrophage type 1; M2, Macrophage type 2; MMPs, Matrix metalloproteinase; EVs, Extracellular vesicles.

DCs produce more TGF-b and IL-10 than conventional DCs and stimulate the differentiation of CD4 $^+$ T cells into Treg cells (110). Therefore, these dendritic cells help improve inflammatory damage in the liver by suppressing the activity and differentiation of inflammatory T cells, including Th1 cells (109).

4.1.2 Impact on Macrophages

MSCs play an essential role in modulating macrophages' M1/M2 axis. It has been shown that the co-culture of bone marrow-derived macrophages with MSCs directs their differentiation through the Hippo-dependent pathway to M2 (111).

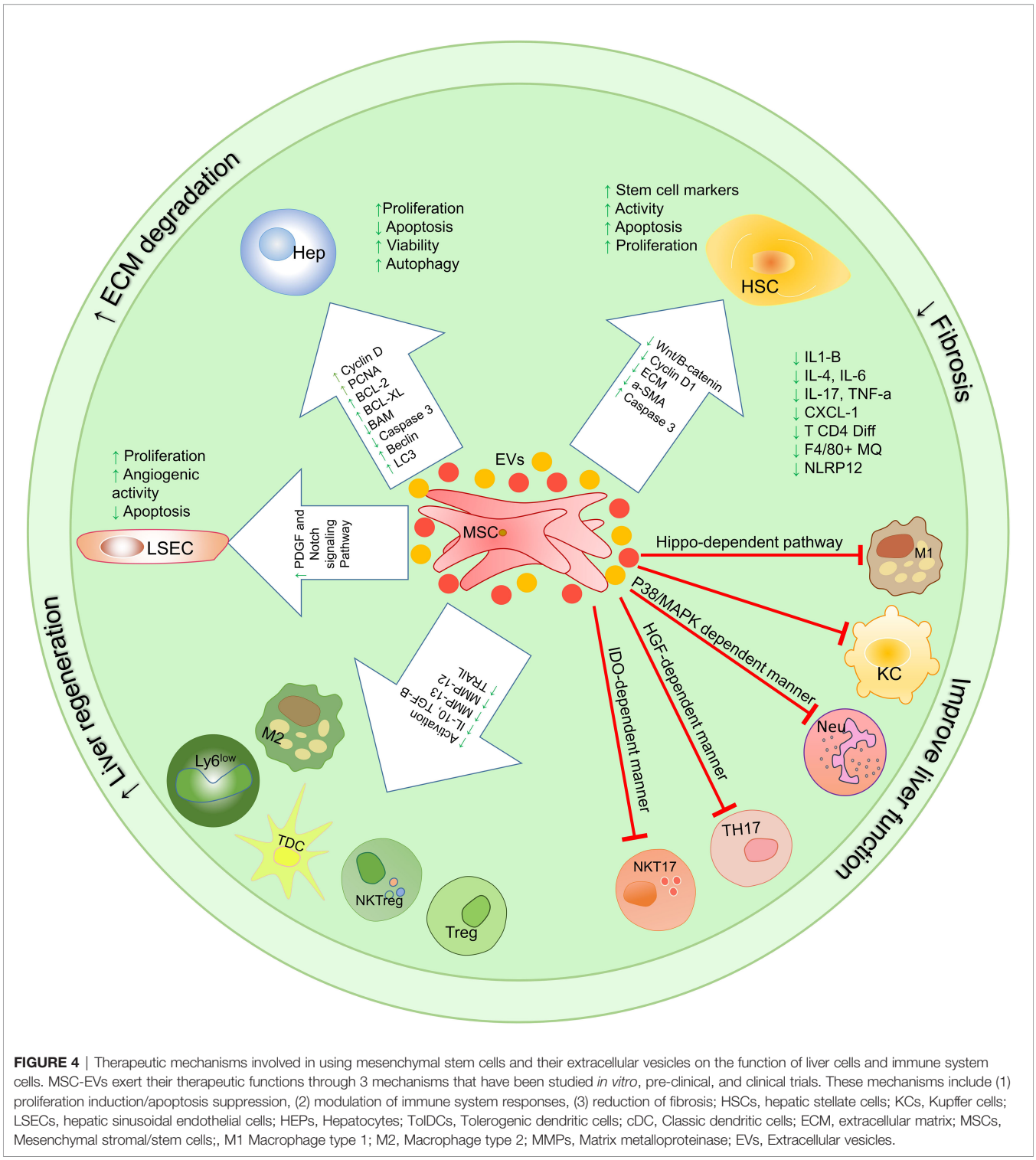

FIGURE 4 | Therapeutic mechanisms involved in using mesenchymal stem cells and their extracellular vesicles on the function of liver cells and immune system cells. MSC-EVs exert their therapeutic functions through 3 mechanisms that have been studied *in vitro*, pre-clinical, and clinical trials. These mechanisms include (1) proliferation induction/apoptosis suppression, (2) modulation of immune system responses, (3) reduction of fibrosis; HSCs, hepatic stellate cells; KCs, Kupffer cells; LSECs, hepatic sinusoidal endothelial cells; HEPs, Hepatocytes; TolDCs, Tolerogenic dendritic cells; cDC, Classic dendritic cells; ECM, extracellular matrix; MSCs, Mesenchymal stromal/stem cells;, M1 Macrophage type 1; M2, Macrophage type 2; MMPs, Matrix metalloproteinase; EVs, Extracellular vesicles.

As mentioned, monocytes/macrophages play a very important role in liver fibrosis. In mice, Ly6C^{hi} macrophages activate HSCs by producing various cytokines and chemokines, including TGF-β, TNF-α, PDGF, MCP1, IL-1β, CCL5, and CCL3 (62). However, Ly6C^{lo} macrophages suppress the functions of HSCs and stimulate apoptosis in these cells by producing and secreting MMPs 12 and 13 and positive regulation of TNF-induced apoptosis ligand (TRAIL) (112). A study by Yuan-hui Li et al. Showed that transplantation of bone marrow-derived MSCs (BM-MSCs) in C57BL/6 J mice with liver fibrosis reduces serum alanine aminotransferase (ALT) levels and collagen deposition in the liver tissue. A sharp decrease in

profibrogenic cytokines including IL-1β, TNF-α, and PDGF derived from profibrotic cells such as Ly6C^{hi} macrophages has also been observed in mice receiving MSCs (113). In fact, transplantation of BM-MSCs has prevented the activation of HSCs through an indirect mechanism by inhibiting Ly6C^{hi} macrophages' function. These macrophages are the most common cells in the fibrotic liver, which increase in proportion to the healthy liver as the liver fibrosis. It is noteworthy that during the treatment of these mice with BM-MSCs, a phenotypic change occurs in macrophages from the Ly6C^{hi} profibrotic subtype to the regenerative Ly6C^{low}, IL-4, IL-10 producing subtype. After BM-MSC transplantation in these mice, the ratio of Ly6C^{hi}/Ly6C^{low} macrophages was reduced by 51% compared to the PBS-treated control group. Therefore, treatment of mouse liver fibrosis model with allogeneic BM-MSCs helps improve liver tissue by suppressing cells involved in liver fibrosis on the one hand and by expanding fibrosis inhibitory cells on the other hand (113).

4.1.3 Neutrophils Migration Suppression

The results of previous studies show that in IRI-related liver injury, innate immune responses play a significant role in inflammatory responses (114). Neutrophils are the most abundant in the bloodstream and reach the site of liver damage as the first leukocytes (115). It has been reported that the severity of the disease and liver damage in I/R and alcoholic liver disease, the amount of neutrophils in the liver tissue is directly related to the severity of the injury (115, 116). However, the induction of liver damage in animals whose neutrophils decreased before induction leads to the limitation of liver damage (117). Therefore, suppressing the harmful responses of these cells can help improve the disease condition (118). The results of a study conducted in 2018 by Shihui Li et al. Show that the use of mesenchymal stem cells in rats with induced liver damage reduces liver damage by lowering neutrophil recruitment and chemotaxis compared to the control group (119).

A chemokine receptor called CXC chemokine receptor 2 (CXCR2) regulates the neutrophil release from bone marrow and its chemotaxis to the inflammation site (120). This study shows that the expression of this receptor on neutrophils in rats with liver damage is significantly reduced after the injection of MSCs (119). In addition, the expression of CXCL2, which is one of the most important chemokines in neutrophil recruitment, decreases in liver ischemic lobes compared to the control group in the experiment. Further analysis of neutrophils isolated from rats with liver damage treated with MSCs showed that p38 MAPK phosphorylation in these neutrophils was the main cause of decreased CXCR2 expression at the cell surface. Interestingly, inhibition of the MAPK p38 phosphorylating enzyme reduces the therapeutic potential of MSCs (119). In addition, since liver macrophages are the main sources of CXCL2-producing and neutrophil recruiting (94), treatment with MSCs by inhibiting NF-κB p65 phosphorylation has been shown to reduce the expression and production of CXCL2 by these cells. Therefore, in general, the use of MSCs reduces the migration of neutrophils to the liver and limits liver damage by reducing the expression of CXCR2 on the surface of neutrophils and reducing the CXCL2 expression and production by liver macrophages. As a result of MSCs therapy, the concentration of liver enzymes in plasma reduces (119). Also, a reduction in hepatocyte apoptosis, improvement in liver function, and a pathological improvement in liver tissue are seen.

4.1.4 Suppression of Activation and Migration of CD4$^+$ T Cells

In general, the use of MSCs to treat liver disease has been shown to reduce the activation and chemotaxis of TCD4$^+$ cells (121). Examination of the expression of different markers of TCD4$^+$ cells isolated from liver injury mice treated with MSCs shows that the expression of CCR7, CXCR3 and CCR5 chemokine receptors is significantly reduced. Also, the production of CXCL9, CCL3, CXCL10, and CCL21 chemokines in the mice's damaged liver is reduced in the treatment with MSCs. In addition, CD69 and CD44 expression are reduced in MSCs treated mice, thereby suppressing TCD4 + cell activation. Serum concentrations of IFN-γ and TNF-α cytokines in these mice also indicate suppression of CD4 + T cell differentiation into Th1 cells (109, 122).

4.1.5 Impact on the Th17/Treg Axis

Due to the importance of the proven role of IL-17 in liver disease (123), the study of MSCs' effects on the IL-17 producing cells is of particular significance. As shown in previous studies, the imbalance in Treg/TH17 is associated with many liver diseases, including autoimmune hepatitis, alcoholic liver disease, and chronic hepatitis B (124).

A study by Qi-Hong Chen et al. Shows that the co-culture of MSCs with LPS-stimulated CD4 + T cell populations can induce plasticity in completely differentiated Th17 cells and convert them into functional Treg cells. The use of an anti-HGF antibody to eliminate and inhibit the effects of this factor leads to the inhibition of the modulatory effects of MSCs by regulating the Th17/Treg equilibrium (125).

In a study by Neda Milosavljevic et al., The effect of transplanted MSCs on Th17 cell responses in liver injury was investigated. IL-17 produced by Th17 cells by activating HSCs increases their production of a-SMA, type 1 collagen and TGF-b1. Intravascular injection of BM-MSCs in the calcium tetrachloride(CCL4)-induced fibrotic liver C57BL/6 mice showed a decrease in the number of IL-17 producing Th17 cells and IL-17 serum level, and also an increase in the serum level immune system suppressory factors such as IL-10, IDO and quinornine. Evaluation of liver tissue damage by H&E staining (to evaluate hepatocyte damage and lobular centre congestion with inflammatory cell infiltration) and Sirius red staining (to assess collagen deposition) in hepatic tissue of MSCs treated mice compared with CCL4-induced mice showed a significant reduction in the size of the stained area in dense fibrous tissue (126).

4.1.6 Impact on the NKT17/NKTreg Axis

In addition to Th17 cells, NKT cells also play a role in the production of IL-17 involved in the pathogenesis of the liver disease (127). Intracellular staining of mononuclear cells

(MNCs) isolated from damaged liver indicates that most of the IL17-producing cells in liver damage are NKT cells. A study by Neda Milosavljevic et al. showed that intravenous injection of MSCs into liver induced injuries with CCL4 and (a-GalCer) a-galactoceramide in C57BL/6 mice decreases inflammatory NKT cell function. The study results show that serum IL-17 levels are reduced in disease-induced mice treated with MSCs. Further studies show that in mice treated with MSCs compared to disease-induced mice, there was a significant reduction in IL-17-producing NKT CD49b$^+$ CD31$^+$ (NKT17) cells (128).

Interestingly, the application of MSCs to treat liver disease in mice treated with a-GalCer1MSC is associated with a significantly higher number of regulatory NKT FOXP3$^+$ IL10$^+$ (NKTreg) cells (128). Therefore, the results of this study suggest that MSCs help improve liver treatment by modulating the NKT17/NKTreg axis and reducing the harmful inflammatory responses (128). It is noteworthy that the co-culture of hepatic NKT cells *in vitro* also confirms the results obtained from the *In Vivo* studies. This function of MSCs is related to IDO and iNOS because of the presence of methyl-DL-tryptophan-1 (IDO inhibitor) and L-N^G-monomethyl arginine citrate (iNOS inhibitor) in the cells and supernatant of injected MSCs imped the protective effect of MSCs on mice. As a result, MSC protects against acute liver damage by reducing the cytotoxicity and capacity of liver NKT17 cells to produce inflammatory cytokines in an IDO-dependent manner (128) (**Figure 3**).

4.2 The Role of MSCs in Liver Tissue Repair and Regeneration

Mesenchymal stem cells help repair liver tissue through various mechanisms, and there is a very complex relationship to their therapeutic function, which is discussed in more detail below.

4.2.1 Reduction of Fibrosis and Impact on the Function of HSCs

MSCs co-culture with HSCs promotes their apoptosis and reduce the production of ECM components such as collagen from these cells. Reducing the synthesis of ECM components is very important in preventing fibrosis progression and can play an essential role in improving the disease (87, 129). In addition, the indirect culture of MSCs with HSC-related LX2 cell lines has been shown to reduce the proliferation of these cells by producing and secreting inflammatory factors such as IL-6, IL-8, and HGF (130). The results of recent studies show that MSCs suppress the activation of HSCs by producing TNFα-stimulated gene-6 (TSG6) and increase the expression of some stem cell markers in these cells (131). *In vitro* studies show that HSCs-derived stem cell-like cells can form organoids that help liver tissue regeneration.

4.2.2 Impact on LSECs

Co-culture of MSCs with endothelial progenitor cells to investigate the effects of these cells on hepatic sinusoidal epithelial cells has been shown to increase endothelial precursor cell proliferation and angiogenic capacity by affecting PDGF and Notch-associated receptors and their downstream signaling pathways (132).

Injection of MSCs into concanavalin-A (Con-A) induced liver disease mice improves liver disease by suppressing apoptosis in LSECs and hepatocytes and lowering serum transaminase enzyme levels (133).

4.2.3 Effect on Hepatocytes

The ability of MSC to differentiate into hepatocyte-like cells has been demonstrated in the *in vivo* and *in vitro* studies. This ability compensates for hepatocyte reduction through apoptosis during various liver damage. Experimental results show that MSCs can differentiate into hepatocyte-like cells (HLCs) in the presence of specific growth factors such as EGF, OSM, HGF and FGF (134, 135). Also, mimicry of the hepatic fibrosis microenvironment stimulates the differentiation of MSCs into hepatocyte-like cells by using 50 g/l of fibrotic tissue extract of rat liver at a faster rate than growth factors (136).

After differentiation, MSCs exhibit the morphology and function of hepatocytes. Analysis of differentiated cells after human Wharton's jelly-derived MSCs (hWJ-MSCs) transplantation in rats shows the presence of cells in rat liver with the expression of human hepatocyte markers such as alpha photoprotein (AFP), CK18, CK19 and albumin. These newly differentiated cells have no sign of rat hepatocyte markers, indicating that hWJ-MSCs differentiate into hepatocyte-like cells after migration to the liver (137, 138). Also, the results of a study conducted by Jae Yeon Kim show that injection of MSCs and their supernatant into (D-galactosamine (D-gal) mediated liver damage) rats reduces hepatocytes apoptosis, and a threefold increase occurs in their proliferation. MSCs appear to increase hepatocyte proliferation by activating the IL-6 signaling pathway mediated by rno-miR-21-5p (139).

Therefore, in general, it can be said that the use of MSCs induces the repair and regeneration of liver tissue through immune responses modulation, differentiation into HLCs, increased proliferation and decreased apoptosis in hepatocytes, increased apoptosis and reduced function of HSCs and improve the function of LSECs.

5 CLINICAL APPLICATIONS OF MSCS FOR THE TREATMENT OF LIVER DISEASE

5.1 Cell Source, Injection Method and Injection Dose

According to our search in the National Institutes of Health (NIH), there are currently 61 active clinical trials using MSCs to treat various liver diseases, including Cirrhosis, fibrosis, acute-on-chronic Liver Failure, and hepatitis viruses related liver failure. **Table 3** summarizes some of these studies. MSCs in these studies were isolated from various tissues, including umbilical cord (UC), bone marrow (BM) and adipose tissue (AD). According to the results of multiple studies on the function of MSCs derived from different tissues, UC-MSCs are used in clinical applications more than others due to features such as (1) providing significant amounts of MSCs compared to BM (2) non-invasive isolation method (3) higher self-renewability and differentiation capacity of UC-MSCs in

TABLE 3 | MSCs based clinical trails.

Liver diseases	Intervention Model	Estimated Enrollment	Source of MSCs	Route	Phase	Dose	Date	NTC number
Acute-on-Chronic Liver Failure	Parallel Assignment	45	N/A	Intravenous (peripheral vein)	Phase 1 and Phase 2	once a week for 4 weeks, 1-10 × 10^5 cell/kg	2019	NCT03863002
Acute-on-chronic Liver Failure	Parallel Assignment	200	N/A	Intravenous (peripheral vein)	N/A	3 times at week 0, 4 and 8, 1 × 10^6 cell/kg	2018	NCT03668171
Alcoholic Liver Cirrhosis	Single Group Assignment	10	Bone Marrow	Hepatic Artery injection	Phase 1	A single dose of 4.5-5.5 × 10^7 cell	2019	NCT03838250
Decompensate Cirrhotic Patients With Pioglitazone	Single Group Assignment	3	Bone Marrow	Intravenous (portal vein)	Phase 1	2 doses at with week intervals	2014	NCT01454336
Decompensated Alcoholic Cirrhosis	Sequential Assignment	36	Umbilical Cord	Intravenous	Phase 1	0.5-2 × 10^6 cell/kg	2021	NCT05155657
Decompensated Hepatitis B Cirrhosis	Single Group Assignment	30	Umbilical Cord	Intravenous	N/A	2 doses with 24 week intervals, 1 × 10^8 cell	2021	NCT05106972
Decompensated liver Cirrhosis	Parallel Assignment	240	Umbilical Cord	Intravenous	Phase 2	3 doses at week 0, week 4, week 8, 6 × 10^7 cell/kg	2021	NCT05121870
Decompensated Liver Cirrhosis	Parallel Assignment	45	Umbilical Cord	Intravenous	Phase 1 and Phase 2	3 doses with 4 week intervals, 0.5 × 10^6 cell/kg	2011	NCT01342250
End-stage Liver Disease (Cirrhosis)	Single Group Assignment	30	N/A	Intravenous	Phase 1 and Phase 2	N/A	2018	NCT03460795
HBV-Related Acute-on-Chronic Liver Failure	Parallel Assignment	261	Umbilical Cord Blood	Intravenous (peripheral vein)	Phase 2	1. 1.once a week for 4 weeks 2. once a week for 8 weeks	2016	NCT02812121
HBV-related Liver Cirrhosis	Parallel Assignment	240	Umbilical cord	Intravenous	Phase 1 and Phase 2	1 × 10^6 cell/kg	2012	NCT01728727
Hepatitis B mediated Liver Cirrhosis	Single Group Assignment	12	Umbilical Cord	Intravenous	Phase 1 and Phase 2	A single dose of 1 × 10^8 cell	2020	NCT04357600
Liver Cirrhosis	Single Group Assignment	30	Bone marrow	Intravenous (peripheral or the portal vein)	Phase 1 and Phase 2	3-4 × 10^7	2007	NCT00420134
Liver Cirrhosis	Single Group Assignment	50	Menstrual Blood	Intravenous	Phase 1 and Phase 2	4 time in 2 week 1 × 10^6 cell/kg	2012	NCT01483248
Liver Cirrhosis	Parallel Assignment	200	Umbilical Cord	Intravenous	Phase 2	3 doses with 3 week intervals, 1 × 10^6 cell/kg	2019	NCT03945487
Liver Cirrhosis	Single Group Assignment	20	bone marrow	Intravenous	Phase 1 and Phase 2	A single dose of 0.5 - 1×10^6 cell/kg	2018	NCT03626090
Liver Cirrhosis	Parallel Assignment	266	Umbilical Cord	Intravenous	Phase 1 and Phase 2	3 doses with 4 week intervals, 0.5 × 10^6 cell/kg	2018	NCT01220492
Liver Cirrhosis	Single Group Assignment	4	Adipose tissue	Intrahepatic Arterial Administration	N/A	N/A	2010	NCT01062750

HBV, Hepatitis B virus; MSCs, Mesenchymal stromal/stem cells; EVs, Extracellular vesicles; TGF-β, Transforming growth factor-beta; NF-kB, Nuclear factor kappa-B; MMPs, Matrix metalloproteinase; NLRP, Nucleotide-binding oligomerization domain; ALT, alanine aminotransferase; AST, Aspartate transaminase; ALP, Alkaline Phosphatase; BM, Bone marrow; UC, umbilical cord; AD, adipose tissue; N/A, Not Applicable.

comparison with BM-MSCs and (4) lower immunogenicity (140, 141).

Injection methods such as intravenous (portal vein or peripheral), intrahepatic artery and intrasplenic injection are used in the transplantation of MSCs. The intravenous (IV) peripheral injection is more used in studies due to ease of identification and less invasive method. However, animal studies have shown that approximately 60% of IV-injected cells never reach the liver and accumulate in tissues like the lungs and kidneys. Due to the existence of different injection methods, in a study conducted by MEM Amer et al., It was shown that injection of MSCs through the portal vein shows better therapeutic results in patients compared to intrasplenic injection (142). As shown in **Table 3**, the number of injections doses, the time interval between injections, and the number of injection cells in the studies vary depending on the different groups' set-up protocols.

5.2 Mechanisms Involved in Liver Disease Treatment After MSCs Transplantation

A phase 1 clinical trial conducted by Kharaziha et al. Showed that the use of BM-MSCs improved patients' symptoms of

uncompensated Cirrhosis. Various scores related to liver healing indicate improvement of the disease without side effects (143). Also, the results of phase 2 of this study, which was performed on patients with alcoholic cirrhosis, showed a reduction in tissue fibrosis and improved liver histology in patients after mesenchymal stem cell transplantation through the hepatic artery (143, 144). Due to the importance of safety in cell therapy studies, a study conducted by Alimoghaddam K et al. has examined this issue in the transplantation of MSCs in various liver diseases, which shows the improvement of liver function in patients without any side effects (145).

A study by Ani Sun et al. Showed that patients receiving routine treatment (RT) in combination with autologous BM-MSCs transplantation had better clinical symptoms such as decreased fatigue and ascites, increased appetite, and abdominal distension than patients receiving only routine treatment. This study also showed that liver function significantly improved in patients receiving combination therapy in terms of MELD (model for end-stage liver disease) and Child-Pugh scores, serum albumin, total bilirubin, aspartate aminotransferase(AST), alanine aminotransferase(ALT), and coagulation function (146).

As mentioned in the *in vitro* studies and animal models of liver disease, the application of MSCs helps improve liver function with different mechanisms in humans. A study conducted by Lanman Xu in 2014 showed that BM-MSCs improve the symptoms of patients with HBV associated Cirrhosis. The findings in this study showed that the number and ratio of Treg cells in PBMCs isolated from patients increased; however, the number of Th17 cells in patients treated with BM-MSCs decreased. Also, extraction of total RNA and evaluation of the expression of Foxp3 and RORγt transcription factors by Real-time polymerase chain reaction (RT-PCR) showed an increase in Foxp3 expression and a decrease in RORγt expression compared to the control group. Also, examination of patients' serum in the first week after transplantation showed an increase in TGF-B and a decrease in inflammatory cytokines such as IL1-B, IL-6 and TNF-a. Therefore, in general, transplantation of MSCs by modulating the Treg/Th17 axis and modulating the production of inflammatory cytokines helps improve liver inflammation and patient conditions (147).

The results of a study conducted in 2020 by Federica Casiraghi et al. Show that intravenous injection of MSCs before liver transplantation does not improve the parameters of chance tissue compared to the group that received this treatment. However, a one-year follow-up of patients shows a slight increase in the circulating Treg/memory Treg and tolerant NK subset ($CD56^{bright}$ NK cells) over baseline (not significant) in MSC-treated compared to the control group (148).

As shown in **Table 2**, the disadvantages of using MSCs, encourage researchers to find safer and more efficient methods. As has been proven in many studies, MSCs perform their therapeutic functions after transplantation in two ways: cell-to-cell communication and secretion of soluble factors (paracrine effect). EVs are one of the main factors in this type (149).

6 MSCS-DERIVED EVS APPLICATION IN LIVER DISEASE TREATMENT

EVs are a significant component of intercellular communication that affect the actions of the target cell by transporting various substances, including proteins, lipids, and nucleic acids, from the producing cell to the target cell (150). These vesicles are divided into microvesicles (MVs), apoptotic bodies and exosomes according to their size, internal contents, biogenesis and different surface markers (151). However, the fourth group of these vesicles, smaller than the rest, has been identified as named exomer (152). Each of these vesicles has different contents, typically containing various proteins (including enzymes, cytokines, growth factors and heat shock proteins), different types of nucleic acids (including DNA, microRNA and lncRNAs) and different types of lipids (153). These molecules change target cell function after transferring by EVs bilipid membrane. As a consequence, and depending on the cell type and its physiological conditions, exosomes can lead to differentiation, increase proliferation and survival, or lead to increased apoptosis and decreased cell activity (154).

Many studies have examined the therapeutic effects of MSC derived EVs (MSC-EVs) in different diseases such as pulmonary fibrosis, osteoporosis, skin diseases, cardiovascular diseases, and various liver-related diseases. The results of new studies show that the application of MSCs-EVs has similar therapeutic effects to MSCs (155–157). In fact, the use of EVs is cell-free cell therapy because it preserves the benefits associated with cell therapy and bypasses its disadvantages. These benefits include: (1) lack of immunogenicity, (2) the ability to store them easily, (3) drug loading and increase their efficiency as a drug delivery system and (4) application as a ready-to-use drug (cryopreservation of EVs) (158).

Given that the results of many *in vitro* and animal model studies have shown that MSCs can migrate to TME, it is thought to be they can be used as carriers for tumor-targeted therapies (159). However, there is little clinical evidence of MSCs recruitment in hepatocellular carcinoma (160). Also, due to the proliferative and differentiating characteristics of MSCs, considering the possibility of malignant transformation and promotion of tumor progression by these cells, most studies are still in the preclinical stage (159). Therefore, to use the therapeutic properties of these cells, researchers used MSC-EVs that do not have these deficiencies (161). Recent studies show that adipose tissue MSCs derived exosomes (MSC-Ex) can increase the chemical sensitivity of liver cancer cells by affecting the mTOR related signaling pathway and leading to increased expression of chemo-sensitive related genes in cancer cells (162). Further studies have shown that these exosomes perform this function by transferring miR-199a to cancer cells (162). MiR-222-3p in BM-MSC-Ex has also been shown to inhibit cancer cell proliferation and increase their apoptosis (163). Another study showed that miR-302a, carried by UC-MSC-Ex, suppressed cyclin D1 as well as the AKT signaling pathway and thereby suppress tumor progression (164). Also, various anti-tumour drugs can be loaded into exosomes

and used as targeted therapy (165). In addition, it has been shown that exosomes can be engineered to migrate to the target site, integrate with cancer cells, and deliver anti-tumor drugs to them (166, 167). However, the application of MSC-Ex is still in its initiation, and further studies are needed for their optimal use.

As mentioned, due to the size of MSCs, when injected intravenously, they accumulate in the lungs while EVs are much smaller and can migrate to the site of injury (168). MSC-EVs exert their therapeutic functions through 3 mechanisms that have been studied *in vitro*, pre-clinical, and clinical trials. These mechanisms include (1) proliferation induction/apoptosis suppression, (2) modulation of immune system responses, (3) reduction of fibrosis. **Table 4** summarizes several new studies on the application of MSC-EVs (**Figure 4**).

6.1 Stimulation of Proliferation/ Suppression of Apoptosis in Hepatocytes

Examination of the effects of MSCs-derived exosomes *in vivo* shows that these vesicles suppress acetaminophen and H2O2-induced apoptosis in hepatocytes by positively regulating Bcl-xl expression (175). Also, the study shows that MSC-Ex stimulates hepatocytes proliferation in CCL4-induced liver damage in mice. Further studies show that the exosomes positively regulate the priming phase genes, which is subsequently increases the expression of Proliferating cell nuclear antigen (PCNA) and cyclin D1 in the treated group compared to the control group (175).

The results of new studies show that the use of BM-MSCs-Ex reduces apoptosis by increasing autophagy in hepatocytes. A study by Shuxian Zhao et al. Shows that the use of BM-MSCs-Ex reduces D-GaIN/LPS-induced apoptosis in rats hepatocytes. Further studies show that autophagy-related markers such as LC3 and Beclin-1 are increased and have led to autophagosomes formation by hepatocytes. Also, the expression level of apoptosis-related proteins such as Bax and cleaved caspase 3 was decreased, and the expression level of Bcl-2 (anti-apoptotic protein) was increased. Because the use of 3-Methyladenine (3-MA), an autophagy inhibitor, limited the therapeutic effects of BM-MSCs-Ex, this study attributed the main therapeutic mechanism of these vesicles to the regulation of apoptosis in an autophagy-dependent manner (176).

A study conducted by Yinpeng Jin et al. In 2018 shows that the use of AD-MSCs-EVs in the model of acute liver failure in rats increases the survival rate by more than 70% compared to the control group. Liver sequencing of rats treated with AD-MSCs-EVs demonstrated an increase in a non-coding long-stranded RNA (lncRNA) called lncRNA H19 (H19), and when the coding sequence of H19 in AD-MSCs of EVs source was knocked off, survival rates could be 40% higher than the control group. In fact, H19 encoding gene silencing reduces the survival of rats compared to the AD-MSCs-EVs treated group. The results of hepatocytes Co-culture with normal AD-MSCs-EVs and manipulated AD-MSCs-EVs (lacking H19) indicate that this lncRNA increases the proliferation of hepatocytes by the HGF/c-Met signaling pathway as well as reducing apoptosis (177).

6.2 Immunomodulatory Properties

The results of a study by H Haga et al. show that administration of BM-MSC-derived EVs to mice with liver injury induced by Intraperitoneal (IP) injection of TNF-a and D-gal increases the migration of protective macrophages to damaged liver tissue. Another study showed that injections of MSC-EVs into a mouse model of ischemic-reperfusion injury helped reduce inflammatory responses by modulating the expression of NLRP12 and CXCL1. This study also showed that the frequency of $F4/80^+$ cells (expressed in protective macrophages) in the damaged liver increased significantly after MSCs-EVs injection (178).

Con-A-induced liver injury studies in C57/B6 male mice show extensive modulation of the immune system by AD-MSCs-Ex in the treatment group compared to the control group. The analyses showed that the expression of IL-2 (a pro-inflammatory cytokine) was associated with a significant decrease. On the other hand, the expression of cytokine TGF-β and HGF was upregulated. Also, the percentage of Treg cells among non-parenchymal liver cells (NPCs) in the three doses of AD-MSCs-Ex treated group increased significantly. Treg has been reported to be required to induce immune tolerance in this liver injury model (179). This study also compared the therapeutic effects of AD-MSC injection and one-dose injection of AD-MSCs-Ex with 3-dose injection. The present results of the study show a significant difference in the therapeutic application 3-dose injection of AD-MSCs-Ex with other groups. Histological and serum analysis also confirmed a decrease in fibrotic and necrotic areas of the liver and a decrease in ALT levels in the treated groups (177).

Using the protein chip method by Xiaoli Rong et al. showed that in treatment of D-GaIN/LPS induced damages in rats with AD-MSCs-EVs, the expression of inflammatory cytokines including IL-6, IL-1α, IL-1β, IL-1ra and IL-17 in was significantly lower than in the Phosphate-buffered saline (PBS) treatment group. Also, the level of inflammatory chemokines such as CXCL7, CXCL9, CXCL10, CCL20, CX3CL1, CINC-3, CINC-2α/β, CINC-1, CNTF, and LECAM-1 decreases in the AD-MSCs-Ev treated group compared to the control group PBS treated group. Simultaneous reduction of inflammatory cytokines and chemokines ultimately leads to a reduction in liver tissue necrosis and an increase in the survival rate of rats (180). Evaluation of inflammatory cytokines including TNF-α, IL-1, IL-2, IL-6, IL-8, and IL-10 and in liver tissue using RT-PCR showed a significant reduction in rats treated by hBM-MSCs and hBM-MSCs-Ex. However, the results of this study showed that the expression of IL-6 and IL-1 in the hBM-MSCs-Ex treatment group was significantly lower than in the hBM-MSCs treated group (181).

Also, the study of malondialdehyde (MDA) levels, which is the end product of membrane lipid peroxidation, can be used as a marker for oxidative stress and liver cell damage. Analysis in hBM-MSCs-Ex treated rats (CCL4-induced liver injury) showed a significant reduction in MDA level (181).

6.3 Reduce Hepatic Fibrosis

The results of a study conducted in 2019 (181) show that the administration of hBM-MSCs-Ex to rats with CCL4-induced

TABLE 4 | Example of studies in the field of MSC-EV application in experimental models of liver injury and their therapeutic mechanisms.

Injury model	Source of MSCs	Acute Or chronic phase	EVs type	Route of administration	Dosage (vesicles/ animal)	Effect(s)	Mechanism(s)	Year	Ref.
CCl4-induced acute liver injury(mouse)	hUC-MSCs	Chronic	Exosome	Intrahepatic	250 μg	1. Inhibited hepatocyte apoptosis 2. Reduce liver fibrosis 3. Reduce the serum levels of HA	1. Suppressed TGF-b signaling and inhibited EMT 2. Reduced collagen-1 and 3 expression	2013	(169)
Hepatic ischemia-reperfusion (mouse)	mBM-MSC	Acute	EVs	Intravenous	2×10^{10}	1. Reduction of inflammatory mediators 2. inhibition of Apoptosis 3. Increase the number of F4/80 positive cells	1. Suppress NF-κB activity 2. increased CXCL1 release from AML12 hepatocytes *in vitro*	2017	(170)
In vitro ischemia/ reperfusion Partial hepatectomy (mouse)	mAD-MSC	Acute	Secretome (EVs + other soluble factors)	Intravenous	N/A	1. Reduce serum IL-6 and TNF-a levels 2. Reduce serum transaminases 3. Accelerate liver regeneration 4. Increase the hepatocyte proliferation	1. Increased p-STAT3 and PCNA expression 2. Decreased hepatic expression of SOCS3 3. increased SIRT1 Increase in survival genes (e.g., Bcl-xL and Mcl-1)	2017	(171)
Thioacetamide induced (rat)	Human embryonic MSC	Chronic	EVs	Intrahepatic	350 μg	1. Reduction of fibrosis 2. Reduction inflammation	1. upregulation in MMP9 and MMP13 2. upregulation of BCL-2 3. upregulation of TGF-β1 and IL-10 4. downregulation of Col1α, αSMA and TIMP1 5. downregulation BAX, TNFα and IL-2	2018	(172)
CCl4-induced acute liver injury(mouse)	hUC-MSCs	Acute	Exosome	Intravenous Or intragastric	8, 16, and 32 mg/kg	1. Reduction of oxidative stress 2. inhibition of Apoptosis 3. Increased cell viability	1. Reduced levels of ROS 2. Upregulated Bcl2 expression	2017	(173)
S.japonicum-infected mice	hUC-MSCs	Chronic	EVs	intravenous	3×10^{9}	1. Reduce liver fibrosis 2. suppress HSCs function 3. Reduction inflammation	1. Reduced collagen-1 and 3 expression 2. Reduced α-SMA expression 3. significantly decrease TNF-α and IL-1β expression	2020	(174)

MSCs, Mesenchymal stromal/stem cells; EVs, Extracellular vesicles; TGF-β, Transforming growth factor-beta; NF-kB, Nuclear factor kappa-B; MMPs, Matrix metalloproteinase; NLRP, Nucleotide-binding oligomerization domain; ALT, alanine aminotransferase; AST, Aspartate transaminase; ALP, Alkaline Phosphatase; BM, Bone marrow; UC, umbilical cord; AD, adipose tissue; N/A, Not Applicable.

liver damage effectively reduces liver fibrosis. Visual examination showed that the liver of mice treated with hBM-MSCs-Ex had a smooth, uniform surface and softer tissue than the control group. Sirus red and H&E staining show reduction of fibrous areas and collagen deposition in the treated liver. In addition, comparing the therapeutic effects of hBM-MSCs-Exo and hBM-MSCs indicates the better therapeutic outcome in the application of hBM-MSCs-Ex due to the collagen deposition level and Ishak fibrosis score. Examination of the hydroxyproline levels, unnecessary amino acid and a major component of collagen also shows a decrease in this amino acid in the treated group and indicates a reduction in collagen deposition. In this study, the biochemical analysis showed that the level of AST, ALT, ALP, total bilirubin (TBIL) and gamma-glutamyl transferase (γ-GT) decreases, and serum total protein (TP) levels increases in serum. Examination of Wnt/β-catenin signaling related factors including PPARγ, Wnt10b, Wnt3a, β-catenin, and WISP1 in both *in vivo* and *in vitro* conditions indicates the use of hBM-MSCs and hBM-MSCs-Ex (have better therapeutic results) reduce the expression of these factors in HSCs (*in vitro*) and

with rat fibrous liver. Due to the reduction of collagen deposition and fibrotic tissue in the damaged liver, the results of this study suggest using hBM-MSCs-Ex leads to decreased HSCs function and reduced fibrosis by inhibiting the Wnt/β-catenin signaling pathway (181).

7 CONCLUSIONS AND FUTURE PROSPECTS

Due to the urgent need to treat tissue degenerative diseases, methods that can accelerate tissue repair are of great value. Using MSCs as multipotent stem cells is one of these widely used methods due to its properties. As mentioned, these cells uses different mechanisms such as differentiation into hepatocyte-like cells, reducing apoptosis and increasing hepatocyte proliferation, reducing inflammation, suppressing tissue-damaging immune cells, producing various growth factors, suppressing the function of HSC, and improving the function of LSECs to improve liver diseases. The use of these cells not only prevents further damage to the liver tissue but also accelerates and increases the repair of liver tissue. MSCs migrate to the site of liver injury after intravenous injection due to their chemokine receptors and perform their therapeutic actions there. As mentioned earlier, due to the limitations of cell therapy, MSC-EVs are used today. Many studies have been conducted on the application of MSC-EVs in preclinical studies. The results of these studies indicate the potential ability of these vesicles to improve liver cell function and modulate the immune system (182). Some studies comparing the therapeutic effect of MSCs and MSC-EVs have shown that MSC-EVs have a higher therapeutic potential and better outcomes. Although the therapeutic effects of EVs on liver repair in this study are divided into three distinct mechanisms, these processes are interrelated and complement each other's functions. In fact, the therapeutic potential of MSC-EVs likely lies in their ability to act simultaneously through multiple signaling pathways. Therefore, using these vesicles does not have cell therapy disadvantages. Due to its benefits, it can perform better therapeutic performance in liver injury animals models.

Although there are numerous clinical trials on the use of MSCs in the treatment of liver disease, to date, no clinical trials have been performed on the use of MSC-EVs despite their benefits. However, it has been used to treat many disorders, including orthopaedic disease (151), neurodegenerative disease (183), myocardial disease (184), renal disease, graft versus host disease (GvHD), pancreatic cancer and type 1 diabetes and has shown promising results (185). Despite the therapeutic potential of MSC-EVs and their beneficial effects in preclinical studies, several issues related to the clinical use of these vesicles remain unresolved. Exosomes as an EV circulate in the blood and transfer their cargos to the target cell through phagocytosis, receptor-mediated endocytosis, fusion, micropinocytosis (186). In the body, the half-life of EVs is estimated at a few minutes and are removed from the bloodstream within a few hours. Therefore, we need multiple injections to treat diseases. Due to this issue, producing EVs in an industrial scale and repeatable method is significant. It is also important to note that despite effective and proven results in animal models, the improvement of these models is usually incomplete. Therefore, more research is needed to investigate the long-term effects of MSC-EVs.

AUTHOR CONTRIBUTIONS

AH: Conceptualization, Investigation, Writing - original draft, Writing - review and editing, Validation. KM: Writing - review and editing, Validation. SS: Edited final version of the manuscript. SH: Supervision and final approval of the manuscript. All authors contributed to the article and approved the submitted version.

REFERENCES

1. Ertek S, Cicero A. Impact of Physical Activity on Inflammation: Effects on Cardiovascular Disease Risk and Other Inflammatory Conditions. *Arch Med Sci: AMS* (2012) 8(5):794. doi: 10.5114/aoms.2012.31614
2. Kiecolt-Glaser JK, Gouin J-P, Hantsoo L. Close Relationships, Inflammation, and Health. *Neurosci Biobehav Rev* (2010) 35(1):33–8. doi: 10.1016/j.neubiorev.2009.09.003
3. Verhamme P, Hoylaerts MF. Hemostasis and Inflammation: Two of a Kind? *Thromb J* (2009) 7(1):1–3. doi: 10.1186/1477-9560-7-15
4. Starlinger P, Luyendyk JP, Groeneveld DJ eds. Hemostasis and Liver Regeneration. In: *Seminars in Thrombosis and Hemostasis*. Thieme Medical Publishers.
5. Ang CH, Hsu SH, Guo F, Tan CT, Victor CY, Visvader JE, et al. Lgr5+ Pericentral Hepatocytes Are Self-Maintained in Normal Liver Regeneration and Susceptible to Hepatocarcinogenesis. *Proc Natl Acad Sci* (2019) 116 (39):19530–40. doi: 10.1073/pnas.1908099116
6. Fausto N, Campbell JS, Riehle KJ. Liver Regeneration. *J Hepatol* (2012) 57 (3):692–4. doi: 10.1016/j.jhep.2012.04.016
7. Laleman W, Claria J, van der Merwe S, Moreau R, Trebicka J. Systemic Inflammation and Acute-on-Chronic Liver Failure: Too Much, Not Enough. *Can J Gastroenterol Hepatol* (2018) 2018:1027152. doi: 10.1155/2018/1027152
8. Stravitz RT, Lee WM. Acute Liver Failure. *Lancet* (2019) 394(10201):869–81. doi: 10.1016/S0140-6736(19)31894-X
9. Anderson SH, Richardson P, Wendon J, Pagliuca A, Portmann B. Acute Liver Failure as the Initial Manifestation of Acute Leukaemia. *Liver* (2001) 21(4):287–92. doi: 10.1034/j.1600-0676.2001.021004287.x
10. Shakil AO, Kramer D, Mazariegos GV, Fung JJ, Rakela J. Acute Liver Failure: Clinical Features, Outcomeanalysis, and Applicability of Prognostic Criteria. *Liver Transplant* (2000) 6(2):163–9. doi: 10.1016/S1527-6465(00)80005-2
11. Jalan R. Acute Liver Failure: Current Management and Future Prospects. *J Hepatol* (2005) 42(1):S115–S23. doi: 10.1016/j.jhep.2004.11.010
12. Kanjo A, Ocskay K, Gede N, Kiss S, Szakács Z, Párniczky A, et al. Efficacy and Safety of Liver Support Devices in Acute and Hyperacute Liver Failure: A Systematic Review and Network Meta-Analysis. *Sci Rep* (2021) 11(1):1–10. doi: 10.1038/s41598-021-83292-z
13. Bernal W, Wendon J. Acute Liver Failure. *N Engl J Med* (2013) 369 (26):2525–34. doi: 10.1056/NEJMra1208937
14. Bataller R, Brenner DA. Liver Fibrosis. *J Clin Invest* (2005) 115(2):209–18. doi: 10.1172/JCI24282
15. Tripodi A, Mannucci PM. The Coagulopathy of Chronic Liver Disease. *N Engl J Med* (2011) 365(2):147–56. doi: 10.1056/NEJMra1011170
16. Tsukada S, Parsons CJ, Rippe RA. Mechanisms of Liver Fibrosis. *Clin Chim Acta* (2006) 364(1-2):33–60. doi: 10.1016/j.cca.2005.06.014

17. Skrypnyk NI, Harris RC, de Caestecker MP. Ischemia-Reperfusion Model of Acute Kidney Injury and Post Injury Fibrosis in Mice. *J Vis Exp: JoVE* (2013) 78:e50495. doi: 10.3791/50495
18. Vasarmidi E, Tsitoura E, Spandidos DA, Tzanakis N, Antoniou KM. Pulmonary Fibrosis in the Aftermath of the COVID-19 Era. *Exp Ther Med* (2020) 20(3):2557–60. doi: 10.3892/etm.2020.8980
19. Renk H, Regamey N, Hartl D. Influenza A (H1N1) Pdm09 and Cystic Fibrosis Lung Disease: A Systematic Meta-Analysis. *PloS One* (2014) 9(1): e78583. doi: 10.1371/journal.pone.0078583
20. Sadeghi S, Soudi S, Shafiee A, Hashemi SM. Mesenchymal Stem Cell Therapies for COVID-19: Current Status and Mechanism of Action. *Life Sci* (2020) 262:118493. doi: 10.1016/j.lfs.2020.118493
21. Khosrojerdi A, Soudi S, Hosseini AZ, Khaligh SG, Hashemi SM. Imipenem Alters Systemic and Liver Inflammatory Responses in CLP-Induced Sepsis Mice in a Dose-Dependent Manner. *Int Immunopharmacol* (2021) 93:107421. doi: 10.1016/j.intimp.2021.107421
22. Yang X, Meng Y, Han Z, Ye F, Wei L, Zong C. Mesenchymal Stem Cell Therapy for Liver Disease: Full of Chances and Challenges. *Cell Biosci* (2020) 10(1):1–18. doi: 10.1186/s13578-020-00480-6
23. Lee SM, Lee SD, Wang SZ, Sarkar D, Lee HM, Khan A, et al. Effect of Mesenchymal Stem Cell in Liver Regeneration and Clinical Applications. *Hepatoma Res* (2021) 7:53. doi: 10.20517/2394-5079.2021.07
24. Kaushal S, Amiel GE, Guleserian KJ, Shapira OM, Perry T, Sutherland FW, et al. Functional Small-Diameter Neovessels Created Using Endothelial Progenitor Cells Expanded *Ex Vivo*. *Nat Med* (2001) 7(9):1035–40. doi: 10.1038/nm0901-1035
25. Asahara T, Murohara T, Sullivan A, Silver M, van der Zee R, Li T, et al. Isolation of Putative Progenitor Endothelial Cells for Angiogenesis. *Science* (1997) 275(5302):964–6. doi: 10.1126/science.275.5302.964
26. Martinez-Agosto JA, Mikkola HK, Hartenstein V, Banerjee U. The Hematopoietic Stem Cell and Its Niche: A Comparative View. *Genes Dev* (2007) 21(23):3044–60. doi: 10.1101/gad.1602607
27. Panteleev A, Vorob'ev I. Expression of Early Hematopoietic Markers in Cord Blood and Mobilized Blood. *Tsitologiia* (2012) 54(10):774–82. doi: 10.21037/atm.2020.03.218
28. Lázaro CA, Rhim JA, Yamada Y, Fausto N. Generation of Hepatocytes From Oval Cell Precursors in Culture. *Cancer Res* (1998) 58(23):5514–22.
29. Zaret KS, Grompe M. Generation and Regeneration of Cells of the Liver and Pancreas. *Science* (2008) 322(5907):1490–4. doi: 10.1126/science.1161431
30. Weber A, Touboul T, Mainot S, Branger J, Mahieu-Caputo D. Human Foetal Hepatocytes: Isolation, Characterization, and Transplantation. *Hepatocytes: Springer;* (2010) p:41–55. doi: 10.1007/978-1-60761-688-7_2
31. Forbes SJ, Gupta S, Dhawan A. Cell Therapy for Liver Disease: From Liver Transplantation to Cell Factory. *J Hepatol* (2015) 62(1):S157–S69. doi: 10.1016/j.jhep.2015.02.040
32. Zhou H, Liu H, Ezzelarab M, Schmelzer E, Wang Y, Gerlach J, et al. Experimental Hepatocyte Xenotransplantation—A Comprehensive Review of the Literature. *Xenotransplantation* (2015) 22(4):239–48. doi: 10.1111/xen.12170
33. Mizukoshi E, Kaneko S. Immune Cell Therapy for Hepatocellular Carcinoma. *J Hematol Oncol* (2019) 12(1):1–11. doi: 10.1186/s13045-019-0742-5
34. Medvedev S, Shevchenko A, Zakian S. Induced Pluripotent Stem Cells: Problems and Advantages When Applying Them in Regenerative Medicine. *Acta Naturae (англоязычная версия)* (2010) 2(2):18–28.
35. Yu Y, Fisher JE, Lillegard JB, Rodysill B, Amiot B, Nyberg SL. Cell Therapies for Liver Diseases. *Liver Transplant* (2012) 18(1):9–21. doi: 10.1002/lt.22467
36. Satija NK, Singh VK, Verma YK, Gupta P, Sharma S, Afrin F, et al. Mesenchymal Stem Cell-Based Therapy: A New Paradigm in Regenerative Medicine. *J Cell Mol Med* (2009) 13(11-12):4385–402. doi: 10.1111/j.1582-4934.2009.00857.x
37. Huang L, Zhang C, Gu J, Wu W, Shen Z, Zhou X, et al. A Randomized, Placebo-Controlled Trial of Human Umbilical Cord Blood Mesenchymal Stem Cell Infusion for Children With Cerebral Palsy. *Cell Transplant* (2018) 27(2):325–34. doi: 10.1177/0963689717729379
38. Hu C, Zhao L, Zhang L, Bao Q, Li L. Mesenchymal Stem Cell-Based Cell-Free Strategies: Safe and Effective Treatments for Liver Injury. *Stem Cell Res Ther* (2020) 11(1):1–12. doi: 10.1186/s13287-020-01895-1
39. Kang SH, Kim MY, Eom YW, Baik SK. Mesenchymal Stem Cells for the Treatment of Liver Disease: Present and Perspectives. *Gut Liver* (2020) 14 (3):306. doi: 10.5009/gnl18412
40. Bernardo ME, Cometa AM, Pagliara D, Vinti L, Rossi F, Cristantielli R, et al. *Ex Vivo* Expansion of Mesenchymal Stromal Cells. *Best Pract Res Clin Haematol* (2011) 24(1):73–81. doi: 10.1016/j.beha.2010.11.002
41. Ozougwu JC. Physiology of the Liver. *Int J Res Pharm Biosci* (2017) 4 (8):13–24.
42. Wu Z, Han M, Chen T, Yan W, Ning Q. Acute Liver Failure: Mechanisms of Immune-Mediated Liver Injury. *Liver Int* (2010) 30(6):782–94. doi: 10.1111/j.1478-3231.2010.02262.x
43. Gao B. Basic Liver Immunology. *Cell Mol Immunol* (2016) 13(3):265–6. doi: 10.1038/cmi.2016.09
44. Bernal W, Auzinger G, Dhawan A, Wendon J. Acute Liver Failure. *Lancet* (2010) 376(9736):190–201. doi: 10.1016/S0140-6736(10)60274-7
45. Rutherford A, Chung RT eds. Acute Liver Failure: Mechanisms of Hepatocyte Injury and Regeneration. In: *Seminars in Liver Disease*. Thieme Medical Publishers.
46. Ramadori G, Moriconi F, Malik I, Dudas J. Physiology and Pathophysiology of Liver Inflammation, Damage and Repair. *J Physiol Pharmacol* (2008) 59 (Suppl 1):107–17.
47. Lazo M, Hernaez R, Bonekamp S, Kamel IR, Brancati FL, Guallar E, et al. Non-Alcoholic Fatty Liver Disease and Mortality Among US Adults: Prospective Cohort Study. *BMJ* (2011) 343:d6891. doi: 10.1136/bmj.d6891
48. Marjot T, Moolla A, Cobbold JF, Hodson L, Tomlinson JW. Nonalcoholic Fatty Liver Disease in Adults: Current Concepts in Etiology, Outcomes, and Management. *Endocr Rev* (2020) 41(1):66–117. doi: 10.1210/endrev/bnz009
49. Asrih M, Jornayvaz FR. Inflammation as a Potential Link Between Nonalcoholic Fatty Liver Disease and Insulin Resistance. *J Endocrinol* (2013) 218(3):R25–36. doi: 10.1530/JOE-13-0201
50. Lin R, Wu D, Wu F-J, Meng Y, Zhang J-H, Wang X-G, et al. Non-Alcoholic Fatty Liver Disease Induced by Perinatal Exposure to Bisphenol a Is Associated With Activated mTOR and TLR4/NF-κb Signaling Pathways in Offspring Rats. *Front Endocrinol* (2019) 10:620. doi: 10.3389/fendo.2019.00620
51. Arshad MI, Piquet-Pellorce C, Samson M. IL-33 and HMGB 1 Alarmins: Sensors of Cellular Death and Their Involvement in Liver Pathology. *Liver Int* (2012) 32(8):1200–10. doi: 10.1111/j.1478-3231.2012.02802.x
52. McDonald B, Pittman K, Menezes GB, Hirota SA, Slaba I, Waterhouse CC, et al. Intravascular Danger Signals Guide Neutrophils to Sites of Sterile Inflammation. *Science* (2010) 330(6002):362–6. doi: 10.1126/science.1195491
53. Mihm S. Danger-Associated Molecular Patterns (DAMPs): Molecular Triggers for Sterile Inflammation in the Liver. *Int J Mol Sci* (2018) 19 (10):3104. doi: 10.3390/ijms19103104
54. Nguyen-Lefebvre AT, Horuzsko A. Kupffer Cell Metabolism and Function. *J Enzymol Metab* (2015) 1(1):101.
55. Kisseleva T, Brenner D. Molecular and Cellular Mechanisms of Liver Fibrosis and Its Regression. *Nat Rev Gastroenterol Hepatol* (2021) 18 (3):151–66. doi: 10.1038/s41575-020-00372-7
56. He Y, Jin L, Wang J, Yan Z, Chen T, Zhao Y. Mechanisms of Fibrosis in Acute Liver Failure. *Liver Int* (2015) 35(7):1877–85. doi: 10.1111/liv.12731
57. Poynard T, Mathurin P, Lai C-L, Guyader D, Poupon R, Tainturier M-H, et al. A Comparison of Fibrosis Progression in Chronic Liver Diseases. *J Hepatol* (2003) 38(3):257–65. doi: 10.1016/S0168-8278(02)00413-0
58. Ramos-Tovar E, Muriel P. Molecular Mechanisms That Link Oxidative Stress, Inflammation, and Fibrosis in the Liver. *Antioxidants* (2020) 9 (12):1279. doi: 10.3390/antiox9121279
59. Lemoinne S, Cadoret A, El Mourabit H, Thabut D, Housset C. Origins and Functions of Liver Myofibroblasts. *Biochim Biophys Acta (BBA)-Mol Basis Dis* (2013) 1832(7):948–54. doi: 10.1016/j.bbadis.2013.02.019
60. Lu D-H, Guo X-Y, Qin S-Y, Luo W, Huang X-L, Chen M, et al. Interleukin-22 Ameliorates Liver Fibrogenesis by Attenuating Hepatic Stellate Cell Activation and Downregulating the Levels of Inflammatory Cytokines. *World J Gastroenterol: WJG* (2015) 21(5):1531. doi: 10.3748/wjg.v21.i5.1531
61. Gandhi CR. Hepatic Stellate Cell Activation and Pro-Fibrogenic Signals. *J Hepatol* (2017) 67(5):1104–5. doi: 10.1016/j.jhep.2017.06.001

62. Tsuchida T, Friedman SL. Mechanisms of Hepatic Stellate Cell Activation. *Nat Rev Gastroenterol Hepatol* (2017) 14(7):397–411. doi: 10.1038/nrgastro.2017.38
63. Shi H, Dong L, Dang X, Liu Y, Jiang J, Wang Y, et al. Effect of Chlorogenic Acid on LPS-Induced Proinflammatory Signaling in Hepatic Stellate Cells. *Inflamm Res* (2013) 62(6):581–7. doi: 10.1007/s00011-013-0610-7
64. Pinzani M, Rosselli M, Zuckermann M. Liver Cirrhosis. *Best Pract Res Clin Gastroenterol* (2011) 25(2):281–90. doi: 10.1016/j.bpg.2011.02.009
65. He G, Karin M. NF-κb and STAT3–key Players in Liver Inflammation and Cancer. *Cell Res* (2011) 21(1):159–68. doi: 10.1038/cr.2010.183
66. Wu W-Y, Li J, Wu Z-S, Zhang C-L, Meng X-L. STAT3 Activation in Monocytes Accelerates Liver Cancer Progression. *BMC Cancer* (2011) 11 (1):1–10. doi: 10.1186/1471-2407-11-506
67. Finkin S, Pikarsky E. NF-κb in Liver Cancer: The Plot Thickens. *NF-kB Health Dis* (2010) 349:185–96. doi: 10.1007/82_2010_104
68. Bishayee A. The Inflammation and Liver Cancer. *Inflamm Cancer* (2014) 816:401–35. doi: 10.1007/978-3-0348-0837-8_16
69. Ölander M, Wiśniewski JR, Artursson P. Cell-Type-Resolved Proteomic Analysis of the Human Liver. *Liver Int* (2020) 40(7):1770–80. doi: 10.1111/liv.14452
70. Knolle P, Löhr H, Treichel U, Dienes H, Lohse A, Schlaack J, et al. Parenchymal and Nonparenchymal Liver Cells and Their Interaction in the Local Immune Response. *Z fur Gastroenterol* (1995) 33(10):613–20.
71. Kimura T, Flynn CT, Whitton JL. Hepatocytes Engulf and Rapidly Silence Coxsackievirus, Protecting the Host Against Systemic Viral Pathology. *Am Assoc Immnol* (2020) 3:1–10. doi: 10.1038/s42003-020-01303-7
72. Zhou Z, Xu M-J, Gao B. Hepatocytes: A Key Cell Type for Innate Immunity. *Cell Mol Immunol* (2016) 13(3):301–15. doi: 10.1038/cmi.2015.97
73. Kubes P, Mehal WZ. Sterile Inflammation in the Liver. *Gastroenterology* (2012) 143(5):1158–72. doi: 10.1053/j.gastro.2012.09.008
74. Kushner I, Mackiewicz A. The Acute Phase Response: An Overview. *Acute Phase Proteins* (2020), 3–19. doi: 10.1201/9781003068587-2
75. Fazel Modares N, Polz R, Haghighi F, Lamertz L, Behnke K, Zhuang Y, et al. IL-6 Trans-Signaling Controls Liver Regeneration After Partial Hepatectomy. *Hepatology* (2019) 70(6):2075–91. doi: 10.1002/hep.30774
76. Crispe IN. Hepatocytes as Immunological Agents. *J Immunol* (2016) 196 (1):17–21. doi: 10.4049/jimmunol.1501668
77. Kenna T, Golden-Mason L, Norris S, Hegarty JE, O'Farrelly C, Doherty DG. Distinct Subpopulations of γδ T Cells Are Present in Normal and Tumor-Bearing Human Liver. *Clin Immunol* (2004) 113(1):56–63. doi: 10.1016/j.clim.2004.05.003
78. Benseler V, Warren A, Vo M, Holz LE, Tay SS, Le Couteur DG, et al. Hepatocyte Entry Leads to Degradation of Autoreactive CD8 T Cells. *Proc Natl Acad Sci* (2011) 108(40):16735–40. doi: 10.1073/pnas.1112251108
79. Ebrahimkhani MR, Mohar I, Crispe IN. Cross-Presentation of Antigen by Diverse Subsets of Murine Liver Cells. *Hepatology* (2011) 54(4):1379–87. doi: 10.1002/hep.24508
80. Duarte N, Coelho IC, Patarrão RS, Almeida JI, Penha-Gonçalves C, Macedo MP. How Inflammation Impinges on NAFLD: A Role for Kupffer Cells. *BioMed Res Int* (2015) 2015:984578. doi: 10.1155/2015/984578
81. Ma Y-Y, Yang M-Q, He Z-G, Wei Q, Li J-Y. The Biological Function of Kupffer Cells in Liver Disease. *Biol Myelomonocytic Cells* (2017) 2. doi: 10.5772/67673
82. Li W, Deng M, Loughran PA, Yang M, Lin M, Yang C, et al. LPS Induces Active HMGB1 Release From Hepatocytes Into Exosomes Through the Coordinated Activities of TLR4 and Caspase-11/GSDMD Signaling. *Front Immunol* (2020) 11:229. doi: 10.3389/fimmu.2020.00229
83. Gaskell H, Ge X, Nieto N. High-Mobility Group Box-1 and Liver Disease. *Hepatol Commun* (2018) 2(9):1005–20. doi: 10.1002/hep4.1223
84. Reynaert H, Thompson M, Thomas T, Geerts A. Hepatic Stellate Cells: Role in Microcirculation and Pathophysiology of Portal Hypertension. *Gut* (2002) 50(4):571–81. doi: 10.1136/gut.50.4.571
85. Fujita T, Narumiya S. Roles of Hepatic Stellate Cells in Liver Inflammation: A New Perspective. *Inflamm Regen* (2016) 36(1):1–6. doi: 10.1186/s41232-016-0005-6
86. Fujita T, Soontrapa K, Ito Y, Iwaisako K, Moniaga CS, Asagiri M, et al. Hepatic Stellate Cells Relay Inflammation Signaling From Sinusoids to Parenchyma in Mouse Models of Immune-Mediated Hepatitis. *Hepatology* (2016) 63(4):1325–39. doi: 10.1002/hep.28112
87. Higashi T, Friedman SL, Hoshida Y. Hepatic Stellate Cells as Key Target in Liver Fibrosis. *Adv Drug Deliv Rev* (2017) 121:27–42. doi: 10.1016/j.addr.2017.05.007
88. Peralta C, Jiménez-Castro MB, Gracia-Sancho J. Hepatic Ischemia and Reperfusion Injury: Effects on the Liver Sinusoidal Milieu. *J Hepatol* (2013) 59(5):1094–106. doi: 10.1016/j.jhep.2013.06.017
89. Reifart J, Rentsch M, Mende K, Coletti R, Sobocan M, Thasler WE, et al. Modulating CD4+ T Cell Migration in the Postischemic Liver: Hepatic Stellate Cells as New Therapeutic Target? *Transplantation* (2015) 99(1):41–7. doi: 10.1097/TP.0000000000000461
90. Feng M, Wang Q, Wang H, Wang M, Guan W, Lu L. Adoptive Transfer of Hepatic Stellate Cells Ameliorates Liver Ischemia Reperfusion Injury Through Enriching Regulatory T Cells. *Int Immunopharmacol* (2014) 19 (2):267–74. doi: 10.1016/j.intimp.2014.01.006
91. Heymann F, Hamesch K, Weiskirchen R, Tacke F. The Concanavalin A Model of Acute Hepatitis in Mice. *Lab Anim* (2015) 49(1_suppl):12–20. doi: 10.1177/0023677215572841
92. Mizuhara H, O'Neill E, Seki N, Ogawa T, Kusunoki C, Otsuka K, et al. T Cell Activation-Associated Hepatic Injury: Mediation by Tumor Necrosis Factors and Protection by Interleukin 6. *J Exp Med* (1994) 179(5):1529–37. doi: 10.1084/jem.179.5.1529
93. Stark K, Eckart A, Haidari S, Tirniceriu A, Lorenz M, von Brühl M-L, et al. Capillary and Arteriolar Pericytes Attract Innate Leukocytes Exiting Through Venules And'instruct'them With Pattern-Recognition and Motility Programs. *Nat Immunol* (2013) 14(1):41–51. doi: 10.1038/ni.2477
94. Qin C-C, Liu Y-N, Hu Y, Yang Y, Chen Z. Macrophage Inflammatory Protein-2 as Mediator of Inflammation in Acute Liver Injury. *World J Gastroenterol* (2017) 23(17):3043. doi: 10.3748/wjg.v23.i17.3043
95. Lim HK, Jeffrey GP, Ramm GA, Soekmadji C. Pathogenesis of Viral Hepatitis-Induced Chronic Liver Disease: Role of Extracellular Vesicles. *Front Cell Infect Microbiol* (2020) 10. doi: 10.3389/fcimb.2020.587628
96. Marrone G, Shah VH, Gracia-Sancho J. Sinusoidal Communication in Liver Fibrosis and Regeneration. *J Hepatol* (2016) 65(3):608–17. doi: 10.1016/j.jhep.2016.04.018
97. Gracia-Sancho J, Caparrós E, Fernández-Iglesias A, Francés R. Role of Liver Sinusoidal Endothelial Cells in Liver Diseases. *Nat Rev Gastroenterol Hepatol* (2021) 18(6):411–31. doi: 10.1038/s41575-020-00411-3
98. Xie G, Wang X, Wang L, Wang L, Atkinson RD, Kanel GC, et al. Role of Differentiation of Liver Sinusoidal Endothelial Cells in Progression and Regression of Hepatic Fibrosis in Rats. *Gastroenterology* (2012) 142(4):918–27. e6. doi: 10.1053/j.gastro.2011.12.017
99. Lisman T, Luyendyk JP eds. Platelets as Modulators of Liver Diseases. In: *Seminars in Thrombosis and Hemostasis*. Thieme Medical Publishers.
100. Benedicto A, Herrero A, Romayor I, Marquez J, Smedsrød B, Olaso E, et al. Liver Sinusoidal Endothelial Cell ICAM-1 Mediated Tumor/Endothelial Crosstalk Drives the Development of Liver Metastasis by Initiating Inflammatory and Angiogenic Responses. *Sci Rep* (2019) 9(1):1–12. doi: 10.1038/s41598-019-49473-7
101. Géraud C, Mogler C, Runge A, Evdokimov K, Lu S, Schledzewski K, et al. Endothelial Transdifferentiation in Hepatocellular Carcinoma: Loss of Stabilin-2 Expression in Peri-Tumourous Liver Correlates With Increased Survival. *Liver Int* (2013) 33(9):1428–40. doi: 10.1111/liv.12262
102. Cogger VC, Arias IM, Warren A, McMahon AC, Kiss DL, Avery VM, et al. The Response of Fenestrations, Actin, and Caveolin-1 to Vascular Endothelial Growth Factor in SK Hep1 Cells. *Am J Physiol Gastrointest Liver Physiol* (2008) 295(1):G137–45. doi: 10.1152/ajpgi.00069.2008
103. Gracia-Sancho J, Laviña B, Rodríguez-Vilarrupla A, García-Calderó H, Bosch J, García-Pagán JC. Enhanced Vasoconstrictor Prostanoid Production by Sinusoidal Endothelial Cells Increases Portal Perfusion Pressure in Cirrhotic Rat Livers. *J Hepatol* (2007) 47(2):220–7. doi: 10.1016/j.jhep.2007.03.014
104. Rosado E, Rodríguez-Vilarrupla A, Gracia-Sancho J, Monclús M, Bosch J, García-Pagán JC. Interaction Between NO and COX Pathways Modulating Hepatic Endothelial Cells From Control and Cirrhotic Rats. *J Cell Mol Med* (2012) 16(10):2461–70. doi: 10.1111/j.1582-4934.2012.01563.x
105. Marrone G, Russo L, Rosado E, Hide D, García-Cardeña G, García-Pagán JC, et al. The Transcription Factor KLF2 Mediates Hepatic Endothelial

Protection and Paracrine Endothelial–Stellate Cell Deactivation Induced by Statins. *J Hepatol* (2013) 58(1):98–103. doi: 10.1016/j.jhep.2012.08.026
106. Forbes SJ, Newsome PN. New Horizons for Stem Cell Therapy in Liver Disease. *J Hepatol* (2012) 56(2):496–9. doi: 10.1016/j.jhep.2011.06.022
107. Zhang S, Yang Y, Fan L, Zhang F, Li L. The Clinical Application of Mesenchymal Stem Cells in Liver Disease: The Current Situation and Potential Future. *Ann Trans Med* (2020) 8(8):565. doi: 10.21037/atm.2020.03.218
108. Taghavi-Farahabadi M, Mahmoudi M, Soudi S, Hashemi SM. Hypothesis for the Management and Treatment of the COVID-19-Induced Acute Respiratory Distress Syndrome and Lung Injury Using Mesenchymal Stem Cell-Derived Exosomes. *Med Hypotheses* (2020) 144:109865. doi: 10.1016/j.mehy.2020.109865
109. Zhang Y, Cai W, Huang Q, Gu Y, Shi Y, Huang J, et al. Mesenchymal Stem Cells Alleviate Bacteria-Induced Liver Injury in Mice by Inducing Regulatory Dendritic Cells. *Hepatology* (2014) 59(2):671–82. doi: 10.1002/hep.26670
110. Zhang Y, Yoneyama H, Wang Y, Ishikawa S, Hashimoto S-i, Gao J-L, et al. Mobilization of Dendritic Cell Precursors Into the Circulation by Administration of MIP-1α in Mice. *J Natl Cancer Inst* (2004) 96(3):201–9. doi: 10.1093/jnci/djh024
111. Vasandan AB, Jahnavi S, Shashank C, Prasad P, Kumar A, Prasanna SJ. Human Mesenchymal Stem Cells Program Macrophage Plasticity by Altering Their Metabolic Status *via* a PGE 2-Dependent Mechanism. *Sci Rep* (2016) 6(1):1–17. doi: 10.1038/srep38308
112. Taimr P, Higuchi H, Kocova E, Rippe RA, Friedman S, Gores GJ. Activated Stellate Cells Express the TRAIL Receptor-2/Death Receptor-5 and Undergo TRAIL-Mediated Apoptosis. *Hepatology* (2003) 37(1):87–95. doi: 10.1053/jhep.2003.50002
113. Li Y-H, Shen S, Shao T, Jin M-T, Fan D-D, Lin A-F, et al. Mesenchymal Stem Cells Attenuate Liver Fibrosis by Targeting Ly6Chi/lo Macrophages Through Activating the Cytokine-Paracrine and Apoptotic Pathways. *Cell Death Discov* (2021) 7(1):1–16. doi: 10.1038/s41420-021-00584-z
114. Saidi RF, Kenari SKH. Liver Ischemia/Reperfusion Injury: An Overview. *J Invest Surg* (2014) 27(6):366–79. doi: 10.3109/08941939.2014.932473
115. Cannistrà M, Ruggiero M, Zullo A, Gallelli G, Serafini S, Maria M, et al. Hepatic Ischemia Reperfusion Injury: A Systematic Review of Literature and the Role of Current Drugs and Biomarkers. *Int J Surg* (2016) 33:S57–70. doi: 10.1016/j.ijsu.2016.05.050
116. Shi X-L, Gu J-Y, Han B, Xu H-Y, Fang L, Ding Y-T. Magnetically Labeled Mesenchymal Stem Cells After Autologous Transplantation Into Acutely Injured Liver. *World J Gastroenterol: WJG* (2010) 16(29):3674. doi: 10.3748/wjg.v16.i29.3674
117. Maher JJ, Scott MK, Saito JM, Burton MC. Adenovirus-Mediated Expression of Cytokine-Induced Neutrophil Chemoattractant in Rat Liver Induces a Neutrophilic Hepatitis. *Hepatology* (1997) 25(3):624–30. doi: 10.1002/hep.510250322
118. Hewett JA, Schultze AE, VanCise S, Roth R. Neutrophil Depletion Protects Against Liver Injury From Bacterial Endotoxin. *Lab Invest J Tech Methods Pathol* (1992) 66(3):347–61.
119. Li S, Zheng X, Li H, Zheng J, Chen X, Liu W, et al. Mesenchymal Stem Cells Ameliorate Hepatic Ischemia/Reperfusion Injury via Inhibition of Neutrophil Recruitment. *J Immunol Res* (2018) 2018:7283703. doi: 10.1155/2018/7283703
120. Eash KJ, Greenbaum AM, Gopalan PK, Link DC. CXCR2 and CXCR4 Antagonistically Regulate Neutrophil Trafficking From Murine Bone Marrow. *J Clin Invest* (2010) 120(7):2423–31. doi: 10.1172/JCI41649
121. Yi T, Song SU. Immunomodulatory Properties of Mesenchymal Stem Cells and Their Therapeutic Applications. *Arch Pharm Res* (2012) 35(2):213–21. doi: 10.1007/s12272-012-0202-z
122. Wang H, Zhang H, Huang B, Miao G, Yan X, Gao G, et al. Mesenchymal Stem Cells Reverse High–Fat Diet–Induced Non–Alcoholic Fatty Liver Disease Through Suppression of CD4+ T Lymphocytes in Mice. *Mol Med Rep* (2018) 17(3):3769–74. doi: 10.3892/mmr.2017.8326
123. Lafdil F, Miller AM, Ki SH, Gao B. Th17 Cells and Their Associated Cytokines in Liver Diseases. *Cell Mol Immunol* (2010) 7(4):250–4. doi: 10.1038/cmi.2010.5
124. Jin Z, You J, Wang H. The Role of the Balance Between Th17 and Treg in Liver Disease. *Zhonghua Gan Zang Bing Za Zhi= Zhonghua Ganzangbing Zazhi= Chin J Hepatol* (2017) 25(8):637–40. doi: 10.3760/cma.j.issn.1007-3418.2017.08.017
125. Chen Q-H, Wu F, Liu L, H-b C, Zheng R-Q, Wang H-L, et al. Mesenchymal Stem Cells Regulate the Th17/Treg Cell Balance Partly Through Hepatocyte Growth Factor *In Vitro*. *Stem Cell Res Ther* (2020) 11(1):1–11. doi: 10.1186/s13287-020-01612-y
126. Milosavljevic N, Gazdic M, Simovic Markovic B, Arsenijevic A, Nurkovic J, Dolicanin Z, et al. Mesenchymal Stem Cells Attenuate Liver Fibrosis by Suppressing Th17 Cells–an Experimental Study. *Transplant Int* (2018) 31(1):102–15. doi: 10.1111/tri.13023
127. Yan S, Wang L, Liu N, Wang Y, Chu Y. Critical Role of Interleukin-17/Interleukin-17 Receptor Axis in Mediating Con A-Induced Hepatitis. *Immunol Cell Biol* (2012) 90(4):421–8. doi: 10.1038/icb.2011.59
128. Milosavljevic N, Gazdic M, Simovic Markovic B, Arsenijevic A, Nurkovic J, Dolicanin Z, et al. Mesenchymal Stem Cells Attenuate Acute Liver Injury by Altering Ratio Between Interleukin 17 Producing and Regulatory Natural Killer T Cells. *Liver Transplant* (2017) 23(8):1040–50. doi: 10.1002/lt.24784
129. Mazhari S, Gitiara A, Baghaei K, Hatami B, Rad RE, Asadirad A, et al. Therapeutic Potential of Bone Marrow-Derived Mesenchymal Stem Cells and Imatinib in a Rat Model of Liver Fibrosis. *Eur J Pharmacol* (2020) 882:173263. doi: 10.1016/j.ejphar.2020.173263
130. Chen L, Zhang C, Chen L, Wang X, Xiang B, Wu X, et al. Human Menstrual Blood-Derived Stem Cells Ameliorate Liver Fibrosis in Mice by Targeting Hepatic Stellate Cells *via* Paracrine Mediators. *Stem Cells Trans Med* (2017) 6(1):272–84. doi: 10.5966/sctm.2015-0265
131. Wang S, Kim J, Lee C, Oh D, Han J, Kim T-J, et al. Tumor Necrosis Factor-Inducible Gene 6 Reprograms Hepatic Stellate Cells Into Stem-Like Cells, Which Ameliorates Liver Damage in Mouse. *Biomaterials* (2019) 219:119375. doi: 10.1016/j.biomaterials.2019.119375
132. Liang T, Zhu L, Gao W, Gong M, Ren J, Yao H, et al. Coculture of Endothelial Progenitor Cells and Mesenchymal Stem Cells Enhanced Their Proliferation and Angiogenesis Through PDGF and Notch Signaling. *FEBS Open Bio* (2017) 7(11):1722–36. doi: 10.1002/2211-5463.12317
133. Hu C, Li L. The Immunoregulation of Mesenchymal Stem Cells Plays a Critical Role in Improving the Prognosis of Liver Transplantation. *J Trans Med* (2019) 17(1):1–12. doi: 10.1186/s12967-019-02167-0
134. Pournasr B, Mohamadnejad M, Bagheri M, Aghdami N, Shahsavani M, Malekzadeh R, et al. *In Vitro* Differentiation of Human Bone Marrow Mesenchymal Stem Cells Into Hepatocyte-Like Cells. *Arch Iranian Med* (2011) 14(4):0–.
135. Yin L, Zhu Y, Yang J, Ni Y, Zhou Z, Chen Y, et al. Adipose Tissue-Derived Mesenchymal Stem Cells Differentiated Into Hepatocyte-Like Cells *In Vivo* and *In Vitro*. *Mol Med Rep* (2015) 11(3):1722–32. doi: 10.3892/mmr.2014.2935
136. Yin F, Wang W-Y, Jiang W-H. Human Umbilical Cord Mesenchymal Stem Cells Ameliorate Liver Fibrosis *In Vitro* and *In Vivo*: From Biological Characteristics to Therapeutic Mechanisms. *World J Stem Cells* (2019) 11(8):548. doi: 10.4252/wjsc.v11.i8.548
137. Khodabandeh Z, Vojdani Z, Talaei-Khozani T, Jaberipour M, Hosseini A, Bahmanpour S. Comparison of the Expression of Hepatic Genes by Human Wharton's Jelly Mesenchymal Stem Cells Cultured in 2D and 3D Collagen Culture Systems. *Iranian J Med Sci* (2016) 41(1):28.
138. Anzalone R, Iacono ML, Corrao S, Magno F, Loria T, Cappello F, et al. New Emerging Potentials for Human Wharton's Jelly Mesenchymal Stem Cells: Immunological Features and Hepatocyte-Like Differentiative Capacity. *Stem Cells Dev* (2010) 19(4):423–38. doi: 10.1089/scd.2009.0299
139. Kim JY, Jun JH, Park SY, Yang SW, Bae SH, Kim GJ. Dynamic Regulation of miRNA Expression by Functionally Enhanced Placental Mesenchymal Stem Cells Promotes Hepatic Regeneration in a Rat Model With Bile Duct Ligation. *Int J Mol Sci* (2019) 20(21):5299. doi: 10.3390/ijms20215299
140. Lu L-L, Liu Y-J, Yang S-G, Zhao Q-J, Wang X, Gong W, et al. Isolation and Characterization of Human Umbilical Cord Mesenchymal Stem Cells With Hematopoiesis-Supportive Function and Other Potentials. *Haematologica* (2006) 91(8):1017–26.
141. Deuse T, Stubbendorff M, Tang-Quan K, Phillips N, Kay MA, Eiermann T, et al. Immunogenicity and Immunomodulatory Properties of Umbilical Cord Lining Mesenchymal Stem Cells. *Cell Transplant* (2011) 20(5):655–67. doi: 10.3727/096368910X536473

142. Amer M-EM, El-Sayed SZ, Abou El-Kheir W, Gabr H, Gomaa AA, El-Noomani N, et al. Clinical and Laboratory Evaluation of Patients With End-Stage Liver Cell Failure Injected With Bone Marrow-Derived Hepatocyte-Like Cells. *Eur J Gastroenterol Hepatol* (2011) 23(10):936–41. doi: 10.1097/MEG.0b013e3283488b00
143. Kharaziha P, Hellström PM, Noorinayer B, Farzaneh F, Aghajani K, Jafari F, et al. Improvement of Liver Function in Liver Cirrhosis Patients After Autologous Mesenchymal Stem Cell Injection: A Phase I–II Clinical Trial. *Eur J Gastroenterol Hepatol* (2009) 21(10):1199–205. doi: 10.1097/MEG.0b013e32832a1f6c
144. Suk KT, Yoon JH, Kim MY, Kim CW, Kim JK, Park H, et al. Transplantation With Autologous Bone Marrow-Derived Mesenchymal Stem Cells for Alcoholic Cirrhosis: Phase 2 Trial. *Hepatology* (2016) 64(6):2185–97. doi: 10.1002/hep.28693
145. Mohamadnejad M, Bashtar M, Ardeshir G, Malekzadeh R. 106: Phase 1 Trial of Autologous Bone Marrow Mesenchymal Stem Cell Transplantation in Patients With Decompensated. *Arch Iranian Med* (2007) 10(4):459–66.
146. Sun A, Gao W, Xiao T. Autologous Bone Marrow Stem Cell Transplantation *via* the Hepatic Artery for the Treatment of Hepatitis B Virus-Related Cirrhosis: A PRISMA-Compliant Meta-Analysis Based on the Chinese Population. *Stem Cell Res Ther* (2020) 11(1):1–17. doi: 10.1186/s13287-020-01627-5
147. Xu L, Gong Y, Wang B, Shi K, Hou Y, Wang L, et al. Randomized Trial of Autologous Bone Marrow Mesenchymal Stem Cells Transplantation for Hepatitis B Virus Cirrhosis: Regulation of T Reg/T H17 Cells. *J Gastroenterol Hepatol* (2014) 29(8):1620–8. doi: 10.1111/jgh.12653
148. Casiraghi F, Perico N, Podestà MA, Todeschini M, Zambelli M, Colledan M, et al. Third-Party Bone Marrow–Derived Mesenchymal Stromal Cell Infusion Before Liver Transplantation: A Randomized Controlled Trial. *Am J Transplant* (2021) 21(8):2795–809. doi: 10.1111/ajt.16468
149. Fan X-L, Zhang Y, Li X, Fu Q-L. Mechanisms Underlying the Protective Effects of Mesenchymal Stem Cell-Based Therapy. *Cell Mol Life Sci* (2020) 77(14):2771–94. doi: 10.1007/s00018-020-03454-6
150. Zarà M, Guidetti GF, Camera M, Canobbio I, Amadio P, Torti M, et al. Biology and Role of Extracellular Vesicles (EVs) in the Pathogenesis of Thrombosis. *Int J Mol Sci* (2019) 20(11):2840. doi: 10.3390/ijms20112840
151. Malekpour K, Hazrati A, Zahar M, Markov A, Zekiy AO, Navashenaq JG, et al. The Potential Use of Mesenchymal Stem Cells and Their Derived Exosomes for Orthopedic Diseases Treatment. *Stem Cell Rev Rep* (2021), 1–19. doi: 10.1007/s12015-021-10185-z
152. Anand S, Samuel M, Mathivanan S. Exomeres: A New Member of Extracellular Vesicles Family. *Subcell Biochem* (2021) 97:89–97. doi: 10.1007/978-3-030-67171-6_5
153. Pegtel DM, Gould SJ. Exosomes. *Annu Rev Biochem* (2019) 88:487–514. doi: 10.1146/annurev-biochem-013118-111902
154. Jabbari N, Akbariazar E, Feqhhi M, Rahbarghazi R, Rezaie J. Breast Cancer-Derived Exosomes: Tumor Progression and Therapeutic Agents. *J Cell Physiol* (2020) 235(10):6345–56. doi: 10.1002/jcp.29668
155. Lai P, Weng J, Guo L, Chen X, Du X. Novel Insights Into MSC-EVs Therapy for Immune Diseases. *biomark Res* (2019) 7(1):1–10. doi: 10.1186/s40364-019-0156-0
156. Alcaraz MJ, Compañ A, Guillén MI. Extracellular Vesicles From Mesenchymal Stem Cells as Novel Treatments for Musculoskeletal Diseases. *Cells* (2020) 9(1):98. doi: 10.3390/cells9010098
157. Khoei SG, Dermani FK, Malih S, Fayazi N, Sheykhhasan M. The Use of Mesenchymal Stem Cells and Their Derived Extracellular Vesicles in Cardiovascular Disease Treatment. *Curr Stem Cell Res Ther* (2020) 15(7):623–38. doi: 10.2174/1574888X15666200501235201
158. Rostom DM, Attia N, Khalifa HM, Abou Nazel MW, El Sabaawy EA. The Therapeutic Potential of Extracellular Vesicles Versus Mesenchymal Stem Cells in Liver Damage. *Tissue Eng Regen Med* (2020) 17:537–52. doi: 10.1007/s13770-020-00267-3
159. Yin Z, Jiang K, Li R, Dong C, Wang L. Multipotent Mesenchymal Stromal Cells Play Critical Roles in Hepatocellular Carcinoma Initiation, Progression and Therapy. *Mol Cancer* (2018) 17(1):1–17. doi: 10.1186/s12943-018-0926-6
160. Shojaei S, Hashemi SM, Ghanbarian H, Salehi M, Mohammadi-Yeganeh S. Effect of Mesenchymal Stem Cells-Derived Exosomes on Tumor Microenvironment: Tumor Progression Versus Tumor Suppression. *J Cell Physiol* (2019) 234(4):3394–409. doi: 10.1002/jcp.27326
161. Zhang F, Guo J, Zhang Z, Qian Y, Wang G, Duan M, et al. Mesenchymal Stem Cell-Derived Exosome: A Tumor Regulator and Carrier for Targeted Tumor Therapy. *Cancer Lett* (2022) 526:29–40. doi: 10.1016/j.canlet.2021.11.015
162. Lou G, Chen L, Xia C, Wang W, Qi J, Li A, et al. MiR-199a-Modified Exosomes From Adipose Tissue-Derived Mesenchymal Stem Cells Improve Hepatocellular Carcinoma Chemosensitivity Through mTOR Pathway. *J Exp Clin Cancer Res* (2020) 39(1):1–9. doi: 10.1186/s13046-019-1512-5
163. Zhang F, Lu Y, Wang M, Zhu J, Li J, Zhang P, et al. Exosomes Derived From Human Bone Marrow Mesenchymal Stem Cells Transfer miR-222-3p to Suppress Acute Myeloid Leukemia Cell Proliferation by Targeting IRF2/INPP4B. *Mol Cell Probes* (2020) 51:101513. doi: 10.1016/j.mcp.2020.101513
164. Li X, Wang K, Ai H. Human Umbilical Cord Mesenchymal Stem Cell-Derived Extracellular Vesicles Inhibit Endometrial Cancer Cell Proliferation and Migration Through Delivery of Exogenous miR-302a. *Stem Cells Int* (2019) 2019:8108576. doi: 10.1155/2019/8108576
165. Bagheri E, Abnous K, Farzad SA, Taghdisi SM, Ramezani M, Alibolandi M. Targeted Doxorubicin-Loaded Mesenchymal Stem Cells-Derived Exosomes as a Versatile Platform for Fighting Against Colorectal Cancer. *Life Sci* (2020) 261:118369. doi: 10.1016/j.lfs.2020.118369
166. Nitzsche F, Müller C, Lukomska B, Jolkkonen J, Deten A, Boltze J. Concise Review: MSC Adhesion Cascade—Insights Into Homing and Transendothelial Migration. *Stem Cells* (2017) 35(6):1446–60. doi: 10.1002/stem.2614
167. Wu Q, Zhou L, Lv D, Zhu X, Tang H. Exosome-Mediated Communication in the Tumor Microenvironment Contributes to Hepatocellular Carcinoma Development and Progression. *J Hematol Oncol* (2019) 12(1):1–11. doi: 10.1186/s13045-019-0739-0
168. Borrelli DA, Yankson K, Shukla N, Vilanilam G, Ticer T, Wolfram J. Extracellular Vesicle Therapeutics for Liver Disease. *J Control Release* (2018) 273:86–98. doi: 10.1016/j.jconrel.2018.01.022
169. Li T, Yan Y, Wang B, Qian H, Zhang X, Shen L, et al. Exosomes Derived From Human Umbilical Cord Mesenchymal Stem Cells Alleviate Liver Fibrosis. *Stem Cells Dev* (2013) 22(6):845–54. doi: 10.1089/scd.2012.0395
170. Haga H, Yan IK, Borrelli DA, Matsuda A, Parasramka M, Shukla N, et al. Extracellular Vesicles From Bone Marrow–Derived Mesenchymal Stem Cells Protect Against Murine Hepatic Ischemia/Reperfusion Injury. *Liver Transplant* (2017) 23(6):791–803. doi: 10.1002/lt.24770
171. Lee SC, Kim K-H, Kim O-H, Lee SK, Hong H-E, Won SS, et al. Determination of Optimized Oxygen Partial Pressure to Maximize the Liver Regenerative Potential of the Secretome Obtained From Adipose-Derived Stem Cells. *Stem Cell Res Ther* (2017) 8(1):1–12. doi: 10.1186/s13287-017-0635-x
172. Mardpour S, Hassani SN, Mardpour S, Sayahpour F, Vosough M, Ai J, et al. Extracellular Vesicles Derived From Human Embryonic Stem Cell-MSCs Ameliorate Cirrhosis in Thioacetamide-Induced Chronic Liver Injury. *J Cell Physiol* (2018) 233(12):9330–44. doi: 10.1002/jcp.26413
173. Yan Y, Jiang W, Tan Y, Zou S, Zhang H, Mao F, et al. hucMSC Exosome-Derived GPX1 is Required for the Recovery of Hepatic Oxidant Injury. *Mol Ther* (2017) 25(2):465–79. doi: 10.1016/j.ymthe.2016.11.019
174. Dong L, Pu Y, Chen X, Qi X, Zhang L, Xu L, et al. hUCMSC-Extracellular Vesicles Downregulated Hepatic Stellate Cell Activation and Reduced Liver Injury in S. Japonicum-Infected Mice. *Stem Cell Res Ther* (2020) 11(1):1–11.
175. Tan CY, Lai RC, Wong W, Dan YY, Lim S-K, Ho HK. Mesenchymal Stem Cell-Derived Exosomes Promote Hepatic Regeneration in Drug-Induced Liver Injury Models. *Stem Cell Res Ther* (2014) 5(3):1–14. doi: 10.1186/scrt465
176. Zhao S, Liu Y, Pu Z. Bone Marrow Mesenchymal Stem Cell-Derived Exosomes Attenuate D-GaIN/LPS-Induced Hepatocyte Apoptosis by Activating Autophagy *In Vitro*. *Drug Design Dev Ther* (2019) 13:2887. doi: 10.2147/DDDT.S220190
177. Tamura R, Uemoto S, Tabata Y. Immunosuppressive Effect of Mesenchymal Stem Cell-Derived Exosomes on a Concanavalin A-Induced Liver Injury Model. *Inflamm Regen* (2016) 36(1):1–11. doi: 10.1186/s41232-016-0030-5

178. Haga H, Yan IK, Takahashi K, Matsuda A, Patel T. Extracellular Vesicles From Bone Marrow-Derived Mesenchymal Stem Cells Improve Survival From Lethal Hepatic Failure in Mice. *Stem Cells Trans Med* (2017) 6 (4):1262–72. doi: 10.1002/sctm.16-0226
179. You Q, Cheng L, Kedl RM, Ju C. Mechanism of T Cell Tolerance Induction by Murine Hepatic Kupffer Cells. *Hepatology* (2008) 48(3):978–90. doi: 10.1002/hep.22395
180. Jin Y, Wang J, Li H, Gao S, Shi R, Yang D, et al. Extracellular Vesicles Secreted by Human Adipose-Derived Stem Cells (hASCs) Improve Survival Rate of Rats With Acute Liver Failure by Releasing lncRNA H19. *EBioMedicine* (2018) 34:231–42. doi: 10.1016/j.ebiom.2018.07.015
181. Rong X, Liu J, Yao X, Jiang T, Wang Y, Xie F. Human Bone Marrow Mesenchymal Stem Cells-Derived Exosomes Alleviate Liver Fibrosis Through the Wnt/β-Catenin Pathway. *Stem Cell Res Ther* (2019) 10(1):1–11. doi: 10.1186/s13287-019-1204-2
182. Heidari N, Abbasi-Kenarsari H, Namaki S, Baghaei K, Zali MR, Ghaffari Khaligh S, et al. Adipose-Derived Mesenchymal Stem Cell-Secreted Exosome Alleviates Dextran Sulfate Sodium-Induced Acute Colitis by Treg Cell Induction and Inflammatory Cytokine Reduction. *J Cell Physiol* (2021) 236 (8):5906–20. doi: 10.1002/jcp.30275
183. Chen Y-A, Lu C-H, Ke C-C, Liu R-S. Mesenchymal Stem Cell-Derived Extracellular Vesicle-Based Therapy for Alzheimer's Disease: Progress and Opportunity. *Membranes* (2021) 11(10):796. doi: 10.3390/membranes11100796
184. Liu C, Bayado N, He D, Li J, Chen H, Li L, et al. Therapeutic Applications of Extracellular Vesicles for Myocardial Repair. *Front Cardiovasc Med* (1802) 2021:8. doi: 10.3389/fcvm.2021.758050
185. Maumus M, Rozier P, Boulestreau J, Jorgensen C, Noël D. Mesenchymal Stem Cell-Derived Extracellular Vesicles: Opportunities and Challenges for Clinical Translation. *Front Bioeng Biotechnol* (2020) 8:997. doi: 10.3389/fbioe.2020.00997
186. Jadli AS, Ballasy N, Edalat P, Patel VB. Inside (Sight) of Tiny Communicator: Exosome Biogenesis, Secretion, and Uptake. *Mol Cell Biochem* (2020) 467 (1):77–94. doi: 10.1007/s11010-020-03703-z

Conflict of Interest: The authors declare that the research was conducted in the absence of any commercial or financial relationships that could be construed as a potential conflict of interest.

Publisher's Note: All claims expressed in this article are solely those of the authors and do not necessarily represent those of their affiliated organizations, or those of the publisher, the editors and the reviewers. Any product that may be evaluated in this article, or claim that may be made by its manufacturer, is not guaranteed or endorsed by the publisher.

frontiers | Frontiers in Immunology

ORIGINAL RESEARCH
published: 13 May 2022
doi: 10.3389/fimmu.2022.859231

Cytosolic p53 Inhibits Parkin-Mediated Mitophagy and Promotes Acute Liver Injury Induced by Heat Stroke

Wei Huang[1,2], Weidang Xie[1], Hanhui Zhong[3], Shumin Cai[1], Qiaobing Huang[4], Youtan Liu[5], Zhenhua Zeng[1] and Yanan Liu[1]**

[1] Department of Critical Care Medicine, Nanfang Hospital, Southern Medical University, Guangzhou, China, [2] The First School of Clinical Medicine, Southern Medical University, Guangzhou, China, [3] Department of Anesthesiology, Affiliated Hospital of Guangdong Medical University, Zhanjiang, China, [4] Guangdong Provincial Key Lab of Shock and Microcirculation, Department of Pathophysiology, Southern Medical University, Guangzhou, China, [5] Department of Anesthesiology, Shenzhen Hospital, Southern Medical University, Shenzhen, China

OPEN ACCESS

Edited by:
Yu Shi,
Zhejiang University, China

Reviewed by:
Robert Weil,
INSERM U1135 Centre d'Immunologie et de Maladies Infectieuses, France
Yihua Wu,
Zhejiang University, China

***Correspondence:**
Zhenhua Zeng
zhenhuazeng.2008@163.com
Yanan Liu
lyn21100145@i.smu.edu.cn

Specialty section:
This article was submitted to Inflammation, a section of the journal Frontiers in Immunology

Received: *21 January 2022*
Accepted: *20 April 2022*
Published: *13 May 2022*

Citation:
Huang W, Xie W, Zhong H, Cai S, Huang Q, Liu Y, Zeng Z and Liu Y (2022) Cytosolic p53 Inhibits Parkin-Mediated Mitophagy and Promotes Acute Liver Injury Induced by Heat Stroke. Front. Immunol. 13:859231. doi: 10.3389/fimmu.2022.859231

Heat stroke (HS) is a severe condition characterized by increased morbidity and high mortality. Acute liver injury (ALI) is a well-documented complication of HS. The tumor suppressor p53 plays an important role in regulation of mitochondrial integrity and mitophagy in several forms of ALI. However, the role of p53-regulated mitophagy in HS-ALI remains unclear. In our study, we discovered the dynamic changes of mitophagy in hepatocytes and demonstrated the protective effects of mitophagy activation on HS-ALI. Pretreatment with 3-MA or Mdivi-1 significantly exacerbated ALI by inhibiting mitophagy in HS-ALI mice. Consistent with the animal HS-ALI model results, silencing Parkin aggravated mitochondrial damage and apoptosis by inhibiting mitophagy in HS-treated normal human liver cell line (LO2 cells). Moreover, we described an increase in the translocation of p53 from the nucleus to the cytoplasm, and cytosolic p53 binds to Parkin in LO2 cells following HS. p53 overexpression using a specific adenovirus or Tenovin-6 exacerbated HS-ALI through Parkin-dependent mitophagy both *in vivo* and *in vitro*, whereas inhibition of p53 using siRNA or PFT-α effectively reversed this process. Our results demonstrate that cytosolic p53 binds to Parkin and inhibits mitophagy by preventing Parkin's translocation from the cytosol to the mitochondria, which decreases mitophagy activation and leads to hepatocyte apoptosis in HS-ALI. Overall, pharmacologic induction of mitophagy by inhibiting p53 may be a promising therapeutic approach for HS-ALI treatment.

Keywords: mitophagy, acute liver injury, p53, Parkin, apoptosis

INTRODUCTION

Heat stroke (HS) is the most serious heat-related illness, defined as having elevated core body temperature (Tc) >40°C with central nervous system dysfunction (1). Recently, HS incidence rates have increased, especially with the growing frequency of heatwaves (2). Of note, HS is associated with multiple organ dysfunction syndrome (MODS), increased morbidity, and high mortality due to the

combined effects of heat cytotoxicity, coagulopathies, and systemic inflammatory response syndrome (SIRS) (3). Acute liver injury (ALI) is a well-documented complication of HS and is strongly predictive of mortality (4). Importantly, the initial dysregulation of hepatocellular function has been associated with problematic microcirculation and a cytokine storm during early progression of HS (5). Massive pathological changes in hepatocytes are directly correlated with the pathogenesis of heat stroke, including cell death and the inflammatory response (6, 7). However, the mechanisms mediating HS-induced hepatocyte injury remain largely unexplored.

Mitochondria are both primary sources and targets of reactive oxygen species (ROS), and mitochondrial dysfunction is a hallmark of HS-mediated pathology (8). Increased oxidative injury following HS exacerbates mitochondrial compromise, and subsequent resultant mitochondrial inefficacy could cause additional increased ROS levels (9). Notably, mitophagy has been identified as an important response of self-regulating mitochondrial quality control and mitochondrial ROS by selectively removing impaired mitochondria (10). Furthermore, mitophagy is the most important mechanism for removing dysfunctional mitochondria, its dysfunction may result in accumulation of damaged mitochondria, release of excessive ROS, and activation of apoptosis-inducing factors (11). PTEN-induced putative kinase 1 (PINK1)-parkin RBR E3 ubiquitin protein ligase (Parkin)-mediated mitophagy is a Parkin-dependent pathway of mitophagy and one of the most recognized mitophagy pathways (12). When mitochondria are impaired and lose their membrane potential, PINK1 accumulates in the outer mitochondrial membrane and then recruits and phosphorylates ubiquitin and the E3 ubiquitin ligase Parkin, leading to the ubiquitination of various mitochondrial proteins, including the outer membrane proteins VDAC1 and mitofusin 1/2 (Mfn1/2) (13). This modification recruits the autophagy adaptor, such as molecule sequestosome 1 (p62/SQSTM1), Nuclear Domain 10 Protein 52 (NDP52), and Optineurin (OPTN), then they bind LC3 protein on autophagosomal membranes, ultimately triggering selective removal of damaged mitochondria by mitophagy (14).

p53 has been well characterized for its response to different cellular stresses, including induction of tumor suppression, growth arrest, senescence, and cell death (15). Upregulation of p53 is involved in triggering HS-induced apoptosis (16). Moreover, recent research found that p53 binds to Parkin's really interesting new gene 0 (RING 0) region, which impairs the removal of damaged mitochondria by blocking Parkin mitochondrial translocation (17, 18). Parkin has been shown to have important roles in the induction of mitophagy, labeling damaged mitochondria for autophagic removal *via* its ubiquitin ligase activity (19). Other recent studies also indicated that binding of cytosolic p53 to Parkin inhibits mitochondrial translocation of Parkin and activation of Parkin's E3 ubiquitin ligase, consequently disrupting Parkin-mediated mitophagy (20, 21). A previous study also demonstrated that the PINK1-Parkin-dependent pathway of mitophagy was increased in HS-induced hypothalamic injury (22). However, the role of Parkin-mediated mitophagy in HS-ALI remains largely unknown.

The purpose of this study was to explore the involvement and regulation of mitophagy in HS-ALI. We further attempted to determine the effect of p53-Parkin coregulation of mitophagy on mitochondrial damage and apoptosis in HS-ALI. Our study reveals critical roles for p53 and Parkin in HS-induced mitophagy and provides an opportunity for developing new therapeutics for HS.

MATERIALS AND METHODS

Animals

C57BL/6 mice (aged 10 to 12 weeks) used in this study were obtained from the Experimental Animal Center of Southern Medical University. All mice were housed under a controlled 12/12-h light/dark cycle at a constant temperature (24 ± 1°C) and (54 ± 2%) relative humidity with free access to a pelleted rodent diet and water. All protocols of animal experiments followed the guidelines approved by the Chinese Association of Laboratory Animal Care and were approved by the Ethical Committee for Animal Experimentation of Nanfang Hospital.

HS Protocol for Animals

HS-ALI models were induced in mice as previously described in our reported method (23). Animals were placed in a climate chamber that was maintained at a constant temperature of 39.5 ± 0.2°C with 60 ± 5% relative humidity in the absence of food or water, and rectal temperature (Tc) was measured at intervals of ten minutes. The time point at which the Tc reached 42.5°C was used as a reference point of HS onset. All mice were then returned to their original cages in an environment at 25°C with water after HS. The control group underwent the same procedure without HS treatment. Chemical reagents at doses of 20 mg/kg for 3-methyladenine (3-MA), 25 mg/kg for Mdivi-1, 25 mg/kg for Tenovin-6, or 2.2 mg/kg for pifithrin-α (PFT-α) were intraperitoneally injected 2 h before HS as required. All groups of mice were sacrificed at time points as indicated after 1.0% pentobarbital sodium (5 mg/100 g.BW, i.p.) administration to harvest the serum and liver tissues.

Cell Culture, Treatment, and Transfection With siRNA or Adenovirus

Normal human liver (LO2) cells were purchased from the Laboratory of iCell Biotechnology Company (Shanghai, China). LO2 cells were cultured in Dulbecco's modified Eagle's medium (DMEM) with 10% fetal bovine serum (FBS). LO2 cells were maintained in a humidified CO_2 incubator at 37°C. For HS treatment *in vitro*, the culture medium was replaced with fresh medium, and then cells were placed in an incubator containing 5% CO_2 at 42 ± 0.5°C for 3 h. Subsequently, the cells were incubated in a normal incubator at 37°C and 5% CO_2. For treatment with PFT-α, cells were pretreated with PFT-α (20 μM, Sigma-Aldrich) 2 h before HS treatment. Lipofectamine 2000 reagent (L3000008, Thermo Fisher Scientific) was used to transiently transfect LO2 cells with short interfering RNA (siRNA) oligonucleotides against Parkin, p53, and negative control siRNA. The siRNAs were synthesized by Gene Pharma

(Shanghai, China), and the sequences of siRNA oligonucleotides were as follows: Parkin siRNA 5′-GAGUAGCCG CAAAUGUG CUUCAUCU-3′, p53 siRNA 5′-UCCAGCUCAAGGAGGU GG UUGCUAA-3′; negative control siRNA, 5′-UUCUCCGAACG UCACGU-3'. After cells were transfected for 72 h, subsequent experiments were performed. The adenoviral vector expressing Flag- and GFP-tagged wild-type p53 (Ad-p53) was provided by Gene Pharma (Shanghai, China).

Western Blot Analysis

Cytoplasmic and nuclear fractions of LO2 cells were obtained using a Nuclear and Cytoplasmic Protein Extraction kit (Beyotime Biotechnology, China). For whole-cell lysates, liver tissues and LO2 cells were harvested using radioimmunoprecipitation assay (RIPA) lysis buffer containing 1× protease inhibitor cocktail. After separation by sodium dodecyl sulfate (SDS)-polyacrylamide gel electrophoresis, the proteins were transferred to polyvinylidene difluoride (PVDF) membranes. Subsequently, the membranes were blocked in 5% bovine serum albumin (BSA) at room temperature (RT) for 1 h followed by immunoblotting at 4°C overnight with primary antibodies. The membranes were then incubated with secondary antibodies for one hour. Target protein was detected using enhanced chemiluminescence reagents. The primary antibodies were as follows: anti-Parkin (4211, Cell Signaling), anti-PINK1 (6946, Cell Signaling), anti-p53 (60283-2, Proteintech), anti-SQSTM1/p62 (A7758, ABclonal), anti-LC3-II/I (12741, Cell Signaling), anti-LaminB1 (23498-1-AP, Proteintech), anti-BAX (50599-2-Ig, Proteintech), anti-Bcl2 (12789-1-AP, Proteintech), anti-GAPDH (AC002, ABclonal), and anti-VDAC1 (55259-1-AP, Proteintech). The secondary antibodies were horseradish peroxidase-labeled goat anti-mouse (AS014, ABclonal) and anti-rabbit (AS003, ABclonal) antibodies. Quantification was performed by measuring the density of blot bands using ImageJ software. Protein expression levels were normalized relative to the levels of VDAC, LaminB1, or GAPDH.

Histopathology and Immunofluorescence Staining

Fresh liver tissues were fixed in 10% formaldehyde, dehydrated, embedded in paraffin, sectioned, and stained with hematoxylin and eosin (H&E). H&E staining of livers was assessed under an optical microscope (Zeiss, Thuringia Germany). Liver injury scores were evaluated in 8 randomly selected, nonoverlapping fields at 200× magnification in each section. The sections were analyzed by two professional pathologists who were blinded to the experimental protocol and scored the liver damage.

To visualize the mitochondria, cells were cultured on cover slips and then incubated using a MitoTracker Red fluorescent probe kit (300 nM at 37°C for 30 minutes; Invitrogen, Waltham, USA). For immunostaining, the cells were fixed in 4% paraformaldehyde for 15 minutes and permeabilized with 0.1% Triton X-100 at RT. Cells were incubated with the specific primary antibody anti-LC3-II/I (12741, Cell Signaling) at 4°C overnight followed by incubation with a fluorescent secondary antibody. After counterstaining with 4' 6-diamidino-2-phenylindole (DAPI), the slides were observed using a confocal inverted laser microscope (Zeiss, Germany).

Mitochondrial Membrane Potential (JC-1) Assay

Mitochondrial membrane potential ($\Delta\Psi m$) was measured by monitoring the fluorescent aggregates of JC-1 using a JC-1 detection kit (Beyotime Biotechnology, China) according to the manufacturer's instructions. We washed cells with PBS buffer three times and prepared the JC-1 fluorescent probe. After staining at 37°C for 30 minutes, relative fluorescence was analyzed by flow cytometry (BD Dickinson, USA).

Detection of Apoptosis and Intracellular ROS

Apoptosis was assessed using the Annexin V-FITC Apoptosis Detection Kit (BestBio, China). Cells were collected and resuspended in binding buffer containing Annexin V-FITC. After a 15-min incubation at RM in darkness, the buffer was degraded by centrifugation, and the cells were then resuspended in propidium iodide (PI) solution for 10 minutes. Then, the cells were immediately analyzed using flow cytometry (Becton Dickinson, USA) to quantify levels of apoptosis. Annexin V (+)/PI (-) and Annexin V (+)/PI (+) cells in the right quadrant were considered apoptotic.

Cells were pretreated with Parkin siRNA or PFT-α and then cultured at 42°C for 3 h. After staining with 2'-7'-dichlorofluorescin diacetate (Beyotime Institute of Biotechnology) at 37°C for 20 minutes in the dark, relative fluorescence was measured by flow cytometry (BD Dickinson, USA).

Mitochondria Protein Extraction

Mitochondrial and cytosolic fractions were isolated from LO2 cells using the Cell Mitochondria Isolation Kit (Beyotime Biotechnology, China) according to the manufacturer's protocols. Lysed cells were resuspended in mitochondrial isolation reagent and centrifuged at 600 × g at 4°C for 10 minutes to obtain the supernatant. Supernatants were then centrifuged at 13,000 g for 5 min to obtain a pellet containing the mitochondria. Protein concentrations were quantified using a bicinchoninic acid (BCA) assay (Beyotime Biotechnology, China) and stored at -80°C.

Liver Function Assessment

Blood samples were collected 12 h after HS and then centrifuged at 3,000 rpm for 10 min at RT to obtain the serum. Plasma alanine aminotransferase (ALT) and aspartate aminotransferase (AST) levels were analyzed using an automatic biochemical analyzer (Chemray 240, Shenzhen, China).

Caspase 3 Activity Assay

Caspase 3 activity in cytosolic extracts was determined using the Caspase 3 Activity Assay kit (Beyotime Biotechnology, China) according to the manufacturer's protocols. Briefly, supernatants from cell lysates were treated with a fluorogenic substrate of caspase 3, Ac-DEVE-MCA, at 37°C for 30 mins. Caspase 3 activity is represented as the relative cumulative fluorescence of

the kinetic reaction and is expressed as the relative value normalized to untreated controls, which was measured using a microplate reader (Multiskan MK3, Thermo) at 405 nm.

Transmission Electron Microscopy

Fresh liver tissues of 1 mm^3 were harvested and then fixed in 2% formaldehyde and 2.5% glutaraldehyde. The tissue blocks were then fixed in 1% osmic acid, dehydrated with ethanol and acetone gradients, and embedded in epoxy resin and propylene oxide overnight. Samples were then cut into 70-nm-thick ultrathin sections. The sections were then observed under an H-7650 transmission electron microscope (Hitachi, Tokyo, Japan) at low magnification (×8,000) and then analyzed at high magnification (×40,000) to observe mitochondrial autophagosomes and autophagolysosomes. Two professional pathologists analyzed the images in a blinded manner.

Co-Immunoprecipitation (Co-IP) Assays

Cells were pretreated with 5 mM MG132, a proteasome inhibitor, before exposure to HS. Cell lysates were incubated with 4 μg anti-Parkin or anti-VDAC antibody overnight at 4°C. Then, 50 μl of protein A+G agarose beads was added and centrifuged at 4°C for 3 h. After centrifugation, the supernatant was discarded to obtain immunocomplexes, and the beads were then resuspended in 1× lysis buffer for western blotting analysis using the indicated antibodies. IgG served as the negative control.

Statistical Analysis

Results are expressed as the mean ± standard deviation. Student's t test was used to analyze differences between two groups. Statistical comparisons of three or more groups were performed using one-way analysis of variance (ANOVA), followed by *post hoc* analysis. Quantitative data are from at least three separate experiments performed in duplicate. All tests for statistical significance were performed using GraphPad software (La Jolla, CA). P values < 0.05 were considered statistically significant.

RESULTS

Mitophagy Is Induced by HS *In Vivo* and *In Vitro*

To clarify the role of mitophagy in HS-ALI, we first demonstrated the occurrence of mitophagy in the liver following HS. As shown in **Figure 1A**, TUNEL staining revealed an increase in TUNEL-positive cells following HS treatment in a time-dependent manner, indicating the occurrence of apoptosis compared to the controls. TEM revealed mitochondrial swelling, loss of mitochondrial cristae, and formations of mitophagosomes and mitophagolysosomes in hepatocytes in HS-treated mice, which were rarely observed in controls (**Figure 1B**). Immunoblot analysis of the mitophagy biomarkers Parkin and PINK1 gradually increased at 0-6 h, and returned to baseline by 24 h; mitochondrial protein Translocase of outer mitochondrial membrane 20 (TOM20) gradually decreased at 0-6 h, and returned to baseline by 24 h. In contrast, p62 expression reached the lowest levels at 12 h after HS, and LC3-II expression gradually increased at 6-12h then slightly decreased following HS (**Figures 1C**, **S1A**), suggesting that mitophagy was induced in HS-ALI mice.

Compared to the control group, flow cytometry analysis showed an increase in apoptotic cells following HS in a time-dependent manner, indicating that apoptosis was induced in LO2 cells by HS (**Figures 1D, G**). The mitophagy biomarkers Parkin and PINK1 gradually increased at 0-6 h, and returned to baseline by 24 h; mitochondrial protein TOM20 gradually decreased at 0-6 h, and returned to baseline by 24 h. In contrast, p62 expression reached the lowest levels at 12 h after HS, and LC3-II expression gradually increased at 6-12 h then slightly decreased following HS (**Figures 1E**, **S1B**). Interestingly, immunoblot analysis indicated an increase of PINK1 expression levels in the mitochondria at 6 h after HS, and an increase in the translocation of Parkin from the cytoplasm to the mitochondria *in vivo* and *in vitro* (**Figures S1C, D**), suggesting that HS stabilized PINK1 at the outer mitochondrial membrane and thereby recruits more Parkin to mitochondria. To further evaluate HS-induced mitophagy, we used double staining of LC3B and MitoTracker, a mitochondrial marker, in HS-treated LO2 cells. Confocal imaging revealed that staining for the autophagosome marker LC3B was distinctively colocalized with MitoTracker at 0-6 h following HS, indicating the formation of mitophagosomes induced by HS (**Figures 1F, H**). Collectively, these findings indicate that mitophagy is temporarily enhanced and then continues to decline in HS-ALI.

Mitophagy-Deficiency Increases Apoptosis in HS-ALI

Mitophagy was reported to be essential for selectively eliminating damaged mitochondria through autophagy (24). To explore the role and regulation of mitophagy in acute liver damage in HS-ALI mice, the autophagy inhibitor 3-MA was used to inhibit the autophagic process of damage mitochondria clearance. TEM examinations revealed that 3-MA inhibited the formation of autophagosomes in hepatocytes and exacerbated mitochondrial damage, as demonstrated by the presence of fragmentation, swelling, and vacuoles in the mitochondrial matrix, which further aggravated acute liver injury in response to HS (**Figure 2A**). Furthermore, 3-MA significantly decreased mitophagy, as indicated by the downregulation of mitophagy-related proteins in mitochondria in the liver tissues (**Figures 2B, C**). 3-MA pretreatment significantly exacerbated acute liver damage and increased apoptosis in HS-treated mice, as evidenced by increased liver histological scores, TUNEL-positive cells, Caspase 3 activity, and serum ALT and AST levels (**Figures 2D–H**). Two major proteins of intrinsic apoptosis pathway are apoptosis-related proteins BCL-2 Associated X Protein (BAX) as a proapoptotic protein and B-cell lymphoma 2 (Bcl2) as an antiapoptotic one (25). Correspondingly, 3-MA significantly exacerbated apoptosis in HS-induced mice, as evidenced by the upregulate of BAX and downregulate of Bcl2 levels (**Figure 2I**). In agreement with these results above, Mdivi-1, a dynamin-related protein 1/mitophagy inhibitor, significantly

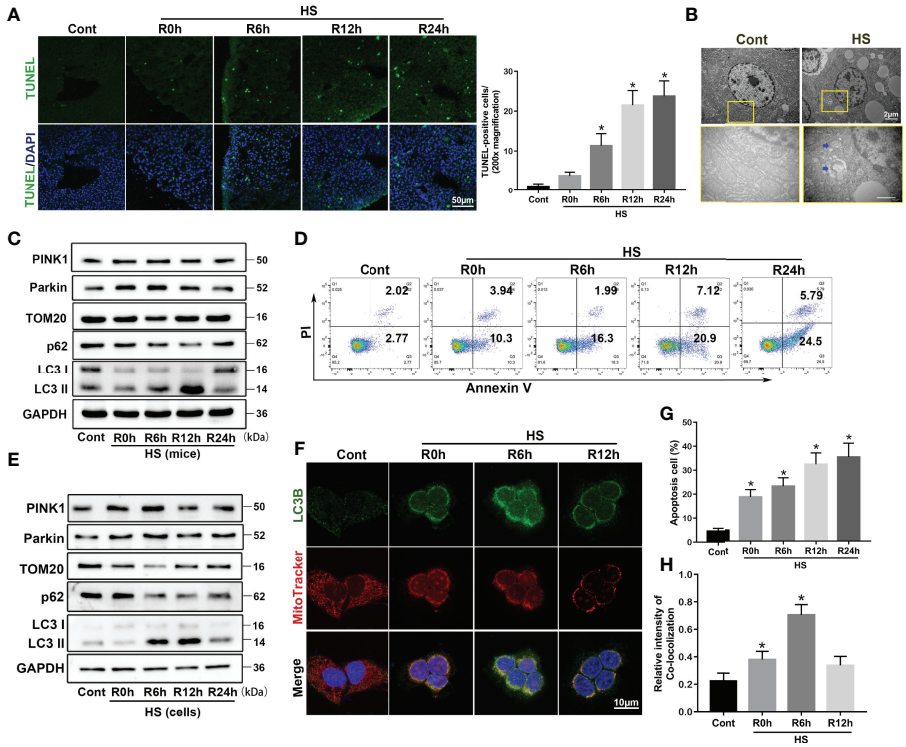

FIGURE 1 | Parkin-mediated mitophagy is induced by HS *in vivo* and *in vitro*. Mitophagy is induced by HS-ALI *in vivo* and *in vitro*. Liver tissues were obtained from HS and sham control mice at the time point of HS onset (0 h) and 6 h, 12 h, and 24 h later. LO2 cells were cultured at 42°C for 3 h to simulate HS followed by incubation at 37°C for 0, 6, 12, and 24 h **(A)** Apoptosis observed by TUNEL staining of liver tissues with quantification of TUNEL-positive cells. Scale bar: 50 μm. **(B)** Representative TEM images of mitochondrial morphology in hepatocytes at 6 h following HS. Blue arrows: mitophagosome and mitolysosome. Scale bar: 2 μm. **(C)** Immunoblot analysis of mito/autophagy-related proteins, including PINK1, Parkin, TOM20, p62, and LC3-II, in liver tissues following HS. **(D, G)** Apoptosis was assessed using Annexin V-FITC/PI staining. **(E)** Immunoblot analysis of mito/autophagy-related proteins, including PINK1, Parkin, TOM20, p62, and LC3-II in HS-induced LO2 cells. **(F, H)** Representative images and quantification of immunofluorescence double-labeling LC3B (green) and MitoTracker (red) in HS-treated LO2 cells, scale bar: 10 μm. Data are shown as the mean ± SD. n = 4. *p < 0.05.

inhibited mitophagy as indicated by western blotting of mito/autophagy-related proteins as well as the formation of autophagosome containing damaged mitochondria (**Figures S2A–C**). Mdivi-1 also exacerbated apoptosis in HS-induced mice, as shown by western blotting of apoptosis-related proteins and Caspase 3 activity (**Figures S2D–H**). Therefore, these results suggest that mitophagy-deficiency exacerbates hepatocyte apoptosis in HS-ALI mice.

Parkin Deficiency Exacerbates Apoptosis and Mitochondrial Damage in HS-Induced LO2 Cells

To determine the role and function of Parkin-mediated mitophagy in HS-treated LO2 cells, siRNA was used to silence Parkin. siRNA transfection successfully inhibited protein levels of Parkin in LO2 cells (**Figure S3A**). Parkin knockdown dramatically reduced mitophagy activation by p62 and LC3-II in mitochondria in LO2 cells following HS (**Figure 3A**). Parkin knockdown also decreased the ubiquitination levels of VDAC (**Figure 3B**). In addition, colocalization of LC3B and MitoTracker revealed reduced formation of mitophagosomes after silencing Parkin (**Figures 3C, D**), suggesting that Parkin-dependent mitophagy was activated by HS and then prevented by silencing Parkin. Furthermore, silencing Parkin remarkably exacerbated apoptosis in LO2 cells following HS, as shown by western blotting and Caspase 3 activity assays (**Figures 3E, F**, **S3B**). Taken together, these data suggested that Parkin-mediated mitophagy deficiency exacerbates hepatocyte apoptosis after HS.

Increased ROS release is positively correlated with cell death and pathological disorders (26). Oxidative stress levels, as assessed using the ROS probe DHE, was agitated by HS and further exacerbated by silencing Parkin (**Figure 3G**). We measured changes in ΔΨm using JC-1 staining. As shown in **Figure 3H**, HS significantly decreased ΔΨm, which was further exacerbated by silencing Parkin. Together, these data demonstrate that Parkin-mediated mitophagy deficiency may exacerbate HS-induced mitochondrial damage.

Cytosolic p53 Binds to Parkin Following HS

p53 is reported to be an important molecule for the crosstalk of autophagy and apoptosis (27). Cytosolic p53 has been shown to bind to Parkin and disrupt the clearance of damaged mitochondria

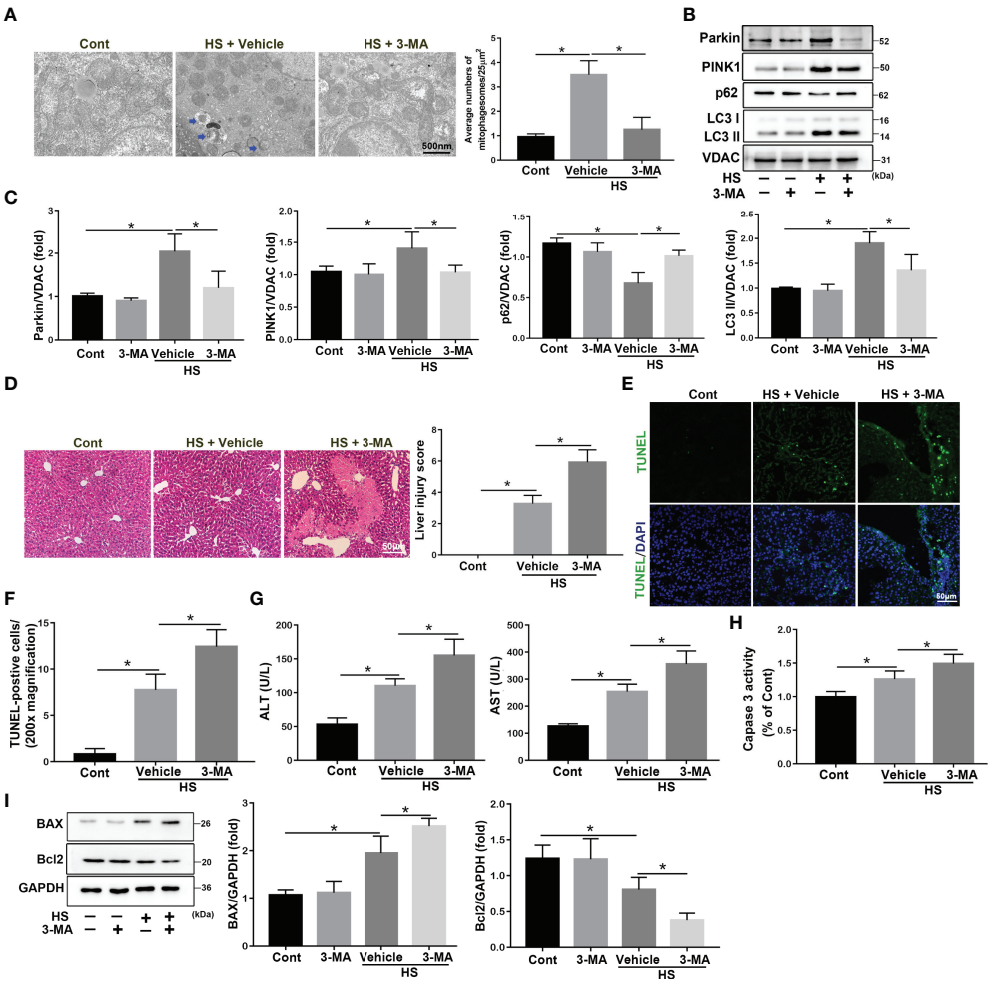

FIGURE 2 | 3-MA treatment increases apoptosis in HS-ALI. Mice were pretreated with 3-MA (20 mg/kg, i.p.) for 2 h and then subjected to sham-untreated or HS. Livers and serum were collected 6 hours after HS. **(A)** Representative TEM images of mitochondrial morphology in hepatocytes after HS. Blue arrows: mitophagosome and mitolysosome. Scale bar: 500nm. **(B, C)** Immunoblot analysis and quantification of mito/autophagy-related proteins, including Parkin, PINK1, p62, and LC3-II, in the mitochondrial fractions of livers. **(D)** Representative histology and pathological score of liver samples by H&E staining. Scale bar: 50 μm. **(E, F)** Apoptosis was observed by TUNEL staining of liver tissues and quantification of TUNEL-positive cells. Scale bar: 50 μm. **(G)** Relative serum ALT and AST levels. **(H)** The enzymatic activity of Caspase 3 was subsequently measured. **(I)** Immunoblot analysis and quantification of BAX and Bcl2 in liver tissues. n = 4. Data are shown as the mean ± SD. n = 4. *p < 0.05.

by Parkin-mediated mitophagy in diabetic islets (28). Other recent studies also reported that p53 exerts distinct cellular functions depending on its cellular concentration and distribution (29, 30). Here, we found that p53 protein levels gradually increased after HS compared to the controls *in vivo* and *in vitro* (**Figures S4A, B**). To further assess whether the intracellular distribution of p53 was altered and whether cytosolic p53 binds to Parkin in HS-induced LO2 cells, immunoblotting analysis and immunofluorescence staining were used. Nuclear p53 protein levels were progressively reduced, and cytoplasmic levels of p53 gradually increased, suggesting an increase in the translocation of p53 from the nucleus to the cytoplasm at 0-6 h following HS (**Figures 4A, B**). In particular, the endogenous Parkin-p53 complex was identified in immunoprecipitants of endogenous Parkin and p53, as well as in the cytosolic lysate of LO2 cells after HS (**Figures 4C–E**). Moreover, colocalization of p53 and Parkin suggested that p53 could bind to Parkin in HS-treated LO2 cells, as indicated by immunofluorescence staining (**Figure 4F**). These data demonstrate that cytosolic p53 binds to Parkin in HS-treated LO2 cells.

p53 Regulates Parkin-Dependent Mitophagy and Apoptosis in HS-ALI

Crosstalk between cytosolic p53 and Parkin-dependent mitophagy has been reported (31). To investigate the role of p53 in regulating mitophagy in HS-ALI, the p53 agonist Tenovin-6 and the selective p53 inhibitor PFT-α were used in HS-ALI mice. TEM revealed that p53 activation by Tenovin-6 prevented the formation of mitochondrial autophagosomes in hepatocytes and exacerbated mitochondrial damage (**Figure 5A**). Correspondingly, Tenovin-6 pretreatment significantly inhibited mitophagy, as indicated by the

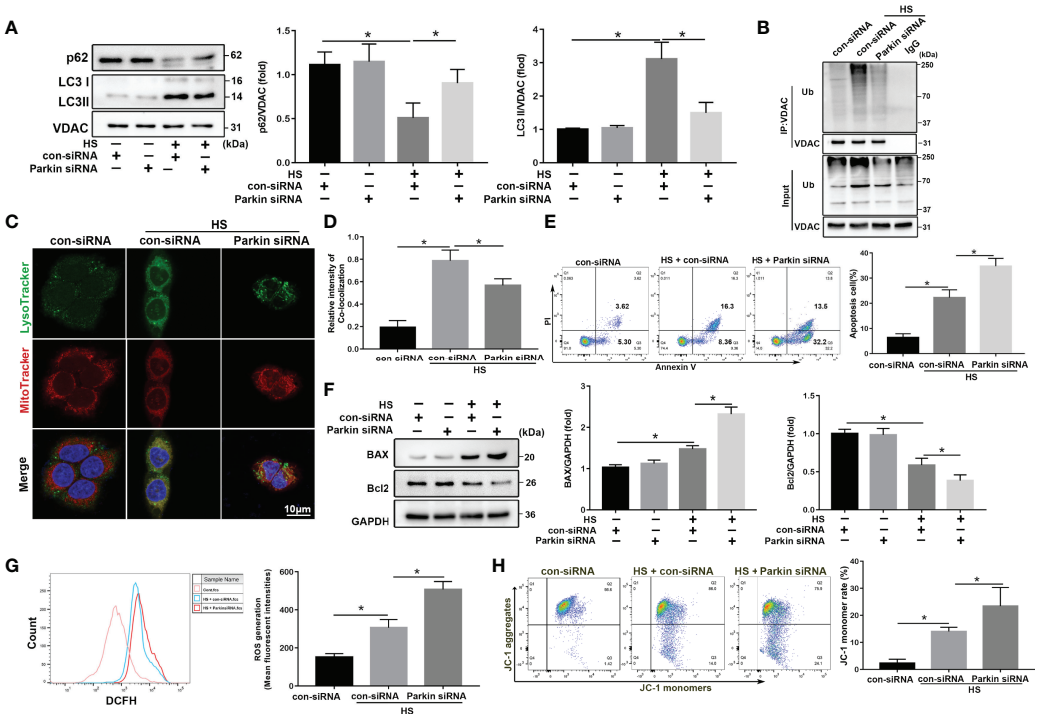

FIGURE 3 | Parkin deficiency exacerbates apoptosis and mitochondria damage in HS-induced LO2 cells. After transfection with con-siRNA or Parkin siRNA for 8 h, LO2 cells were exposed to 42°C for 3 h and then incubated at 37°C for 6 h **(A)** Immunoblot analysis and quantification of mito/autophagy-related proteins, including Parkin, p62, and LC3-II, in the mitochondrial fractions of LO2 cells. **(B)** Immunoprecipitation (IP) analysis of VDAC ubiquitination levels. **(C, D)** Representative images and quantification of immunofluorescence double-labeling LysoTracker (green) and MitoTracker stains (red) in HS-treated LO2 cells. Scale bar: 5 μm. **(E)** Apoptosis was assessed using Annexin V-FITC/PI staining. **(F)** Immunoblot analysis and quantification of BAX and Bcl2 in HS-treated LO2 cells. **(G)** Representative images and quantification of the ROS probe DHE staining in HS-treated LO2 cells. **(H)** Flow cytometry analysis of ΔΨm in LO2 cells stained with JC-1. The percentage represents LO2 cells with damaged mitochondria (low ΔΨm). Data are shown as the mean ± SD. n = 4. *p < 0.05.

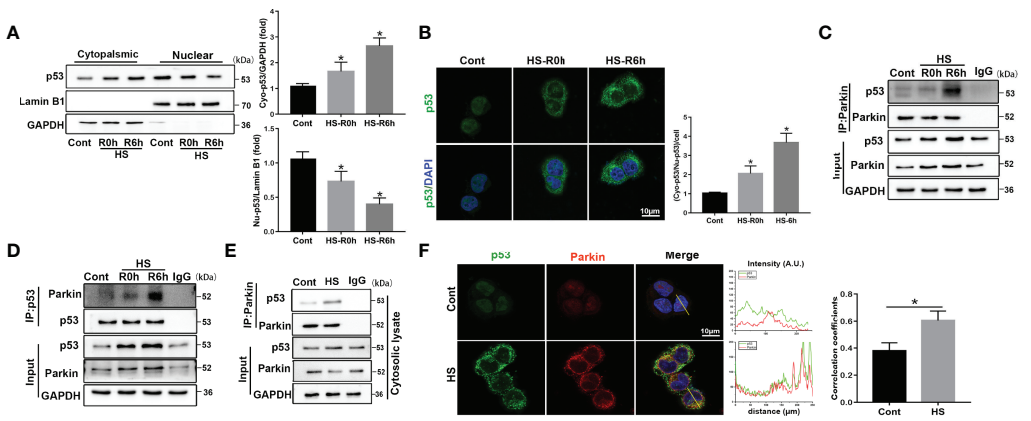

FIGURE 4 | Translocation of p53 from the nucleus to the cytoplasm and cytosolic p53 binding to Parkin following HS. LO2 cells were exposed to 42°C for 3 h for HS treatment and then incubated at 37°C for 0 or 6 h **(A)** Immunoblot analysis and quantification of p53 in the nucleus and cytoplasm after HS. **(B)** Representative images of immunofluorescence labeling of p53 in the nucleus and cytoplasm in HS-treated LO2 cells with quantification of the ratio of fluorescence intensity of cytoplasmic p53 to nuclear p53 in LO2 cells. Scale bar: 10 μm. **(C, D)** Endogenous Parkin-p53 complex in total lysates of HS-treated LO2 cells. **(E)** The endogenous Parkin-p53 complex in cytosolic lysates of LO2 cells following HS. **(F)** Representative images and quantification of immunofluorescence double-labeling p53 and Parkin in HS-treated LO2 cells. Scale bar: 10 μm. Data are shown as the mean ± SD. n = 4. *p < 0.05.

downregulation of Parkin, LC3-II, and upregulation of p62 protein expression in mitochondria in the livers of HS-induced mice (**Figures 5B, C**). In addition, Tenovin-6 exacerbated HS-ALI, as evidenced by increased liver histological scores, TUNEL-positive cells, and serum ALT and AST levels (**Figures 5D, E**, **S4C, D**). Tenovin-6 also exacerbated HS-induced apoptosis in HS-ALI mice (**Figures 5F–H**). In contrast, the p53 inhibitor PFT-α attenuated apoptosis in HS-ALI by improving Parkin-dependent mitophagy (**Figures 5A–H**). Collectively, these data suggest that p53 regulates Parkin-dependent mitophagy and apoptosis in HS-ALI.

p53 Regulates Parkin-Dependent Mitophagy and Apoptosis in HS-Treated LO2 Cells

Next, to further assess the regulation of Parkin-mediated mitophagy by p53 in LO2 cells following HS, a specific adenovirus was used Rya Marasiganto achieve p53 overexpression (**Figure S4E**). p53 overexpression strongly inhibited HS-induced translocation of Parkin from the cytoplasm to the mitochondria (**Figure 6A**). Furthermore, p53 overexpression markedly suppressed expression levels of mitophagy-related proteins in LO2 cells following HS (**Figure 6B**). p53 overexpression also decreased VDAC ubiquitination levels and formations of mitophagosomes (**Figures 6C, D**). Moreover, p53 overexpression significantly increased hepatocyte apoptosis (**Figures 6E–H**).

We speculated that p53 deletion would enhance Parkin-mediated mitophagy activation in LO2 cells following HS. To test this hypothesis, p53 siRNA was used to inhibit p53 expression in LO2 cells (**Figure S4F**). As expected, knockdown of p53 markedly promoted HS-induced translocation of Parkin from the cytoplasm to the mitochondria (**Figure 7A**) and significantly enhanced mitophagy activation in HS-treated LO2 cells (**Figures 7B–D**). In addition, p53 deletion also inhibited HS-induced apoptosis in HS-treated LO2 cells (**Figures 7E–H**). Taken together, these results suggest that Parkin-dependent

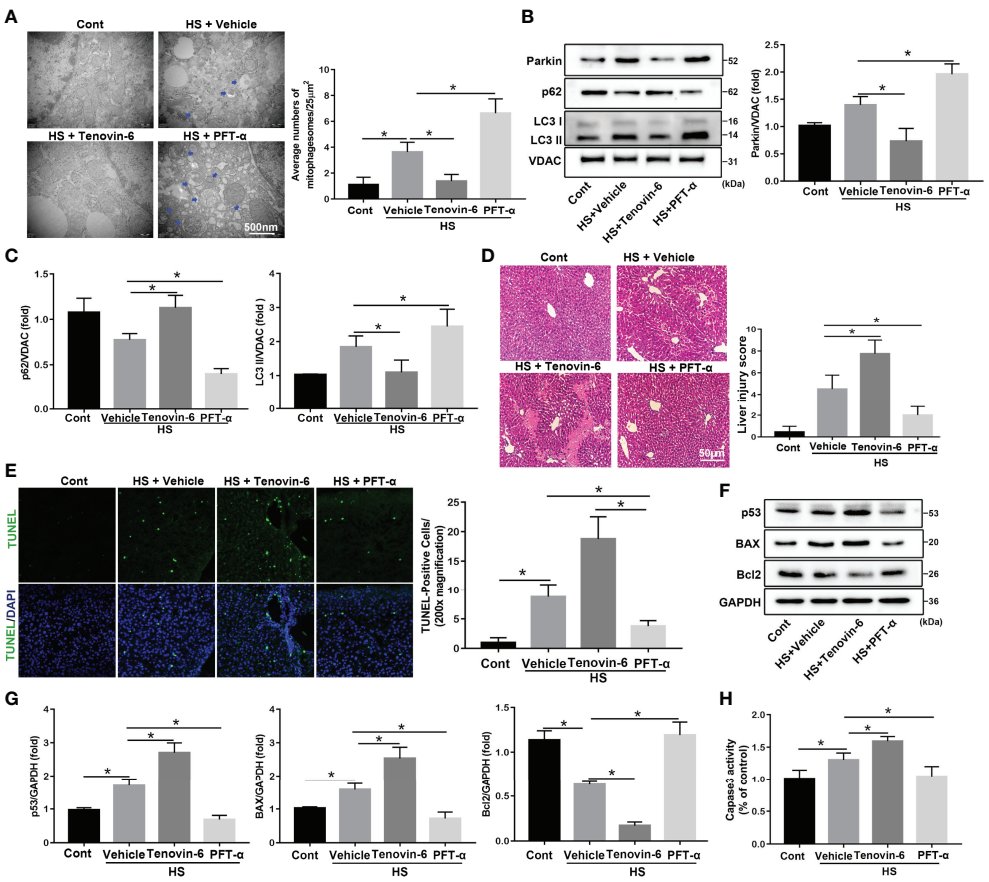

FIGURE 5 | p53 regulates Parkin-dependent mitophagy and apoptosis in HS-ALI. Mice were pretreated with the selective p53 agonist Tenovin-6 (25 mg/kg, i.p.) or the p53 inhibitor PFT-α (2.2 mg/kg, i.p.) for 2 h and then subjected to HS, these livers and blood were collected 6 hours after HS. **(A)** Representative TEM images of mitochondrial morphology in hepatocytes after HS. Blue arrows: mitophagosome and mitolysosome. Scale bar: 500 nm. **(B, C)** Immunoblot analysis and quantification of mito/autophagy-related proteins, including Parkin, p62, and LC3-II, in the mitochondrial fractions of livers. **(D)** Representative histology and pathological score of liver samples by H&E staining. Scale bar: 50 μm. **(E)** Apoptosis was observed by TUNEL staining of liver tissues and quantification of TUNEL-positive cells. Scale bar: 50 μm. **(F, G)** Immunoblot analysis and quantification of p53, BAX, and Bcl2 proteins in liver tissues. **(H)** The enzymatic activity of Caspase 3 was determined. Data are shown as the mean ± SD. n = 4. *p < 0.05.

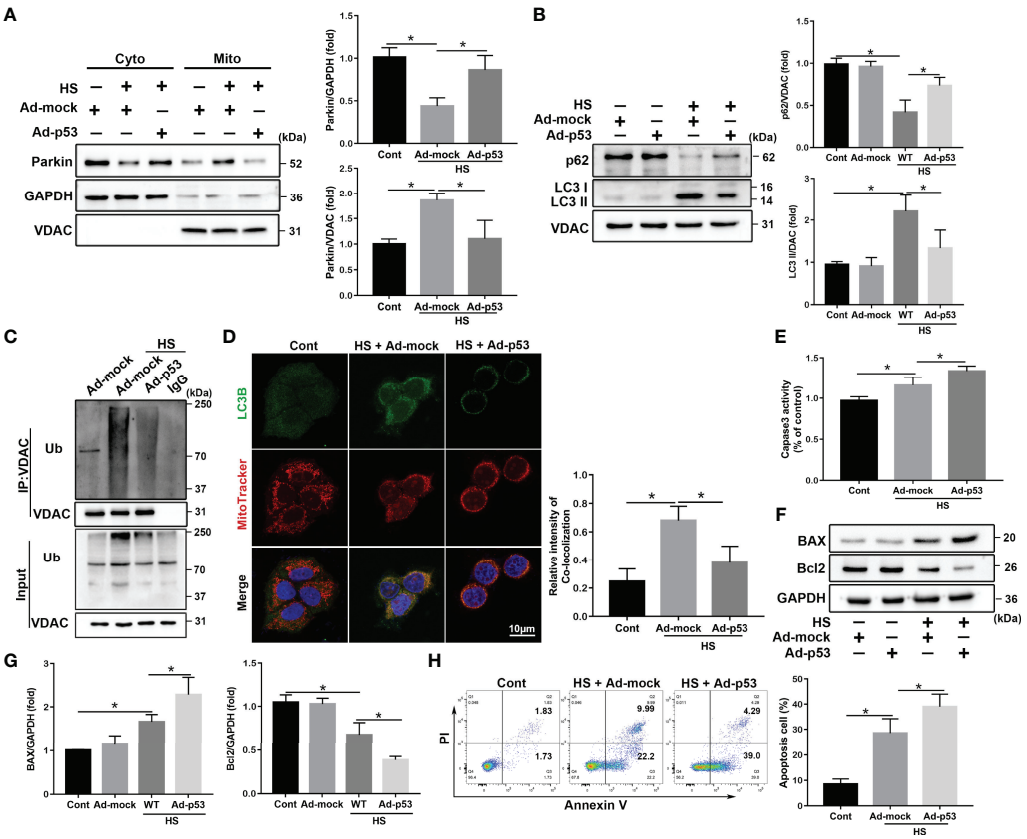

FIGURE 6 | p53 overexpression exacerbates apoptosis through Parkin-dependent mitophagy *in vitro*. After transfection with the empty adenovirus (Ad-mock) or p53 adenovirus (Ad-p53) Ad-p53 for 8 h, LO2 cells were exposed to 42°C for 3 h for HS treatment followed by incubation at 37°C for 6 h **(A)** Immunoblot analysis and quantification of Parkin in the cytoplasm and mitochondrial fractions after HS. **(B)** Immunoblot analysis and quantification of autophagy-related proteins p62 and LC3-II in the mitochondrial fractions of LO2 cells. **(C)** Immunoprecipitation analysis of VDAC ubiquitination levels. **(D)** Representative images and quantification of immunofluorescence double-labeling LC3B (green) and MitoTracker stains (red) in HS-treated LO2 cells. Scale bar: 10 μm. **(E)** The enzymatic activity of Caspase 3 was subsequently determined. **(F, G)** Immunoblot analysis and quantification of BAX and Bcl2 in HS-treated LO2 cells. **(H)** Apoptosis was measured using Annexin V-FITC/PI staining. Data are shown as the mean ± SD. n = 4. *p < 0.05.

mitophagy and apoptosis are activated by HS, which are further exacerbated by p53 overexpression in HS-treated LO2 cells, whereas inhibition of p53 may effectively reverse this process.

p53 Regulates Mitophagy and Mitochondrial Damage *via* Parkin

We subsequently explored the molecular mechanisms by which p53 regulates mitophagy and oxidative stress *via* Parkin. p53 inhibitor PFT-α significantly enhanced mitophagy activation in LO2 cells following HS (**Figure 8A**). Consistent with the immunoblotting results, colocalization of LC3B and MitoTracker demonstrated increased formations of mitophagosomes (**Figure 8B**). However, the protective effect of PFT-α was eliminated in Parkin siRNA-treated LO2 cells (**Figures 8A, B**). Similar results were also observed with respect to mitochondrial damage as assessed by flow cytometry analysis. As shown in **Figures 8C, D**, PFT-α also upregulated mitochondrial ΔΨm and decreased ROS production, which were effectively reversed by silencing Parkin. Overall, these results demonstrate that PFT-α treatment ameliorates mitochondrial damage through Parkin-mediated mitophagy in HS-induced LO2 cells.

DISCUSSION

It is well known that mitophagy, the principal mechanism to eliminate impaired mitochondria, is important for the regulation of mitochondrial function and cellular homeostasis (32, 33). Here, our results indicated an increase of PINK1 expression levels in the mitochondria at 6 h after HS, and an increase in the translocation of Parkin from the cytoplasm to the mitochondria *in vivo* and *in vitro*, suggesting that HS treatment stabilized PINK1 at the outer mitochondrial membrane and thereby recruits more Parkin to damage mitochondria. Interestingly, Recent evidence has suggested a linear PINK1-Parkin mitophagy pathway, which places PINK1 as a critical upstream molecule for Parkin recruitment (34). PINK1-mediated phosphorylation recruits the E3 ubiquitin ligase Parkin, leading

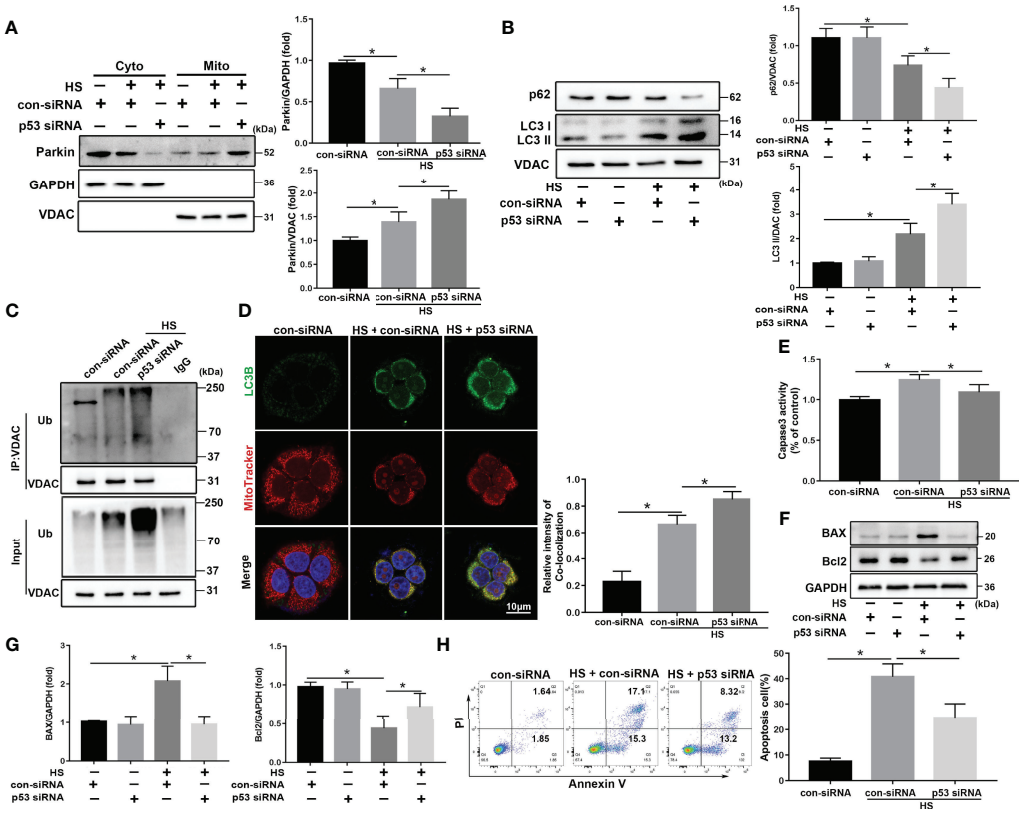

FIGURE 7 | p53 knockdown attenuates apoptosis through Parkin-dependent mitophagy *in vitro*. After transfection with con-siRNA or p53 siRNA for 8 h, LO2 cells were exposed to 42°C for 3 h for HS treatment followed by incubation at 37°C for 6 h **(A)** Immunoblot analysis and quantification of Parkin in the cytoplasm and mitochondrial fractions after HS. **(B)** Immunoblot analysis and quantification of autophagy-related proteins p62 and LC3-II in the mitochondrial fractions of LO2 cells. **(C)** Immunoprecipitation analysis of VDAC ubiquitination levels. **(D)** Representative images and quantification of immunofluorescence double-labeling LC3B (green) and MitoTracker stains (red) in HS-treated LO2 cells. Scale bar: 10 μm. **(E)** The enzymatic activity of Caspase 3 was subsequently assessed. **(F, G)** Immunoblot analysis and quantification of BAX and Bcl2 in HS-treated LO2 cells. **(H)** Apoptosis was measured using Annexin V-FITC/PI staining. Data are shown as the mean ± SD. n = 4. *p < 0.05.

to ubiquitination of substrates on damaged mitochondria (35). Meanwhile, one recent study demonstrated the protective role of Parkin-mediated mitophagy in Contrast-induced acute kidney injury (CI-AKI) (36). Parkin-mediated mitophagy was also indicated that contribution to liver pathophysiology (37). Our data also demonstrated that Parkin-mediated mitophagy deficiency may exacerbate HS-induced hepatocyte apoptosis by using Parkin siRNA. Thus, Parkin also plays an important role in the induction of mitophagy. In addition, we observed that mitochondrial dysfunction was necessary for cellular injury or death in response to HS. Meanwhile, although both hepatocyte apoptosis and mitophagy increased at 0-6 h after HS treatment, mitophagy deficiency exacerbated hepatocyte injury and apoptosis after HS, supporting a protective role of mitophagy in HS-ALI. Moreover, we demonstrated cytosolic p53 inhibited Parkin's mitochondrial translocation, preventing the removal of damaged mitochondria and exacerbating hepatocyte apoptosis and oxidative stress. These findings provide a mechanistic explanation for the observed HS-induced compromise of mitochondrial integrity and functional decline in HS-ALI.

Emerging evidence indicates that mitophagy plays a crucial role in the regulation of liver homeostasis (38, 39). Impaired mitophagy is known to contribute to several liver pathologies, including drug-induced liver injury, hepatic ischemia-reperfusion injury (IR), alcoholic liver disease (ALD), nonalcoholic fatty liver disease (NAFLD), and viral hepatitis (40). In IR-ALI, Xu et al. found that increased hepatic mitophagy is induced at the early stages of IR, both *in vivo* and *in vitro*, which is linked to elevated cell death and aggregated liver injury (41). In drug-induced liver injury, acetaminophen (APAP) administration enhances Parkin's mitochondrial translocation and concurrently mitophagy induction in mouse livers (42). However, the role of mitophagy in HS-AL remains unknown. Notably, we provide additional mechanistic evidence that Parkin-mediated mitophagy was activated in hepatocytes exposed to HS-ALI, as illustrated by Parkin deletion, Mdivi-1, and 3-MA treatment. Our data demonstrated that defective Parkin-mediated mitophagy resulted in excessive accumulation of damaged mitochondria, leading to ROS generation and ΔΨm depolarization. Inhibition of mitophagy resulted in increased

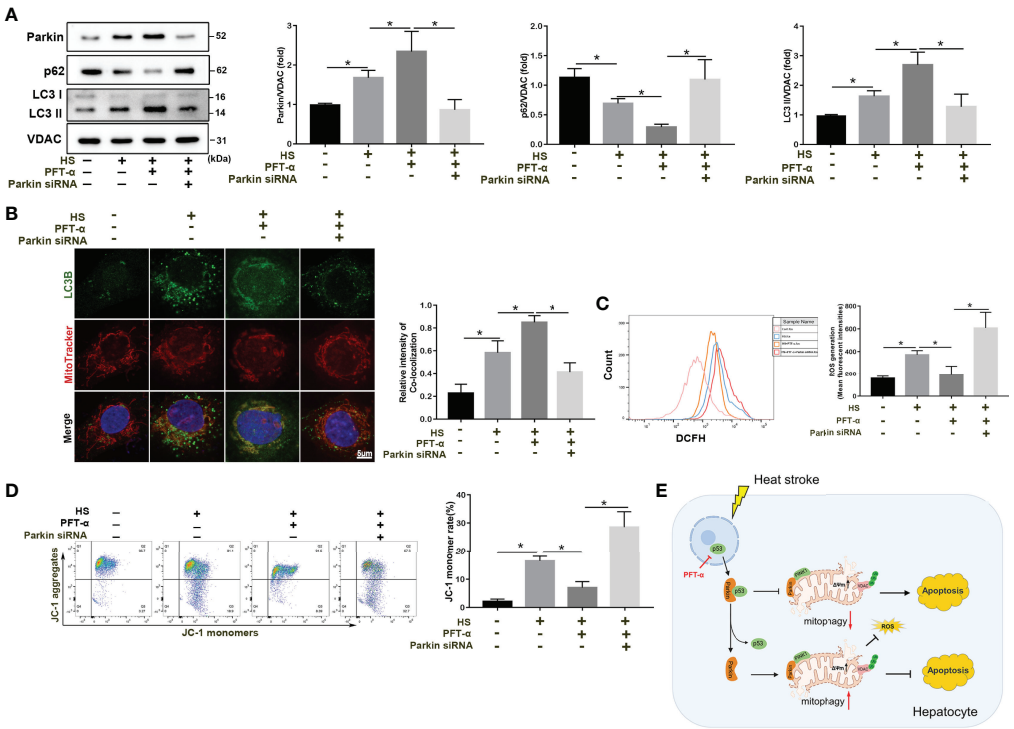

FIGURE 8 | p53 regulates mitophagy and mitochondrial damage through Parkin. After transfection with con-siRNA or p53 siRNA for 8 h, LO2 cells were pretreated with the p53 inhibitor PFT-α (20 μM) and then subjected to HS. **(A)** Immunoblot analysis and quantification of mito/autophagy-related proteins, including Parkin, p62, and LC3-II, in the mitochondrial fractions of LO2 cells. **(B)** Representative images and quantification of immunofluorescence double-labeling LC3B (green) and MitoTracker stains (red) in HS-treated LO2 cells. Scale bar: 5 μm. **(C)** Representative images and quantification of the ROS probe DHE staining in HS-treated LO2 cells. **(D)** Flow cytometry analysis of $\Delta\Psi m$ in LO2 cells stained with JC-1. **(E)** Proposed mechanism by which p53-Parkin-mediated mitophagy alleviates hepatocyte apoptosis in HS-ALI. In response to HS, increased translocation of p53 from the nucleus to the cytoplasm is induced. Subsequently, cytosolic p53 binds to Parkin, which blocks Parkin mitochondrial translocation and reduces VDAC ubiquitination levels, leading to inhibition of mitophagy, upregulation of ROS production, and ultimately exacerbating hepatocyte apoptosis. Of note, p53 deficiency effectively reverses this process. Data are shown as the mean ± SD. n =4. *p < 0.05.

levels of apoptosis and mitochondrial injury in hepatocytes following HS, indicating a protective role of mitophagy in HS-ALI by restraining apoptosis and mitochondrial injury in hepatocytes.

With respect to the regulatory pathways that influence mitochondrial integrity and function, we found that p53 was potently activated in HS-treated hepatocytes. Growing evidence suggests that p53 is a transcription factor that is activated by multiple different stresses, including DNA damage, oncogene activation, oxidative stress, and disruption of nucleolar function (43, 44). In addition, p53 exerts differential effects on cellular function according to its cellular concentration and distribution. Genotoxic stress provokes p53 accumulation in both the nucleus and cytosol, and endogenous cytosolic p53 directly activates BAX to induce apoptosis (45). p53 is also known to restrict autophagy activation through a cytosolic effect (46). The direct molecular link between p53 activation and Parkin-mediated mitophagy deficiency contributes to the mitochondrial compromise associated with aging-related and doxorubicin (DOX)-mediated decreases in cardiac contractility (47). Here, we found that p53 translocation from the nucleus to the cytoplasm was increased by HS in a time-dependent manner. The endogenous Parkin-p53 complex was identified in immunoprecipitants of endogenous Parkin and p53 in the cytosolic lysate, as well as colocalization of p53 and Parkin indicated by immunofluorescence staining, indicating that cytosolic p53 binds to Parkin in HS-treated LO2 cells. Consistent with previous studies, our results also demonstrated that p53 inhibits mitophagy by inhibiting Parkin's translocation from the cytosol to mitochondria, which in turn reduces VDAC ubiquitination levels. Previous studies demonstrated that p53 can bind to the RING0 region of Parkin, disrupting Parkin's biological function and affecting damaged mitochondrial clearance and cellular redox homeostasis (28, 48). Whether this also occurs in HS-treated hepatocytes requires further study.

Although these findings demonstrated the key role of p53 in Parkin-dependent mitophagy, to the best of our knowledge, the exact mechanism whereby p53 controls mitochondrial homeostasis remains unclear. In particular, previous studies have demonstrated that p53 regulates mitochondrial homeostasis through nuclear, cytosolic or intramitochondrial sites of action (49, 50). A recent study demonstrated that nuclear p53 decreases the specialized

autophagy-related mitophagy response by transcriptionally downregulating PINK1 (51). Consistently, the p53-dependent anti-autophagic phenotype exclusively accounts for cytosolic p53 in sepsis-induced acute kidney injury, which may promote proteasomal degradation of the autophagic protein Beclin1 (52). p53 preserves mitochondrial biogenesis and function in the setting of the telomeric DNA damage response (DDR) (53). Of note, the mechanism underlying the role of p53 on different cellular distributions in regulating mitochondrial homeostasis remains unclear, and further studies are needed to address these gaps in knowledge. In this study, p53 overexpression using a specific adenovirus or Tenovin-6 exacerbated hepatocyte apoptosis and oxidative stress through habiting Parkin-dependent mitophagy in HS-ALI, whereas inhibition of p53 using siRNA or PFT-α effectively reversed this process. Consequently, it appears certain that the mitochondria-related functions of p53 have broader implications than previously thought in HS-ALI, providing new therapeutic targets for treatment.

In summary, our present study provides a molecular understanding of Parkin-dependent mitophagy in HS-ALI. We uncovered a novel concept, as shown in **Figure 8E**, whereby increased cytosolic p53 inhibits Parkin-mediated mitophagy and provokes mitochondrial compromise in response to HS-ALI. In particular, the enhancement of p53 activation and Parkin-mediated mitophagy deficiency aggravated apoptosis and ROS production following HS. And p53 deficiency effectively with inhibitor reverses this process. Therefore, our study shows that p53 has a previously undescribed pathogenic effect on HS-treated hepatocytes in which cytosolic p53 aggravates apoptosis by inhibiting Parkin-mediated mitophagy. p53-parkin-mediated mitophagy may represent a novel target for attenuating HS-ALI.

DATA AVAILABILITY STATEMENT

The raw data supporting the conclusions of this article will be made available by the authors, without undue reservation.

ETHICS STATEMENT

The animal study was reviewed and approved by Ethical Committee for Animal Experimentation of Nanfang Hospital.

AUTHOR CONTRIBUTIONS

WH and WX were involved in conception and design, performance of experiments, and composition of this manuscript. HZ and SC performed all the experiments and analyzed our results. YoL, QH, and YaL were involved in the data acquisition. YaL and ZZ confirmed the authenticity of the raw data. All authors analyzed the data, and reviewed and approved the final manuscript.

FUNDING

This study was supported by grants from the National Natural Science Foundation of China (81701955, 81871604, and 82172181).

SUPPLEMENTARY MATERIAL

The Supplementary Material for this article can be found online at: https://www.frontiersin.org/articles/10.3389/fimmu.2022.859231/full#supplementary-material

REFERENCES

1. Bouchama A, Knochel JP. Heat Stroke. *N Engl J Med* (2002) 346(25):1978–88. doi: 10.1056/NEJMra011089
2. Alele FO, Malau-Aduli BS, Malau-Aduli AEO, J Crowe M. Epidemiology of Exertional Heat Illness in the Military: A Systematic Review of Observational Studies. *Int J Environ Res Public Health* (2020) 17(19). doi: 10.3390/ijerph17197037
3. Liu Z-F, Ji J-J, Zheng D, Su L, Peng T. Calpain-2 Protects Against Heat Stress-Induced Cardiomyocyte Apoptosis and Heart Dysfunction by Blocking P38 Mitogen-Activated Protein Kinase Activation. *J Cell Physiol* (2019) 234 (7):10761–70. doi: 10.1002/jcp.27750
4. Xuan B, Park J, Choi S, You I, Nam B-H, Noh ES, et al. Draft Genome of the Korean Smelt Hypomesus Nipponensis and its Transcriptomic Responses to Heat Stress in the Liver and Muscle. *G3 (Bethesda)* (2021) 11(9). doi: 10.1093/g3journal/jkab147
5. Hirao H, Nakamura K, Kupiec-Weglinski JW. Liver Ischaemia-Reperfusion Injury: A New Understanding of the Role of Innate Immunity. *Nat Rev Gastroenterol Hepatol* (2021) 19(4):239–56. doi: 10.1038/s41575-021-00549-8
6. Vescia FG, Peck OC. Liver Disease From Heat Stroke. *Gastroenterology* (1962) 43:340–3. doi: 10.1055/s-0038-1670656
7. Bi X, Deising A, Frenette C. Acute Liver Failure From Exertional Heatstroke Can Result in Excellent Long-Term Survival With Liver Transplantation. *Hepatol (Baltimore Md)* (2020) 71(3):1122–3. doi: 10.1002/hep.30938
8. Dokladny K, Myers OB, Moseley PL. Heat Shock Response and Autophagy–Cooperation and Control. *Autophagy* (2015) 11(2):200–13. doi: 10.1080/15548627.2015.1009776
9. Li L, Su Z, Zou Z, Tan H, Cai D, Su L, et al. Ser46 Phosphorylation of P53 is an Essential Event in Prolyl-Isomerase Pin1-Mediated P53-Independent Apoptosis in Response to Heat Stress. *Cell Death Dis* (2019) 10(2):96. doi: 10.1038/s41419-019-1316-8
10. Youle RJ. Mitochondria-Striking a Balance Between Host and Endosymbiont. *Science (New York NY)* (2019) 365(6454):eaaw9855. doi: 10.1126/science.aaw9855
11. Samaiya PK, Krishnamurthy S, Kumar A. Mitochondrial Dysfunction in Perinatal Asphyxia: Role in Pathogenesis and Potential Therapeutic Interventions. *Mol Cell Biochem* (2021) 476(12):4421–34. doi: 10.1007/s11010-021-04253-8
12. Bader V, Winklhofer KF. PINK1 and Parkin: Team Players in Stress-Induced Mitophagy. *Biol Chem* (2020) 401(6-7):891–9. doi: 10.1515/hsz-2020-0135
13. Deshwal S, Fiedler KU, Langer T. Mitochondrial Proteases: Multifaceted Regulators of Mitochondrial Plasticity. *Annu Rev Biochem* (2020) 89:501–28. doi: 10.1146/annurev-biochem-062917-012739
14. Song Y, Xu Y, Liu Y, Gao J, Feng L, Zhang Y, et al. Mitochondrial Quality Control in the Maintenance of Cardiovascular Homeostasis: The Roles and Interregulation of UPS, Mitochondrial Dynamics and Mitophagy. *Oxid Med Cell Longev* (2021) 2021:3960773. doi: 10.1155/2021/3960773
15. Fu X, Wu S, Li B, Xu Y, Liu J. Functions of P53 in Pluripotent Stem Cells. *Protein Cell* (2020) 11(1):71–8. doi: 10.1007/s13238-019-00665-x
16. Chen Y, Yu T. Involvement of P53 in the Responses of Cardiac Muscle Cells to Heat Shock Exposure and Heat Acclimation. *J Cardiovasc Transl Res* (2020) 13(6):928–37. doi: 10.1007/s12265-020-10003-w
17. Song YM, Lee WK, Lee Y-H, Kang ES, Cha B-S, Lee B-W. Metformin Restores Parkin-Mediated Mitophagy, Suppressed by Cytosolic P53. *Int J Mol Sci* (2016) 17(1):122. doi: 10.3390/ijms17010122

18. Zhang F, Peng W, Zhang J, Dong W, Wu J, Wang T, et al. P53 and Parkin Co-Regulate Mitophagy in Bone Marrow Mesenchymal Stem Cells to Promote the Repair of Early Steroid-Induced Osteonecrosis of the Femoral Head. *Cell Death Dis* (2020) 11(1):42. doi: 10.1038/s41419-020-2238-1
19. Agarwal S, Muqit MMK. PTEN-Induced Kinase 1 (PINK1) and Parkin: Unlocking a Mitochondrial Quality Control Pathway Linked to Parkinson's Disease. *Curr Opin Neurobiol* (2021) 72:111–9. doi: 10.1016/j.conb.2021.09.005
20. Jung YY, Son DJ, Lee HL, Kim DH, Song MJ, Ham YW, et al. Loss of Parkin Reduces Inflammatory Arthritis by Inhibiting P53 Degradation. *Redox Biol* (2017) 12:666–73. doi: 10.1016/j.redox.2017.04.007
21. Li Y, Ma Y, Song L, Yu L, Zhang L, Zhang Y, et al. SIRT3 Deficiency Exacerbates P53/Parkin-Mediated Mitophagy Inhibition and Promotes Mitochondrial Dysfunction: Implication for Aged Hearts. *Int J Mol Med* (2018) 41(6):3517–26. doi: 10.3892/ijmm.2018.3555
22. Chen Y, Yu T, Deuster P. Astaxanthin Protects Against Heat-Induced Mitochondrial Alterations in Mouse Hypothalamus. *Neuroscience* (2021) 476:12–20. doi: 10.1016/j.neuroscience.2021.09.010
23. Geng Y, Ma Q, Liu Y-N, Peng N, Yuan F-F, Li X-G, et al. Heatstroke Induces Liver Injury *via* IL-1β and HMGB1-Induced Pyroptosis. *J Hepatol* (2015) 63 (3):622–33. doi: 10.1016/j.jhep.2015.04.010
24. Kouroumalis E, Voumvouraki A, Augoustaki A, Samonakis DN. Autophagy in Liver Diseases. *World J Hepatol* (2021) 13(1):6–65. doi: 10.4254/wjh.v13.i1.6
25. Tian S, Yu H. Atractylenolide II Inhibits Proliferation, Motility and Induces Apoptosis in Human Gastric Carcinoma Cell Lines HGC-27 and AGS. *Molecules* (2017) 22(11):1886. doi: 10.3390/molecules22111886
26. Choudhury FK. Mitochondrial Redox Metabolism: The Epicenter of Metabolism During Cancer Progression. *Antioxid (Basel)* (2021) 10 (11):1838. doi: 10.3390/antiox10111838
27. Saleem S. Apoptosis, Autophagy, Necrosis and Their Multi Galore Crosstalk in Neurodegeneration. *Neuroscience* (2021) 469:162–74. doi: 10.1016/j.neuroscience.2021.06.023
28. Hoshino A, Ariyoshi M, Okawa Y, Kaimoto S, Uchihashi M, Fukai K, et al. Inhibition of P53 Preserves Parkin-Mediated Mitophagy and Pancreatic β-Cell Function in Diabetes. *Proc Natl Acad Sci USA* (2014) 111(8):3116–21. doi: 10.1073/pnas.1318951111
29. Carlsen L, El-Deiry WS. Differential P53-Mediated Cellular Responses to DNA-Damaging Therapeutic Agents. *Int J Mol Sci* (2021) 22(21):11828. doi: 10.3390/ijms222111828
30. Mehta S, Campbell H, Drummond CJ, Li K, Murray K, Slatter T, et al. Adaptive Homeostasis and the P53 Isoform Network. *EMBO Rep* (2021) 22 (12):e53085. doi: 10.15252/embr.202153085
31. Venderova K, Park DS. Programmed Cell Death in Parkinson's Disease. *Cold Spring Harb Perspect Med* (2012) 2(8):a009365. doi: 10.1101/cshperspect.a009365
32. Ma X, McKeen T, Zhang J, Ding W-X. Role and Mechanisms of Mitophagy in Liver Diseases. *Cells* (2020) 9(4):837. doi: 10.3390/cells9040837
33. Li R, Toan S, Zhou H. Role of Mitochondrial Quality Control in the Pathogenesis of Nonalcoholic Fatty Liver Disease. *Aging* (2020) 12(7):6467–85. doi: 10.18632/aging.102972
34. Thangaraj A, Periyasamy P, Guo M-L, Chivero ET, Callen S, Buch S. Mitigation of Cocaine-Mediated Mitochondrial Damage, Defective Mitophagy and Microglial Activation by Superoxide Dismutase Mimetics. *Autophagy* (2020) 16:289–312. doi: 10.1080/15548627.2019.1607686
35. Zhang S, Wang Y, Cao Y, Wu J, Zhang Z, Ren H, et al. Inhibition of the PINK1-Parkin Pathway Enhances the Lethality of Sorafenib and Regorafenib in Hepatocellular Carcinoma. *Front Pharmacol* (2022) 13:851832. doi: 10.3389/fphar.2022.851832
36. Lin Q, Li S, Jiang N, Shao X, Zhang M, Jin H, et al. PINK1-Parkin Pathway of Mitophagy Protects Against Contrast-Induced Acute Kidney Injury *via* Decreasing Mitochondrial ROS and NLRP3 Inflammasome Activation. *Redox Biol* (2019) 26:101254. doi: 10.1016/j.redox.2019.101254
37. Wang S, Tao J, Chen H, Kandadi MR, Sun M, Xu H, et al. Ablation of Akt2 and AMPK2 Rescues High Fat Diet-Induced Obesity and Hepatic Steatosis Through Parkin-Mediated Mitophagy. *Acta Pharm Sin B* (2021) 11:3508–26. doi: 10.1016/j.apsb.2021.07.006
38. Ke P-Y. Mitophagy in the Pathogenesis of Liver Diseases. *Cells* (2020) 9 (4):831. doi: 10.3390/cells9040831
39. Williams JA, Ding W-X. Targeting Pink1-Parkin-Mediated Mitophagy for Treating Liver Injury. *Pharmacol Res* (2015) 102:264–9. doi: 10.1016/j.phrs.2015.09.020
40. Ezhilarasan D. Mitochondria: A Critical Hub for Hepatic Stellate Cells Activation During Chronic Liver Diseases. *Hepatobil Pancreat Dis Int* (2021) 20(4):315–22. doi: 10.1016/j.hbpd.2021.04.010
41. Xu M, Hang H, Huang M, Li J, Xu D, Jiao J, et al. DJ-1 Deficiency in Hepatocytes Improves Liver Ischemia-Reperfusion Injury by Enhancing Mitophagy. *Cell Mol Gastroenterol Hepatol* (2021) 12(2):567–84. doi: 10.1016/j.jcmgh.2021.03.007
42. Tan Q, Liu Y, Deng X, Chen J, Tsai P-J, Chen P-H, et al. Autophagy: A Promising Process for the Treatment of Acetaminophen-Induced Liver Injury. *Arch Toxicol* (2020) 94(9):2925–38. doi: 10.1007/s00204-020-02780-9
43. Achanta G, Sasaki R, Feng L, Carew JS, Lu W, Pelicano H, et al. Novel Role of P53 in Maintaining Mitochondrial Genetic Stability Through Interaction With DNA Pol Gamma. *EMBO J* (2005) 24(19):3482–92. doi: 10.1038/sj.emboj.7600819
44. Eliaš J, Macnamara CK. Mathematical Modelling of P53 Signalling During DNA Damage Response: A Survey. *Int J Mol Sci* (2021) 22(19):10590. doi: 10.3390/ijms221910590
45. Banfi F, Rubio A, Zaghi M, Massimino L, Fagnocchi G, Bellini E, et al. SETBP1 Accumulation Induces P53 Inhibition and Genotoxic Stress in Neural Progenitors Underlying Neurodegeneration in Schinzel-Giedion Syndrome. *Nat Commun* (2021) 12(1):4050. doi: 10.1038/s41467-021-24391-3
46. Tang C, Ma Z, Zhu J, Liu Z, Liu Y, Liu Y, et al. P53 in Kidney Injury and Repair: Mechanism and Therapeutic Potentials. *Pharmacol Ther* (2019) 195:5–12. doi: 10.1016/j.pharmthera.2018.10.013
47. Hoshino A, Mita Y, Okawa Y, Ariyoshi M, Iwai-Kanai E, Ueyama T, et al. Cytosolic P53 Inhibits Parkin-Mediated Mitophagy and Promotes Mitochondrial Dysfunction in the Mouse Heart. *Nat Commun* (2013) 4:2308. doi: 10.1038/ncomms3308
48. Manzella N, Santin Y, Maggiorani D, Martini H, Douin-Echinard V, Passos JF, et al. Monoamine Oxidase-A Is a Novel Driver of Stress-Induced Premature Senescence Through Inhibition of Parkin-Mediated Mitophagy. *Aging Cell* (2018) 17(5):e12811. doi: 10.1111/acel.12811
49. Suzuki N, Johmura Y, Wang T-W, Migita T, Wu W, Noguchi R, et al. TP53/p53-FBXO22-TFEB Controls Basal Autophagy to Govern Hormesis. *Autophagy* (2021) 17(11):3776–93. doi: 10.1080/15548627.2021.1897961
50. Shi T, Dansen TB. Reactive Oxygen Species Induced P53 Activation: DNA Damage, Redox Signaling, or Both? *Antioxid Redox Signal* (2020) 33(12):839–59. doi: 10.1089/ars.2020.8074
51. Goiran T, Duplan E, Rouland L, El Manaa W, Lauritzen I, Dunys J, et al. Nuclear P53-Mediated Repression of Autophagy Involves PINK1 Transcriptional Down-Regulation. *Cell Death Differ* (2018) 25(5):873–84. doi: 10.1038/s41418-017-0016-0
52. Sun M, Li J, Mao L, Wu J, Deng Z, He M, et al. P53 Deacetylation Alleviates Sepsis-Induced Acute Kidney Injury by Promoting Autophagy. *Front Immunol* (2021) 12:685523. doi: 10.3389/fimmu.2021.685523
53. Schank M, Zhao J, Wang L, Li Z, Cao D, Nguyen LN, et al. Telomeric Injury by KML001 in Human T Cells Induces Mitochondrial Dysfunction Through the P53-PGC-1α Pathway. *Cell Death Dis* (2020) 11(12):1030. doi: 10.1038/s41419-020-03238-7

Conflict of Interest: The authors declare that the research was conducted in the absence of any commercial or financial relationships that could be construed as a potential conflict of interest.

frontiers | Frontiers in Immunology

ORIGINAL RESEARCH
published: 16 May 2022
doi: 10.3389/fimmu.2022.885829

Granulocyte Colony-Stimulating Factor Accelerates the Recovery of Hepatitis B Virus-Related Acute-on-Chronic Liver Failure by Promoting M2-Like Transition of Monocytes

Jingjing Tong[1,2,3†], Hongmin Wang[4†], Xiang Xu[5], Zhihong Wan[6], Hongbin Fang[7], Jing Chen[1,2], Xiuying Mu[4], Zifeng Liu[1], Jing Chen[1], Haibin Su[2], Xiaoyan Liu[2], Chen Li[2], Xiaowen Huang[1] and Jinhua Hu[1,2,4]*

[1] Chinese PLA Medical School, Beijing, China, [2] Senior Department of Hepatology, the Fifth Medical Center of PLA General Hospital, Beijing, China, [3] Department of Infectious Diseases, Beijing Jishuitan Hospital, Beijing, China, [4] Peking University 302 Clinical Medical School, Beijing, China, [5] Laboratory of Translational Medicine, Medical Innovation Research Division of Chinese PLA General Hospital, Beijing, China, [6] Center for Drug Evaluation, National Medical Products Administration, Beijing, China, [7] Department of Biostatistics, Bioinformatics and Biomathematics, Georgetown University Medical Center, Washington, DC, United States

OPEN ACCESS

Edited by:
Yu Shi,
Zhejiang University, China

Reviewed by:
Yu Chen,
Capital Medical University, China
Tao Chen,
Huazhong University of Science and Technology, China

***Correspondence:**
Jinhua Hu
13910020608@163.com

†These authors have contributed equally to this work and share first authorship

Specialty section:
This article was submitted to Inflammation, a section of the journal Frontiers in Immunology

Received: 28 February 2022
Accepted: 20 April 2022
Published: 16 May 2022

Citation:
Tong J, Wang H, Xu X, Wan Z, Fang H, Chen J, Mu X, Liu Z, Chen J, Su H, Liu X, Li C, Huang X and Hu J (2022) Granulocyte Colony-Stimulating Factor Accelerates the Recovery of Hepatitis B Virus-Related Acute-on-Chronic Liver Failure by Promoting M2-Like Transition of Monocytes. Front. Immunol. 13:885829. doi: 10.3389/fimmu.2022.885829

Background and Aim: Acute-on-chronic liver failure (ACLF) has a high mortality rate. The role of granulocyte colony-stimulating factor (G-CSF) in ACLF remains controversial. Monocytes/macrophages are core immune cells, which are involved in the initiation and progression of liver failure; however, the effect of G-CSF on monocytes/macrophages is unclear. The study aimed to verify the clinical efficacy of G-CSF and explore the effect of it on monocytes in hepatitis B virus (HBV)-related ACLF (HBV-ACLF) paitents.

Methods: We performed a large randomized controlled clinical trial for the treatment of HBV-ACLF using G-CSF. A total of 111 patients with HBV-ACLF were prospectively randomized into the G-CSF group (5 μg/kg G-CSF every day for 6 days, then every other day until day 18) or the control group (standard therapy). All participants were followed up for at least 180 days. The relationship between monocyte count and mortality risk was analyzed. The effect of G-CSF on the phenotype and function of monocytes from patients with HBV-ACLF was evaluated using flow cytometry *in vivo* and *in vitro* experiments.

Results: The survival probability of the G-CSF group at 180 days was higher than that of the control group (72.2% vs. 53.8%, $P = 0.0142$). In the G-CSF-treated group, the monocyte counts on days 0 and 7 were independently associated with an evaluated mortality risk in the fully adjusted model (Model 3) [at day 0: hazard ratio (HR) 95% confidence interval (CI): 15.48 (3.60, 66.66), $P = 0.0002$; at day 7: HR (95% CI): 1.10 (0.50, 2.43), $P=0.8080$]. Further analysis showed that after treatment with G-CSF in HBV-ACLF patients, the expression of M1-like markers (HLA-DR and CD86) in monocytes decreased (HLA-DR: $P = 0.0148$; CD86: $P = 0.0764$). The expression of MerTK (M2-like marker) increased ($P = 0.0002$). The secretion of TNF-α, IL-6, and IL-10 from monocytes decreased without lipopolysaccharide (LPS)

stimulation (TNF-α: $P < 0.0001$; IL-6: $P = 0.0025$; IL-10: $P = 0.0004$) or with LPS stimulation (TNF-α: $P = 0.0439$; $P = 0.0611$; IL-10: $P = 0.0099$). Similar effects were observed *in vitro* experiments.

Conclusion: G-CSF therapy confers a survival benefit to patients with HBV-ACLF. G-CSF can promote the anti-inflammatory/pro-restorative phenotype (M2-like) transition of monocytes, which may contribute to the recovery of ACLF.

Clinical Trial Registration Number: ClinicalTrials.gov, identifier (NCT02331745).

Keywords: acute-on-chronic liver failure, granulocyte colony stimulating factor, monocytes, hepatitis B virus, inflammation, prognosis, cytokine

INTRODUCTION

Acute-on-chronic liver failure (ACLF) is a clinical syndrome characterized by severe hepatic dysfunction resulting from acute injury to an underlying chronic liver disease and a substantially high short-term mortality rate (1, 2). The hallmark of ACLF is the large-area necrosis of liver tissue and severe inflammation. However, current treatment for ACLF focuses on targeting the triggering insult and optimizing the clinical management of complications (3). Efficacious therapeutic strategies, aimed at promoting liver regeneration and restricting inflammation, remain limited. Currently, liver transplantation is the only effective therapy to prevent ACLF; however, its application may not be generalizable because of its cost prohibitive nature and the insufficiency of donors (4). Therefore, there is an unmet need for novel treatment approaches.

Although traditionally considered a hematopoietic regulator, granulocyte colony stimulating factor (G-CSF) has been regarded as a candidate treatment for ACLF recently. Several studies have established the efficacy and safety of G-CSF in the management of ACLF (5–9). However, a recent study showed no significant survival benefit of G-CSF in individuals with ACLF (10). Therefore, more well-conducted investigations are required.

The role of G-CSF in liver tissue regeneration and in regulation of the immune response has been shown. Studies in animals and humans indicate that G-CSF can promote the migration of hematopoietic stem cells as well as the proliferation and differentiation of hepatic progenitor cells during liver failure (5, 11, 12). Other studies have demonstrated the useful effects of G-CSF on dendritic cells and neutrophils in ACLF (13, 14). However, as the core immune cells involved in the development and progression of liver failure (15–17), the effects of G-CSF on monocytes/macrophages in ACLF patients remain unexplored. Monocytes/macrophages are characterized by high diversity and plasticity (18). Monocytes are classically categorized into three subgroups: $CD14^{++}CD16^{-}$ (classical), $CD14^{++}CD16^{+}$ (intermediate), and $CD14^{+}CD16^{++}$ (non-classical) (19, 20). Monocytes can also be classified into M1 (pro-inflammatory) and M2 (anti-inflammatory/pro-restorative) subtypes, based on their differentiation status. M1 monocytes highly express HLA-DR and CD86 on their surface, and secrete pro-inflammatory TNF-α and IL-6 as the dominant cytokines, whereas M2 monocytes overexpress CD163 and MerTK and mainly secrete anti-inflammatory factors such as IL-10 (17). Therefore, monocyte plasticity could be a potential therapeutic target for immune regulation in ACLF. Nonetheless, the effect of G-CSF on monocytes in ACLF patients warrants further investigation.

In Asia, the main etiology of ACLF is chronic hepatitis B virus (HBV) infection (21–23). The purpose of our study was to provide new data on the treatment of HBV-related ACLF (HBV-ACLF) using G-CSF. Here, we discuss the efficacy and safety of G-CSF, investigate the effect of G-CSF on monocytes in HBV-ACLF patients, and explore the underlying mechanisms of action of G-CSF.

PATIENTS AND METHODS

The current study includes a clinical trial and basic experiments. The former was a randomized, controlled, open-label trial to evaluate the efficacy of G-CSF for HBV-ACLF. Then, we evaluated the effect of G-CSF on the phenotype and function of monocytes from patients with HBV-ACLF.

Patients

In the clinical trial, all participants were recruited from the Fifth Medical Center of the People's Liberation Army (PLA) General Hospital for screening from June 2014 to September 2016. Eligible patients met the diagnostic criteria for ACLF, suggested by the Asian Pacific Association for the Study of the Liver (APASL) (1, 24), which are: (i) pre-existing diagnosed or undiagnosed chronic liver disease; (ii) acute deterioration with exacerbating jaundice (serum total bilirubin ≥ 5 mg/dL); (iii) international standard ratio (INR) ≥ 1.5 or plasma prothrombin activity (PTA; <40%); and (iv) comply with ascite and/or encephalopathy within 4 weeks. The inclusion criteria were as

Abbreviations: ACLF, acute-on-chronic liver failure; G-CSF, granulocyte colony-stimulating factor; HBV-ACLF, hepatitis B virus (HBV)-related ACLF; APASL, Asian-Pacific Association for the Study of the Liver; PBMCs, peripheral blood mononuclear cells; LPS, lipopolysaccharide; MELD, Model for End-Stage Liver Disease; MELD-Na, MELD-sodium; CLIF-SOFA, Chronic Liver Failure-Sequential Organ Failure Assessment; CTP, Child-Turcotte-Pugh; EASL-CLIF, European Association for the Study of the Liver -Chronic Liver Failure; IQR, interquartile range; HR, hazard risk; CI, confidence interval.

follows: (i) 18–70-year-old male or female; and (ii) serum hepatitis B surface antigen or HBV DNA was detected for at least 6 months. The exclusion criteria were as follows: (i) super-infection or co-infection with other hepatotropic and non-hepatotropic virus; (ii) a previous application of any immune modulator or cytotoxic/immunosuppressive therapy within the previous 12 months; (iii) hepatocellular carcinoma or extrahepatic malignancy; (iv) co-existence of severe renal, lung, brain,or heart disease or other liver disease such as alcoholic liver disease, Wilson disease, drug-induced liver injury, or autoimmune hepatitis; (v) presence of sepsis; (vi) malignant jaundice leaded by obstructive or hemolytic jaundice; and (vii) prolonged prothrombin time due to hematologic system disease.

Ascites was identified by clinical manifestations, diagnostic paracentesis, and abdominal imaging examination; Acute kidney injury was diagnosed according to the International Club of Ascites (ICA) corresponding standard (25); A West Haven classification was applied in the diagnosis of hepatic encephalopathy (26); Corresponding formulas were applied for calculation of the model for end-stage liver disease (MELD), MELD-sodium (MELD-Na), and chronic liver failure-sequential organ failure assessment (CLIF-SOFA) scores (3, 27, 28).

Diagnosis of infection was made based on clinical presentation, laboratory values and imaging examination. (i) spontaneous bacterial peritonitis: polymorphonuclear cell count in ascitic fluid ≥250/mm^3. (ii) pneumonia: pulmonary imaging changes (infiltration, consolidation, or cavitation) plus at least 1 of the following presentation (fever ≥38°C, leucocyte count >12,000/mm^3 or <4,000/mm^3) plus at least 1 of the following symptoms or signs (new cough, sputum production, dyspnea, rales or bronchial breath sounds, etc.) and/or etiological evidence. (iii) urinary tract infection: Patient had at least 1of the following clinical presentations (fever, urinary tract irritation or suprapubic tenderness, etc.) and positive urine culture; or at least 2 of the above presentations and more than 10 leukocytes/μL in urine. (iv)bacteremia: positive blood culture (29, 30).

Study Design and Follow-Up of the Clinical Trial

PASS 11.0 software (NCSS, Kaysville, UT, USA) was used to calculate the sample size. Based on our previous study, we expected that G-CSF therapy could improve the survival rate at 180 days by approximately 20% in the G-CSF group compared to that in the control group. With a statistical power of 80%, we required 52 patients in each group to detect this meaningful difference at a significance level of 5%. Considering the possible loss of patients to follow-up (10%), 114 patients were included in this study. The computer-generated randomization number code was prepared for each patient. The patients were randomly allocated to the G-CSF group (receive G-CSF therapy plus standard medical therapy) or control group (only receive standard medical therapy).

G-CSF (SL Pharm, Beijing, China) was injected subcutaneously at a dose of 5 μg/kg every day for 6 days and then every other day until day 18 (total 12 doses) in G-CSF group patients; thereafter, physical examination and laboratory tests were conducted. All patients received standard medical therapy, including intensive care monitoring, antiviral therapy, supportive therapy, and prevention and treatment for complications. All patients with infection were treated with antibiotics. Patients received albumin, terlipressin, and so on if required.

A total of 114 patients meeting the inclusion and exclusion criteria were enrolled in the study (**Figure 1**). Of these, 56 patients received both standard medical therapy and G-CSF treatment (G-CSF group), and 58 patients received standard medical therapy only (control group). All patients were followed up for at least 180 days after treatment commencement. During the follow-up period, one patient in the G-CSF group discontinued treatment, and one patient each in the G-CSF group and control group underwent liver transplantation. Thus, 111 patients were included in the final analysis.

Peripheral blood samples were obtained from the enrolled patients and loaded into 10 mL heparin anticoagulant tubes for the following experiments.

Phenotyping of Monocytes and Measurement of Cytokine Expression in G-CSF-Treated Patients

Peripheral blood mononuclear cells (PBMCs) were obtained from patients with HBV-ACLF (n = 12), before and after G-CSF treatment, to evaluate the effect of G-CSF on monocytes. Surface markers and intracellular cytokine expression in monocytes, expressed as frequency or mean fluorescence intensity (MFI), were measured using flow cytometry on the BD FACSymphony A5 analyzer (BD Biosciences, UK). Data were analyzed using the FlowJo software (Tristar, San Carlos, CA, USA).

For surface marker staining, APC-Cy7-conjugated anti-CD45 (BD Biosciences), PerCP-Cy5.5-conjugated anti-CD14 (BD Biosciences), APC-conjugated anti-CD16 (BD Biosciences), BV711-conjugated anti-HLA-DR (BD Biosciences), PE-conjugated anti-MerTK (R&D Systems), PE-Cy7-conjugated anti-CD163 (eBioscience), BV421-conjugated anti-CCR2 (BioLegend), FITC-conjugated anti-CX3CR1 (BioLegend), and BUV-737-conjugated anti-CD86 (BD Biosciences) antibodies were used. For intracellular cytokine staining (ICCS), BV-421-conjugated anti-IL-6 (BD Biosciences), PE-CF594-conjugated anti-IL-10 (BD Biosciences), and BV-510-conjugated anti-TNF-α (BioLegend) were used. Dead cells were excluded using Fixable Viability Stain 440UV (BD Bioscience).

For surface marker labeling, PBMCs were incubated with surface fluorescent-labeled monoclonal antibodies. For intracellular staining, PBMCs were incubated with or without 100 ng/mL lipopolysaccharide (LPS) and protein transport inhibitor (1μL/mL, BD GolgiPlug) for 6 h, followed by staining with surface markers, and fixation, permeabilization, and staining with the corresponding fluorescent intracellular antibodies.

Effect of G-CSF on Monocyte Phenotype and Cytokine Secretion *In Vitro*

PBMCs were obtained from patients with HBV-ACLF who did not receive G-CSF therapy. CD14$^+$ monocytes were further

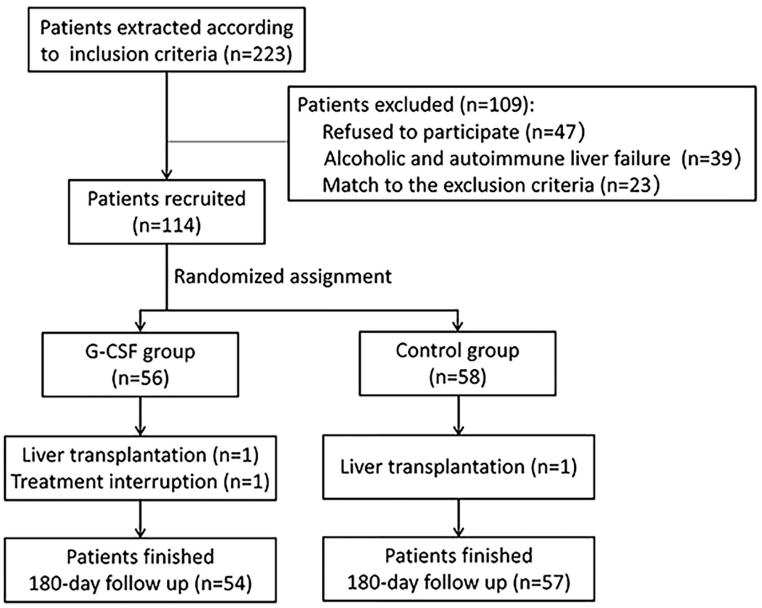

FIGURE 1 | Flowchart of screening and recruitment of patients with HBV-ACLF.

isolated using magnetic bead separation (Miltenyi, Bergisch Gladbach, Germany). The purity of monocyte separation was examined using flow cytometry, and $CD14^+$ monocytes with a purity >95% were used *in vitro* experiments. Isolated monocytes were incubated in complete media with 20 ng/mL G-CSF or an equivalent volume of PBS (control) for 24 h for surface staining. For intracellular staining, the isolated $CD14^+$ monocytes were stimulated with G-CSF (20 ng/ml) for 18 h. After 18 h incubation, LPS (100 ng/ml) and protein transport inhibitor (1μL/mL, BD GolgiPlug) was added and continue to incubation for 6 h, followed by staining with surface markers, and fixation, permeabilization, and staining with the corresponding fluorescent intracellular antibodies. After all the above steps, the monocytes were harvested and analyzed for their surface phenotype and intracellular cytokine levels using flow cytometry. Staining was performed as previously described.

Phagocytosis and Oxidative Burst Assays

The effect of G-CSF therapy on monocyte phagocytosis and the oxidative burst capacity of patients with HBV-ACLF was evaluated. Monocyte phagocytosis and oxidative burst capacity were tested using the PHAGOTEST kit (CELONIC, Germany) and PHAGOBURST kit (CELONIC, Germany) following the manufacturer's protocol, respectively, and then assessed by flow cytometry.

Ethics

The study protocol and informed consent form were approved by the Human Ethics Committee of the Fifth Medical Center of the PLA General Hospital. All the procedures were in accordance with the ethical guidelines of Declaration of Helsinki. Written informed consent was obtained from patients or their guardians before enrollment. This trial was registered at ClinicalTrials.gov (NCT02331745).

Statistical Analysis

In the clinical trial, continuous variables with normal distribution and skewed distribution were expressed as mean ± standard deviation (SD) and median [interquartile range (IQR)], respectively. Categorical variables were expressed as numbers and percentages. The chi-square test (for categorical variables) and Student's *t*-test (for continuous variables, normal distribution) or Mann–Whitney *U* test (for continuous variables, skewed distribution) were used to compare differences between the two groups. Patients lost to follow-up contributed to the censored data. Survival rates were calculated using the Kaplan–Meier method and compared using the Log-Rank test. In the crude model and three multivariate adjusted models, Cox proportional hazards model was used for multivariate regression analysis to estimate the hazard ratios (Hazard Ratio, HRs) and 95% confidence intervals (Confidence Interval, CIs) for the risk of 180-day mortality. Statistical analyses and graphing were conducted using the statistical packages R version 3.4.3 (The R Foundation, Vienna, Austria), EmpowerStats (X&Y Solutions, Inc., Boston, MA, USA) and the MedCalc 15.2.2 (Ostend, Belgium). Statistical significance was set at $P < 0.05$.

In the Experimental section, statistical analysis was performed using GraphPad Prism 7.00 (GraphPad Software Inc., La Jolla, CA, USA). Data are presented as median (IQR). Non-parametric analyses, such as Kruskal–Wallis and Mann–Whitney *U* tests, were applied to comparisons across the different groups. Comparisons within the same individual were performed using Wilcoxon's matched-pair test. Statistical significance was set at $P < 0.05$.

RESULTS

Baseline Clinical Characteristics of Enrolled Patients

As shown in **Table 1**, the median age was 43.9 years [n = 91 men (82.0%) and 20 women (18.0%)]. Seventy patients (63.1%) patients had liver cirrhosis. MELD, MELD-Na and CLIF-SOFA scores were 23.7 (21.0–26.4), 22.9 (17.6–29.2), and 7.2 ± 1.0, respectively. The most common complication was ascites (88.3%), followed by infection (36.9%). Serum bilirubin and CRP in the G-CSF group were higher than those in the control group, but the differences were not statistically significant ($P = 0.066$ and 0.051, respectively). Meanwhile, the serum creatinine level in the control group was slightly higher than that in the G-CSF group, but both were within the normal range, and no statistical difference was detected ($P = 0.090$). **Table 1** shows that there were no significant differences in the patients' demographic and clinical characteristics between the control and G-CSF groups.

Adverse Effects and Main Complications During the First Month Follow-Up

The patients tolerated the treatment well, and no severe side effects were observed. One of the patients developed a mild rash during the follow-up and discontinued all drugs, including G-CSF. However, no evidence was shown that the rash was induced by G-CSF. The results showed that the G-CSF treatment protocol was safe.

During the first month, the main new-onset complications were infection, hepatic encephalopathy, and acute kidney injury (**Supplementary Table 1**). The frequency of complications was not significantly different ($P > 0.05$) between the control and G-CSF groups.

Kaplan–Meier Comparative Survival Analysis of the Control and G-CSF Group

Of the 111 patients, 66 survived, 40 died, and 5 lost to 180 days of follow-up; thus, the survival probability at day 180 was 62.6%. In the G-CSF group, 36 patients survived, 14 patients died, and 4 patients lost to follow-up; hence, the survival probability at day 180 was 72.2%. In the control group, 30 patients survived, 26 patients died, and 1 patient lost to follow-up, with a survival probability of 53.8%. The differences between the two groups were statistically significant ($P = 0.0242$; **Figure 2**).

Association Between Monocyte Count and 180-Day Mortality in HBV-ACLF Patients Treated With or Without G-CSF

We further explored the association between baseline and day 7 monocyte count and 180-day mortality in HBV-ACLF patients treated with or without G-CSF. As shown in **Table 2**, in both the crude and adjusted models (Models 1, 2, and 3), the baseline monocyte count was positively correlated with the 180-day mortality risk of HBV-ACLF [HR: 2.90 (1.41, 5.93), $P = 0.0036$ in Model 3], and the stratification analyses showed that this positive correlation was mainly contributed by patients in the G-CSF group [HR: 15.48 (3.60, 66.66), $P = 0.0002$ in Model 3]. However, after six consecutive days of treatment, the control

TABLE 1 | Demographical and clinical characteristic of patients in control and G-CSF Group.

Variable	Total	G-CSF group	Control group	p-value
No. of patients	111	54	57	
Age (year)	43.9 ± 10.4	42.5 ± 10.2	45.3 ± 10.6	0.154
Male, n (%)	91 (82.0%)	44 (81.5%)	47 (82.5%)	0.894
Liver Cirrhosis, n (%)	70 (63.1%)	33 (61.1%)	37 (64.9%)	0.678
White Blood Cells (10^9/L)	6.0 (4.3-8.3)	5.9 (4.1-8.3)	6.4 (4.5-8.3)	0.439
Neutrophile (10^9/L)	3.6 (2.5-5.6)	3.5(2.5-4.9)	4.0(2.6-5.9)	0.221
Monocyte (10^9/L)	0.6 (0.4-0.9)	0.5 (0.4-0.9)	0.6 (0.4-0.8)	0.779
Platelets(10^9/L)	85.0 (53.0-123.5)	90.0 (55.2-133.5)	85.0 (46.0-121.0)	0.362
Albumin (g/L)	29.0 (26.0-31.0)	29.0 (27.0-33.0)	28.0 (26.0-31.0)	0.123
Alanine aminotransferase (IU/L)	125.0 (64.0-314.5)	111.0 (62.5-300.0)	143.0 (75.0-316.0)	0.440
Aspartate transaminase (IU/L)	149.5 (90.2-285.8)	150.0 (94.0-250.0)	149.0 (89.0-288.0)	0.928
Total bilirubin (μmol/L)	291.0 (214.5-391.2)	324.4 (244.9-395.1)	273.0 (190.3-377.5)	0.066
Creatinine (μmol/L)	84.0 (72.0-97.5)	83.0 (69.2-92.0)	85.0 (74.0-108.0)	0.090
Triglycerides (mmol/L)	1.0 (0.6-1.4)	1.2 (0.7-1.6)	0.8 (0.6-1.3)	0.124
Sodium (mmol/L)	135.1 ± 4.3	135.4 ± 4.3	134.7 ± 4.3	0.373
Prothrombin activity (%)	37.2 (30.5-43.3)	38.0 (29.3-43.3)	36.4 (30.9-43.3)	0.786
International normalized ratio	1.9 (1.6-2.1)	1.8 (1.6-2.1)	1.9 (1.7-2.2)	0.263
C- reactive protein (mg/L)	12.8 (8.0-20.6)	15.6 (8.6-22.5)	10.0 (8.1-14.2)	0.051
HBV DNA (Log10 IU/mL)	4.0 (2.0-5.2)	3.8 (1.9-5.5)	4.0 (2.4-4.9)	0.674
Ascites, n (%)	98 (88.3%)	45 (83.3%)	53 (93.0%)	0.114
Infection, n (%)	41 (36.9%)	18 (33.3%)	23 (40.4%)	0.444
Acute kidney injury, n (%)	13 (11.7%)	5 (9.3%)	8 (14.0%)	0.434
Hepatic encephalopathy, n (%)	18 (16.2%)	8 (14.8%)	10 (17.5%)	0.697
MELD	23.7 (21.0-26.4)	22.8 (20.7-26.0)	24.1 (21.6-27.1)	0.261
MELD Na	22.9 (17.6-29.2)	21.8 (16.8-25.6)	23.7 (17.8-31.2)	0.152
CLIF-SOFA	7.2 ± 1.0	7.1 ± 0.9	7.3 ± 1.1	0.335

All data were present as mean ± SD, median (IQR) or number (%). G-CSF, Granulocyte-colony stimulating factor; MELD, model for end-stage liver disease; MELD-Na, MELD-sodium; CLIF-SOFA, chronic liver failure-sequential organ failure assessment.

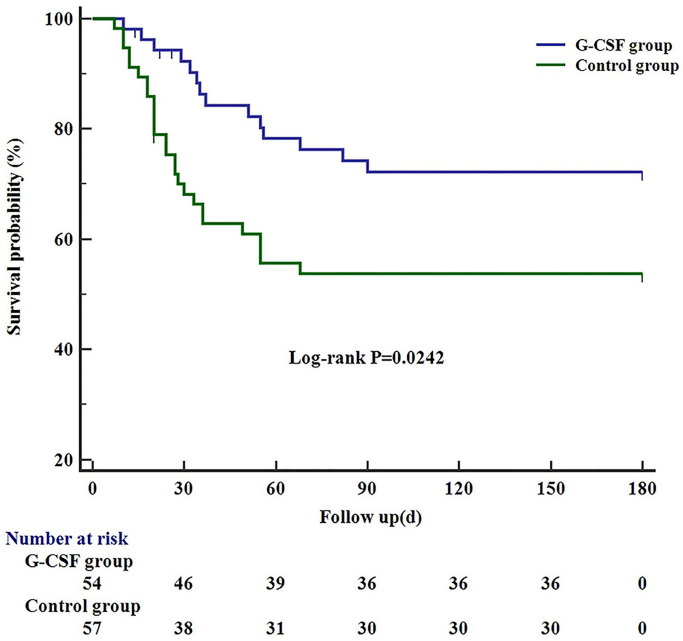

FIGURE 2 | Kaplan–Meier curve showing the 180-day survival in G-CSF group, compared with the control group. G-CSF, Granulocyte-colony stimulating factor.

group did not demonstrate significant changes, whereas the positive association between monocyte count on day 7, and the risk of death was significantly weakened in the G-CSF-treated group [HR: 1.10 (0.50, 2.43), P = 0.8080 in Model 3]. Similar relationship was observed between monocyte count and 90-day mortality (**Supplementary Table 2**). Therefore, we speculate that G-CSF may benefit patients with HBV-ACLF by altering the number or function of monocytes.

Shift in the Monocyte Subpopulations After G-CSF Treatment

According to traditional gating, monocyte subtypes can be identified by the expression of CD14 and CD16 (**Figure 3A**). We evaluated the frequencies of the three monocyte subsets (described above). As shown in **Figure 3B**, although there was no significant difference in the proportion of classic, intermediate, and non-classical monocytes before (day 0) and after G-CSF treatment (P = 0.8981, 0.7113 and 0.9953, respectively), the intermediate and non-classical monocytes demonstrated a decreasing trend, whereas classical monocytes demonstrated an increasing trend. Thus, a shift in monocyte subpopulations was detected after G-CSF treatment.

G-CSF Therapy Induces an Anti-Inflammatory/Pro-Restorative (M2-Like) Monocyte Phenotype in HBV-ACLF Patients

To fully evaluate the effect of G-CSF on monocytes in HBV-ACLF, we designed detailed immunophenotypic analyses to detect the levels of activation/inflammation markers (HLA-DR, CD86, MerTK, and CD163) and tissue-homing markers (CCR2 and CX3CR1) before (day 0) and after the administration of G-

TABLE 2 | Association between monocyte count and 180-day mortality in HBV-ACLF patients.

Model	Total	G-CSF group	Control group
Monocytes on day 0 ($\times10^9$/L)			
Crude model	2.42 (1.38, 4.24) 0.0020	5.19 (2.10, 12.82) 0.0004	1.72 (0.81, 3.65) 0.1599
Model 1	2.83 (1.58, 5.07) 0.0005	5.41 (2.10, 13.89) 0.0005	2.13 (0.94, 4.83) 0.0690
Model 2	2.86 (1.59, 5.12) 0.0004	5.25 (2.05, 13.46) 0.0006	2.32 (1.05, 5.12) 0.0365
Model 3	2.90 (1.41, 5.93) 0.0036	15.48 (3.60, 66.66) 0.0002	2.43 (0.72, 8.20) 0.1531
Monocytes on day 7 ($\times10^9$/L)			
Crude model	1.79 (1.11, 2.90) 0.0180	1.30 (0.69, 2.45) 0.4117	3.09 (1.42, 6.71) 0.0044
Model 1	1.93 (1.17, 3.19) 0.0106	1.27 (0.64, 2.51) 0.4972	3.36 (1.44, 7.85) 0.0051
Model 2	1.96 (1.17, 3.26) 0.0102	1.25 (0.63, 2.47) 0.5177	3.73 (1.58, 8.82) 0.0027
Model 3	1.42 (0.77, 2.61) 0.2590	1.10 (0.50, 2.43) 0.8080	2.57 (0.79, 8.44) 0.1184

Data are presented as HR (95% CI) and P value. Model 1 was adjusted for age and sex; Model 2 was adjusted for Model 1+ liver cirrhosis; Model 3 was adjusted for Model 2+ total bilirubin and international normalized ratio, and infection, acute kidney injury, and hepatic encephalopathy presence. G-CSF, Granulocyte-colony stimulating factor.

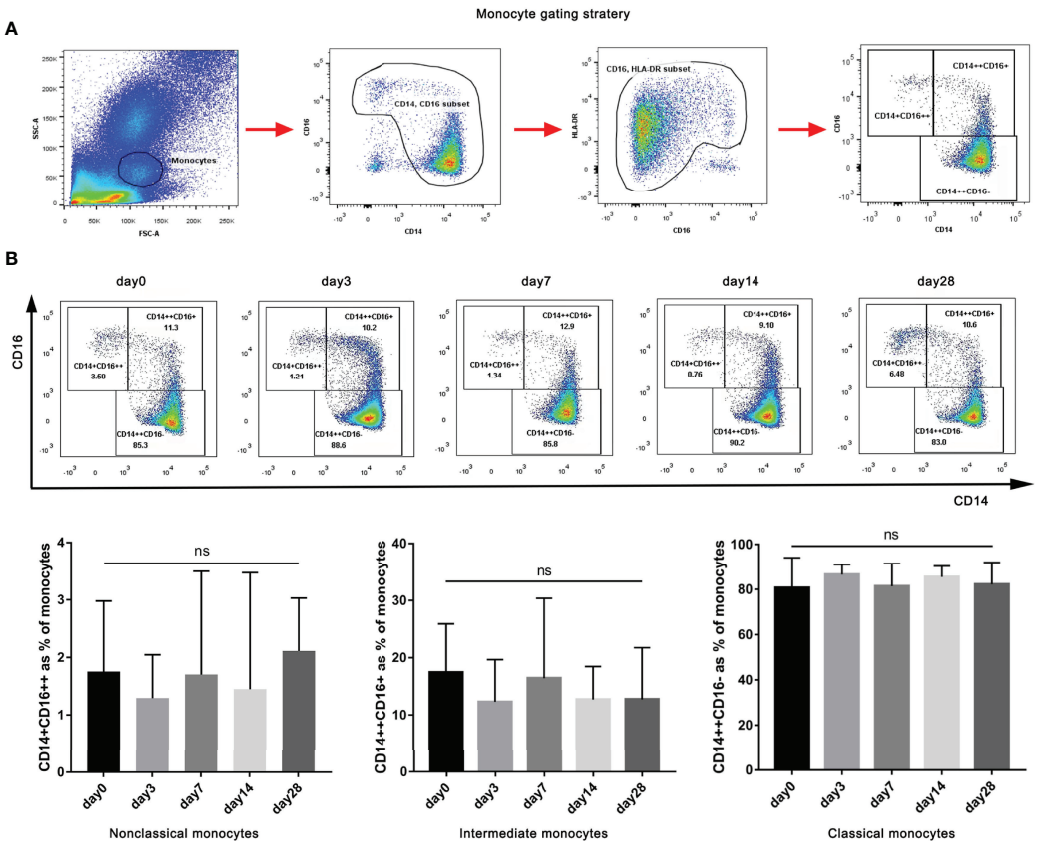

FIGURE 3 | Gating of monocytes and effect of G-CSF on monocyte subtypes in patients with HBV-ACLF. **(A)** Flow cytometry analysis and gating strategy used to determine monocytes and their subsets. **(B)** Effect of G-CSF on monocyte subtypes in patients with HBV-ACLF (n=12). Non-parametric (Wilcoxon's matched-pair test) statistical analysis was used. Data presented as median with interquartile range. ns represents P >0.05; G-CSF, Granulocyte-colony stimulating factor; HBV-ACLF, hepatitis B virus-related acute-on -chronic liver failure.

CSF (n = 12). As shown in **Figure 4**, after treatment with G-CSF, the expression of M1-like markers (HLA-DR and CD86) in monocytes decreased (HLA-DR: day 0 vs. day 3 vs. day 7 vs. day 14 vs. day 28 = 94.9% vs. 78.5% vs. 80.1% vs. 82.1% vs. 92.6%, respectively; $P = 0.0148$; CD86: day 0 vs. day 3 vs. day 7 vs. day 14 vs. day 28 = 57.1% vs. 30.5% vs. 28.6% vs. 43% vs. 40.3%, respectively; $P = 0.0764$), whereas the expression of M2-like marker (MerTK) increased (day 0 vs. day 3 vs. day 7 vs. day 14 vs. day 28 = 39.3% vs. 71.5% vs. 56.3% vs. 55.4% vs. 37.5%, respectively; $P = 0.0002$). There was no significant change in the expression of CCR2 and CX3CR1 in monocytes according to MFI before and after G-CSF treatment ($P = 0.1074$ and 0.8889, respectively). The above results indicate that circulating monocytes after G-CSF therapy showed an anti-inflammatory/pro-restorative phenotype in patients with HBV-ACLF.

G-CSF Therapy Attenuated Cytokine Secretion in Monocytes Obtained From HBV-ACLF Patients With or Without LPS Stimulation

We evaluated whether G-CSF treatment in patients with HBV-ACLF modulated the ability of monocytes to produce IL-6, TNF-α, and IL-10 following LPS challenge or not. As shown in **Figure 5**, the secretion of TNF-α, IL-6, and IL-10 by monocytes decreased after G-CSF therapy without LPS stimulation (TNF-α: day 0 vs. day 3 vs. day 7 vs. day 14 vs. day 28 = 6.6% vs. 1.6% vs. 2.0% vs. 1.6% vs. 12.5%, respectively; $P < 0.0001$; IL-6: day 0 vs. day 3 vs. day 7 vs. day 14 vs. day 28 = 24.0% vs. 7.5% vs. 10.9% vs. 8.4% vs. 44.6%, respectively; $P = 0.0025$; IL-10: day 0 vs. day 3 vs. day 7 vs. day 14 vs. day 28 = 0.9% vs. 0.5% vs. 0.2% vs. 0.5% vs. 1.6%, respectively; $P = 0.0004$). In contrast to pre-treatment (day 0), cytokine secretion in monocytes showed a decreased response to LPS stimulation after G-CSF treatment (TNF-α: day 0 vs. day 3 vs. day 7 vs. day 14 vs. day 28 = 30.8% vs. 18.8% vs. 21.0% vs. 23.6% vs. 26.3%, respectively; $P = 0.0439$; IL-6: day 0 vs. day 3 vs. day 7 vs. day 14 vs. day 28 = 69.4% vs. 64.5% vs. 61.8% vs. 72.3% vs. 74.7%, respectively; $P = 0.0611$; IL-10: day 0 vs. day 3 vs. day 7 vs. day 14 vs. day 28 = 4.2% vs. 2.7% vs. 3.0% vs. 4.5% vs. 4.6%, respectively; $P = 0.0099$). Hence, G-CSF reduces the inflammatory response of monocytes in HBV-ACLF patients.

G-CSF Induces M2-Like Phenotype and Functional Transition of Monocytes From HBV-ACLF Patients *In Vitro*

We performed *in vitro* experiments to further clarify the effect of G-CSF on the phenotype and function of monocytes in patients

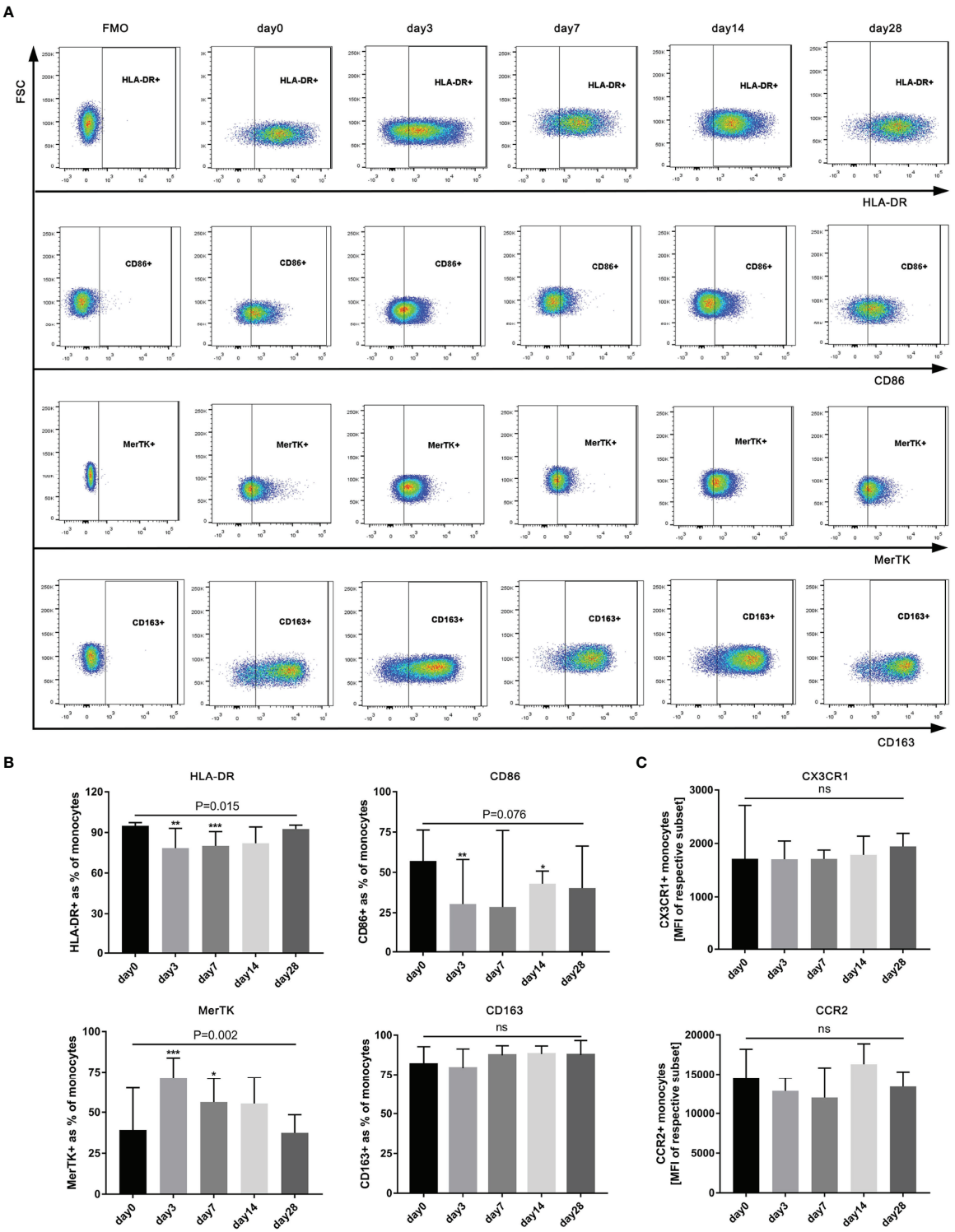

FIGURE 4 | Phenotype of circulating monocytes in HBV-ACLF patients (n=12) before (day 0) and after G-CSF treatment. **(A)** Expression of CD86、HLA-DR、MerTK, and CD163 on monocytes in HBV-ACLF before and after G-CSF treatment. **(B)** Phenotypic alterations on monocytes after treated with G-CSF. **(C)** Expression of tissue-homing receptors on monocytes after treated with G-CSF. Non-parametric (Wilcoxon's matched-pair test) statistical analysis was used. Data presented as median with interquartile range. Compared with day 0, $^{*}P < 0.05$, $^{**}P < 0.01$, $^{***}P < 0.001$. ns represents $P > 0.05$. G-CSF, Granulocyte-colony stimulating factor; HBV-ACLF, hepatitis B virus-related acute-on -chronic liver failure; FSC, forward scatter.

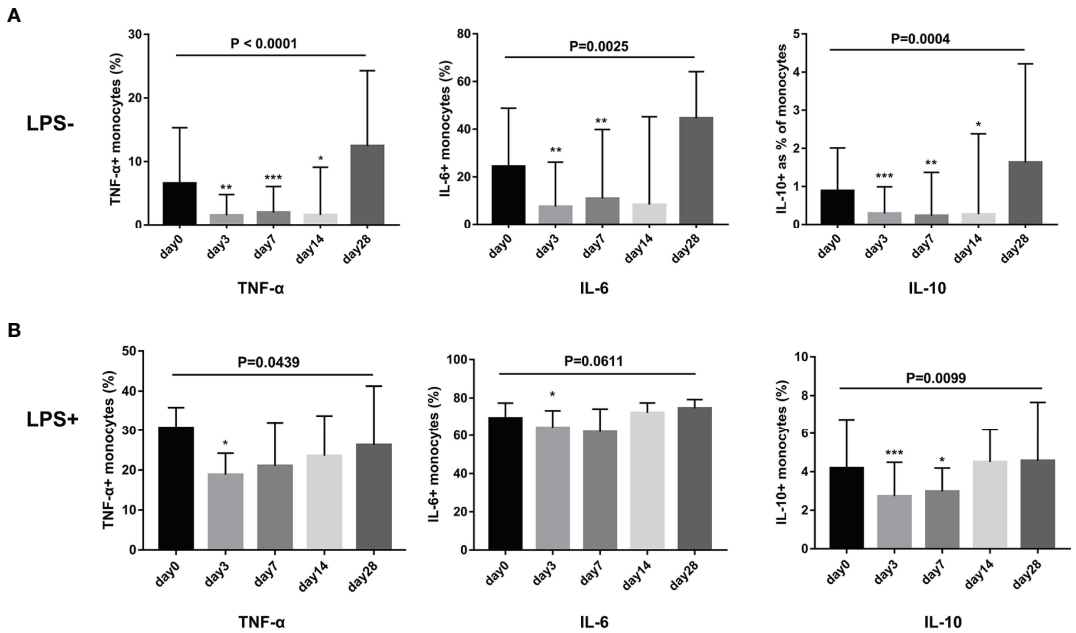

FIGURE 5 | G-CSF therapy attenuated cytokine secretion in monocytes with or without LPS stimulation in HBV-ACLF patients (n=12). **(A)** Cytokine secretion in monocytes without LPS stimulation. **(B)** Cytokine secretion in monocytes with LPS stimulation. Non-parametric (Wilcoxon's matched-pair test) statistical analysis was used. Data presented as median with interquartile range. Compared with day 0, $^{*}P < 0.05$, $^{**}P < 0.01$, $^{***}P < 0.001$. G-CSF, Granulocyte-colony stimulating factor; HBV-ACLF, hepatitis B virus-related acute-on-chronic liver failure; LPS, lipopolysaccharide.

with HBV-ACLF. As shown in **Figure 6**, after exogenous addition of G-CSF to monocytes from HBV-ACLF patients, the expression of M1-type markers (HLA-DR and CD86) decreased, whereas the expression of M2-type markers (CD163 and MerTK) increased ($P < 0.01$). There was no significant difference in the expression of homing receptors CCR2 and CX3CR1 between the two groups ($P > 0.05$; **Figure 6C**). Concurrently, although no statistically significant difference was detected, G-CSF decreased the secretion of pro-inflammatory factors (IL-6 and TNF-α) after LPS stimulation, whereas IL-10 secretion was slightly increased (**Figure 6D**). Except for the secretion of IL-10, these results were consistent with those observed *in vivo*. G-CSF tend to promote the transition of monocytes to M2 type in HBV-ACLF patient.

Influence of G-CSF on Phagocytosis and Oxidative Burst Function of Monocytes in HBV-ACLF

We tested and compared phagocytosis (**Figure 7A**) and oxidative burst (**Figure 7B**) of monocytes freshly isolated from HBV-ACLF patients before (day 0) and after G-CSF treatment. It was observed that phagocytosis of monocytes showed an upward trend, whereas oxidative burst showed a downward trend after the administration of G-CSF; however, the discrepancies were not statistically significant in view of the small numbers (P all <0.05).

DISCUSSION

In the present study, we conducted a randomized clinical trial to treat HBV-ACLF patients with G-CSF. We showed that G-CSF significantly improved the survival of HBV-ACLF patients. In addition, Cox regression analysis showed that G-CSF treatment attenuated the positive correlation coefficient between monocyte count and 180-day mortality risk in patients with HBV-ACLF. Further analyses demonstrated that after treatment with G-CSF, the phenotype and function of monocytes in HBV-ACLF tended to an anti-inflammatory/pro-restorative (M2-like) phenotype, which may contribute to the attenuation of liver injury and promote recovery of ACLF. These novel findings expand our knowledge of the role of G-CSF in the treatment of liver failure and provide new evidence that G-CSF may contribute to protection against liver damage.

In the current study, we observed a survival benefit in patients with HBV-ACLF after G-CSF therapy. This result was in agreement with those of several previous studies (5, 6). A study performed by Garg et al. (6) showed that the 60-day survival rate was significantly higher in ACLF patients treated with G-CSF than in the placebo group (69.6% vs. 29.2%; $P = 0.001$). Another study also revealed superior 90-day survival (5) of HBV-ACLF patients treated with G-CSF compared to those treated with the placebo (64.3% vs. 28.6%; $P = 0.04$). In addition, these two studies showed improvement in liver function, as indicated by

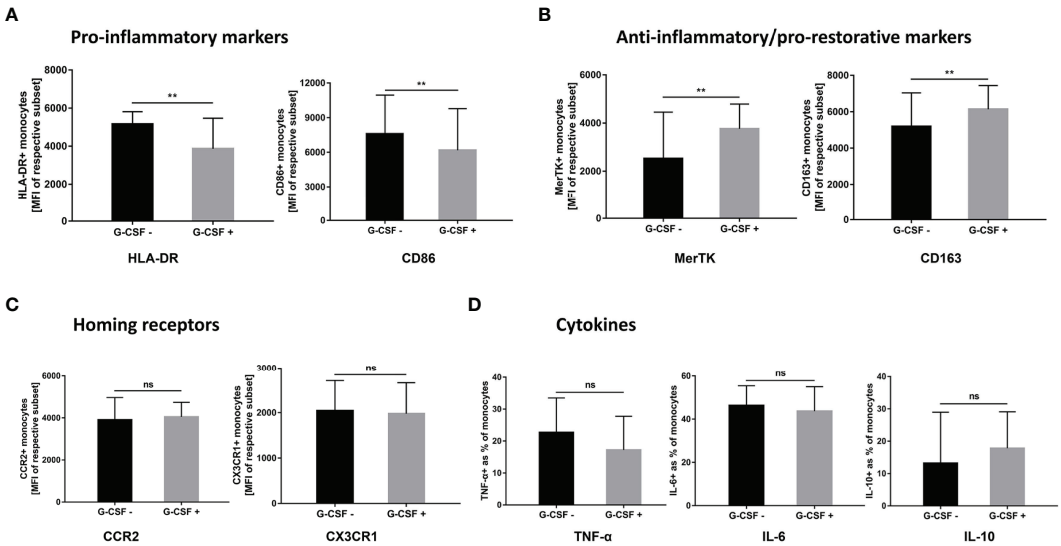

FIGURE 6 | G-CSF induces M2-like phenotype and functional transition of monocytes from HBV-ACLF patients *in vitro*. **(A)** G-CSF decreased the expression of pro-inflammatory markers on monocytes (n=9). **(B)** G-CSF elevated the expression of anti-inflammatory/pro-restorative markers on monocytes (n=9). **(C)** Effect of G-CSF on the expression of homing receptors on monocytes (n=9). **(D)** G-CSF attenuated pro-inflammatory cytokine secretion in monocytes (n=5). Non-parametric (Wilcoxon's matched-pair test) statistical analysis was used. Data presented as median with interquartile range. ** represents compared with day 0, $P<0.01$; ns represents $P>0.05$; G-CSF, Granulocyte-colony stimulating factor; HBV-ACLF, hepatitis B virus-related acute-on -chronic liver failure.

the MELD and Child-Turcotte-Pugh (CTP) scores. However, a European study by Engelmann et al. (10) failed to demonstrate better efficacy of G-CSF than standard medical therapy in ACLF patients (90-day transplant-free survival rates: 34.1% vs. 37.5%; $P = 0.805$). The liver function scores also did not improve in the G-CSF treatment group. The positive effect of G-CSF has only been confirmed in Asian studies, and not in the European study.

A major potential factor that may have contributed to this discrepancy is that the inclusion criteria were different. In the studies conducted by Gerg and Duan (5, 6), ACLF was defined according to the APASL criteria, in which patients with pre-exiting decompensated cirrhosis and sepsis were not included. The European study enrolled patients with acute decompensation of cirrhosis, utilizing the European Association for the Study of the Liver -Chronic Liver Failure (EASL-CLIF) criteria. APASL criteria focuses on liver failure, and severe liver necroinflammation is regarded as the core feature of ACLF. However, organ failure, whether hepatic or extrahepatic, was the predominant feature according to the EASL-CLIF criteria (31). ACLF patients, who meet EASL-CLIF criteria, are typically and more irreversibly at the "end-stage." G-CSF is regarded as a growth factor in hepatic regeneration and an immunomodulatory agent in ACLF (2). Garg et al. (6) showed that the number of $CD34^+$ cells markedly increased in the liver tissue after G-CSF therapy in patients with ACLF. Subsequently, they demonstrated that G-CSF enhanced the mobilization of

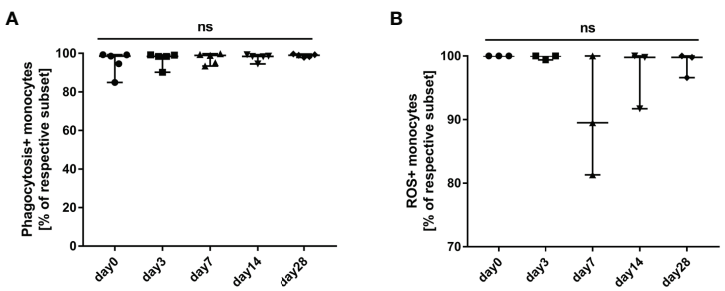

FIGURE 7 | Influence of G-CSF on phagocytosis and oxidative burst function of monocytes in HBV-ACLF. **(A)** Effect of G-CSF on phagocytosis function of monocytes (n=5). **(B)** Effect of G-CSF on oxidative burst function of monocytes (n=3). ns represents $P>0.05$; G-CSF, Granulocyte-colony stimulating factor; HBV-ACLF, hepatitis B virus-related acute-on -chronic liver failure.

bone marrow hematopoietic stem cells and promoted their homing in the hepatic parenchyma. G-CSF therapy was also shown to enhance dendritic cell recruitment to the liver and suppress interferon-γ secretion by $CD8^+$ T cells to attenuate hepatocellular injury (13). The purpose of G-CSF in patients with ACLF is to enhance liver regeneration and regulate the immune and inflammatory responses. Hence, G-CSF should be used in patients with early stage ACLF, where it can offer excellent regenerative potential. However, in the study by Engelmann (10), all G-CSF-treated ACLF patients had a poor pre-existing liver base (liver cirrhosis), more than 65.9% suffered from extrahepatic organ failure, and up to 56.8% had bacterial infection at baseline. Thus, it may have been too late for G-CSF to exert a therapeutic effect. In a comment on this study, Sarin (32) offers a similar opinion. Therefore, the differences in the definition of ACLF between the East and the West also directly led to the discrepancy in understanding the pathophysiological process, therapeutic strategies, and treatment effects in ACLF.

Our study also showed that the baseline monocyte count was positively associated with the 180-day mortality risk of HBV-ACLF patients, while the stratified analysis showed that this positive correlation was mainly contributed by the patients in the G-CSF group. Interestingly, after 6 days of continuous treatment, the control group did not demonstrate significant changes, whereas the positive association between monocyte count on day 7 and the risk of death was significantly weakened in the G-CSF-treated group. Therefore, we speculate that G-CSF may benefit HBV-ACLF patients by altering the number or function of monocytes.

Monocyte/macrophage dysfunction plays a core role in the progression of ACLF (17). These cells have plastic phenotypes and diverse roles in ACLF, from pro-inflammatory (M1-like) to anti-inflammatory/pro-restorative (M2-like), depending on the microenvironment. To better understand the mechanism of action of G-CSF, we investigated its effect on the phenotype and function of monocytes in ACLF patients. Our study demonstrated that after treatment with G-CSF, the expression of M1-like markers (HLA-DR and CD86) in monocytes decreased, whereas expression of MerTK (M2-like marker) increased. Weise et al. (33) detected a similar phenomenon in mouse models of ischemic stroke. After administration of G-CSF, the expression of $Ly6c^+$ (M1-like marker) in monocytes was markedly suppressed (33). Similarly, in another study performed by Fadini, circulating M2-like phenotype monocytes were evaluated after G-CSF treatment (34). Our study also showed that the secretion of TNF-α, IL-6, and IL-10 by monocytes decreased after G-CSF therapy with or without LPS stimulation in patients with ACLF. This indicates that G-CSF could attenuate the monocyte immune response in the basal state in ACLF. Moreover, the response to further LPS stimuli was reduced, which indicated LPS tolerance. Interestingly, *in vitro* experiments, we found that the IL-10 level was slightly increased by G-CSF after LPS stimulation. Weise et al. also found that G-CSF may promote the production of IL-10 (an M2-like cytokine) in monocytes in animal models of ischemic stroke (33). This discrepancy may be related to the methodological limitations of the studies. The microenvironment is also different *in vivo* vs. *in vitro*, and monocytes in patients may also be affected by other stimuli. What is more, several studies have detected an anti-inflammatory effect of monocytes mediated by G-CSF, which is characterized by the reduction of LPS-induced TNF-α (M1-like cytokine) production (35, 36). These findings appear to be compatible with our results. It means that G-CSF appears to impair antimicrobial defenses while attenuating monocyte inflammatory responses in ACLF. However, our study also found that after G-CSF treatment, the phagocytic function of monocytes in patients tended to be elevated, while the oxidative burst capacity decreased. Due to the small sample size, these differences were not statistically significant. Therefore, further studies may be required to assess whether G-CSF has a negative effect on the antimicrobial defense capacity of monocytes. Collectively, these results indicate that G-CSF seems to induce monocytes to exert immunosuppressive effects. From this perspective, it supports the argument that G-CSF should be used in the early phase of ACLF, when the pro-inflammatory/injury response is dominant (37).

Our study had several limitations. Firstly, this was a single-center study, and a larger multicenter trial should be conducted. Secondly, the relatively small sample size in the experimental study may have led to statistical fluctuations. Finally, because liver tissues were unavailable, we only investigated the effect of G-CSF on circulating monocytes in ACLF patients, and lacked macrophages. This issue will be resolved in future animal experiments.

In summary, our study validated the efficacy of G-CSF in patients with HBV-ACLF. In addition, the effects of G-CSF on monocytes in ACLF were explored. G-CSF can promote the anti-inflammatory/pro-restorative phenotype (M2-like) transition of monocytes, which may contribute to the recovery of ACLF. However, owing to heterogeneity, monocytes play distinct roles in ACLF, from pro-inflammatory to pro-resolution, depending on the microenvironment. Therefore, a full understanding of the pathophysiological processes and developmental stages of ACLF may help to select the right patients for appropriate therapy.

DATA AVAILABILITY STATEMENT

The raw data supporting the conclusions of this article will be made available by the authors, without undue reservation.

ETHICS STATEMENT

The studies involving human participants were reviewed and approved by the Human Ethics Committee of the Fifth Medical Center of the PLA General Hospital. The patients/participants provided their written informed consent to participate in this study.

AUTHOR CONTRIBUTIONS

JT, HW, XX, JC (6th author), XM, ZL, HS, XL and CL participated in the data acquisition. JH, ZW, HF and JT designed the study. JT, HW and HF performed analyses and interpretation of data. JT, HW, XM, JC (9th author) and HXW completed the experiments. JT, HW,

ZW wrote the first draft of the manuscript and incorporated revisions. JT, HW and JH prepared the final version. All authors contributed to the article and approved the submitted version.

FUNDING

This work was supported by a grant from the Capital's Funds for Health Improvement and Research, China (NO.2020-1-5031) and National Clinical Research Center for Infectious Diseases (NCRC-ID202106).

ACKNOWLEDGMENTS

The authors thank all the participants of this study for their contribution.

SUPPLEMENTARY MATERIAL

The Supplementary Material for this article can be found online at: https://www.frontiersin.org/articles/10.3389/fimmu.2022.885829/full#supplementary-material

REFERENCES

1. Sarin SK, Choudhury A, Sharma MK, Maiwall R, Al Mahtab M, Rahman S, et al. Acute–on–Chronic Liver Failure: Consensus Recommendations of the Asian Pacific Association for the Study of the Liver (APASL): An Update. *Hepatol Int* (2019) 13(4):353–90. doi: 10.1007/s12072-019-09946-3
2. Sarin SK, Choudhury A. Acute–on–Chronic Liver Failure: Terminology, Mechanisms and Management. *Nat Rev Gastroenterol hepatol* (2016) 13 (3):131–49. doi: 10.1038/nrgastro.2015.219
3. Moreau R, Jalan R, Gines P, Pavesi M, Angeli P, Cordoba J, et al. Acute–on–Chronic Liver Failure is a Distinct Syndrome That Develops in Patients With Acute Decompensation of Cirrhosis. *Gastroenterol* (2013) 144(7):1426–37.e1421–1429. doi: :10.1053/j.gastro.2013.02.042
4. Bernal W, Jalan R, Quaglia A, Simpson K, Wendon J, Burroughs A. Acute–on–Chronic Liver Failure. *Lancet (Lond Engl)* (2015) 386(10003):1576–87. doi: 10.1016/S0140-6736(15)00309-8
5. Duan XZ, Liu FF, Tong JJ, Yang HZ, Chen J, Liu XY, et al. Granulocyte–Colony Stimulating Factor Therapy Improves Survival in Patients With Hepatitis B Virus–Associated Acute–on–Chronic Liver Failure. *World J Gastroenterol* (2013) 19(7):1104–10. doi: 10.3748/wjg.v19.i7.1104
6. Garg V, Garg H, Khan A, Trehanpati N, Kumar A, Sharma BC, et al. Granulocyte Colony–Stimulating Factor Mobilizes CD34(+) Cells and Improves Survival of Patients With Acute–on–Chronic Liver Failure. *Gastroenterol* (2012) 142(3):505–12.e501. doi: 10.1053/j.gastro.2011.11.027
7. Singh V, Sharma AK, Narasimhan RL, Bhalla A, Sharma N, Sharma R. Granulocyte Colony–Stimulating Factor in Severe Alcoholic Hepatitis: A Randomized Pilot Study. *Am J Gastroenterol* (2014) 109(9):1417–23. doi: 10.1038/ajg.2014.154
8. Di Campli C, Zocco MA, Saulnier N, Grieco A, Rapaccini G, Addolorato G, et al. Safety and Efficacy Profile of G–CSF Therapy in Patients With Acute on Chronic Liver Failure. *Digest Liver Dis* (2007) 39(12):1071–6. doi: 10.1016/j.dld.2007.08.006
9. Saha BK, Mahtab MA, Akbar SMF, Noor ESM, Mamun AA, Hossain SMS, et al. Therapeutic Implications of Granulocyte Colony Stimulating Factor in Patients With Acute–on–Chronic Liver Failure: Increased Survival and Containment of Liver Damage. *Hepatol Int* (2017) 11(6):540–6. doi: 10.1007/s12072-017-9814-1
10. Engelmann C, Herber A, Franke A, Bruns T, Reuken P, Schiefke I, et al. Granulocyte–Colony Stimulating Factor (G–CSF) to Treat Acute–on–Chronic Liver Failure: A Multicenter Randomized Trial (GRAFT Study). *J Hepatol* (2021) 75(6):1346–54. doi: 10.1016/j.jhep.2021.07.033
11. Theocharis SE, Papadimitriou LJ, Retsou ZP, Margeli AP, Ninos SS, Papadimitriou JD. Granulocyte–Colony Stimulating Factor Administration Ameliorates Liver Regeneration in Animal Model of Fulminant Hepatic Failure and Encephalopathy. *Digest Dis Sci* (2003) 48(9):1797–803. doi: 10.1023/a:1025463532521
12. Spahr L, Lambert JF, Rubbia-Brandt L, Chalandon Y, Frossard JL, Giostra E, et al. Granulocyte–Colony Stimulating Factor Induces Proliferation of Hepatic Progenitors in Alcoholic Steatohepatitis: A Randomized Trial. *Hepatol (Baltimore Md)* (2008) 48(1):221–9. doi: 10.1002/hep.22317
13. Khanam A, Trehanpati N, Garg V, Kumar C, Garg H, Sharma BC, et al. Altered Frequencies of Dendritic Cells and IFN–Gamma–Secreting T Cells With Granulocyte Colony–Stimulating Factor (G–CSF) Therapy in Acute–on–Chronic Liver Failure. *Liver Int* (2014) 34(4):505–13. doi: 10.1111/liv.12415
14. Moreau R, Rautou PE. G–CSF Therapy for Severe Alcoholic Hepatitis: Targeting Liver Regeneration or Neutrophil Function? *Am J Gastroenterol* (2014) 109(9):1424–6. doi: 10.1038/ajg.2014.250
15. Krenkel O, Tacke F. Liver Macrophages in Tissue Homeostasis and Disease. *Nat Rev Immunol* (2017) 17(5):306–21. doi: 10.1038/nri.2017.11
16. Heymann F, Tacke F. Immunology in the Liver–From Homeostasis to Disease. *Nat Rev Gastroenterol Hepatol* (2016) 13(2):88–110. doi: 10.1038/nrgastro.2015.200
17. Triantafyllou E, Woollard KJ, McPhail MJW, Antoniades CG, Possamai LA. The Role of Monocytes and Macrophages in Acute and Acute–On–Chronic Liver Failure. *Front Immunol* (2018) 9:2948. doi: 10.3389/fimmu.2018.02948
18. Youn JI, Kumar V, Collazo M, Nefedova Y, Condamine T, Cheng P, et al. Epigenetic Silencing of Retinoblastoma Gene Regulates Pathologic Differentiation of Myeloid Cells in Cancer. *Nat Immunol* (2013) 14(3):211–20. doi: 10.1038/ni.2526
19. Jakubzick CV, Randolph GJ, Henson PM. Monocyte Differentiation and Antigen–Presenting Functions. *Nat Rev Immunol* (2017) 17(6):349–62. doi: 10.1038/nri.2017.28
20. Bernsmeier C, van der Merwe S, Périanin A. Innate Immune Cells in Cirrhosis. *J Hepatol* (2020) 73(1):186–201. doi: 10.1016/j.jhep.2020.03.027
21. You S, Rong Y, Zhu B, Zhang A, Zang H, Liu H, et al. Changing Etiology of Liver Failure in 3,916 Patients From Northern China: A 10–Year Survey. *Hepatol Int* (2013) 7(2):714–20. doi: 10.1007/s12072-013-9424-5
22. Matsushita M, Freigang S, Schneider C, Conrad M, Bornkamm GW, Kopf M. T Cell Lipid Peroxidation Induces Ferroptosis and Prevents Immunity to Infection. *J Exp Med* (2015) 212(4):555–68. doi: 10.1084/jem.20140857
23. Yu Z, Li J, Ren Z, Sun R, Zhou Y, Zhang Q, et al. Switching From Fatty Acid Oxidation to Glycolysis Improves the Outcome of Acute–On–Chronic Liver Failure. *Adv Sci (Weinheim Baden–Wurttemberg Germany)* (2020) 7 (7):1902996. doi: 10.1002/advs.201902996
24. Sarin SK, Kumar A, Almeida JA, Chawla YK, Fan ST, Garg H, et al. Acute–On–Chronic Liver Failure: Consensus Recommendations of the Asian Pacific Association for the Study of the Liver (APASL). *Hepatol Int* (2009) 3(1):269–82. doi: 10.1007/s12072-008-9106-x
25. Angeli P, Ginès P, Wong F, Bernardi M, Boyer TD, Gerbes A, et al. Diagnosis and Management of Acute Kidney Injury in Patients With Cirrhosis: Revised Consensus Recommendations of the International Club of Ascites. *J Hepatol* (2015) 62(4):968–74. doi: 10.1016/j.jhep.2014.12.029
26. Patidar KR, Bajaj JS. Covert and Overt Hepatic Encephalopathy: Diagnosis and Management. *Clin Gastroenterol Hepatol* (2015) 13(12):2048–61. doi: 10.1016/j.cgh.2015.06.039
27. Kamath PS, Kim WR. The Model for End–Stage Liver Disease (MELD). *Hepatol (Baltimore Md)* (2007) 45(3):797–805. doi: 10.1002/hep.21563
28. Kim WR, Biggins SW, Kremers WK, Wiesner RH, Kamath PS, Benson JT, et al. Hyponatremia and Mortality Among Patients on the Liver–Transplant

Waiting List. *N Engl J Med* (2008) 359(10):1018–26. doi: 10.1056/NEJMoa0801209
29. Piano S, Singh V, Caraceni P, Maiwall R, Alessandria C, Fernandez J, et al. Epidemiology and Effects of Bacterial Infections in Patients With Cirrhosis Worldwide. *Gastroenterol* (2019) 156(5):1368–80.e1310. doi: 10.1053/j.gastro.2018.12.005
30. Zhang Z, Yang Z, Cheng Q, Hu X, Liu M, Liu Y, et al. Establishment and Validation of a Prognostic Model for Hepatitis B Virus–Related Acute–on–Chronic Liver Failure Patients With Bacterial Infection. *Hepatol Int* (2022) 16 (1):38–47. doi: 10.1007/s12072-021-10268-6
31. Bajaj JS. Defining Acute–on–Chronic Liver Failure: Will East and West Ever Meet? *Gastroenterol* (2013) 144(7):1337–9. doi: 10.1053/j.gastro.2013.04.024
32. Jindal A, Sarin SK. G–CSF in Acute–on–Chronic Liver Failure – Art of 'Patient Selection' is Paramount! *J Hepatol* (2022) 76(2):472–3. doi: 10.1016/j.jhep.2021.08.022
33. Weise G, Pösel C, Möller K, Kranz A, Didwischus N, Boltze J, et al. High–Dosage Granulocyte Colony Stimulating Factor Treatment Alters Monocyte Trafficking to the Brain After Experimental Stroke. *Brain Behav Immun* (2017) 60:15–26. doi: 10.1016/j.bbi.2016.08.008
34. Fadini GP, De Kreutzenberg SV, Boscaro E, Albiero M, Cappellari R, Kränkel N, et al. An Unbalanced Monocyte Polarisation in Peripheral Blood and Bone Marrow of Patients With Type 2 Diabetes has an Impact on Microangiopathy. *Diabetologia* (2013) 56(8):1856–66. doi: 10.1007/s00125-013-2918-9
35. Boneberg EM, Hareng L, Gantner F, Wendel A, Hartung T. Human Monocytes Express Functional Receptors for Granulocyte Colony–Stimulating Factor That Mediate Suppression of Monokines and Interferon–Gamma. *Blood* (2000) 95 (1):270–6. doi: 10.1182/blood.V95.1.270.001k39_270_276
36. Nishiki S, Hato F, Kamata N, Sakamoto E, Hasegawa T, Kimura-Eto A, et al. Selective Activation of STAT3 in Human Monocytes Stimulated by G–CSF: Implication in Inhibition of LPS–Induced TNF–Alpha Production. *Am J Physiol Cell Physiol* (2004) 286(6):C1302–1311. doi: 10.1152/ajpcell.00387.2003
37. Chen P, Wang YY, Chen C, Guan J, Zhu HH, Chen Z. The Immunological Roles in Acute–on–Chronic Liver Failure: An Update. *Hepatobil Pancreat Dis Int: HBPD Int* (2019) 18(5):403–11. doi: 10.1016/j.hbpd.2019.07.003

Conflict of Interest: The authors declare that the research was conducted in the absence of any commercial or financial relationships that could be construed as a potential conflict of interest.

Publisher's Note: All claims expressed in this article are solely those of the authors and do not necessarily represent those of their affiliated organizations, or those of the publisher, the editors and the reviewers. Any product that may be evaluated in this article, or claim that may be made by its manufacturer, is not guaranteed or endorsed by the publisher.

frontiers | Frontiers in Immunology

ORIGINAL RESEARCH
published: 03 June 2022
doi: 10.3389/fimmu.2022.856587

Bioenergetic Failure Drives Functional Exhaustion of Monocytes in Acute-on-Chronic Liver Failure

Deepanshu Maheshwari[1†], Dhananjay Kumar[1†], Rakesh Kumar Jagdish[2], Nidhi Nautiyal[1], Ashinikumar Hidam[1], Rekha Kumari[1], Rashi Sehgal[1], Nirupama Trehanpati[1], Sukriti Baweja[1], Guresh Kumar[1], Swati Sinha[3], Meenu Bajpai[4], Viniyendra Pamecha[5], Chhagan Bihari[6], Rakhi Maiwall[2], Shiv Kumar Sarin[2] and Anupam Kumar[1*]*

[1] Department of Molecular and Cellular Medicine, Institute of Liver and Biliary Sciences, New Delhi, India, [2] Department of Hepatology, Institute of Liver and Biliary Sciences, New Delhi, India, [3] Department of Obstetrics and Gynaecology, Sitaram Bhartia Institute of Science and Research, New Delhi, India, [4] Department of Transfusion Medicine, Institute of Liver and Biliary Sciences, New Delhi, India, [5] Department of Hepato-Pancreato-Biliary (HPB) Surgery and Liver Transplant, Institute of Liver and Biliary Sciences, New Delhi, India, [6] Department of Pathology, Institute of Liver and Biliary Sciences, New Delhi, India

Objective: The monocyte–macrophage system is central to the host's innate immune defense and in resolving injury. It is reported to be dysfunctional in acute-on-chronic liver failure (ACLF). The disease-associated alterations in ACLF monocytes are not fully understood. We investigated the mechanism of monocytes' functional exhaustion and the role of umbilical cord mesenchymal stem cells (ucMSCs) in re-energizing monocytes in ACLF.

Design: Monocytes were isolated from the peripheral blood of ACLF patients ($n = 34$) and matched healthy controls ($n = 7$) and patients with compensated cirrhosis ($n = 7$); phagocytic function, oxidative burst, and bioenergetics were analyzed. In the ACLF mouse model, ucMSCs were infused intravenously, and animals were sacrificed at 24 h and day 11 to assess changes in monocyte function, liver injury, and regeneration.

Results: Patients with ACLF (alcohol 64%) compared with healthy controls and those with compensated cirrhosis had an increased number of peripheral blood monocytes ($p < 0.0001$) which displayed significant defects in phagocytic ($p < 0.0001$) and oxidative burst capacity ($p < 0.0001$). ACLF patients also showed a significant increase in the number of liver macrophages as compared with healthy controls ($p < 0.001$). Bioenergetic analysis showed markedly reduced oxidative phosphorylation ($p < 0.0001$) and glycolysis ($p < 0.001$) in ACLF monocytes. Patients with monocytes having maximum mitochondrial respiration of <37.9 pmol/min [AUC = 0.822, hazard ratio (HR) = 4.5] and baseline glycolysis of ≤42.7 mpH/min (AUC = 0.901, HR = 9.1) showed increased 28-day mortality ($p < 0.001$). Co-culturing ACLF monocytes with ucMSC showed improved mitochondrial respiration ($p < 0.01$) and phagocytosis ($p < 0.0001$). Furthermore, ucMSC therapy increased monocyte energy ($p < 0.01$) and phagocytosis ($p < 0.001$), reduced hepatic injury, and enhanced hepatocyte regeneration in ACLF animals.

OPEN ACCESS

Edited by:
Yu Shi,
Zhejiang University, China

Reviewed by:
Maria-Rosa Sarrias,
Germans Trias i Pujol Health Science Research Institute (IGTP), Spain
Tao Chen,
Huazhong University of Science and Technology, China

***Correspondence:**
Anupam Kumar
dr.anupamkumar.ilbs@gmail.com
Shiv Kumar Sarin
shivsarin@gmail.com

[†]These authors have contributed equally to this work

Specialty section:
This article was submitted to Inflammation, a section of the journal Frontiers in Immunology

Received: *17 January 2022*
Accepted: *27 April 2022*
Published: *03 June 2022*

Citation:
Maheshwari D, Kumar D, Jagdish RK, Nautiyal N, Hidam A, Kumari R, Sehgal R, Trehanpati N, Baweha S, Kumar G, Sinha S, Bajpai M, Pamecha V, Bihari C, Maiwall R, Sarin SK and Kumar A (2022) Bioenergetic Failure Drives Functional Exhaustion of Monocytes in Acute-on-Chronic Liver Failure. Front. Immunol. 13:856587. doi: 10.3389/fimmu.2022.856587

Conclusion: Bioenergetic failure drives the functional exhaustion of monocytes in ACLF. ucMSCs resuscitate monocyte energy and prevent its exhaustion. Restoring monocyte function can ameliorate hepatic injury and promote liver regeneration in the animal model of ACLF.

Keywords: bioenergetics, ucMSC therapy, regeneration, acute-on-chronic liver failure (ACLF), monocyte

INTRODUCTION

Acute-on-chronic liver failure (ACLF) is a life-threatening condition caused by acute hepatic injury in patients with underlying chronic liver disease resulting in liver failure (1–6). Unresolved injury, poor infection control, and liver regeneration result in persistent systemic inflammation and cytokine storm, which subsequently lead to systemic inflammatory response syndrome (SIRS) resulting in multiple organ failure, septic shock, and death in ACLF (1, 4, 5, 7–9). Nearly 74% of ACLF patients initially diagnosed without SIRS or sepsis develop SIRS by day 7 which increases the onset of secondary organ failure and sepsis with high short-term mortality (9). About 25%–37% of these patients show the presence of infection/sepsis at the time of presentation and nearly 46% of the remaining patients develop infection/sepsis by day 28, which further increases secondary organ failure and lowers the 90-day probability of survival (9–12). The precise mechanism of poor resolution of infection and ongoing hepatic injury that accounts for SIRS and the subsequent onset of sepsis and secondary organ failure in ACLF is not clear.

Liver macrophages [Kupffer cells (KCs)] along with bone marrow (BM) monocytes play an important role in the host's innate immune defense against pathogens and injury (13–16). Although the number of KCs increases in ACLF compared to healthy (8), they fail to clear the infection and resolve the injury. Previous studies have shown that monocytes in ACLF show a suppressive phenotype with reduced human leucocyte antigen-DR (HLA-DR) expression, antigen presentation, and impaired pro-inflammatory cytokine production in response to bacterial components (17–21). These cells also show significantly low expression of toll-like receptors 2/4 (TLR-2/TLR-4) and defects in their phagocytic and oxidative burst functions (22) necessary for the identification, engulfment, and killing of bacteria, respectively. The underlying cause for these defects is still not clear.

Functional heterogeneity of monocytes/macrophages is regulated at the transcriptional and metabolic levels (23). Monocytes/macrophages adopt a distinct metabolic pathway upon encountering pathogen/tissue damage and use a variety of carbon sources to fuel their diverse functions (24). In response to infection or necrotic stimuli, these cells mainly rely on glycolysis for ATP requirement (25) and execute their pro-inflammatory and bacterial killing function by remodeling the TCA cycle and electron transport chain (26–28). On the other hand, anti-inflammatory monocytes maintain basal levels of glycolysis for sustaining oxidative phosphorylation (OXPHOS) but prefer fatty acid oxidation for producing ATP and anti-inflammatory cytokines such as IL-10 (25, 29–31).

Monocyte functions such as phagocytosis, efferocytosis, and oxidative burst are highly energy-demanding processes. Infections are associated with broad defects in energy metabolism in a dose-dependent manner leading to immune paralysis as seen in sepsis (32, 33). ACLF patients have intestinal barrier failure which may increase the exposure of monocytes to bacteria and bacterial products (34–36). In ACLF, it is unclear whether there is metabolic dysfunction or metabolic exhaustion of monocytes, responsible for the poor response to infection. In this study, we aimed to analyze the changes in the energy metabolism of monocytes during ACLF progression and their impact on monocyte functions. We also investigated whether restoring ACLF monocyte bioenergetics by using mesenchymal stem cells (MSCs) could resuscitate their phagocytic function. These results may provide new insights into the pathophysiology of innate immune dysfunction and the therapeutic use of MSCs for the management of ACLF.

MATERIALS AND METHODS

Patients

We recruited ACLF patients ($n = 34$) from the Institute of Liver and Biliary Sciences, India, between July 2017 and January 2021. Patients were characterized according to the Asian Pacific Association for the Study of the Liver (APASL)-ACLF criteria (2). Patients were excluded based on the following criteria: were <18 years of age; had autoimmune hepatitis, septic shock, extrahepatic malignancies, or prior liver transplant; were pregnant; and did not provide consent. Patients with ACLF were stratified into ACLF-systemic inflammatory response syndrome (ACLF-SIRS) (SIRS is defined as the presence of any of the two criteria from the following: temperature >104.4 or <96.8°F, heart rate >90/min, respiratory rate >20/min, TLC >12), ACLF-sepsis (infection with or without SIRS), and ACLF (having no SIRS and infection). Baseline blood was

Abbreviations: ACLF, acute-on-chronic liver failure; ucMSCs, umbilical cord mesenchymal stem cells; CCl_4, carbon tetrachloride; APAP, acetaminophen; LPS, lipopolysaccharide; OCR, oxygen consumption rate; ECAR, extracellular acidification rate; SIRS, systemic inflammatory response; TUNEL, terminal deoxynucleotidyl transferase; APASL, Asian Pacific Association for the Study of the Liver; AARC, APASL ACLF Research Consortium; AUROC, area under the receiver operating characteristic curve; BM, bone marrow; HLA-DR, human leucocyte antigen-DR; TLR, toll-like receptor; TCA, tricarboxylic acid cycle; ROS, reactive oxygen species; MSC, mesenchymal stem cell; INR, international normalized ratio; LDLT, live donor liver transplant; OXPHOS, oxidative phosphorylation; FCCP, fluorocarbonyl cyanide phenylhydrazone; 2-DG, 2-deoxy-D-glucose; MR, maximum respiration; MTG, MitoTracker Green; MTR, MitoTracker Red CMXRos; PGE2, prostaglandin E2.

collected at the time of admission before initiating therapy. In consenting patients, blood was also collected at 24 and 72 h to study the cellular kinetics. Blood and urine cultures were obtained, ascitic fluid was collected for analysis, and a chest X-ray was performed to confirm infections and pulmonary infiltrates as per standard care. The blood from age- and gender-matched healthy volunteers ($n = 7$) and patients with compensated cirrhosis ($n = 7$) was taken as the control for the analysis of monocyte energy and function.

Explant liver tissues from ACLF patients ($n = 8$) who had undergone live donor liver transplant (LDLT) and liver tissues of healthy controls [$n = 5$; cadaveric liver unfit for transplant = 1; discarded donor liver tissue after trimming during adult to pediatric (>2 months) LDLT = 4] were collected to analyze the distribution and function of liver macrophages.

Written informed consent was obtained from all patients or their designated family members. The study protocol conformed to the ethical guidelines of the 1975 Declaration of Helsinki as reflected in the *a-priori* approval by the appropriate institutional review committee. No donor organs were obtained from executed prisoners or other institutionalized persons.

Monocyte Isolation and Culture

Blood was collected from healthy donors and ACLF patients in EDTA-coated vacutainers (BD Biosciences, New Jersey, USA). Plasma was separated and collected for further analysis. $CD14^+$ monocytes were isolated using a positive selection procedure according to the manufacturer's specification (Miltenyi CD14 MicroBeads, human, Miltenyi Biotec, Bergisch Gladbach, Germany). For bioenergetic analysis, freshly isolated monocytes were used. Monocytes were cultured in RPMI medium (Gibco, USA) containing antibiotics (1% penicillin and streptomycin) and further supplemented with either plasma from healthy donors or plasma from patients with ACLF at a final concentration of 10% by volume with or without LPS (Sigma Aldrich, Missouri, USA) (100 ng/ml) to study the effect of ACLF plasma and endotoxins on the energy metabolism of healthy monocytes (22). Patient plasma used in these experiments represents a pool of six healthy donors or ACLF (without SIRS or sepsis). Plasma was heat-inactivated (56 C for 30 min) and passed through a 0.22-μM filter prior to use. Following a 6-h incubation time (37 C, 5% CO_2), the cells were harvested and used for bioenergetic analysis. To study the effect of glycolysis and OXPHOS on monocyte phagocytic and oxidative burst function, cells were pre-incubated with RPMI medium containing 1.0 μM oligomycin, 0.75 μM FCCP, or 0.5 μM rotenone + antimycin A for the inhibition of OXPHOS or 50 mM 2-deoxy-2-glucose (2-DG) for the inhibition of glycolysis for 30 min (37 C, 5% CO_2), and then monocytes were analyzed for phagocytic capacity (Cayman Chemicals, Michigan, USA) and ROS production (Sigma Aldrich, Missouri, USA). Pre- and post-treatment cells were stained with annexin V to analyze the effect of OXPHOS and glycolysis inhibitors on cell death using a flow cytometer.

Cellular Bioenergetic Studies

Oxygen consumption rate (OCR) and extracellular acidification rate (ECAR) were measured using Seahorse XFe24 Extracellular Flux Analyzer (Agilent Technologies, California, USA) as readout for OXPHOS and glycolysis, respectively. An equal number (3×10^5/well) of viable $CD14^+$ monocytes (as assessed by trypan blue dye exclusion assay) were seeded on CellTak (Corning)-coated plates in XF-Base Media (Agilent Technologies) containing 2.5 mM glucose, 1 mM sodium pyruvate, and 2 mM glutamine. OCR and ECAR were measured sequentially at the basal level and following the addition of 1.0 μM oligomycin, 0.75 μM FCCP (fluorocarbonyl cyanide phenylhydrazone), and 0.5 μM rotenone + antimycin to analyze changes in glycolysis and various mitochondrial respiratory parameters. The plate was read three times each at baseline and after the addition of drugs. Data were analyzed using Wave 2.6.1 and GraphPad Prism.

Monocyte–Mesenchymal Stem Cell Co-Culture

Prior to monocyte co-culture, MSCs were seeded in Transwell inserts at a ratio of 1:5 (MSCs to monocytes) and incubated in complete alpha-MEM (containing 10% FBS, 1% GlutaMAX, 1% non-essential amino acids, and 1% PSA) for 24 h. MSCs in Transwell were co-cultured with monocytes in TexMACS™ Medium (Miltenyi Biotec, California, USA) (without MCSF) for 24 h. After 24 h, monocytes were harvested and analyzed for mitochondrial bioenergetics using Seahorse XFe24 Extracellular Flux Analyzer (Agilent Technologies). Cells were also analyzed for mitochondrial biomass and mitochondrial membrane potential using MitoTracker dyes. To study the mitochondria transfer from MSC to monocyte, MSCs were pre-incubated with 300 nm MitoTracker Red CMXRos (Life Technologies, California, USA) for 2 h and washed three times with PBS to remove any unbound dye. MSCs were then co-cultured with monocytes for 24 h. The cells were then assayed for fluorescence by BD FACSAria and by confocal microscopy.

ACLF Murine Model and MSC Administration

Six- to 8-week-old male C57Bl6 mice (Liveon Biolabs Pvt. Ltd., Karnataka, India) were used to develop the animal model of ACLF as described previously (37). All the animals were housed in the institutional animal facility in a clean, temperature-controlled environment with a 12-h light and dark cycle and were provided with free access to regular laboratory chow diet and water. All animals received humane care according to the criteria outlined in the "Guide for the Care and Use of Laboratory Animals," and all experimental procedures were approved by the Institutional Animal Ethics Committee (IAEC) under project approval (IAEC/ILB/17/03). To develop the ACLF animal model, 8–10-week-old male C57BL6/J mice ($n = 24$) were first subjected to carbon tetrachloride (CCl_4)-induced chronic liver injury for 10 weeks. Following 10 weeks of chronic liver injury, a single dose of acetaminophen (350 mg/kg bw) and LPS (100 μg/kg bw) was given to induce ACLF. Sixteen hours post-ACLF injury, animals were divided into two groups. Group 1 received ucMSCs (1×10^6/kg wt), while group 2 received 200 μl PBS as a control. Mice were sacrificed by an overdose of ketamine post-24 h and day 11 of cell therapy, blood was

collected through retro-orbital bleeding, and BM and liver were harvested for cell isolation and histology.

Statistical Analysis

Data were analyzed using SPSS version 22 (IBM Corp. Ltd., USA). Categorical data were compared using chi-square test and continuous data were compared by using one-way ANOVA/Kruskal–Wallis test, wherever applicable followed by *post-hoc* comparison by the Bonferroni method. Log transformation was applied wherever necessary. Univariate and multivariate analyses were carried out using multinomial logistic regression and expressed as odds ratio (OR, 95 CL). Diagnostic tests were applied to find out the area under the curve (AUROC) and Kaplan–Meier was used to find out the survival probabilities. Statistical analysis and graphical generation of data were done with GraphPad Prism software (San Diego, CA, USA). The exact values of n (the number of one sample or an individual animal) and statistical significance are depicted in the figures. Error bars represent standard deviation of the mean (SD). Significant difference in means is indicated as follows: $^{*}p < 0.05$, $^{**}p < 0.01$, $^{***}p < 0.001$, and $^{****}p < 0.0001$.

Detailed methodology for the development of the ACLF animal model; isolation, culture, and characterization of umbilical cord mesenchymal stem cells; isolation of monocytes from peripheral blood and their phenotypic characterization; monocyte–MSC co-culture; phagocytic and oxidative burst assay; mitochondrial staining; estimation of plasma cytokines and endotoxin; and histopathology, immunohistochemistry, and TUNEL assay are provided in the Online **Supplementary Methods**.

Study Approval

All experiments were conducted in accordance with the National Ethical Guidelines for Biomedical and Health Research and the Committee for the Purpose of Control and Supervision of Experiments on Animals (CPCSEA) Govt. of India and were approved by the Ethics Committee of the Institute of Liver and Biliary Sciences, New Delhi, India (IEC/2017/50/NA02; IAEC/ILB/17/03; 9/ILBS/IC-SCR/2017).

RESULTS

Patient Demographics

Of the 34 ACLF patients, 13 had SIRS (ACLF-SIRS), 13 had sepsis (ACLF-sepsis), and 8 had neither sepsis nor SIRS (ACLF). The clinical characteristics with circulating biochemical and immunological parameters of the ACLF cohort are summarized in **Supplementary Table S1**. Eight of the 34 ACLF patients underwent LDLT. While blood was obtained from all 34 patients, liver tissue could be obtained from those who underwent LDLT. Of the seven cirrhosis patients (median age 64 years), five patients had cirrhosis secondary to alcoholic liver disease (ALD; 71.4%), one secondary to non-alcoholic fatty liver disease (NAFLD; 14.3%), and one cryptogenic (14.3%) with a median model for end-stage liver disease prognostic score of 9.1 [interquartile range (IQR) 7.1–10.2].

Defective Phagocytic and Oxidative Burst Functions of Peripheral Blood Monocyte and Liver Macrophages in ACLF

To identify the underlying cause of monocyte dysfunction, we first evaluated the changes in peripheral blood monocyte distribution and their phagocytic and oxidative burst function with SIRS and sepsis. Flow cytometric analysis of monocyte distribution showed a significant increase in monocytes in ACLF compared with healthy monocytes ($p < 0.0001$) and compensated cirrhosis ($p < 0.0001$) (**Figure 1A**), which was mainly contributed by intermediate monocytes (**Figures S1A, B**). Within the ACLF cohort, the number of monocytes was comparable between ACLF and ACLF-SIRS but was significantly ($p < 0.0001$) decreased in ACLF-sepsis (**Figure 1B**).

Next, we assessed the phagocytic and oxidative burst capacity of these cells on exposure to *Escherichia coli*. ACLF monocytes featured a significantly impaired phagocytic ($p < 0.0001$) and oxidative burst ($p < 0.0001$) capacity compared with healthy monocytes ($p < 0.0001$) and compensated cirrhosis ($p < 0.0001$) (**Figure 1C**). In comparison to healthy monocytes, there was a significant decrease in monocyte phagocytosis in cirrhosis which further decreased in ACLF (**Figure 1C**). Within the ACLF cohort, in comparison to ACLF, the monocytes from ACLF-SIRS showed a significant decrease in their phagocytosis ($p < 0.01$) and oxidative burst ($p < 0.001$). Between ACLF-SIRS and ACLF-sepsis, while phagocytosis further decreased ($p < 0.001$) in ACLF-sepsis, oxidative burst was comparable (**Figure 1D**), suggesting the loss of monocyte phagocytic and oxidative burst function with the onset of SIRS and sepsis.

To further understand monocyte–macrophage dysfunction in ACLF, we compared the distribution and phagocytic function of liver macrophages/KCs in ACLF with healthy monocytes ($n = 5$). Flow cytometric analysis of liver cells showed a significant ($p < 0.001$) increase in the number of $CD68^{+}$ KCs and $CD14^{+}$ monocytes in ACLF (**Figures 1E**, **S1C**). Out of the total $CD68^{+}$ KCs, while the number of yolk-sac KCs (YC-KC; $CD68^{+}$ $Cd14^{-}CD16^{-}$) significantly ($p < 0.001$) decreased, the number of BM-monocyte-derived KCs (BM-KC; $CD68^{+}CD14^{+}/CD16^{+}$) was significantly ($p < 0.01$) increased in ACLF (**Figure S1D**). Furthermore, $CD68^{+}$ KCs also showed significant ($p < 0.0001$) defects in phagocytosis (**Figure 1F**), suggesting that, though the number of macrophages increases in ACLF liver, these cells were defective in their phagocytic function.

Broad Defect in Energy Metabolism Drives the Loss of Phagocytic and Oxidative Burst Function in ACLF Monocytes

Phagocytosis and oxidative burst function are energy-demanding processes. To understand the metabolic processes required for these functions, we inhibited glycolysis using 2-DG and OXPHOS using rotenone/antimycin and oligomycin and studied their effect on phagocytosis and oxidative burst in healthy monocytes. Treatment with rotenone/antimycin ($p < 0.01$), oligomycin ($p < 0.01$), and 2-DG ($p < 0.05$) significantly reduced the phagocytic capacity of healthy monocytes (**Figure 2A**). However, reduction in phagocytosis in response

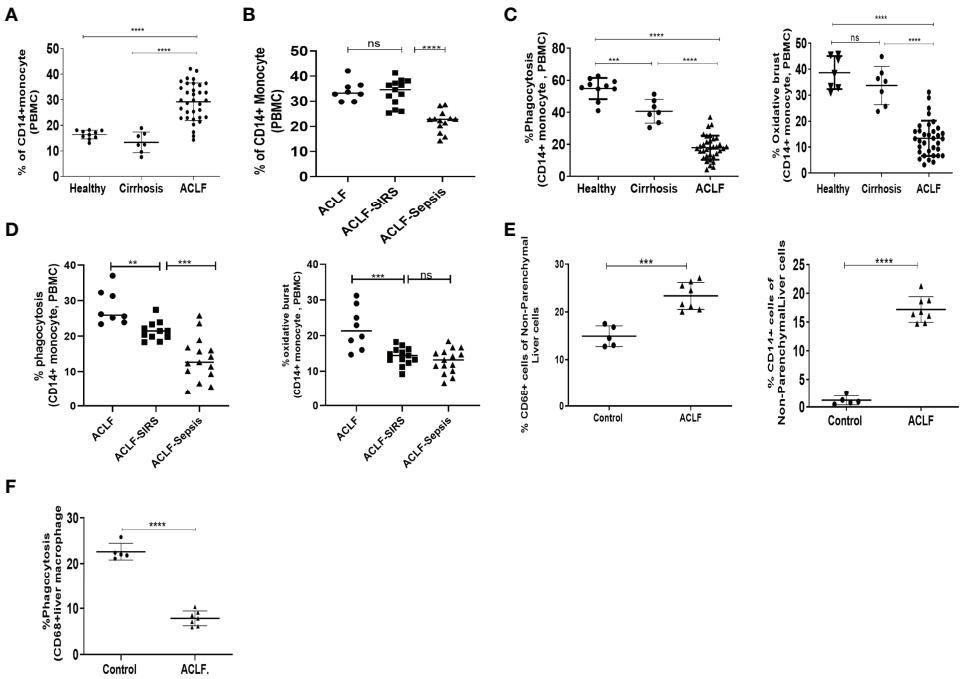

FIGURE 1 | Distribution and function of peripheral blood monocytes and liver macrophages in healthy controls and acute-on-chronic liver failure (ACLF) patients. **(A)** Dot plot showing changes in the percentage of peripheral blood CD14$^+$ monocytes in ACLF compared with healthy controls and those with cirrhosis. **(B)** Dot plot showing changes in the percentage of peripheral blood CD14$^+$ monocytes between subgroups of ACLF (ACLF, ACLF-SIRS, and ACLF-sepsis). **(C)** Dot plot showing the percentage changes in phagocytosis (left) and oxidative burst (right) of peripheral blood CD14$^+$ monocytes in ACLF compared with healthy controls and those with cirrhosis. **(D)** Dot plot showing the percentage changes in phagocytosis (left) and oxidative burst (right) of peripheral blood CD14$^+$ monocytes between subgroups of ACLF (ACLF, ACLF-SIRS, and ACLF-sepsis). **(E)** Dot plot showing the percentage changes in the distribution of CD68$^+$ macrophage (left) and CD14$^+$ monocyte (right) in ACLF compared with healthy controls. **(F)** Dot plot showing the percentage changes in phagocytosis of CD68$^+$ liver macrophages in ACLF compared with healthy controls (*$p < 0.05$; **$p < 0.01$; ***$p < 0.001$; ****$p < 0.0001$). n.s. stands for non-significant.

to inhibitors of mitochondrial respiration and glycolysis was comparable, suggesting that oxidative phosphorylation of glucose facilitates phagocytosis. Oxidative burst in response to *E. coli* was comparable between control, rotenone/antimycin A, and oligomycin; however, it was significantly ($p < 0.001$) reduced in monocytes treated with 2-DG (**Figure 2B**). Treatment of healthy monocytes with rotenone/antimycin, oligomycin, or 2-DG did not affect cell death, as assessed by annexin V staining (**Figure S2A**), indicating that anaerobic glycolysis is required to facilitate the oxidative burst function of monocytes.

To check the status of energy metabolism, we analyzed ACLF and healthy and cirrhotic monocytes for changes in glycolysis and OXPHOS. In comparison to healthy monocytes, there was a significant decrease in both OXPHOS ($p < 0.01$) and glycolysis ($p < 0.0001$) in cirrhotic monocytes. In comparison to cirrhosis, while OXPHOS ($p < 0.001$) further decreases in ACLF, glycolysis was comparable (**Figure 2C**), suggesting a broad defect in ACLF monocyte energy metabolism which becomes evident even at the stage of cirrhosis. Further analysis of different OXPHOS parameters showed a significant decrease in maximum respiration (MR, $p < 0.0001$) and ATP production (ATP, $p < 0.001$) between healthy and cirrhotic monocytes and in proton leak (PL, $p < 0.001$) between healthy and ACLF monocytes (**Figure S2B**), suggesting loss of mitochondrial function in ACLF monocytes, which is independent of ACLF etiology (**Figure S2C**).

Within the ACLF cohort, in comparison to ACLF, both ACLF-SIRS and ACLF-sepsis monocytes showed a significant reduction in basal, maximal, ATP, PL-linked OXPHOS (**Figures 2D**, **S2D**, **Table S2**), and glycolysis (**Figure 2E**, **Table S2**). Between ACLF-SIRS and ACLF-sepsis, while there was further reduction of basal ($p = 0.05$) and ATP ($p < 0.05$)-linked OXPHOS (**Figure 2D**, **Table S2**) in ACLF-sepsis, glycolysis was comparable (**Figure 2E**, **Table S2**). In further nominal logistic regression analysis, a progressive decrease in various OXPHOS parameters and glycolysis of ACLF monocytes were significantly ($p < 0.05$) associated with the development of SIRS and sepsis (**Table S3**), explaining the changes observed in ACLF monocyte phagocytosis and oxidative burst with the onset of SIRS and sepsis. The AUROC and cutoff values of various OXPHOS parameters and glycolysis for the onset of SIRS and sepsis are summarized in **Table S4**.

To investigate whether the loss of OXPHOS in ACLF monocytes resulted from the loss of mitochondrial mass or accumulation of dysfunctional mitochondria, we stained cells with MitoTracker Green (MTR, $\Delta\Psi$m-independent mitochondrial stain) and MitoTracker Red CMXRos (MTR, $\Delta\Psi$m-dependent mitochondrial stain). In comparison to control, ACLF monocytes

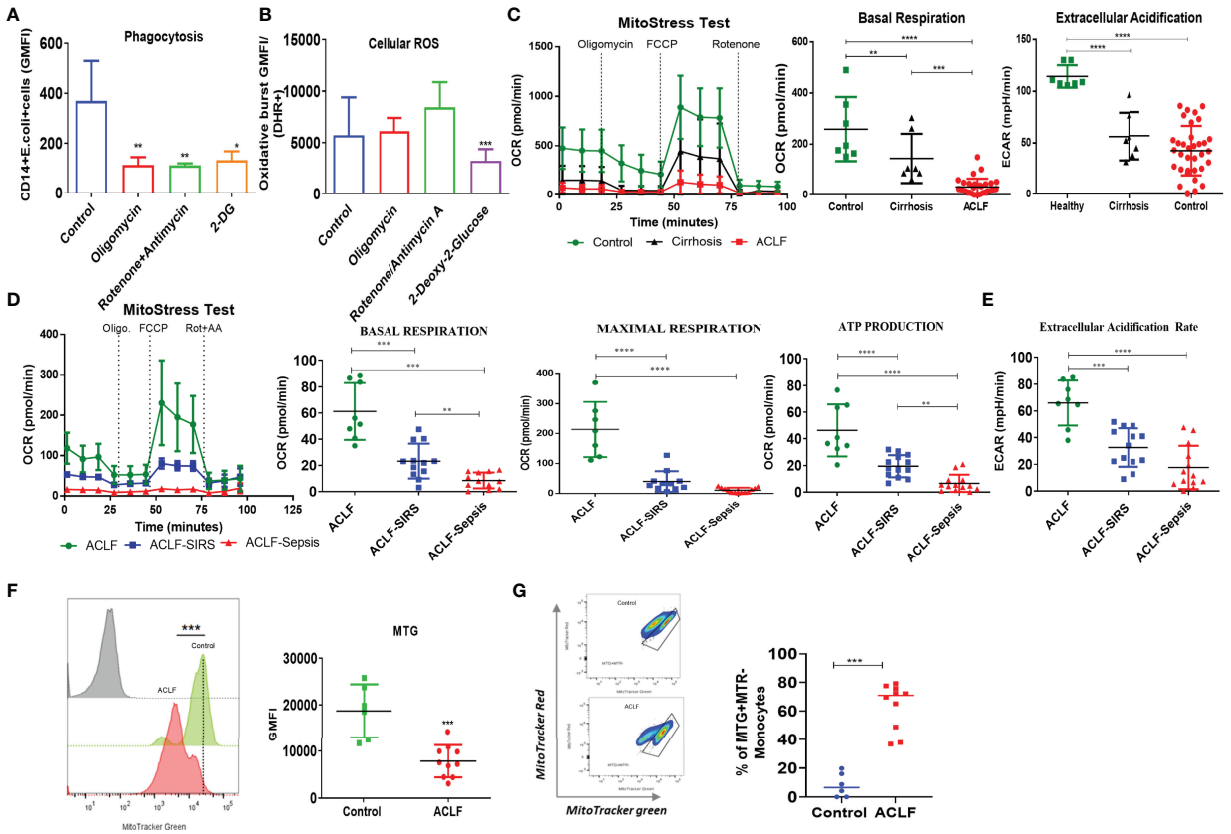

FIGURE 2 | Energy metabolism of healthy and ACLF monocytes. **(A, B)** Bar graph showing changes in median fluorescence intensity of **(A)** phagocytosis and **(B)** cellular ROS of healthy CD14$^+$ monocytes in the presence of inhibitors of mitochondria and glycolysis. **(C)** Real-time changes in oxygen consumption rate (OCR) with subsequent treatment with oligomycin (Oligo.) FCCP and rotenone and antimycin A (Rot. + AA.) in ACLF, cirrhosis, and healthy monocytes (left). Dot plot showing changes in basal mitochondrial respiration (middle) and glycolysis (right) in ACLF monocytes compared with healthy controls and those with cirrhosis. **(D)** Real-time changes in OCR and dot plot showing changes in the given mitochondrial respiratory parameter of monocytes in the ACLF subgroups (ACLF, ACLF-SIRS, and ACLF-sepsis). **(E)** Dot plot showing changes in glycolysis (extracellular acidification rate) of monocytes in the ACLF subgroups (ACLF, ACLF-SIRS, and ACLF-sepsis). **(F)** MitoTracker Green staining and **(G)** mitochondrial functionality based on MitoTracker Red vs. MitoTracker Green percentage in ACLF monocytes compared with healthy controls (*$p < 0.05$; **$p < 0.01$; ***$p < 0.001$; ****$p < 0.0001$).

showed a significant decrease ($p < 0.001$) in total mitochondrial mass (**Figure 2F**) with accumulation ($p < 0.001$) of dysfunctional mitochondria (MTG$^+$MTR$^-$) (**Figure 2G**). Together, these observations suggest that the loss of functional mitochondria leads to an OXPHOS defect that drives the defect in ACLF monocyte phagocytosis.

Association of Systemic Inflammation and Endotoxemia With Defect in Monocyte OXPHOS

Systemic endotoxemia and cytokine surge have been associated with ACLF and have shown to dampen monocyte phagocytosis (22). Next, to check how the plasma level of cytokines and endotoxin changes with the development of SIRS and sepsis in ACLF, we measured the levels of 24 different pro- and anti-inflammatory cytokines and endotoxin in the same patients. Interestingly, we observed that the plasma levels of all 24 different cytokines were comparable in ACLF, ACLF-SIRS, and ACLF-sepsis (**Figures 3A**, **S3**), while endotoxin significantly increases from ACLF to ACLF-SIRS ($p < 0.05$) and ACLF-SIRS to ACLF-sepsis ($p < 0.0001$) (**Figure 3B**).

To explore the impact of these factors on monocyte OXPHOS, we devised an *in-vitro* model of ACLF-mimic by culturing the freshly isolated healthy monocytes with pooled ACLF (no-SIRS, no-sepsis) plasma alone or with LPS for 6 h. Monocytes treated with healthy plasma were taken as control. Exposure of ACLF plasma alone significantly ($p < 0.001$) decreased the OXPHOS of monocytes, which was further dampened ($p < 0.0001$) in the presence of LPS (**Figure 3C**). Taken together, these data suggest that during ACLF, circulating plasma-derived factors suppress monocyte OXPHOS which are further dampened by systemic endotoxemia.

Dynamic Assessment of Mitochondrial Function in ACLF Monocytes and Its Impact on Patient Outcome

We observed a significant decrease in monocyte OXPHOS from ACLF to ACLF-sepsis. To understand how it changes with the

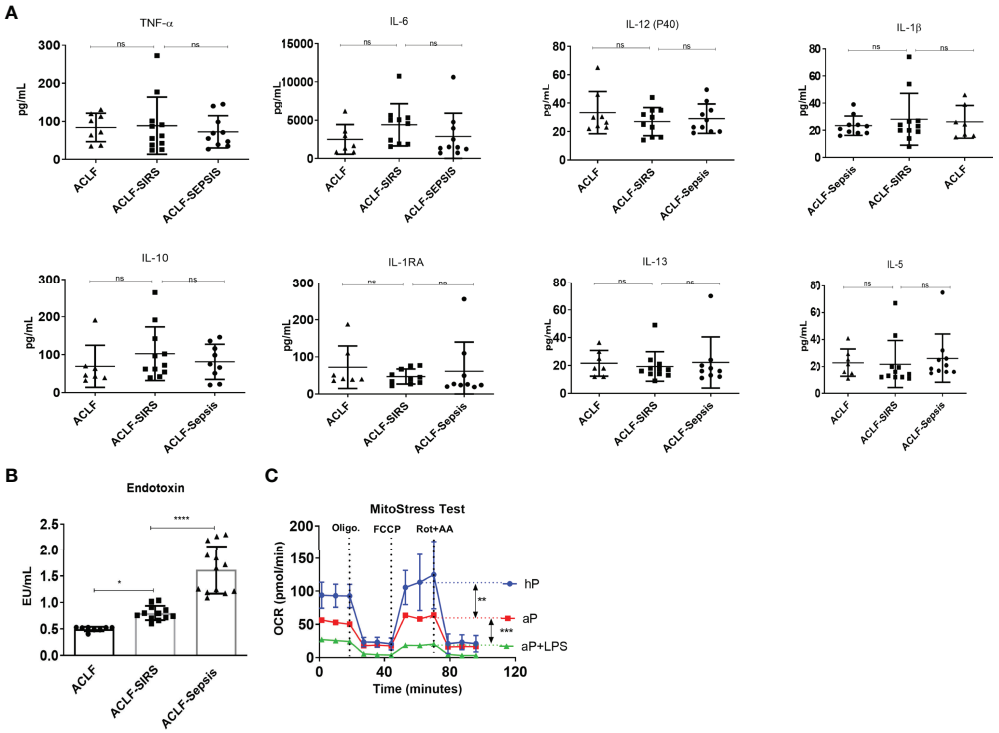

FIGURE 3 | Association of systemic inflammation and endotoxemia with monocyte mitochondrial respiration defects in patients with ACLF. **(A)** Dot plot showing changes in plasma level of pro-inflammatory and anti-inflammatory cytokines [tumor necrosis factor-alpha (TNF-α); interleukins (IL), 6, 12, 1β, 10, 1RA, 13, and 5] in the ACLF subgroups (ACLF, ACLF-SIRS, and ACLF-sepsis). **(B)** Dot plot showing changes in plasma endotoxin levels in the ACLF subgroups (ACLF, ACLF-SIRS, and ACLF-sepsis). **(C)** Real-time changes in oxygen consumption rate (OCR) with subsequent treatment with oligomycin (Oligo.) FCCP and rotenone and antimycin A (Rot. + AA.) in healthy monocytes treated with healthy plasma (hP), ACLF plasma (aP), and ACLF plasma with LPS (aP + LPS) (*$p < 0.05$; **$p < 0.01$; ***$p < 0.001$; ****$p < 0.0001$). n.s. stands for non-significant.

progression of ACLF, we followed the changes in monocyte OXPHOS till 72 h from the time of admission. Due to the limited availability of repeated blood samples, we were able to analyze kinetic changes (baseline, 24 h, and 72 h) in eight patients. Out of these eight ACLF patients, six had sepsis and two had no sepsis at the time of presentation. All patients received albumin; three patients also received plasma exchange together with albumin. With further therapeutic intervention, six (four with sepsis and two without sepsis) of eight patients showed improvement in monocyte OXPHOS, out of which one patient subsequently succumbed to COVID-19 and the remaining five recovered and were discharged. Two sepsis patients did not show any improvement in monocyte OXPHOS by 72 h and died within a week of admission (**Figure S4**).

Out of the 34 ACLF patients in which monocyte bioenergetics was done at the time of admission, 22 died or underwent transplant (non-survivors) and 12 were alive (survivors) at 28 days of follow-up. In comparison to survivors, the monocytes of non-survivors showed a significant reduction in both OXPHOS [BR–, $p < 0.001$; MR, $p < 0.001$ (**Figure 4A**)] and glycolysis [$p < 0.001$ (**Figure 4B**)]. In the univariate Cox regression analysis, both glycolysis [hazard ratio (HR) = 9.1] and OXPHOS (BR, HR = 4.9; MR, HR = 3.5) significantly correlated with short-term (28 days) mortality in ACLF patients (**Table S5**). ACLF patients with monocyte glycolysis of ≤42.7 mpH/min (AUROC = 0.901, sensitivity 86.9%, specificity 83.3%) and with OXPHOS [BR ≤ 22.5 pmol/min (AUROC = 0.81, sensitivity 75%, specificity 77.3%); MR ≤ 37.9 pmol/min (AUROC = 0.82, sensitivity 77.3%, specificity 75%)] showed a significant increase in short-term mortality (**Figure 4C**). Together, these data suggest that loss of monocyte bioenergy adversely affects the outcome of ACLF patients.

Umbilical Cord Mesenchymal Stem Cells and Monocyte Co-Culture Restore ACLF Monocyte Bioenergetics and Function

Our data showed that OXPHOS fuels monocyte phagocytosis and loss of total and functional mitochondria is associated with defective OXPHOS in ACLF monocytes. Recently, a number of studies have shown that mitochondrial transfer from MSCs improves the energy metabolism of various cells (38–40). We hypothesized that mitochondrial transfer from MSCs could restore ACLF monocyte OXPHOS and their phagocytosis. MSCs isolated from the umbilical cord showed characteristic fibroblast-like spindle-shaped morphology with >90% positive expression of MSC surface markers CD90, CD73, and CD105 and <1% expression of CD14/20/34/45 (**Figures S5A, B**). Passage 3 ucMSCs were labeled

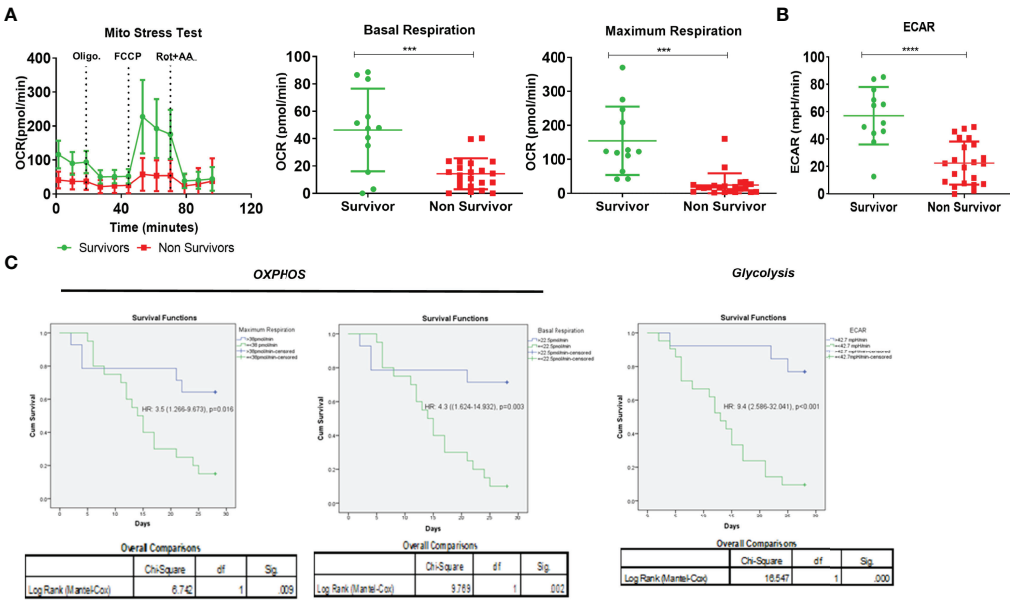

FIGURE 4 | Effect of monocyte energy metabolism on ACLF patients' outcomes. **(A)** Real-time changes in oxygen consumption rate (OCR) with subsequent treatment with oligomycin (Oligo.) FCCP and rotenone and antimycin A (Rot. + AA.) (left). Dot plot showing changes in basal mitochondrial respiration (middle) and maximum mitochondrial respiration (right) of monocytes in ACLF survivors and non-survivors. **(B)** Dot plot showing changes in glycolysis (extracellular acidification rate) of monocytes in ACLF survivors and non-survivors. **(C)** Kaplan–Meyer survivorship graph showing changes in monocyte maximal respiration, basal respiration, and glycolysis (extracellular acidification rate) in ACLF survivors vs. non-survivors (*$p < 0.05$; **$p < 0.01$; ***$p < 0.001$; ****$p < 0.0001$).

withMTR and co-cultured with ACLF monocytes. Using immunofluorescence imaging, we observed that after an overnight co-culture with ucMSCs, most of the ACLF monocytes acquire MTR^+ MSC mitochondria (**Figure 5A**). Flow cytometry analysis showed that >70% ($p < 0.01$) of $CD14^+$ ACLF monocytes were positive for MTR^+ ucMSC mitochondria (**Figure 5B**), suggesting the transfer of mitochondria from ucMSC to ACLF monocytes. Post-ucMSC co-culture, there was a significant increase in both total (MTG^+) ($p < 0.01$) and functional (MTG^+MTR^+) ($p < 0.001$) mitochondrial mass in ACLF monocytes (**Figure 5C**). Next, to evaluate whether this increase in functional mitochondrial mass can translate to an increase in ACLF monocyte energy and function, we determine the changes in monocyte OXPHOS and phagocytosis with and without ucMSCs. *In-vitro* overnight co-culture with ucMSCs significantly improved OXPHOS ($p < 0.001$; **Figure 5D**) and phagocytosis ($p < 0.0001$; **Figure 5E**) of ACLF monocytes. Together, these data showed that mitochondrial transfer from ucMSC restores ACLF monocyte OXPHOS and phagocytic function.

ucMSC Therapy Resuscitates Monocyte Bioenergetics, Decreases Hepatocyte Injury, and Potentiates Regeneration in the ACLF Animal

To check whether MSCs could restore monocyte energy and function *in vivo*, we analyzed the effect of MSC therapy on the change in monocyte phagocytosis, bioenergetics, and its impact on liver injury and regeneration in the animal model of ACLF. Firstly, we showed that human ucMSC infusion was well tolerated by healthy C57BL/6J mice, showing no changes in body weight (**Figure S6A**), AST, ALT (**Figure S6B**), and blood circulating lymphocytes (**Figure S6C**) and no histological change in the liver, kidney, and lung at 24 h or day 7 post-injection (**Figure S6D**). Next, we tested the therapeutic efficacy of ucMSC for restoring monocyte function in ACLF animals (**Figure 6A**). ucMSC-treated animals showed a significant increase in monocyte phagocytosis [24 h, $p < 0.001$; day 11, $p < 0.0001$ (**Figure 6B**)] and OXPHOS [24 h, $p < 0.001$ (**Figure 6C**)] compared with control. ucMSC-treated animals also showed a significant increase in the number of $F4/80^+$ liver macrophages (24 h, $p < 0.001$; day 11, $p < 0.001$) and their phagocytosis (day 11, $p < 0.01$) compared with control (**Figure 6D**). This suggests that ucMSCs can resuscitate monocyte bioenergetics and prevent their dysfunction in ACLF. Further analysis of liver tissue showed a significant reduction in hepatocyte ballooning at 24 h, $TUNEL^+$ hepatocyte, and fibrosis at day 11 in ucMSC-treated animals compared with control (**Figures 6E**, **S7**). They also showed a significant increase in the number of $PCNA^+$ hepatocytes both at 24 h ($p < 0.01$) and day 11 ($p < 0.001$) in comparison with control. From 24 h to day 11 while control animals showed significant ($p < 0.0001$) loss of hepatocyte proliferation, animals with ucMSC therapy showed further increase in PCNA positivity (**Figure 6F**). These combined data suggest that ucMSC therapy not only rejuvenates monocyte bioenergetics and function but also reduces liver injury and potentiates native liver regeneration in the animal model of ACLF.

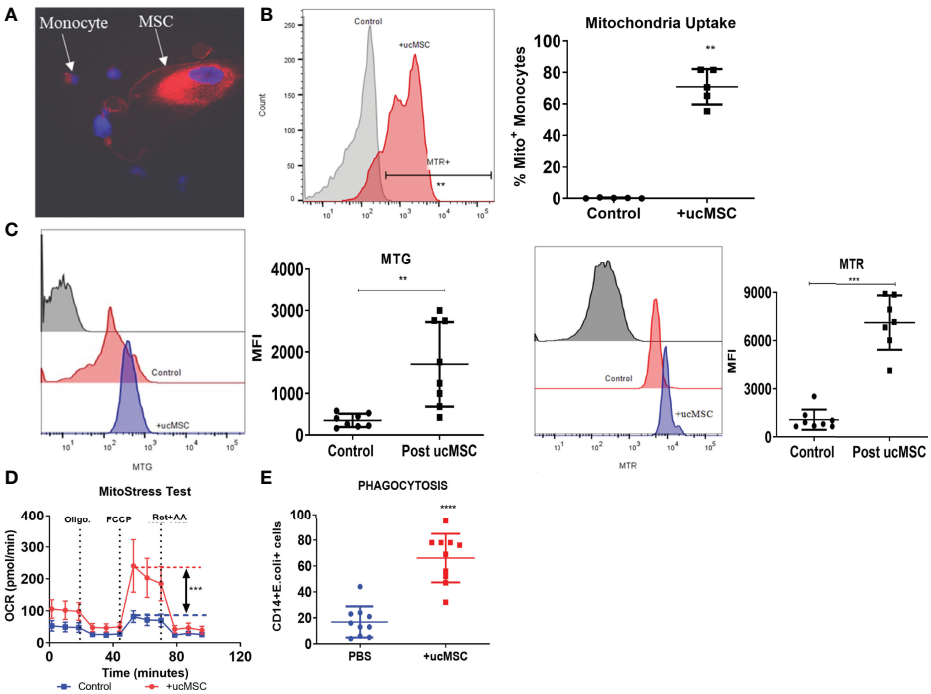

FIGURE 5 | Effect of umbilical cord mesenchymal stem cells (ucMSCs) on ACLF monocyte bioenergy and function. **(A)** Representative immunofluorescence confocal image of MSC donating its mitochondria to the ACLF monocyte (×60). **(B)** Representative histogram (left) and dot plot (right) showing mitochondrial uptake by ACLF monocytes measured through flow cytometry. **(C)** Representative histograms and dot plot showing changes in MitoTracker Green (total mitochondria) and MitoTracker Red (functional mitochondria) intensity in ACLF monocytes co-cultured with ucMSCs. **(D)** Real-time changes in oxygen consumption rate (OCR) with subsequent treatment with oligomycin (Oligo.) FCCP and rotenone and antimycin A (Rot. + AA.) in ACLF patients' monocytes co-cultured with ucMSC, compared with control. **(E)** Dot plot showing changes in phagocytic activity of ACLF monocytes co-cultured with ucMSCs compared with control (*$p < 0.05$; **$p < 0.01$; ***$p < 0.001$; ****$p < 0.0001$).

DISCUSSION

Aggravated systemic inflammatory and oxidative stresses due to uncontrolled liver injury and poor infection control are associated with regeneration failure, multi-organ dysfunction, septic shock, and death in ACLF (34, 36, 41). The underlying mechanisms of the host's innate immune failure to resolve liver injury and infection in ACLF are partially understood. Here, we demonstrate that bioenergetic failure drives the functional exhaustion of monocytes in ACLF. We further demonstrate the importance of monocyte bioenergetics in the spontaneous recovery of ACLF and show that rejuvenating monocyte bioenergetics by ucMSC improves monocyte phagocytic function, prevents liver injury, and potentiates regeneration in ACLF (**Figure 7**).

Liver macrophages together with monocytes play an important role in the host's innate immune defense (13–16). In our study, we observed that while the number of monocytes–macrophages in the liver and peripheral blood increased in ACLF, they displayed profound defects in *ex-vivo* phagocytic and oxidative burst capacity. To understand the underlying defects, we focused on the energy metabolism of monocytes and showed that while OXPHOS fuels the phagocytosis, glycolysis fuels the oxidative burst function of monocytes. In comparison to healthy monocytes, ACLF monocytes showed significant defects in glycolysis and OXPHOS with loss of total and functional mitochondria, suggesting that broad defects in monocyte energy metabolism drive the loss of monocyte phagocytic and oxidative burst function in ACLF.

During ACLF, acute insult in chronic liver injury leads to the development of SIRS and the subsequent progression of secondary organ dysfunction and/or sepsis (9). In comparison to healthy and cirrhotic monocytes, ACLF showed a marked increase in plasma levels of various inflammatory and anti-inflammatory cytokines (8, 42), which is thought to induce innate immune dysfunction in ACLF. However, in ACLF, it is unclear whether patients succumb to infection due to failure of monocytes/macrophages to effectively clear the invading pathogen leading to sepsis and organ failure or whether prolonged anti-inflammatory response renders the patient incapable to respond to secondary infections. Our data showed a significant reduction in monocyte bioenergetics and its phagocytic and oxidative burst function in cirrhosis which were further compromised in ACLF and worsened with the onset of SIRS and sepsis. In this study, we observed that while the plasma levels of pro- and anti-inflammatory cytokines were comparable, there was a significant increase in endotoxin from ACLF to ACLF-SIRS and ACLF-SIRS to ACLF-sepsis. We further demonstrated that treatment of healthy monocytes with ACLF plasma significantly reduced OXPHOS which was further dampened with LPS, suggesting the potential role of systemic inflammation and

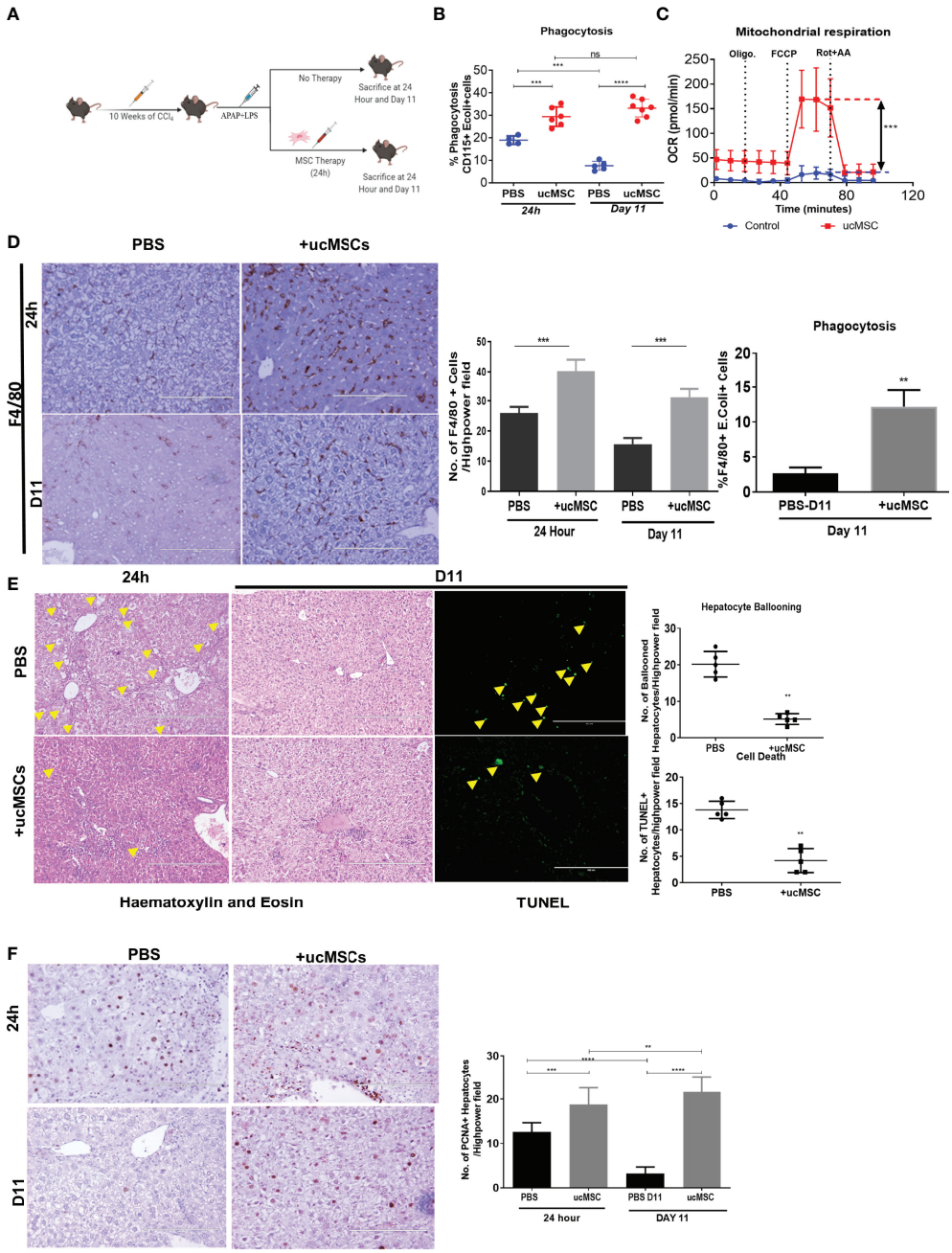

FIGURE 6 | Effect of ucMSC therapy on monocyte energy and function, liver injury, and regeneration in the animal model of ACLF. **(A)** Schematic diagram of MSC therapy in the ACLF animal model. **(B)** Dot plot showing changes in $CD115^+$ bone marrow monocyte phagocytosis at 24 h and day 11 in control and ucMSC-treated animals. **(C)** Real-time changes in oxygen consumption rate (OCR) with subsequent treatment with oligomycin (Oligo.) FCCP and rotenone and antimycin A (Rot. + AA.) in $CD115^+$ bone marrow monocytes in control and ucMSC-treated animals. **(D)** Representative images showing $F4/80^+$ liver macrophages in liver tissue sections (left) and bar graphs showing changes in the number of $F4/80^+$ cells (middle) and $F4/80^+$ liver macrophage phagocytosis (right) in control and ucMSC-treated animals at the given time points. **(E)** Representative images showing hematoxylin and eosin staining of liver tissue and $TUNEL^+$ hepatocytes (left). Dot plot showing the number of ballooned hepatocytes and $TUNEL^+$ hepatocytes (right) in control and ucMSC-treated animals at the given time points. **(F)** Representative images showing $PCNA^+$ hepatocytes in liver tissue sections (left). Bar graph showing changes in the number of $PCNA^+$ hepatocytes (right) in control and ucMSC-treated animals at the given time points (*$p < 0.05$; **$p < 0.01$; ***$p < 0.001$; ****$p < 0.0001$). n.s. stands for non-significant.

endotoxemia in bioenergetic suppression of monocytes in ACLF. Previous studies showed that increased prostaglandin E2 (PGE2) and EP2-mediated signaling in response to acute injury dampened the monocyte–macrophage function (43, 44) and drove the immunosuppression in ACLF (20). Recently, PGE2–EP2 signaling has been shown to dampen both glycolysis and OXPHOS of

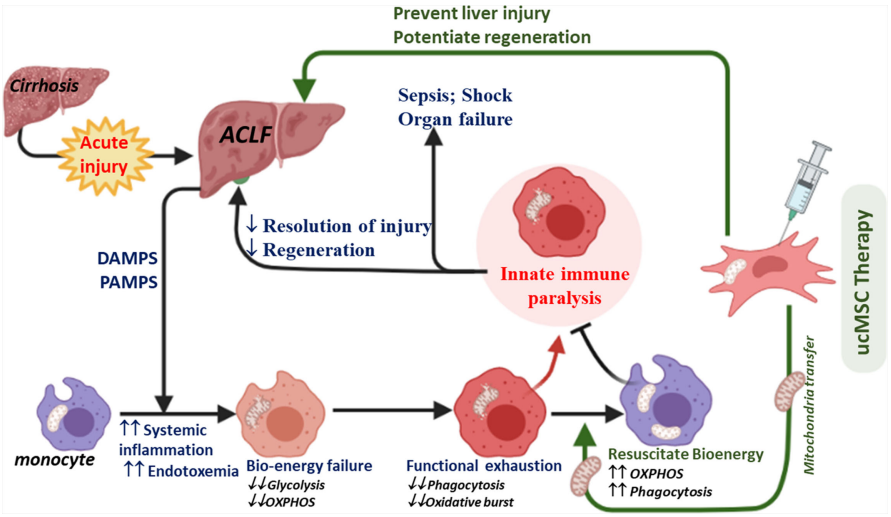

FIGURE 7 | Diagram showing the proposed mechanism of ucMSC therapy in ACLF. Increased systemic accumulation of DAMPS, PAMPS, and inflammatory mediators in response to acute liver injury in cirrhosis (a condition called ACLF) induces mitochondrial damage and bioenergy failure in monocytes. A broad defect in energy metabolism drives the exhaustion of phagocytic and oxidative burst function of monocytes in ACLF, required for the effective clearance of pathogens and cellular debris. This may account for the poor resolution of liver injury and infection, leading to regeneration failure, sepsis, shock, and death in ACLF. ucMSCs rejuvenate monocyte energy and function, prevent liver injury, and potentiate regeneration in ACLF animals.

macrophages by reducing the glucose flux and mitochondrial respiration (45). Indeed, patients with ACLF have shown an increase in glucose flux to pentose and D-glucuronate pathways (46). Similarly, LPS-induced suppression of *de-novo* NAD synthesis dampens the macrophage OXPHOS and phagocytosis in a dose-dependent manner (47), leading to immune paralysis in sepsis (33). Taken together, it is tempting to speculate that a profound increase in plasma inflammatory mediators like PGE2 in response to acute liver injury may lead to bioenergetic suppression of ACLF monocytes. This results in the maladaptive immune response against infection and a rise in systemic endotoxemia which further drives the loss of monocyte bioenergy and function during the course of ACLF. This may account for the poor resolution of injury and infection, leading to sepsis, secondary organ failure, shock, and death in ACLF. Indeed, our data showed that the loss of monocyte bioenergetics adversely affects the ACLF outcome. There was a progressive improvement in monocyte OXPHOS in patients with spontaneous recovery; however, patients who failed to improve showed early mortality. Recently, we have shown that ACLF patients that fail to improve monocyte energy and function do not respond to plasma exchange therapy even with the dampening of cytokines and endotoxin (48). This further highlights the clinical importance of monocyte energy metabolism and the need for a therapeutic strategy that can rejuvenate the monocyte energy metabolism in ACLF.

MSCs have been shown to improve the energy metabolism of various cells including monocytes–macrophages by donating their mitochondria (38–40). ACLF patients showed a significant loss of mitochondrial mass and function; hence, we investigated whether ucMSCs could resuscitate ACLF monocyte bioenergetics and phagocytosis. *In-vitro* co-culture with ucMSCs significantly improved the monocyte OXPHOS and phagocytic function. ucMSCs transferred their mitochondria and resuscitated the functional mitochondrial mass of monocytes. Further ucMSC therapy in ACLF animals showed improvement of monocyte energy and phagocytosis. Hence, ucMSCs can be used to resuscitate monocyte energy and phagocytic function in ACLF. Interestingly, similar to ACLF, patients with late-stage sepsis also show defects in mitochondrial energy metabolism in monocytes (33), and the use of MSCs has shown promising results in the practical model of sepsis (49). MSC therapy has also been shown to be safe and improves the outcome in ACLF (50, 51). Our data also showed significant reduction in liver injury and improvement of hepatocyte regeneration with ucMSC therapy. However, our data do not explain whether improvement in liver injury and regeneration in ACLF animals are due to improved monocyte energy and function or other immunomodulatory and paracrine functions of MSCs. Supplementing and resolving macrophage function in acute liver injury have recently been shown to improve the resolution of liver injury and regeneration (52), and we observed a significant increase in liver macrophage number and their phagocytic function with ucMSC therapy. Hence, improved monocyte energy and function may contribute to the observed reduction of liver injury and improvement of regeneration in ACLF animals.

In conclusion, broad defects in energy metabolism drive the exhaustion of phagocytic and oxidative burst function of ACLF monocytes. Our study provides new insight into the pathophysiology of innate immune dysfunction in ACLF along with evidence that approaches like MSC therapy can correct this problem. This also highlights the importance of bioenergetic

rejuvenating therapeutic strategies in the treatment of ACLF. It will be intriguing for future work to further fine-tune and develop this approach as a potential interventional strategy to treat and/or prevent immune dysfunction in ACLF.

DATA AVAILABILITY STATEMENT

The raw data supporting the conclusions of this article will be made available by the authors, without undue reservation.

ETHICS STATEMENT

The studies involving human participants were reviewed and approved by the Institutional Ethics Committee. The patients/participants provided their written informed consent to participate in this study. The animal study was reviewed and approved by the Institutional Animal Ethics Committee, Institute of Liver and Biliary Sciences.

AUTHOR CONTRIBUTIONS

AK and SKS contributed to the design of the studies. DM and DK performed most of the experiments, with the assistance from RJ, NN, RK, AH, and RS. GK performed the statistical analysis. CB helped in the histopathology analysis. SS recruited patients for umbilical cord samples. RM, SKS, and RK were responsible for the recruitment, diagnosis, and clinical management of ACLF patients. VP provided the explant ACLF and healthy human liver. MB provided the healthy donor blood. NT and SS helped in the FACS analysis. AK, RM, and SKS assisted with the interpretation of the findings. The manuscript was written by AK and DM with critical input from SKS and RM. All authors contributed to the article and approved the submitted version.

FUNDING

This work was supported by the Science and Engineering Research Board (SERB-DST), Government of India (Grant IR/SB/EF/02/2016), and the Department of Biotechnology, Government of India (Grant BT/PR21543/MED/31/351/2016).

SUPPLEMENTARY MATERIAL

The Supplementary Material for this article can be found online at: https://www.frontiersin.org/articles/10.3389/fimmu.2022.856587/full#supplementary-material

REFERENCES

1. Moreau R, Jalan R, Gines P, Pavesi M, Angeli P, Cordoba J, et al. Acute-on-Chronic Liver Failure is a Distinct Syndrome That Develops in Patients With Acute Decompensation of Cirrhosis. *Gastroenterology* (2013) 144(7):1426–37 37.e1-9. doi: 10.1053/j.gastro.2013.02.042
2. Sarin SK, Choudhury A, Sharma MK, Maiwall R, Al Mahtab M, Rahman S, et al. Acute-On-Chronic Liver Failure: Consensus Recommendations of the Asian Pacific Association for the Study of the Liver (APASL): An Update. *Hepatol Int* (2019) 13(4):353–90. doi: 10.1007/s12072-019-09946-3
3. Choudhury A, Jindal A, Maiwall R, Sharma MK, Sharma BC, Pamecha V, et al. Liver Failure Determines the Outcome in Patients of Acute-on-Chronic Liver Failure (ACLF): Comparison of APASL ACLF Research Consortium (AARC) and CLIF-SOFA Models. *Hepatol Int* (2017) 11(5):461–71. doi: 10.1007/s12072-017-9816-z
4. Tandon P, Garcia-Tsao G. Bacterial Infections, Sepsis, and Multiorgan Failure in Cirrhosis. *Semin Liver Dis* (2008) 28(1):26–42. doi: 10.1055/s-2008-1040319
5. Sarin SK, Choudhury A. Acute-on-Chronic Liver Failure: Terminology, Mechanisms and Management. *Nat Rev Gastroenterol Hepatol* (2016) 13 (3):131–49. doi: 10.1038/nrgastro.2015.219
6. Meersseman P, Langouche L, du Plessis J, Korf H, Mekeirele M, Laleman W, et al. The Intensive Care Unit Course and Outcome in Acute-on-Chronic Liver Failure are Comparable to Other Populations. *J Hepatol* (2018) 69 (4):803–9. doi: 10.1016/j.jhep.2018.04.025
7. Arroyo V, Moreau R, Jalan R. Acute-On-Chronic Liver Failure. *N Engl J Med* (2020) 382(22):2137–45. doi: 10.1056/NEJMra1914900
8. Shubham S, Kumar D, Rooge S, Maras JS, Maheshwari D, Nautiyal N, et al. Cellular and Functional Loss of Liver Endothelial Cells Correlates With Poor Hepatocyte Regeneration in Acute-on-Chronic Liver Failure. *Hepatol Int* (2019) 13(6):777–87. doi: 10.1007/s12072-019-09983-y
9. Choudhury A, Kumar M, Sharma BC, Maiwall R, Pamecha V, Moreau R, et al. Systemic Inflammatory Response Syndrome in Acute-on-Chronic Liver Failure: Relevance of 'Golden Window': A Prospective Study. *J Gastroenterol Hepatol* (2017) 32(12):1989–97. doi: 10.1111/jgh.13799
10. Fernandez J, Acevedo J, Wiest R, Gustot T, Amoros A, Deulofeu C, et al. Bacterial and Fungal Infections in Acute-on-Chronic Liver Failure: Prevalence, Characteristics and Impact on Prognosis. *Gut* (2018) 67 (10):1870–80. doi: 10.1136/gutjnl-2017-314240
11. Wong F, Piano S, Singh V, Bartoletti M, Maiwall R, Alessandria C, et al. Clinical Features and Evolution of Bacterial Infection-Related Acute-on-Chronic Liver Failure. *J Hepatol* (2021) 74(2):330–9. doi: 10.1016/j.jhep.2020.07.046
12. Mucke MM, Rumyantseva T, Mucke VT, Schwarzkopf K, Joshi S, Kempf VAJ, et al. Bacterial Infection-Triggered Acute-on-Chronic Liver Failure Is Associated With Increased Mortality. *Liver Int* (2018) 38(4):645–53. doi: 10.1111/liv.13568
13. Zeng Z, Surewaard BG, Wong CH, Geoghegan JA, Jenne CN, Kubes P. CRIg Functions as a Macrophage Pattern Recognition Receptor to Directly Bind and Capture Blood-Borne Gram-Positive Bacteria. *Cell Host Microbe* (2016) 20(1):99–106. doi: 10.1016/j.chom.2016.06.002
14. Broadley SP, Plaumann A, Coletti R, Lehmann C, Wanisch A, Seidlmeier A, et al. Dual-Track Clearance of Circulating Bacteria Balances Rapid Restoration of Blood Sterility With Induction of Adaptive Immunity. *Cell Host Microbe* (2016) 20(1):36–48. doi: 10.1016/j.chom.2016.05.023
15. You Q, Holt M, Yin H, Li G, Hu CJ, Ju C. Role of Hepatic Resident and Infiltrating Macrophages in Liver Repair After Acute Injury. *Biochem Pharmacol* (2013) 86(6):836–43. doi: 10.1016/j.bcp.2013.07.006
16. Triantafyllou E, Pop OT, Possamai LA, Wilhelm A, Liaskou E, Singanayagam A, et al. MerTK Expressing Hepatic Macrophages Promote the Resolution of Inflammation in Acute Liver Failure. *Gut* (2018) 67(2):333–47. doi: 10.1136/gutjnl-2016-313615
17. Shi Y, Wu W, Yang Y, Yang Q, Song G, Wu Y, et al. Decreased Tim-3 Expression is Associated With Functional Abnormalities of Monocytes in

Decompensated Cirrhosis Without Overt Bacterial Infection. *J Hepatol* (2015) 63(1):60–7. doi: 10.1016/j.jhep.2015.02.020
18. Antoniades CG, Wendon J, Vergani D. Paralysed Monocytes in Acute on Chronic Liver Disease. *J Hepatol* (2005) 42(2):163–5. doi: 10.1016/j.jhep.2004.12.005
19. Bernsmeier C, Triantafyllou E, Brenig R, Lebosse FJ, Singanayagam A, Patel VC, et al. CD14(+) CD15(-) HLA-DR(-) Myeloid-Derived Suppressor Cells Impair Antimicrobial Responses in Patients With Acute-on-Chronic Liver Failure. *Gut* (2018) 67(6):1155–67. doi: 10.1136/gutjnl-2017-314184
20. O'Brien AJ, Fullerton JN, Massey KA, Auld G, Sewell G, James S, et al. Immunosuppression in Acutely Decompensated Cirrhosis Is Mediated by Prostaglandin E2. *Nat Med* (2014) 20(5):518–23. doi: 10.1038/nm.3516
21. Bernsmeier C, Pop OT, Singanayagam A, Triantafyllou E, Patel VC, Weston CJ, et al. Patients With Acute-on-Chronic Liver Failure Have Increased Numbers of Regulatory Immune Cells Expressing the Receptor Tyrosine Kinase MERTK. *Gastroenterology* (2015) 148(3):603–15.e14. doi: 10.1053/j.gastro.2014.11.045
22. Korf H, du Plessis J, van Pelt J, De Groote S, Cassiman D, Verbeke L, et al. Inhibition of Glutamine Synthetase in Monocytes From Patients With Acute-on-Chronic Liver Failure Resuscitates Their Antibacterial and Inflammatory Capacity. *Gut* (2019) 68(10):1872–83. doi: 10.1136/gutjnl-2018-316888
23. O'Neill LA, Hardie DG. Metabolism of Inflammation Limited by AMPK and Pseudo-Starvation. *Nature* (2013) 493(7432):346–55. doi: 10.1038/nature11862
24. Zhu X, Meyers A, Long D, Ingram B, Liu T, Yoza BK, et al. Frontline Science: Monocytes Sequentially Rewire Metabolism and Bioenergetics During an Acute Inflammatory Response. *J Leukoc Biol* (2019) 105(2):215–28. doi: 10.1002/JLB.3HI0918-373R
25. Biswas SK, Mantovani A. Orchestration of Metabolism by Macrophages. *Cell Metab* (2012) 15(4):432–7. doi: 10.1016/j.cmet.2011.11.013
26. Garaude J, Acin-Perez R, Martinez-Cano S, Enamorado M, Ugolini M, Nistal-Villan E, et al. Mitochondrial Respiratory-Chain Adaptations in Macrophages Contribute to Antibacterial Host Defense. *Nat Immunol* (2016) 17(9):1037–45. doi: 10.1038/ni.3509
27. Tannahill GM, Curtis AM, Adamik J, Palsson-McDermott EM, McGettrick AF, Goel G, et al. Succinate is an Inflammatory Signal That Induces IL-1beta Through HIF-1alpha. *Nature* (2013) 496(7444):238–42. doi: 10.1038/nature11986
28. Mills EL, Kelly B, Logan A, Costa ASH, Varma M, Bryant CE, et al. Succinate Dehydrogenase Supports Metabolic Repurposing of Mitochondria to Drive Inflammatory Macrophages. *Cell* (2016) 167(2):457–70.e13. doi: 10.1016/j.cell.2016.08.064
29. Rodriguez-Prados JC, Traves PG, Cuenca J, Rico D, Aragones J, Martin-Sanz P, et al. Substrate Fate in Activated Macrophages: A Comparison Between Innate, Classic, and Alternative Activation. *J Immunol* (2010) 185(1):605–14. doi: 10.4049/jimmunol.0901698
30. Zhang S, Weinberg S, DeBerge M, Gainullina A, Schipma M, Kinchen JM, et al. Efferocytosis Fuels Requirements of Fatty Acid Oxidation and the Electron Transport Chain to Polarize Macrophages for Tissue Repair. *Cell Metab* (2019) 29(2):443–56.e5. doi: 10.1016/j.cmet.2018.12.004
31. Zhao Q, Chu Z, Zhu L, Yang T, Wang P, Liu F, et al. 2-Deoxy-D-Glucose Treatment Decreases Anti-Inflammatory M2 Macrophage Polarization in Mice With Tumor and Allergic Airway Inflammation. *Front Immunol* (2017) 8:637. doi: 10.3389/fimmu.2017.00637
32. Lachmandas E, Boutens L, Ratter JM, Hijmans A, Hooiveld GJ, Joosten LA, et al. Microbial Stimulation of Different Toll-Like Receptor Signalling Pathways Induces Diverse Metabolic Programmes in Human Monocytes. *Nat Microbiol* (2016) 2:16246. doi: 10.1038/nmicrobiol.2016.246
33. Cheng SC, Scicluna BP, Arts RJ, Gresnigt MS, Lachmandas E, Giamarellos-Bourboulis EJ, et al. Broad Defects in the Energy Metabolism of Leukocytes Underlie Immunoparalysis in Sepsis. *Nat Immunol* (2016) 17(4):406–13. doi: 10.1038/ni.3398
34. Wiest R, Lawson M, Geuking M. Pathological Bacterial Translocation in Liver Cirrhosis. *J Hepatol* (2014) 60(1):197–209. doi: 10.1016/j.jhep.2013.07.044
35. Schierwagen R, Alvarez-Silva C, Madsen MSA, Kolbe CC, Meyer C, Thomas D, et al. Circulating Microbiome in Blood of Different Circulatory Compartments. *Gut* (2019) 68(3):578–80. doi: 10.1136/gutjnl-2018-316227
36. Hackstein CP, Assmus LM, Welz M, Klein S, Schwandt T, Schultze J, et al. Gut Microbial Translocation Corrupts Myeloid Cell Function to Control Bacterial Infection During Liver Cirrhosis. *Gut* (2017) 66(3):507–18. doi: 10.1136/gutjnl-2015-311224
37. Nautiyal N, Maheshwari D, Tripathi DM, Kumar D, Kumari R, Gupta S, et al. Establishment of a Murine Model of Acute-on-Chronic Liver Failure With Multi-Organ Dysfunction. *Hepatol Int* (2021) 15(6):1389–1401. doi: 10.21203/rs.3.rs-438031/v1
38. Islam MN, Das SR, Emin MT, Wei M, Sun L, Westphalen K, et al. Mitochondrial Transfer From Bone-Marrow-Derived Stromal Cells to Pulmonary Alveoli Protects Against Acute Lung Injury. *Nat Med* (2012) 18(5):759–65. doi: 10.1038/nm.2736
39. Phinney DG, Di Giuseppe M, Njah J, Sala E, Shiva S, St Croix CM, et al. Mesenchymal Stem Cells Use Extracellular Vesicles to Outsource Mitophagy and Shuttle microRNAs. *Nat Commun* (2015) 6:8472. doi: 10.1038/ncomms9472
40. Li C, Cheung MKH, Han S, Zhang Z, Chen L, Chen J, et al. Mesenchymal Stem Cells and Their Mitochondrial Transfer: A Double-Edged Sword. *Biosci Rep* (2019) 39(5):BSR20182417. doi: 10.1042/BSR20182417
41. Xiang X, Feng D, Hwang S, Ren T, Wang X, Trojnar E, et al. Interleukin-22 Ameliorates Acute-on-Chronic Liver Failure by Reprogramming Impaired Regeneration Pathways in Mice. *J Hepatol* (2020) 72(4):736–45. doi: 10.1016/j.jhep.2019.11.013
42. Claria J, Stauber RE, Coenraad MJ, Moreau R, Jalan R, Pavesi M, et al. Systemic Inflammation in Decompensated Cirrhosis: Characterization and Role in Acute-on-Chronic Liver Failure. *Hepatology* (2016) 64(4):1249–64. doi: 10.1002/hep.28740
43. Serezani CH, Chung J, Ballinger MN, Moore BB, Aronoff DM, Peters-Golden M. Prostaglandin E2 Suppresses Bacterial Killing in Alveolar Macrophages by Inhibiting NADPH Oxidase. *Am J Respir Cell Mol Biol* (2007) 37(5):562–70. doi: 10.1165/rcmb.2007-0153OC
44. Aronoff DM, Canetti C, Peters-Golden M. Prostaglandin E2 Inhibits Alveolar Macrophage Phagocytosis Through an E-Prostanoid 2 Receptor-Mediated Increase in Intracellular Cyclic AMP. *J Immunol* (2004) 173(1):559–65. doi: 10.4049/jimmunol.173.1.559
45. Minhas PS, Latif-Hernandez A, McReynolds MR, Durairaj AS, Wang Q, Rubin A, et al. Restoring Metabolism of Myeloid Cells Reverses Cognitive Decline in Ageing. *Nature* (2021) 590(7844):122–8. doi: 10.1038/s41586-020-03160-0
46. Moreau R, Claria J, Aguilar F, Fenaille F, Lozano JJ, Junot C, et al. Blood Metabolomics Uncovers Inflammation-Associated Mitochondrial Dysfunction as a Potential Mechanism Underlying ACLF. *J Hepatol* (2020) 72(4):688–701. doi: 10.1016/j.jhep.2019.11.009
47. Minhas PS, Liu L, Moon PK, Joshi AU, Dove C, Mhatre S, et al. Macrophage *De Novo* NAD(+) Synthesis Specifies Immune Function in Aging and Inflammation. *Nat Immunol* (2019) 20(1):50–63. doi: 10.1038/s41590-018-0255-3
48. Maiwall R, Bajpai M, Choudhury AK, Kumar A, Sharma MK, Duan Z, et al. Therapeutic Plasma-Exchange Improves Systemic Inflammation and Survival in Acute-on-Chronic Liver Failure: A Propensity-Score Matched Study From AARC. *Liver Int* (2021) 41(5):1083–96. doi: 10.1111/liv.14806
49. Horak J, Nalos L, Martinkova V, Benes J, Stengl M, Matejovic M. Mesenchymal Stem Cells in Sepsis and Associated Organ Dysfunction: A Promising Future or Blind Alley? *Stem Cells Int* (2017) 2017:7304121. doi: 10.1155/2017/7304121
50. Shi M, Zhang Z, Xu R, Lin H, Fu J, Zou Z, et al. Human Mesenchymal Stem Cell Transfusion Is Safe and Improves Liver Function in Acute-on-Chronic Liver Failure Patients. *Stem Cells Transl Med* (2012) 1(10):725–31. doi: 10.5966/sctm.2012-0034
51. Li YH, Xu Y, Wu HM, Yang J, Yang LH, Yue-Meng W. Umbilical Cord-Derived Mesenchymal Stem Cell Transplantation in Hepatitis B Virus Related Acute-On-Chronic Liver Failure Treated With Plasma Exchange and Entecavir: A 24-Month Prospective Study. *Stem Cell Rev Rep* (2016) 12(6):645–53. doi: 10.1007/s12015-016-9683-3

52. Starkey Lewis P, Campana L, Aleksieva N, Cartwright JA, Mackinnon A, O'Duibhir E, et al. Alternatively Activated Macrophages Promote Resolution of Necrosis Following Acute Liver Injury. *J Hepatol* (2020) 73(2):349–60. doi: 10.1016/j.jhep.2020.02.031

Conflict of Interest: The authors declare that the research was conducted in the absence of any commercial or financial relationships that could be construed as a potential conflict of interest.

Publisher's Note: All claims expressed in this article are solely those of the authors and do not necessarily represent those of their affiliated organizations, or those of the publisher, the editors and the reviewers. Any product that may be evaluated in this article, or claim that may be made by its manufacturer, is not guaranteed or endorsed by the publisher.

frontiers | Frontiers in Immunology

ORIGINAL RESEARCH
published: 08 July 2022
doi: 10.3389/fimmu.2022.901566

Hepatocyte-Conditional Knockout of Phosphatidylethanolamine Binding Protein 4 Aggravated LPS/D-GalN-Induced Acute Liver Injury *via* the TLR4/NF-κB Pathway

Xiao-qin Qu[1†], Qiong-feng Chen[1,2†], Qiao-qing Shi[1†], Qian-qian Luo[1], Shuang-yan Zheng[3], Yan-hong Li[4], Liang-yu Bai[5], Shuai Gan[5] and Xiao-yan Zhou[1,6]*

[1] Department of Pathophysiology, Medical College of Nanchang University, Nanchang, China, [2] Department of Pathology, Medical College of Nanchang University, Nanchang, China, [3] The Center of Laboratory Animal Science, Nanchang University, Nanchang, China, [4] Department of Forensic Medicine, Medical College of Nanchang University, Nanchang, China, [5] The Second Clinical Medical College, Nanchang University, Nanchang, China, [6] Jiangxi Province Key Laboratory of Tumor Etiology and Molecular Pathology, Medical College of Nanchang University, Nanchang, China

OPEN ACCESS

Edited by:
Xiaogang Xiang,
Shanghai Jiao Tong University, China

Reviewed by:
Feng Ren,
Capital Medical University, China
Xia Gong,
Chongqing Medical University, China

***Correspondence:**
Xiao-yan Zhou
zhouxiaoyan@ncu.edu.cn

[†]These authors have contributed equally to this work

Specialty section:
This article was submitted to Inflammation, a section of the journal Frontiers in Immunology

Received: *22 March 2022*
Accepted: *13 June 2022*
Published: *08 July 2022*

Citation:
Qu X-q, Chen Q-f, Shi Q-q, Luo Q-q, Zheng S-y, Li Y-h, Bai L-y, Gan S and Zhou X-y (2022) Hepatocyte-Conditional Knockout of Phosphatidylethanolamine Binding Protein 4 Aggravated LPS/D-GalN-Induced Acute Liver Injury via the TLR4/NF-κB Pathway. Front. Immunol. 13:901566. doi: 10.3389/fimmu.2022.901566

Acute liver injury (ALI) is a disease that seriously threatens human health and life, and a dysregulated inflammation response is one of the main mechanisms of ALI induced by various factors. Phosphatidylethanolamine binding protein 4 (PEBP4) is a secreted protein with multiple biological functions. At present, studies on PEBP4 exist mainly in the field of tumors and rarely in inflammation. This study aimed to explore the potential roles and mechanisms of PEBP4 on lipopolysaccharide (LPS)/D-galactosamine (D-GalN)-induced ALI. PEBP4 was downregulated after treatment with LPS/D-GalN in wild-type mice. PEBP4 hepatocyte-conditional knockout (CKO) aggravated liver damage and repressed liver functions, including hepatocellular edema, red blood cell infiltration, and increased aspartate aminotransferase (AST)/alanine aminotrans-ferase (ALT) activities. The inflammatory response was promoted through increased neutrophil infiltration, myeloperoxidase (MPO) activities, and cytokine secretions (interleukin-1β, IL-1β; tumor necrosis factor alpha, TNF-α; and cyclooxygenase-2, COX-2) in PEBP4 CKO mice. PEBP4 CKO also induced an apoptotic effect, including increasing the degree of apoptotic hepatocytes, the expressions and activities of caspases, and pro-apoptotic factor Bax while decreasing anti-apoptotic factor Bcl-2. Furthermore, the data demonstrated the levels of Toll-like receptor 4 (TLR4), phosphorylation-inhibitor of nuclear factor kappaB Alpha (p-IκB-α), and nuclear factor kappaB (NF-κB) p65 were upregulated, while the expressions of cytoplasmic IκB-α and NF-κB p65 were downregulated after PEBP4 CKO. More importantly, both the NF-κB inhibitor (Ammonium pyrrolidinedithiocarbamate, PDTC) and a small-molecule inhibitor of TLR4 (TAK-242) could inhibit TLR4/NF-κB signaling activation and reverse the effects of PEBP4

CKO. In summary, the data suggested that hepatocyte-conditional knockout of PEBP4 aggravated LPS/D-GalN-induced ALI, and the effect is partly mediated by activation of the TLR4/NF-κB signaling pathway.

Keywords: PEBP4, acute liver injury, TLR4, NF-κB, inflammation, apoptosis

INTRODUCTION

Acute liver injury (ALI) is a disease characterized by the destruction of liver defense function and the induction of uncontrolled inflammation (1). Following severe or persistent liver injury will ultimately provoke acute liver failure (ALF). Once ALI or ALF occurs, the affected individual's life and health become seriously threatened (2, 3). So far, no specific drugs for ALI or ALF exist for use as clinical treatments. Therefore, it is vital to explore specific intervention targets and design more effective therapeutic drugs.

Inflammation and apoptosis are the main pathological manifestations of ALI (4, 5). The injection of LPS/D-GalN can induce the most classic and common model of ALI (6–8). The TLR4/NF-κB signaling pathway plays the most important role in the inflammatory response (9–11). TLR4, a member of the Toll-like protein family, could bind to LPS on the cell membrane, then activate NF-κB (12). The activation of NF-κB promotes the expression of pro-inflammatory cytokines and further aggravates the inflammatory process (13). Moreover, NF-κB can also regulate apoptosis-related hydrolytic protein caspases along with apoptosis-related genes, such as Bax and Bcl-2 (14, 15). Uncontrollable inflammatory and apoptotic responses ultimately lead to liver injury (16, 17).

PEBP4, a member of the PEBP family, is a secreted protein widely expressed in multiple organs of the human body (18). At present, studies on PEBP4 have mostly focused on cancers (19–23). In addition, members of the PEBP family, such as Raf kinase inhibitor protein (RKIP) and PEBP1, can regulate microglia inflammation by inhibiting the NF-κB signaling pathway (24, 25), and RKIP is known to be closely associated with ALF (26). Furthermore, PEBP4 can also regulate the apoptotic process (27, 28). Based on these prior studies, we speculated about PEBP4 may exacerbate liver injury by facilitating the inflammation release and apoptosis, and the effect was achieved through TLR4/NF-κB signaling pathway. To explore the effects and mechanism of PEBP4 in ALI hepatocyte-conditional knockout of PEBP4 mice were established, and the mouse model of ALI was built *via* the administration of D-GalN combined with LPS. Our research is the first to focus PEBP4 on the field of inflammatory diseases, which will provide a new experimental basis for clinical treatment.

MATERIALS AND METHODS

Reagents

LPS (Escherichia coli, O55: B5), D-GalN and PDTC were obtained from Sigma-Aldrich (St. Louis, MO, USA). TAK-242 was acquired from Abmole Bioscience Inc (Houston, TX, USA). Kits for the detection of AST, ALT and MPO detection kits were purchased from Nanjing Jiancheng Bioengineering Institute (Nanjing, China). Enzyme-linked immunosorbent assay (ELISA) kits for IL-1β and TNF-α were provided by Invitrogen (Carlsbad, CA, USA). Trizol reagents, EasyScript One-Step gDNA Removal, and cDNA Synthesis Super Mix, and PerfectStart Green qPCR Super Mix were produced by TransGen Biotech (Beijing, China). Kits for the detection of caspase-3 and -9 activity came from Abcam (Cambridge, England). A caspase-8 activity detection kit was sourced from BioVision (San Francisco, CA, USA). A transferase-mediated dUTP-biotin nick end labeling assay (TUNEL) kit was acquired from Servicebio Biotech (Wuhan, China). PEBP4 antibody was obtained from RayBiotech (Atlanta, USA). The antibodies of IκB-α and p-IκB-α were produced by Cell Signaling Technology (Boston, MA, USA). Finally, the antibodies of NF-κB p65; caspases-3, -8, and -9; lamin B1; ATP1A1; and GAPDH were provided by Proteintech (Chicago, IL, USA).

Animals and ALI Model

C57BL/6N WT mice were purchased from Jiangsu Jicui Yaokang Biotechnology Co., Ltd (Jiangsu, China). $PEBP4^{flox/+}$ mice, and Alb-Cre^{+} mice were supplied by Saiye Biotechnology Co., Ltd (Jiangsu, China) (The loxP sequences with the *PEBP4* gene were introduced by CRISPR/Cas9 technology to allow for the conditional deletion of exon 3, which would result in a null allele upon Cre recombinase-mediated excision. Mutant PEBP4-floxed offspring were generated on a C57BL/6N background and identified by genotyping. All mice were maintained under 25°C and 12h day/night rhythm with sufficient food and sterile water, and the research was approved by the Animal Protection Committee of Jiangxi Medical College of Nanchang University.

After one week of adaptive feeding, $PEBP4^{flox/flox}$ mice were obtained from the offspring of male and female mice with the $PEBP4^{flox/+}$ gene, and Alb-Cre^{+} mice were intercrossed with $PEBP4^{flox/flox}$ mice to obtain $PEBP4^{flox/+;Alb\text{-}Cre+}$ mice. The $PEBP4^{flox/flox;Alb\text{-}Cre+}$ (PEBP4 CKO) mice were generated by breeding male and female $PEBP4^{flox/+;Alb\text{-}Cre+}$ mice together. Finally, PEBP4 CKO mice were used in this experiment. The genotype was identified by polymerase chain reaction (PCR). Sequences of forward and reverse primers are list in the **Table 1**. When enough WT and PEBP4 CKO mice were obtained, each type of mouse was randomly divided into the following four groups(n=12 per group): (1) a control group, which received an intraperitoneal injection with normal saline, (2) an LPS/D-GalN group, which received an intraperitoneal injection with 5 μg/kg of LPS and 300 mg/kg of D-GalN, (3) an LPS/D-GalN+PDTC (NF-κB inhibitor) group, which received 60 mg/kg of PDTC by

TABLE 1 | Sequence used for PCR.

No	Primer name	Primer sequence (5'-3')	Band size
1	loxp F	GATCCTGGAGCTACTGAAAGCACTGAG	Flox=251 bp
	loxp R	GCTATTTACACCACCATGCCCTGC	WT=188 bp
2	Alb-Cre F	GAAGCAGAAGCTTAGGAAGATGG	Alb-Cre=390 bp
	Alb-Cre R	TTGGCCCCTTACCATAACTG	
3	PEBP4 dellele F	GATCCTGGAGCTACTGAAAGCACTGAG	PEBP4 KO=277 bp
	PEBP4 dellele R	ACAACCAGAAGGATGAAATCGGAAAC	

intraperitoneal injection 30 min prior to receiving 5 μg/kg of LPS and 300 mg/kg of D-GalN; and (4) an LPS/D-GalN+TAK-242 (TLR4 inhibitor) group, which received 3 mg/kg of TAK-242 by intraperitoneal injection 30 min prior to receiving 5 μg/kg of LPS and 300 mg/kg of D-GalN. Half of the mice in each group were sacrificed at 6 h, and their blood and liver tissues were collected (10); the other half were sacrificed at 1.5 h, and their serum was harvested for TNF-α detection.

Hematoxylin and Eosin (H&E) Staining

H&E staining was performed according to Yan at el. (7). In a word, liver tissue blocks (approximately 0.5 × 0.5 cm size) were selected at the same position on the right lobe, then steeped in 4% paraformaldehyde for fixation for 24 h. The 4-6μm tissue sections were stained with H&E using a common protocol. To evaluate the degree of acute liver injury, each sample was independently observed by 3 pathologists under a light microscope (Olympus Corporation, Tokyo, Japan) and made an injury score according to hepatocellular edema, red blood cell infiltration, neutrophil infiltration, and liver structural disorders.

Western Blotting

Western blot was performed according to the standard protocol. Briefly, the total protein, membrane protein, and nuclear protein from tissues were extracted according to the protein extraction kit instructions, then the protein concentrations were detected with a BCA kit (Solarbio, China). Protein extracts (40μg) were fractionated on 12% polyacrylamide-sodium dodecyl sulfate gel, then transferred to nitrocellulose membranes. Non-specific binding to the membrane was blocked by incubation in 5% (w/v) fat-free milk in TBST buffer, followed by incubation with a rabbit or mouse primary polyclonal antibody (1:1000, except for PEBP4 at 1:750) at 4°C overnight. The next day, the membranes were treated with horseradish peroxidase-conjugated goat anti-rabbit or goat anti-mouse secondary antibody (1:5000). Finally, the protein expressions were observed in a gel imaging system (BioRad Laboratories, Hercules, CA, USA) and performed quantitative analysis using the ImageJ software (U.S. National Institutes of Health, Bethesda, MD, USA).

Real-Time Quantitative PCR Analysis

Total RNA was extracted from liver tissue using Trizol reagents according to the manufacturer's instructions. The expressions of gene messenger RNA were measured by real-time PCR using the PerfectStart Green qPCR Master Mix. The gene expressions were calculated by using the comparative $2^{-\Delta\Delta CT}$ method and GAPDH as a reference gene. The primer sequences of GAPDH (as the reference gene) and candidate genes were listed in **Table 2**.

ALT/AST Measurement

After the mice were sacrificed, the blood was placed on ice for 1 h, and then the supernatant was acquired by a cryogenic ultracentrifuge run at 3,000 rpm, 4°C for 10 min. The supernatant was used to detect the activity of ALT and AST according to the manufacturer's recommendations.

MPO Activity Measurement

100 mg of liver tissues were accurately weighed out, added a homogenate medium at a weight-to-volume ratio of 1:19, and obtained 5% tissue homogenate. MPO activities were measured by following the instructions of the activity detection kits.

ELISA

According to the manufacturer's instructions, standards were serially diluted at 1:1 dilution and the serum was diluted 10-fold by the sample diluent; then 100 μL of various concentrations of standards (0-2000 pg/mL) and serum were pipetted into the 96-well ELISA plate in duplicate. The plates were incubated at room temperature (18°C-25°C) for 2 h with 50 μL of biotin-conjugate. After that, the microwell strips were washed 6 times with approximately 400 μL of wash buffer per well, then added 100 μL of diluted streptavidin-horseradish peroxidase for 1 h at room temperature. Then, the plates were washed again and treated them with 100 μL of TMB substrate solution for 30 min without intense light. The enzymatic reaction was terminated with 100 μL of stop solution, and the absorbance at 450 nm was recorded with a microplate reader (Molecular Devices, American).

TUNEL

TUNEL was performed using an apoptosis detection kit according to the manufacturer's instruction. First, the paraffin sections were placed in xylene and gradient alcohol for dehydration, and washed in distilled water. Secondly, proteinase K repair solution was dropped for antigen retrieval and then 0.1% Triton for permeabilization. Subsequently, reaction solution (TDT enzyme:dUTP:buffer, 1:5:50) was added and incubated sections for 2h at 37°C. Finally, nuclei ware stained with DAPI and coverslip covered sections with anti-fade mounting medium. All images were acquired using a fluorescence microscope (Olympus, Japan).

TABLE 2 | The primers sequence used for real-time quantitative PCR.

Name	Primer
GAPDH	F:5'-AGGTCGGTGTGAACGGATTTG-3'
	R:5'-TGTAGACCATGTAGTTGAGGTCA-3'
Bcl-2	F:5'-CCGGGAGAACAGGGTATGATAA-3'
	R:5'-CCCACTCGTAGCCCCTCTG-3'
Bax	F:5'-AGGATGCGTCCACCAAGAAGCT-3'
	R:5'-TCCGTGTCCACGTCAGCAATCA-3'

Measurement of Caspase-3, -8, and -9 Activities

In according with the kit instructions, the kits were taken out of the refrigerator at -20°C and slowly melted. At the same time, the liver tissues were taken out of the refrigerator at -80°C, 400 μL of pre-cooled cell lysate was added and repeatedly ground, and then placed in a 4°C centrifuge at 10,000 g for 1 min. Subsequently, the supernatant was acquired, and the protein concentrations was immediately detected. Next, 50 μL (50-200 μg) sample or 2× reaction buffers was added to the well, respectively, and 50 μL of reaction mix and 5 μL of DEVD-p-NA substrate were added successively. The mixture was shook horizontally and then placed in a constant-temperature water bath at 37°C for 2 h. Finally, the OD value of each well was detected with a microplate reader (Molecular Devices, American) at a wavelength of 405 nm.

Statistical Analysis

All data were expressed as mean ± standard deviation (SD) values. GraphPad Prism version 8.0 (GraphPad Software, San Diego, CA, USA) was used for mapping, and the results were statistically analyzed by one-way analysis of variance using SPSS version 26.0 (IBM Corporation, Armonk, NY, USA). $P < 0.05$ indicated that the difference was statistically significant.

RESULTS

Constructed and Identified the PEBP4 Hepatocyte-Conditional Knockout (CKO) Mice

To explore the relationship of PEBP4 with ALI, LPS/D-GalN was used to establish an ALI model among WT mice, and then the protein expressions of PEBP4 were detected by western blotting. The results showed PEBP4 was decreased in ALI ($P < 0.01$, **Figure 1A**). Based on the results of **Figure 1A**, we designed PEBP4 CKO mice to explore the role of PEBP4 in ALI. In this study, we used CRISPR/Cas9 technology to construct *PEBP4*$^{flox/+}$ mice, which were maintained with a C57BL/6N background, and

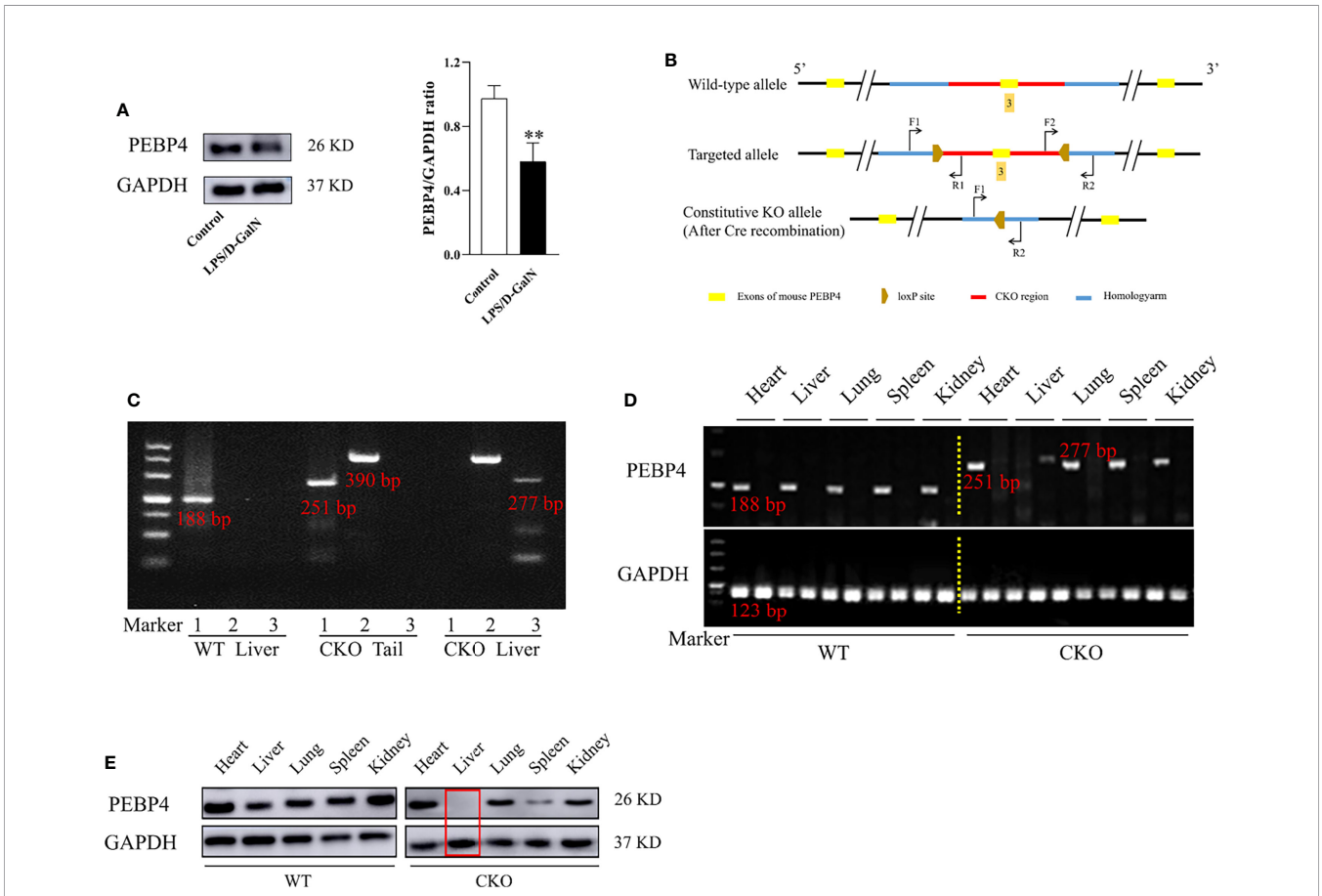

FIGURE 1 | PEBP4 hepatocyte-conditional knockout (CKO) mice were constructed and identified. **(A)**: Western blotting was used to detect the expression of PEBP4. **(B)**: The undisturbed *PEBP4* gene in WT mice (top panel), schematic of loxP sites introduced into exon 3 of the PEBP4 locus for the generation of *PEBP4*$^{flox/flox}$ mice (middle panel), and schematic for the generation of PEBP4CKO mice (bottom panel). **(C)**: The LoxP sites flanking the PEBP4 gene, the Cre transgene and PEBP4 allele were detected by PCR analysis of tail DNA and liver DNA. **(D)**: Agarose gel electrophoresis was employed to examine the gene expression of PEBP4 in the heart, liver, lungs, spleen, and kidneys of WT and CKO mice. **(E)**: PEBP4 protein expression was tested by western blotting in the heart, liver, lungs, spleen, and kidneys of WT and CKO mice. Data are presented as mean ± SD values (n = 3). $^{**}P < 0.01$ compared to WT mice in the control group.

then bred *PEBP4*$^{flox/flox}$ mice with Alb-Cre mice to obtain PEBP4 CKO mice (**Figure 1B**). Agarose gel electrophoresis and western blotting during the experiment both suggested that the PEBP4 CKO mice were successfully created (**Figures 1C–E**).

PEBP4 CKO Could Aggravate LPS/D-GalN-Induced ALI

According to **Figure 1**, PEBP4 CKO mice were successfully acquired. The liver tissue sections and the results of biochemical kits suggested that there were no significant changes in liver tissue and functions after PEBP4 CKO ($^{NS}P > 0.05$, **Figures 2A, B**). To explore the potential influence of PEBP4 on ALI, the model was induced by injections of LPS/D-GalN in WT mice and PEBP4 CKO mice. Histological changes were detected by H&E staining, and the results showed that, compared with WT mice, LPS/D-GalN aggravated hepatocellular edema, red blood cell infiltration, neutrophil infiltration, and liver structural disorders in the PEBP4 CKO mice (**Figure 2A**). ALT/AST activities were also tested, and data were consistent with the changes in liver pathological damage (**Figure 2B**). Inflammation and apoptosis are two of the most important features in LPS/D-GalN-induced ALI. To assess the degree of the inflammatory response, the levels of MPO, IL-1β, TNF-α, and cyclooxygenase-2 (COX-2) were examined. The results demonstrated the activities of MPO and the expressions of IL-1β, TNF-α, and COX-2 were improved in the LPS/D-GalN groups, although the changes were more obvious in the PEBP4 CKO mice (**Figures 2C–F**). Subsequently, the degree of apoptotic response was evaluated through TUNEL; the expressions and activities of cleaved caspase-3, -8, and -9; and the apoptotic regulatory proteins (Bax and Bcl-2). The results suggested that LPS/D-GalN could induce hepatocyte apoptosis, and a more severe apoptosis response could be observed in PEBP4 CKO mice too (**Figures 2G–I**). Meanwhile, real-time PCR indicated that the expression of Bax was higher and that of Bcl-2 was lower in the PEBP4 CKO mice (**Figure 2J**).

PEBP4 CKO Activated the TLR4/NF-κB Signaling Pathway

The TLR4/NF-κB signaling pathway is one of the important signaling pathways in the regulation of inflammation. In this study, the protein expressions of TLR4, p-IκB-α, and NF-κB p65 were examined. As shown in **Figure 3**, compared to WT mice, LPS/D-GalN could more significantly increase TLR4, p-IκB-α, and nuclear protein NF-κB p65 expressions ($P < 0.01$), and the cytoplasmic protein of IκB-α and NF-κB p65 expression were decreased more obviously in CKO mice ($P < 0.01$). These data indicated that PEBP4 CKO might activate the TLR4/NF-κB signaling pathway.

TLR4/NF-κB Signaling Pathway Inhibitor Could Partially Reverse the Effects of PEBP4 CKO on LPS/D-GalN-Induced ALI

To further clarify the effects and mechanisms of PEBP4, PDTC and TAK-242 were utilized, and the results showed that both could partially reverse the effects of PEBP4 CKO on ALI, including liver pathological changes (**Figure 4A**); the activities of ALT/AST and MPO (**Figures 4B, C**); the expression levels of inflammatory factors (**Figures 4D, E**); hepatocyte apoptosis (**Figure 4F**); and the expressions and activities of caspases-3, -8, and -9 (**Figures 4G, H**). To provide further evidence regarding the regulatory effect on TLR4/NF-κB signaling, the levels of TLR4, IκB-α, p-IκB-α, and NF-κB p65 were also examined after treatment with PDTC and TAK-242, and the results proved that the phosphorylation and degradation of levels of IκB-α and the nuclear translocation of NF-κB were decreased in the PDTC and TAK-242 intervention groups (**Figure 4I**).

DISCUSSION

The combined administration of LPS and D-GalN to induce ALI has been widely considered as a model given the pathological changes are similar to endotoxin-induced ALI in humans, and this approach could be utilized to explore the exact pathogenesis of ALI (6, 29). In this study, we first established the model in WT mice and found that PEBP4 expression was significantly inhibited in ALI. The results suggested PEBP4 may be a possible intervention target for ALI. PEBP4 is a secreted protein with a variety of biological functions. Available studies on PEBP4 have mainly focused on cancers, and PEBP4 is highly expressed in cancer tissues (19–23), but the effects of PEBP4 expression on tissue damage have not been reported, which attracted our attention. To investigate the effects of PEBP4 on ALI and the potential mechanisms, PEBP4 CKO mice were established and liver damage was observed after LPS/D-GalN treatment. The results of pathological changes showed that the LPS/D-GalN group of PEBP4 CKO mice had more red blood cell infiltration in liver tissues and more serious hepatocellular edema than that in WT mice. In addition, the activities of ALT and AST were higher in PEBP4 CKO mice. These results indicated that PEBP4 CKO aggravated liver damage and reduced liver function.

The inflammatory response is the major contributing factor in the development of LPS/D-GalN-induced ALI. Various pro-inflammatory cytokines, such as TNF-α and IL-1β, are secreted, and then neutrophil activation and infiltration are elicited by TNF-α, which has been considered an important hinge in the progress of LPS/D-GalN-induced ALI (30–33). The results in this research coincided with this point. In this study, the activity of MPO, which reflected the degree of neutrophil infiltration, and the expressions of inflammatory factors (IL-1β, TNF-α, and COX-2) were all increased in PEBP4 CKO mice. Some studies have reported that PEBP family member PEBP1 and RIPK have anti-inflammatory roles, but little is known about the impact of PEBP4 in inflammation (24, 25). In this experiment, the data demonstrated that, after hepatocyte-conditional knockout of PEBP4, all the inflammatory indicators (pathological changes,

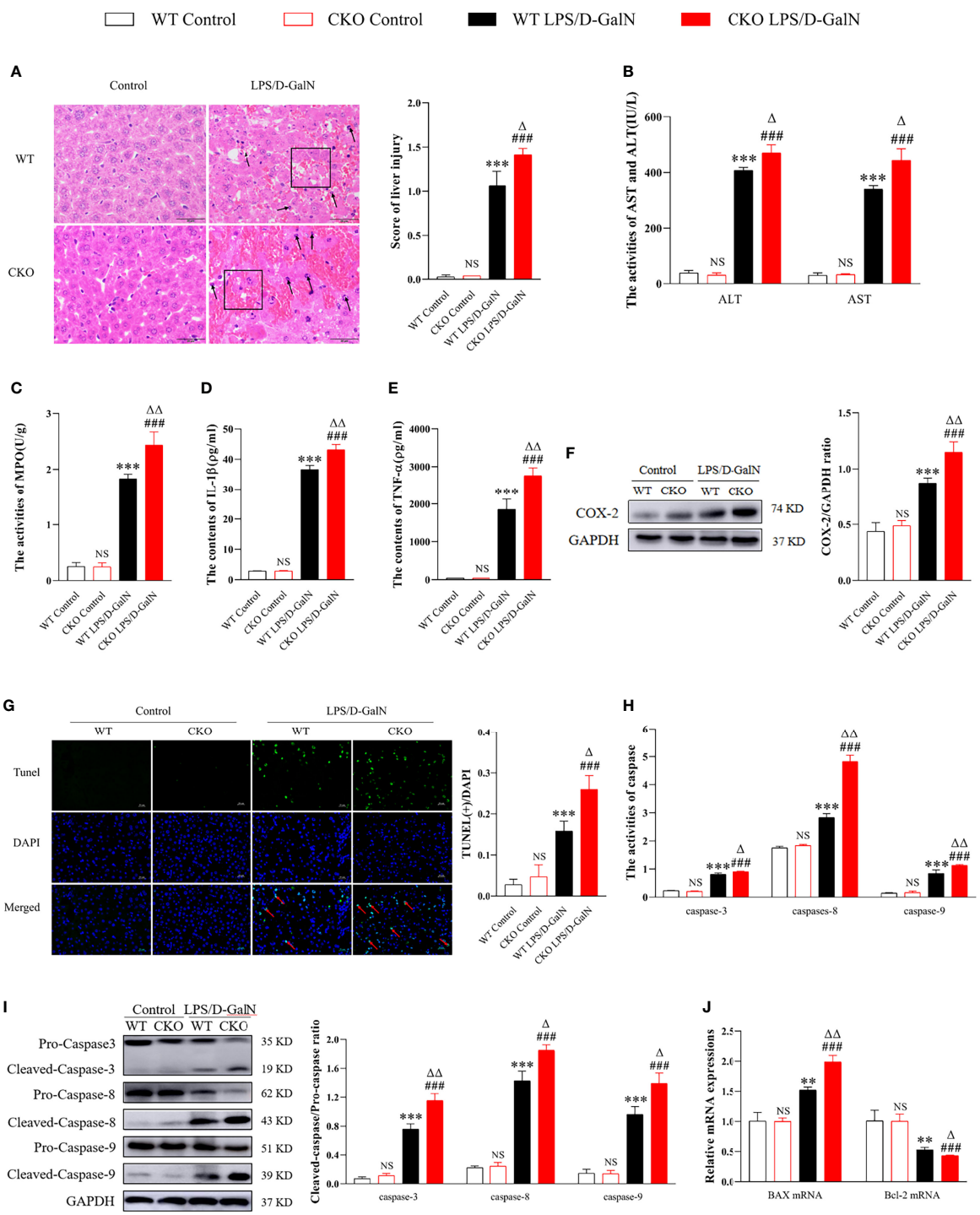

FIGURE 2 | PEBP4 CKO could aggravate LPS/D-GalN–induced ALI. **(A)**: Histological changes of liver tissue (H&E staining, ×400) and the injury scores of HE were quantifies, ↑ for inflammatory cell infiltration, □ for hepatocyte degeneration and red blood cell infiltration. **(B)**: We detected the activities of AST and ALT in serum (n = 6). **(C)**: MPO activities were tested in liver tissue (n = 6). **(D, E)**: The levels of IL-1β and TNF-α in serum were detected by ELISA (n = 6); **(F)**: Western blot was used to examine the expression of COX-2 (n = 3). **(G)**: The apoptotic level of hepatocytes was detected with a TUNEL fluorescence detection kit (the DAPI-stained nuclei were blue and apoptotic nuclei were green, ×400) and positive cells of TUNEL were quantified, ↑ for TUNEL (+) cells. **(H, I)**. The activities and protein expression of caspase-3, -8, and -9 were detected by the activity test kit (n = 6) and western blotting (n = 3), respectively; **(J)**. The mRNA expression levels of Bax and Bcl-2 were detected by real-time PCR. Data are presented as mean ± SD values. $^{NS}P > 0.05$, $^{**}P < 0.01$, and $^{***}P < 0.001$ compared to the WT control group; $^{###}P < 0.001$ compared to the CKO control group; and $^{\Delta}P < 0.05$ and $^{\Delta\Delta}P < 0.01$ compared to the WT LPS/D-GalN group.

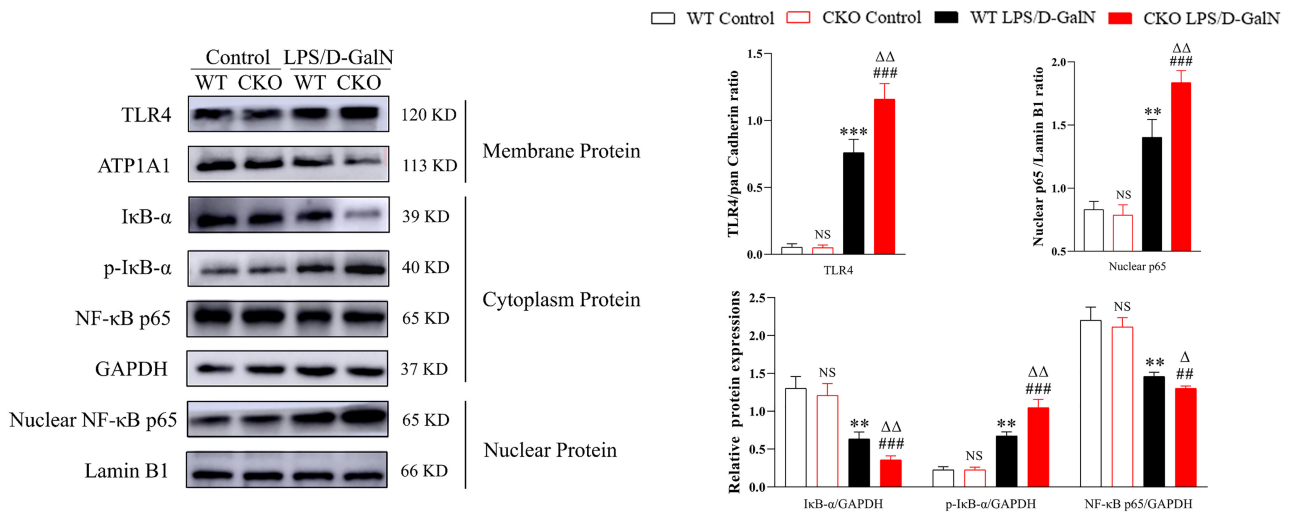

FIGURE 3 | PEBP4 CKO could activate the TLR4/NF-κB signaling pathway. Western blotting was employed to examine the expressions of TLR4, IκB-α, p-IκB-α, nuclear protein NF-κB p65, and cytoplasmic protein NF-κB p65. Data are presented as mean ± SD values (n = 3). $^{NS}P > 0.05$, $^{**}P < 0.01$, and $^{***}P < 0.001$ compared to the WT control group; $^{\#\#\#}P < 0.001$ compared to the CKO control group; and $^{\Delta}P < 0.05$ and $^{\Delta\Delta}P < 0.01$ compared to the WT LPS/D-GalN group.

MPO activity, IL-1β, TNF-α, and COX-2) were more significantly serious in CKO mice, suggesting PEBP4 CKO could promote inflammation and PEBP4 may be a target to control ALI. On the other hand, hepatocyte apoptosis is a common phenomenon in LPS/D-GalN-induced ALI models, and it is also the cause of liver function decrease and even death. Therefore, controlling apoptosis is also a key target for mitigating liver damage (34, 35). TNF-α initiated the death receptor-dependent apoptosis pathway through its receptors, leading to the activation of the caspase cascade (36–38). The results in this research indicated that PEBP4 CKO increased TNF-α secretion. In addition, it has been reported that PEBP4 could enhance cell resistance to TNF-α-induced apoptosis (39). So, we also speculate that PEBP4 is involved in the regulation of apoptosis in LPS/D-GalN-induced ALI in this investigation. TUNEL staining and the activities and expressions of apoptosis-related factors were examined in this study. The data suggested the number of TUNEL (+) cells in hepatic tissues; the expression levels of cleaved caspase-3, -8, and -9; and the activities of caspase-3, -8, and -9 were increased in PEBP4 CKO mice after treatment with LPS/D-GalN. Meanwhile, the expression of pro-apoptotic Bax was upregulated, while that of anti-apoptotic factor Bcl-2 was downregulated. This suggested that PEBP4 CKO could facilitate LPS/D-GalN-induced hepatocyte apoptosis and PEBP4 may be a target to resist ALI also.

A large number of studies have shown that the TLR4/NF-κB signaling pathway plays an important role in the development of ALI induced by LPS/D-GalN (10, 40, 41). TLR4 is a transmembrane receptor existing in Kupffer cells whose natural ligand is LPS. When TLR4 combines with LPS, the innate immune and inflammatory responses of liver tissue are initiated (42–44). NF-κB, an important transcription factor, could be activated by TLR4, and then NF-κB p65 is transferred from the cytoplasm to the nucleus to regulate the expression of inflammatory cytokines, such as IL-1β, IL-6, TNF-α, caspases, Bax, and Bcl-2 (14, 15, 45, 46). In this study, TLR4/NF-κB signaling pathway-related proteins were detected, and it was found that TLR4 and nuclear NF-κB p65 protein expression increased and IκB-α and cytoplasm NF-κB p65 expression decreased in PEBP4 CKO mice, suggesting that PEBP4 deficiency may activate the TLR4/NF-κB signaling pathway. To further clarify the effects and mechanisms of PEBP4, PDTC and TAK-242 were used. Subsequently, the data hinted that phosphorylation and degradation of IκB were inhibited and the level of NF-κB translocation into the nucleus was reduced. More importantly, the activities of MPO and ALT/AST decreased, the secretion levels of TNF-α and IL-1β reduced, the number of TUNEL (+) cells fell, and the level of cleaved caspase-3 dropped in the two inhibitor groups. All these data suggest that both inhibitors could partially reverse PEBP4 CKO induced activation of the TLR4/NF-κB signaling pathway and then restrain inflammation and apoptosis.

In this study, we found that PEBP4 expression was decreased in ALI and PEBP4 CKO aggravated ALI, contrasting with the increased expressions of PEBP4 in tumor tissues and PEBP4's promotion of tumor development. The different effects may be mainly related to the expression levels. PEBP4 could have a protective effect at a low or normal expression level. However, once PEBP4 was overexpressed, it would adopt different or even completely opposite biological effects, and the specific mechanisms, including the interaction between PEBP4 and TLR4, need to be further investigated and explored.

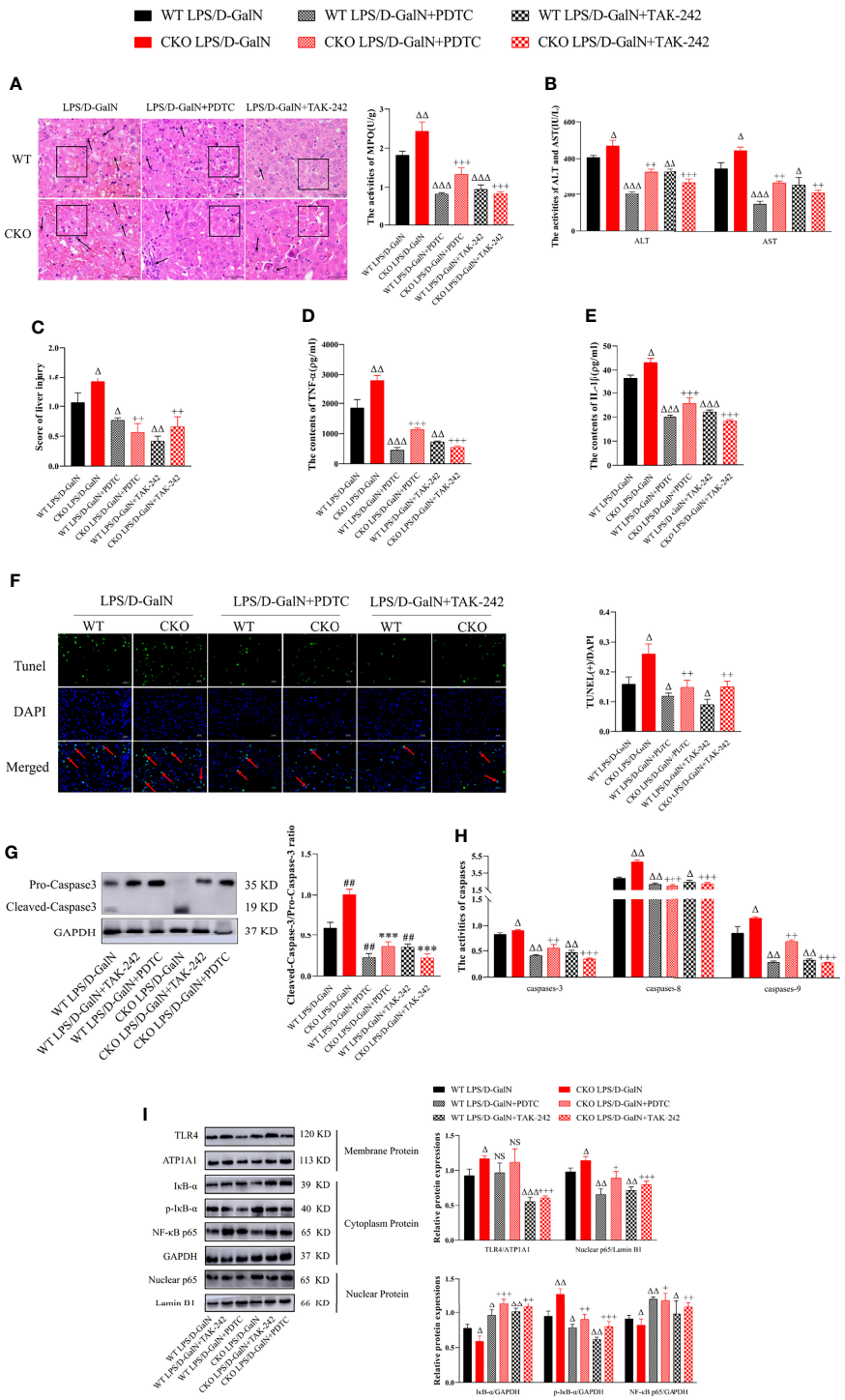

FIGURE 4 | PDTC and TAK-242 could partially counteract TLR4/NF-κB signaling activation induced by PEBP4 CKO in ALI. **(A)**: Histological changes of liver tissue (H&E staining, ×400) and the injury scores of HE was quantifies, ↑ for inflammatory cell infiltration, □ for hepatocyte degeneration and red blood cell infiltration. **(B)**: Serum ALT/AST activities (n = 6). **(C)**: Liver MPO activities (n = 6). **(D, E)**: The contents of serum TNF-α and IL-1β (n = 6). **(F)**: TUNEL staining results of liver tissue (×400) and positive cells of TUNEL were quantified, ↑ for TUNEL (+) cells. **(G)**: The expressions of cleaved caspase-3/pro–caspase-3 (n = 3); **(H)**: The activities of caspase-3, -8, and -9 in liver tissue (n = 6). **(I)**: The expression levels of TLR4, IκB-α, p-IκB-α, NF-κB p65, and nuclear protein NF-κB p65 were detected by western blotting, and the gray levels were analyzed (n = 3). Data are presented as mean ± SD values. $^{\Delta}P < 0.05$, $^{\Delta\Delta}P < 0.01$, and $^{\Delta\Delta\Delta}P < 0.001$ compared to the WT LPS/D-GalN group, $^{+}P < 0.05$, $^{++}P < 0.01$, and $^{+++}P < 0.001$ compared to CKO LPS/D-GalN group. NS, no significance.

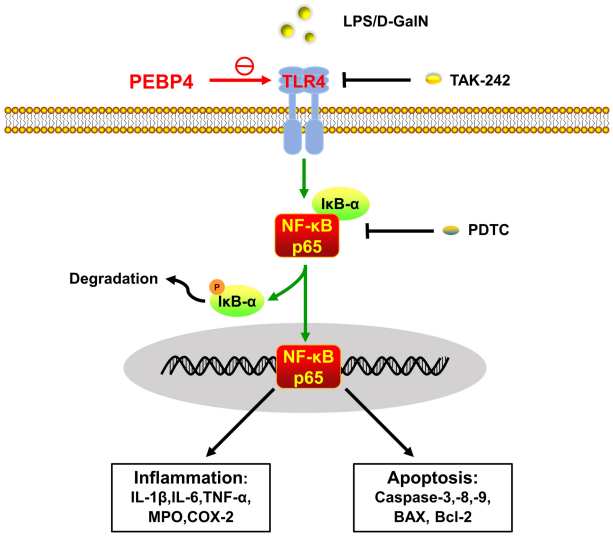

FIGURE 5 | Schematic of PEBP4-driven TLR4/NF-κB signaling pathway-associated inflammatory and apoptotic talk in LPS/D-GalN-induced ALI. PEBP4 CKO could activate the TLR4/NF-κB signaling pathway, promote NF-κB translocation into the nucleus, and then regulate the transcription of inflammatory factors and apoptotic genes to mediate acute liver injury (ALI) from both inflammation and apoptosis. TLR4 inhibitor (TAK-242) and NF-κB inhibitor (PDTC) could partially reverse these effects.

Furthermore, the defect of this article is that the cell experiment is not completed synchronously, which will be further improved in the later stage.

In conclusion, this research demonstrated that PEBP4 CKO aggravated LPS/D-GalN-induced ALI by promoting inflammatory mediators release and apoptosis. Mechanistically, the effect achieves through activation of the TLR4/NF-κB signaling pathway (**Figure 5**).

DATA AVAILABILITY STATEMENT

The original contributions presented in the study are included in the article/supplementary material. Further inquiries can be directed to the corresponding author.

ETHICS STATEMENT

All animal experiment was approved by the Animal Protection Committee of Jiangxi Medical College of Nanchang University.

AUTHOR CONTRIBUTIONS

X-qQ, Q-fC, Q-qS and Q-qL: build model, western blot, RT-PCR, statistical analyses and writing the article. S-yZ, Y-hL, L-yB, and SG: HE staining, TUNEL staining, and Kits assay. Q-fC: modified the article and submitted the article. X-yZ: oversaw the study, designed the experiments, modified the article, and funding acquisition. All authors take responsibility for the manuscript.

FUNDING

This work was supported by the National Natural Science Foundation of China (No. 81760117 and No. 81460126), Natural Science Foundation of Jiangxi province (No. 20181BAB205012), National College Students' innovation and entrepreneurship training program (No. 202010403006), and Jiangxi Students' innovation and entrepreneurship training program (No.S202010403056).

ACKNOWLEDGMENTS

We thank LetPub (www.letpub.com) for its linguistic assistance during the preparation of this manuscript.

REFERENCES

1. Percy AK, Dirk W. Immunological Functions of Liver Sinusoidal Endothelial Cells. *Cell Mol Immunol* (2016) 13:347–53. doi: 10.1038/cmi.2016.5
2. William ML, Robert HS, Scott LN, Edward D, Jay HH. Acute Liver Failure: Summary of a Workshop. *Hepatology* (2008) 47:1401–15. doi: 10.1002/hep.22177
3. Yang S, Kuang G, Zhang LK, Wu SW, Zhao ZZ, Wang B, et al. Mangiferin Attenuates LPS/D-Galn-Induced Acute Liver Injury by Promoting HO-1 in Kupffer Cells. *Front Immunol* (2020) 11:285. doi: 10.3389/fimmu.2020.00285
4. Tao YC, Wang ML, Wu DB, Luo C, Tang H, Chen EQ. Apolipoprotein A5 Alleviates LPS/D-Galn-Induced Fulminant Liver Failure in Mice by Inhibiting TLR4-Mediated NF-κb Pathway. *J Transl Med* (2019) 17:151. doi: 10.1186/s12967-019-1900-9
5. Li RD, Yang WC, Yin YP, Zhang P, Wang YX, Tao KX. Protective Role of 4-Octyl Itaconate in Murine LPS/D-Galn-Induced Acute Liver Failure *via* Inhibiting Inflammation, Oxidative Stress, and Apoptosis. *Oxid Med Cell Longev* (2021) 2021:9932099. doi: 10.1155/2021/9932099

6. Silverstein R. D-Galactosamine Lethality Model: Scope and Limitations. *J Endotoxin Res* (2004) 10:147–62. doi: 10.1179/096805104225004879
7. Yan D, Liu HL, Yu ZJ, Huang YH, Gao D, Hao H, et al. BML-111 Protected LPS/D-Galn-Induced Acute Liver Injury in Rats. *Int J Mol Sci* (2016) 17:1114. doi: 10.3390/ijms17071114
8. Gong XB, Yang Y, Huang LG, Zhang QY, Wan RZ, Zhang P, et al. Antioxidation, Anti-Inflammation and Anti-Apoptosis by Paeonol in LPS/D-Galn-Induced Acute Liver Failure in Mice. *Int Immunopharmacol* (2017) 46:124–32. doi: 10.1016/j.intimp.2017.03.003
9. Chen YE, Lu YY, Pei CY, Liang J, Ding P, Chen SX, et al. Monotropein Alleviates Secondary Liver Injury in Chronic Colitis by Regulating TLR4/NF-κb Signaling and NLRP3 Inflammasome. *Eur J Pharmacol* (2020) 883:173358. doi: 10.1016/j.ejphar
10. Wang HY, Wei XG, Wei X, Sun XM, Huang XK, Liang YQ, et al. 4-Hydroxybenzo [D] Oxazol-2 (3H)-One Ameliorates LPS/D-Galn-Induced Acute Liver Injury by Inhibiting TLR4/NF-κb and MAPK Signaling Pathways in Mice. *Int Immunopharmacol* (2020) 83:106445. doi: 10.1016/j.intimp.2020.106445
11. Ayman MM, Ekram MD, Walaa GH, May BJ, El-Shaymaa EN, Hanan AS, et al. Mesoporous Silica Nanoparticles Trigger Liver and Kidney Injury and Fibrosis *via* Altering TLR4/NF-κb, JAK2/STAT3 and Nrf2/HO-1 Signaling in Rats. *Biomolecules* (2019) 9:528. doi: 10.3390/biom9100528
12. Joh EH, Gu W, Kim DH. Echinocystic Acid Ameliorates Lung Inflammation in Mice and Alveolar Macrophages by Inhibiting the Binding of LPS to TLR4 in NF-κb and MAPK Pathways. *Biochem Pharmacol* (2012) 84:331–40. doi: 10.1016/j.bcp.2012.04.020
13. Qi M, Zheng LL, Qi Y, Han X, Xu YW, Xu L, et al. Corrigendum to" Dioscin Attenuates Renal Ischemia/Reperfusion Injury by Inhibiting Thetlr4/Myd88 Signaling Pathway *via* Up-Regulation of HSP70". *Pharmacol Res* (2019) 150:104449. doi: 10.1016/j.phrs.2019.104449. [Pharmacol. Res. 100 (2015) 341-352].
14. Zhang Q, Lenardo MJ, Baltimore D. 30 Years of NF-κb: A Blossoming of Relevance to Human Pathobiology. *Cell* (2017) 168:37–57. doi: 10.1016/j.cell.2016.12.012
15. Xu NN, Lu MM, Wang JX, Li YJ, Yang XT, Wei XJ, et al. Ivermectin Induces Apoptosis of Esophageal Squamous Cell Carcinoma *via* Mitochondrial Pathway. *BMC Cancer* (2021) 21:1307. doi: 10.1186/s12885-021-09021-x
16. Han H, Romain D, Sukanta D, Song ZL, Dipti A, Ge XD, et al. Danger Signals in Liver Injury and Restoration of Homeostasis. *J Hepatol* (2020) 73:933–51. doi: 10.1016/j.jhep.2020.04.033
17. Susana O, Andrew O. RIPK3 in Cell Death and Inflammation: The Good, the Bad, and the Ugly. *Immunol Rev* (2017) 277:102–12. doi: 10.1111/imr.12536
18. He H, Liu D, Lin H, Jiang SS, Ying Y, Chun S, et al. Phosphatidylethanolamine Binding Protein 4 (PEBP4) Is a Secreted Protein and has Multiple Functions. *Biochim Biophys Acta* (2016) 1863:1682–9. doi: 10.1016/j.bbamcr.2016.03.022
19. Wu ZJ, Liu B, Zheng XM, Hou HJ, Li Y. Role of the PEBP4 Protein in the Development and Metastasis of Gastric Cancer. *Oncotarget* (2017) 8:18177–84. doi: 10.18632/oncotarget.15255
20. Wang SC, Zhou F, Zhou ZY, Hu Z, Chang L, Ma MD. Knockdown of PEBP4 Suppresses Proliferation, Migration and Invasion of Human Breast Cancer Cells. *BioMed Pharmacother* (2017) 90:659–64. doi: 10.1016/j.biopha.2017.03.098
21. Zhang DX, Dai YD, Cai YK, Suo T, Liu H, Wang YQ, et al. PEBP4 Promoted the Growth and Migration of Cancer Cells in Pancreatic Ductal Adenocarcinoma. *Tumour Biol* (2016) 37:1699–705. doi: 10.1007/s13277-015-3906-0
22. Yu GP, Zhong N, Huang B, Mi YD. PEBP4 Gene Expression in Lung Squamous Cell Carcinoma: A Meta-Analysis-Based Study of the Molecular Pathways Involved. *Oncol Lett* (2020) 19:2825–31. doi: 10.3892/ol.2020.11386
23. Yu GP, Huang B, Chen GQ, Mi YD. Phosphatidylethanolamine-Binding Protein 4 Promotes Lung Cancer Cells Proliferation and Invasion *via* PI3K/Akt/Mtor Axis. *J Thorac Dis* (2015) 7:1806–16. doi: 10.3978/j.issn.2072-1439.2015.10.17
24. Wang J, Du J, Miao C, Lian H. Raf-Kinase Inhibitor Protein Attenuates Microglia Inflammation in an *In Vitro* Model of Intracerebral Hemorrhage. *Cell Mol Biol* (2016) 62:86–91. doi: 10.14715/cmb/2016.62.6.16
25. Yang XY, Wang YN, Lu PP, Shen YZ, Zhao XY, Zhu YQ, et al. PEBP1 Suppresses HIV Transcription and Induces Latency by Inactivating MAPK/NF-κb Signaling. *EMBO Rep* (2020) 21:e49305. doi: 10.15252/embr.201949305
26. Lin X, Wei JB, Nie JL, Bai FC, Zhu XS, Zhuo L, et al. Inhibition of RKIP Aggravates Thioacetamide-Induced Acute Liver Failure in Mice. *Exp Ther Med* (2018) 16:2992–8. doi: 10.3892/etm.2018.6542
27. Yu GP, Shen ZY, Chen GQ, Teng XM, Hu YQ, Huang B. PEBP4 Enhanced HCC827 Cell Proliferation and Invasion Ability and Inhibited Apoptosis. *Tumour Biol* (2013) 34:91–8. doi: 10.1007/s13277-012-0514-0
28. Huang RQ, Wang SQ, Zhu QB, Guo SC, Shi DL, Chen F, et al. Knockdown of PEBP4 Inhibits Human Glioma Cell Growth and Invasive Potential *via* ERK1/2 Signaling Pathway. *Mol Carcinog* (2019) 58:135–43. doi: 10.1002/mc.22915
29. Yuan ZQ, Zhang HR, Muhammad H, Ding JX, Chen X, Liang PS, et al. A New Perspective of Triptolide-Associated Hepatotoxicity: Liver Hypersensitivity Upon LPS Stimulation. *Toxicology* (2019) 414:45–56. doi: 10.1016/j.tox.2019.01.005
30. Fu TH, Li HJ, Zhao Y, Cai EB, Zhu HY, Li PY, et al. Hepatoprotective Effect of α-Mangostin Against Lipopolysaccharide/D-Galactosamine-Induced Acute Liver Failure in Mice. *Biomed Pharmacother* (2018) 106:896–901. doi: 10.1016/j.biopha.2018.07.034
31. Yang X, Masayoshi F, Teizo Y, Toshiaki O, Miwa S, Megumi M, et al. Spred2 Deficiency Exacerbates D-Galactosamine/Lipopolysaccharide-Induced Acute Liver Injury in Mice *via* Increased Production of Tnfα. *Sci Rep* (2018) 8:188. doi: 10.1038/s41598-017-18380-0
32. He YT, Xia ZJ, Yu DQ, Wang JK, Jin L, Huang D, et al. Hepatoprotective Effects and Structure Activity Relationship of Five Flavonoids Against Lipopolysaccharide/D-Galactosamine Induced Acute Liver Failure in Mice. *Int Immunopharmacol* (2019) 68:171–8. doi: 10.1016/j.intimp.2018.12.059
33. Tang FY, Fan KF, Wang KL, Bian CZ. Amygdalin Attenuates Acute Liver Injury Induced by D-Galactosamine and Lipopolysaccharide by Regulating the NLRP3, NF-κb and Nrf2/NQO1 Signalling Pathways. *BioMed Pharmacother* (2019) 111:527–36. doi: 10.1016/j.biopha.2018.12.096
34. Luo YS, Yang YQ, Shen Y, Li LJ, Huang JY, Tang L, et al. Luzindole Attenuates LPS/D-Galactosamine -Induced Acute Hepatitis in Mice. *Innate Immunol* (2020) 26:319–27. doi: 10.1177/1753425919890912
35. Zhou D, Ai Q, Lin L, Gong XQ, Ge P, Che Q, et al. 5- Aminoimidazole-4-Carboxamide-1-β-D-Ribofuranoside-Attenuates LPS/D-Gal-Induced Acute Hepatitis in Mice. *Innate Immunol* (2015) 21:698–705. doi: 10.1177/1753425915586231
36. Wen JJ, Lin HF, Zhao MS, Tao L, Yang YX, Xu X, et al. Piceatannol Attenuates D-Galn/LPS-Induced Hepatoxicity in Mice: Involvement of ER Stress, Inflammation and Oxidative Stress. *Int Immunopharmacol* (2018) 64:131–9. doi: 10.1016/j.intimp.2018.08.037
37. Beverley K, Erica LWL, William ML, Hanje AJ, Stravitz RT, Safwat G, et al. Acute Liver Failure From Tumor Necrosis Factor-α Antagonists: Report of Four Cases and Literature Review. *Dig Dis Sci* (2018) 63:1654–66. doi: 10.1007/s10620-018-5023-6
38. Liu YM, Zhu LL, Liang ST, Yao SS, Li R, Liu SH, et al. Galactose Protects Hepatocytes Against TNF-α-Induced Apoptosis by Promoting Activation of the NF-κb Signaling Pathway in Acute Liver Failure. *Lab Invest* (2015) 95:504–14. doi: 10.1038/labinvest.2015.34
39. Rania B, David E, Anita H, Andrea G, Vladimir M, Mark M, et al. Quantitative Proteomics of Cerebrospinal Fluid Using Tandem Mass Tags in Dogs With Recurrent Epileptic Seizures. *J Proteomics* (2021) 231:103997. doi: 10.1016/j.jprot.2020.103997
40. Xie YL, Chu JG, Jian XM, Dong JZ, Wang LP, Li GX, et al. Curcumin Attenuates Lipopolysaccharide/D-Galactosamine-Induced Acute Liver Injury by Activating Nrf2 Nuclear Translocation and Inhibiting NF-κb Activation. *BioMed Pharmacother* (2017) 91:70–7. doi: 10.1016/j.biopha.2017.04.070
41. Pan CW, Yang SX, Pan ZZ, Zheng B, Wang JZ, Lu GR, et al. Andrographolide Ameliorates D-Galactosamine/Lipopolysaccharide-Induced Acute Liver Injury by Activating Nrf2 Signaling Pathway. *Oncotarget* (2017) 8:41202–10. doi: 10.18632/oncotarget.17149
42. Zhou J, Peng ZL, Wang J. Trelagliptin Alleviates Lipopolysaccharide (LPS) -Induced Inflammation and Oxidative Stress in Acute Lung Injury Mice. *Inflammation* (2021) 44:1507–17. doi: 10.1007/s10753-021-01435-w

43. Guo SX, Guo LS, Fang Q, Yu MR, Zhang LP, You CG, et al. Astaxanthin Protects Against Early Acute Kidney Injury in Severely Burned Rats by Inactivating the TLR4/Myd88/NF-κb Axis and Upregulating Heme Oxygenase-1. *Sci Rep* (2021) 11:6679. doi: 10.1038/s41598-021-86146-w
44. Liu YL, Zhang QZ, Wang YR, Fu LN, Han JS, Zhang J, et al. Astragaloside IV Improves High-Fat Diet-Induced Hepatic Steatosis in Nonalcoholic Fatty Liver Disease Rats by Regulating Inflammatory Factors Level *via* TLR4/NF-κb Signaling Pathway. *Front Pharmacol* (2020) 11:6050 64. doi: 10.3389/fphar.2020.605064
45. Naoko K, Bibo K, Amir AG, Shen XD, Ronald WB, Cheng GH, et al. ASC/Caspase-1/IL-1β Signaling Triggers Inflammatory Responses by Promoting HMGB1 Induction in Liver Ischemia/Reperfusion Injury. *Hepatology* (2013) 58:351–62. doi: 10.1002/hep.26320
46. Heyninck K, Wullaert A, Beyaert R. Nuclear Factor-Kappa B Plays a Central Role in Tumour Necrosis Factor-Mediated Liver Disease. *Biochem Pharmacol* (2003) 66:1409–15. doi: 10.1016/s0006-2952(03)00491-x

Conflict of Interest: The authors declare that the research was conducted in the absence of any commercial or financial relationships that could be construed as a potential conflict of interest.

Publisher's Note: All claims expressed in this article are solely those of the authors and do not necessarily represent those of their affiliated organizations, or those of the publisher, the editors and the reviewers. Any product that may be evaluated in this article, or claim that may be made by its manufacturer, is not guaranteed or endorsed by the publisher.

frontiers | Frontiers in Immunology

REVIEW
published: 14 July 2022
doi: 10.3389/fimmu.2022.935160

The Immune Pathogenesis of Acute-On-Chronic Liver Failure and the Danger Hypothesis

Rui Qiang[1], *Xing-Zi Liu*[2] *and Jun-Chi Xu*[1,3]*

[1] The Affiliated Infectious Diseases Hospital, Suzhou Medical College of Soochow University, Suzhou, China, [2] Key Laboratory of Oral Diseases Research of Anhui Province, College and Hospital of Stomatology, Anhui Medical University, Hefei, China, [3] Key Laboratory of Infection and Immunity of Suzhou City, The Fifth People's Hospital of Suzhou, Suzhou, China

Acute-on-chronic liver failure (ACLF) is a group of clinical syndromes related to severe acute liver function impairment and multiple-organ failure caused by various acute triggering factors on the basis of chronic liver disease. Due to its severe condition, rapid progression, and high mortality, it has received increasing attention. Recent studies have shown that the pathogenesis of ACLF mainly includes direct injury and immune injury. In immune injury, cytotoxic T lymphocytes (CTLs), dendritic cells (DCs), and $CD4^+$ T cells accumulate in the liver tissue, secrete a variety of proinflammatory cytokines and chemokines, and recruit more immune cells to the liver, resulting in immune damage to the liver tissue, massive hepatocyte necrosis, and liver failure, but the key molecules and signaling pathways remain unclear. The "danger hypothesis" holds that in addition to the need for antigens, damage-associated molecular patterns (DAMPs) also play a very important role in the occurrence of the immune response, and this hypothesis is related to the pathogenesis of ACLF. Here, the research status and development trend of ACLF, as well as the mechanism of action and research progress on various DAMPs in ACLF, are summarized to identify biomarkers that can predict the occurrence and development of diseases or the prognosis of patients at an early stage.

Keywords: ACLF, DAMPs, danger hypothesis, inflammatory cytokine storm, biological target molecules

OPEN ACCESS

Edited by:
Olaf Tyc,
University Hospital Frankfurt, Germany

Reviewed by:
Albrecht Piiper,
University Hospital Frankfurt, Germany
Alessandra Fiore,
Max Planck Institute of Biochemistry, Germany

***Correspondence:**
Jun-Chi Xu
xujunchi19850504@126.com

Specialty section:
This article was submitted to Inflammation, a section of the journal Frontiers in Immunology

Received: *03 May 2022*
Accepted: *20 June 2022*
Published: *14 July 2022*

Citation:
Qiang R, Liu X-Z and Xu J-C (2022) The Immune Pathogenesis of Acute-on-Chronic Liver Failure and the Danger Hypothesis. Front. Immunol. 13:935160. doi: 10.3389/fimmu.2022.935160

HIGHLIGHTS

- Immune damage is an important factor in the occurrence of ACLF, but the immune mechanism is unclear.
- The DAMP cycle and immune damage are important factors leading to cytokine storms.
- According to the "danger hypothesis," DAMP release, inflammatory cytokine storms, and the occurrence of ACLF are closely related.
- Intrahepatic infiltration and hyperfunction of immune cells caused by DAMPs are important factors leading to the occurrence of ACLF.

- DAMPs can be biological target molecules for the early diagnosis and treatment of ACLF.

As a group of complex clinical syndromes related to severe acute liver function impairment and multiple-organ failure caused by various acute triggering factors on the basis of chronic liver disease, ACLF is characterized by severe disease, rapid progression, and high mortality. Currently, there are four categories of liver failure worldwide, namely, acute liver failure (ALF) (1), subacute liver failure (SALF) (2), ACLF (3), and chronic liver failure (CLF) (4), among which ACLF is a common type of liver failure. Additionally, chronic viral hepatitis, drug-induced hepatitis, and alcoholic hepatitis are major diseases induced by ACLF.

Immune damage is an important mechanism for the occurrence of ACLF. Recent studies have shown that intrahepatic immune cell infiltration and cytokine storms are important factors, but the key molecules involved in immune hyperfunction in ACLF remain unclear. "The danger hypothesis" holds that in addition to the antigens that the immune system responds to when detected, the DAMP-mediated injury-hyperimmunity cycle coincides with the mechanism of ACLF; thus, DAMPs may be closely related to the occurrence of ACLF. This paper summarizes the research status and development trends related to ACLF, as well as the mechanism of action and research progress on various DAMPs in ACLF.

1 THE DEFINITION, INDUCEMENT, TREATMENT, RESEARCH STATUS, AND DEVELOPMENT TRENDS OF ACLF

1.1 The Controversial Definition of ACLF

Liver failure is a group of clinical syndromes in which severe liver damage caused by many factors results in severe dysfunction or decompensation of synthesis, detoxification, metabolism, and biotransformation, with jaundice, coagulation disorders, hepatorenal syndrome, hepatic encephalopathy (HE), and ascites as the main manifestations (5). ACLF, as the most common severe liver disease syndrome in clinical practice, has various causes, complex clinical manifestations, and high mortality.

Currently, the definitions of ACLF in different areas of research are controversial, which mainly results from differences in patients in Europe, America, Asia Pacific, and other regions, as well as medical histories, diagnostic criteria, and acute inducing factors. The European Association for the Study of the Liver-Chronic Liver Failure (EASL-CLIF) defines ACLF as a severe syndrome in patients with liver cirrhosis that has three typical characteristics: acute liver decompensation, organ failure, and short-term high mortality. This definition not only includes intrahepatic symptoms but also reflects the damage caused by ACLF to multiple organs or systems including the liver and other tissues (6). The North American Consortium for the Study of End-Stage Liver Disease (NACSELD) defines ACLF as involving two or more extrahepatic organ failures, excluding changes in liver function and the coagulation system (7). The definition of ACLF by the Asian Pacific Association for the Study of the Liver (APASL) was published in 2009 (8) and updated in 2014 (9) and 2019 (10), including patients with liver cirrhosis (compensatory period) or chronic liver disease who have or not been diagnosed in the past, acute liver injury complicated with jaundice (serum bilirubin ≥ 5 mg/dl (85 μmol/l), and coagulation disorders (international normalized ratio ≥ 1.5 or prothrombin activity < 40%), ascites and/or HE within 4 weeks; no history of decompensation and extrahepatic sediment, renal failure, and circulatory or respiratory failure are excluded from the definition, and the mortality rate within 28 days is usually high.

1.2 Inducement and Treatment Status of ACLF

According to recent clinical studies, the main causes of death in ACLF patients include hepatitis virus reactivation, sepsis caused by bacterial infection, severe alcoholic liver disease, and drug toxicity and side effects.

Currently, the treatment of ACLF generally includes medical support treatment, artificial liver treatment, and liver transplantation treatment, but ACLF is still characterized by severe illness, rapid progression, and high mortality in the clinic (5). Treatment studies of liver failure have been continuously developed to further clarify the pathogenesis of ACLF, explore related factors of its prognosis, find early diagnosis and treatment targets, predict patient outcomes such that clinical intervention treatment can be carried out in a timely manner, improve prognosis, and reduce mortality.

1.3 Research Status and Development Trends of the Immune Pathogenesis of ACLF

At present, the pathogenesis of ACLF remains unclear, although recent studies have shown that the pathogenesis of ACLF mainly includes direct injury and immune injury. Pathogen-associated molecular patterns (PAMPs) released by pathogens themselves or DAMPs induced by various factors bind to receptors and stimulate the release of proinflammatory cytokines such as interleukin (IL)-1β, IL-6, and IL-8, leading to immune disorders and thus causing a "cytokine inflammatory storm," sepsis, tissue hypoperfusion, and mitochondrial dysfunction, all of which can culminate in multiple-organ failure and ACLF (11–13).

From the perspective of immune cell function, cellular immunity mediated by CTLs is the main factor causing massive hepatocyte necrosis (14). Studies have shown that IFN-γ and TNF-α expression in the liver of ACLF patients is markedly upregulated, which is significantly related to accumulation of $CD4^+$ and $CD8^+$ T cells (15). Some studies have found that the expression level of programmed cell death protein 1 (PD-1) on $CD8^+$ T cells decreases significantly in the early stage of ACLF, which diminishes the negative regulation of CTL immune activity and promotes disease aggravation (16). In addition, some studies have found that DCs migrate from the blood to the liver in ACLF patients, inhibiting IFN-γ secretion by $CD8^+$ T cells and reducing liver damage (17). $CD4^+$ T cells are also an important factor in the occurrence of ACLF. Compared with

healthy people and chronic hepatitis B (CHB) patients, regulatory T cells (Tregs) in the peripheral blood of ACLF patients are significantly increased, which correlates positively with the viral nucleic acid load, suggesting that it may be related to disease severity (18). Other studies have observed immune imbalance between Th17 and Treg cells in ACLF patients. When ACLF occurs, there are asynchronous increases in Th17 cells and decreases in Treg cells, and prognosis is poor when the ratio of Treg/Th17 cells is low (19, 20). Some scholars have studied the number and function of peripheral blood mononuclear cells in the course of ACLF, with human leukocyte antigen–DR isotype (HLA-DR) showing a downward trend with disease aggravation; the proinflammatory factors IL-1β and TNF-α secreted by monocytes are also increased in the early stage and decreased in the late stage. The immune state of the body changes from a severe proinflammatory reaction at the beginning of the disease to an anti-inflammatory reaction stage, which enhances the risk of infection and further aggravates the disease (21). Moreover, some scholars have put forward the "triple attack theory," which suggests that the occurrence of liver failure includes a triple attack of immune injury, ischemia, and hypoxia injury and endotoxemia. On this basis, it is proposed that immunotherapy for ACLF should be carried out in stages, that is, immunosuppressive therapy should be given at the initial stage and immune enhancement therapy should be given at the middle and late stages (22).

In addition to various immune cells, many cytokines are involved in the occurrence and development of ACLF. Compared with acute hepatitis B patients, CHB patients, and healthy controls, the serum IL-1Rα level in HBV-ACLF patients is significantly increased, although the ratio of IL-1Rα/IL-1β is significantly decreased. Further follow-up has shown that the level of IL-1Rα and the IL-1Rα/IL-1β ratio are closely related to survival time, and many proinflammatory cytokines, such as IL-6, IL-8, and IL-23, are significantly related to the occurrence and prognosis of ACLF (14, 20, 21).

In summary, a variety of immune cells and cytokines are involved in the pathogenesis of ACLF. In the early stage, CTLs, DCs, and $CD4^+$ T cells accumulate in the liver tissue, secrete a variety of proinflammatory cytokines and chemokines, and recruit more immune cells to the liver, resulting in immune damage to the liver and leading to massive hepatocyte necrosis and liver failure. In general, the key factors leading to aggravation of immune injury can be identified by further understanding the immune mechanism of ACLF, which will provide an important theoretical basis for early treatment of liver failure and curb its further development.

2 TYPES AND FUNCTIONS OF INFLAMMATORY FACTORS RELATED TO THE DANGER HYPOTHESIS

Dr. Matzinger first put forward the "danger hypothesis" in 1994, which holds that the immune system will respond only when it detects danger; otherwise, it is immune tolerant (23). Subsequently, Dr. Matzinger put forward the "danger model" in 2002, which shows that the immune system is more concerned about the danger signals generated by cell damage or stress, than with unconditionally recognizing and removing foreign substances. Regardless of whether danger signals are exogenous pathogens released from necrotic cells or chemicals synthesized or modified by endogenous cells themselves, they can trigger immune responses through tissue damage or cell stress and are not emitted by healthy cells or cells in a normal physiological death state (24). Necrosis of cells can result in the generation of danger signals, which will promote secretion of cytokines by immune cells, further aggravate immune damage to cells, form a cycle of tissue damage, and lead to the generation of a cytokine storm and massive tissue necrosis (**Figure 1**).

There is no clear definition of the properties of danger signaling molecules, which can be divided into physical, chemical, and biological molecular forms according to different inducements. A large class of danger signaling molecules, DAMPs belong to the immune stimulation molecular model in aseptic inflammation, which is different from the microbial model and is usually related to injury (25). DAMPs are produced by necrotic and stressed cells or tissues and can bind to host pattern recognition receptors (PRRs) and other receptors, transmitting proinflammatory signals and promoting secretion of inflammatory factors and the inflammatory response. DAMPs are mainly derived from the nucleus, cytoplasm, organelles, or extracellular matrix and include uric acid, mitochondrial DNA (mtDNA), ATP, heat shock proteins (HSPs), amyloid β, S100 protein, high-mobility group box chromosomal protein 1 (HMGB1), ECM protein, IL-1α, IL-33, genomic DNA, cyclophilic protein A, fibrous actin (F-actin), and calreticulin (26, 27). DAMPs are associated with LF occurrence and development. All studies of IL-33, IL-1α, S100 protein, and mitochondrial DNA and 75% of those of histones have shown that DAMP expression is elevated during ACLF and correlates positively with disease severity. Studies of HSPs and 25% of studies of histones found that expression is decreased, which might prevent the occurrence of ACLF (**Table 1**). Therefore, analysis of the relationship between DAMPs and ACLF may be of great significance to elucidate the pathogenesis of ACLF.

3 TYPES AND FUNCTIONS OF DAMPS RELATED TO ACLF

3.1 Interleukin-1 Family Cytokines

In recent years, increasing attention has been given to the relationship between the function of IL-1 superfamily members and the occurrence of ACLF. IL-1 superfamily members are involved in many inflammatory diseases, such as obesity, cardiovascular diseases, cancer, viral or parasitic infections, autoinflammatory syndrome, and liver diseases (102). The role of the IL-1 superfamily in liver diseases can be protective or proinflammatory, and two members, namely, IL-33 and IL-1α, which have been studied the most, are considered bifunctional cytokines. In addition to their functions as classical cytokines, as part of the DAMP process, IL-33 and IL-1α are early warning

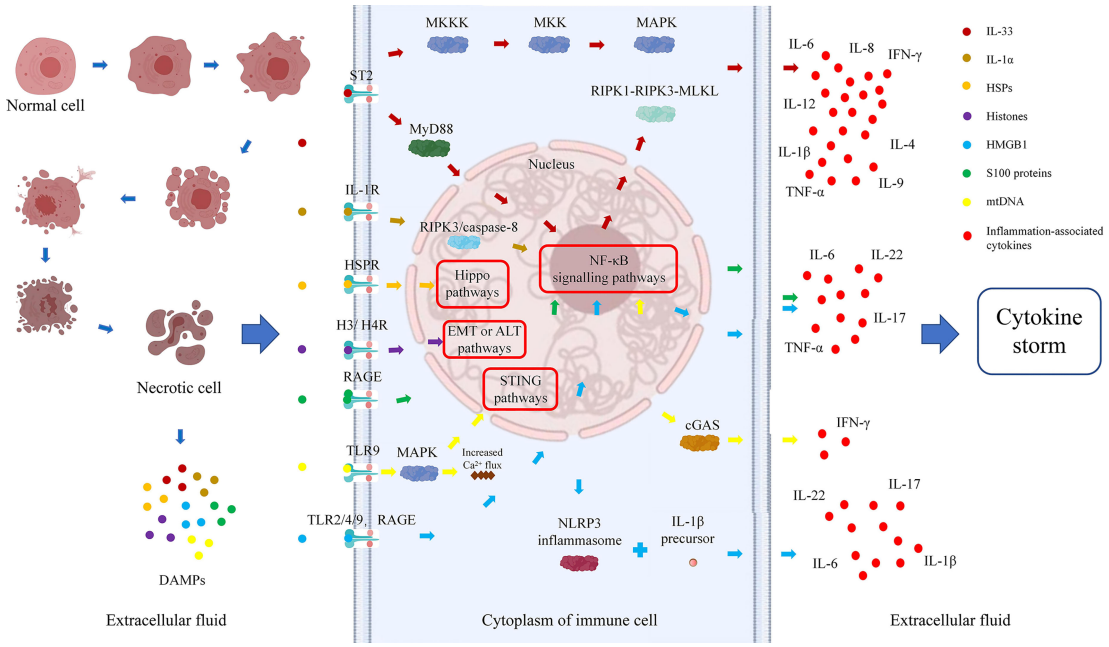

FIGURE 1 | Danger signal cycle: relationships among cell necrosis, DAMPs, and cytokine storms.

signals of cell injury (102). The IL-33/ST2 pathway has a bidirectional regulatory role in acute hepatocyte injury and chronic liver fibrosis, and the IL-1α/IL-1R1 axis promotes massive necrosis of hepatocytes and infiltration of inflammatory cells into liver tissue, leading to organ failure. Such enhanced immune cell tissue infiltration and cytokine secretion abilities may play an important role in liver immune injury.

Knowledge of effects of the IL-33/ST2 axis and IL-1α/IL-1R1 axis on ACLF will be helpful to reveal the pathogenesis of ACLF to provide a new target for early diagnosis and treatment of ACLF.

3.1.1 Interleukin-33

IL-33 is a member of the IL-1 superfamily. As a tissue-derived nuclear cytokine, it is mainly derived from endothelial cells, epithelial cells, and fibroblasts during inflammation. Its receptor ST2 is a member of the Toll-like receptor superfamily and is expressed on the surface of many immune cells, such as mast cells, type II intrinsic lymphocytes (ILC2s), Tregs, helper T cells, $CD8^+$ T cells, natural killer cells, B cells, and macrophages (103).

Kotsiou et al. summarized previous studies and found that acute large-scale liver injury could result in release of IL-33 from cells, which might be an activator of tissue self-protection and repair (35) or an anti-inflammatory factor marker of M2 macrophages (36). However, IL-33 acts as a liver fibrosis factor to aggravate liver deterioration in chronic liver injury (36). Rickard et al. found that IL-33 released from mouse liver necrosis tissue into the microenvironment forms a coupling complex with myeloid differentiation factor 88 (MyD88), IL-1, and a subset of Toll-like receptors; this process might be regulated by the RIPK1–RIPK3–MLKL axis and drive inflammation (39). Arshad et al. reported that the expression of IL-33 in hepatocytes is partly controlled by perforin and tumor necrosis factor-related apoptosis-inducing ligand (TRAIL) under the regulation of natural killer T cells but that is not controlled by tumor necrosis factor α (TNF-α) or Fas ligand (FasL). IL-33-deficient mice exhibit more severe liver injury than WT mice, suggesting that IL-33 has a protective effect against acute liver injury (37). According to Volarevic et al., acute liver injury induced by concanavalin A can be reduced by activating the IL-33/ST2 axis. ST2-deficient mice developed more severe hepatitis and more liver inflammatory cell infiltration, suggesting the potential of the IL-33/ST2 axis as a therapeutic target (38).

Nevertheless, some studies have shown that the IL-33/ST2 axis has a role in promoting the development of acute liver injury. Kim et al. (40) and Seo et al. (41) found serum levels of HMGB1 and IL-33 to be significantly increased in ALF animal models induced by D-galactosamine (GalN) and lipopolysaccharide (LPS) and that blocking the pathway with inhibitors (such as necrostatin-1) could reduce liver injury. IL-33/ST2 promotes activation of the nuclear factor (NF)-κB, mitogen-activated protein kinase (MAPK), or extracellular signal-regulated kinase (ERK)/p38-MAPK pathways to produce proinflammatory cytokines (IL-6, IL-8) and T helper type 2 (Th2)-related cytokines (IL-4, IL-5, IL-9, IL-13) (104, 105).

At present, there are few studies on the IL-33/ST2 axis in ACLF. Roth et al. found through serological experiments that compared with healthy people, the concentrations of IL-33 and soluble ST2 (sST2) in ALF and ACLF patients are significantly

TABLE 1 | DAMPs associated with ALF.

Intracellular location	DAMPs	NOT ACLF (ALF/ALI)		ACLF	
		Upregulation (protective)	Upregulation (damaging)	Upregulation (protective)	Upregulation (damaging)
Nucleus	IL-33	Animal models: (35–38)	Animal models: (35, 39–41)		Humans: (28–34)
	IL-1α		Animal models: (44–48)		Humans: (42, 43) Animal model: (43)
	Histones		Humans: (49, 50) Animal models: (49, 50, 54)	Animal model: (53)	Humans: (51, 52) Animal model: (55)
	HMGB1		Humans: (56–59) Animal models: (61–66)		Humans: (56, 60) Animal models: (66–68)
Cytosol	HSPs	Humans: (69–71) Animal models: (69, 70, 78–90)	Animal models: (73–77)	Humans: (72) Animal model: (87)	
	ATP			Humans: (91, 92) Animal models: (91, 92)	
	S100 Protein		Humans: (93, 94) Animal model: (97)	Humans: (58, 95, 96) Animal model: (98)	
Mitochondria	Mitochondrial DNA		Human model: (99)		Animal model: (100, 101)

increased, which is helpful for distinguishing acute and chronic liver failure or for monitoring the progression and severity of the disease (28). Subsequently, immunohistochemistry by Lei et al. showed a weak IL-33 expression and high sST2 expression in liver slices of HBV-ACLF patients, suggesting that sST2 can be used as a predictor of disease severity (29). Jiang et al. found no significant difference in serum IL-33 among HBV-ACLF, CHB, and HC groups, even though serum sST2 levels were higher in HBV-ACLF patients, correlated with the survival rate, and decreased after treatment. It was suggested that sST2 can be used as a marker for evaluating disease severity and early recognition (30). In the study of Du et al., the expression level of IL-33/ST2 was significantly increased in the serum and liver tissue of ACLF patients, and the level of serum IL-33 was found to be related to the severity of liver disease. *In vitro* experiments proved that IL-33 enhanced the LPS-stimulated inflammatory storm of monocytes through ERK1/2 activation but not p38 and JNK activation (31). Regarding the course of ACLF caused by CHB, Yuan et al. showed that compared with levels in the CHB group and the pre-ACLF group, serum IL-33 and sST2 were highest in the ACLF group, which could be used to evaluate progression and mortality in patients with multiple biological indicators (32). Gao et al. showed that serum IL-33 and sST2 were highly expressed in HBV-ACLF and that sST2 may be used as a prognostic marker (106).

In conclusion, abundant clinical evidence and experimental data show that the IL-33/ST2 pathway is related to the occurrence and development of various acute liver diseases, but the role of the IL-33/ST2 axis in ALF/ACLF is still controversial. As a DAMP, IL-33 stimulates the immune system to respond to virus invasion through its receptor ST2, drives immune cell infiltration into the liver, increases secretion of cytokines, and causes toxic damage to liver cells. However, some studies have found that the IL-33/ST2 axis can also promote Th2-type responses and hepatic stellate cell activity, promoting the progression of liver fibrosis due to chronic damage, which is a protective mechanism.

3.1.2 Interleukin 1α

IL-1α, a member of the IL-1 superfamily, is released by RIPK3/caspase-8 apoptosis signal transduction in a caspase-1-dependent manner during cell injury or apoptosis, from macrophages undergoing TNF-induced necroptotic death or from apoptotic bodies. IL-1α can trigger an inflammatory response regardless of cell damage or apoptosis (107). The receptors, the IL-1 receptor (IL-1R) family including more than 10 structurally related members such as IL-1R1, IL-1R2, and IL-1R3, which transmit inflammatory signals downstream, induce the accumulation of immune cells and promote the secretion of inflammatory cytokines. IL-1Rs are alert receptors

that play a central role in sensing maladaptive tissue changes from both outside and within the body (108). One study found that IL-1R-/- mice had a higher survival rate than wild-type mice during chronic infection, which was due to the attenuated inflammatory response in the former, allowing them to recover from cachexia (109). As a common proinflammatory factor, IL-1α has been intensely studied in liver injury, mainly with regard to ALF and less so ACLF. In addition, many studies on the IL-1α/IL-1R axis in liver disease have high patient numbers.

Romics et al. used LPS to induce liver injury in mice and found that various serum proinflammatory cytokines (including IL-1α) were significantly increased and that mRNA expression levels of various proinflammatory cytokines in the liver also increased (44). Gehrke et al. showed that inhibiting IL-1R1 by blocking it with IL-1ra can alleviate the severity of ALF but that administration of IL-1α aggravates the degree of liver injury (45). Xiao et al. found that IL-1α can obviously induce and maximize a reduction in the liver inflammatory state (46). *Lactobacillus reuteri* DSM 17938 is a potential probiotic for preventing or treating liver failure. In one study, the serum IL-1α level, the inflammatory state, and acute liver injury decreased significantly in a rat model treated with *Lactobacillus reuteri* DSM 17938 (47). Sultan et al. reported that IL-1α plays a central role in the pathogenesis of fulminant liver failure in mice; the symptoms of ALF in IL-1$\alpha^{-/-}$mice were obviously alleviated, and secretion of inflammatory factors was obviously reduced (48).

Systemic inflammation can easily lead to ACLF, which may be related to activation of inflammatory corpuscles. The research of Monteiro and studies of other animal models have confirmed that development of ACLF in compensated cirrhosis is related to increases in IL-1α and IL-1β (42). Recently, a genetic study found two kinds of gene cluster polymorphisms belonging to the IL-1 superfamily, in which expression of IL-1α-related genes significantly reduced the occurrence of ACLF (43).

In conclusion, it may be a possible approach to treat ALF/ACLF by blocking the IL-1α/IL-1R axis.

3.2 Heat Shock Proteins

HSPs, which are produced by heat shock, ischemia, hypoxia, and other stress factors, participate in the correct folding, modification, and maturation of proteins; assist in the degradation of aging proteins; are expressed during cell stress; and play an important role in regulating antigen presentation, inflammatory signal transduction, and apoptosis (110). HSPs are classified according to their molecular weights as HSP25, HSP27, HSP60, HSP70, HSP90, HSP110, and glucose-regulated protein (GRP), among others. HSPs play an important role in the proliferation, invasion, metastasis, and apoptosis evasion of cancer cells and promote the development of diseases. As a new cancer diagnostic marker and therapeutic target, HSPs play an important role in evaluating the molecular mechanism of cancer development and metastasis (111). Overall, HSPs are very important for cell survival under unfavorable environmental conditions.

HSP27 overexpression is closely related to the tumorigenesis, metastasis, and invasiveness of cancer. For example, the elevated expression of HSP27 increases Salvador–Warts–Hippo pathway (Hippo pathway) nuclear localization, activates related oncogenic and metastatic pathways, including the TGF-B/SMAD, WNT/B-Catenin, and ILK signaling pathways, and leads to increased tumor cell expansion in local tissues (112). HSP70 induces cell proliferation, inhibits apoptosis and oncogene-induced senescence, and is a poor prognostic marker for various cancers (112). HSP70 promotes tumor metastasis and infiltration by upregulating the expression of molecules such as N-cadherin, MMP2, SNAIL, and vimentin (113). To date, there are few studies on the mechanisms of HSPs in ACLF, and those that have been conducted are mainly related to ALI and ALF.

HSPs have been considered to be protective factors in the occurrence of acute liver injury or liver failure. Oda et al. found in 2002 that geranylgeranylacetone (GGA) could prevent ALF after large-scale hepatectomy by inducing and enhancing HSP70 expression in residual liver (78). Subsequently, Kanemura et al. (79) and Kawashima et al. (80) reported that GGA initiated strong cell protection by inhibiting the CXC chemokine GRO1 and inducing HSP27 and HSP70. Sepsis causes acute inflammatory reactions in the liver, which can lead to organ failure and death. According to Peppler et al., exercise has anti-inflammatory and hepatoprotective effects; regular exercise increases liver protein levels, including HSP70, prevents the inflammatory cascade reaction induced by LPS, and weakens the severe inflammatory reaction of the liver caused by sepsis (81). Sumioka et al. showed that HSP25 and HSP70i have protective effects on acute liver injury induced by acetaminophen (APAP) in mice, and their levels might be key in determining the fate of APAP-injured mice (82). ALF induced by APAP damages the mitochondria and activates HSP70 expression, whereas diphenyl diselenide prevents ALF induced by APAP and plays a key role in regulating the cell protection response (83). Excessive production of HSP70 in the liver protects hepatocytes under various pathological conditions. It has been found that prostaglandin E1, a non-toxic HSP inducer, prevents ALF after large-scale hepatectomy by enhancing the production of HSP70 in residual liver (84). Bicyclic alcohol is a new type of hepatoprotective agent that induces the production of heat shock transcription factor 1 (HSF1) and promotes synthesis of HSP70 and the stress response, inducing sex-specific liver protection to prevent liver injury or failure (85). Dai et al. found that bicyclol induces the overexpression of HSP27 in the liver, which significantly enhances the protection of an animal model of acute liver injury induced by D-galactosamine/lipopolysaccharide (86). In the study of Vidyasagar et al., serum HSP25 and HSP27 had antioxidant effects in ALF and CLF patients and reduced the damage caused by reactive oxygen species (ROS) and prevented the occurrence of HE (69). El-Baz et al. showed that *D. salina* hydrochloride increased HSP25 and improved brain histopathological changes in HE patients, benefiting ALF prognosis (70).

Most scholars believe that HSPs are important protective factors in the repair of liver tissue damage and that increases in their levels are helpful for the prognosis of patients and predicting efficacy, but the mechanism of some remains controversial. Ye et al. found that HSP27 accelerated the early

acute liver injury induced by ischemia–reperfusion injury in rats by reducing the number of Treg cells, reducing levels of the stress-protective factors superoxide dismutase (SOD) and glutathione, increasing the level of proinflammatory factors, and aggravating inflammation (73). Wright et al. conducted ACLF-related animal experiments and showed increased HSP25 in the corpus callosum of the bile duct ligation (BDL) rat model, suggesting a cell stress state (such as inflammation and apoptosis) (87).

Other members of the HSP family also play important roles in the development of acute liver injury or liver failure. Some studies have found that GRP78 combined with other preparations can significantly improve the incidence of ALF or prevent aggravation of acute liver injury. GRP78, a member of the HSP70 family, is a molecular chaperone for endoplasmic reticulum stress and stress-induced autophagy. Win et al. showed that Japanese miso extract prepared from rice yeast can enhance the expression of GRP78, inhibiting hepatitis A virus (HAV) replication and reducing ALF (88). Nwe et al. reported that free fatty acids or high concentrations of glucose enhance HAV replication and reduce GRP78 expression but that thapsigargin has the opposite effects, reducing the occurrence of ALF (71). The protective effect of kaempferol in the ALF mouse model occurs through inhibition of hepatocyte apoptosis by increasing the expression of GRP78 (89). Ren et al. found that compared with healthy people and patients with CHB, the expression of GRP78 and GRP94 in ACLF patients decreases gradually, indicating that HSP-mediated stress protection is decreased in ACLF patients and correlates negatively with the degree of liver injury (72).

However, some studies have reported that GRP78 and GRP94 are important factors for acute liver injury or liver failure. Baudi et al. found that acute liver injury induced by IFN-α-mediated virus infection could be alleviated by inhibiting GRP78 through a mechanism that involves IFN-α induction of ER stress-related cell death by reducing the unfolded protein response (UPR), with GRP78 promoting high UPR expression and reducing IFN-α-mediated liver injury in mice (74). Zhang et al. found that peroxisome proliferator-activated receptor α (PPARα) can improve liver injury caused by ALF; the mechanism is mainly to reduce hepatocyte apoptosis by regulating endoplasmic reticulum stress and reducing the expression of GRP78, GRP94, and other proteins (75). According to Blas-Valdivia et al., hypothyroidism reduces cell damage caused by endoplasmic reticulum stress and redox environment changes in an ALF rat model, which might be due to inhibition or decreased protein activation pathways, such as GRP78 (76).

Finally, there are two common HSPs, HSP40 and HSP60, that act as injury factors during acute liver injury or liver failure and play an important role in regulating the acute inflammatory response of the liver. A long-term treatment with isoniazid leads to severe liver injury and ALF. Verma et al. reported the following: the mechanism is that isoniazid prevents Nrf2 translocation and induces oxidative stress and apoptosis by inhibiting ERK1 phosphorylation, thus increasing levels of the stress proteins HSP40 and HSP60 (114). Hu et al. found that chlorogenic acid (CGA) reduces the infiltration of immune cells in the liver, prevents increases in HMGB1 and HSP60, and regulates the Nrf2-mediated HSP60 pathway to alleviate acute liver injury induced by acetaminophen in mice (77).

Studies of the HSP family in ALF/ACLF are relatively scarce, and the role of HSPs in the process of liver tissue injury remains unclear. Due to the lack of basic experiments, more research on HSPs is needed to clarify the mechanism.

3.3 Histones

Histones are an important structural component of eukaryotic chromatin that help regulate gene transcription. Histones are considered key mediators of systemic inflammatory diseases; induce endothelial injury and platelet aggregation and activate coagulation and cytokine production; and may cause sepsis, severe trauma, vasculitis, and acute liver, kidney, brain, and lung injury (115). Silvestre-Roig et al. found that the extracellular histone H4-mediated membrane lysis of smooth muscle cells (SMCs) triggers arterial tissue damage in atherosclerotic mice and attracts neutrophils to exacerbate the inflammatory response and that neutralizing histone H4 can prevent SMC death and stabilize atherosclerotic lesions (116). Ray-Gallet et al. summarized the potential oncogenic roles of histones H3 and H4 and their chaperones in several cancers, indicating that they stimulate the epithelial–mesenchymal transition (EMT) in various ways or the alternative lengthening of telomeres (ALT) pathway to promote tumor progression, illustrating their potential clinical application as biomarkers (117). Despite increasing attention on histone H3, only a few studies have explored the importance of H4 and its chaperones or ways to inhibit their action as a new therapeutic strategy (118).

In recent years, increasing attention has been given to the role of histones as DAMP molecules in acute liver injury, ALF, and ACLF to find potential new biomarkers and therapeutic targets. Extracellular histones, especially H4, have been recognized as important mediators of cell injury under various inflammatory conditions. High expression of extracellular histones is closely related to the development of inflammation in acute liver injury and acute liver failure.

In the ALF mouse model of Ferriero et al., pyruvate dehydrogenase complex (PDHC) and lactate dehydrogenase (LDH) are transferred to the nucleus, which leads to an increase in acetyl coenzyme A and lactic acid concentrations in the nucleus and promotes acetylation of histone H3 and expression of injury-related genes. However, liver injury in ALF mice can be reduced and the survival rate improved by the enzyme inhibitors gamboge and galloflavin (54). Wen et al. (49) and Yang et al. (50) both showed that extracellular histones increase to different degrees in ALF patients and ALF mice, demonstrating that extracellular histones are the main mediator inducing systemic inflammation, cell damage, and multiple-organ failure. Clinical studies by Li et al. highlighted that compared to levels in chronic hepatitis B (CHB), liver cirrhosis, and healthy control groups, plasma histone H4 levels in HBV-ACLF patients are significantly increased, aggravating cell injury and systemic inflammation, and are significantly related to disease severity, systemic inflammation, and outcomes (51). Ding

et al. found that the Qing Chang Li Gan formula (QCLGF) is a good traditional Chinese medicine for treating ACLF, which may be due to its ability to interfere with extracellular histone-mediated cell damage and systemic inflammation. In one study, extracellular histones and proinflammatory cytokines in ACLF patients (conventional drugs + QCLGF) were lower than those in the conventional drug treatment group. *In vivo* experiments have revealed that QCLGF significantly improves the survival rate of concanavalin A-induced liver fibrosis mice, improves hepatotoxicity, and reduces extracellular histone levels and proinflammatory reactions (55).

Histone methylation, phosphorylation, and acetylation are markers of gene transcriptional status in several diseases, and different posttranslational modification patterns are related to some inflammatory diseases (119). Jin et al. found that the whole-genome histone H3 lysine 9 acetylation analysis of $CD4^+$ T cells indicated endoplasmic reticulum stress defects in ACLF patients, which provided a useful clue for further study of the pathogenesis of ACLF (52). Zhang et al.'s research showed that trichostatin A (TSA) reduces the activity of histone deacetylase inhibitors (HDACs) in liver tissue, promotes histone acetylation, inhibits release of various proinflammatory cytokines (TNF-α, IFN-γ, IL-10, and IL-18), and improves the survival rate of ACLF model rats (53).

Although studies of extracellular H3 and H4 in ALF and ACLF are rare and the mechanism is still unclear, some experiments have shown that extracellular histones play an irreplaceable role in liver injury. The importance of histones as proinflammatory proteins in ALF and ACLF should be further explored.

3.4 High-Mobility Group Box Chromosomal Protein 1

HMGB1 is a non-histone chromatin-related protein that is widely distributed in eukaryotic cells. A DAMP, HMGB1 is actively secreted by immunocompetent cells or passively released from apoptotic necrotic cells, which activates the immune response and promotes inflammation and cancer development (120). HMGB1 transmits danger signals by binding with various receptors, thus intensifying a series of cellular reactions that are closely related to inflammatory diseases, autoimmune diseases, and cancer (121). Extracellular HMGB1 transmits danger signals to surrounding cells by interacting with its classical receptors. For example, HMGB1 can bind to the receptor for advanced glycation end products (RAGE) (122) and induce inflammation together with Toll-like receptor 2/4/9 (TLR-2/4/9) (25, 123, 124). HMGB1 is released from damaged host cells and activates PRRs (such as RAGE), which upregulates the expression of NLRP3 and IL-1β precursors, activating the NLRP3 inflammasome and binding with IL-1β to exacerbate immune cell-induced inflammation and cellular damage, which then accelerates cancer progression (125, 126).

In recent years, HMGB1 has been studied in ALF, ALI, ACLF, and CLI, although only the relationship between HMGB1 and ACLF is summarized here. HMGB1 is an important proinflammatory molecule in many inflammatory diseases, but its role in ACLF is not completely clear. The existence of HMGB1 is strongly associated with early liver injury, immune activation, and further immune injury during ACLF.

Some clinical experiments showed that increases in serum or tissue HMGB1 levels correlate positively with the occurrence and development of ACLF inflammation. A meta-analysis of 16 studies by Hu et al. revealed that the serum level of HMGB1 in patients with severe HBV and HBV-ACLF is higher than that in patients with mild and moderate hepatitis, and it was speculated that HMGB1 might be an important diagnostic target for ACLF (56). Jhun et al. showed that the expression of HMGB1, RAGE, and IL-17 increased in the liver tissue of severe HBV patients. IL-17 expression induced by the HMGB1/RAGE axis further aggravates the inflammatory reaction of peripheral blood cells in HBV patients, and downregulation of the HMGB1/RAGE axis may effectively reduce the inflammatory reaction (57). According to Cai et al., compared with levels in the healthy control, liver fibrosis, and CHB groups, the serum HMGB1 levels of ACLF patients are significantly increased, suggesting that HMGB1 can provide diagnostic or prognostic information for HBV-related ACLF (58). However, Wu et al. found levels of proinflammatory cytokines to be significantly increased in ACLF patients, whereas serum HMGB1 levels did not change (67).

The mechanism by which HMGB1 participates in the occurrence of ACLF has been partially confirmed. Xu et al. found that HMGB1 mainly exists in bile duct cells. HMGB1 begins to increase gradually at 4 h after stimulation with LPS or TNF-α in cholangiocarcinoma cell TFK-1 culture until the end of stimulation. Due to ischemia and hypoxia, inflammatory stimulation leads to the death of initial hepatocytes and release of HMGB1, demonstrating that HMGB1 plays a key role in the systemic inflammation related to ACLF (59). Gao et al. reported that the protective effect of the recombinant Ad-HGF-HIL-6 adenovirus with hyper-IL-6 and hepatocyte growth factor can significantly reduce serum HMGB1 and other proteins in ACLF rats as well as liver injury and apoptosis activity (61). Xu et al. found that levels of the serum proinflammatory cytokines IL-22, IL-6, and HMGB1 are significantly decreased in ACLF mice treated with a lncRNA-rich transcript-1 (NEAT1)-related adenovirus because NEAT1 blocks TRAF6 ubiquitination in an ACLF rat model to inhibit the inflammatory response (62). Wang et al. reported that ethyl pyruvate significantly improves liver histopathology and reduces levels of serum endotoxin, inflammatory cytokines, and HMGB1 in liver tissue (63); Fang et al. reported that quercetin reduces oxidative stress and apoptosis by inhibiting HMGB1 and its translocation, thus alleviating liver injury in ACLF rats (64); and Yang et al. reported that plasma-soluble T-cell immunoglobulin and mucin-domain-containing molecule-3 (sTim-3) are significantly increased in ACLF and inhibit the release of HMGB1, alleviating inflammatory reactions and liver injury by promoting autophagy and regulating monocyte/macrophage function (65). The latest research results of Hou et al. (2021) revealed that the thermal apoptosis of hepatocytes induced by HMGB1 enhances the inflammatory reaction to aggravate ACLF and that inhibiting HMGB1 *in vivo* obviously improves liver function and coagulation function in ACLF rats, indicating that it is a potential therapeutic target for ACLF treatment (66).

In conclusion, the mechanism of action of HMGB1 in ACLF is not yet fully understood. Blocking the production of HMGB1 with certain drugs or small-molecule preparations can reduce the inflammatory response in the process of ACLF, which may be a new targeted therapeutic strategy for ACLF.

3.5 S100 Protein

The S100 protein family is the key mediator for initiating and maintaining inflammation, not only amplifying the initial inflammatory signal and inducing inflammatory reactions but also slowing inflammation, promoting tissue repair, and regulating inflammation, cell proliferation and differentiation, energy metabolism, apoptosis, calcium homeostasis, cytoskeletal functions, and microbial resistance under certain conditions. This family is also becoming a new diagnostic marker for identifying and monitoring various diseases (108). The S100 protein is released by a variety of cells in the inflammatory state to promote the expression of inflammation-related genes and cell damage effects, among which S100A12 was the first S100 protein identified as a RAGE ligand (34). ACLF research has mainly focused on serological experiments, and the mechanism involved remains to be further elucidated.

Early studies revealed that serum S100b levels in fulminant hepatitis patients and ACLF patients are higher than those in cirrhosis patients and normal controls and unrelated to survival time (95). Another study showed that compared with 13 cirrhosis patients without HE and 8 healthy subjects, blood levels of S100b in most of the 35 ALF patients studied were increased but unrelated to the survival rate (93). Later, some scholars found that serum S100b is a useful marker of HE in fulminant hepatitis patients (96). Serum S100A12 may reflect the oxidative stress and inflammation levels of HBV-ACLF patients, and an increase in S100A12 may be an important biological index of poor prognosis (58). Others have found that M2 macrophages can alleviate liver injury and play a protective role in ACLF mice by inhibiting the S100A9 protein-related necrotic inflammation axis, which provides new insight for the treatment of ACLF patients (98). In addition, in children with pediatric acute liver failure (PALF), the serum S100 β level may correlate positively with the severity of the disease (94). Researchers have also found that the serum S100 β level is increased at an early stage in animal ALF models and may be used as a marker of HE (97).

On the basis of clinical experiments, S100 proteins can be used as new potential inflammatory markers of ACLF to assist in the diagnosis or assess the prognosis of ACLF.

3.6 Mitochondrial DNA

In recent years, mtDNA, as a DAMP molecule, has been increasingly studied in the context of cell damage. As a proinflammatory mediator, its mechanism in many inflammatory diseases has also been discussed. For example, Tumburu et al. found that mtDNA is a proinflammatory DAMP molecule in sickle cell disease (127) and Todkar et al. reported that mtDNA can enhance the proinflammatory effect in vesicles (116). Zhang et al. reported that mtDNA is greatly increased in systemic inflammatory response syndrome (SIRS), promoting MAPK activity, increasing Ca^{2+} flux and phosphorylation, inducing neutrophil-mediated organ damage, and leading to death in patients by binding with TLR9 and activating human polymorphonuclear neutrophils (PMNs) (117). mtDNA is of concern in genetic diseases and systemic diseases, and its level is related to the severity of inflammation. However, there are few studies on the role of mtDNA in ALF or ACLF.

When hepatocyte damage leads to mitochondrial dysfunction, mtDNA is damaged, consumed, and released into the blood circulation from cells and triggers an inflammatory reaction through TLR9, the inflammatory corpuscle, and the stimulator of interferon genes (STING) pathways, which aggravates hepatocyte damage and even multiple-organ dysfunction (128). McGill et al. reported that compared with survivors, the group of APAP-induced ALF patients who died had higher serum mtDNA levels and that mtDNA could be used as a good biomarker to predict prognosis (99). The mtDNA of DAMPs can be released into the tissue environment by necrotic hepatocytes during liver injury, and free mtDNA can promote the development of inflammation and lead to ACLF by interacting with cyclic GMP-AMP synthase (cGAS) to induce IFN (100). He et al. found that APAP can significantly increase serum mtDNA levels in ALF mice and that mtDNA in necrotic hepatocytes triggers TLR9 on neutrophils, induces expression and infiltration of proinflammatory mediators, and aggravates liver injury (101).

As an inflammatory mediator in the process of hepatocyte injury, mtDNA has received significant attention, but further research is needed to find a stable inflammatory marker for the early diagnosis of ALF or ACLF.

4 SUMMARY AND PERSPECTIVES

Currently, liver transplantation is the most effective treatment for ACLF, but its use is limited by the number of donors. Therefore, finding a treatment that limits excessive systemic inflammation without inducing immunosuppression is important for ACLF treatment. The danger signal theory states that the death of tissue cells causes immune cell activation and release of a large number of cytokines, increases immune damage to organs, and eventually leads to systemic inflammation. Early inflammatory mediators such as TNF-α, IL-1β, IL-17, and IFN-γ are important cytokines leading to ACLF, and DAMPs such as HMGB1 and IL-33 have been shown to regulate early inflammatory mediators through the NF-kB signaling pathway. IL-33 enhances the ability of Tc cells to secrete IFN-γ, NK cells to secrete IL-12, and DCs to secrete TNF-α and IL-1β by binding to ST2 on the surface of immune cells. TNF-α and HMGB1 synergistically promote D-galactosamine/LPS-induced acute lethal liver injury, and blocking TNF-α and HMGB1 synergistically improves liver injury (129) while promoting histone acetylation, inhibiting release of a variety of proinflammatory cytokines (TNF-α, IFN-γ, IL-10, IL-18) (53). DAMP-related molecules have been confirmed to be expressed abnormally in ACLF patients, and IL-33, sST2 (28, 30, 32, 106), and HMGB1 (58) have also been found to be single biomarkers

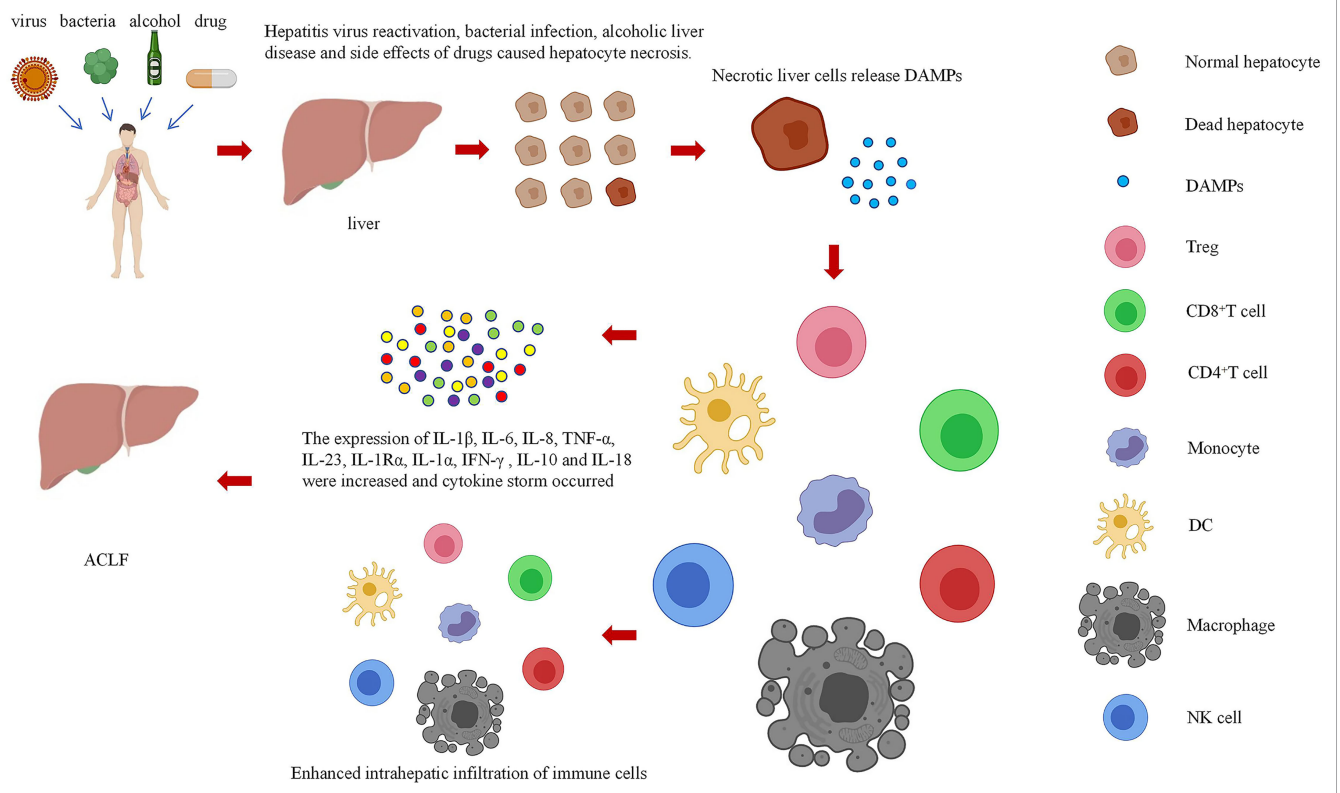

FIGURE 2 | Relationships among cell necrosis, DAMPs, and ACLF.

that predict the prognosis of ACLF. There is currently no ACLF therapy targeting DAMPs, but neutralization of IL-33 (130) using sST2, HMGB1, and IL-33-blocking antibodies (131–133) and TSA-acetylated histones (53) can effectively reduce the inflammatory cytokine storm caused by DAMPs, which shows the potential of ACLF precision immune diagnosis and treatment targeting DAMPs.

In this paper, the relationship between DAMPs and ACLF in the danger hypothesis is systematically analyzed, the possible mechanism of DAMPs participating in the immune mechanism of ACLF is explored, and the role of DAMPs in the occurrence of ACLF is studied systematically and deeply by summarizing various methods related to ACLF research. DAMPs mainly result in the occurrence of ACLF by increasing the infiltration of immune cells into the liver and causing a cytokine storm (**Figure 2**). However, the mechanism of these pathways remains unclear, and research is still in the stages of *in vivo* and *in vitro* experiments. Regarding some of the research results, there are still disputes, and the safety and effectiveness need to be further studied. Therefore, it is necessary to further explore the mechanism of the involvement of DAMPs in ACLF.

ACLF is a disease model of systemic inflammation, and studies on the interaction between DAMPs and ACLF will add value to the study of innate immunology and adaptive immune responses that can be extended to other inflammatory diseases beyond ACLF. Furthermore, ACLF serves as a suitable disease model to study the mechanisms of systemic inflammation and tissue damage, as the relationship of each immune cell to DAMPs during ACLF development is poorly understood. With the development of new research tools, such as single-cell RNA-seq and other cutting-edge technologies, the immunological characteristics of ACLF development will be further determined, and how DAMPs affect immune cell polarization and their subsequent effects on ACLF will be revealed. In conclusion, we conducted a literature review of DAMPs and their interactions in ACLF to increase, updating our understanding of this research area and providing new ideas for finding an appropriate immune intervention for ACLF.

AUTHOR CONTRIBUTIONS

All authors listed have made a substantial, direct, and intellectual contribution to the work, and approved it for publication.

FUNDING

This work was funded by the National Natural Science Foundation (grant number 81900577) and the Science and Technology Plan of Suzhou, China (grant numbers SYS2020192 and GSWS2019067).

REFERENCES

1. Stravitz RT, Lee WM. Acute Liver Failure. *Lancet.* (2019) 394(10201):869–81. doi: 10.1016/s0140-6736(19)31894-x
2. Shah SC, Shah SR, Amarapurkar DN. Subacute Liver Failure. *Lancet.* (1993) 342(8879):1119. doi: 10.1016/0140-6736(93)92105-3
3. Arroyo V, Moreau R, Jalan R. Acute-On-Chronic Liver Failure. *N Engl J Med* (2020) 382(22):2137–45. doi: 10.1056/NEJMra1914900
4. Singanayagam A, Triantafyllou E. Macrophages in Chronic Liver Failure: Diversity, Plasticity and Therapeutic Targeting. *Front Immunol* (2021) 12:661182. doi: 10.3389/fimmu.2021.661182
5. Guideline for Diagnosis and Treatment of Liver Failure. *Clin Hepatobiliary Dis* (2019) 35(01):38–44. doi: 10.3760/cma.j.issn.1674-2397.2018.06.001
6. Moreau R, Jalan R, Gines P, Pavesi M, Angeli P, Cordoba J, et al. Acute-On-Chronic Liver Failure is a Distinct Syndrome That Develops in Patients With Acute Decompensation of Cirrhosis. *Gastroenterology.* (2013) 144 (7):1426–37. doi: 10.1053/j.gastro.2013.02.042
7. Bajaj JS, O'Leary JG, Reddy KR, Wong F, Biggins SW, Patton H, et al. Survival in Infection-Related Acute-on-Chronic Liver Failure Is Defined by Extrahepatic Organ Failures. *Hepatology.* (2014) 60(1):250–6. doi: 10.1002/hep.27077
8. Sarin SK, Kumar A, Almeida JA, Chawla YK, Fan ST, Garg H, et al. Acute-On-Chronic Liver Failure: Consensus Recommendations of the Asian Pacific Association for the Study of the Liver (APASL). *Hepatol Int* (2009) 3(1):269–82. doi: 10.1007/s12072-008-9106-x
9. Sarin SK, Kedarisetty CK, Abbas Z, Amarapurkar D, Bihari C, Chan AC, et al. Acute-On-Chronic Liver Failure: Consensus Recommendations of the Asian Pacific Association for the Study of the Liver (APASL) 2014. *Hepatol Int* (2014) 8(4):453–71. doi: 10.1007/s12072-014-9580-2
10. Sarin SK, Choudhury A, Sharma MK, Maiwall R, Al Mahtab M, Rahman S, et al. Acute-On-Chronic Liver Failure: Consensus Recommendations of the Asian Pacific Association for the Study of the Liver (APASL): An Update. *Hepatol Int* (2019) 13(4):353–90. doi: 10.1007/s12072-019-09946-3
11. Arroyo V, Moreau R, Kamath PS, Jalan R, Ginès P, Nevens F, et al. Acute-On-Chronic Liver Failure in Cirrhosis. *Nat Rev Dis Primers* (2016) 2:16041. doi: 10.1038/nrdp.2016.41
12. Sarin SK, Choudhury A. Acute-On-Chronic Liver Failure: Terminology, Mechanisms and Management. *Nat Rev Gastroenterol Hepatol* (2016) 13 (3):131–49. doi: 10.1038/nrgastro.2015.219
13. Zaccherini G, Weiss E, Moreau R. Acute-On-Chronic Liver Failure: Definitions, Pathophysiology and Principles of Treatment. *JHEP Rep* (2021) 3(1):100176. doi: 10.1016/j.jhepr.2020.100176
14. Wu Z, Han M, Chen T, Yan W, Ning Q. Acute Liver Failure: Mechanisms of Immune-Mediated Liver Injury. *Liver Int* (2010) 30(6):782–94. doi: 10.1111/j.1478-3231.2010.02262.x
15. Zou Z, Li B, Xu D, Zhang Z, Zhao JM, Zhou G, et al. Imbalanced Intrahepatic Cytokine Expression of Interferon-Gamma, Tumor Necrosis Factor-Alpha, and Interleukin-10 in Patients With Acute-on-Chronic Liver Failure Associated With Hepatitis B Virus Infection. *J Clin Gastroenterol* (2009) 43(2):182–90. doi: 10.1097/MCG.0b013e3181624464
16. Liu XY, Shi F, Zhao H, Wang HF. [Research of PD-1 Expression in CD8+ T Cell of Peripheral Blood With HBV-Associated Acute-on-Chronic Liver Failure]. *Zhonghua Shi Yan He Lin Chuang Bing Du Xue Za Zhi.* (2010) 24 (2):125–7. doi: 10.3760/cma.j.issn.1003-9279.2010.02.016
17. Zhang Z, Zou ZS, Fu JL, Cai L, Jin L, Liu YJ, et al. Severe Dendritic Cell Perturbation Is Actively Involved in the Pathogenesis of Acute-on-Chronic Hepatitis B Liver Failure. *J Hepatol* (2008) 49(3):396–406. doi: 10.1016/j.jhep.2008.05.017
18. Yang J, Yi P, Wei L, Xu Z, Chen Y, Tang L, et al. Phenotypes and Clinical Significance of Circulating CD4(+)CD25(+) Regulatory T Cells (Tregs) in Patients With Acute-on-Chronic Liver Failure (ACLF). *J Transl Med* (2012) 10:193. doi: 10.1186/1479-5876-10-193
19. Dong X, Gong Y, Zeng H, Hao Y, Wang X, Hou J, et al. Imbalance Between Circulating CD4+ Regulatory T and Conventional T Lymphocytes in Patients With HBV-Related Acute-on-Chronic Liver Failure. *Liver Int* (2013) 33(10):1517–26. doi: 10.1111/liv.12248
20. Lv H, Pan Z, Hu S, Chen Y, Zhuang Q, Yao X, et al. Relationship Between CD4+CD25+Treg Cells, Th17 Cells and IL-6 and the Prognosis of Hepatitis B Virus-Related Acute-on-Chronic Liver Failure: A Meta-Analysis. *Zhonghua Gan Zang Bing Za Zhi.* (2014) 22(7):493–8. doi: 10.3760/cma.j.issn.1007-3418.2014.07.004
21. Tan W, Xia J, Dan Y, Li M, Lin S, Pan X, et al. Genome-Wide Association Study Identifies HLA-DR Variants Conferring Risk of HBV-Related Acute-on-Chronic Liver Failure. *Gut.* (2018) 67(4):757–66. doi: 10.1136/gutjnl-2016-313035
22. Gao ZN, Ye YN. Triple Attack Theory in the Process of Liver Failure. In: *The Fifth International and National Conference on Liver Failure and Artificial Liver*. Fuzhou, Fujian, China:Science and Technology Association of Zhejiang Province (2009).
23. Matzinger P. Tolerance, Danger, and the Extended Family. *Annu Rev Immunol* (1994) 12:991–1045. doi: 10.1146/annurev.iy.12.040194.005015
24. Matzinger P. The Danger Model: A Renewed Sense of Self. *Science.* (2002) 296(5566):301–5. doi: 10.1126/science.1071059
25. Kono H, Rock KL. How Dying Cells Alert the Immune System to Danger. *Nat Rev Immunol* (2008) 8(4):279–89. doi: 10.1038/nri2215
26. Bertheloot D, Latz E. HMGB1, IL-1α, IL-33 and S100 Proteins: Dual-Function Alarmins. *Cell Mol Immunol* (2017) 14(1):43–64. doi: 10.1038/cmi.2016.34
27. Patel S. Danger-Associated Molecular Patterns (DAMPs): The Derivatives and Triggers of Inflammation. *Curr Allergy Asthma Rep* (2018) 18(11):63. doi: 10.1007/s11882-018-0817-3
28. Roth GA, Zimmermann M, Lubsczyk BA, Pilz J, Faybik P, Hetz H, et al. Up-Regulation of Interleukin 33 and Soluble ST2 Serum Levels in Liver Failure. *J Surg Res* (2010) 163(2):e79–83. doi: 10.1016/j.jss.2010.04.004
29. Lei Z, Mo Z, Zhu J, Pang X, Zheng X, Wu Z, et al. Soluble ST2 Plasma Concentrations Predict Mortality in HBV-Related Acute-on-Chronic Liver Failure. *Mediators Inflamm* (2015) 2015:535938. doi: 10.1155/2015/535938
30. Jiang SW, Wang P, Xiang XG, Mo RD, Lin LY, Bao SS, et al. Serum Soluble ST2 Is a Promising Prognostic Biomarker in HBV-Related Acute-on-Chronic Liver Failure. *Hepatobiliary Pancreat Dis Int* (2017) 16(2):181–88. doi: 10.1016/s1499-3872(16)60185-6
31. Du XX, Shi Y, Yang Y, Yu Y, Lou HG, Lv FF, et al. DAMP Molecular IL-33 Augments Monocytic Inflammatory Storm in Hepatitis B-Precipitated Acute-on-Chronic Liver Failure. *Liver Int* (2018) 38(2):229–38. doi: 10.1111/liv.13503
32. Yuan W, Mei X, Zhang YY, Zhang ZG, Zou Y, Zhu H, et al. High Expression of Interleukin-33/ST2 Predicts the Progression and Poor Prognosis in Chronic Hepatitis B Patients With Hepatic Flare. *Am J Med Sci* (2020) 360(6):656–61. doi: 10.1016/j.amjms.2020.06.023
33. Yu X, Guo R, Ming D, Deng Y, Su M, Lin C, et al. The Transforming Growth Factor β1/Interleukin-31 Pathway Is Upregulated in Patients With Hepatitis B Virus-Related Acute-On-Chronic Liver Failure and Is Associated With Disease Severity and Survival. *Clin Vaccine Immunol* (2015) 22(5):484–92. doi: 10.1128/cvi.00649-14
34. Praktiknjo M, Monteiro S, Grandt J, Kimer N, Madsen JL, Werge MP, et al. Cardiodynamic State Is Associated With Systemic Inflammation and Fatal Acute-on-Chronic Liver Failure. *Liver Int* (2020) 40(6):1457–66. doi: 10.1111/liv.14433
35. Kotsiou OS, Gourgoulianis KI, Zarogiannis SG. IL-33/ST2 Axis in Organ Fibrosis. *Front Immunol* (2018) 9:2432. doi: 10.3389/fimmu.2018.02432
36. Cai SY, Ge M, Mennone A, Hoque R, Ouyang X, Boyer JL. Inflammasome Is Activated in the Liver of Cholestatic Patients and Aggravates Hepatic Injury in Bile Duct-Ligated Mouse. *Cell Mol Gastroenterol Hepatol* (2020) 9(4):679–88. doi: 10.1016/j.jcmgh.2019.12.008
37. Arshad MI, Piquet-Pellorce C, L'Helgoualc'h A, Rauch M, Patrat-Delon S, Ezan F, et al. TRAIL But Not FasL and Tnfα, Regulates IL-33 Expression in Murine Hepatocytes During Acute Hepatitis. *Hepatology.* (2012) 56 (6):2353–62. doi: 10.1002/hep.25893
38. Volarevic V, Mitrovic M, Milovanovic M, Zelen I, Nikolic I, Mitrovic S, et al. Protective Role of IL-33/ST2 Axis in Con A-Induced Hepatitis. *J Hepatol* (2012) 56(1):26–33. doi: 10.1016/j.jhep.2011.03.022
39. Rickard JA, O'Donnell JA, Evans JM, Lalaoui N, Poh AR, Rogers T, et al. RIPK1 Regulates RIPK3-MLKL-Driven Systemic Inflammation and Emergency Hematopoiesis. *Cell.* (2014) 157(5):1175–88. doi: 10.1016/j.cell.2014.04.019
40. Kim SJ, Lee SM. Necrostatin-1 Protects Against D-Galactosamine and Lipopolysaccharide-Induced Hepatic Injury by Preventing TLR4 and

RAGE Signaling. *Inflammation.* (2017) 40(6):1912–23. doi: 10.1007/s10753-017-0632-3
41. Seo MJ, Hong JM, Kim SJ, Lee SM. Genipin Protects D-Galactosamine and Lipopolysaccharide-Induced Hepatic Injury Through Suppression of the Necroptosis-Mediated Inflammasome Signaling. *Eur J Pharmacol* (2017) 812:128–37. doi: 10.1016/j.ejphar.2017.07.024
42. Monteiro S, Grandt J, Uschner FE, Kimer N, Madsen JL, Schierwagen R, et al. Differential Inflammasome Activation Predisposes to Acute-on-Chronic Liver Failure in Human and Experimental Cirrhosis With and Without Previous Decompensation. *Gut.* (2021) 70(2):379–87. doi: 10.1136/gutjnl-2019-320170
43. Alcaraz-Quiles J, Titos E, Casulleras M, Pavesi M, López-Vicario C, Rius B, et al. Polymorphisms in the IL-1 Gene Cluster Influence Systemic Inflammation in Patients at Risk for Acute-on-Chronic Liver Failure. *Hepatology.* (2017) 65(1):202–16. doi: 10.1002/hep.28896
44. Romics LJr., Dolganiuc A, Velayudham A, Kodys K, Mandrekar P, Golenbock D, et al. Toll-Like Receptor 2 Mediates Inflammatory Cytokine Induction But Not Sensitization for Liver Injury by Propioni- Bacterium Acnes. *J Leukoc Biol* (2005) 78(6):1255–64. doi: 10.1189/jlb.0804448
45. Gehrke N, Hövelmeyer N, Waisman A, Straub BK, Weinmann-Menke J, Wörns MA, et al. Hepatocyte-Specific Deletion of IL1-RI Attenuates Liver Injury by Blocking IL-1 Driven Autoinflammation. *J Hepatol* (2018) 68 (5):986–95. doi: 10.1016/j.jhep.2018.01.008
46. Xiao T, Cui Y, Ji H, Yan L, Pei D, Qu S. Baicalein Attenuates Acute Liver Injury by Blocking NLRP3 Inflammasome. *Biochem Biophys Res Commun* (2021) 534:212–18. doi: 10.1016/j.bbrc.2020.11.109
47. Jiang H, Yan R, Wang K, Wang Q, Chen X, Chen L, et al. Lactobacillus Reuteri DSM 17938 Alleviates D-Galactosamine-Induced Liver Failure in Rats. *BioMed Pharmacother* (2021) 133:111000. doi: 10.1016/j.biopha.2020.111000
48. Sultan M, Ben-Ari Z, Masoud R, Pappo O, Harats D, Kamari Y, et al. Interleukin-1α and Interleukin-1β Play a Central Role in the Pathogenesis of Fulminant Hepatic Failure in Mice. *PloS One* (2017) 12(9):e0184084. doi: 10.1371/journal.pone.0184084
49. Wen Z, Lei Z, Yao L, Jiang P, Gu T, Ren F, et al. Circulating Histones are Major Mediators of Systemic Inflammation and Cellular Injury in Patients With Acute Liver Failure. *Cell Death Dis* (2016) 7(9):e2391. doi: 10.1038/cddis.2016.303
50. Yang R, Zou X, Tenhunen J, Tønnessen TI. HMGB1 and Extracellular Histones Significantly Contribute to Systemic Inflammation and Multiple Organ Failure in Acute Liver Failure. *Mediators Inflamm* (2017) 2017:5928078. doi: 10.1155/2017/5928078
51. Li X, Gou C, Yao L, Lei Z, Gu T, Ren F, et al. Patients With HBV-Related Acute-on-Chronic Liver Failure Have Increased Concentrations of Extracellular Histones Aggravating Cellular Damage and Systemic Inflammation. *J Viral Hepat.* (2017) 24(1):59–67. doi: 10.1111/jvh.12612
52. Jin L, Wang K, Liu H, Chen T, Yang Y, Ma X, et al. Genomewide Histone H3 Lysine 9 Acetylation Profiling in CD4+ T Cells Revealed Endoplasmic Reticulum Stress Deficiency in Patients With Acute-On-Chronic Liver Failure. *Scand J Immunol* (2015) 82(5):452–9. doi: 10.1111/sji.12341
53. Zhang Q, Yang F, Li X, Wang LW, Chu XG, Zhang H, et al. Trichostatin A Protects Against Experimental Acute-On-Chronic Liver Failure in Rats Through Regulating the Acetylation of Nuclear Factor-κb. *Inflammation.* (2015) 38(3):1364–73. doi: 10.1007/s10753-014-0108-7
54. Ferriero R, Nusco E, De Cegli R, Carissimo A, Manco G, Brunetti-Pierri N. Pyruvate Dehydrogenase Complex and Lactate Dehydrogenase are Targets for Therapy of Acute Liver Failure. *J Hepatol* (2018) 69(2):325–35. doi: 10.1016/j.jhep.2018.03.016
55. Ding L, Zhang X, Li L, Gou C, Luo X, Yang Y, et al. Qingchangligan Formula Alleviates Acute Liver Injury by Attenuating Extracellular Histone-Associated Inflammation. *BioMed Pharmacother* (2018) 103:140–46. doi: 10.1016/j.biopha.2018.01.121
56. Hu YB, Hu DP, Fu RQ. Correlation Between High Mobility Group Box-1 Protein and Chronic Hepatitis B Infection With Severe Hepatitis B and Acute-on-Chronic Liver Failure: A Meta-Analysis. *Minerva Med* (2017) 108 (3):268–76. doi: 10.23736/s0026-4806.16.04865-5
57. Jhun J, Lee S, Kim H, Her YM, Byun JK, Kim EK, et al. HMGB1/RAGE Induces IL-17 Expression to Exaggerate Inflammation in Peripheral Blood Cells of Hepatitis B Patients. *J Transl Med* (2015) 13:310. doi: 10.1186/s12967-015-0663-1
58. Cai J, Han T, Nie C, Jia X, Liu Y, Zhu Z, et al. Biomarkers of Oxidation Stress, Inflammation, Necrosis and Apoptosis are Associated With Hepatitis B-Related Acute-on-Chronic Liver Failure. *Clin Res Hepatol Gastroenterol* (2016) 40(1):41–50. doi: 10.1016/j.clinre.2015.06.009
59. Xu H, Li H, Qu Y, Zheng J, Lu J. High Mobility Group Box 1 Release From Cholangiocytes in Patients With Acute-on-Chronic Liver Failure. *Exp Ther Med* (2014) 8(4):1178–84. doi: 10.3892/etm.2014.1904
60. He Y, Wang F, Yao N, Wu Y, Zhao Y, Tian Z. Serum Superoxide Dismutase Level Is a Potential Biomarker of Disease Prognosis in Patients With HEV-Induced Liver Failure. *BMC Gastroenterol* (2022) 22(1):14. doi: 10.1186/s12876-022-02095-2
61. Gao DD, Fu J, Qin B, Huang WX, Yang C, Jia B. Recombinant Adenovirus Containing Hyper-Interleukin-6 and Hepatocyte Growth Factor Ameliorates Acute-on-Chronic Liver Failure in Rats. *World J Gastroenterol* (2016) 22(16):4136–48. doi: 10.3748/wjg.v22.i16.4136
62. Xu Y, Cao Z, Ding Y, Li Z, Xiang X, Lai R, et al. Long Non-Coding RNA NEAT1 Alleviates Acute-On-Chronic Liver Failure Through Blocking TRAF6 Mediated Inflammatory Response. *Front Physiol* (2019) 10:1503. doi: 10.3389/fphys.2019.01503
63. Wang LW, Wang LK, Chen H, Fan C, Li X, He CM, et al. Ethyl Pyruvate Protects Against Experimental Acute-on-Chronic Liver Failure in Rats. *World J Gastroenterol* (2012) 18(40):5709–18. doi: 10.3748/wjg.v18.i40.5709
64. Fang P, Dou B, Liang J, Hou W, Ma C, Zhang Q. Quercetin Reduces Oxidative Stress and Apoptosis by Inhibiting HMGB1 and Its Translocation, Thereby Alleviating Liver Injury in ACLF Rats. *Evid Based Complement Alternat Med* (2021) 2021:2898995. doi: 10.1155/2021/2898995
65. Yang Y, Ying G, Wu F, Chen Z. Stim-3 Alleviates Liver Injury *via* Regulation of the Immunity Microenvironment and Autophagy. *Cell Death Discovery* (2020) 6:62. doi: 10.1038/s41420-020-00299-7
66. Hou W, Wei X, Liang J, Fang P, Ma C, Zhang Q, et al. HMGB1-Induced Hepatocyte Pyroptosis Expanding Inflammatory Responses Contributes to the Pathogenesis of Acute-On-Chronic Liver Failure (ACLF). *J Inflammation Res* (2021) 14:7295–313. doi: 10.2147/jir.S336626
67. Wu W, Sun S, Wang Y, Zhao R, Ren H, Li Z, et al. Circulating Neutrophil Dysfunction in HBV-Related Acute-On-Chronic Liver Failure. *Front Immunol* (2021) 12:620365. doi: 10.3389/fimmu.2021.620365
68. Li J, Zhang Q, Gao L, Du Y, Chen Y. Efficacy of Decoction From Jieduan Niwan Formula on Rat Model of Acute-on-Chronic Liver Failure Induced by Porcine Serum. *J Tradit Chin Med* (2020) 40(4):602–12. doi: 10.19852/j.cnki.jtcm.2020.04.009
69. Vidyasagar A, Wilson NA, Djamali A. Heat Shock Protein 27 (HSP27): Biomarker of Disease and Therapeutic Target. *Fibrogenesis Tissue Repair* (2012) 5(1):7. doi: 10.1186/1755-1536-5-7
70. El-Baz FK, Elgohary R, Salama A. Amelioration of Hepatic Encephalopathy Using Dunaliella Salina Microalgae in Rats: Modulation of Hyperammonemia/Tlr4. *BioMed Res Int* (2021) 2021:8843218. doi: 10.1155/2021/8843218
71. Nwe Win N, Kanda T, Nakamura M, Nakamoto S, Okamoto H, Yokosuka O, et al. Free Fatty Acids or High-Concentration Glucose Enhances Hepatitis A Virus Replication in Association With a Reduction in Glucose-Regulated Protein 78 Expression. *Biochem Biophys Res Commun* (2017) 483(1):694–99. doi: 10.1016/j.bbrc.2016.12.080
72. Ren F, Shi H, Zhang L, Zhang X, Wen T, Xie B, et al. The Dysregulation of Endoplasmic Reticulum Stress Response in Acute-on-Chronic Liver Failure Patients Caused by Acute Exacerbation of Chronic Hepatitis B. *J Viral Hepat.* (2016) 23(1):23–31. doi: 10.1111/jvh.12438
73. Ye S, Zhang C, Zhou J, Cheng J, Lv Z, Zhou L, et al. Human Heat Shock Protein 27 Exacerbates Ischemia Reperfusion Injury in Rats by Reducing the Number of T Regulatory Cells. *Mol Med Rep* (2014) 9(5):1998–2002. doi: 10.3892/mmr.2014.2032
74. Baudi I, Isogawa M, Moalli F, Onishi M, Kawashima K, Ishida Y, et al. Interferon Signaling Suppresses the Unfolded Protein Response and Induces Cell Death in Hepatocytes Accumulating Hepatitis B Surface Antigen. *PloS Pathog* (2021) 17(5):e1009228. doi: 10.1371/journal.ppat.1009228
75. Zhang L, Ren F, Zhang X, Wang X, Shi H, Zhou L, et al. Peroxisome Proliferator-Activated Receptor Alpha Acts as a Mediator of Endoplasmic

Reticulum Stress-Induced Hepatocyte Apoptosis in Acute Liver Failure. *Dis Model Mech* (2016) 9(7):799–809. doi: 10.1242/dmm.023242
76. Blas-Valdivia V, Cano-Europa E, Martinez-Perez Y, Lezama-Palacios R, Franco-Colin M, Ortiz-Butron R. Hypothyroidism Minimizes the Effects of Acute Hepatic Failure Caused by Endoplasmic Reticulum Stress and Redox Environment Alterations in Rats. *Acta Histochem* (2015) 117(8):811–9. doi: 10.1016/j.acthis.2015.07.003
77. Hu F, Guo Q, Wei M, Huang Z, Shi L, Sheng Y, et al. Chlorogenic Acid Alleviates Acetaminophen-Induced Liver Injury in Mice *via* Regulating Nrf2-Mediated HSP60-Initiated Liver Inflammation. *Eur J Pharmacol* (2020) 883:173286. doi: 10.1016/j.ejphar.2020.173286
78. Oda H, Miyake H, Iwata T, Kusumoto K, Rokutan K, Tashiro S. Geranylgeranylacetone Suppresses Inflammatory Responses and Improves Survival After Massive Hepatectomy in Rats. *J Gastrointest Surg* (2002) 6 (3):464–72. doi: 10.1016/s1091-255x(01)00043-9
79. Kanemura H, Kusumoto K, Miyake H, Tashiro S, Rokutan K, Shimada M. Geranylgeranylacetone Prevents Acute Liver Damage After Massive Hepatectomy in Rats Through Suppression of a CXC Chemokine GRO1 and Induction of Heat Shock Proteins. *J Gastrointest Surg* (2009) 13(1):66–73. doi: 10.1007/s11605-008-0604-x
80. Kawashima Y, Hisaka T, Horiuchi H, Ishikawa H, Uchida S, Kinugasa T, et al. The Organo- and Cytoprotective Effects of Heat-Shock Protein in Response to Injury Due to Radiofrequency Ablation in Rat Liver. *Anticancer Res* (2016) 36(7):3591–7.
81. Peppler WT, Anderson ZG, Sutton CD, Rector RS, Wright DC. Voluntary Wheel Running Attenuates Lipopolysaccharide-Induced Liver Inflammation in Mice. *Am J Physiol Regul Integr Comp Physiol* (2016) 310 (10):R934–42. doi: 10.1152/ajpregu.00497.2015
82. Sumioka I, Matsura T, Kai M, Yamada K. Potential Roles of Hepatic Heat Shock Protein 25 and 70i in Protection of Mice Against Acetaminophen-Induced Liver Injury. *Life Sci* (2004) 74(20):2551–61. doi: 10.1016/j.lfs.2003.10.011
83. Carvalho NR, Tassi CC, Dobraschinski F, Amaral GP, Zemolin AP, Golombieski RM, et al. Reversal of Bioenergetics Dysfunction by Diphenyl Diselenide Is Critical to Protection Against the Acetaminophen-Induced Acute Liver Failure. *Life Sci* (2017) 180:42–50. doi: 10.1016/j.lfs.2017.05.012
84. Togo S, Chen H, Takahashi T, Kubota T, Matsuo K, Morioka D, et al. Prostaglandin E1 Improves Survival Rate After 95% Hepatectomy in Rats. *J Surg Res* (2008) 146(1):66–72. doi: 10.1016/j.jss.2007.05.003
85. Chen X, Zhang J, Han C, Dai H, Kong X, Xu L, et al. A Sexual Dimorphism Influences Bicyclol-Induced Hepatic Heat Shock Factor 1 Activation and Hepatoprotection. *Mol Pharmacol* (2015) 88(1):38–47. doi: 10.1124/mol.114.097584
86. Dai HJ, Li DW, Wang YX, Sun AJ, Lu YX, Ding X, et al. Induction of Heat Shock Protein 27 by Bicyclol Attenuates D-Galactosamine/Lipopolysaccharide-Induced Liver Injury. *Eur J Pharmacol* (2016) 791:482–90. doi: 10.1016/j.ejphar.2016.09.002
87. Wright GA, Sharifi Y, Newman TA, Davies N, Vairappan B, Perry HV, et al. Characterisation of Temporal Microglia and Astrocyte Immune Responses in Bile Duct-Ligated Rat Models of Cirrhosis. *Liver Int* (2014) 34(8):1184–91. doi: 10.1111/liv.12481
88. Win NN, Kanda T, Nakamoto S, Moriyama M, Jiang X, Suganami A, et al. Inhibitory Effect of Japanese Rice-Koji Miso Extracts on Hepatitis A Virus Replication in Association With the Elevation of Glucose-Regulated Protein 78 Expression. *Int J Med Sci* (2018) 15(11):1153–59. doi: 10.7150/ijms.27489
89. Wang H, Chen L, Zhang X, Xu L, Xie B, Shi H, et al. Kaempferol Protects Mice From D-GalN/LPS-Induced Acute Liver Failure by Regulating the ER Stress-Grp78-CHOP Signaling Pathway. *BioMed Pharmacother* (2019) 111:468–75. doi: 10.1016/j.biopha.2018.12.105
90. Hirao H, Dery KJ, Kageyama S, Nakamura K, Kupiec-Weglinski JW. Heme Oxygenase-1 in Liver Transplant Ischemia-Reperfusion Injury: From Bench-to-Bedside. *Free Radic Biol Med* (2020) 157:75–82. doi: 10.1016/j.freeradbiomed.2020.02.012
91. Xue R, Yang J, Jia L, Zhu X, Wu J, Zhu Y, et al. Mitofusin2, as a Protective Target in the Liver, Controls the Balance of Apoptosis and Autophagy in Acute-On-Chronic Liver Failure. *Front Pharmacol* (2019) 10. doi: 10.3389/fphar.2019.00601
92. Arroyo V, Angeli P, Moreau R, Jalan R, Clària J, Trebicka J, et al. The Systemic Inflammation Hypothesis: Towards a New Paradigm of Acute Decompensation and Multiorgan Failure in Cirrhosis. *J Hepatol* (2021) 74 (3):670–85. doi: 10.1016/j.jhep.2020.11.048
93. Vaquero J, Jordano Q, Lee WM, Blei AT. Serum Protein S-100b in Acute Liver Failure: Results of the US Acute Liver Failure Study Group. *Liver Transpl* (2003) 9(8):887–8. doi: 10.1053/jlts.2003.50172
94. Toney NA, Bell MJ, Belle SH, Hardison RM, Rodriguez-Baez N, Loomes KM, et al. Hepatic Encephalopathy in Children With Acute Liver Failure: Utility of Serum Neuromarkers. *J Pediatr Gastroenterol Nutr* (2019) 69 (1):108–15. doi: 10.1097/mpg.0000000000002351
95. Strauss GI, Christiansen M, Møller K, Clemmesen JO, Larsen FS, Knudsen GM. S-100b and Neuron-Specific Enolase in Patients With Fulminant Hepatic Failure. *Liver Transpl* (2001) 7(11):964–70. doi: 10.1053/jlts.2001.28742
96. Isobe-Harima Y, Terai S, Segawa M, Uchida K, Yamasaki T, Sakaida I. Serum S100b (Astrocyte-Specific Protein) Is a Useful Marker of Hepatic Encephalopathy in Patients With Fulminant Hepatitis. *Liver Int* (2008) 28 (1):146–7. doi: 10.1111/j.1478-3231.2007.01604.x
97. Ytrebø LM, Ingebrigtsen T, Nedredal GI, Elvenes OP, Korvald C, Romner B, et al. Protein S-100beta: A Biochemical Marker for Increased Intracranial Pressure in Pigs With Acute Hepatic Failure. *Scand J Gastroenterol* (2000) 35 (5):546–51. doi: 10.1080/003655200750023831
98. Bai L, Kong M, Duan Z, Liu S, Zheng S, Chen Y. M2-Like Macrophages Exert Hepatoprotection in Acute-on-Chronic Liver Failure Through Inhibiting Necroptosis-S100A9-Necroinflammation Axis. *Cell Death Dis* (2021) 12 (1):93. doi: 10.1038/s41419-020-03378-w
99. McGill MR, Staggs VS, Sharpe MR, Lee WM, Jaeschke H. Serum Mitochondrial Biomarkers and Damage-Associated Molecular Patterns are Higher in Acetaminophen Overdose Patients With Poor Outcome. *Hepatology.* (2014) 60(4):1336–45. doi: 10.1002/hep.27265
100. West AP, Khoury-Hanold W, Staron M, Tal MC, Pineda CM, Lang SM, et al. Mitochondrial DNA Stress Primes the Antiviral Innate Immune Response. *Nature.* (2015) 520(7548):553–7. doi: 10.1038/nature14156
101. He Y, Feng D, Li M, Gao Y, Ramirez T, Cao H, et al. Hepatic Mitochondrial DNA/Toll-Like Receptor 9/MicroRNA-223 Forms a Negative Feedback Loop to Limit Neutrophil Overactivation and Acetaminophen Hepatotoxicity in Mice. *Hepatology.* (2017) 66(1):220–34. doi: 10.1002/hep.29153
102. Barbier L, Ferhat M, Salamé E, Robin A, Herbelin A, Gombert JM, et al. Interleukin-1 Family Cytokines: Keystones in Liver Inflammatory Diseases. *Front Immunol* (2019) 10:2014. doi: 10.3389/fimmu.2019.02014
103. Cayrol C, Girard JP. Interleukin-33 (IL-33): A Nuclear Cytokine From the IL-1 Family. *Immunol Rev* (2018) 281(1):154–68. doi: 10.1111/imr.12619
104. Weiskirchen R, Tacke F. Interleukin-33 in the Pathogenesis of Liver Fibrosis: Alarming ILC2 and Hepatic Stellate Cells. *Cell Mol Immunol* (2017) 14 (2):143–45. doi: 10.1038/cmi.2016.62
105. Tan Z, Liu Q, Jiang R, Lv L, Shoto SS, Maillet I, et al. Interleukin-33 Drives Hepatic Fibrosis Through Activation of Hepatic Stellate Cells. *Cell Mol Immunol* (2018) 15(4):388–98. doi: 10.1038/cmi.2016.63
106. Gao S, Huan SL, Han LY, Li F, Ji XF, Li XY, et al. Overexpression of Serum Sst2 Is Associated With Poor Prognosis in Acute-on-Chronic Hepatitis B Liver Failure. *Clin Res Hepatol Gastroenterol* (2015) 39(3):315–23. doi: 10.1016/j.clinre.2014.10.012
107. Frank D, Vince JE. Pyroptosis Versus Necroptosis: Similarities, Differences, and Crosstalk. *Cell Death Differ* (2019) 26(1):99–114. doi: 10.1038/s41418-018-0212-6
108. Sreejit G, Flynn MC, Patil M, Krishnamurthy P, Murphy AJ, Nagareddy PR. S100 Family Proteins in Inflammation and Beyond. *Adv Clin Chem* (2020) 98:173–231. doi: 10.1016/bs.acc.2020.02.006
109. Melchor SJ, Saunders CM, Sanders I, Hatter JA, Byrnes KA, Coutermarsh-Ott S, et al. IL-1r Regulates Disease Tolerance and Cachexia in Toxoplasma Gondii Infection. *J Immunol* (2020) 204(12):3329–38. doi: 10.4049/jimmunol.2000159
110. Wu J, Liu T, Rios Z, Mei Q, Lin X, Cao S. Heat Shock Proteins and Cancer. *Trends Pharmacol Sci* (2017) 38(3):226–56. doi: 10.1016/j.tips.2016.11.009
111. Yun CW, Kim HJ, Lim JH, Lee SH. Heat Shock Proteins: Agents of Cancer Development and Therapeutic Targets in Anti-Cancer Therapy. *Cells.* (2019) 9(1):1–29. doi: 10.3390/cells9010060

112. Vahid S, Thaper D, Gibson KF, Bishop JL, Zoubeidi A. Molecular Chaperone Hsp27 Regulates the Hippo Tumor Suppressor Pathway in Cancer. *Sci Rep* (2016) 6:31842. doi: 10.1038/srep31842
113. Sun G, Cao Y, Xu Y, Huai D, Chen P, Guo J, et al. Overexpression of Hsc70 Promotes Proliferation, Migration, and Invasion of Human Glioma Cells. *J Cell Biochem* (2019) 120(6):10707–14. doi: 10.1002/jcb.28362
114. Verma AK, Yadav A, Dewangan J, Singh SV, Mishra M, Singh PK, et al. Isoniazid Prevents Nrf2 Translocation by Inhibiting ERK1 Phosphorylation and Induces Oxidative Stress and Apoptosis. *Redox Biol* (2015) 6:80–92. doi: 10.1016/j.redox.2015.06.020
115. Allam R, Kumar SV, Darisipudi MN, Anders HJ. Extracellular Histones in Tissue Injury and Inflammation. *J Mol Med (Berl)* (2014) 92(5):465–72. doi: 10.1007/s00109-014-1148-z
116. Todkar K, Chikhi L, Desjardins V, El-Mortada F, Pépin G, Germain M. Selective Packaging of Mitochondrial Proteins Into Extracellular Vesicles Prevents the Release of Mitochondrial DAMPs. *Nat Commun* (2021) 12 (1):1971. doi: 10.1038/s41467-021-21984-w
117. Zhang Q, Raoof M, Chen Y, Sumi Y, Sursal T, Junger W, et al. Circulating Mitochondrial DAMPs Cause Inflammatory Responses to Injury. *Nature.* (2010) 464(7285):104–7. doi: 10.1038/nature08780
118. Morel D, Jeffery D, Aspeslagh S, Almouzni G, Postel-Vinay S. Combining Epigenetic Drugs With Other Therapies for Solid Tumours - Past Lessons and Future Promise. *Nat Rev Clin Oncol* (2020) 17(2):91–107. doi: 10.1038/s41571-019-0267-4
119. Helin K, Dhanak D. Chromatin Proteins and Modifications as Drug Targets. *Nature.* (2013) 502(7472):480–8. doi: 10.1038/nature12751
120. Wang S, Zhang Y. HMGB1 in Inflammation and Cancer. *J Hematol Oncol* (2020) 13(1):116. doi: 10.1186/s13045-020-00950-x
121. Paudel YN, Angelopoulou E, Piperi C, Vrmt B, Othman I, Shaikh MF. Enlightening the Role of High Mobility Group Box 1 (HMGB1) in Inflammation: Updates on Receptor Signalling. *Eur J Pharmacol* (2019) 858:172487. doi: 10.1016/j.ejphar.2019.172487
122. Hudson BI, Lippman ME. Targeting RAGE Signaling in Inflammatory Disease. *Annu Rev Med* (2018) 69:349–64. doi: 10.1146/annurev-med-041316-085215
123. Medzhitov R. Origin and Physiological Roles of Inflammation. *Nature.* (2008) 454(7203):428–35. doi: 10.1038/nature07201
124. Takeuchi O, Akira S. Pattern Recognition Receptors and Inflammation. *Cell.* (2010) 140(6):805–20. doi: 10.1016/j.cell.2010.01.022
125. Lamkanfi M, Dixit VM. Mechanisms and Functions of Inflammasomes. *Cell.* (2014) 157(5):1013–22. doi: 10.1016/j.cell.2014.04.007
126. Sharma BR, Kanneganti TD. NLRP3 Inflammasome in Cancer and Metabolic Diseases. *Nat Immunol* (2021) 22(5):550–59. doi: 10.1038/s41590-021-00886-5
127. Tumburu L, Ghosh-Choudhary S, Seifuddin FT, Barbu EA, Yang S, Ahmad MM, et al. Circulating Mitochondrial DNA Is a Proinflammatory DAMP in Sickle Cell Disease. *Blood.* (2021) 137(22):3116–26. doi: 10.1182/blood.2020009063
128. Zhang X, Wu X, Hu Q, Wu J, Wang G, Hong Z, et al. Mitochondrial DNA in Liver Inflammation and Oxidative Stress. *Life Sci* (2019) 236:116464. doi: 10.1016/j.lfs.2019.05.020
129. Wang W, Sun L, Deng Y, Tang J. Synergistic Effects of Antibodies Against High-Mobility Group Box 1 and Tumor Necrosis Factor-α Antibodies on D-(+)-Galactosamine Hydrochloride/Lipopolysaccharide-Induced Acute Liver Failure. *FEBS J* (2013) 280(6):1409–19. doi: 10.1111/febs.12132
130. Matsumoto K, Kouzaki H, Kikuoka H, Kato T, Tojima I, Shimizu S, et al. Soluble ST2 Suppresses IL-5 Production by Human Basophilic KU812 Cells, Induced by Epithelial Cell-Derived IL-33. *Allergol Int* (2018) 67s:S32–s37. doi: 10.1016/j.alit.2018.05.009
131. Kim YH, Yang TY, Park CS, Ahn SH, Son BK, Kim JH, et al. Anti-IL-33 Antibody has a Therapeutic Effect in a Murine Model of Allergic Rhinitis. *Allergy.* (2012) 67(2):183–90. doi: 10.1111/j.1398-9995.2011.02735.x
132. Luo Y, Yoneda J, Ohmori H, Sasaki T, Shimbo K, Eto S, et al. Cancer Usurps Skeletal Muscle as an Energy Repository. *Cancer Res* (2014) 74(1):330–40. doi: 10.1158/0008-5472.Can-13-1052
133. Allinne J, Scott G, Lim WK, Birchard D, Erjefält JS, Sandén C, et al. IL-33 Blockade Affects Mediators of Persistence and Exacerbation in a Model of Chronic Airway Inflammation. *J Allergy Clin Immunol* (2019) 144(6):1624–37.e10. doi: 10.1016/j.jaci.2019.08.039

Conflict of Interest: The authors declare that the research was conducted in the absence of any commercial or financial relationships that could be construed as a potential conflict of interest.

GLOSSARY

ACLF	acute-on-chronic liver failure
CTL	cytotoxic T lymphocyte
DC	dendritic cell
DAMPs	damage-associated molecular patterns
ALF	acute liver failure
SALF	subacute liver failure
CLF	chronic liver failure
HE	hepatic encephalopathy
EASL-CLIF	European Association for the Study of the Liver-Chronic Liver Failure
NACSELD	North American Consortium for the Study of End-stage Liver Disease
APASL	Asian Pacific Association for the Study of the Liver
PAMPs	pathogen-associated molecular patterns
PD-1	programmed cell death protein 1
Tregs	regulatory T cells
HLA-DR	human leukocyte antigen-DR isotype;
PRR	pattern recognition receptors
mtDNA	mitochondrial DNA
HSPs	heat shock proteins
HMGB1	high mobility group box chromosomal protein 1
F-actin	fibrous actin
ILC2	type II intrinsic lymphocytes
MyD88	myeloid differentiation factor 88
TRAIL	tumor necrosis factor-related apoptosis inducing ligand
TNF-α	tumor necrosis factor α
FasL	Fas ligand
GalN	D-galactosamine
LPS	lipopolysaccharide
NF	nuclear factor
MAPKs	mitogen-activated protein kinases
ERK	extracellular signal-regulated kinase
Th2	T helper type 2
sST2	soluble ST2
IL-1R	IL-1 receptor
GRP	glucose-regulated protein
GGA	geranylgeranylacetone
APAP	acetaminophen
HSF1	heat shock transcription factor 1
ROS	reactive oxygen species
SOD	superoxide dismutase
BDL	bile duct junction
HAV	hepatitis A virus
UPR	unfolded protein response
PPARα	peroxisome proliferator-activated receptor α
CGA	chlorogenic acid
SMCs	smooth muscle cells
EMT	mesenchymal transition
ALT	alternative lengthening of telomeres
PDHC	pyruvate dehydrogenase complex
LDH	lactate dehydrogenase
CHB	chronic hepatitis B
QCLGF	Qing Chang Li Gan formula
TSA	trichostatin A
HDAC	histone deacetylase inhibitors
RAGE	receptor for advanced glycation end products
TLR	toll-like receptor
NEAT1	lncRNA rich transcript-1
PALF	pediatric acute liver failure
SIRS	systemic inflammatory response syndrome
PMN	polymorphonuclear neutrophils
STING	stimulator of interferon genes
cGAS	cyclic GMP-AMP synthase.
sTim-3	soluble T-cell immunoglobulin and mucin-domain containing molecule-3

frontiers | Frontiers in Immunology

TYPE Original Research
PUBLISHED 04 October 2022
DOI 10.3389/fimmu.2022.988668

OPEN ACCESS

EDITED BY
Xiaogang Xiang,
Shanghai Jiao Tong University, China

REVIEWED BY
Wei Hou,
Beijing Youan Hospital, Capital Medical University, China
Jun Yin,
First Affiliated Hospital of Anhui Medical University, China

*CORRESPONDENCE
Hong Tang
htang6198@hotmail.com
En-Qiang Chen
chenenqiang1983@hotmail.com

SPECIALTY SECTION
This article was submitted to Inflammation, a section of the journal Frontiers in Immunology

RECEIVED 07 July 2022
ACCEPTED 15 September 2022
PUBLISHED 04 October 2022

CITATION
Tao Y-C, Wang Y-H, Wang M-L, Jiang W, Wu D-B, Chen E-Q and Tang H (2022) Upregulation of microRNA-125b-5p alleviates acute liver failure by regulating the Keap1/Nrf2/HO-1 pathway.
Front. Immunol. 13:988668.
doi: 10.3389/fimmu.2022.988668

Upregulation of microRNA-125b-5p alleviates acute liver failure by regulating the Keap1/Nrf2/HO-1 pathway

Ya-Chao Tao[1,2], Yong-Hong Wang[1,2], Meng-Lan Wang[1,2], Wei Jiang[1,2], Dong-Bo Wu[1,2], En-Qiang Chen[1,2]* and Hong Tang[1,2]*

[1]Center of Infectious Diseases, West China Hospital, Sichuan University, Chengdu, China, [2]Division of Infectious Diseases, State Key Laboratory of Biotherapy, Sichuan University, Chengdu, China

Background: Acute liver failure (ALF) and acute-on-chronic liver failure (ACLF) are the two most common subtypes of liver failure. They are both life-threatening clinical problems with high short-term mortality. Although liver transplantation is an effective therapeutic, its application is limited due to the shortage of donor organs. Given that both ACLF and ALF are driven by excessive inflammation in the initial stage, molecules targeting inflammation may benefit the two conditions. MicroRNAs (miRNAs) are a group of small endogenous noncoding interfering RNA molecules. Regulation of miRNAs related to inflammation may serve as promising interventions for the treatment of liver failure.

Aims: To explore the role and mechanism of miR-125b-5p in the development of liver failure.

Methods: Six human liver tissues were categorized into HBV-non-ACLF and HBV-ACLF groups. Differentially expressed miRNAs (DE-miRNAs) were screened and identified through high-throughput sequencing analysis. Among these DE-miRNAs, miR-125b-5p was selected for further study of its role and mechanism in lipopolysaccharide (LPS)/D-galactosamine (D-GalN) -challenged Huh7 cells and mice *in vitro* and *in vivo*.

Results: A total of 75 DE-miRNAs were obtained. Of these DE-miRNAs, miR-125b-5p was the focus of further investigation based on our previous findings and preliminary results. We preliminarily observed that the levels of miR-125b-5p were lower in the HBV-ACLF group than in the HBV-non-ACLF group. Meanwhile, LPS/D-GalN-challenged mice and Huh7 cells both showed decreased miR-125b-5p levels when compared to their untreated control group, suggesting that miR-125b-5p may have a protective role against liver injury, regardless of ACLF or ALF. Subsequent results revealed that miR-125b-5p not only inhibited Huh7 cell apoptosis *in vitro* but also relieved mouse ALF *in vivo* with evidence of improved liver histology, decreased alanine aminotransferase (ALT) and aspartate

aminotransferase (AST) levels, and reduced tumor necrosis factor-α (TNF-α) and IL-1β levels. Based on the results of a biological prediction website, microRNA.org, Kelch-like ECH-associated protein 1 (Keap1) was predicted to be one of the target genes of miR-125b-5p, which was verified by a dual-luciferase reporter gene assay. Western blot results *in vitro* and *in vivo* showed that miR-125b-5p could decrease the expression of Keap1 and cleaved caspase-3 while upregulating the expression of nuclear factor (erythroid-derived 2)-like 2 (Nrf2) and heme oxygenase-1(HO-1).

Conclusion: Upregulation of miR-125b-5p can alleviate acute liver failure by regulating the Keap1/Nrf2/HO-1 pathway, and regulation of miR-125b-5p may serve as an alternative intervention for liver failure.

KEYWORDS

acute liver failure, acute-on-chronic liver failure, microRNA-125b-5p, Kelch-like ECH-associated protein 1, high-throughput sequencing, inflammation

Introduction

Liver failure is a life-threatening clinical problem with high short-term mortality. It can present as acute liver failure (ALF, without pre-existing chronic liver disease), acute-on-chronic liver failure (ACLF, an acute deterioration of underlying chronic liver disease) or an acute decompensation of an end-stage liver disease (1). Liver transplantation is an effective therapeutic option, irrespective of the etiology of liver failure. However, the application of liver transplantation is limited due to the shortage of donor organs (2). Thus, liver failure is still a severe clinical challenge, and other interventions assisting alleviating liver injury are being explored.

ALF and ACLF are the most widely discussed owing to their high incidence worldwide. Better knowledge of the pathophysiology of these diseases can provide insights into novel therapies. It has been reported that the development of both ALF and ACLF is driven by immune dysfunction and inflammatory imbalance, although the conditions are distinct clinical entities (3–5). The immune and inflammatory status of the diseases is dynamic, progressing from intensive inflammation to the development of immunoparalysis (3, 4, 6). In the initial phase of ALF, immune cells participating in the innate response are activated to produce proinflammatory mediators, which can stimulate a systemic inflammatory response. Patients with ACLF display an excessive innate immune response, which is characterized by leukocytosis, neutrophilia and lymphopenia, together with high levels of inflammatory mediators (7, 8). Initial systemic inflammatory response syndrome (SIRS) due to acute insult and/or subsequent secondary infection due to immunoparalysis can lead to extrahepatic organ failure (4, 9, 10). Thus, strategies modulating immune and proinflammatory mediators can be potential targets to alleviate liver failure.

MicroRNAs (miRNAs) are a class of small endogenous noncoding interfering RNA molecules and can induce gene silencing and translational repression by binding specific sequences in target mRNAs, thereby playing key roles in biological processes and in the development of various diseases (11). Accumulating studies have demonstrated that miRNAs are involved in the modulation of immunity and inflammation, and regulation of these miRNAs may be potential therapeutics for clinical problems (12–14). For instance, inhibition of miR-34b-5p could attenuate inflammation and apoptosis in acute lung injury, and thus miR-34b-5p and its target progranulin might be a potential intervention pathway for the treatment of acute lung injury (15). Thus, the regulation of miRNAs and their target genes may improve the outcome of various diseases by regulating immunity and inflammation.

In the present study, we identified miRNAs that were differentially expressed in human HBV-ACLF tissues compared to HBV-non-ACLF tissues. Then, we further explored the role of a certain miRNA in the development of liver failure, aiming to determine whether the miRNA may improve liver failure by regulating intensive inflammation, hoping to pave the way for miRNA-targeting therapies for liver failure.

Materials and methods

Study population

Six patients with chronic HBV infection were enrolled. They all received antiviral therapy with nucleos(t)ide analogs. They were

divided into HBV-non-ACLF (n=3) and HBV-ACLF (n=3) groups based on their liver histopathology and liver function. The histological assessments were performed using the METAVIR scoring system. Briefly, the degree of inflammation in the liver biopsies was assessed with the standard METAVIR histology activity index scoring system, defined as A0, no inflammation; A1, mild inflammation; A2, moderate inflammation, and A3, severe inflammation. The histological appearance of fibrosis was classified as F0 to F4, ranging from no fibrosis to cirrhosis (16).

HBV-non-ACLF referred to patients with chronic hepatitis B (CHB) who had abnormal liver function and mild-to-moderate inflammatory activity (≤A2) in the liver tissue due to HBV infection, but did not meet the diagnostic criteria of ACLF.

ACLF is diagnosed according to the recommendations of the Asian Pacific Association for the Study of the Liver (APASL) (1). Herein, patients who were previously diagnosed with CHB or cirrhosis belonged to the HBV-ACLF group if they manifested with jaundice (bilirubin>5 mg/dL), coagulopathy [prolonged international normalized ratio (INR)>1.5], encephalopathy, and ascites within 4 weeks. The histopathological findings of the HBV-ACLF group showed evident infiltration of inflammatory cells (A3), accompanied by the formation of pseudolobuli (F4). All HBV-ACLF patients later received liver transplantation.

Patients were excluded if they had any of the following conditions: (1) infections with other hepatitis viruses (including A, C, D, and E) or human immunodeficiency virus (HIV); (2) evidence of drug-induced liver injury, alcoholic liver disease, autoimmune liver diseases, severe systemic illnesses; (3) malignancies, such as hepatocellular carcinoma.

This study was carried out in accordance with the Declaration of Helsinki. All patients provided verbal informed consent. Detailed information about the study cohort is described in Table 1.

High-throughput sequencing

Total RNA was extracted using TRIzol reagent (Invitrogen, Carlsbad, CA, USA) according to the manufacturer's instructions. The quantity and purity of total RNA were analyzed with an Agilent 2100 Bioanalyzer (Agilent, USA) with RIN> 6.5. Small RNAs of different length were separated using denaturing polyacrylamide gel electrophoresis (PAGE). Fragments between 18 and 30 nt in length were gel-purified and ligated to adaptors at both the 3′- and 5′-ends. The ligation products were subsequently reverse- transcribed into cDNA, and PCR amplification was performed using an Illumina sequencing kit (Illumina, USA) to generate a cDNA library according to previous studies (17, 18).

High-throughput sequencing was performed by Chengdu Life Baseline Technology Co., Ltd. As shown in Supplement 1, the raw read sequences were filtered to remove low-quality reads, 5′ adaptor contaminant reads, reads without 3' adaptor sequences, reads containing poly (A) and adapter sequences, sequences <18 nt and sequences >32 nt. The clean reads were obtained and their length distributions were calculated using Fastx-Toolkit (19). Then, the clean reads were mapped and aligned to the human reference genome group and other small RNA databases using Bowtie2 software (20). The known miRNAs and novel miRNAs were identified and predicted using miRbase and miRDeep2, respectively (21, 22).

The miRNA expression levels between the two groups were compared to identify differentially expressed (DE)-miRNAs. The expression of miRNA was normalized using transcripts per million (TPM) as the following formula: TPM = (mapped read count/total clean read count) $\times 10^6$ (23). DE-miRNAs were defined as |log2 (fold change)| >1 between two groups with a false discovery rate (FDR) of <0.05.

Bioinformatics analysis for DE-miRNAs

To understand the functions of these DE-miRNAs, their potential target genes were predicted by RNAhybrid (https://bibiserv.cebitec.uni-bielefeld.de/rnahybrid/) and miRanda (http://www.microrna.org/microrna/home.do) (24, 25). Only the target genes predicted by both methods were considered reliable targets for further analysis. Gene ontology (GO)

TABLE 1 Clinical characteristics of the two groups of patients.

Groups	Patients	Gender	Age (year)	ALT (IU/L)	AST (IU/L)	TBil(μmoL/mL)	INR	HBV-DNA (log10 IU/mL)	Inflammation activity index	Fibrosis score
HBV-non-ACLF	Patient 1	male	39	50	44	9.9	1.24	4.049	A1	F0
	Patient 2	male	40	59	56	14.9	1.10	3.328	A2	F1
	Patient 3	male	46	114	93	14.0	1.05	3.755	A2	F1
HBV- ACLF	Patient 4	male	47	559	353	326.6	2.07	2.538	A3	F4
	Patient 5	male	52	442	293	396.3	1.95	2.661	A3	F4
	Patient 6	male	46	417	356	402.6	2.23	3.326	A3	F4

Upper limit of normal (ULN) of ALT: 50 IU/mL for male; ULN of TB: 28 μmol/L. HBV DNA<100 IU/mL is defined as undetectable serum HBV DNA.
ALT, Alanine aminotransferase; TBil, total bilirubin. INR, International Normalized Ratio.

functional enrichment analysis and Kyoto Encyclopedia of Genes and Genomes (KEGG) pathway enrichment analysis were performed on these target genes (26, 27). GO analysis was conducted to provide functional annotation for predicted target genes of miRNAs by analyzing the classifications of Biological Process, Cellular Component and Molecular Function. Pathway analysis was based on KEGG, which is a database resource for understanding the high-level functions and utilities of biological systems. $p<0.05$ was regarded as the cutoff to select significantly enriched terms.

Cell culture and transfection

The human HCC cell line Huh7 was preserved in our laboratory. Cells were cultured in Dulbecco's modified Eagle's medium (DMEM, D6429, Sigma, USA) containing 10% fetal bovine serum (12103C, Sigma, USA) and 1% penicillin/streptomycin under standard culture conditions (a humidified 5% carbon dioxide incubator at 37°C).

The miR-125b-5p overexpression vector and negative control (NC) vector were designed and provided by *Heyuan Biotechnology* (OBIO, Shanghai, China). After growth to 60%-70% confluence in six-well plates, Huh7 cells were transfected with miR-125b-5p vector or NC vector using Lipofectamine™ 2000 (11668019, Invitrogen, USA). On the following day, the cells were incubated with normal medium.

Flow cytometric analysis

Apoptotic cells were assessed using an Annexin V-Fluorescein isothiocyanate (FITC) apoptosis detection kit (APOAF, Sigma, USA) according to the manufacturer's protocol. Huh7 cells were collected and washed twice with PBS. Then, the cells were resuspended in 500 µL of 1× binding buffer and stained with 5 µL of Annexin V-FITC conjugate and 10 µL of PI solution. After incubation for 15 min in the dark at room temperature, stained cells were analyzed by flow cytometry (BD Accuri™ C6 flow cytometer).

Real–time quantitative PCR analysis

Total RNA was extracted from Huh7 cells and liver tissues using TRIzol Reagent (15596026, Invitrogen, USA) according to the manufacturer's instructions. Reverse transcription was performed using a First Strand cDNA Synthesis Kit (B300537, Sangon Biotech, China). The expression of miR-125b-5p was determined by quantitative real-time PCR using a miRNA qPCR detection kit (B532461, Sangon Biotech, China), as previously reported (28). The forward primer sequence for miR-125b-5p was CGTCCCTGAGA-CCCTAACTTGTGA. The reverse primers for miR-125b-5p were universal adaptor primers designed and provided by Sangon Biotech Company (Shanghai, China). The level of miR-125b-5p was calculated using the relative quantification $2^{-\Delta\Delta CT}$ method and normalized to the U6 transcript (Bio-Rad CFX Manager software), as previously described (29, 30)

Animals

Male C57BL/6J mice (6-8 weeks old, weighing 20-25 g) were purchased from Huaxi Laboratory Animal Center of Sichuan University (Chengdu, China). All mice were maintained under controlled conditions (24°C, 55% humidity and 12-h day/night rhythm) and given free access to water and food. The mice received humane care under guidance from the Institutional Review Board in accordance with the Animal Protection Art of Sichuan University. After 1 week of acclimation, the mice were prepared for further study.

Mouse model of acute liver failure

The mouse model of ALF was established using lipopolysaccharide (LPS) and D-galactosamine (D-GalN) as previously described (31). In brief, C57BL/6J mice were given 700 mg/kg D-GalN (G0500, Sigma, USA) and 10 µg/kg LPS (*Escherichia coli*, 0111:B4, L2630, Sigma, USA) by intraperitoneal injection. Mice in the present study were randomly divided into four groups (n = 8/group): a normal control group, an LPS/D-GalN group, an LPS/D-GalN+ negative control (NC) group and an LPS/D-GalN+ miR-125b-5p group.

The miR-125b-5p overexpression vector or negative control vector was administered to mice *via* tail vein prior to the establishment of ALF as previously reported (32, 33). Seven hours after ALF model establishment, all mice were sacrificed, and serum and liver samples were harvested and stored for further analysis.

H&E staining

Liver tissue was obtained and fixed with 4% paraformaldehyde at 4°C for 48 h and then embedded in paraffin. After immobilization, samples were cut into sections and then stained with hematoxylin-eosin (HE) using a standard protocol. The sections were visualized under a light microscope, and representative images are presented.

Biochemical detection of aminotransferase

Serum samples were collected from mice to detect alanine aminotransferase (ALT) and aspartate aminotransferase (AST) by an automatic biochemical analyzer.

Enzyme-linked immunosorbent assay (ELISA)

The levels of serum tumor necrosis factor -α (TNF-α, EMC102a, NeoBioscience, China) and IL-1β (EMC001b, NeoBioscience, China) were detected using ELISA kits according to the manufacturer's instructions.

Western blotting

Protein was extracted from Huh7 cells and liver tissues. The isolated proteins were separated by polyacrylamide gel electrophoresis and then transferred onto polyvinylidene fluoride (PVDF) membranes. Subsequently, the blots were exposed to primary antibodies against Kelch-like ECH-associated protein 1 (Keap1, #8047, CST, USA), nuclear factor (erythroid-derived 2)-like 2 (Nrf2, sc-365949, Santa Cruz, USA), heme oxygenase-1 (HO-1, #43966, CST, USA), and cleaved caspase-3 (#9661, CST, USA). Anti-GAPDH (TA-08), anti-β-tubulin (TA-10) and anti-β-actin (TA-09) were used as internal references, and were purchased from Beijing Zhong Shan-Golden Bridge Biological Technology Co., Ltd. The images of the gels were captured in a Bio-Rad Image Lab (ChemiDoc™ MP Imaging System, Bio-Rad, California, USA).

Dual-luciferase reporter gene assay

A biological prediction website, microRNA.org, was used to analyze the target genes of miR-125b-5p, and a dual-luciferase reporter gene assay was performed to detect whether miR-125b-5p extensively targeted Keap1. The full length of the 3′-untranslated region (3′UTR) (forward primer: GAGGAGTTGTGTTTGTGGAC; reverse primer: TGTAAAACGACGGCCAGT) of the Keap1 gene was amplified clonally. The wild-type (WT) vector of Keap1 (Keap1-WT) and a mutant type vector (Keap1-MUT) were constructed. Bioinformatics software was used to predict the binding sites between miR-125b-5p and Keap1. The vectors were cotransfected with miR-125b-5p mimic and mimic negative control into 293T cells according to the following groups: Keap1-WT+ miR-125b-5p mimic negative control (miR-NC), Keap1-WT+ miR-125b-5p mimic, Keap1-MUT+ miR-NC, and Keap1-MUT+ miR-125b-5p mimic. Firefly and Renilla luciferase activities were measured using a dual luciferase reporter gene detection kit. The experiment was repeated three times in each group.

Statistical analysis

Statistical analysis was performed using SPSS 20.0 software. Data are presented as the mean± deviation (SD) determined from a minimum of three independent experiments each performed with triplicate cultures. One-way ANOVA was performed to evaluate the level of significance, and the results were considered statistically significant if $p<0.05$.

Results

Sequence analysis of small RNAs and identification of DE-miRNAs

Six liver tissues were obtained and categorized into HBV-non-ACLF and HBV-ACLF groups based on the severity of liver injury (Table 1, Figure 1A). The sequences of small RNAs ranged from 18-30 nt in length, of which the majority were 21-23 nt long, and the 22-nt small RNAs were the most abundant (Figure 1B). After removal of the adaptor, insert, poly (A) tail and short RNAs of <18 nt, a total of 59,160,359 and 49,723,211 clean reads were obtained for the two groups, respectively (Supplement 2). Small RNA sequences were searched against the GenBank, Rfam, and Repbase databases by Bowtie2 software, rRNA, snRNA, snoRNA, tRNA, sRNA, etc., were annotated and removed, and the unannotated RNAs were subjected to further analyses for miRNA identification (Figure 1C). We used the software miRbase and miRDeep2 to map the retained sequence reads to identify candidate miRNAs.

DE-miRNAs were obtained when they met the criteria of |log2 (fold change)|>1 between the two groups and FDR<0.05, and these DE-miRNAs are presented in a heatmap (Figure 1D). Compared with the HBV-non-ACLF group, the levels of 28 miRNAs were increased, while the levels of 47 miRNAs were decreased in the HBV-ACLF group. Some of the upregulated and downregulated miRNAs are shown in Tables 2 and 3, respectively.

GO and KEGG enrichment analysis

To further understand the roles of miRNAs in the progression of liver injury, GO and KEGG analyses of putative target genes of these DE-miRNAs were performed. GO describes genes from three aspects, namely molecular function (MF), cellular component (CC) and biological process (BP).

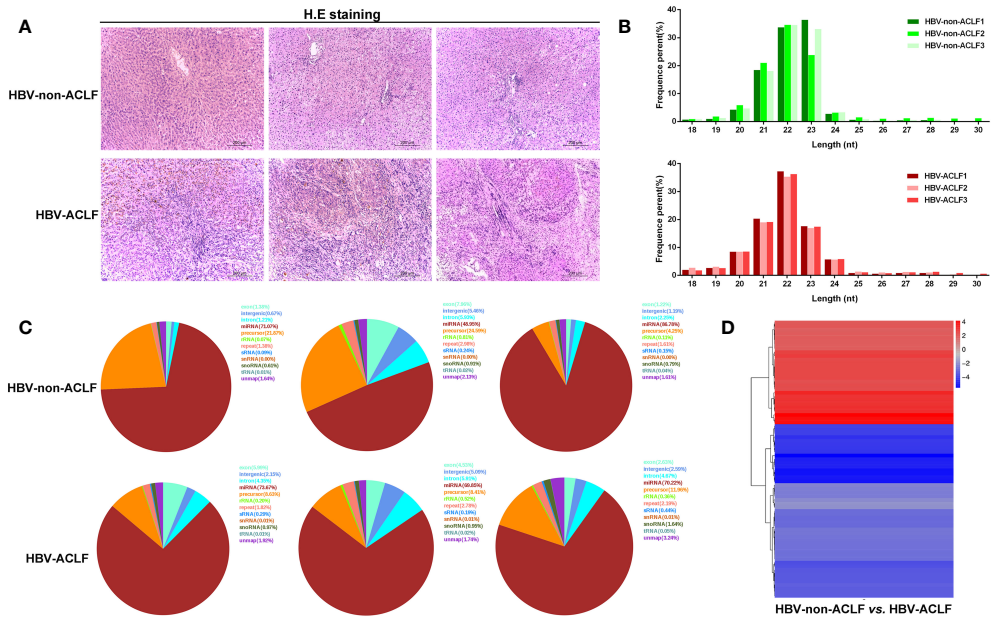

FIGURE 1
Results of high-throughput sequencing and identification of DE-miRNAs. **(A)** H&E staining of liver tissues from HBV-non-ACLF and HBV-ACLF groups; **(B)** Length distribution of the small RNA library; **(C)** Distribution of small RNAs among different categories; **(D)** Heatmap of DE-miRNAs constructed by comparing the levels of miRNAs between the two groups.

Among the DE-miRNA target genes, "binding" was the most represented in the MF category, followed by "catalytic activity", "nucleic acid binding transcription factor activity", "antioxidant activity" and "transporter activity". For the CC category, target genes mostly participated in the "cell", "cell part", "organelle", "organelle part" and "membrane". Genes involved in the "cellular process", "single-organism process", "biological process", "metabolic process" and "regulation of biological process" were notably represented in the BP category (Figure 2A). In the KEGG analysis, target genes were primarily enriched in the "pathways in cancer", "toxoplasmosis", "pertussis", "leishmaniasis" and "microRNAs in cancer" (Figure 2B).

Protective action of miR-125b-5p against ALF both *in vitro* and *in vivo*

We previously proved that serum miR-125b-5p was associated with the severity of HBV-related liver damage, and

TABLE 2 Ten of the upregulated DE-miRNAs in the HBV-ACLF group compared to the HBV-non-ACLF group.

Gene ID	HBV-non-ACLF vs. HBV-ACLF		Regulation
	Log2(HBV-ACLF/HBV-non-ACLF)	FDR	
hsa-miR-1827	3.779564	0.020201	Up
hsa-miR-3934-5p	3.743929	0.020344	Up
novel_mir70	2.968886	0.020482	Up
hsa-miR-548ba	2.846975	0.023141	Up
hsa-miR-329-3p	2.812766	0.005075	Up
hsa-miR-3690	2.577176	0.002611	Up
hsa-miR-147b	2.303872	0.012293	Up
hsa-miR-6718-5p	2.292068	0.000115	Up
hsa-miR-143-5p	2.289669	0.001049	Up
hsa-miR-155-3p	2.301391	0.011031	Up

FDR, false discovery rate.

TABLE 3 Twenty of the downregulated DE-miRNAs in the HBV-ACLF group compared to the HBV-non-ACLF group.

Gene ID	HBV-non-ACLF vs. HBV-ACLF		Regulation
	Log2(HBV-ACLF/HBV-non-ACLF)	FDR	
hsa-miR-378i	-5.58567	1.40E-06	Down
novel_mir3	-5.16057	2.09E-07	Down
hsa-miR-6130	-5.13246	3.08E-06	Down
novel_mir143	-4.98430	6.36E-17	Down
hsa-miR-216a-5p	-4.80066	0.00012	Down
novel_mir211	-4.73787	7.88E-05	Down
hsa-miR-216b-5p	-4.73061	8.89E-07	Down
hsa-miR-216b-3p	-4.3374	1.11E-05	Down
hsa-miR-483-3p	-4.17394	1.89E-09	Down
hsa-miR-4686	-4.08130	1.43E-07	Down
hsa-miR-3591-3p	-3.93922	3.67E-05	Down
hsa-miR-3591-5p	-3.93449	1.23E-08	Down
hsa-miR-375	-3.88737	1.75E-08	Down
hsa-miR-505-5p	-3.56423	1.15E-05	Down
hsa-miR-122-5p	-3.33444	0.002364	Down
hsa-miR-483-5p	-3.30266	1.65E-05	Down
hsa-miR-338-5p	-3.20726	0.00599	Down
hsa-miR-1295a	-3.12447	1.40E-06	Down
hsa-miR-192-3p	-2.85876	2.09E-05	Down
hsa-miR-125b-5p	-2.58513	0.000155	Down

FDR, false discovery rate.

high serum miR-125b-5p might serve as a predictor for poor outcomes in HBV-ACLF cases (28). In the present study, we observed that the levels of hepatic miR-125b-5p were decreased with the aggravation of HBV-induced liver injury based on miRNA array data. Meanwhile, we verified the expression of miR-125b-5p using 20 pairs of liver tissues from patients with HBV-non-ACLF and HBV-ACLF and confirmed that the levels of hepatic miR-125b-5p were lower in HBV-ACLF patients than in HBV-non-ACLF patients (p<0.001, Supplement 3A). In addition, the levels of miR-125b-5p were decreased in LPS/D-

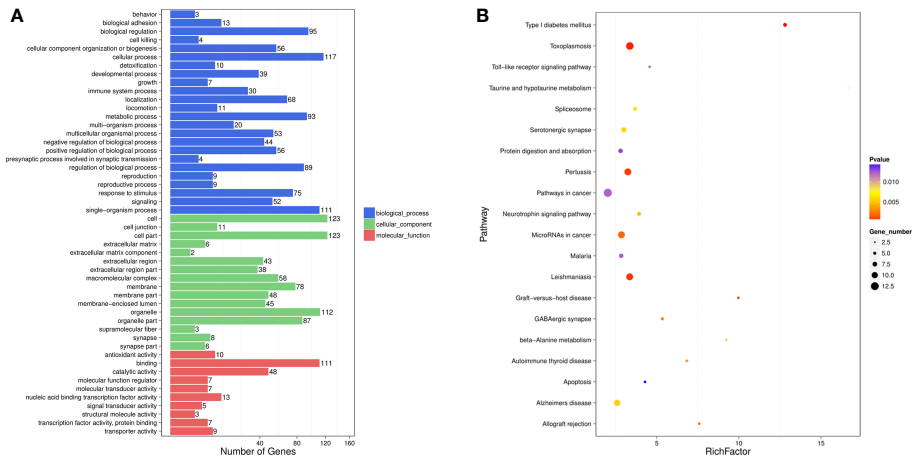

FIGURE 2
GO functional enrichment analysis **(A)** and KEGG pathway analysis **(B)** for DE-miRNAs obtained from the comparsion between HBV-non-ACLF and HBV-ACLF groups. Rich actor is the ratio of the DE gene number to the total gene number in a certain pathway. The size and color of the dots represent the gene number and range of the p value, respectively.

GalN-challenged Huh7 cells (p<0.01, Supplement 3B) and mice (p<0.001, Supplement 3C) compared to those in untreated control groups. Thus, it was well-founded to speculate that miR-125b-5p might play an important role in the development of liver failure, regardless of ACLF or ALF, and we focused on this miRNA for further study.

To determine the role of miR-125b-5p, Huh7 cells were transfected with miR-125b-5p overexpression vector or negative control vector. The expression of miR-125b-5p was significantly increased in the cells of the experimental group compared with the control group (p<0.001, Supplement 3D). Twenty-four hours after transfection with the vector, Huh7 cells were treated with LPS (20 ng/mL)/D-GalN (3 mol/mL) for 36 hours. Cell apoptosis was analyzed using annexin-V flow cytometry. As shown in Figures 3A, B, the apoptosis rates were significantly lower in cells transfected with miR-125b-5p vector before LPS/D-GalN addition than in cells only treated with LPS/D-GalN (29.41% ± 2.61% vs. 44.63% ± 5.45%, p<0.05) and in cells transfected with negative control vector (29.41% ± 2.61% vs. 50.39% ± 6.71%, p<0.01), demonstrating that miR-125b-5p may help to alleviate acute liver injury *in vitro* by inhibiting cell apoptosis.

To further identify the protective role of miR-125b-5p in ALF *in vivo*, we established mouse ALF through intraperitoneal injection of LPS/D-GalN and assessed the improvements in liver histopathology and serum biochemical indicators after administration of the miR-125b-5p overexpression vector. The liver histopathological characteristics of the negative control groups showed no significant differences from those of the LPS/D-GalN-induced ALF groups, whereas administration of the miR-125b-5p vector improved the liver histopathology based on the retained liver structure, decreased inflammatory cell infiltration and reduced hemorrhage (Figure 4A). In addition, miR-125b-5p also reduced ALT and AST levels in mice treated with LPS/D-GalN (p<0.001, Figure 4B). Serum TNF-α and IL-1β levels were enhanced in the LPS/D-GalN-induced ALF group. In contrast, significant decreases in the

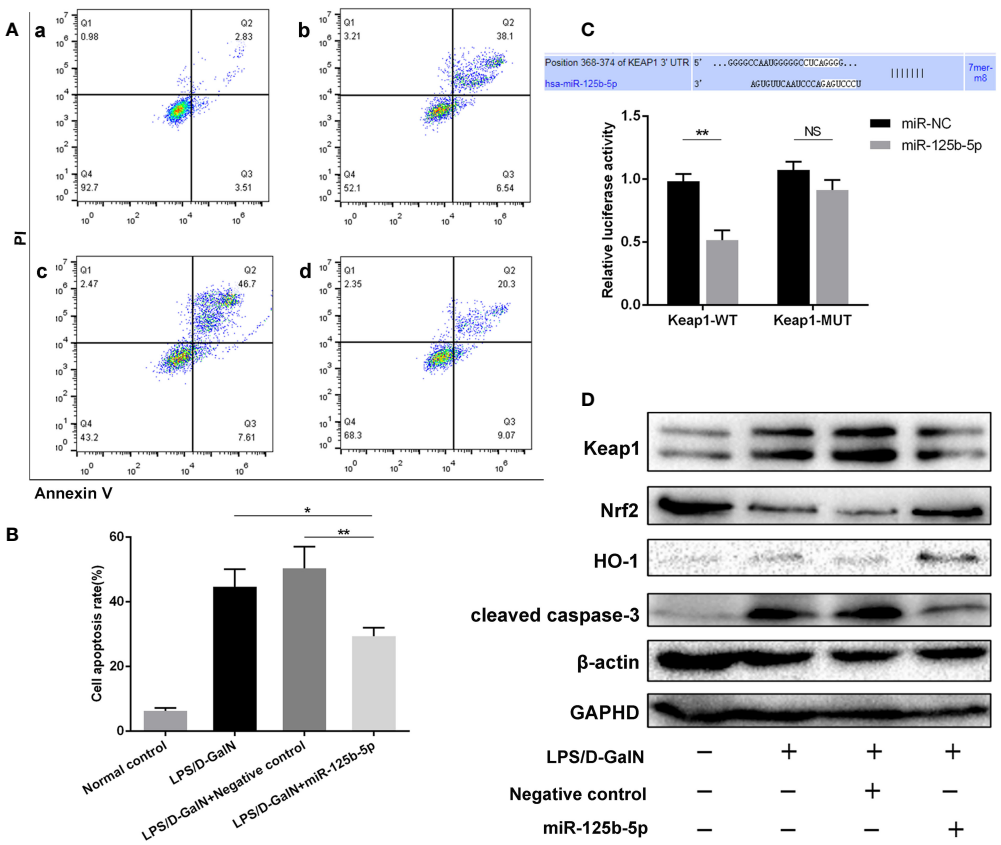

FIGURE 3
Role and mechanism of miR-125b-5p in injured Huh7 cells *in vitro*. **(A)** The cell apoptosis rate was calculated by flow cytometry. a: Normal control; b: LPS/D-GalN; c: LPS/D-GalN+ Negative control vector; d: LPS/D-GalN+ miR-125b-5p. **(B)** The cell apoptosis rate was calculated and compared. **(C)** A luciferase reporter assay was performed to identify the binding sites between human Keap1 and hsa-miR-125b-5p. **(D)** The expression levels of Keap1, Nrf2, HO-1 and cleaved caspase-3 were evaluated by western blotting. NS, no significance. *p < 0.05, **p < 0.01.

two proinflammatory cytokines were observed in the miR-125b-5p treated group (p<0.001, Figure 4C).

MiR-125b-5p alleviated ALF by regulating the Keap1/Nrf2 signaling pathway

A dual-luciferase reporter gene assay was performed to detect whether miR-125b-5p targeted Keap1 through the potential binding site predicted by TargetScan. The luciferase assay activity levels were reduced in the miRNA-125b-5p group compared with the miR-NC group, demonstrating that the 3'–UTR of human Keap1 mRNA was the binding site of miRNA-125b-5p, and unchanged levels of luciferase activity in the presence of the mutated 3'–UTR of Keap1 further confirmed that Keap1 is the target of miR-125b-5p (Figure 3C). We then investigated whether the Keap1 protein and its involved signaling pathway were regulated by miR-125b-5p *in vitro*. Overexpression of miRNA-125b-5p significantly suppressed the protein expression of Keap1. The Keap1/Nrf2 pathway plays a key role in mitigating acute liver injury (34). Our study found that the expression levels of Nrf2 and one of its downstream proteins, HO-1, were upregulated, whereas cleaved caspase-3 was decreased in miRNA-125b-5p-overexpressing cells compared to the control groups (Figure 3D).

We further explored whether miR-125b-5p could improve ALF *in vivo* by targeting Keap1 and its downstream proteins. The dual-luciferase reporter gene assay confirmed the direct binding of miR-125b-5p with the 3'-UTR of mouse Keap1 but not with the mutated 3'-UTR (Figure 4D). Subsequently, we found elevated levels of Nrf2 and HO-1 in miR-125b-5p-treated mice (Figure 4E). The expression of cleaved caspase-3 was significantly decreased in mice administered the miR-125b-5p overexpression vector. Thus, miR-125b-5p can regulate Keap1, which leads to the activation of Nrf2 signaling and hence alleviates LPS/D-GalN-induced ALF.

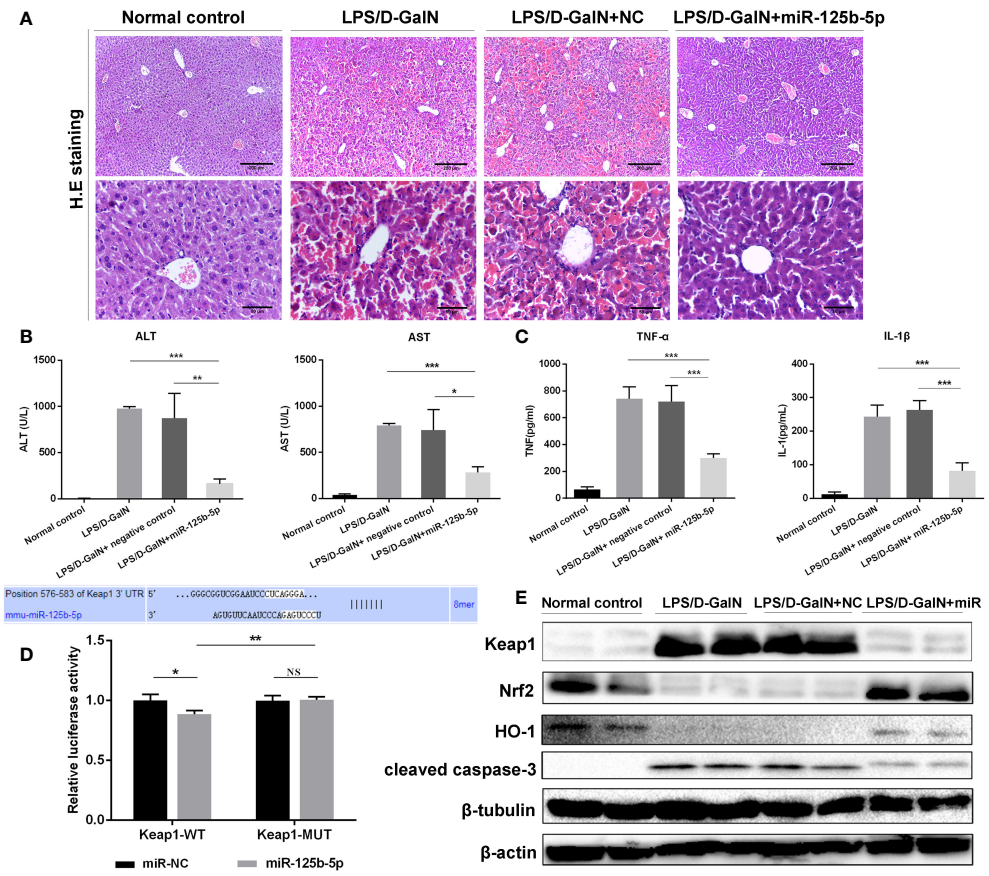

FIGURE 4
Role and mechanism of miR-125b-5p in LPS/D-GalN- induced ALF *in vivo*. **(A)** H&E staining of liver tissue. **(B)** Detection of serum ALF and AST. **(C)** Detection of two serum proinflammtory mediators, TNF-α and IL-1 β, using ELISA. **(D)** A luciferase reporter assay was performed to identify the binding sites between mouse Keap1 and mmu-miR-125b-5p. **(E)** The expression levels of Keap1, Nrf2, HO-1 and cleaved caspase-3 were evaluated by western blotting. NC, negative control. NS, no significance. *p<0.05, **p <0.01, ***p <0.001.

Discussion

Liver failure is a challenging condition with high mortality; thus, the development of novel therapeutic agents for liver failure is crucial. Both ACLF and ALF are driven by dysfunctional immunity and excessive inflammation. Hence, strategies targeting immunity and inflammation may provide new insight into the treatment of liver failure.

In the present study, we screened DE-miRNAs in human liver tissues from patients with HBV-non-ACLF and HBV-ACLF using high-throughput sequencing. To the best of our knowledge, this is the first study that systematically quantifies the expression features of miRNAs by high-throughput sequencing analysis in human HBV-related liver tissue.

A total of 75 DE-miRNAs were ultimately obtained, and subsequent GO analysis revealed that most target genes of these DE-miRNAs were involved in "binding", "cell part", "cellular process" and related categories. KEGG analysis showed that target genes predominantly participated in the "pathways in cancer", "toxoplasmosis", and "microRNAs in cancer". Although the functions of these DE-miRNAs in the development of liver failure remain unclear, several lines of evidence from previous findings suggest that our results are biologically reasonable. For instance, in the present study, the level of hepatic miR-122-5p was downregulated with the aggravation of liver injury. Previous study proved that circulating miR-122-5p might function as a new biomarker for CHB patients with normal or nearly normal ALT levels (35), and miR-122-5p knockdown protected against acetaminophen-induced liver injury (36). Likewise, miR-192-5p was downregulated when liver injury worsened in the present study, while a previous study proved that mR-192-5p was upregulated in serum during liver injury, and downregulation of miR-192-5p might protect against liver cell death (37). Overall, it seems that DE-miRNAs may participate in the development of liver injury, and some of them may be potential targets for the treatment of liver failure.

Of these DE-miRNAs, miR-125b-5p was the focus of further investigation based on our previous findings and preliminary results. We previously documented that circulating miR-125b-5p might be a novel biomarker for liver injury, and high serum miR-125b-5p levels might predict a poor outcome in HBV-ACLF patients (28). In the present study, we preliminarily observed that the hepatic miR-125b-5p levels were lower in the HBV-ACLF group than in the HBV-non-ACLF group. Meanwhile, LPS/D-GalN-challenged mice and Huh7 cells both showed decreased miR-125b-5p levels compared to their untreated control groups. Therefore, it is reasonable to speculate that miR-125b-5p may have a protective role against liver injury, regardless of the presence of ACLF or ALF.

Subsequent experiments were performed to determine the role of miR-125b-5p in acute liver injury both *in vitro* and *in vivo*. We found a reduced apoptosis rate of injured Huh7 cells after transfection with the miR-125b-5p vector, demonstrating that miR-125b-5p was able to ameliorate acute liver injury. Later, using a mouse ALF model induced by LPS/D-GalN, we observed severely damaged liver histology and elevated ALT/AST levels in ALF mice, whereas upregulation of miR-125b-5p reversed the impacts of liver failure, in line with a previous study in which miR-125b-5p was proven to protect against paracetamol- and FAS-induced toxicity in hepatocytes (38).

We next explored the underlying mechanism of miR-125b-5p in relieving ALF. Patients with liver failure, either ALF or ACLF, display evidence of a proinflammatory state in the initial stage. Targeting factors that are involved in the inflammatory response may be an alternative therapeutic for liver failure. Immune dysfunction in ALF and ACLF shares many features with sepsis (3, 4, 39). During sepsis, miRNAs are crucial regulators of immune cell function and participate in the inflammatory response by regulating the production of inflammatory factors, the vascular barrier and endothelial function (40–42). Thus, dysregulated miRNAs may also be involved in the inflammatory response during liver failure. It has been reported that miR-125b-5p may directly or indirectly participate in inflammation (43–45). MiRNA-125b-5p elevation can restrain the inflammatory response and protect against sepsis-induced acute lung injury (43). Correspondingly, dramatic decreases in the levels of serum TNF-α and IL-1β in mice treated with miR-125b-5p were observed in our study; thus, we speculated that miR-125b-5p may alleviate ALF by suppressing inflammation.

Keap1, as a putative target of miR-125b-5p, was verified using a luciferase activity assay in the present study. There was a negative correlation between miR-125b-5p and Keap1 expression in Huh7 cells and liver tissues; thus, miR-125b-5p targeted and negatively regulated Keap1. The Keap1/Nrf2 signaling pathway plays a pivotal role in the maintenance of intracellular redox homeostasis and the regulation of inflammation. Under homeostatic conditions, Nrf2 is mainly retained by Keap1 in the cytoplasm. Upon oxidative stress, Keap1 is inactivated, and Nrf2 dissociates from Keap1. Nrf2 then translocates to the nucleus and binds to antioxidant response elements (AREs), leading to the expression of diverse antioxidant and metabolic genes, such as glutathione S-transferase (GST) and heme oxygenase 1 (HO-1) (46). HO-1 is a critical protective enzyme that inhibits the release of proinflammatory cytokines and activates the anti-inflammatory cytokines (47). The Nrf2/HO-1 axis has been found to reduce the levels of TNF-α, IL-6 and IL-1-β and play a major role in anti-inflammatory function (48).

In the present study, we found that LPS/D-GalN decreased hepatic miR-125b-5p levels to target Keap1 and inhibit the Nrf2 pathway, triggering liver inflammation and cell apoptosis. In contrast, upregulation of miR-125b-5p decreased the level of Keap1 and promoted the expression of Nrf2 and its target HO-1. Hence, miR-125b-5p protects against LPS/D-GalN- induced ALF by targeting Keap1 and disrupting the interaction

between Nrf2 and Keap1, followed by the activation of the Nrf2/HO-1 axis, thereby decreasing the levels of TNF-α and IL-1-β and inhibiting cell apoptosis, which was in accordance with previous evidence that regulation of the Keap1/Nrf2/HO-1 signaling pathway could alleviate acute liver injury (34, 49, 50).

However, only miR-125b-5p was investigated herein, and further studies are needed to disclose the molecular mechanisms by which other miRNAs, individually or cooperatively, contribute to the development of liver injury. Moreover, it may be better to establish a miRNA-network diagram targeting inflammation in the development of liver failure, which may provide new insight into the pathophysiology of liver failure and lay a basis for the study of new therapeutics.

In conclusion, our study provides evidence that miR-125b-5p can alleviate LPS/D-GalN-induced ALF by regulating the Keap1/Nrf2/HO-1 signaling pathway, and therefore, regulation of miR-125b-5p and its downstream target Keap1 may serve as an alternative intervention for liver failure.

Data availability statement

The datasets presented in this study can be found in online repositories. The names of the repository/repositories and accession number(s) can be found below: https://www.ncbi.nlm.nih.gov/, PRJNA885574.

Ethics statement

The animal study was reviewed and approved by animal ethics committee of Sichuan University.

Author contributions

E-QC and HT proposed the study. Y-CT and Y-HW performed the research. Y-CT, M-LW, WJ, and D-BW contributed to the acquisition of data and drafting of the manuscript. All the authors contributed to the analysis and interpretation of data and approved the final version of the manuscript.

Funding

This work was supported by the 1.3.5 project for disciplines of excellence, West China Hospital, Sichuan University (NO.ZYGD20009) and the Science and Technological Supports Project of Sichuan Province, China (NO. 2019YFS0028).

Conflict of interest

The authors declare that the research was conducted in the absence of any commercial or financial relationships that could be construed as a potential conflict of interest.

Publisher's note

All claims expressed in this article are solely those of the authors and do not necessarily represent those of their affiliated organizations, or those of the publisher, the editors and the reviewers. Any product that may be evaluated in this article, or claim that may be made by its manufacturer, is not guaranteed or endorsed by the publisher.

Supplementary material

The Supplementary Material for this article can be found online at: https://www.frontiersin.org/articles/10.3389/fimmu.2022.988668/full#supplementary-material

References

1. Sarin SK, Choudhury A, Sharma MK, Maiwall R, Al Mahtab M, Rahman S, et al. Acute-on-chronic liver failure: consensus recommendations of the Asian pacific association for the study of the liver (APASL): An update. *Hepatol Int* (2019) 13(4):353–90. doi: 10.1007/s12072-019-09946-3

2. Dogan S, Gurakar A. Liver transplantation update: 2014. *Euroasian J Hepatogastroenterol* (2015) 5(2):98–106. doi: 10.5005/jp-journals-10018-1144

3. Hensley MK, Deng JC. Acute on chronic liver failure and immune dysfunction: A mimic of sepsis. *Semin Respir Crit Care Med* (2018) 39(5):588–97. doi: 10.1055/s-0038-1672201

4. Dong V, Nanchal R, Karvellas CJ. Pathophysiology of acute liver failure. *Nutr Clin Pract* (2020) 35(1):24–9. doi: 10.1002/ncp.10459

5. Li J, Hu CH, Chen Y, Zhou MM, Gao ZJ, Fu MJ, et al. Characteristics of peripheral lymphocyte subsets in patients with acute-On-Chronic liver failure associated with hepatitis b. *Front Med (Lausanne)* (2021) 8:689865. doi: 10.3389/fmed.2021.689865

6. Laleman W, Claria J, Van der Merwe S, Moreau R, Trebicka J. Systemic inflammation and acute-on-Chronic liver failure: Too much, not enough. *Can J Gastroenterol Hepatol* (2018) p:1027152. doi: 10.1155/2018/1027152

7. Wu W, Yan H, Zhao H, Sun W, Yang Q, Sheng J, et al. Characteristics of systemic inflammation in hepatitis b-precipitated ACLF: Differentiate it from no-ACLF. *Liver Int* (2018) 38(2):248–57. doi: 10.1111/liv.13504

8. Weiss E, de la Grange P, Defaye M, Lozano JJ, Aguilar F, Hegde P, et al. Characterization of blood immune cells in patients with decompensated cirrhosis including ACLF. *Front Immunol* (2020) 11:619039. doi: 10.3389/fimmu.2020.619039

9. Khanam A, Kottilil S. Abnormal innate immunity in acute-on-Chronic liver failure: Immunotargets for therapeutics. *Front Immunol* (2020) 11:2013. doi: 10.3389/fimmu.2020.02013

10. Antoniades CG, Berry PA, Wendon JA, Vergani D. The importance of immune dysfunction in determining outcome in acute liver failure. *J Hepatol* (2008) 49(5):845–61. doi: 10.1016/j.jhep.2008.08.009

11. Vishnoi A, Rani S. MiRNA biogenesis and regulation of diseases: An overview. *Methods Mol Biol* (2017) 1509:1–10. doi: 10.1007/978-1-4939-6524-3_1

12. Nejad C, Stunden HJ, Gantier MP. A guide to miRNAs in inflammation and innate immune responses. *FEBS J* (2018) 285(20):3695–716. doi: 10.1111/febs.14482

13. Mikami Y, Philips RL, Sciume G, Petermann F, Meylan F, Nagashima H, et al. MicroRNA-221 and -222 modulate intestinal inflammatory Th17 cell response as negative feedback regulators downstream of interleukin-23. *Immunity* (2021) 54(3):514–25.e6. doi: 10.1016/j.immuni.2021.02.015

14. Fu B, Lin X, Tan S, Zhang R, Xue W, Zhang H, et al. MiR-342 controls mycobacterium tuberculosis susceptibility by modulating inflammation and cell death. *EMBO Rep* (2021) 22(9):e52252. doi: 10.15252/embr.202052252

15. Xie W, Lu Q, Wang K, Lu J, Gu X, Zhu D, et al. miR-34b-5p inhibition attenuates lung inflammation and apoptosis in an LPS-induced acute lung injury mouse model by targeting progranulin. *J Cell Physiol* (2018) 233(9):6615–31. doi: 10.1002/jcp.26274

16. Hu Y, Wu X, Ye Y, Ye L, Han S, Wang X, et al. Liver histology of treatment-naive children with chronic hepatitis b virus infection in shanghai China. *Int J Infect Dis* (2022) 123:112–8. doi: 10.1016/j.ijid.2022.08.017

17. Zhang Y, Xiang D, Hu X, Ruan Q, Wang L, Bao Z. Identification and study of differentially expressed miRNAs in aged NAFLD rats based on high-throughput sequencing. *Ann Hepatol* (2020) 19(3):302–12. doi: 10.1016/j.aohep.2019.12.003

18. Ouyang H, He X, Li G, Xu H, Jia X, Nie Q, et al. Deep sequencing analysis of miRNA expression in breast muscle of fast-growing and slow-growing broilers. *Int J Mol Sci* (2015) 16(7):16242–62. doi: 10.3390/ijms160716242

19. Zhao X, Chen Z, Zhou Z, Li Y, Wang Y, Zhou Z, et al. High-throughput sequencing of small RNAs and analysis of differentially expressed microRNAs associated with high-fat diet-induced hepatic insulin resistance in mice. *Genes Nutr* (2019) 14:6. doi: 10.1186/s12263-019-0630-1

20. Langmead B, Salzberg SL. Fast gapped-read alignment with bowtie 2. *Nat Methods* (2012) 9(4):357–9. doi: 10.1038/nmeth.1923

21. Kozomara A, Griffiths-Jones S. miRBase: annotating high confidence microRNAs using deep sequencing data. *Nucleic Acids Res* (2014) 42(Database issue):D68–73. doi: 10.1093/nar/gkt1181

22. Friedlander MR, Mackowiak SD, Li N, Chen W, Rajewsky N. miRDeep2 accurately identifies known and hundreds of novel microRNA genes in seven animal clades. *Nucleic Acids Res* (2012) 40(1):37–52. doi: 10.1093/nar/gkr688

23. Huang J, Li Y, Ma F, Kang Y, Liu Z, Wang J. Identification and characterization of microRNAs in the liver of rainbow trout in response to heat stress by high-throughput sequencing. *Gene* (2018) 679:274–81. doi: 10.1016/j.gene.2018.09.012

24. Wang J, Shao J, Li Y, Elzo MA, Jia X, Lai S. Genome-wide identification and characterization of perirenal adipose tissue microRNAs in rabbits fed a high-fat diet. *Biosci Rep* (2021) 41(4):BSR20204297. doi: 10.1042/BSR20204297

25. Ou N, Song Y, Xu Y, Yang Y, Liu X. Identification and verification of hub microRNAs in varicocele rats through high-throughput sequencing and bioinformatics analysis. *Reprod Toxicol* (2020) 98:189–99. doi: 10.1016/j.reprotox.2020.09.012

26. Gene Ontology C. The gene ontology: enhancements for 2011. *Nucleic Acids Res* (2012) 40(Database issue):D559–64. doi: 10.1093/nar/gkr1028

27. Kanehisa M, Furumichi M, Tanabe M, Sato Y, Morishima K. KEGG: new perspectives on genomes, pathways, diseases and drugs. *Nucleic Acids Res* (2017) 45 (D1):D353–61. doi: 10.1093/nar/gkw1092

28. Tao YC, Wang ML, Wang M, Ma YJ, Bai L, Feng P. Quantification of circulating miR-125b-5p predicts survival in chronic hepatitis b patients with acute-on-chronic liver failure. *Dig Liver Dis* (2019) 51(3):412–8. doi: 10.1016/j.dld.2018.08.030

29. Ganjali S, Aghaee-Bakhtiari SH, Reiner Z, Sahebkar A. Differential expression of miRNA-223 in coronary in-stent restenosis. *J Clin Med* (2022) 11 (3):849. doi: 10.3390/jcm11030849

30. Afonso MB, Rodrigues PM, Simao AL, Gaspar MM, Carvalho T, Borralho P, et al. miRNA-21 ablation protects against liver injury and necroptosis in cholestasis. *Cell Death Differ* (2018) 25(5):857–72. doi: 10.1038/s41418-017-0019-x

31. Wang H, Chen L, Zhang X, Xu L, Xie B, Shi H, et al. Kaempferol protects mice from d-GalN/LPS-induced acute liver failure by regulating the ER stress-Grp78-CHOP signaling pathway. *BioMed Pharmacother* (2019) 111:468–75. doi: 10.1016/j.biopha.2018.12.105

32. Tao YC, Wang ML, Wu DB, Luo C, Tang H, Chen EQ. Apolipoprotein A5 alleviates LPS/D-GalN-induced fulminant liver failure in mice by inhibiting TLR4-mediated NF-kappaB pathway. *J Transl Med* (2019) 17(1):151. doi: 10.1186/s12967-019-1900-9

33. Liu L, Wang P, Wang YS, Zhang YN, Li C, Yang ZY, et al. MiR-130a-3p alleviates liver fibrosis by suppressing HSCs activation and skewing macrophage to Ly6C(lo) phenotype. *Front Immunol* (2021) 12:696069. doi: 10.3389/fimmu.2021.696069

34. Wu CT, Deng JS, Huang WC, Shieh PC, Chung MI, Huang GJ. Salvianolic acid c against acetaminophen-induced acute liver injury by attenuating inflammation, oxidative stress, and apoptosis through inhibition of the Keap1/Nrf2/HO-1 signaling. *Oxid Med Cell Longev 2019* (2019) p:9056845. doi: 10.1155/2019/9056845

35. Cheng JL, Zhao H, Yang SG, Chen EM, Chen WQ, Li LJ Plasma miRNA-122-5p and miRNA-151a-3p identified as potential biomarkers for liver injury among CHB patients with PNALT. *Hepatol Int* (2018) 12(3):277–87. doi: 10.1007/s12072-018-9871-0

36. Yang Z, Wu W, Ou P, Wu M, Zeng F, Zhou B, et al. MiR-122-5p knockdown protects against APAP-mediated liver injury through up-regulating NDRG3. *Mol Cell Biochem* (2021) 476(2):1257–67. doi: 10.1007/s11010-020-03988-0

37. Roy S, Benz F, Alder J, Bantel H, Janssen J, Vucur M, et al. Down-regulation of miR-192-5p protects from oxidative stress-induced acute liver injury. *Clin Sci (Lond)* (2016) 130(14):1197–207. doi: 10.1042/CS20160216

38. Yang D, Yuan Q, Balakrishnan A, Bantel H, Klusmann JH, Manns MP, et al. MicroRNA-125b-5p mimic inhibits acute liver failure. *Nat Commun* (2016) 7:11916. doi: 10.1038/ncomms11916

39. Claria J, Arroyo V, Moreau R. The acute-on-Chronic liver failure syndrome, or when the innate immune system goes astray. *J Immunol* (2016) 197(10):3755–61. doi: 10.4049/jimmunol.1600818

40. Kingsley SMK, Bhat BV. Role of microRNAs in sepsis. *Inflammation Res* (2017) 66(7):553–69. doi: 10.1007/s00011-017-1031-9

41. Zhong L, Simard MJ, Huot J. Endothelial microRNAs regulating the NF-kappaB pathway and cell adhesion molecules during inflammation. *FASEB J* (2018) 32(8):4070–84. doi: 10.1096/fj.201701536R

42. Lee LK, Medzikovic L, Eghbali M, Eltzschig HK, Yuan X. The role of MicroRNAs in acute respiratory distress syndrome and sepsis, from targets to therapies: A narrative review. *Anesth Analg* (2020) 131(5):1471–84. doi: 10.1213/ANE.0000000000005146

43. Jiang L, Ni J, Shen G, Xia Z, Zhang L, Xia S, et al. Upregulation of endothelial cell-derived exosomal microRNA-125b-5p protects from sepsis-induced acute lung injury by inhibiting topoisomerase II alpha. *Inflammation Res* (2021) 70(2):205–16. doi: 10.1007/s00011-020-01415-0

44. Luo X, Hu R, Zheng Y, Liu S, Zhou Z. Metformin shows anti-inflammatory effects in murine macrophages through dicer/microribonucleic acid-34a-5p and microribonucleic acid-125b-5p. *J Diabetes Investig* (2020) 11(1):101–9. doi: 10.1111/jdi.13074

45. Diao W, Lu L, Li S, Chen J, Zen K, Li L, et al. MicroRNA-125b-5p modulates the inflammatory state of macrophages *via* targeting B7-H4. *Biochem Biophys Res Commun* (2017) 491(4):912–8. doi: 10.1016/j.bbrc.2017.07.135

46. Lu MC, Ji JA, Jiang ZY, You QD. The Keap1-Nrf2-ARE pathway as a potential preventive and therapeutic target: An update. *Med Res Rev* (2016) 36 (5):924–63. doi: 10.1002/med.21396

47. Ahmed SM, Luo L, Namani A, Wang XJ, Tang X. Nrf2 signaling pathway: Pivotal roles in inflammation. *Biochim Biophys Acta Mol Basis Dis* (2017) 1863 (2):585–97. doi: 10.1016/j.bbadis.2016.11.005

48. Saha S, Buttari B, Panieri E, Profumo E, Saso L. An overview of Nrf2 signaling pathway and its role in inflammation. *Molecules* (2020) 25(22):5474. doi: 10.3390/molecules25225474

49. Lv H, Xiao Q, Zhou J, Feng H, Liu G, Ci X. Licochalcone a upregulates Nrf2 antioxidant pathway and thereby alleviates acetaminophen-induced hepatotoxicity. *Front Pharmacol* (2018) 9:147. doi: 10.3389/fphar.2018.00147

50. Wang W, Wu L, Li Q, Zhang Z, Xu L, Lin C, et al. Madecassoside prevents acute liver failure in LPS/D-GalN-induced mice by inhibiting p38/NF-kappaB and activating Nrf2/HO-1 signaling. *BioMed Pharmacother* (2018) 103:1137–45. doi: 10.1016/j.biopha.2018.04.162

frontiers | Frontiers in Immunology

TYPE Original Research
PUBLISHED 22 November 2022
DOI 10.3389/fimmu.2022.1002126

OPEN ACCESS

EDITED BY
Jonel Trebicka,
Goethe University Frankfurt, Germany

REVIEWED BY
Rolf Teschke,
Hospital Hanau, Germany
Pragyan Acharya,
All India Institute of Medical Sciences, India

*CORRESPONDENCE
Jian-Qing He
Jianqhe@gmail.com;
jianqing_he@scu.edu.cn

†These authors have contributed equally to this work

SPECIALTY SECTION
This article was submitted to Inflammation, a section of the journal Frontiers in Immunology

RECEIVED 24 July 2022
ACCEPTED 04 November 2022
PUBLISHED 22 November 2022

CITATION
Wang M-G, Wu S-Q, Zhang M-M and He J-Q (2022) Urine metabolomics and microbiome analyses reveal the mechanism of anti-tuberculosis drug-induced liver injury, as assessed for causality using the updated RUCAM: A prospective study.
Front. Immunol. 13:1002126.
doi: 10.3389/fimmu.2022.1002126

Urine metabolomics and microbiome analyses reveal the mechanism of anti-tuberculosis drug-induced liver injury, as assessed for causality using the updated RUCAM: A prospective study

Ming-Gui Wang[1,2†], Shou-Quan Wu[1†], Meng-Meng Zhang[1] and Jian-Qing He[1*]

[1]Department of Respiratory and Critical Care Medicine, West China Hospital, Sichuan University, Chengdu, China, [2]Department of Emergency Medicine, Sichuan Provincial People's Hospital, University of Electronic Science and Technology of China, Chengdu, China

Background: Anti-tuberculosis drug-induced liver injury (ATB-DILI) is one of the most common adverse reactions that brings great difficulties to the treatment of tuberculosis. Thus, early identification of individuals at risk for ATB-DILI is urgent. We conducted a prospective cohort study to analyze the urinary metabolic and microbial profiles of patients with ATB-DILI before drug administration. And machine learning method was used to perform prediction model for ATB-DILI based on metabolomics, microbiome and clinical data.

Methods: A total of 74 new TB patients treated with standard first-line anti-TB treatment regimens were enrolled from West China Hospital of Sichuan University. Only patients with an updated RUCAM score of 6 or more were accepted in this study. Nontargeted metabolomics and microbiome analyses were performed on urine samples prior to anti-tuberculosis drug ingestion to screen the differential metabolites and microbes between the ATB-DILI group and the non-ATB-DILI group. Integrating electronic medical records, metabolomics, and microbiome data, four machine learning methods was used, including random forest algorithm, artificial neural network, support vector machine with the linear kernel and radial basis function kernel.

Results: Of all included patients, 69 patients completed follow-up, with 16 (23.19%) patients developing ATB-DILI after antituberculosis treatment. Finally, 14 ATB-DILI patients and 30 age- and sex-matched non-ATB-DILI patients were subjected to urinary metabolomic and microbiome analysis. A total of 28 major differential metabolites were screened out, involving bile secretion, nicotinate and nicotinamide metabolism, tryptophan metabolism, ABC

transporters, etc. Negativicoccus and Actinotignum were upregulated in the ATB-DILI group. Multivariate analysis also showed significant metabolic and microbial differences between the non-ATB-DILI and severe ATB-DILI groups. Finally, the four models showed high accuracy in predicting ATB-DILI, with the area under the curve of more than 0.85 for the training set and 1 for the validation set.

Conclusion: This study characterized the metabolic and microbial profile of ATB-DILI risk individuals before drug ingestion for the first time. Metabolomic and microbiome characteristics in patient urine before anti-tuberculosis drug ingestion may predict the risk of liver injury after ingesting anti-tuberculosis drugs. Machine learning algorithms provides a new way to predict the occurrence of ATB-DILI among tuberculosis patients.

KEYWORDS

metabolomic, microbiome, anti-tuberculosis drug-induced liver injury (ATB-DILI), machine learning, cohort, updated RUCAM

Introduction

Tuberculosis (TB) is caused by *Mycobacterium tuberculosis* infection, which is an infectious disease with the highest mortality before the novel coronavirus pneumonia pandemic (1). According to the report of the World Health Organization, there were 9.9 million new cases of tuberculosis worldwide, and approximately 1.3 million patients died in 2020 (1). After treatment with a first-line anti-tuberculosis regimen containing isoniazid and rifampicin, 86% of patients were treated successfully (1–3). However, it is often accompanied by various adverse drug reactions, such as gastrointestinal reaction, drug-induced liver injury (DILI), hyperuricemia, leucopenia, allergy, peripheral neuritis and so on (3–7). Anti-tuberculosis drug-induced liver injury (ATB-DILI) is one of the most common adverse reactions in the treatment of tuberculosis (4–6) and may lead to treatment interruption, prolonged treatment time, decreased treatment success rate and increased hospitalization rat (8–10). Early identification and evaluation of ATB-DILI will provide new ideas for the precise treatment of tuberculosis patients.

Currently, the identification of biomarkers by metabolomics has been widely used in pathophysiological mechanisms in many scientific fields, such as plant biology (11), toxicology (12) and disease diagnosis and prognosis (13–16). Ultrahigh performance liquid chromatography tandem mass spectrometry (UPLC-MS) is one of the most effective means of metabolomics research (17). Through metabolomics research, Xie et al. found that 31 metabolites were related to DILI and were closely related to the severity of DILI (18). Prospective studies show that there are significant differences in serum metabolites between the DILI group and the non-DILI group prior to polygonum multiflorum ingestion, and the unique metabolic characteristics may be used to predict the risk of DILI after taking polygonum multiflorum (19). This suggests that metabolomics can be used to evaluate and predict DILI. There are a few clinical and animal experiments using metabolomics to explore the toxic mechanism and biomarkers of ATB-DILI (20–25). Nontargeted metabolomics found that 28 metabolites can be used as important distinguishing factors between ATB-DILI and non-ATB-DILI patients, and ATB-DILI affects the tricarboxylic acid cycle, arginine and proline metabolism, purine metabolism and pentose phosphate pathway (24). In our previous study, 11 urine differential metabolites were identified between ATB-DILI patients and non-ATB-DILI patients by gas chromatography-mass spectrometry (GC-MS) (26). These studies indicate that metabolomics is helpful for a new understanding of the pathophysiological process of ATB-DILI and for screening new markers of ATB-DILI. Moreover, no study has evaluated the metabolic characteristics of ATB-DILI patients and non-ATB-DILI patients before taking anti-tuberculosis drugs.

There are thousands of microbial species in the human microbial ecosystem that play a key role in maintaining host immunity, metabolism, drug metabolism, vitamin production and carbohydrate metabolism (27–29). Research interest has been focused on the interaction between the microbiota and the host, and how the composition of the human microbiota may have a potential impact on the development of certain diseases, such as metabolic syndrome, obesity (30), diabetes (31) and liver injury (26, 32, 33). Previous studies have shown that the

quantities of the urine microbiota differ significantly between patients with ATB-DILI and without ATB-DILI (26).

At present, the data on metabolomic or microbiota changes related to ATB-DILI are limited, especially premedication data. In addition, a model for the prediction of ATB-DILI is lacking. In this study, we hypothesized that the metabolome and microbiome are related to ATB-DILI. Therefore, we performed urine metabolomic and microbiota analyses of ATB-DILI prior to medication. Meanwhile, four machine learning methods was used to establish a clinical prediction model of ATB-DILI based on metabolomics, microbiome and clinical data.

Methods

Study population and sample collection

This prospective cohort study included patients with tuberculosis who visited the tuberculosis clinic of West China Hospital of Sichuan University from March 2021 to December 2021. The study was approved by the Ethics Committee of West China Hospital of Sichuan University. All research subjects were required to sign a written informed consent form by themselves or their representatives before being included in the study. Demographic datasets of patients with laboratory test data were obtained through electronic medical records and questionnaires.

Inclusion criteria are as follows: 1) age≥16 years and <80 years old; 2) newly diagnosed TB patients, including etiologically confirmed, pathologically confirmed and clinically diagnosed cases; 3) standard first-line anti-TB treatment regimens (including 2-month HRZE intensive treatment and at least 4 months of HRE consolidation therapy), and can be followed up regularly; 4) Han nationality in Southwest China; 5) voluntarily participate in this study and sign the informed consent form when included in the study. Those who do not meet the above diagnostic criteria are referred to as non-ATB-DILI.

The exclusion criteria were as follows: 1) abnormal liver function at baseline; 2) concomitant liver diseases such as alcoholic hepatitis, viral hepatitis or liver cirrhosis; 3) taking immunosuppressive drugs, antitumor drugs, and acetaminophen and other drugs that may cause liver damage; 4) patients with diabetes, autoimmune diseases, malignant tumors, or tuberculosis with severe heart, lung, and renal insufficiency; and 5) patients with HIV infection or who died during follow-up from causes other than adverse drug reactions.

The diagnostic criteria for ATB-DILI used in this study are (9, 34–36) as follows: alanine aminotransferase (ALT)≥3 normal upper limit of normal value (ULN) and/or total bilirubin (TBil)≥ 2ULN; or aspartate aminotransferase (AST) or alkaline phosphatase (ALP) and TBil are elevated at the same time, and at least one of them is ≥2 ULN. In addition, considering that the updated Roussel Uclaf Causality Assessment Method (RUCAM) was the recognized standard for the diagnosis of DILI, no matter what drug was used (37). Here, for patients who met the DILI diagnostic criteria (ALT≥5ULN or ALP≥2ULN) in the updated RUCAM, we conducted a subgroup analysis. All patients diagnosed with ATB-DILI completed a causality assessment using the updated RUCAM scale (37). Only patients with a RUCAM score of 6 or more were accepted in this study.

Urine nontargeted metabolomics and microbiome analyses were performed in ATB-DILI and gender and age-matched non-DILI patients, and patients with urinary system diseases were excluded. Urine samples were self-collected from the subjects according to the provided instructions prior to antituberculosis treatment and immediately sent to the laboratory. Once in the laboratory, samples were stored at −80°C until metabolomic and microbiome analysis.

Sample preparation

Urine is the common sample type used to perform metabolomics studies (38, 39). Compared to other samples, urine has easy sampling, low protein levels and less complexity (38). Also the urine metabolites are products of normal and abnormal cellular biological processes and can reflect a wide range of phenotypes including genetic modifications (38). Therefore, urine is more advantageous compared to other sample types and was used as a study sample in this study.

Clean midstream urine from patients before medication was collected, divided into three 1 ml aliquots, and immediately stored at −80°C. We discarded samples that were at room temperature for >2 hours.

Metabolite extraction was primarily performed according to previously reported methods (40, 41). In short, 100 μL samples were extracted by directly adding 300 μL of precooled methanol and acetonitrile (2:1, v/v), and internal standards mix (contains: L-Leucine-d3, L-Phenylalanine (13C9, 99%), L-Tryptophan-d5, Progesterone-2,3,4-13C3) were added for quality control of sample preparation. After vortexing for 1 min and incubating at -20°C for 2 h, the samples were centrifuged for 20 min at 4000 rpm, and the supernatant was then transferred for vacuum freeze drying. The metabolites were resuspended in 150 μL of 50% methanol and centrifuged for 30 min at 4000 rpm, and the supernatants were transferred to autosampler vials for LC–MS analysis. A quality control (QC) sample was prepared by pooling the same volume of each sample to evaluate the reproducibility of the whole LC–MS analysis.

Metabolite detection and comments

This experiment used a Waters 2D UPLC (Waters, USA) tandem Q Exactive HF high resolution mass spectrometer

(Thermo Fisher Scientific, USA) for separation and detection of metabolites. To provide more reliable experimental results during instrument testing, the samples are randomly ordered to reduce system errors. A QC sample was interspersed for every 10 samples.

The samples were analyzed on a Waters 2D UPLC (Waters, USA), coupled to a Q-Exactive mass spectrometer (Thermo Fisher Scientific, USA) with a heated electrospray ionization (HESI) source and controlled by the Xcalibur 2.3 software program (Thermo Fisher Scientific, Waltham, MA, USA). Chromatographic separation was performed on a Waters ACQUITY UPLC BEH C18 column (1.7 µm, 2.1 mm × 100 mm, Waters, USA), and the column temperature was maintained at 45°C. The mobile phase consisted of 0.1% formic acid (A) and acetonitrile (B) in the positive mode, and in the negative mode, the mobile phase consisted of 10 mM ammonium formate (A) and acetonitrile (B). The gradient conditions were as follows: 0-1 min, 2% B; 1-9 min, 2%-98% B; 9-12 min, 98% B; 12-12.1 min, 98% B to 2% B; and 12.1-15 min, 2% B. The flow rate was 0.35 mL/min and the injection volume was 5 µL.

The mass spectrometric settings for positive/negative ionization modes (ESI+/-) were as follows: spray voltage, 3.8/−3.2 kV; sheath gas flow rate, 40 arbitrary units (arb); aux gas flow rate, 10 arb; aux gas heater temperature, 350°C; capillary temperature, 320°C. The full scan range was 70–1050 m/z with a resolution of 70000, and the automatic gain control (AGC) target for MS acquisitions was set to 3e6 with a maximum ion injection time of 100 ms. The top 3 precursors were selected for subsequent MSMS fragmentation with a maximum ion injection time of 50 ms and resolution of 30,000, and the AGC was 1e5. The stepped normalized collision energy was set to 20, 40 and 60 eV.

LC–MS/MS analysis

The original data (raw file) collected byLC-MS/MS were imported into Compound Discoverer 3.1 (Thermo Fisher Scientific, USA) for data processing, including peak extraction, retention time correction, background peak labeling, and metabolite identification. We calculate the coefficient of variation of the relative peak area in all QC samples, and delete the compounds with coefficient of variation greater than 30%. The identification of metabolites was a combined result of the BGI Metabolome Database (BMDB), mzCloud and ChemSpider (Human Metabolome Database (HMDB), Kyoto Encyclopedia of Genes and Genomes (KEGG), LipidMaps) databases. Main parameters of metabolite identification: Precursor Mass Tolerance <5 ppm, Fragment Mass Tolerance <10 ppm, RT Tolerance <0.2 min. The identification level of metabolites was divided into five confidence levels, and the credibility of Level 1 to Level 5 decreased in order. The original data exported by LipidSearch were imported into metaX for data preprocessing and subsequent analysis (42). Multivariate statistical analysis (principal component analysis (PCA) and partial least squares-discriminant analysis (PLS-DA)), and univariate analysis (fold-change, FC and Student's t test) were combined to screen for differential metabolites between groups. Differential metabolite screening conditions: 1) variable projected importance (VIP) ≥ 1, 2) fold-change ≥ 1.2 or ≤ 0.83, 3) p-value <0.05. Metabolic pathway enrichment analysis of differential metabolites was performed based on the KEGG database.

Urine DNA extraction and 16S sequencing

Microbial genomic DNA extraction was performed as described previously (43). Urine microbial DNA was extracted using a Qiagen Mini Kit (Qiagen, Hilden, Germany) following the manufacturer's instructions. Primers targeting the hypervariable V3+V4 region of the 16S gene were used to amplify the extracted DNA samples (the forward primer was 5′- ACTCCTACGGGAGGCAGCA -3′, and the reverse primer was 5′- GGACTACHVGGGTWTCTAAT -3′). All samples were sequenced *via* Illumina HiSeq 2500.

Sequencing data analysis

Cutadapt v2.6 software was used to process the raw data to obtain fragments of the target region. FLASH (Fast Length Adjustment of Short reads, v1.2.11) was used for sequence splicing, and UCHIME (v4.2.40) software was used to remove chimeras. Sequences were clustered with a 97% similarity level by using USEARCH (v7.0.1090_i86linux32) to cluster the spliced tags into OTUs. The OTU representative sequences were aligned with the database for species annotation by RDP classifier (1.9.1) software, and the confidence threshold was set to 0.6. The VennDiagram package of R (v3.1.1) software was used to display the number of common and unique OTUs for each group. Principal coordinate analysis was performed using QIIME (v1.80) software to present similarities or differences in data. Line Discriminant Analysis (LDA) Effect Size (LEFSE) was used to calculate the differences in species abundance between the two groups and then to research the biomarkers related to ATB-DILI.

Statistical analysis

Differences between two groups were compared by using Student's t test for normal continuous variables and $\chi 2$-test for categorical variables. Differences with a p value <0.05 (two-

sided) were considered statistically significant. Statistical analyses were performed using SPSS V.21.0 for Windows (SPSS, Chicago, Illinois, USA). Moreover, correlations between the microbiota and metabolites and between the metabolites and clinical parameters were analyzed. Integrating electronic medical records, metabolomic and microbiome data, and machine learning methods was used to establish a clinical prediction model of ATLI. We used four machine learning algorithms: random forest, artificial neural network, support vector machine (SVM) with the linear kernel (SVM-linear), and SVM with radial basis function kernel (SVM-rbf) (44). The stratified sampling method was used to divide the training set (80%) and the validation set (20%), and the R4.1.2 software (R Foundation for Statistical Computing, Vienna, Austria) was used for data screening and model building. The importance of each feature in the occurrence of ATB-DILI was scored, and area under receiver operating characteristic (ROC) curves were employed to assess the accuracy of the models.

Results

Baseline characteristics

A total of 74 patients diagnosed with TB were recruited for this study from March 2021 to December 2021 at West China Hospital of Sichuan University (Sichuan Province, China). Finally, 5 patients were lost to follow-up. Of the remaining 69 patients, 16 (23.19%) developed ATB-DILI after antituberculosis treatment (Supplementary Figure 1). The general clinical characteristics of the two groups and the results of liver function tests when DILI occurred are shown in Table 1. Compared with the non-ATB-DILI group, the levels of albumin (43.2(40.1-44.4)g/L vs. 44.9(42.2-46.8)g/L, *P*: 0.033) and hemoglobin (125.5(118.5-135.8)g/L vs. 137.0(128.5-145.5) g/L, *P*: 0.019) were significantly lower in the ATB-DILI group. No significant differences were observed in other baseline characteristics between the two groups of patients (*P*>0.05).

TABLE 1 Clinical characteristics of 69 tuberculosis patients.

Characteristic	ATB-DILI (n=16)	Non-ATB-DILI (n=53)	*P*
Age, years, median(IQR)	39.0(24.0-53.8)	33.0(27.0-52.0)	0.717
Females, n(%)	11(68.75)	30(56.60)	0.386
Weight, kg, median(IQR)	51.0(50.0-55.0)	55.0(49.0-60.0)	0.289
BMI, kg/m2, median(IQR)	19.9(18.9-20.9)	20.0(18.6-21.9)	0.771
Smoking, n(%)	1(6.25)	7(13.21)	0.527
Drinking, n(%)	0(0.00)	7(13.21)	0.210
Extrapulmonary tuberculosis, n(%)	5(31.25)	14(26.42)	0.704
Baseline laboratory examination, median(IQR)			
TBil umol/L	8.1(6.6-12.5)	9.2(7.0-12.1)	0.495
ALT IU/L	14.5(12.3-16.8)	14.0(10.0-20.5)	0.499
AST IU/L	21.5(15.3-26.0)	19.0(16.0-23.0)	0.339
Alkaline phosphatase, IU/L	74.5(57.8-89.0)	75.0(66.5-107.0)	0.518
Glutamyltranspeptidase, IU/L	18.0(11.8-34.3)	19.5(11.3-32.3)	0.750
Albumin, g/L	43.2(40.1-44.4)	44.9(42.2-46.8)	0.033
Creatinine, μmol/L	66.5(59.0-78.3)	67.0(58.5-76.0)	0.915
Uric acid, mmol/L	265.5(227.8-373.0)	314.0(265.5-370.0)	0.191
Hemoglobin, g/L	125.5(118.5-135.8)	137.0(128.5-145.5)	0.019
White blood cell ×10^12/L	6.8(5.4-8.5)	6.0(4.9-7.5)	0.060
Platelet×10^9/	242.5(182.0-417.3)	249.5(202.0-282.5)	0.937
ESR mm/h	20.0(10.8-83.3)	14.0(9.3-29.3)	0.098
C-reactive protein, mg/L	3.8(2.8-27.1)	3.4(2.1-8.6)	0.359
Triglyceride, mmol/L	1.1(0.7-1.5)	1.1(0.8-1.5)	0.889
Circumstances of DILI, median (IQR)			
Onset time, days	29.0(14.0-44.3)		
ALT, IU/L	168.0(129.0-331.0)		
AST, IU/L	155.0(122.0-362.0)		
TBil, umol/L	14.1(9.5-17.9)		
Alkaline phosphatase, IU/L	90.0(74.0-122.0)		

ALT, alanine aminotransferase; AST, aspartate aminotransferase; TBil, total bilirubin; ESR, erythrocyte sedimentation rate; BMI, body mass index; IQR, Interquartile distance.

The median time to DILI occurred on day 29 after taking anti-TB drugs (Table 1).

After excluding patients with urinary system diseases, 14 ATB-DILI patients and 30 age- and sex- matched non-ATB-DILI patients were included for urinary metabolomics and microbiome analysis (Supplementary Figure 1). It is important to note that of these 14 patients, 8 met the definition of liver adaptation (45). The other 6 patients with ALT≥5 times the upper limit of normal were stopped using antituberculosis drugs according to Chinese guidelines, so it was hard to distinguish which were liver adaptation (36).

As shown in Table 2, there were no significant differences in sex, age, body weight, BMI, body mass index (BMI), smoking, drinking or tuberculosis site between the two groups of patients who underwent urine nontargeted metabolome and microbiome analysis (P>0.05). All participants had normal liver function before anti-tuberculosis drug ingestion. It was suggested that the general conditions of the two groups were consistent and comparable.

Metabonomic analysis of urine

PCA and OPLS-DA were performed for both positive ion mode (ESI+) and negative ion mode (ESI−). As shown in the figure (Figures 1A, B), the QC samples (blue circles) were significantly aggregated, indicating that the instrument was stable and that the reproducibility of the acquired data was good. The ATB-DILI (n=14, red circles) and tolerance groups (n=30, green circles) were not well separated in PCA. As shown (Figures 1C, D), the PLS-DA model clearly separated the ATB-DILI and non-ATB-DILI groups in both ionization modes. Differential metabolites between the two groups were screened according to multivariate and univariate statistical significance criteria (VIP≥1, FC≥1.2 or ≤ 0.83, and P<0.05). In general, there were 1256 urine differential metabolites screened in the positive ion mode and 334 in the negative ion mode (Figure 2). Finally, 28 differential metabolites with secondary classification names and reliable identification results (Level 1-3) were selected (Table 3), including choline, cherry base, N-acetyl, pseudohadine, N8-acetyl spermamine, glycolic acid, etc. As shown in Table 4, a total of 7 significant enrichment pathways for differential metabolites were found in both positive and negative ion modes. The differential metabolites were mainly involved in the metabolism of bile secretion, nicotinate and nicotinamide metabolism, tryptophan metabolism, ABC transporters, neuroactive ligand-receptor interaction, arginine and proline metabolism, and porphyrin and chlorophyll metabolism (P<0.05, Count≥2) (Table 4).

Correlation analysis of metabolic and clinical data

Correlation analysis was conducted between urine differential metabolites and clinical data, including baseline ALT, AST, TBIL, Alkaline phosphatase, hemoglobin, uric acid and albumin. We found that many different metabolites were significantly correlated with clinical data (Supplementary Table 1). The urine differential metabolite 11 dehydrothromboxane B2 was positively correlated with the baseline total bilirubin concentration, while the urine differential metabolite N8-acetylspermidine was negatively correlated with the hemoglobin content, and uric acid was also negatively correlated with the baseline serum uric acid level (Supplementary Table 2).

Microbiome analysis of urine

As shown in the Figure (Figure 3A), 1079 OTUs were shared between the ATB-DILI group and the non-ATB-DILI group, 607 OTUs were unique to the non-ATB-DILI group, and the other 189 OTUs were unique to the ATB-DILI group. The Shannon curve (Figure 3B) shows that the amount of sequencing data in this study was large enough to reflect the vast majority of microbial information in the sample. The top 10 key species between the two groups are shown in Figure 3C. Weighted UniFrac principal coordinate analysis (PCoA) was applied to detect the changes in microbial community structures

TABLE 2 Clinical characteristics of the two groups of matched patients.

Characteristic	Non-ATB-DILI group (n=30)	ATB-DILI group (n=14)	*P*
Age, years, median(IQR)	33.0 (27.0-52.0)	43.5 (22.8-55.5)	0.772
Females, n(%)	16(53.3)	9(64.3)	0.495
Weight, kg, median(IQR)	52.8(48.0-58.8)	50.0(49.9-55.0)	0.495
BMI, kg/m2, median(IQR))	19.9(18.6-22.0)	19.5(18.7-20.1)	0.473
Smoking, n(%)	2(6.7)	1(7.1)	0.976
Drinking, n(%)	2(6.7)	0(0.0)	0.314
Extrapulmonary tuberculosis, n(%)	23(76.7)	11(78.6)	0.888

IQR, Interquartile distance.

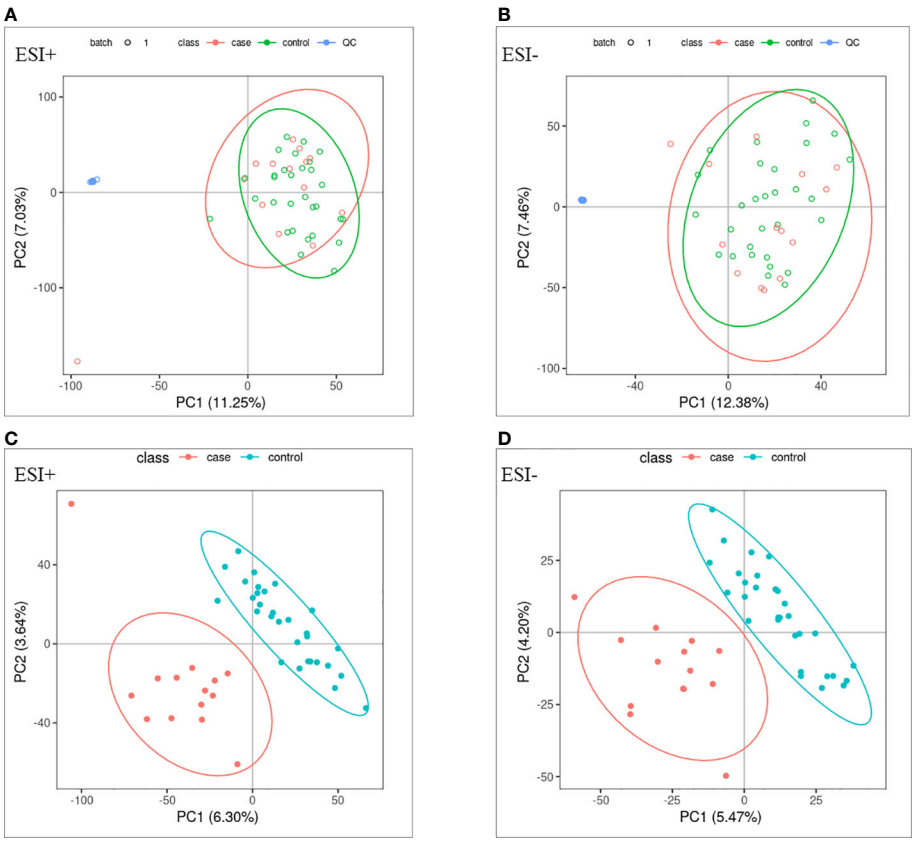

FIGURE 1
Multivariate statistical analysis. **(A, B)** principal component analysis scores scatter plots of the two groups. **(C, D)** partial least squares-discriminant analysis score scatter plots of the two groups. QC (blue circles), control group (n = 30, green circles), ATB-DILI group (n =14, red circles).

(Supplementary Figure 3). The results indicate that the ATB-DILI group and the control group were significantly separated along the PC2 axis, which explained 19.79% of the total variation. LEFSE analysis was used to determine the key attribute differences between the two groups. The differential microbiota (LDA score>2) screened between the two groups were Negativicoccus and Actinotignum, which were all upregulated in the ATB-DILI group (Figure 3D).

Correlation of the urine microbiota and metabolism

We further investigated the correlation of urinary differential metabolites with altered urinary microbiota. Significant correlations were found between some differential metabolites and microbial groups by calculating rank correlation coefficients (Figure 4 and Supplementary Table 2). Carbendazim was positively correlated with synergistia but negatively correlated with mollicutes ($p<0.05$) (Supplementary Table 2). D-(-)-lyxose was positively correlated with four microbial groups, including synergistia, ktedonobacteria, fibrobacteria and fusobacteriia ($p<0.05$) (Supplementary Table 2). Altogether, these results showed that distinctive metabolites were closely related to urinary microbiome variation, and distinctive metabolites and microbiomes were closely related to the occurrence of ATB-DILI.

Subgroup analysis

According to RUCAM criteria, metabolome and microbiome analysis were performed between the ALT≥5 ULN group and normal patients. Significant metabolic differences were observed between the two groups, there were 1122 different metabolites were screened in positive ion mode and 386 in negative ion mode (Supplementary Figure 3). Finally, 26 different metabolites were selected, including choline, 11-dehydrothromboxane b2, and N8-acetylspermidine. (Supplementary Table 3). Consistent with our results in Section 3.2, 8 common different metabolites were found in the

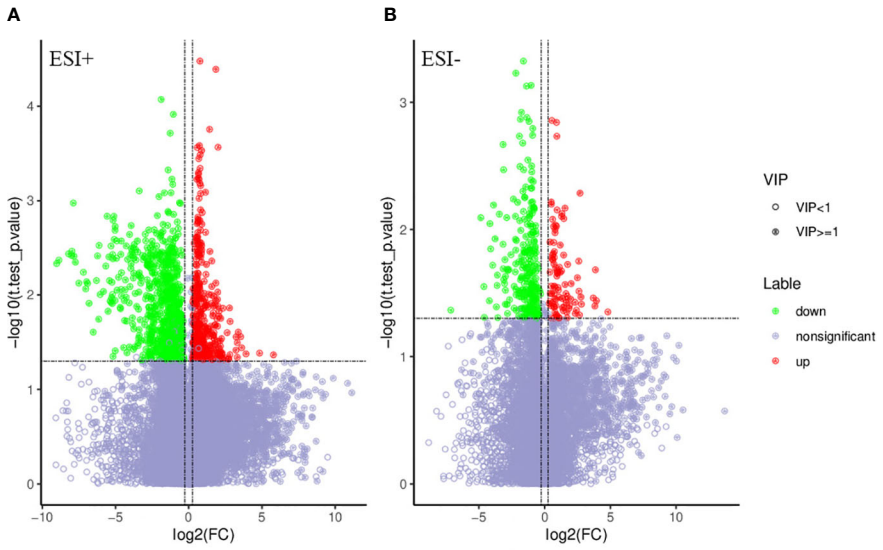

FIGURE 2
Volcano map of differential metabolites. Green is the down-regulated differential metabolite (labeled green), red is the up-regulated differential metabolite (labeled red), and metabolites without difference are labeled purple-gray. **(A)** positive ion mode, **(B)** negative ion mode.

subgroup analysis to be related to liver injury after medication, especially when ALT>5ULN occurred (Table 3 and Supplementary Table 3). The eight differential metabolites were choline, N8-acetylspermidine, carbendazim, N-acetylputrescine, 1-methylnicotinamide, creatine, porphobilinogen, and nonanoic acid (Table 3 and Supplementary Table 3). And these different metabolites had the same label direction in the two groups of patients with liver injury (Table 3 and Supplementary Table 3).

There were 795 OTUs shared between the DILI patients with ALT ≥ 5 ULN and normal patients, 68 OTUs were unique to the DILI group, and the other 891 OTUs were unique to the control group (Supplementary Figure 4-A). The top 10 key species between the two groups are shown in Supplementary Figure 4-B. Finally, 3 differential microbiotas (LDA score>2) were found between the two groups (Supplementary Figure 4-B). The Actinotignum was down regulated in DILI group, while the Bradyrhizobiaceae, and Bradyrhizobium were upregulated in the non-DILI group (Supplementary Figures 4-C). Combined with the results in Section 3.4, we have sufficient evidence to show that Actinotignum was closely related to the occurrence of liver injury after medication, regardless of the DILI standards.

Comparison of the models for the prediction of ATB-DILI

Random forest analysis was performed on the screened differential metabolites (Table 3), differential microbiota (Figure 2), and relevant clinical data of 44 patients. For clinical characteristics, we included albumin and hemoglobin, which were significantly different between the two groups, as well as other factors that may be associated with the occurrence of ATB-DILI (including age, sex, BMI, baseline ALT, AST, and TBil). A total of 38 variables are included. When ntree=500 and mtry=6, the model reaches the optimum. The score of the 38 variables was shown in Figure 5A. The larger the absolute value is, the greater the importance of the indicator. After sorting the variables from high to low according to the absolute value, the cross-validation curve was obtained by performing tenfold cross-validation repeated 5 times (Supplementary Figure 5). The top 10 variables were selected for model building with the lowest error (Supplementary Figure 5). The area under the ROC curve of the four models were shown in Table 5. At training set, the random forest model performed significantly better than the remaining three models (area under the curve 0.98 vs. 0.87 (ANN), 0.89 (SVM-linear) and 0.89 (SVM-rbf) (Table 5). Overall, random forest model, artificial neural network model and two support vector machine models (both SVM-linear and SVM-rbf) all have excellent prediction value for the validation set (Figure 5B and Table 5). The consistent results between the training set and the validation set indicate that those models have high accuracy for predicting the occurrence of ATB-DILI.

Discussion

Evidence that the human urine microbiome and metabolome contribute to the development of ATB-DILI is

10.3389/fimmu.2022.1002126

TABLE 3 Identified differential metabolites between two groups.

Name	MW	RT	VIP	FC	P	Label
Choline	103.1	0.7	3.3	1.79	0.003	Up
Trigonelline	137.0	0.7	2.1	3.19	0.016	up
N-acetylputrescine	130.1	0.7	1.8	1.23	0.009	up
Pseudoephedrine	165.1	3.3	2.5	0.01	0.009	down
N8-acetylspermidine	187.2	0.7	2.4	1.43	0.004	up
Glycocholate	465.3	8.0	2.2	4.06	0.013	up
Uric acid	168.0	1.0	1.9	1.66	0.021	up
Ecgonine	185.1	4.9	1.8	1.96	0.028	up
1-methylnicotinamide	136.1	0.8	1.8	2.09	0.012	up
6-methylquinoline	143.1	3.5	1.6	0.63	0.035	down
Sebacic acid	202.1	6.4	1.6	1.97	0.049	up
Picolinic acid	123.0	3.5	1.5	0.64	0.012	down
3-hydroxyanthranilic acid	153.0	2.8	1.1	1.26	0.049	up
Mannitol	182.1	0.7	1.9	1.57	0.022	up
Carbendazim	191.1	0.7	1.6	0.15	0.023	down
Lipoamide	205.1	4.0	1.4	1.78	0.033	up
Ophthalmic acid	289.1	2.4	1.4	0.47	0.041	down
Valerophenone	162.1	5.5	1.2	0.71	0.030	down
D-(-)-lyxose	150.1	0.7	1.0	0.77	0.030	down
Creatine	131.1	0.7	1.6	0.32	0.030	down
L-glutamic acid	147.1	0.7	1.1	0.71	0.029	down
Methylmalonic acid	118.0	0.7	1.9	0.46	0.014	down
Porphobilinogen	226.1	0.7	1.5	0.49	0.001	down
Epinephrine	183.1	3.9	2.2	2.44	0.008	up
Heptanoic acid	130.1	5.4	1.4	0.50	0.047	down
11-dehydrothromboxane b2	368.2	6.8	1.1	1.40	0.040	up
Nonanoic acid	158.1	6.9	1.5	0.51	0.004	down
Taurolithocholic acid 3-sulfate	563.3	7.8	2.2	1.53	0.017	up

VIP, variable important for the projection; FC, fold-change; MW, molecular weight; RT, retention time.

accumulating. Thus, characterization of the urinary microbiota and metabolites in ATB-DILI is highly warranted, especially before medication. Herein, we first reported the characterization of urine metabolomics and the microbiome in patients with ATB-DILI before medication and identified key metabolites and bacteria that may be involved in the development of ATB-DILI. Meanwhile, we first proposed and successfully built four ATB-DILI clinical prediction models using our metabolomics, microbiome and clinical data.

In this study, the levels of ALT, AST, TBil or ALP were within the normal range in all enrolled patients before ingestion of anti-tuberculosis drugs. Approximately 23.2% of the patients had markedly elevated ALT and AST after ingesting anti-tuberculosis drugs. According to China's 2019 guidelines for

TABLE 4 Differential metabolite pathway analysis.

Pathway	Ion modes	Count	Count All	P
Bile secretion	positive	4	97	<0.001
Nicotinate and nicotinamide metabolism	positive	2	55	0.001
Tryptophan metabolism	positive	2	81	0.002
ABC transporters	positive	2	124	0.005
Neuroactive ligand-receptor interaction	negative	2	52	<0.001
Arginine and proline metabolism	negative	2	78	<0.001
Porphyrin and chlorophyll metabolism	negative	2	142	0.003

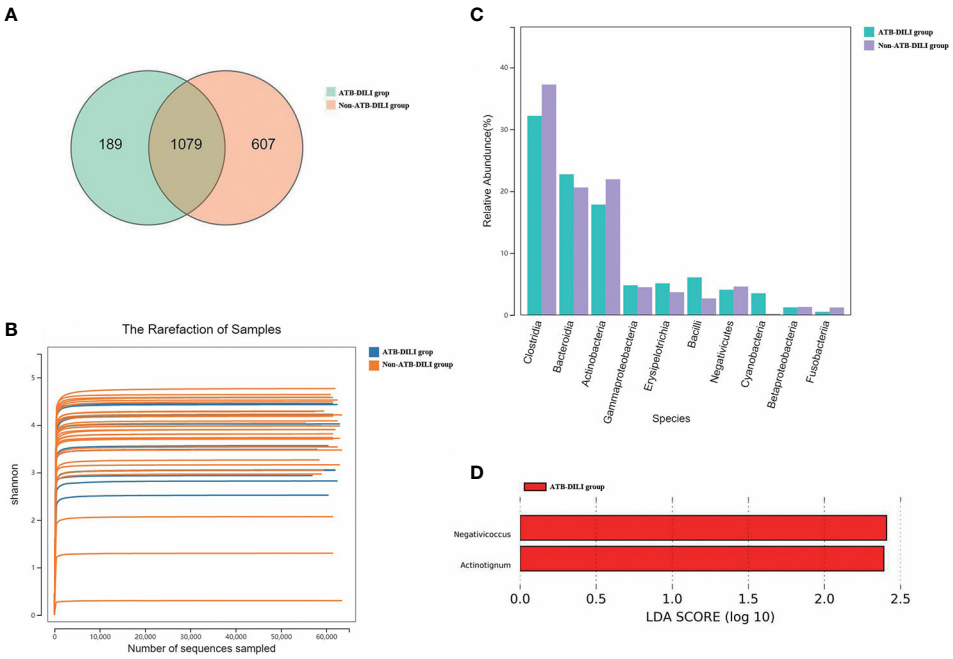

FIGURE 3
Comparison between 16S sequencing data of urine samples from non-ATB-DILI patients (n = 30) and ATB-DILI patients (n = 14). **(A)** Venn diagram. The left is the ATB-DILI group, the right is the control group. **(B)** α-diversity (Shannon curve). **(C)** Difference comparison of key species. **(D)** LEfSe analysis. Species with LDA greater than the set value of 2 are presented. The length of the bar indicates the magnitude of LDA influence.

the diagnosis and treatment of ATB-DILI (36), for DILI caused by anti-tuberculosis drugs, when ALT≥3ULN or TBil≥2ULN, the relevant anti-tuberculosis drugs need to be discontinued, and when ALT≥5ULN or TBil≥3ULN, it is necessary to stop all anti-tuberculosis drugs. Indicates that DILI needs to be taken seriously in TB patients. Therefore, we first analyzed the characteristics of the metabolomics and microbiome of DILI patients with ALT≥3 ULN. As a large number of domestic and foreign studies both recommend the use of RUCAM to assess DIL (46–48), we did a subgroup analysis for those DILI was defined as serum ALT level ≥5ULN. What was exciting was that no matter which DILI standard, we have found the same differential metabolites and microorganisms.

Metabolomics and the microbiome were used to analyze the urine of the ATB-DILI susceptible group and normal liver function control group, and the two groups could be distinguished significantly on the PLS-DA scatter plot. Consistent with those of a previous study (23, 24, 26), our results also indicated that ATB-DILI susceptible individuals may have specific metabolomic and microbiological patterns. We identified 28 major differential metabolites between the two groups in urine, including choline, trigonelline, N-acetylputrescine, uric acid, etc. The biological properties of each metabolite were searched from the human metabolome database (https://hmdb.ca/), and summarized in Supplementary Table 4. The differential metabolites selected in this study were consistent with the biospecimen locations in the database. This process involves bile secretion, nicotinate and nicotinamide metabolism, tryptophan, ABC transporters, neuroactive ligand-receptor interaction, arginine and proline metabolism, porphyrin and chlorophyll metabolism. Two major differential microbial, Negativicoccus and Actinotignum, were identified between the two groups.

As an essential nutrient, choline in the urine of patients with overactive bladder was 34.8% lower in urine metabolomic analysis than patients without overactive bladder ($P = 0.014$) (49). The urinary excretion of choline metabolites in term breast-fed infants was significantly higher than that in term formula-fed infants ($P < 0.05$) (50). This study found that urinary choline levels may be a noninvasive biomarker for predicting ATB-DILI. For the first time, upregulated trigonelline in urine before medication was found to be associated with ATB-DILI in TB patients. This may be related to the possible inhibition of key enzymes in lipid metabolism and absorption by trigonelline (51). Previous studies have found that glycocholic acid levels were significantly increased in DILI (52, 53), and the increased levels were positively correlated with the severity of DILI (52). Combined with the results of this study, glycocholic acid may have a role as a biomarker for DILI. As a proinflammatory and proapoptotic molecule, uric acid

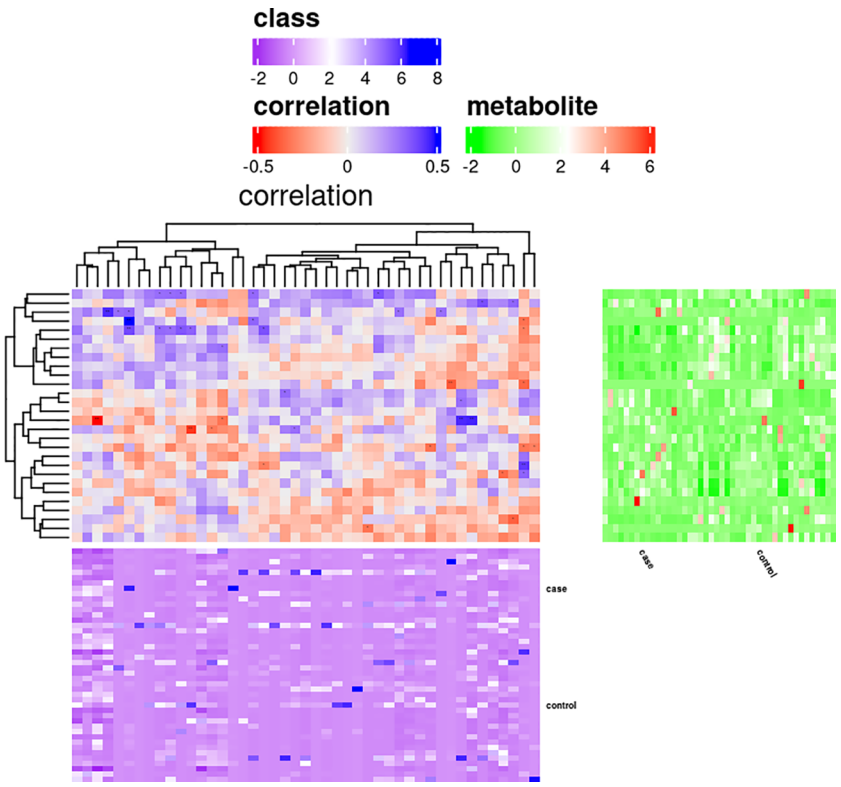

FIGURE 4
Correlation analysis of differential metabolites and microbiota.

plays an intermediary role in the process of liver and kidney injury (54, 55), and animal experiments have shown that the elevation of uric acid may lead to alcohol-induced steatosis, endoplasmic reticulum stress, and cell apoptosis. death and liver damage (56). Cao et al. found that uric acid levels in urine can be used to differentiate ATB-DILI from non-ATB-DILI patients (24). In this study, we found that uric acid in urine generation before medication could be used as a biomarker to predict the occurrence of ATB-DILI after medication, indicating that uric acid in urine metabolism may have great potential in predicting and identifying ATLI.

Additionally, differential metabolite enrichment analysis showed that metabolic pathways, including bile secretion, niacin and nicotinamide metabolism, ABC transporters, and etc., were involved in the occurrence of ATB-DILI after medication. Impaired bile secretion has been observed in mouse models of liver injury (57), which leads to intrahepatic bile accumulation (58). Studies have found that the bile secretion pathway is involved in psoralen (59) and liver injury induced by baklavaine (60). Our study found that abnormalities in the bile secretion pathway existed before liver injury occurred and before drug administration. It has also been shown that liver damage can be alleviated by improving bile secretion (61). Therefore, this pathway may provide a new target for the prevention and treatment of ATB-DILI. Consistent with our earlier study, niacin and nicotinamide metabolism were involved in the occurrence of ATB-DILI in this study (26). The difference is that a previous study found that the niacin and nicotinamide metabolism pathways were significantly altered when liver injury occurred, and this study found that this pathway abnormality existed long before liver injury occurred. Herein, the niacin and nicotinamide metabolic pathways play an important role in the development and progression of ATLI. The specific mechanism needs further study.

Each disease has its own unique microbial alterations (29, 62). Microorganisms in the gut originate from the digestive system, while urine microorganisms reflect the entire body including the intestinal tract, oral system, respiratory system, etc (63). Studies have shown that the urinary microbiota is associated with diseases outside the urinary system (64, 65). Previous studies have indicated that microbiota alterations are associated with drug-induced liver injury (26, 32, 33). Our previous study found that six microbiota including o_Bacteroidales, f_Prevotellaceae, etc., were associated with ATB-DILI (26). Compared with control group, this prospective study found that the Negativicoccus and

10.3389/fimmu.2022.1002126

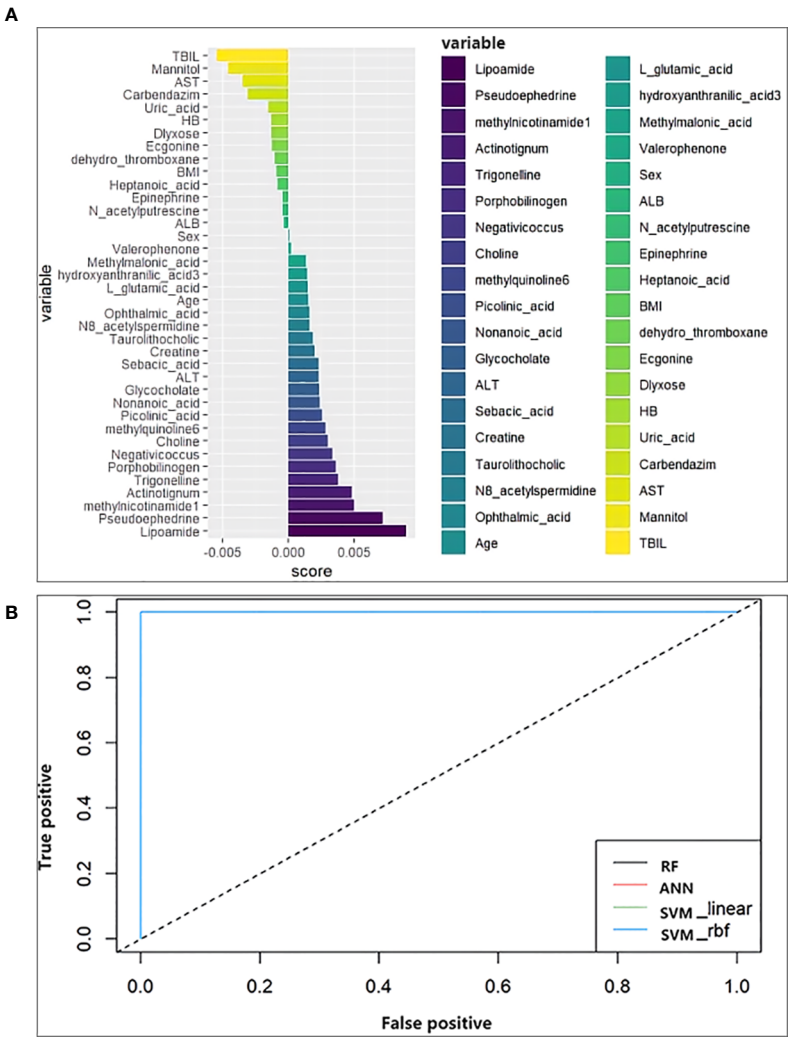

FIGURE 5
Machine learning models. **(A)** Score the importance of variables. The larger the value, the more important the variable is. **(B)** Receiver operating characteristic curve for the models developed with the top 10 important variables as inputs. ALT, alanine aminotransferase; AST, aspartate aminotransferase; TBIL, total bilirubin; ALB, albumin; BMI, body mass index; HB, hemoglobin.

TABLE 5 The area under the curve of machine learning models.

Model	AUC	
	Training set	Test set
RF	0.98	1
ANN	0.87	1
SVM_linear	0.89	1
SVM_rbf	0.89	1

AUC, area under the curve; RF, random forest; ANN, artificial neural network; SVM, support vector machine; SVM_rbf, support vector machine with radial basis function kernel.

Actinotignum were upregulated in the ATB-DILI group before medication. Negativicoccus was found to be significantly increased in the oral cavity of hamsters using smokeless tobacco products (66). Among patients with nonmuscle-invasive bladder cancer, BCG-vaccinated patients had significantly more negativicoccus in their urine than nonvaccinated BCG patients (67). Negativicoccus was also found to be one of the core flora in all ground glass nodules and normal tissue samples (68). However, studies have proven that Negativicoccus and Actinotignum are associated with ATB-DILI.

Furthermore, our results also suggested that there may be specific metabolomic and microbiological patterns in individuals

susceptible to severe ATB-DILI when compared with the mild ATB-DILI group. The discovery of these biomarkers may help with the early identification of TB patients at risk of developing severe DILI, thus providing new ideas for the individualized treatment of TB. However, due to the limited sample size, the results of this study cannot be directly generalized to other populations.

This study is the first to establish the early prediction models of ATB-DILI by combining clinical data and metabolomics and microbiology data using a machine learning method. The random forest algorithm was used to analyze multiple variables, the importance of each variable was scored, and the optimal variable (top 10) combination was obtained by adjusting the parameters to form the ATB-DILI prediction models. The results of the training set and the validation set were consistent (all ROC ≥ 0.85) (Table 5). Based on clinical and genomic data, researchers from Taipei Medical University compared the accuracy of multiple machine learning methods in predicting ATB-DILI, among which the artificial neural network showed the best prediction performance (69). In their study, the area under the ROC curve of the training set in the random forest algorithm was 0.724 and 0.718 for the validation set (69). Combined with our study, machine learning techniques show great potential in predicting ATB-DILI and may provide new opportunities for the diagnosis and treatment of ATB-DILI.

This study has some limitations. First, the number of participants was limited. However, this was a prospective study, which enhanced reliability of the results. Further validation in more centers with more patients needs to be verified in the future. Second, even though this study adds to the understanding of metabolome and microbiological patterns on the progress of ATD-DILI, this study only analyzed predose characteristics and lacked data at multiple time points after drug use. There is much work yet to be performed to understand these changes entirely. Finally, the current study obtained good predictive value in both the training set and the validation set, but limited by the limited sample size and geographical limitations, further verification is required in studies with more regions and larger samples in the future.

Conclusion

In conclusion, our findings extend our knowledge of the relationship between urinary metabolites and microbiota and host ATB-DILI susceptibility, indicating that certain metabolomic and microbiome changes from the host can be used to identify and predict an individual's susceptibility to ATB-DILI. In the future, prospective cohorts with a larger number of subjects are needed to investigate the potential clinical utility of metabolic markers in the identification of susceptible individuals. Prospective cohorts with more subjects and more time points are needed to investigate the potential clinical utility of metabolic markers and key microbiota in identifying susceptible individuals.

Data availability statement

The original contributions presented in the study are publicly available. This data can be found here: https://www.ncbi.nlm.nih.gov/, PRJNA870240.

Ethics statement

The studies involving human participants were reviewed and approved by West China Hospital of Sichuan University [Approval No.: 761 (2019)]. The patients/participants provided their written informed consent to participate in this study.

Author contributions

All authors contributed substantially to the study design, data interpretation, and the writing of the manuscript. J-QH contributed to the study design. M-GW and S-QW contributed to data collection and analysis and completed the full text. M-MZ contributed to data collection. All authors contributed to the article and approved the submitted version.

Funding

This work was supported by the National Natural Science Foundation of China (Grant No. 81870015).

Conflict of interest

The authors declare that the research was conducted in the absence of any commercial or financial relationships that could be construed as a potential conflict of interest.

Publisher's note

Supplementary material

The Supplementary Material for this article can be found online at: https://www.frontiersin.org/articles/10.3389/fimmu.2022.1002126/full#supplementary-material

SUPPLEMENTARY FIGURE 1
Flow chart.

SUPPLEMENTARY FIGURE 2
Volcano map of differential metabolites in subgroup analysis.

SUPPLEMENTARY FIGURE 3
Principal co-ordinates analysis.

SUPPLEMENTARY FIGURE 4
Subgroup analysis of 16S sequencing data of urine samples. **(A)** Venn diagram. The left is the severe DILI group, the right is the non-DILI group. **(B)** Difference comparison of the top 10 key species. **(C)** LEfSe analysis. Species with LDA greater than the set value of 2 are presented. The length of the bar indicates the magnitude of LDA influence.

SUPPLEMENTARY FIGURE 5
Cross validation curve. The abscissa is the number of variables, and the ordinate is the cross-validation error rate.

References

1. World Health Organization. *Global tuberculosis report 2021*. (Geneva: World Health Organization) (2021).

2. World Health Organization *Global tuberculosis report 2020*. (Geneva: World Health Organization) (2020).

3. Nahid P, Dorman SE, Alipanah N, Barry PM, Brozek JL, Cattamanchi A, et al. Official American thoracic Society/Centers for disease control and Prevention/ Infectious diseases society of America clinical practice guidelines: Treatment of drug-susceptible tuberculosis. *Clin Infect Dis* (2016) 63:e147–95. doi: 10.1093/cid/ciw376

4. El Hamdouni M, Ahid S, Bourkadi JE, Benamor J, Hassar M, Cherrah Y. Incidence of adverse reactions caused by first-line anti-tuberculosis drugs and treatment outcome of pulmonary tuberculosis patients in Morocco. *Infection* (2020) 48:43–50. doi: 10.1007/s15010-019-01324-3

5. Zhang T, Du J, Yin X, Xue F, Liu Y, Li R, et al. Adverse events in treating smear-positive tuberculosis patients in China. *Int J Environ Res Public Health* (2015) 13:86. doi: 10.3390/ijerph13010086

6. Wu S, Wang Y, Zhang M, Wang M, He JQ. Transforming growth factor-beta 1 polymorphisms and anti-tuberculosis drug-induced liver injury. polymorphisms in TGFbeta1 and its relationship with anti-tuberculosis drug-induced liver injury. *Therapie* (2019) 74:399–406. doi: 10.1016/j.therap.2018.07.003

7. Zhang D, Hao J, Hou R, Yu Y, Hu B, Wei L. The role of NAT2 polymorphism and methylation in anti-tuberculosis drug-induced liver injury in Mongolian tuberculosis patients. *J Clin Pharm Ther* (2020) 45:561–9. doi: 10.1111/jcpt.13097

8. Jindani A, Nunn AJ, Enarson DA. Two 8-month regimens of chemotherapy for treatment of newly diagnosed pulmonary tuberculosis: international multicentre randomised trial. *Lancet* (2004) 364:1244–51. doi: 10.1016/S0140-6736(04)17141-9

9. Shang P, Xia Y, Liu F, Wang X, Yuan Y, Hu D, et al. Incidence, clinical features and impact on anti-tuberculosis treatment of anti-tuberculosis drug induced liver injury (ATLI) in China. *PloS One* (2011) 6:e21836. doi: 10.1371/journal.pone.0021836

10. Wang S, Shangguan Y, Ding C, Li P, Ji Z, Shao J, et al. Risk factors for acute liver failure among inpatients with anti-tuberculosis drug-induced liver injury. *J Int Med Res* (2020) 48:300060518811512. doi: 10.1177/0300060518811512

11. Schauer N, Fernie AR. Plant metabolomics: towards biological function and mechanism. *Trends Plant Sci* (2006) 11:508–16. doi: 10.1016/j.tplants.2006.08.007

12. Clarke CJ, Haselden JN. Metabolic profiling as a tool for understanding mechanisms of toxicity. *Toxicol Pathol* (2008) 36:140–7. doi: 10.1177/0192623307310947

13. Brindle JT, Antti H, Holmes E, Tranter G, Nicholson JK, Bethell HW, et al. Rapid and noninvasive diagnosis of the presence and severity of coronary heart disease using 1H-NMR-based metabonomics. *Nat Med* (2002) 8:1439–44. doi: 10.1038/nm1202-802

14. Crestani E, Harb H, Charbonnier LM, Leirer J, Motsinger-Reif A, Rachid R, et al. Untargeted metabolomic profiling identifies disease-specific signatures in food allergy and asthma. *J Allergy Clin Immunol* (2020) 145:897–906. doi: 10.1016/j.jaci.2019.10.014

15. Bowerman KL, Rehman SF, Vaughan A, Lachner N, Budden KF, Kim RY, et al. Disease-associated gut microbiome and metabolome changes in patients with chronic obstructive pulmonary disease. *Nat Commun* (2020) 11:5886. doi: 10.1038/s41467-020-19701-0

16. van Laarhoven A, Dian S, Aguirre-Gamboa R, Avila-Pacheco J, Ricano-Ponce I, Ruesen C, et al. Cerebral tryptophan metabolism and outcome of tuberculous meningitis: an observational cohort study. *Lancet Infect Dis* (2018) 18:526–35. doi: 10.1016/S1473-3099(18)30053-7

17. Yu M, Zhu Y, Cong Q, Wu C. Metabonomics research progress on liver diseases. *Can J Gastroenterol Hepatol* (2017) 2017:8467192. doi: 10.1155/2017/8467192

18. Xie Z, Chen E, Ouyang X, Xu X, Ma S, Ji F, et al. Metabolomics and cytokine analysis for identification of severe drug-induced liver injury. *J Proteome Res* (2019) 18:2514–24. doi: 10.1021/acs.jproteome.9b00047

19. Zhang L, Niu M, Wei AW, Tang JF, Tu C, Bai ZF, et al. Risk profiling using metabolomic characteristics for susceptible individuals of drug-induced liver injury caused by polygonum multiflorum. *Arch Toxicol* (2020) 94:245–56. doi: 10.1007/s00204-019-02595-3

20. Zhao H, Si ZH, Li MH, Jiang L, Fu YH, Xing YX, et al. Pyrazinamide-induced hepatotoxicity and gender differences in rats as revealed by a (1)H NMR based metabolomics approach. *Toxicol Res (Camb)* (2017) 6:17–29. doi: 10.1039/C6TX00245E

21. Ruan LY, Fan JT, Hong W, Zhao H, Li MH, Jiang L, et al. Isoniazid-induced hepatotoxicity and neurotoxicity in rats investigated by (1)H NMR based metabolomics approach. *Toxicol Lett* (2018) 295:256–69. doi: 10.1016/j.toxlet.2018.05.032

22. Rawat A, Chaturvedi S, Singh AK, Guleria A, Dubey D, Keshari AK, et al. Metabolomics approach discriminates toxicity index of pyrazinamide and its metabolic products, pyrazinoic acid and 5-hydroxy pyrazinoic acid. *Hum Exp Toxicol* (2018) 37:373–89. doi: 10.1177/0960327117705426

23. Liu L, Li X, Huang C, Bian Y, Liu X, Cao J, et al. Bile acids, lipid and purine metabolism involved in hepatotoxicity of first-line anti-tuberculosis drugs. *Expert Opin Drug Metab Toxicol* (2020) 16:527–37. doi: 10.1080/17425255.2020.1758060

24. Cao J, Mi Y, Shi C, Bian Y, Huang C, Ye Z, et al. First-line anti-tuberculosis drugs induce hepatotoxicity: A novel mechanism based on a urinary metabolomics platform. *Biochem Biophys Res Commun* (2018) 497:485–91. doi: 10.1016/j.bbrc.2018.02.030

25. Brewer CT, Kodali K, Wu J, Shaw TI, Peng J, Chen T. Toxicoproteomic profiling of hPXR transgenic mice treated with rifampicin and isoniazid. *Cells* (2020) 9:1654. doi: 10.3390/cells9071654

26. Wu S, Wang M, Zhang M, He JQ. Metabolomics and microbiomes for discovering biomarkers of antituberculosis drugs-induced hepatotoxicity. *Arch Biochem Biophys* (2022) 716:109118. doi: 10.1016/j.abb.2022.109118

27. Jandhyala SM, Talukdar R, Subramanyam C, Vuyyuru H, Sasikala M, Nageshwar Reddy D. Role of the normal gut microbiota. *World J Gastroenterol* (2015) 21:8787–803. doi: 10.3748/wjg.v21.i29.8787

28. Pickard JM, Zeng MY, Caruso R, Nunez G. Gut microbiota: Role in pathogen colonization, immune responses, and inflammatory disease. *Immunol Rev* (2017) 279:70–89. doi: 10.1111/imr.12567

29. Dominguez-Bello MG, Godoy-Vitorino F, Knight R, Blaser MJ. Role of the microbiome in human development. *Gut* (2019) 68:1108–14. doi: 10.1136/gutjnl-2018-317503

30. Sergeev IN, Aljutaily T, Walton G, Huarte E. Effects of synbiotic supplement on human gut microbiota, body composition and weight loss in obesity. *Nutrients* (2020) 12:222. doi: 10.3390/nu12010222

31. Harsch IA, Konturek PC. The role of gut microbiota in obesity and type 2 and type 1 diabetes mellitus: New insights into "Old" diseases. *Med Sci (Basel)* (2018) 6:32. doi: 10.3390/medsci6020032

32. Sun J, Zhang J, Wang X, Ji F, Ronco C, Tian J, et al. Gut-liver crosstalk in sepsis-induced liver injury. *Crit Care* (2020) 24:614. doi: 10.1186/s13054-020-03327-1

33. Gong S, Lan T, Zeng L, Luo H, Yang X, Li N, et al. Gut microbiota mediates diurnal variation of acetaminophen induced acute liver injury in mice. *J Hepatol* (2018) 69:51–9. doi: 10.1016/j.jhep.2018.02.024

34. Saukkonen JJ, Cohn DL, Jasmer RM, Schenker S, Jereb JA, Nolan CM, et al. An official ATS statement: hepatotoxicity of antituberculosis therapy. *Am J Respir Crit Care Med* (2006) 174:935–52. doi: 10.1164/rccm.200510-1666ST

35. Tostmann A, Boeree MJ, Aarnoutse RE, de Lange WC, van der Ven AJ, Dekhuijzen R. Antituberculosis drug-induced hepatotoxicity: concise up-to-date review. *J Gastroenterol Hepatol* (2008) 23:192–202. doi: 10.1111/j.1440-1746.2007.05207.x

36. C.S.o.T.o.C.M. Association. Guidelines for the diagnosis and treatment of anti-tuberculosis drug-induced liver injury (2019 edition). *Chinese Journal of Tuberculosis and Respiratory*. (2019) 42(5):343–56. doi: 10.3760/cma.j.issn.1001-0939.2019.05.007

37. Danan G, Teschke R. RUCAM in drug and herb induced liver injury: The update. *Int J Mol Sci 17* (2015) 17:14. doi: 10.3390/ijms17010014

38. Zhang A, Sun H, Wang P, Han Y, Wang X. Recent and potential developments of biofluid analyses in metabolomics. *J Proteomics* (2012) 75:1079–88. doi: 10.1016/j.jprot.2011.10.027

39. Araujo AM, Carvalho M, Carvalho F, Bastos ML, Guedes de Pinho P. Metabolomic approaches in the discovery of potential urinary biomarkers of drug-induced liver injury (DILI). *Crit Rev Toxicol* (2017) 47:633–49. doi: 10.1080/10408444.2017.1309638

40. Dunn WB, Broadhurst D, Begley P, Zelena E, Francis-McIntyre S, Anderson N, et al. Procedures for large-scale metabolic profiling of serum and plasma using gas chromatography and liquid chromatography coupled to mass spectrometry. *Nat Protoc* (2011) 6:1060–83. doi: 10.1038/nprot.2011.335

41. Sarafian MH, Gaudin M, Lewis MR, Martin FP, Holmes E, Nicholson JK, et al. Objective set of criteria for optimization of sample preparation procedures for ultra-high throughput untargeted blood plasma lipid profiling by ultra performance liquid chromatography-mass spectrometry. *Anal Chem* (2014) 86:5766–74. doi: 10.1021/ac500317c

42. Wen B, Mei Z, Zeng C, Liu S. metaX: a flexible and comprehensive software for processing metabolomics data. *BMC Bioinf* (2017) 18:183. doi: 10.1186/s12859-017-1579-y

43. Ren Z, Wang H, Cui G, Lu H, Wang L, Luo H, et al. Alterations in the human oral and gut microbiomes and lipidomics in COVID-19. *Gut* (2021) 70:1253–65. doi: 10.1136/gutjnl-2020-323826

44. Boobier S, Hose DRJ, Blacker AJ, Nguyen BN. Machine learning with physicochemical relationships: solubility prediction in organic solvents and water. *Nat Commun* (2020) 11:5753. doi: 10.1038/s41467-020-19594-z

45. Dara L, Liu ZX, Kaplowitz N. Mechanisms of adaptation and progression in idiosyncratic drug induced liver injury, clinical implications. *Liver Int* (2016) 36:158–65. doi: 10.1111/liv.12988

46. Teschke R, Danan G. Idiosyncratic drug-induced liver injury (DILI) and herb-induced liver injury (HILI): Diagnostic algorithm based on the quantitative roussel uclaf causality assessment method (RUCAM). *Diagnostics (Basel)* (2021) 11:458. doi: 10.3390/diagnostics11030458

47. Teschke R, Eickhoff A, Schulze J, Danan G. Herb-induced liver injury (HILI) with 12,068 worldwide cases published with causality assessments by roussel uclaf causality assessment method (RUCAM): an overview. *Transl Gastroenterol Hepatol* (2021) 6:51. doi: 10.21037/tgh-20-149

48. Teschke R, Danan G. Worldwide use of rucam for causality assessment in 81,856 idiosyncratic dili and 14,029 hili cases published 1993-mid 2020: a comprehensive analysis. *Medicines (Basel)* (2020) 7:62. doi: 10.3390/medicines7100062.

49. Sheyn D, Hijaz AK, Hazlett FEJr., Dawodu K, El-Nashar S, Mangel JM, et al. Evaluation of urine choline levels in women with and without overactive bladder syndrome. *Female Pelvic Med Reconstr Surg* (2020) 26:644–8. doi: 10.1097/SPV.0000000000000639

50. Shoji H, Taka H, Kaga N, Ikeda N, Hisata K, Miura Y, et al. Choline-related metabolites influenced by feeding patterns in preterm and term infants. *J Matern Fetal Neonatal Med* (2020) 33:230–5. doi: 10.1080/14767058.2018.1488165

51. Lang R, Yagar EF, Eggers R, Hofmann T. Quantitative investigation of trigonelline, nicotinic acid, and nicotinamide in foods, urine, and plasma by means of LC-MS/MS and stable isotope dilution analysis. *J Agric Food Chem* (2008) 56:11114–21. doi: 10.1021/jf802838s

52. Ma Z, Wang X, Yin P, Wu R, Zhou L, Xu G, et al. Serum metabolome and targeted bile acid profiling reveals potential novel biomarkers for drug-induced liver injury. *Med (Baltimore)* (2019) 98:e16717. doi: 10.1097/MD.0000000000016717

53. Slopianka M, Herrmann A, Pavkovic M, Ellinger-Ziegelbauer H, Ernst R, Mally A, et al. Quantitative targeted bile acid profiling as new markers for DILI in a model of methapyrilene-induced liver injury in rats. *Toxicology* (2017) 386:1–10. doi: 10.1016/j.tox.2017.05.009

54. Gilbert K, Rousseau G, Bouchard C, Dunberry-Poissant S, Baril F, Cardinal AM, et al. Caspase-(8/3) activation and organ inflammation in a rat model of resuscitated hemorrhagic shock: A role for uric acid. *J Trauma Acute Care Surg* (2019) 86:431–9. doi: 10.1097/TA.0000000000002152

55. Khazoom F, L'Ecuyer S, Gilbert K, Gagne MA, Bouchard C, Rose CF, et al. Impact of uric acid on liver injury and intestinal permeability following resuscitated hemorrhagic shock in rats. *J Trauma Acute Care Surg* (2020) 89:1076–84. doi: 10.1097/TA.0000000000002868

56. Wang M, Chen WY, Zhang J, Gobejishvili L, Barve SS, McClain CJ, et al. Elevated fructose and uric acid through aldose reductase contribute to experimental and human alcoholic liver disease. *Hepatology* (2020) 72:1617–37. doi: 10.1002/hep.31197

57. Pradhan-Sundd T, Vats R, Russell JO, Singh S, Michael AA, Molina L, et al. Dysregulated bile transporters and impaired tight junctions during chronic liver injury in mice. *Gastroenterology* (2018) 155:1218–1232.e24. doi: 10.1053/j.gastro.2018.06.048

58. Vats R, Liu S, Zhu J, Mukhi D, Tutuncuoglu E, Cardenes N, et al. Impaired bile secretion promotes hepatobiliary injury in sickle cell disease. *Hepatology* (2020) 72:2165–81. doi: 10.1002/hep.31239

59. Duan J, Dong W, Xie L, Fan S, Xu Y, Li Y. Integrative proteomics-metabolomics strategy reveals the mechanism of hepatotoxicity induced by fructus psoraleae. *J Proteomics* (2020) 221:103767. doi: 10.1016/j.jprot.2020.103767

60. Li ZQ, Wang LL, Zhou J, Zheng X, Jiang Y, Li P, et al. Integration of transcriptomics and metabolomics profiling reveals the metabolic pathways affected in dictamnine-induced hepatotoxicity in mice. *J Proteomics* (2020) 213:103603. doi: 10.1016/j.jprot.2019.103603

61. Xiao Q, Zhang S, Ren H, Du R, Li J, Zhao J, et al. Ginsenoside Rg1 alleviates ANIT-induced intrahepatic cholestasis in rats *via* activating farnesoid X receptor and regulating transporters and metabolic enzymes. *Chem Biol Interact* (2020) 324:109062. doi: 10.1016/j.cbi.2020.109062

62. Schneider KM, Candels LS, Hov JR, Myllys M, Hassan R, Schneider CV, et al. Gut microbiota depletion exacerbates cholestatic liver injury *via* loss of FXR signalling. *Nat Metab* (2021) 3:1228–41. doi: 10.1038/s42255-021-00452-1

63. Gottschick C, Deng ZL, Vital M, Masur C, Abels C, Pieper DH, et al. The urinary microbiota of men and women and its changes in women during bacterial vaginosis and antibiotic treatment. *Microbiome* (2017) 5:99. doi: 10.1186/s40168-017-0305-3

64. Lee Y, Park JY, Lee EH, Yang J, Jeong BR, Kim YK, et al. Rapid assessment of microbiota changes in individuals with autism spectrum disorder using bacteria-derived membrane vesicles in urine. *Exp Neurobiol* (2017) 26:307–17. doi: 10.5607/en.2017.26.5.307

65. Liu F, Ling Z, Xiao Y, Lv L, Yang Q, Wang B, et al. Dysbiosis of urinary microbiota is positively correlated with type 2 diabetes mellitus. *Oncotarget* (2017) 8:3798–810. doi: 10.18632/oncotarget.14028

66. Jin J, Guo L, VonTungeln L, Vanlandingham M, Cerniglia CE, Chen H. Smokeless tobacco impacts oral microbiota in a Syrian golden hamster cheek pouch carcinogenesis model. *Anaerobe* (2018) 52:29–42. doi: 10.1016/j.anaerobe.2018.05.010

67. Hussein AA, Elsayed AS, Durrani M, Jing Z, Iqbal U, Gomez EC, et al. Investigating the association between the urinary microbiome and bladder cancer: An exploratory study. *Urol Oncol* (2021) 39:370.e9–370.e19. doi: 10.1016/j.urolonc.2020.12.011

68. Ren Y, Su H, She Y, Dai C, Xie D, Narrandes S, et al. Whole genome sequencing revealed microbiome in lung adenocarcinomas presented as ground-glass nodules. *Transl Lung Cancer Res* (2019) 8:235–46. doi: 10.21037/tlcr.2019.06.11

69. Lai NH, Shen WC, Lee CN, Chang JC, Hsu MC, Kuo LN, et al. Comparison of the predictive outcomes for anti-tuberculosis drug-induced hepatotoxicity by different machine learning techniques. *Comput Methods Programs BioMed* (2020) 188:105307. doi: 10.1016/j.cmpb.2019.105307

Frontiers in Immunology

Explores novel approaches and diagnoses to treat immune disorders.

The official journal of the International Union of Immunological Societies (IUIS) and the most cited in its field, leading the way for research across basic, translational and clinical immunology.

Discover the latest Research Topics

See more →

Frontiers

Avenue du Tribunal-Fédéral 34
1005 Lausanne, Switzerland
frontiersin.org

Contact us

+41 (0)21 510 17 00
frontiersin.org/about/contact